The biodiversity of the Dinosaur Provincial Park ecosystem and its vicinity in the Late Cretaceous (Campanian) of western Canada through space, time, and energy flow

Alexandre Vitruve Demers-Potvin
Department of Biology
McGill University, Montreal

August 2024

A thesis submitted to McGill University in partial fulfillment of the requirements of the degree of
Doctor of Philosophy

Table of Contents

CHAPTER 1. General introduction and literature review

CHAPTER 2. Occurrence of *Centrosaurus apertus* (Ceratopsidae: Centrosaurinae) in Saskatchewan, Canada, and expanded dinosaur diversity in the easternmost exposure of the Late Cretaceous (Campanian) Dinosaur Park Formation

CHAPTER 3. Insights into the temporal resolution of the Late Cretaceous (Campanian) Dinosaur Provincial Park biota (Alberta, Canada) from 3-D stratigraphic mapping

CHAPTER 4. Tyrannosaurs were dragons, not lions: food webs reveal the ecological role of apex predators in the Dinosaur Provincial Park biota

4.2 Material and methods

4.3 Results

APPENDICES

ABSTRACT

Over the past few decades, palaeontology has increasingly contributed to present biological conservation issues by revealing past biotic responses to environmental change at vast temporal scales and at a global spatial scale to guide predictions of long-term biodiversity patterns. However, such patterns should be explored in greater detail at more constrained spatiotemporal scales to increase the relevance of palaeontology to more urgent challenges to specific ecosystems. Unfortunately, diversity estimates from the fossil record are notoriously hindered by reduced temporal resolution relative to the present combined with highly variable preservation potential across the tree of life. For this thesis, I argue that Dinosaur Provincial Park, along with its coeval fossil localities in Alberta and Saskatchewan, Canada, preserves one of the world's few ancient ecosystems known from the Mesozoic Era with a geological and palaeontological heritage that is sufficiently informative to reduce these shortfalls to deep-time biodiversity knowledge on a regional to local scale over a relatively short time interval (~2.5 million years). Based on a rich research history spanning more than a century, my main objective is to gain further knowledge on three of the dimensions through which the biodiversity of the Dinosaur Provincial Park (DPP) ecosystem can be studied: space, time, and energy flux (i.e. trophic interactions). First, I investigate the spatial dimension of that diversity by documenting the first confirmed occurrence of two dinosaur species in the easternmost outcrop of the Dinosaur Park Formation among a vertebrate fauna preserved in a Saskatchewan bonebed, thus expanding their known palaeogeographical range into a more coastal palaeoenvironment at a time of higher sea levels. I then turn to DPP itself to investigate the temporal resolution of diversity by examining sedimentary rock sequences that host several of my research group's field sites. Using 3-D digital outcrop models created through photogrammetry from images acquired through drone flights in the field, I find that established stratigraphic (and therefore temporal) distributions of individual fossil quarries based on a geological datum that separates the Oldman Formation from the overlying Dinosaur Park Formation contain major uncertainties because of a previously overlooked local variability in the absolute elevation of that datum. Instead, I propose that the Dinosaur Park Formation can be subdivided into at least three successive sedimentary architectural units that contain promising marker beds that could constrain those stratigraphic distributions more rigorously with a more extensive aerial coverage of the Park. Finally, I explore the energy flow dimension of the DPP ecosystem by creating the first trophic networks and resulting trophic biomass pyramids ever attempted for this locality at a species-level taxonomic resolution based on feasible trophic interactions inferred from the very high quality of its fossil record. These novel food webs reveal that the tyrannosaurid dinosaurs at the top of DPP's food chains were more analogous to Komodo dragons than to carnivoran mammals by displaying a marked shift in trophic level through their ontogeny. In conclusion, this thesis opens promising research trajectories to further establish Dinosaur Provincial Park as a model palaeoecological system for studying biodiversity patterns over deep time at a local to regional spatial scale.

RÉSUMÉ

Au cours des dernières décennies, la paléontologie a contribué de plus en plus à des questions de conservation biologique en révélant des réactions biotiques à des changements environnementaux à de vastes échelles temporelles et à une échelle spatiale globale pour guider des prédictions de tendances de biodiversité à long terme. Toutefois, de telles tendances devraient être explorées plus en détail à des échelles spatiotemporelles plus limitées pour augmenter la pertinence de la paléontologie à des défis plus urgents pour des écosystèmes spécifiques. Malheureusement, les estimations de diversité à partir du registre fossile sont notoirement entravées par une résolution temporelle réduite par rapport au présent en plus d'un potentiel de préservation très variable à travers l'arbre de la vie. Pour cette thèse, j'argumente que le Parc provincial Dinosaur, en plus de localités fossiles d'âge semblable en Alberta et en Saskatchewan, Canada, préserve un des rares écosystèmes anciens connus de l'ère Mésozoïque avec un patrimoine géologique et paléontologique suffisamment informatif pour réduire ces lacunes aux connaissances de la biodiversité du temps profond à une échelle locale et régionale sur un intervalle de temps relativement court (~2,5 millions d'années). Basé sur une riche histoire de recherche étendue sur plus d'un siècle, mon objectif principal est d'acquérir plus de connaissances sur trois des dimensions à travers lesquelles la biodiversité de l'écosystème du Parc provincial Dinosaur (DPP) peut être étudiée : l'espace, le temps et le flux d'énergie (soit les interactions trophiques). Premièrement, j'enquête sur la dimension spatiale de cette diversité en documentant la première présence confirmée de deux espèces de dinosaures dans l'affleurement le plus oriental de la formation Dinosaur Park parmi une faune de vertébrés préservés dans un lit de fossiles de Saskatchewan, étendant ainsi leur répartition paléogéographique connue dans un paléoenvironnement plus côtier à une époque où le niveau de la mer était plus élevé. Je me tourne ensuite vers DPP même pour enquêter sur la résolution temporelle de la diversité en examinant des séquences de roches sédimentaires qui contiennent plusieurs des sites de terrain de mon groupe de recherche. En utilisant des modèles 3-D d'affleurements digitaux créés par photogrammétrie à partir d’images acquises durant des vols de drones sur le terrain, je découvre que les répartitions stratigraphiques (et donc temporelles) de carrières de fossiles individuelles basées sur une frontière géologique qui sépare la formation Oldman de la formation Dinosaur Park sus-jacente contiennent des incertitudes majeures à cause d’une variabilité locale auparavant négligée dans l’altitude absolue de cette frontière. Au lieu de cela, je propose que la formation Dinosaur Park soit divisible en au moins trois unités architecturales sédimentaires successives qui contiennent des couches marquantes prometteuses qui pourraient cerner ces répartitions stratigraphiques plus rigoureusement avec une couverture aérienne plus étendue du Parc. Finalement, j’explore la dimension du flux d’énergie de l’écosystème de DPP en créant les premiers réseaux trophiques et pyramides trophiques de biomasse résultantes jamais tentés pour cette localité à une résolution taxonomique au niveau de l’espèce basé sur des interactions trophiques réalistes déduites à partir de la qualité très élevée de son registre fossile. Ces nouveaux réseaux révèlent que les dinosaures tyrannosauridés au sommet des chaînes alimentaires de DPP étaient plus analogues au dragon de Komodo qu’aux grands mammifères carnivores en ayant un changement marqué de niveau trophique à travers leur ontogénie. En conclusion, cette thèse ouvre des trajectoires de recherche prometteuses pour poursuivre l’établissement du Parc provincial Dinosaur en tant que système paléoécologique moderne pour étudier la biodiversité à travers le temps profond à une échelle spatiale locale et régionale.

ACKNOWLEDGEMENTS

Discussion and support

First of all, I wish to thank my doctoral supervisor, Hans C.E. Larsson, as well as the other members of my supervisory committee, Philip J. Currie and Laura Pollock, and my thesis defence committee, including examiners Corwin Sullivan and Galen Halverson, and members Christopher Cameron, Irene Gregory-Eaves and Frédéric Guichard, for their valuable and multidisciplinary knowledge and insights which repeatedly propelled this thesis in inspiring directions. I also acknowledge that the field research presented in this thesis was conducted on ancestral lands of the *Niitsitapi* (i.e., the Blackfoot Confederacy) and of the Plains Cree, which are now located on territories covered by Treaty No. 4 and Treaty No. 7 in Alberta and Saskatchewan.

Chapter 2 has been decades in the making when accounting for the initial exploration of Saskatchewan's scattered Dinosaur Park Formation outcrops. One of the most important contributions came from Tim Tokaryk, who initially re-discovered the Lake Diefenbaker ceratopsian bonebed in 1990. This fossil collection could not have been assembled without the tireless contributions of the graduate and undergraduate students who participated in the 2012, 2013, 2014, 2015, 2017, and 2018 editions of McGill University's Vertebrate Palaeontology field course. Special thanks are dedicated to Emily Bamforth, who was a key member of each of these excursions to the site and kindly provided access to her field notes and quarry maps to complete this project. Preparation and imaging of the majority of the specimens would not have been completed without the contributions of Chantal Montreuil (Redpath Museum) and of the following volunteers: Gabrielle Bonin, Robert Bourque, Isabel Fernandez-McAuley, Holly Ghandhi, Audrey Gray, André Mueller, Sofia Mucci, and Anthony Smith. Thanks are extended to Editor J. Brendan Murphy and two anonymous reviewers for their insightful comments which greatly improved this manuscript for publication, as well as Ryan McKellar and Wes Long (Royal Saskatchewan Museum) for providing access to museum collections, and finally Saskatchewan Landing Provincial Park for granting land access.

Chapter 3 would not have been possible without the contributions of all crew members of the 2021, 2022 and 2023 editions of the McGill University Vertebrate Palaeontology field course, especially Aidan O. Howenstine, Anthony Smith, Robert Bourque, Hoai-Nam Bui, Anthony Zerafa, Victoria Crozier, José Avila Cervantes, and Luca Larsson. The authors would also like to thank Caleb Brown (Royal Tyrrell Museum of Palaeontology (TMP)), Paul Durkin (University of Manitoba), and David Eberth for helpful discussions, as well as Allison Vitkus (TMP) for sharing a digital elevation model (DEM) covering the entirety of Dinosaur Provincial Park and Tim Elrick (Geographic Information Centre, McGill University) for providing software access and data storage space. Thanks are extended to Alberta Parks and Dinosaur Provincial Park (Research permits 21-227, 22-022, 23-016 and 23-329), as well as Lane and Jean Lucas, for land access.

As for Chapter 4, I wish to thank Don Brinkman (TMP), Dominique Caron and Michael Catchen (McGill University), as well as Francis Banville, Corinne Soucy, and Timothée Poisot (Université de Montréal) for helpful discussions and code availability which greatly stimulated this research. The following must also be acknowledged for additional discussions which greatly improved each chapter: Louis-Philippe Bateman, Gregory Funston, Christiana Garros, Jack Milligan, Khoi Nguyen, Mark Powers, and Henry Sharpe. Specimen access was also provided by Brandon Strilisky, Rebecca Sanchez and Tom Courtenay (Royal Tyrrell Museum of Palaeontology). Finally, I wish to thank my friends, family, and, most of all, my parents for their invaluable advice which guided me throughout this incredible adventure.

Funding

My thesis research was supported by the following funding sources awarded to me: doctoral scholarships from the National Science and Engineering Research Council (NSERC PGSD3-559424) and the *Fonds de recherche Nature et technologies du Québec* (FRQNT 289816), funding from the

Dinosaur Research Institute (2017, 2021, 2022 and 2023), a Quebec Center for Biodiversity Science Excellence Award and two Redpath Museum Class of 66 Awards. Additionally, I benefited from a Canadian Foundation for Innovation Grant (Project 36146) and NSERC Discovery Grant (RGPIN-2016-06724), both awarded to Hans Larsson.

CONTRIBUTION TO ORIGINAL KNOWLEDGE

This research provides several distinct contributions to knowledge and original scholarship. It constitutes a unique outlook on the Late Cretaceous (Campanian) Belly River Group palaeobiota, one of Canada's (and of the world's) most universally recognized ancient ecosystems known from the fossil record, using a particularly diverse array of sedimentological, palaeobiological, and quantitative ecological methods to study various aspects of its past biodiversity. Chapter 2 constitutes the most detailed description of a dinosaur bonebed for all of Saskatchewan, which now includes the most complete record of the ceratopsian dinosaur *Centrosaurus apertus* from this province based on diagnostic anatomical characters preserved among some of the specimens uncovered there. The identification of that species also leads to the first reassessment of the relative age of that locality relative to Dinosaur Provincial Park in Alberta. Chapter 3 constitutes the first application of structure-from-motion photogrammetry of badlands landscapes (based on images acquired in the field with unmanned aerial vehicles) aimed at addressing the stratigraphic distributions of Cretaceous vertebrate taxa in Dinosaur Provincial Park. In this way, this research has initiated the assembly of the most detailed and expansive 3-D reconstruction and orthomosaic of the Park's fossil-bearing outcrops ever attempted. This is also where the high local variability of the elevation of the contact between the Oldman and Dinosaur Park Formations, which has been the main landmark used to measure the stratigraphic heights of fossil quarries in the Park for more than 30 years, has been quantified for the first time, which now leads to an alternative method relying on the identification of laterally continuous marker beds. Chapter 4 provides the first site-specific quantitative highly resolved trophic networks (and derived biomass pyramids) ever produced for the Dinosaur Provincial Park palaeocommunity, or for any non-marine Mesozoic biota. It is also the first research ever to measure trophic levels in any non-avian dinosaur, and to compare them with trophic levels derived from modern food webs, as well as the very first research to account for dietary shifts through ontogeny in any ancient ecosystem.

CONTRIBUTION OF AUTHORS

Chapter 2, *Occurrence of* Centrosaurus apertus *(Ceratopsidae: Centrosaurinae) in Saskatchewan, Canada, and expanded dinosaur diversity in the easternmost exposure of the Late Cretaceous (Campanian) Dinosaur Park Formation*, is a co-authored manuscript published at the *Canadian Journal of Earth Sciences*. I am the first author on this article, with Hans Larsson as co-author. I conceptualized the study, curated the study material (including preparing and imaging fossil specimens), acquired funding, participated in fieldwork, analyzed the data, and wrote the original manuscript draft. Hans Larsson conceptualized the study, acquired funding, directed fieldwork and reviewed and edited the manuscript.

Chapter 3*, Insights into the temporal resolution of the Late Cretaceous (Campanian) Dinosaur Provincial Park biota (Alberta, Canada) from 3-D stratigraphic mapping*, largely consists of a co-authored manuscript currently in review. I am the first author on this article, with Hans Larsson as co-author. This chapter also contains additional data and text intended to contribute to three supplementary co-authored manuscripts. I conceptualized the study, acquired funding, co-directed fieldwork, analyzed the data, and wrote the original draft of this chapter. Hans Larsson conceptualized the study, acquired funding, co-directed fieldwork and reviewed and edited the manuscript.

Chapter 4, *Tyrannosaurs were dragons, not lions: food webs reveal the ecological role of apex predators in the Dinosaur Provincial Park biota*, is a co-authored manuscript in preparation for submission. I am the first author on this article, with Hans Larsson as co-author. I conceptualized the study, acquired funding, collected and analyzed the data, and wrote the original manuscript draft. Hans Larsson conceptualized the study and reviewed and edited the manuscript.

I prepared all other components of this thesis, including the general introduction and literature review (Chapter 1), the comprehensive discussion (Chapter 5), and the final conclusion and appendices.

LIST OF FIGURES AND TABLES

LIST OF ABBREVIATIONS

	General
BB	Bonebed
BRG	Belly River Group
DPP	Dinosaur Provincial Park
DPF	Dinosaur Park Formation
Ka	Thousand years
LCZ	Lethbridge Coal Zone
MAZ	Megaherbivore assemblage zone
Ma/Myr	Million years
$\mathbf{O_2}$	Atmospheric dioxygen
OF	Oldman Formation
$\boldsymbol{p}\mathbf{CO_2}$	Carbon dioxide partial pressure
ppm	Parts per millions
U-Pb	Uranium-lead

	Institutions
CMN	Canadian Museum of Nature
NHMUK	Natural History Museum, London
RM	Redpath Museum
RSKM	Royal Saskatchewan Museum
TMP	Royal Tyrrell Museum of Palaeontology
UALVP	University of Alberta Laboratory for Vertebrate Palaeontology

	Chapter 2
ACE	Abundance Coverage Estimator
LDB	Lake Diefenbaker Bonebed
P*n*	Parietal process on locus *n*
WIS	Western Interior Seaway

	Chapter 3
ANOVA	Analysis of variance
DEM	Digital elevation model
DOM	Digital outcrop model
DGPS	Differential GPS receiver
DTM	Digital terrain model
dF	Digital facies
GCP	Ground control point
IBS	Inclined bedding sandstone
IHS	Inclined heterolithic strata
MUD	Mudstone
MVS	Multiview stereo
RMSE	Root mean square error
SfM	Structure-from-motion
TX	Trough cross-bedded sandstone
UAV	Unmanned aerial vehicle

	Chapter 4
CL	Chain length
PATL	Prey-averaged trophic level

We shall not cease from exploration
And the end of all our exploring
Will be to arrive where we started
And know the place for the first time

– T.S. Eliot, from “Little Gidding”, *Four Quartets* (1943)

CHAPTER 1. GENERAL INTRODUCTION AND LITERATURE REVIEW

1.1 General introduction

The badlands of Dinosaur Provincial Park (DPP) in southern Alberta, Canada, have arguably become one of the world's most fascinating places to study ancient life. Sustained palaeontological research conducted there since the latest nineteenth century has revealed a vertebrate fossil assemblage of almost unparalleled diversity, providing one of the most detailed glimpses available into a terrestrial ecosystem during the Late Cretaceous Epoch. Palaeontology in DPP has especially contributed to our knowledge of dinosaur anatomy, systematics, evolution and palaeoecology, and of local biodiversity patterns on a geological temporal scale. Extensive taxon descriptions, diversity analyses and geochronological advances now lay foundations to ask more complex questions about this spectacular ancient ecosystem. First, we are beginning to understand how biodiversity varied across the coastal floodplain surrounding DPP during the Late Cretaceous, from the emerging Rocky Mountains to the epicontinental Western Interior Seaway. However, the relative lack of satellite fossil localities along that spatial gradient leads us to ask whether new discoveries will reveal more or less faunal overlap than is currently appreciated. Second, what is the highest temporal resolution available from the Park's geological record to track biodiversity change through time? Third, what will the connection of the Park's fossil fauna and flora into food webs created by inferring interspecific trophic interactions reveal about the structure of that community?

These are just a selection of outstanding questions on the palaeoecology of Dinosaur Provincial Park. The original research chapters in the following thesis will address these questions by investigating changes in the biodiversity of that locality through three dimensions: space, time, and energy flow (the latter via trophic interactions).

In Chapter 1, I review the contribution of palaeontology to addressing biodiversity shortfalls in the fossil record. I place particular emphasis on the necessity to measure and compare biodiversity patterns revealed from a variety of diversity measurement methods in different localities across deep time at relatively constrained spatiotemporal scales due to their potential to showcase biotic responses to a variety of environmental perturbations. In the second part of this chapter, I demonstrate why the Belly River Group of Dinosaur Provincial Park constitutes an ideal system for such a research program. Our knowledge of the Park's palaeoecology has accumulated over 130 years of palaeontological research, and now combines a well-described stratigraphic succession that records a significant landscape change, a relatively precise and accurate absolute age to calibrate ecological (and possibly evolutionary) change in time, and, above all, an incredibly rich terrestrial and aquatic fossil record spanning most of the ecological niches and trophic levels that formed this Cretaceous community. By outlining our current state of knowledge on DPP, this review lays a foundation for the original research at the core of my thesis.

In Chapter 2, I explore the biodiversity of the Belly River Group biota through space since I venture away from DPP to investigate the faunal composition of a nearby coeval community. It is preserved in the Lake Diefenbaker Bonebed in Saskatchewan Landing Provincial Park, a locality that would have lain on the eastern shore of Laramidia by the Western Interior Seaway, downstream from DPP along a broad coastal plain. Among the abundant dinosaur remains uncovered at this site over the past decade, I dedicate particular attention to ceratopsid skull fragments that I assign to *Centrosaurus apertus*. I then discuss the implications of this discovery for the palaeogeographical distribution of *Centrosaurus*, since this is one of the most abundant dinosaurs known from late Campanian Alberta, and this study now presents the most complete record of this species in nearby Saskatchewan, in a far more coastal palaeoenvironment than the localities in which it was previously reported. This study ultimately contributes to characterizing the similarities and differences between the DPP and Lake Diefenbaker biotas along a coastal-inland spatial gradient.

In Chapter 3, I explore the biodiversity of the Belly River Group biota through time by investigating the time resolution of the formations that host its fossil record in Dinosaur Provincial Park. This is the chapter where I ask whether it is possible to stratigraphically correlate each of the Park's known fossil quarries and bonebeds by identifying marker beds across all of its exposures, a feat that has proven impossible to achieve from traditional ground-based observations alone. I begin to address this question by creating digital elevation models and orthomosaics assembled from drone images I acquired in the field, which together allow me to characterize local sedimentary successions around some of the quarries and bonebeds I investigated with my crew over three field seasons in DPP. The geological maps I present in this chapter have a small geographical area and should be considered as a proof of concept before achieving a more extensive aerial coverage of the Park. Nonetheless, the largest of these maps, centered around a mixed faunal bonebed we have been exploring since 2018, reveals two interesting patterns. The first is that the Oldman-Dinosaur Park Formation contact, which is the established datum for measuring the stratigraphic position of the Park's quarries, has a highly variable local elevation, which raises uncertainties about this method for estimating the relative ages of these sites. The second pattern consists of the identification of successive sedimentary architectural units on a local scale, which suggests that at least some of them are promising candidate marker beds for a more expansive correlation that could be achieved across DPP as a whole.

In Chapter 4, I explore the biodiversity of the Belly River Group biota through energy flow by assembling the first quantitative food webs achieved at a high taxonomic resolution for Dinosaur Provincial Park. This ecological network lays the groundwork to investigate the ecological role of a keystone apex predator in this ancient community, the tyrannosaurid dinosaur *Gorgosaurus libratus*, by tracing its trophic level through its ontogeny. The trophic interactions between each of the network's constituent species were determined by a review of the extensive palaeontological literature assembled for DPP, fossil localities of similar faunal composition, and close extant relatives of some fossil species. A comparison between the DPP food webs and extant food webs which I also assembled reveals that the trophic level of *G. libratus* shifted markedly from juvenile to adult life stages, following a pattern more similar to the Komodo dragon than to any extant carnivoran mammal. This study also resulted in the first estimate of the standing terrestrial vertebrate biomass of the DPP biota distributed along a trophic pyramid, which confirms previous findings that DPP likely sustained a much higher predator-prey ratio than that seen in extant communities with large carnivorans as apex predators. Therefore, it leads me to propose that the ecological impact of the tyrannosaurids of the DPP palaeobiota was more similar overall to that of the Komodo dragon than to that of extant carnivoran mammals despite having a very different suite of life history traits. Looking forward, the inclusion of intraspecific variation through ontogeny in the food webs presented in this study is expected to attract increased interest in future palaeoecological network analyses.

Chapter 5 consists of a general discussion and conclusions on the long-term outcomes of the results of my thesis. First, I demonstrate that the large-scale mapping project of the Belly River Group's outcrops in Dinosaur Provincial Park has great potential to shed greater certainty on the stratigraphic distributions of several of its vertebrate (especially dinosaur) species, with important ecological and macroevolutionary implications. Second, I lay a case to increase research efforts on mixed faunal macrofossil-bearing bonebeds after the experience I gained working on two localities that conform to this oft-overlooked taphonomic mode among Mesozoic fluvial deposits. Lastly, I propose that the ecological network of the DPP biota which I created for this thesis now lays a new foundation to investigate palaeocommunity structure throughout (and likely beyond) the Cretaceous Period.

The appendices that complement the chapters of this thesis are as follows: Appendix I is a brief timeline of the history of research in Dinosaur Provincial Park. Appendix II presents the database of all currently known quarries, bonebeds, plant and invertebrate localities of DPP, which I updated as part of my field- and museum collections-based research. Appendix III is a supplementary table for Chapter 2 listing all fossil occurrences from the Lake Diefenbaker Bonebed. Appendix IV details additional drone surveys conducted in DPP as part of my 2021 fieldwork which were deemed beyond the scope of Chapter 3. Appendix V is a detailed justification for all nodes and trophic links included in the DPP food webs presented in Chapter 4. Appendix VI is a series of tables listing references for occurrence, trophic links and body size for all nodes included in the DPP, Serengeti and Komodo food webs. The bibliography at the end of this thesis contains references for chapters 1 and 5 and appendices I, II and V. Chapters 2, 3 and 4 each have a distinct reference list.

1.2 Diving into 'shallow' deep time towards mesoeco-evolutionary dynamics

Palaeontology is the scientific field dedicated to the study of ancient life using fossil material preserved in the rock record. It was arguably recognized as a science when naturalists such as Georges Cuvier introduced the concept of biotic extinction following the realization during the late eighteenth to early nineteenth centuries that a fossil record that was only beginning to be explored contained species that went extinct long before human origins (Rudwick 1997). The scientific foundations of palaeontology were then consolidated by geological advances revealing the ancient age of planet Earth (Lyell 1830, 1832), and by biological advances developing the theory of evolution as a driver for the origin of species (Darwin 1859; Laland *et al.* 2015). As this discipline has evolved over the last 200 years, its scientific value is becoming ever more appreciated by using the fossil record to reveal trends in ecology and evolution otherwise imperceptible on a historical time scale, let alone human lifetimes. These biological trends often have similar durations to long-term geological and atmospheric processes and are thus considered to operate at a 'deep time' scale (Dobzhansky 1937: 12). This is usually the most insight-rich temporal scale to discern macroevolution, i.e. evolution above the species level where entire species and potentially clades (as opposed to individuals *within* species as in microevolution) are the unit of selection (Stanley 1975; Hautmann 2020). Likewise, palaeomacroecology is focused on investigating biodiversity patterns over deep time (Vavrek 2010), and explicitly integrates the geological and palaeontological record to questions on the causes and drivers of biodiversity across large spatial, temporal and taxonomic scales which define macroecology (Brown & Maurer 1989; Blackburn & Gaston 2002).

The single greatest contribution of palaeomacroecology to humanity may yet reside in the exploration of global climate and diversity trends over deep time (Sepkoski *et al.* 1981; Conway Morris 1995; Zachos *et al.* 2001; Alroy *et al.* 2008; Mayhew *et al.* 2012; Song *et al.* 2021), especially when environmental perturbations can be identified as very plausible causal mechanisms for past biotic responses such as diversification, invasion and extinction. The fact that the rate and magnitude of those responses hold potential to set baselines against which current biodiversity patterns can be compared, as well as to guide predictions of future biodiversity patterns at a time of unprecedented anthropogenic activity (i.e. the Anthropocene epoch (Crutzen 2006)), is becoming ever more recognized across the scientific community (Barnosky *et al.* 2011; Jaramillo & Cárdenas 2013; Ceballos *et al.* 2015; Keller *et al.* 2018; IPCC 2023). While this extremely long-term perspective is proving highly informative to biologists, the following chapter will defend the value of palaeoecology on a more constrained spatiotemporal scale focused on detailed studies of changes in outstanding ancient ecosystems displaying a detailed fossil record in specific localities across disparate geological intervals spanning a few million years at a resolution of 10^5-10^6 years. This is because this research may offer a long-term perspective to current environmental challenges specific to different biomes on a scale that is far more relatable to the Holocene and Anthropocene epochs. In this regard, now that palaeontology has revealed macroevolution and 'deep time' macroecology, I suggest that this field should direct itself more towards an intermediate temporal scale to the geological and historical time scales, in other words a *meso*eco-evolutionary time scale. If the various temporal scales of Earth's history are analogous to different pelagic ocean zones, the historical time scale is equivalent to the surface while deep time is equivalent to all depths below the photic zone. Therefore, the mesoeco-evolutionary time scale would be restricted to the ocean's epipelagic zone, i.e. 'shallow' deep time. I will also explain why it is essential to conduct this research beyond the Neogene Period and to investigate other geological time intervals with highly disparate biotic and abiotic conditions while accounting for the limitations of the fossil record. This will eventually lead me to propose the palaeobiota of the Late Cretaceous (Campanian) Belly River Group revealed from the badlands of Dinosaur Provincial Park, Alberta, Canada, as an ideal study system to investigate biotic responses on a mesoeco-evolutionary time scale.

Before going further, it is worth reiterating a fundamental question which has driven palaeontology at least since the 1960s and which has established foundations for modern palaeoecology: which processes are the main causes of biodiversity change in deep time? The fossil record tends to provide evidence for abiotic factors as the main cause by detecting correlations between perturbations in the physical environment and extreme biotic turnover. The most spectacular evidence in this regard comes from the detection of five mass extinction events at the Ordovician-Silurian, Devonian-Carboniferous, Permian-Triassic, Triassic-Jurassic, and Cretaceous-Paleogene boundaries (Raup & Sepkoski 1984; Marshall 2023). While each of these occurred under a different set of abiotic conditions, they seem to share at least one factor in common consisting of abrupt shifts in global temperature and atmospheric composition derived from a combination of volcanic activity, marine regressions and changes in oceanic circulation, which themselves seemed driven by continental drift operating at longer time scales (Caplan & Bustin 1999; Wignall 2001; Archibald *et al.* 2010; Jaraula *et al.* 2013; Ghienne *et al.* 2014; Brusatte *et al.* 2015; Burgess & Bowring 2015; Schoene *et al.* 2019). More frequent minor extinction events are also usually attributed to disturbances in the physical environment, such as the Carboniferous Rainforest Collapse, the Jurassic-Cretaceous transition, or the mammal cladal turnover known as *La Grande Coupure* at the Eocene-Oligocene transition (Legendre & Hartenberger 1992; Tennant *et al.* 2017; Pardo *et al.* 2019). Outside mass and minor extinction events, the dual forces of continental drift and climate change likely caused origination and extinction events consistently at a ‘background’ rate (Jablonski 1986, 2005) by triggering allopatric speciation through vicariance or dispersal. For instance, shallow epicontinental seas have often been proposed as ideal cradles for evolution and diversification (Bardet *et al.* 2014; Sallan *et al.* 2018), while the global reduction of the area of oceans’ neritic zone due to sea level fall at the end of the Pliocene is cited as the likely cause of a marine megafaunal extinction event at that time (Pimiento *et al.* 2017). As another example, phyletic splitting of some dinosaur lineages appears to track shifting landmasses (Sereno 1999; Upchurch *et al.* 2002; Sereno *et al.* 2004). Lastly, biotic interactions have been demonstrated to be major micro- and macroevolutionary factors by evolutionary biologists (Ehrlich & Raven 1964; Wilcox *et al.* 2018; Harmon *et al.* 2019; Agrawal & Zhang 2021). Moreover, their stabilizing effect on diversity over deep time is hard to deny since they were likely essential to the maintenance of ecosystem resilience against minor perturbations, thus explaining the long periods of ecological stasis suggested by the fossil record (Sheehan 1996; Roopnarine & Banker 2021).

Questions on the causes of biodiversity in deep time have thus fostered a longstanding debate on the tempo and mode of evolution as the driver of biodiversity (Simpson 1944). Proponents of the primacy of biotic interactions (most notably predation and interspecific competition) historically favoured a Darwinian gradualistic model of macroevolution, where diversification rates remained fairly stable over time, as in the Red Queen hypothesis (Van Valen 1973). However, this paradigm is somewhat divorced from the pattern offered by the fossil record, which seems to support a model of punctuated equilibria where bursts in evolution and diversification rates could only realistically be caused by abiotic perturbations triggering allopatric speciation (Eldredge & Gould 1972; Gould & Eldredge 1977). This dichotomy has since evolved into more nuanced paradigms such as Gould's tiers of time (Gould 1985), according to which evolutionary processes occurring at the first tier (i.e. a historical time scale) caused by biotic factors are undone either by punctuated equilibria occurring at a second tier over deep time (corresponding to the background diversification/extinction rate), or mass extinctions occurring at the third tier at a much lower frequency throughout Earth's history. The turnover-pulse hypothesis is also related to the paradox of the third tier in proposing that physical change initiates biotic changes, which themselves trigger species turnover (Vrba 1993). While the debate on the necessity of abiotic disturbances to stimulate diversity change has understandably been focused on extinction events, it is also relevant for understanding the causes of adaptive radiations at high origination rates. This process has often been explained by the creation of new ecological opportunities such as niche vacancies following mass extinctions, or the advent of more favourable climate conditions, as was likely the case for the Carnian Pluvial Event and the Great Ordovician

Biodiversification Event (Stigall *et al.* 2019; Dal Corso *et al.* 2020). However, other radiations may have been caused instead by developmental evolutionary novelties arising independently from the physical environment (following sufficient morphological character accumulation), notably the Cambrian explosion (Erwin 2007, 2015). All these questions have historically been asked from an evolutionary perspective, yet they have clear macroecological implications as well since evolutionary trends are indisputably influenced to some extent by prevailing ecological conditions (whether biotic or abiotic factors), and in turn have affected diversity patterns to this day. While the intensity and duration of the states of these ecological conditions likely had a decisive influence on biodiversity patterns through deep time, these dimensions remain incredibly difficult to quantify to achieve any meaningful comparison between successive organismal assemblages.

While the causes of diversity have been intensely investigated, so have efforts been made to reconcile the mechanisms behind its main driver, i.e. phenotypic and molecular micro- and macroevolution (Rolland *et al.* 2023). Ecological and evolutionary processes operating at disparate spatiotemporal scales can now be integrated further by the application of hierarchy theory to biology (Congreve *et al.* 2018): genealogical hierarchies (through which information is transferred from the codon to clade level) are joined to ecological hierarchies (through which energy and matter is transferred from enzyme to ecosystem level) at the only level shared by both parallel scales (the organism). In this way, genetics and palaeontology can find common ground since ‘changes occurring at lower hierarchical levels can have unexpected, complex effects at higher scales due to emergent interactions between simple systems’ (Congreve *et al.* 2018: 811). As an example of the power of this theory, these authors demonstrate that the primary causal mechanism of biotic extinction, termed ‘multi-generational attritional loss of reproductive fitness’ (Wiens & Worsley 2016), operates at the organism level as a symptom of natural selection, while still resulting in differential survival outcomes for higher levels (e.g. species or clades) according to the intensity and duration of a given disturbance.

The remainder of this chapter is firmly focused on palaeontology from an ecological angle, as the study of entire ecosystems through time has become increasingly appreciated to a similar degree as the study of macroevolution. In this respect, this entire thesis aims to contribute to a fundamental question at the core of 'evolutionary palaeoecology' (Wing *et al.* 1992) as this subdiscipline was originally intended: how do ecosystems respond in the long term to changing biotic and abiotic conditions? This question has driven research on the causes of biotic decline and recovery before and after mass extinction events (Johnson *et al.* 1989; Benton *et al.* 2004; Chen & Benton 2012; Congreve 2013; Scheyer *et al.* 2014; Field *et al.* 2018; Carvalho *et al.* 2021; Huang *et al.* 2021), temporal shifts in biomes and latitudinal and altitudinal climate and diversity gradients (Jablonski *et al.* 2006; Hoorn *et al.* 2010; Mannion *et al.* 2014; Rolland *et al.* 2018; Rahbek *et al.* 2019), and global ecosystem assembly rules throughout the Phanerozoic Eon (Benton 2010; Judson 2017; Knoll & Nowak 2017; Close *et al.* 2019; DiMichele *et al.* 2023). All these topics can arguably provide a much-needed long-term perspective on modern biotic responses, and eventually contribute to answering another essential question in palaeoecology: which dimension of biodiversity matters for the resilience of communities to perturbations and ultimately their persistence (or at least relative stasis) on geological time scales? This problem has been indirectly addressed in the past, notably with the recognition of chronofaunas, i.e. geographically restricted faunal assemblages that maintained their basic structure (i.e. functional richness) over a geologically significant period of time despite species turnover (Olson 1952), as well as Ecological Evolutionary Units, which span much longer periods reflective of global evolutionary trends (Boucot 1990; Sheehan 1996). There is an emerging consensus that the stability of functional diversity is far more essential than that of taxonomic diversity (i.e. species richness) to the maintenance of ecological guilds, nutrient cycling and trophic pathways which ensure ecosystem stability regardless of the species that compose a community (DiMichele *et al.* 2004; Blanco *et al.* 2021; Roopnarine & Banker 2021). In this regard, quantitative trophic network reconstructions are being implemented on fossil assemblages with increasing frequency and add yet another dimension to functional diversity by providing diversity metrics which account for interspecific interactions as well as comparing the trophic positions of possible functional analogues along their respective food chains in palaeocommunities separated by space and time (Banker *et al.* 2022; Cortés & Larsson 2023).

Another question derived from this avenue of research is whether interspecific interactions can persist long enough to produce significant long-term evolutionary effects on lineages and ecological structure (DiMichele *et al.* 2004). Advances in aforementioned trophic network analysis methods, as well as birth-death sampling and phylogenetic comparative approaches, now reveal that the influence of biotic interactions can indeed be detected in evolutionary patterns found in the fossil record (Jablonski & Sepkoski 1996; Fraser *et al.* 2021). As an example, mammaliaform ecomorphological disparity across Jurassic, Cretaceous and Eocene localities appears shaped by coevolution with angiosperms and competition with other vertebrates (Chen *et al.* 2019). Conversely, we can ask whether the geological record preserves evidence of the impact of evolutionary novelties on ecosystem structure, including the physical environment beyond its biotic components. For instance, there is tantalizing evidence that the origination of trees with complex rooting systems during the Devonian considerably modified palaeosol geochemistry, thus shaping nutrient cycling and weathering rates for the remainder of the Phanerozoic Eon (Morris *et al.* 2015). In this respect, these questions apply the field of eco-evolutionary dynamics, i.e. the feedback between ecological and evolutionary processes (Hendry 2016), on a macroevolutionary scale. Ultimately, the emerging field of phylogenetic palaeoecology may provide insights on 'macro' eco-evolutionary dynamics in deep time (Lamsdell *et al.* 2017) by using phylogenetic relationships to distinguish biodiversity patterns caused by similar interactions with the environment from those that are caused by shared evolutionary history.

1.2.1 Why 'shallow' deep time matters for ecology

The aforementioned palaeoecological questions have often been investigated by examining biodiversity patterns on a global spatial and on extremely long temporal scales, which have added invaluable knowledge on the evolution of life on Earth. However, with the knowledge that diversity is influenced by different processes depending on spatial scales, it can be argued that more efforts should be directed at diversity analyses on local and regional scales which could detect trends that would otherwise be lost amid the noise of a global signal (Vermeij & Leighton 2003; Gotelli *et al.* 2010; McGill 2010; Sreekar *et al.* 2018; Benson *et al.* 2021). Likewise, I argue in this chapter that exploring these local and regional trends at a much higher temporal resolution (along short geological time intervals) could reveal biotic responses for specific biomes that would be more relevant to urgent specific conservation challenges, at more constrained temporal scales which would not appear so vastly distant from historical time scales. This call has already been answered in conservation palaeobiology, a subdiscipline characterized by the use of the geohistorical record as a means to inform modern conservation practices (Willis & Birks 2006; Dietl & Flessa 2011; Polly *et al.* 2011; Dietl *et al.* 2015; Barnosky *et al.* 2017; Kiessling *et al.* 2019).

The Plio-Pleistocene and early Holocene fossil and subfossil record has proven particularly useful in conservation palaeobiology due to its high degree of completeness (including ancient DNA) combined with an abundance of available absolute dating methods (most significantly carbon 14), which have provided a high time resolution unmatched for any more distant period (e.g. Barnett *et al.*, 2020; Groff *et al.*, 2020; Guthrie, 2006; Mann *et al.*, 2015; Wooller *et al.*, 2021; Zazula *et al.*, 2014). For instance, it revealed that large mammalian hypercarnivores likely exerted top-down control on megaherbivore populations due to their higher species richness and the greater degree of interspecific competition that came with it (Van Valkenburgh *et al.* 2016). That is not the case of modern ecosystems where top-down control by apex predators is limited to smaller herbivore species (Sinclair *et al.* 2003). In this way, Pleistocene fossil assemblages have shown that extinct predators occupying a similar guild to extant relatives had a distinct ecological impact on the rest of their community. Elsewhere, several independent studies which estimate changes in alpha and beta diversity as well as species' abundance, interspecific interactions, functional richness and food web properties before and after megafaunal extinctions at the end of the last Ice Age together reveal the impoverished state of postglacial land mammal communities (Sandom *et al.* 2014; Lyons *et al.* 2016; Smith *et al.* 2016; Tóth *et al.* 2019; Pires *et al.* 2020; Fricke *et al.* 2022). As an example of palaeoecology on a local scale at a high time resolution, accurate radiocarbon dates from Rancho La Brea led to the detection of a clear relationship between megafaunal extinctions and an increase in fire frequency changing habitat conditions in conjunction with the arrival of *Homo sapiens* (O'Keefe *et al.* 2023). Considering the overwhelming complexity of the debate on the respective causes of end-Pleistocene megafaunal extinctions, this study may lead the way as an example of more spatially constrained palaeoecological studies that tackle one set of problems at a time to avoid the confounding signals observed on a global scale.

Some studies have gone further back in time on a more regional spatial scale to track mammal community evolution. For example, mammalian response to global warming during the Miocene around the Rocky Mountains demonstrated a predictable pattern where the magnitude of biotic change increased along with the temporal scale over which it was detected, from variation in phenotype and population density at a 10^2-year scale to near-total species turnover at a 10^5 to 10^6-year scale (Barnosky *et al.* 2003). A more recent one has shown evidence of punctuated equilibrium at the community level (beyond the species level at which this theory was originally developed (Eldredge & Gould 1972; Gould & Eldredge 1977)) by tracking functional diversity in a mammal chronofauna on the Iberian Peninsula for the past 21 Ma (Blanco *et al.* 2021). Elsewhere in the world, a study of the late Miocene to recent African large mammal fossil record uncovered a relationship between species loss and a shift in biomass distributions towards smaller-bodied species (Bibi & Cantalapiedra 2023), and palaeomagnetostratigraphy temporally calibrated the biostratigraphy of the late Miocene Siwalik Hills of Pakistan to establish first- and last (estimated) appearance dates and up to four intervals of faunal turnover (Barry *et al.* 1985).

Travelling even deeper into Earth's past, the limitations of the fossil record become more salient due to the dual impacts of taphonomic filters and time averaging. Even our knowledge of *modern* biodiversity remains beset by at least seven major shortfalls (Hortal *et al.* 2015): the Linnean shortfall on species taxonomy, the Wallacean shortfall on their geographical distribution, the Prestonian shortfall on their abundance and population dynamics, the Darwinian shortfall on their evolutionary relationships, the Hutchinsonian shortfall on their abiotic tolerances, the Eltonian shortfall on their biotic interactions, and the Raunkiæran shortfall on species' traits. When accounting for time resolution and fossilization potential in biodiversity estimates, these shortfalls unsurprisingly become even more problematic. Henceforth, the Gouldian shortfall on species' stratigraphic (and by extension temporal) distributions is now introduced in recognition of Stephen Jay Gould's development of the theory of punctuated equilibrium (Eldredge & Gould 1972; Gould & Eldredge 1977), which decisively shifted the accepted paradigm on the tempo and mode of evolution by examining the fossil record.

The depositional environment of a fossil community formed from any death assemblage has long been known to affect the probability of preservation of different organic tissues depending on its hydraulic regime, its geochemical properties (such as pH and oxygen levels) and its exposure to external pre- and postburial perturbations (Behrensmeyer & Hook 1992; Behrensmeyer *et al.* 2000). This usually induces a taphonomic bias against certain materials or groups of organisms (e.g. soft tissues or delicate skeletal remains), which creates an offset between diversity observed in the fossil assemblage and the palaeobiota's true past diversity. While taphonomic biases usually result in underestimating diversity, the relatively low time resolution which prevails in pre-Quaternary deposits causes uncertainties on the absolute geological ages of specific localities, which can lead to time averaging between communities that did not truly coexist (Behrensmeyer 1982; Behrensmeyer & Hook 1992). Therefore, time averaging tends to result in overestimating diversity on every spatial scale, which then obscures local and global variability in those measurements (Kidwell & Flessa 1995). Although the joint forces of taphonomic biases and time averaging could theoretically yield a fairly realistic absolute species richness estimate for a given time interval, several members and guilds would certainly be over- or underrepresented in almost any fossil assemblage (e.g. Damuth 1982). This is the main reason why several authors consider community properties such as alpha diversity, morphological disparity or body size distributions to be fundamentally incomparable between fossil and extant assemblages (Behrensmeyer *et al.* 1979; Fürsich & Aberhan 1990; Wilson & Moore 2016). Understanding the influence of taphonomy is thus key to increasing our confidence in the fossil record and quantifying probabilities of preservation to correct species' distributions in space and time, as well as the diversity estimates derived from the latter (Kidwell & Holland 2002). There is also an enduring collection bias where Europe and North America are overrepresented in the fossil record as the cradles of modern palaeontology within a historical context of colonial imperialism (Raja *et al.* 2022). In contrast, landmasses that used to form the southern supercontinent of Gondwana (e.g. Africa, South America, India, Australia and Antarctica) are underrepresented (Benson *et al.* 2013, 2021), which can distort our perception of global diversity patterns and of the structure of a typical community in any distant geological time interval given the profoundly distinct evolutionary history of the lineages that evolved there. Older rocks (particularly from the Precambrian eons and the Paleozoic and Mesozoic eras) may well have yielded a sufficient quality and quantity of fossils to document landmark events in the history of life, but the fact remains that they preserve less information in absolute terms (Benton *et al.* 2000).

In light of these concerns, it could be argued that the Neogene (i.e. the last 23 Ma from the Miocene epoch to the present) is the only period in Earth's deep history that should get any sustained focus in evolutionary palaeoecology due to its unrivalled fossil record and time resolution. Nonetheless, I counter that fossil ecosystems preserved at a reasonably high time resolution (from tens of thousands to a few million years) in Earth's distant past are still worth seeking. This is where the concept of 'shallow' deep time is introduced as an intermediate between the time scale of the

Pleistocene fossil record, whose lowest resolution is 10^4 years, and the deepest of deep time scales, whose lowest resolution is around 10^8 years (DiMichele *et al.* 2004). This is because a sufficiently detailed and calibrated fossil record can show a range of possible scenarios of biotic responses to environmental change that can theoretically add further context to the current biodiversity crisis. As was written succinctly before, 'ancient ecosystems may differ from those of today in a variety of unexpected ways' (Conway Morris 1995): tectonic activity influences sea level trends as well as landmass and ocean locations, which in turn affect global climate patterns. First, atmospheric carbon dioxide (CO_2) concentrations were frequently half as low during the Pleistocene ice ages compared to the Anthropocene (Royer *et al.* 2004; Foster & Rohling 2013). Therefore, we must go at least ~2.5 Ma back in time to study ecosystems evolving under a pCO_2 at least at a similar level to the 420 ppm we are currently experiencing (Martínez-Botí *et al*. 2015). Concurrently, studying past communities evolving in the context of decreasing atmospheric oxygen concentrations might be an even more urgent priority considering projected drops in O_2 levels caused in large part by the reduction of vegetation cover worldwide over the past 20 years (Conway Morris 1995; Martin *et al.* 2017). For that matter, the Permo-Triassic mass extinction event may prove informative considering the likely role of habitat loss triggered by the sharp advent of anoxic and dysoxic conditions in the decimation of marine invertebrate faunas (Wignall & Hallam 1993). Elsewhere, the Paleocene-Eocene Thermal Maximum has been proposed as the best-case analogous scenario for our present global warming trend, while the Cretaceous-Paleogene mass extinction event would be among the worst-case realistic analogous scenarios as an ominous warning sign for species loss (Keller *et al.* 2018), especially large-bodied species including our very own.

Second, faunal and floral replacement occurred repeatedly within several ecological niches which were successively occupied by species from phylogenetically distant lineages (Benton 1979, 2010; Behrensmeyer *et al.* 1992). The contrasting evolutionary histories of these lineages thus caused the development of diverging life history traits and likely differential impacts on community structure and energy flux in ecosystems. This resulted in a multitude of ancient ecosystems which lack any clear modern analogue, yet ultimately faced the same universal environmental pressures. For example, how did the community structure of shallow seas differ between the Cambrian and the Ordovician considering that the former lacked corals among its reef-building metazoan taxa (Fagerstrom 1987)? How did the body size and biomass distribution of a typical terrestrial community differ along trophic levels between the Mesozoic and the Cenozoic considering the contrasting developmental and reproductive strategies of large dinosaurs and mammals as potential keystone species (Codron *et al.* 2012, 2013; Benson 2018; Schroeder *et al.* 2021)? How did Cretaceous polar forest ecosystems function with dinosaurs as the main land vertebrates under a regime of high sunlight seasonality in a warmer and more equable climate (Herman & Spicer 1997; Fiorillo *et al.* 2016; Herman *et al.* 2016; Chiarenza *et al.* 2020)? As another example, extraordinary discoveries of Devonian floras including some of the oldest petrified tree trunks and roots raise an opportunity to compare the complexity of the first true forests' palaeosol and vegetation structure to that of more recent floras (Stein *et al.* 2012, 2019; Morris *et al.* 2015; Wang *et al.* 2019).

It must be acknowledged that only a select few extinct ecosystems have the right conditions to investigate biotic responses on 'shallow' deep time scales. These require fossil assemblages with limited preservation biases combined with high spatiotemporal fidelity that limits time averaging. Localities where fossil remains include tissues that are rarely biomineralized elsewhere, known as Konservat-Lagerstätten (Seilacher *et al.* 1985), almost always fulfill the former condition since their high preservation quality enables diversity to be measured in their community beyond metrics limited to taxonomic richness, and into the realms of morphological disparity and even ecological network properties accounting for (usually feasible, i.e. not realized) interspecific interactions (e.g. Dunne *et al.* 2008, 2014; Kempf *et al.* 2020). This is because specimens uncovered from these localities are often preserved in an articulated state and display fossilized soft tissues as well as occasional direct evidence of inter- or intraspecific interactions such as traces of food resources in abdominal contents (Kobayashi *et al.* 1999; Vullo 2011; Rose 2012; Xing *et al.* 2012; Zheng *et al.* 2018; O'Connor 2019; White *et al.* 2022; Wu *et al.* 2023). For example, the diminutive dromaeosaurid *Microraptor*, from the Early Cretaceous Jehol biota of northeastern China, is known from so many remarkably preserved skeletons that they have offered direct evidence of a highly generalist diet that could not be tested optimally based on ecomorphological inferences alone (O'Connor *et al.* 2011, 2019; Xing *et al.* 2013; Hone *et al.* 2022). Conversely, some of these sites have an equally high value for resolving evolutionary relationships since they often host fossil specimens that provide a disproportionately high frequency of anatomical characters for phylogenetic analyses (Woolley *et al.* 2024). Many Lagerstätten are found in lacustrine deposits, which often have a sufficiently high temporal resolution to show cyclic faunal and floral changes correlated with seasonal sedimentary cycles, but an insufficient duration (on the 10^6-yr scale at the most) to detect broader directional patterns of ecosystem change (Olsen *et al.* 1978; Fürsich *et al.* 2007). Only a select few Konservat-Lagerstätten combine a high spatiotemporal resolution with a stratigraphic succession that enables the observation of more permanent palaeoecological successions in a comparable level of detail to the most complete Quaternary localities such as Rancho La Brea: these include Grube Messel in Germany, which provides an unparalleled window into an early Eocene tropical forest community rich in birds and mammals (Dunne *et al.* 2014; Lenz & Wilde 2018); the Burgess Shale of the Canadian Rocky Mountains, which remains the primary source for understanding the Cambrian Explosion (Caron & Jackson 2008); and the Rhynie Chert of Scotland, which documents the first complex terrestrial floras as well as the oldest known insects during the early Devonian (Selden & Nudds 2012).

Other localities have offered uniquely detailed glimpses into the biotic consequences of abrupt perturbations throughout the Phanerozoic. For instance, the exquisite preservation of vertebrate, invertebrate and plant remains in Wyoming's Bighorn and Clarks Fork basins has revealed regional shifts in species' geographical ranges and even phenotypic evolution rates in response to the Paleocene-Eocene Thermal Maximum, a global warming event which only lasted around 200 Ka (Gingerich &

Gunnell 1995; Wilf 2000; Wing *et al.* 2005; Currano *et al.* 2008; Smith *et al.* 2009; Secord *et al.* 2012; Bowen *et al.* 2015). The Denver Basin in Colorado preserves a recently discovered Paleocene community which reveals a surprisingly rapid mammal radiation following the Cretaceous-Paleogene mass extinction event with a robust time calibration (Fuentes *et al.* 2019; Lyson *et al.* 2019). Biotic collapse and recovery before and after the Permo-Triassic mass extinction event can also be examined in great detail in a few regions around the world: South Africa's Karoo Basin has become a model system for community persistence through perturbations (Roopnarine & Angielczyk 2015; Codron *et al.* 2017; Roopnarine *et al.* 2017, 2019; Viglietti *et al.* 2021), and a sequence of newly explored localities in southern China shows that marine communities regained their pre-extinction complexity more rapidly than expected (Hu *et al.* 2011; Benton *et al.* 2013; Dai *et al.* 2023; Huang *et al.* 2023). Likewise, the Ordovician-Silurian mass extinction event is extremely well documented and time-constrained on Anticosti Island, Québec (Barnes 1988; Knaust & Desrochers 2019).

Despite exciting advances in functional diversity and network complexity metrics to measure ancient community diversity based on the known fossil record, a final word must be dedicated to the essential nature of palaeontological fieldwork to provide ever more anatomical data which lay the foundation of macroevolutionary and palaeoecological analyses. New discoveries presented over the last 10 years alone have revealed entirely new lineages, functional guilds and ecosystems, including a new Cambrian Lagerstätte, a completely new radiodont body plan that endured into the Early Ordovician, a rare non-avialan theropod with swimming adaptations, and a gigantic Eocene early whale (Van Roy *et al.* 2015; Brown *et al.* 2017; Clack *et al.* 2017; Fu *et al.* 2019; Luque *et al.* 2019; Moysiuk & Caron 2019; Krause *et al.* 2020; Lamsdell *et al.* 2020; Spiekman *et al.* 2020; Qvarnström *et al.* 2021; Allain *et al.* 2022; Lee *et al.* 2022; Bianucci *et al.* 2023). Far more exploration will be required for most of the source localities of these new fossils to have a suitable record for the type of palaeoecological analysis defended in this chapter, and we can only guess at the next corner of the world that will take us on a dive into 'shallow' deep time on a mesoeco-evolutionary scale.

1.2.2 Dinosaur Provincial Park: a model system to study non-marine Mesozoic biodiversity

In the following section, we argue that the exposures of the Judith River (Belly River) Group (BRG) outcropping along the Red Deer River in Dinosaur Provincial Park (DPP), Alberta, Canada, constitute one of the world's ideal localities to study biotic responses in an ancient non-marine ecosystem from the Late Cretaceous Epoch. This may be the one non-marine Mesozoic locality that holds the greatest promise to provide a baseline for modern biotic responses at a background extinction rate. One way in which the Cretaceous stands out compared to other geological periods is in the sheer amount of diversity and productivity that ecosystems seemed to reach. This ~80 Ma long period was generally characterized by warm mean global temperatures with an equable latitudinal climate gradient caused by high atmospheric greenhouse gas concentrations (including $p\mathrm{CO}_2$ levels often four times higher than in the present) combined with fluctuating sea levels and widespread epicontinental seas between evenly distributed landmasses across the globe (Hay & Floegel 2012; Hong & Lee 2012; Boucot *et al.* 2013; Hay 2017; Scotese *et al.* 2021). This setting is thought to have created a 'perfect storm' for evolutionary innovation by creating a mosaic of habitats undergoing pulses of spatial connection and isolation, which likely accelerated origination rates as has been shown throughout Earth's history (Davis *et al.* 2005; Rolland & Condamine 2019; Congreve *et al.* 2021; Jablonski & Edie 2023). For instance, it took almost 100 Ma of evolution for dinosaur faunas to reach a high level of regionalization during the Early Cretaceous, at the onset of the fragmentation of the Laurasian and Gondwanan supercontinents which had persisted throughout much of the Jurassic (Sereno 1999; Upchurch *et al.* 2002). It was on that greenhouse (or occasionally hothouse) planet that the radiations of angiosperms, of pollinating and eusocial insects, and of birds and modern mammal lineages (collectively known as the Cretaceous Terrestrial Revolution) occurred to lay the final foundations of modern ecosystems as a possible example of the long-term effects of biotic interactions on macroevolutionary trends (Grimaldi 1999; Labandeira & Currano 2013; Barba-Montoya *et al.* 2018;

Zhang *et al.* 2018; Benton *et al.* 2022; Weaver *et al.* 2024). A similar hypothesis has revolved around the convergent diversification of several herbivorous dinosaur lineages, with hadrosaurids and ceratopsians in particular being proposed to co-evolve with angiosperms (Bakker 1978; Butler *et al.* 2009; Barrett 2014), although it is nearly impossible to test rigorously due to the lack of close extant relatives with any similar morphology for these non-avialan dinosaurs. The positive feedback between high greenhouse gas concentrations and angiosperm diversification is oft-cited as a very likely contributing factor to the high frequency of wildfires, which seemed particularly characteristic of Cretaceous Earth systems compared to other periods (Bond & Scott 2010; Brown *et al.* 2012). It is reasonable to suggest that radiations at low trophic levels increased primary productivity and energy flux from producers to consumers along food chains across entire food webs since that is the main hypothesis behind the consistently high abundance of apex predators in marine as well as terrestrial Cretaceous ecosystems, from Morocco’s Cenomanian Kem Kem Beds to the Western Interior Seaway that divided North America into Appalachia and Laramidia during the Late Cretaceous (Nicholls & Russell 1990; Hassler *et al.* 2018; Ibrahim *et al.* 2020; Cortés & Larsson 2023). On the one hand, several Cretaceous biotas had many features in common with modern ones (especially in the Campanian and Maastrichtian) as angiosperms rose to ecological prominence. On the other hand, however, the vertebrate fauna would still have looked very alien to a modern visitor with the prevalence of non-avian dinosaurs, pterosaurs, notosuchian and pholidosaurid crocodyliforms, plesiosaurs, and mosasaurs, all of which lacked any phylogenetically near modern relatives.

The Western Interior of North America lays a particularly compelling case for high alpha, beta and gamma diversity during the Campanian Stage of the Cretaceous based on the presence of distinct endemic dinosaur faunal provinces (including the BRG biota of Alberta and Saskatchewan) distributed along a palaeolatitudinal gradient along the Laramidian coastal plain between the emerging Rocky Mountains and the Western Interior Seaway (Ostrom 1963; Lehman 2001; Gates & Sampson 2007; Gates *et al.* 2010; Sampson *et al.* 2010; Loewen *et al.* 2013; Mallon *et al.* 2016; Arbour & Evans

2017). The lack of any discernible physical barrier as a possible cause of allopatric speciation combined with an equable climate gradient renders this palaeobiogeographical pattern highly unusual and may suggest that dinosaurs had fundamentally narrower biotic and abiotic niche breadths than the large mammals that succeeded them. There is evidence that the Campanian overcontributes to total Mesozoic dinosaur diversity due to a combination of rock accumulation and subsidence rates favourable to fossilization in several parts of the world, especially North America's Western Interior (Chiarenza *et al.* 2019). However, the relatively low dinosaur beta diversity observed in that same region during the Maastrichtian Stage does support the hypothesis that species richness in that clade was already decreasing by the end of the Campanian, likely due to a sea level fall which increased continental interconnectedness combined with global cooling (Lehman 1987; Barrett *et al.* 2009; Vavrek & Larsson 2010; Brusatte *et al.* 2012; Condamine *et al.* 2021). Conversely, that hypothesis is challenged by evidence for higher available fossil-bearing outcrop area in the Campanian than in the Maastrichtian of the Western Interior (Chiarenza *et al*. 2019). Therefore, diversity comparisons within the Campanian of North America (let alone among distinct Cretaceous time intervals) are still hindered by collecting biases between discrete fossil localities (Benson *et al.* 2013; Maidment *et al.* 2021). Ultimately, our ability to investigate whether spatial biotic heterogeneity was a consistent feature of the Cretaceous Period or whether it was especially high during the Campanian Stage due to an ideal combination of high sea levels and warm and equable global climate conditions remains limited.

In this respect, the major palaeontological value of Dinosaur Provincial Park lies in a fossil record that provides an almost unparalleled glimpse of vertebrate biodiversity (around 166 species) in a Campanian non-marine ecosystem with robust spatiotemporal constraints as a result of more than 120 years of exploration (Osborn & Lambe 1902; Sternberg 1917; Russell 1966; Dodson 1983; Brinkman 1990; Currie 2005; Currie & Koppelhus 2005 and papers therein; see Appendix I). Among these taxa, non-avialan dinosaurs are particularly well represented since 50 species are represented in DPP (depending on taxonomic validity), an impressive 7% of the world's total (Dodson 1983; Ryan &

Russell 2001; Wang & Dodson 2006; Benton 2008, Brown *et al.* 2013*b*). This exceptional ancient biodiversity record is the main criterion for the status of DPP as one of the world's few fossil localities to be included in the list of UNESCO World Heritage Sites in 1979 (Currie 2005). The largest dinosaur species found there are known from a density of well-preserved (often articulated) skeletons unmatched anywhere in the world and are far more abundant than other partial to complete vertebrate remains in the local fossil record due to a taphonomic bias favouring large skeletons in fluvial channel deposits whose high-energy sedimentary flow can readily disarticulate and even destroy more delicate skeletons (Currie & Russell 2005, Brown *et al.* 2013*b*). No other place on Earth has yielded such a high dinosaur species richness, with some time intervals (such as the lower Dinosaur Park Formation) having as many as three ceratopsid species, three hadrosaurid species and three ankylosaur species co-occurring (Mallon *et al.* 2012; Mallon 2019). As a result, DPP has become one of the world's most important localities to understand all aspects of the biology of tyrannosaurid, hadrosaurid, ceratopsid and ankylosaurian dinosaurs, whether anatomy, systematics, functional morphology or development through ontogeny (Sternberg 1935, 1940*a*; Ostrom 1961; Russell 1970; Dodson 1975; Coombs 1978; Godfrey & Holmes 1995, Currie 2003*a*, *b*; Ryan *et al.* 2007; Arbour *et al.* 2009; Evans *et al.* 2009; Arbour & Currie 2013; Frederickson & Tumarkin-Deratzian 2014; Currie *et al.* 2016; LeBlanc *et al.* 2016, Brown *et al.* 2020*a*, 2022*a*; Therrien *et al.* 2021). As one example, the holotype of *Gorgosaurus libratus* was the first known tyrannosaurid skeleton to be sufficiently complete to reveal that this theropod family had evolved peculiarly reduced forelimbs (Lambe 1914*a*, 1917).

Smaller-bodied dinosaurs are not preserved as frequently in the Park's badlands outcrops yet have proven essential to understanding their own lineages' ecology and evolution. In the Ornithischia clade, these lineages include Pachycephalosauridae, Leptoceratopsidae and Thescelosauridae (Gilmore 1924*a*; Ryan *et al.* 2012, Brown *et al.* 2013*a*; Dyer *et al.* 2022). In the Theropoda clade, these include Ornithomimidae, Caenagnathidae, Troodontidae, Dromaeosauridae, and a few problematic taxa (Sternberg 1932; Colbert & Russell 1969; Russell 1969, 1972*a*; Nicholls & Russell 1981; Currie 1995;

Sankey *et al.* 2002; Longrich 2008; Longrich & Currie 2009; Funston & Currie 2014, 2020; Currie & Evans 2020; Funston 2020). Troodontid remains from the Park, especially braincases, hold a special place in the history of vertebrate palaeontology since they provided key evidence supporting the evolution of birds within dinosaurs prior to the discovery of 'feathered dinosaurs' in China's Jehol biota (Currie 1985, 1987; Currie & Zhao 1993). Birds are among the most poorly represented vertebrate clades in the DPP fauna, yet their presence has still been demonstrated by rare, isolated elements usually assigned to morphotaxa (Longrich 2009; Mohr *et al.* 2020).

Other vertebrates are represented in the DPP fossil assemblage to complete the picture of this late Campanian North American fauna. Pterosaurs are very rarely found due to the fragility of their bones, but still have a respectable record (Currie & Godfrey 2005; Hone *et al.* 2019). One tibia now assigned to the giant azhdarchid *Cryodrakon boreas* even bears tooth marks attributed to the dromaeosaurid *Saurornitholestes langstoni* (Currie & Jacobsen 1995), thus providing tentative evidence of a predator-prey interaction in the Park's fossil record. Moving away from Ornithodira to Crurotarsi within Archosauria, crocodilians are not represented by a single associated skeleton but are known at least from several complete skulls which together reveal that *Leidyosuchus canadensis* was the most plesiomorphic member of superfamily Alligatoroidea (Wu *et al.* 2001; Wu 2005; Lee & Yates 2018). DPP is one of those Late Cretaceous and Paleogene localities where crocodilians coexisted with *Champsosaurus*, another diapsid clade superficially similar to modern gharials that seems to have evolved convergently within Choristodera (Russell 1956; Gao & Fox 1996; Dudgeon *et al.* 2020). The river channels in which so many carcasses were preserved throughout the Park were also populated by plesiosaurs (almost exclusively long-necked elasmosaurids) which appeared to tolerate freshwater (Sato *et al.* 2005). Squamates are abundant as isolated jaws found in vertebrate microfossil localities, which reveal a diverse fauna composed of anguids, teiids, xenosaurids, helodermatids, and monstersaurs such as *Palaeosaniwa canadensis* (Gao & Fox 1996; Caldwell 2005). Turtles may well be the second-best represented animal group in the Park's entire fossil assemblage (after large ornithischians) considering their high density of complete skulls and skeletons: up to twelve species are currently recognized, up to five of which are assigned to family Trionychidae (soft-shelled turtles) alone, and all but one species (the large tortoise *Basilemys variolosa*) interpreted to have a semiaquatic lifestyle (Gilmore 1923; Brinkman & Nicholls 1991, 1993; Gardner *et al.* 1995; Brinkman 2003, 2005; Parham & Hutchison 2003). Amphibian remains are all isolated microfossils recovered from microsites, yet are extremely abundant, and have even revealed a fully edentulous frog named *Tyrrellbatrachus brinkmani* (Gardner 2005, 2015; Gardner *et al.* 2016). A diverse fish fauna spanning Holostei, Teleostei and Elasmobranchii is also known from the Park, although most species are represented by extremely isolated elements such as jaws and centra in vertebrate microfossil localities (Wilson *et al.* 1992; Neuman & Brinkman 2005; Brinkman 2019). Only three fish species are known from articulated skeletons in DPP: the large teleost *Paratarpon apogerontus*, the sturgeon *Anchiacipenser acanthaspis*, and the ray *Myledaphus bipartitus* (Bardack 1970; Neuman & Brinkman 2005; Sato *et al.* 2018). Lastly, mammals are another elusive vertebrate group in the DPP fossil record yet are still represented by up to 13 species distributed among the major eutherian, metatherian and multituberculate lineages (Fox 2005; Sankey *et al.* 2005; Scott & Fox 2015). Despite their very fragmentary nature, they still offer one of the most complete windows into mammal evolution in Late Cretaceous North America.

The aforementioned vertebrate groups all have varying preservation potential in the successions of channel meander belts that form the badlands of DPP, and a wide range of facies types among fluvial channel deposits has enabled some of the world's most detailed studies on the influence of sedimentological setting on vertebrate taphonomy (Dodson 1971; Wood *et al.* 1988; Eberth & Currie 2005). For instance, most of the articulated skeletons for which the Park remains most famous are only regularly preserved under palaeochannel point bars with a sufficiently high sedimentation rate combined with sufficient isolation from decomposers (Wood *et al.* 1988; Eberth & Currie 2005). DPP has also been one of the world's foremost locations to study dense aggregations of medium to large bones (i.e. bonebeds), particularly those dominated by ceratopsid species considering the invaluable information they provide on intraspecific variation and behavioural inferences within those populations, as well as the (likely) catastrophic causes of their mass death assemblages (Currie & Dodson 1984; Visser 1986; Sampson *et al.* 1997; Ryan *et al.* 2001; Eberth & Getty 2005; Ryan & Russell 2005; Eberth *et al.* 2007; Eberth 2015, Brown *et al.* 2020*b*). Several vertebrate microfossil localities also revealed clear associations between their sedimentological setting and their faunal composition (Brinkman 1990; Eberth 1990, Brinkman *et al.* 2005*b, a*), thus helping to disentangle ecological from taphonomic signals in palaeodiversity estimates.

Beyond vertebrates, plants and invertebrates are admittedly poorly represented in the DPP fossil assemblage. The latter are mostly represented by mass death assemblages of clams and mussels, which are perhaps the single most understudied animal group of that biota considering their relative fossil abundance (Johnston & Hendy 2005). Arthropods are even more scarcely reported, with only a millipede and an aphid (the latter referred to family Cretamyzidae) presently known from the entire Park (Johnston & Hendy 2005; McKellar *et al.* 2019). Most of the plant diversity is found in the palynoflora (Jarzen 1982; Braman 2005), with only a few dozen recurring morphotypes reported among the angiosperm and conifer leaf macroflora (Koppelhus 2005). Petrified wood is highly abundant throughout the Park's exposures and is exclusively assigned to large conifers such as *Sequoia*, which likely persisted in forming the bulk of the canopy late into the Cretaceous (Ramanujam 1972; Koppelhus 2005). Considering how few quantitative estimates have been made to infer the palaeoclimate of the DPP biota (Barrick *et al.* 1999; Bamforth & Koppelhus 2018), plant and invertebrate taxa deserve increased scientific attention since they have potential to be at least as informative as the vertebrate species with evolutionarily near extant relatives on this matter.

Other dinosaur-rich sedimentary units around the globe arguably have a vertebrate diversity on par with the Belly River Group of Dinosaur Provincial Park. Particularly noteworthy formations include the Late Jurassic Morrison Formation of the U.S. Western Interior (Dodson *et al.* 1980; Foster 2003; Farlow *et al.* 2010; Whitlock *et al.* 2018; Woodruff 2019), the latest Maastrichtian Hell Creek Formation of the north-central U.S.A. (Sheehan *et al.* 1991; White *et al.* 1998; Hartman *et al.* 2002, Wilson *et al.* 2014*b*, Brown *et al.* 2022*b*), the Barremian-Aptian Jehol biota of China (Zhou *et al.* 2003; Chang *et al.* 2008; Yang *et al.* 2020), and the Nemegt and Djadokhta Formations of Mongolia, the latter being of similar age to the BRG (Jerzykiewicz *et al.* 1993; Dashzeveg *et al.* 1995; Eberth 2018; Fanti *et al.* 2018). However, what makes the Dinosaur Provincial Park biota particularly outstanding is its high spatial fidelity and temporal resolution, which together remain unmatched in these other stratigraphic units. First, the near totality of the Park's individual fossil quarries (around 600 collected and uncollected associated and/or articulated skeletons and more than 300 bonebeds) are located within an ~80 km^2 area of badlands along the Red Deer River (Dodson 1971; Béland & Russell 1978; Currie & Russell 2005). An estimated 50% of these quarries have been (re)located with highly precise GPS coordinates in an unprecedented effort to document their geographical and stratigraphic distribution (Currie 2005; MacDonald *et al.* 2005; Tanke 2005). This detailed historical record was initiated by a foresighted quarry staking program led by C.M. and Levi Sternberg (Geological Survey of Canada), as well as W.A. Parks (Royal Ontario Museum), in 1935 and 1936 (Sternberg 1936, 1950; Tanke 2005). It was then completed with differential GPS surveys conducted from 1999 to 2003 combined with relocations of previously 'lost quarries' (MacDonald *et al.* 2005; Tanke 2005). The database resulting from this ambitious survey has since been created by Philip Currie (Currie & Koppelhus 2005: Supplementary CD-ROM) and is constantly being expanded with the discoveries of new specimens and localities (Appendix II).

Second, the 100 m thick succession of sedimentary horizons hosting these quarries has a well constrained geological age since it is known to represent 2.429 ± 0.024 Ma based on the latest U-Pb zircon geochronology of five stratigraphically distinct beds of bentonite mudstone ranging across nearly the entire stratigraphic breadth of the BRG in the Park (Thomas *et al.* 1990; Ramezani *et al.*

2022; Eberth *et al.* 2023). The Oldman Formation contains the Field Station Tuff (dated at 76.718 ± 0.020 Ma); the Dinosaur Park Formation (which is has an estimated duration of 2.065 ± 0.059 Ma) contains the Jackson Coulee Tuff (76.354 ± 0.057 Ma, in the lower DPF), the Plateau Tuff (75.639 ± 0.025 Ma, around halfway up the formation), and the Lethbridge Coal Zone Tuff (75.017 ± 0.020 Ma, in the uppermost DPF); lastly, the Bearpaw Formation contains the Bearpaw Tuff (74.289 ± 0.014 Ma). The highly precise and accurate absolute ages of these horizons (for such a distant geological time period), combined with stratigraphic heights of individual fossil quarries, may tentatively suggest that accurate relative ages could be obtained from estimated rock accumulation rates between stratigraphically separate specimens (Eberth 2005; Eberth *et al.* 2023). However, their preservation in fluvial or deltaic depositional settings characteristic of badlands induces major uncertainties in those relative ages due to frequent downcutting of muddy overbank deposits by overlying channel deposits (Wood *et al.* 1988; Eberth & Getty 2005; Brown 2013: Ch. 4). Nonetheless, the current constraints on the temporal resolution of biotic change in DPP pale in comparison to similar constraints encountered in other dinosaur-bearing formations. For instance, the Morrison Formation, whose dinosaur diversity has been directly compared to that of DPP, has a reasonably detailed fossil quarry record (Dodson *et al.* 1980; Leach *et al.* 2021; Farlow *et al.* 2022), but it extends spatially for ~1.2 million km^2 from Montana to Arizona, and extends temporally for as much as 7 Ma (Trujillo & Kowallis 2015; Maidment & Muxworthy 2019). The Jehol biota may have far better-preserved fossil remains than could ever be expected in DPP due to its lacustrine and lahar/ash flow deposits (Zhou 2014), yet the latest radioisotopic dates for one of its formations suggest it lasted as long as 15 Ma (Yang *et al.* 2020) and the availability of its respective quarries' locality data is far less consistent. The Hell Creek Formation may have a more comparable biota to DPP since its duration of ~1.6 Ma is on a similar order of magnitude (Fowler 2017), yet it has a much lower spatial resolution since several of its most important fossil localities are scattered over an area spanning eastern Montana and western North and South Dakota (Johnson & Hickey 1990, Wilson *et al.* 2014*b*; During *et al.* 2022).

As radiometric dating projects are currently being coordinated with increasing precision between geographically distant Campanian dinosaur-bearing formations (such as the DPF, Kaiparowits, Two Medicine, Judith River and Fruitland-Kirtland), they now contribute decisively to a longstanding debate on the extent of dinosaur endemism in Late Cretaceous North America (Lehman 2001; Sampson *et al.* 2010; Loewen *et al.* 2013; Fowler 2017). The latest dates now confirm that the temporal ranges of all these formations overlapped (albeit to a lesser extent for the Fruitland-Kirtland Formation) (Ramezani *et al.* 2022), thus strongly supporting the idea that megafaunal dinosaur species had remarkably constrained geographical distributions in the late Campanian of eastern Laramidia, at least compared to extant terrestrial animals of similar body size. This finding raises tantalizing questions about the causes and drivers of such a high beta diversity along Laramidia's palaeolatitudinal gradient despite the absence of any clear geographical barrier that could have triggered allopatric speciation among those dinosaur lineages.

In addition to having a remarkable fossil heritage with a strongly constrained geochronology, the lithostratigraphic succession of the Belly River Group observed in DPP has been shown to record gradual palaeoenvironmental change during the last major transgression of the Western Interior Seaway (Kauffman & Caldwell 1993; Eberth 2005). At the bottom of the Red Deer River valley, the Oldman Formation (OF) is the lowest sedimentary unit of the BRG to outcrop in the Park and is characterized by exclusively sandy facies indicative of a depositional environment dominated by alluvial channels on a relatively well-drained floodplain (Eberth & Hamblin 1993; Eberth 2005). Only the uppermost 10 m of the OF are usually exposed in the Park, and its upper stratigraphic boundary is marked by a sharp facies transition from its pale ochre sandstones to a mosaic of pale grey sandstones which is characteristic of the Dinosaur Park Formation (DPF) (Eberth & Hamblin 1993; Eberth 2005). The DPF extends for the next ~80 m of the Park's stratigraphic section and displays a mosaic of facies representing alluvial, deltaic and paralic environments (Eberth & Hamblin 1993; Eberth 2005; Eberth *et al.* 2023). Its proportion of sandy relative to muddy facies gradually decreases up section, and the dominance of the former in its lower horizons likely explains the particularly high abundance of articulated vertebrate skeletons recovered there since they represent an ideal burial setting of channel lags and point bars (Wood *et al.* 1988; Currie & Russell 2005). The higher proportion of muddy lithological facies in the upper DPF indicates a transition from a well-drained to a lesser drained floodplain, which culminates in the swampy environment of the Lethbridge Coal Zone (LCZ) in the formation's uppermost ~20 m, when DPP would have been located on the coastal margin of Laramidia at a time of rising eustatic sea level (Kauffman & Caldwell 1993, Brinkman *et al.* 2005*b*; Eberth 2005). The most extreme palaeoenvironmental change occurred at the contact between the LCZ and the marine shales of the Bearpaw Formation, by which time most of southern Alberta lay at the bottom of the Bearpaw Sea (Beavan & Russell 1999, Brinkman *et al.* 2005*b*).

The combination of the Park's geological and palaeontological records created the opportunity to investigate stratigraphic distributions of species (and occasionally of entire faunal assemblages) with robust stratigraphic control rarely achieved in any non-marine Mesozoic locality, in coincidence with a regional sea level rise (Brinkman 1990; Mallon *et al.* 2012; Cullen & Evans 2016; Cullen *et al.* 2021). Some of the most significant advances in those fields resulted in the detection of patterns of vertebrate faunal turnover from different taphonomic modes across the Belly River Group's exposures. First, vertebrate microfossil localities reveal a significant shift in rank abundance and relative abundance over time from vertebrate taxa indicative of coastal and inland conditions in response to the aforementioned perturbation (Brinkman 1990; Brinkman *et al.* 1998; Cullen & Evans 2016; but see also Oreska & Carrano 2019). As an example, the abundance of sharks (such as *Hybodus montanensis*) and rays (such as *Myledaphus bipartitus*) increases considerably in microsites located in the upper DPF along with that of gar (family Lepisosteidae) and other holostean fishes, crocodilians and champsosaurs, as saltwater conditions typical of marginal marine habitats set in progressively. In contrast, the abundance of groups associated with freshwater (and highly sensitive to salinity), such as frogs and scapherpetontid salamanders, falls steeply from the lower to the upper DPF, along with that of bowfins (family Amiidae) and teleost fishes such as *Coriops*. Moreover, the palaeodiversity of DPP's vertebrate microfossil localities has also been compared to that of neighbouring coeval late Campanian fossil localities in Alberta and Saskatchewan such as Irvine, Onefour, Manyberries, Sandy Point and Unity, which together reveal a similar pattern of biotic turnover along a spatial gradient across the width of the Laramidian coastal plain (Brinkman *et al.* 1998, 2004; Peng *et al.* 2001; Cullen & Evans 2016).

Second, the distribution of associated and articulated dinosaur skeletons suggests the presence of at least four megaherbivore assemblage zones across the Oldman and Dinosaur Park Formations collectively forming a possible chronofauna, each of which are now proposed to have durations varying between ~650 and ~700 Ka (Mallon *et al.* 2012; Mallon 2019; Eberth *et al.* 2023). The stratigraphically lowest of these zones is associated with the upper Oldman Formation exposed in the Park (with a duration of at least ~333 Ka), and is characterized by the occurrence of the centrosaurine *Coronosaurus brinkmani* and of the hadrosaurine *Brachylophosaurus canadensis*. The Dinosaur Park Formation is then subdivided into three biozones: the lowest of which is characterized by the lambeosaurine *Corythosaurus* spp. and the centrosaurine *Centrosaurus apertus* (duration ~700 Ka); it is then overlain by a zone characterized by the hadrosaurine *Prosaurolophus maximus* and the centrosaurine *Styracosaurus albertensis* (below the Lethbridge Coal Zone, duration ~672 Ka); and the uppermost zone is associated with the LCZ (duration >658 Ka), and is characterized by the unique occurrences of the lambeosaurine *Lambeosaurus magnicristatus*, a centrosaurine ceratopsid (tribe Pachyrhinosaurini) similar to *Achelousaurus*, and the chasmosaurine ceratopsid *Chasmosaurus irvinensis*. However, it remains unclear which process drives this particular faunal turnover pattern between evolutionary change and ecological replacement in response to climate or habitat change (Ryan & Evans 2005; Evans *et al.* 2009, 2015; Mallon *et al.* 2012; Lowi-Merri & Evans 2020). Since the megaherbivore turnover rate in the Oldman and Dinosaur Park Formations appears higher than the rate of environmental change detected from the rock record alone (unlike the pattern observed in Western Interior formations of relatively similar age and faunal composition such as central Alberta's Horseshoe Canyon Formation (Eberth *et al.* 2013)), it is likely that increased macroevolutionary rates may also be operating. Speciation in response to sexual selection has been cited as one of these possible drivers, especially considering that almost all osteological interspecific variation within the Park's hadrosaurid and ceratopsid families appears to lie within cranial ornamentation (such as crests for the former and frills and horns for the latter) which likely had limited functions for feeding or even defensive behaviour affecting natural selection (Lull & Wright 1942; Dodson 1975; Knapp *et al.* 2018; Campbell *et al.* 2019, Brown *et al.* 2020*a*). Interestingly, faunal turnover patterns have only been convincingly proposed for hadrosaurs and ceratopsians. Otherwise, ankylosaurs and tyrannosaurs show more tentative trends (Currie & Russell 2005; Arbour & Currie 2013): the only realistic case of turnover among those groups consists of the replacement of the tyrannosaurine *Daspletosaurus torosus* (characteristic of the upper Oldman Formation exposed in the Park) by an undescribed species of *Daspletosaurus* found in the lower DPF and time-equivalent Oldman Formation deposits of the Manyberries area in southeastern Alberta (Currie 2003*a*; Paulina Carabajal *et al.* 2021; Scherer & Voiculescu-Holvad 2024). Small theropods such as ornithomimids, caenagnathids, troodontids and dromaeosaurids either display no faunal turnover pattern at all or have been recovered too rarely to establish any meaningful biostratigraphic hypothesis (Funston 2020; Cullen *et al.* 2021). Overall, though, the shifts in species' abundance and in faunal composition observed over the duration of the DPP biota make this ecosystem stand out compared to Hell Creek, the latter of which is likely the only other Mesozoic ecosystem to be known to a similar degree of scientific detail (Hartman *et al.* 2002, Wilson *et al.* 2014*b*). This is because the Hell Creek and Fort Union Formations document biodiversity before, during and after a mass extinction event while DPP, by contrast, offers a rare, detailed glimpse into a palaeocommunity undergoing changes at a 'background' extinction rate. While successive taxonomic faunas together forming a chronofauna have already been documented (and time-calibrated) in far more recent mammal assemblages (Barry *et al.* 1985; Behrensmeyer *et al.* 1997; Blanco *et al.* 2021), DPP may be the world's only pre-Neogene fossil locality with a sedimentological, geochronological and palaeontological record of sufficient quality to make investigations of similar ecological stasis and persistence in deep time realistically feasible.

Together, these lines of evidence suggest that Dinosaur Provincial Park is one of the world's few fossil localities to have the potential to document the local response of a long-extinct community to a perturbation that is becoming ever more prevalent on our planet today (Kirwan & Megonigal 2013; Barnard *et al.* 2021). The Bearpaw marine transgression admittedly occurred over ~2 Myr, on a much deeper temporal scale than the present sea level rises triggered by anthropogenic global warming (Haq 2014; Ray *et al.* 2019), yet it may still be relevant to the present in showing how a community responds to that change at a time of background extinction rate. This may be the most promising baseline that the DPP ecosystem can offer for modern conservation biology, although the spatial and temporal scales of the ecological (whether biotic or abiotic) and (potentially) macroevolutionary changes that occurred there must be determined more accurately to become sufficiently informative.

After praising the geological and palaeontological heritage of Dinosaur Provincial Park, the fact remains that it is not perfect. For example, small-bodied terrestrial vertebrates remain vastly underrepresented in alpha diversity and relative abundance relative to large dinosaurs, thus skewing the true species' body size distribution of that locality (Brown *et al.* 2013*b, a*). However, this limitation is characteristic of almost every terrestrial fossil vertebrate assemblage (Damuth 1982; Benson 2018, Brown *et al.* 2022*b*; but see also Leach *et al.* 2021 for exception). Moreover, the Park's vertebrate fossil specimens have a highly skewed stratigraphic distribution, where about 80% of them have been found in the lower half (40 m) of the Dinosaur Park Formation alone (Eberth & Currie 2005; Henderson & Tanke 2010). This means that the upper horizons of the DPF are poorly represented in the entire chronofauna, especially the Lethbridge Coal Zone, due to a gradual decrease up section in the proportion of sandstone facies favourable to skeleton preservation. Even more problematic from a nonvertebrate palaeontological perspective is the relatively poor plant and invertebrate fossil record as mentioned previously. In any case, these taphonomic biases are arguably outweighed in DPP by the uniquely high geographical and stratigraphic control achieved for this locality outlined above. Overall, this review has presented the strong palaeontological foundations of the DPP biota, which make this ancient ecosystem among the most informative for studying biotic patterns in deep time with a high degree of spatial and temporal fidelity.

Decades of intensive palaeontological research conducted in the Park have already answered fundamental questions about its biodiversity, to a greater extent than is possible in most of the world's fossil localities. In reference to the biodiversity shortfalls mentioned earlier in this chapter (Hortal *et al.* 2015), much of the research undertaken in DPP has addressed the Linnaean, Darwinian, and (to a lesser extent) Raunkiæran shortfalls of that ecosystem. The Gouldian shortfall on the Park's vertebrate species stratigraphic (and by extension temporal) distributions has also been addressed, but these arguably need revision (see Chapter 3). All this work as a whole now raises the possibility to ask even more advanced questions to further develop our knowledge of those diversity trends across spatial and temporal scales, and also to connect the anatomical and morphological descriptions of its fauna (especially its vertebrates) by inferring interspecific interactions. In a way, our understanding of the palaeoecology of DPP remains beset by all biodiversity shortfalls outlined above at varying orders of magnitude. Consequently, it is our responsibility as palaeoecologists to identify the shortfalls that can be addressed most realistically considering the taphonomic biases that affect the Park's fossil record, while distinguishing those that built conservatively upon previous advances from those that will lead to truly groundbreaking questions which have not yet been asked explicitly about that ancient ecosystem. Based on the geological and palaeontological knowledge outlined above, this thesis will address the Wallacean biodiversity shortfall (on species' geographical distribution, see Chapter 2), the Gouldian shortfall (on species' stratigraphic and temporal distribution, see Chapter 3), and the Eltonian shortfall (on species' interactions, see Chapter 4) on the biodiversity of Dinosaur Provincial Park and its vicinity.

BRIDGING TEXT

While Dinosaur Provincial Park has an exceptional fossil record to study the biodiversity of Late Cretaceous Canada, the faunal composition of its community cannot be assumed to represent a regional trend. This is because the region of southern Alberta that now contains DPP lay in a broad floodplain near the Western Interior Seaway, along an inland-coastal palaeoenvironmental gradient. Therefore, investigating the past biodiversity of the region surrounding DPP could reveal patterns of spatial faunal turnover that reflect greater or lesser proximity to this epicontinental sea. Isolated bonebeds and vertebrate microfossil localities of the Dinosaur Park Formation have been documented to the North, South and East of DPP and have revealed some variation in alpha diversity and relative taxon abundances. However, none so far have been as surprising as the marginal marine community preserved in the Lake Diefenbaker Bonebed of Saskatchewan Landing Provincial Park, due to its peculiar combination of marine animals among its microfossil assemblage and of dinosaurs identifiable to the species level in its macrofossil assemblage. The following chapter now reveals a fossil assemblage which remains unique to the Belly River Group ecosystem across southern Alberta and southwestern Saskatchewan, and thus contributes to addressing the Wallacean biodiversity shortfall on dinosaur species' geographical distribution across the region surrounding Dinosaur Provincial Park.

CHAPTER 2. Occurrence of *Centrosaurus apertus* (Ceratopsidae: Centrosaurinae) in Saskatchewan, Canada, and expanded dinosaur diversity in the easternmost exposure of the Late Cretaceous (Campanian) Dinosaur Park Formation

Abstract

Late Campanian terrestrial communities of western Canada are best known from the fluvial-paralic deposits of the Dinosaur Park Formation (DPF) in Dinosaur Provincial Park (DPP), Alberta. However, a growing list of localities from isolated DPF outcrops, outside of the DPP area, offers a glimpse into palaeocommunities that evolved isochronously with DPP biotas in greater proximity to the Western Interior Seaway. Over the past decade, one such locality was explored along Lake Diefenbaker in Saskatchewan Landing Provincial Park. The initial palaeoecological analysis of this marginal marine community was based on palynomorph and vertebrate microfossil diversity and has laid a foundation for the current study of its monodominant ceratopsian bonebed. The latter has resulted in new occurrences of *Centrosaurus apertus* and of the elmisaurine *Citipes elegans* for Saskatchewan based on incomplete yet diagnostic specimens. *C. apertus* is unequivocally identified by a parietal bar bearing two prominent P1 and P2 hooks, which expands the geographical and habitat range of this species to the most coastal environment known from the DPF. Furthermore, the presence of *C. apertus* suggests that the DPF in this region of Saskatchewan is closer in age to the lower DPF than to the uppermost DPF in DPP, which is at odds with a previous palynostratigraphic interpretation. The faunal composition of this bonebed also supports the presence of a widely distributed metacommunity across these deposits. This contribution demonstrates how evidence from multiple localities in the DPF along a spatial gradient, beyond the temporal gradient available within DPP alone, expands the picture of this metacommunity as a potential model system for biotic turnover in response to sea level rise at a geological temporal scale.

2.1 Introduction

After more than a century of exploration, the late Campanian Belly River Group (BRG) in Canada's Western Interior Basin has a remarkable fossil record distributed over a well constrained ~2.43 Myr time interval (Russell 1966; Ramezani *et al.* 2022; Eberth *et al.* 2023). The badlands of Dinosaur Provincial Park (DPP) in southern Alberta preserve the BRG's best-known communities (Currie & Koppelhus 2005) and therefore constitute an excellent study system for biotic turnover through time, as a westward transgression of the Western Interior Seaway (WIS) is documented by the succession from the fluvial deposits of the Oldman Formation into the mixed fluvial/paralic transition of the Dinosaur Park Formation (DPF), up to the final advance of the marine Bearpaw Formation (Béland & Russell 1978; Brinkman 1990; Eberth 2005; Mallon *et al.* 2012; Cullen & Evans 2016; Cullen *et al.* 2021). This sea level rise occurred over approximately 2.4 Myr (Haq 2014; Ray *et al.* 2019; Eberth *et al.* 2023), yet its profound biotic consequences for the composition of the community inhabiting the region arguably produced a rare model system suited to investigating biodiversity patterns in response to a gradual habitat change at a geological time scale.

The BRG is also represented in isolated localities scattered along a ~250 km transect between DPP and western Saskatchewan (Figure 2.1). So far, the faunal variation along that inland-coastal palaeoenvironmental gradient between the nonmarine communities of DPP and the marine communities of the Bearpaw Sea has only been explicitly investigated once (Brinkman *et al.* 1998), thus it has attracted less interest than the faunal variation observed over time within DPP itself. Since the nonmarine communities along that gradient were approximately contemporaneous and have several species in common, they can be considered to collectively form a metacommunity, defined in ecology as a group of local communities linked by dispersal of potentially interacting species (Leibold *et al.* 2004). The BRG is well exposed in the Milk and South Saskatchewan river basins of southeastern Alberta, where the Irvine vertebrate microfossil locality has produced invaluable mammal and lizard specimens among a diverse fauna (Gao & Fox 1996; Fox 2005), and where the Onefour, Manyberries, Sandy Point and White Rock Coulee areas have produced abundant microfossils and ceratopsian bonebeds (Brinkman *et al.* 1998; Evans & Reisz 2007; Eberth *et al.* 2010; Chiba *et al.* 2015). However, these exposures become extremely rare and isolated in southwestern Saskatchewan, which is problematic from the perspective of palaeoecological reconstructions. This is precisely where the palaeocoastline of Laramidia persisted the longest during the late Campanian Stage, despite minor fluctuations in sea level, until the onset of the Bearpaw marine transgression (Eberth & Hamblin 1993; Gilbert *et al.* 2019), and thus where faunas with highly mixed habitat preferences should be found. Saskatchewan's late Campanian – early Maastrichtian fossil record is better known for the spectacular marine reptiles recovered from its Bearpaw Formation outcrops, notably the mosasaurid *Tylosaurus saskatchewanensis* found near Herbert Ferry (Jiménez-Huidobro *et al.* 2019), the elasmosaurid *Terminonatator ponteixensis* found near Ponteix (Sato 2003), and the polycotylid *Dolichorhynchops herschelensis* found near Herschel (Sato 2005), as well as a rare plesiosaur-dominated marine bonebed located near that same settlement (Street *et al.* 2019). Furthermore, Bearpaw Formation exposures in the West Block of Grasslands National Park are beginning to yield new discoveries (Bamforth 2022).

Nevertheless, a few localities in southwestern Saskatchewan offer a glimpse into the most marginal nonmarine communities known from the DPF: these include the Unity Bonebed in the most northerly exposure of that formation (Eberth *et al.* 1990), as well as an isolated outcrop just below a DPF-Bearpaw contact near Herschel which preserves an indeterminate disarticulated ceratopsid skeleton (Mucci *et al.* 2022). Most recently, research conducted throughout the past decade has revealed a diverse bonebed in Saskatchewan Landing Provincial Park, on the northern shore of the South Saskatchewan River's Lake Diefenbaker, amid the easternmost known outcrops of the DPF (Gilbert *et al.* 2018; Figure 2.2A). This locality has the potential to fill an important gap in the known record of the metacommunity of the Belly River Group, where the DPF is poorly exposed, on the eastern coast of Laramidia.

2.1.1 History of research at the Lake Diefenbaker Bonebed

The first recorded palaeontological research around Lake Diefenbaker dates from 1935, when Roy Graham found a bonebed along the South Saskatchewan River from which C. M. Sternberg later collected the posterior section of a frill that would become the paratype of *Chasmosaurus russelli* (Sternberg 1940). It was later referred to '*Mojoceratops perifania'* (Longrich 2010) until that taxon was declared a junior synonym of *C. russelli* (Campbell *et al.* 2019). Efforts to relocate the quarry that yielded this important specimen have proven fruitless so far, yet it is reasonable to assume that it is part of the same bonebed as the site of the current study, based on Sternberg's field notes (J. Mallon, pers. comm., 2023). Subsequent fossil surface collecting efforts for the Royal Saskatchewan Museum (RSKM) were led by N. Yurchyshyn (1975); T. Tokaryk, D. Taylor and N. Yurchyshyn (1990); T. Tokaryk, J. Storer and G. Schutte (1992); and W. Long and M. Caldwell (2002) (Gilbert *et al.* 2018). These resulted in the first discoveries of shark teeth, plesiosaur remains and a *Baptornis* (Aves: Hesperornithiformes) dorsal vertebra among this apparently ceratopsian-dominated bonebed, which led to the first suggestion that this fossil assemblage had formed in a nearshore environment (Tokaryk & Harington 1992). It was not until 2012 that the Lake Diefenbaker Bonebed was explored more systematically, when H. Larsson began leading a survey of this locality as a major objective of his annual palaeontology field course at McGill University for the next six years. As these crews significantly expanded the vertebrate microfossil sample through bulk and surface collecting, the macrofossil bone layer was progressively exposed (Figure 2.2). This project led to a palaeoecological analysis that documented the sedimentological setting and palynomorph and microvertebrate diversity of this ecosystem (Gilbert *et al.* 2018). In that study, the first complete census of the bonebed's vertebrate microfossil diversity revealed a faunal composition that reflected its marginal marine palaeogeographical position and its proximity to a DPF-Bearpaw Formation contact. It confirmed the occurrence of a highly mixed coastal and marine faunal assemblage almost unknown in approximately coeval Alberta localities (Brinkman 1990; Brinkman *et al.* 2004, 2005), except for the Onefour mud-filled incised valley system in the Lethbridge Coal Zone (Eberth & Brinkman 1997). Having established the palaeoecology of the easternmost outcrop of the DPF lays a foundation to investigate what the first significant non-avian dinosaur macrofossils found at the Lake Diefenbaker Bonebed since the days of C. M. Sternberg contribute to the diversity of an ancient community that evolved at an ecotone between the eastern Laramidian coastal plain and the Bearpaw Sea during the late Campanian Stage. In the following paper, this faunal assemblage will be shown to reveal new occurrences of the ceratopsid *Centrosaurus apertus* and of the elmisaurine caenagnathid *Citipes elegans* in Saskatchewan.

Institutional abbreviations: CMN, Canadian Museum of Nature, Ottawa, ON, Canada; RM, Redpath Museum, Montréal, QC, Canada; RSKM, Royal Saskatchewan Museum, Regina, SK, Canada.

2.2 Material and methods

2.2.1 *Fieldwork in Saskatchewan Landing Provincial Park*

The Lake Diefenbaker Bonebed was excavated from the year of its re-discovery in June 2012 to the closure of its main quarry in June 2018. Prospecting efforts during those seasons revealed the presence of seven distinct macrofossil sites in the same depositional horizon, labeled A-G. A master quarry stake was planted as a georeference point for quarry maps, and grids for each of the latter were drawn originating from their own distinct quarry stakes (Figure 2.2B-E). Overburden was removed each summer throughout the 2013, 2014, 2015, 2017 and 2018 field seasons, exposing an ever-greater portion of the bone layer. The final map of the most extensive quarry (Quarry C) was aggregated from grid squares drawn annually (Figure 2.3). The total excavated area of the seven main sites (Quarries A-G) amounted to ~70 m^2 over an East-West transect of ~200 m (Figure 2.2B). In addition to quarry mapping, stratigraphic sections were measured at Quarry C during the 2012 field season. The master section was published in Gilbert *et al*. (2018), but two more constrained sections were also measured at the northern and southern extremities of Quarry C to study more subtle facies variation immediately above and below the bonebed horizon. Fieldwork was conducted under Saskatchewan Palaeontological Resources and Investigation Permits 13-P003, 14-P007, 15-P006 and 18-P003, along with Saskatchewan Landing Provincial Park Research Permits – 2013, 2014, 2015 and 2018.

2.2.2 Fossil preparation and imaging

All specimens collected *in situ* were assigned a field number according to their quarry map location. They were accessioned at the RSKM and loaned to the RM for preparation and study, in compliance with Saskatchewan fossil heritage laws. Adhesion, consolidation, filling and labelling of the most scientifically significant specimens was not completed until the 2020-21 and 2021-22 academic years. The most complete and taxonomically informative specimens that were selected for the present study were accessioned into the RSKM collections, which also include most of the previously studied specimens from a vertebrate microsite within the same bonebed (Gilbert *et al.* 2018), as RSKM P3193 and P3217.

Some of the catalogued specimens were imaged for this study using up to three methods: photographs were taken using a Canon Rebel T6 macro lens (or a Canon EOS 70D lens for the largest specimens) (Canon, Tokyo, Japan), often stitched for the same specimen via focus stacking using Helicon Focus 7 (Helicon Soft, Kharkiv, Ukraine); line drawings were made from photographs using Adobe Fresco (Adobe Inc., San Jose, USA); and surface scans were produced using a Go!Scan Spark handheld surface scanner and the VxModel 3D scanning software (both from Creaform, Lévis, Canada). Scanning resolution was 0.4 mm / voxel for the majority of specimens and 0.2 mm / voxel for the smallest (usually <10 cm in length), using the 'Targets only' positioning method. The scans were then decimated and rendered in Meshlab (Cignoni *et al.* 2008).

2.2.3 Alpha diversity analyses

The identification of all elements recovered *in situ* from the macrofossil bonebed created an opportunity to update the Lake Diefenbaker Bonebed's overall alpha (within-site) diversity. As in Gilbert *et al*. (2018), the Chao-1 (Chao, 1984), Jackknife-2 (Smith & van Belle 1984) and Abundance-based Coverage Estimator (ACE) (Chao & Lee 1992) were selected to count the number of rare taxa (singletons or doubletons) in the locality's fossil assemblage and thus extrapolate its theoretical 'missing' diversity (Vavrek 2010; Bamforth 2013). Of all non-parametric species richness estimators, these three have been shown to produce the most realistic alpha diversity estimates for palaeontological samples, which have a notoriously high quantity of rare taxon occurrences (Colwell & Coddington 1994; Hammer & Harper 2006; Hortal *et al.* 2006). The results of these estimators were compared between the following datasets: a dataset created from the locality's microfossil taxon frequencies reported in Gilbert *et al*. (2018); a dataset that combined the aforementioned microfossils with macrofossils collected before this study (such as the *Chasmosaurus russelli* posterior parietals, see Introduction) and the newly reported fossil occurrences from the bonebed; a dataset containing only dinosaur occurrences from the Lake Diefenbaker Bonebed (whether macro- or microfossil, including birds); and finally datasets of dinosaur abundances for three DPP bonebeds as a point of comparison of dinosaur taxonomic diversity with Lake Diefenbaker within the DPF. The selected DPP bonebeds were the heavily ceratopsid-dominated Bonebed 043 (data obtained from Ryan *et al.* 2001), the marginally ceratopsid-dominated Bonebed 042 (data obtained from Visser 1986: figure 29) and the multigeneric Bonebed 047 (data obtained from Tumarkin-Deratzian 1997: figure 23, appendix B).

All diversity estimates were calculated in the 'fossil' package (Vavrek 2011) in R statistical software (R Core Team 2023), version 4.2.2. Diversity was estimated at the family level in order to include macrofossils and microfossils of the same family (e.g. Ceratopsidae) within the same operational taxonomic unit in this analysis, despite the potential of the macrofossil assemblages to contain dinosaur elements identifiable at lower taxonomic levels. The only exceptions were in the separation of carpet sharks (Orectolobidae) from the microsite into *Cretorectolobus olsoni* and *Eucrossorhinus microcuspidatus* and of scapherpetontid salamanders into *Scapherpeton tectum* and *Lisserpeton bairdi* since all elements representing these families were identifiable at the species level (Gilbert *et al.* 2018). As in the aforementioned study, elements unidentifiable at the family level were excluded from each dataset. The taxon counts from the BB047 dataset were also adjusted. First, only one of its 64 ankylosaurian specimens was identified by Tumarkin-Deratzian (1997) as nodosaurid, the remainder being assigned to Ankylosauridae by default. We elected to retain this single nodosaurid tooth as a separate operational taxonomic unit in the dataset (despite clearly underestimating nodosaurid abundance) since it would still lead to more realistic alpha diversity estimates. Similarly, we elected to keep the single indeterminate bird fossil reported from that same collection (identified as an ulna, see Royal Tyrrell Collections 2024) as a taxonomic unit separate from Dromaeosauridae since the latter family would otherwise have been the only representative of small theropods.

2.3 Results

2.3.1 Geological setting and taphonomic observations

The broader sedimentological setting of the Lake Diefenbaker Bonebed and of the DPF-Bearpaw Formation transition at Saskatchewan Landing Provincial Park was presented in Gilbert *et al.* (2018). In that study, the bonebed was located within a lithological unit termed ‘Facies 1’, which is dominated by silty and sandy inclined heterolithic stratification (see Thomas *et al.* 1987 for definition). This facies was interpreted as laterally migrating tidally influenced point bar deposits within channel fills in a coastal plain. A recent sedimentological and ichnological review of the DPF in southwestern Saskatchewan proposed that its depositional environments were not part of a delta system (as was previously hypothesized), but instead were tidal flats in a complex of estuary basins and lagoons protected from storms by barrier island bars (Gilbert *et al.* 2019). In this revised interpretation, the Lake Diefenbaker Bonebed appears to have been deposited in a wave-dominated, tide-influenced, fluvially affected marginal marine depositional environment, i.e. ‘Facies association 3’. As noted by these authors, the corollary would be that this stretch of the eastern Laramidian coastline was shaped primarily by wave energy and secondarily by tides and fluvial energy.

The present study has prompted the publication of more constrained stratigraphic sections that highlight the sedimentary succession immediately above and below the bonebed layer at Quarry C (Figure 2.4). These reveal fine-scale variation in facies dominated by sandy and silty inclined heterolithic stratification. The section measured at the northern edge of the quarry is the thicker of the two and extends for 1.2 m, which represents roughly a third of the thickness of Facies 1 identified by Gilbert *et al*. (2018). The base of that section lies almost 70 cm below the bone layer, and its lower half is dominated by a shaley purple organic-rich mudstone interspersed in places with a clay-pebble conglomerate with ironstone nodules. This facies is interrupted first by a ~10 cm thick bright orange, very fine muddy siltstone emerging ~40 cm below the bone layer, and then by a much shallower, slightly coarser fine-grained sandstone layer. It is also interrupted by a 10 cm thick fine-grained sandstone bracketed by ironstone nodules extending up to ~8 cm below the bone layer. Fossils from Quarry C are spread among three distinct successively stacked horizons: the lowest is the clay-pebble conglomerate and contains the majority of collected microfossils. The middle horizon lies directly over that clay-pebble conglomerate and constitutes the main bonebed layer, containing the most complete and best-preserved elements. Lastly, a sandstone layer directly above the middle horizon preserves mostly rounded, broken bones. The upper two layers are within an unstructured ~30 cm fine sandstone unit and are separated by a ~1 cm thick mudstone stripe. The uppermost fossil-bearing horizon of Quarry C is overlain by a dark grey fine-grained mudstone. These three layers do not include an even higher sandstone horizon from which a hesperornithiform pelvis (cf. *Baptornis*) was collected (Gilbert *et al.* 2018). It must be noted that all bones found in quarries A, B, C and D lie within the middle bonebed horizon. Quarry E, as well as a 3 m long outcrop lying around halfway between quarries C and D, is located in the thicker mudstone unit that overlies the sandstone units.

The stratigraphic section drawn at the southern edge of Quarry C is even less extensive yet has a higher facies diversity. Its base lies within <40 cm of the bonebed layer and is composed of alternating fine-grained shales and muds, with a very fine-grained siltstone overlying the lowest 10 cm. Above these sediments lies what is probably the same orange siltstone as in the northern stratigraphic section, although here it is divided by a dark mud-rich organic shale interspersed with ironstone beds. This siltstone is then succeeded by the same mudstone as in the northern section, divided by a similar very fine-grained sandstone. In the southern section, this unit fines upward from a dark grey fine-grained mudstone to the same purple organic-rich mudstone with clay-pebble conglomerates as in the northern section. The latter is interrupted by another very fine-grained sandstone. The remainder of the southern section is almost identical to the northern section, in that the bone layer lies once again at the base of the same thick very fine-grained sandstone, just overlying the top of an organic-rich mudstone. Overall, the observed variations in sedimentary facies may be very local, and in any case do not change the original interpretation of the bonebed's immediate depositional environment.

A total of 337 individual fossil bones and teeth have been excavated from the Lake Diefenbaker Bonebed's main bone layer (Figures 2.2, 2.3; Appendix III). Even though a quantitative taphonomic study of the site is beyond the scope of this paper, a few preliminary observations are deemed noteworthy. First, the bones uncovered in Quarry C display nearly the entire possible range of long-axis orientations (Figure 2.3). Second, most of the bonebed's largest elements (>20 cm in length) are complete or near-complete, and the vast majority in that size category show little to no sign of abrasion or weathering (see descriptions below). However, the smaller size classes are dominated by indeterminate sharply broken fragments and bone pebbles. Several specimens were found with a thick coat of ironstone on their underside, which is likely the same material that forms the dense ironstone beds around the bonebed layers. The ironstone varies from a coarse-grained, almost sandy, texture to a hard, almost muddy, texture, sometimes along the length of a single fossil specimen. Lastly, some elements bear tooth marks attributed to scavenging, as well as deep rounded holes interpreted as borings formed by insects, such as dermestid beetle larvae, as suggested for other localities (Rogers 1992; Hasiotis *et al.* 1999).

2.3.2 Dinosaur macrofossil descriptions

The following section presents summary descriptions of the most taxonomically significant dinosaur fossil bones uncovered from the Lake Diefenbaker Bonebed. These constitute the most essential contributions of the macrofossil assemblage to the diversity of the Campanian community preserved in Saskatchewan Landing Provincial Park. All described and figured specimens have been returned to the RSKM collections.

Ceratopsids

Frill elements. One of the most taxonomically informative elements recovered from the Lake Diefenbaker Bonebed consists of the medial section of a right ceratopsid parietal that displays intact first and second parietal processes, henceforth referred to as P1 and P2 *sensu* Sampson *et al*. (1997) (RSKM P3217.500, Figure 2.5). P1 forms an elongated rostroventrally curving hook with a length of 19.2 cm and a width of 11.2 cm at its locus origin. P2 forms a much shorter, medially curving hook 9 cm long, and 9 cm wide at locus origin. Both parietal processes are carved longitudinally by shallow sulci constituting vascular channels for bloodflow that would have supplied keratin sheaths covering each process. The most rounded transverse fracture in the specimen is a break in the posterior transverse ramus of the parietal, which has an anteroposterior diameter of 6 cm and a dorsoventral diameter of 5.2 cm and is near-cylindrical in cross-section as in all centrosaurines (Figure 2.5F, K-L). Conversely, the break on the opposite side has a more linear shape that corresponds to the medial edge of the parietal’s lateral ramus, with an anteroposterior diameter of 2.8 cm and a dorsoventral diameter of 8.5 cm (Figure 2.5F, J). This specimen displays the main diagnostic characters of *Centrosaurus apertus* (Lambe 1904, 1910). The medial edge of P1 stretches towards the sagittal midline over the only preserved fragment of the median parietal bar's posterior extremity (Figure 2.5C) and the base of P1 completely overlies what is left of the ventral flange of the posterior transverse ramus (Figure 2.5F, H). The diameter of the posterior transverse ramus combined with the length of P1 demonstrate that this specimen likely had reached adult size at the time of death. Both parietal processes are nearly fully formed, providing another indication that the individual had reached skeletal maturity at time of death, yet their surficial texture remains relatively smooth and displays none of the rugosities and deep sulci observed in the oldest known *Centrosaurus* individuals (see Frederickson & Tumarkin-Deratzian 2014). This evidence indicates that RSKM P3217.500 died as a young adult. In some *Centrosaurus* specimens, both P1 processes are connected by a sharp-edged flange that overlies the median parietal bar, but RSKM P3217.500 has such a smooth P1 medial edge that it likely would not display this character state were the left parietal preserved (Figure 2.5B, L). Both processes will henceforth be designated as epiparietals, following recent arguments defending the hypothesis that they fused to the parietal during ontogeny in a manner homologous to the mode of fusion that characterized less prominent epiparietals (with a less controversial developmental sequence) along the more lateral loci of the frill (Mallon *et al.* 2023).

A median parietal bar was recovered that lacked both extremities, had heavily abraded margins, was pierced by multiple insect borings, and displayed a relatively sharp sagittal ridge (despite taphonomic abrasion) coupled with a distinct ventral groove (RSKM P3217.473, Figure 2.6A-F). A convex parietal bar coupled with a concave ventral groove is a feature characteristic of centrosaurines (Lull 1933). A clear ridge running longitudinally down the midline of the specimen has previously been observed on more complete frills belonging to young juvenile *Centrosaurus* individuals previously identified as *Monoclonius* and *Brachyceratops* (Dodson & Currie 1988; Sampson *et al.* 1997). The preserved portion of the bar has a long axis length of 21 cm and its dorsoventral thickness of approximately 0.75 cm remains relatively uniform throughout (Figure 2.6E-F). Assuming a few centimetres are missing at either extremity, the length of this bar falls well within the size range of the aforementioned young juvenile centrosaurine specimens. The absence of any preserved lateral margin to the bar could be explained by the fact that it had not even formed by the time of the individual's death due to an incomplete opening of the parietal fenestrae. Furthermore, its surface displays a radiating long-grained texture, which has been shown to be a size-independent indicator of juvenile status in previous studies of centrosaurine craniofacial ontogeny (Sampson *et al.* 1997; Brown *et al.* 2009). Therefore, these lines of evidence confirm that this median parietal bar belongs to a juvenile, making it one of the least skeletally mature ceratopsid individuals known from the Lake Diefenbaker Bonebed.

Another noteworthy frill component consists of a partial right squamosal retaining only the posteroventral corner from the infratemporal fenestra to the second episquamosal locus (RSKM P3217.418, Figure 2.6G-K). The sinusoidal curve comprising the jugal notch and the squamosal corner is relatively smooth with a wide arc, more akin to centrosaurines than to chasmosaurines such as *Chasmosaurus russelli* (Longrich 2010; Campbell *et al.* 2018). The sutural surfaces for contact with the quadrate (a wide and deep cotyle) and exoccipitals (a narrow ridge with a rugose texture) remain clearly visible. A more fragmentary specimen is also identified as a centrosaurine left squamosal corner (RSKM P3217.368, Figure 2.6O-S). It has similar proportions to RSKM P3217.418, with a concave lateral side, a convex medial side, a slightly concave ventral margin contributing to the jugal notch, and a convex posterior margin with a swelling that would have supported an episquamosal. However, its increased dimensions indicate it belongs to a much larger individual, especially considering that only the posterior part of the jugal notch margin appears preserved. The identification of this specimen remains more tentative because of heavy abrasion on nearly every broken edge combined with several insect borings.

A small isolated subtriangular bone displaying a slightly pointed extremity with vascular channels radiating from it is almost certainly a ceratopsid cranial epiossification (RSKM P3217.589, Figure 2.6L-N). Its compressed shape suggests it is more likely to be an epiparietal than an epijugal.

Other cranial elements. A few ceratopsid skull (excluding frill) elements have been recovered from the Lake Diefenbaker Bonebed, including a well-preserved right nasal horncore (RSKM P3217.464, Figure 2.7A-F). It was separated sagittally from the corresponding left nasal at the median suture, indicating that the fusion of the nasals from the tip down had not begun by the time of the individual's death. The laterally compressed and recurved shape of the horn, combined with the presence of well-defined vascular grooves and its position overlying most of the narial opening, further suggest that this individual was osteologically immature (see Sampson *et al.* 1997). Conversely, the specimen is close to the full size that would be expected at maturity, suggesting it belonged to a subadult. These observations collectively suggest that this right nasal belonged to a subadult centrosaurine rather than an adult chasmosaurine.

One partial right maxilla was also recovered (RSKM P3217.426, Figure 2.7M-O). The middle third of the bone is preserved and all the teeth were shed, leaving the alveoli clearly preserved. A prominent ridge forms a concave posterior margin for the lateral surface of the maxilla and widens transversely at its dorsal extremity into the sutural surface for the jugal. Two quadrates with almost pristine articular surfaces for the mandible were also collected (RSKM P3217.475 and RSKM P3217.558, Figure 2.7P-U): the left quadrate displays a more complete lateral margin, revealing the sutural surface with the paroccipital process, as well as a more complete pterygoid sutural surface on its medial side (Figure 2.7P-R).

One element is clearly part of a skull roof between the orbits and the base of the frill due to its densely grooved texture (RSKM P3217.552, Figure 2.7G-I). It is tentatively proposed to constitute the posteromedial edge of the left frontal that contributes to the margin of the supracranial cavity, which opens on the skull roof via the frontal fontanelle (Dodson *et al.* 2004: 501-2). The anteroventral face of the specimen has a particularly smooth texture, is pierced by two foramina, and would have contributed to the left orbit (Figure 2.7H). The braincase itself is represented by a fragment that could constitute the base of a paroccipital process (RSKM P3217.479, Figure 2.7J), as well as a near-complete basioccipital uncovered during Tim Tokaryk's initial surveys of the region (RSKM P2199.3, Figure 2.7K-L).

Mandibular elements. Three relatively well-preserved ceratopsid dentaries are known from the Lake Diefenbaker Bonebed (RSKM P3217.586, RSKM P3217.371 and RSKMP3217.587, Figure 2.8A-H). They are all assigned to Ceratopsidae on the basis of their coronoid processes having a pointed, nearly hooked, rostral extremity and a faintly pointed dorsal extremity. The most complete of these dentaries (RSKM P3217.586) affirms this identification with the presence of the anterior half of a single toothless alveolar row with a slight posteroventral slope, as well as a slightly rounded predentary sutural surface on its rostral extremity (Figure 2.8A-D). The taphonomic loss of the posterior half of the alveolar row, and much of the mandibular ramus' posterolingual surface, exposes the mandibular fossa at the base of the coronoid process. The posterior dentary RSKM P3217.371 is characterized by a relatively high density of insect borings (Figure 2.8E-F).

Non-dentary mandibular elements are represented by a left surangular-articular complex (RSKM P3217.530, Figure 2.8I-O) and a right angular (RSKM P3217.383, Figure 2.8P-R). As is characteristic of Ceratopsidae, the articular bears a wide glenoid fossa and the surangular's contribution to the coronoid process is reduced to a mediolaterally thin lamina with pointed tips at its dorsal and anterior extremities, rising from the adductor fossa. The prearticular is visible as a short process emerging rostrally from the adductor fossa. The angular is identified as ceratopsid due to the presence of a distinct flange on the posterior margin that would have accommodated the posterior extremity of the surangular. Furthermore, its externally visible surface has a smooth texture interspersed with faint grooves and occasional vasculature, all of which are characteristic of ceratopsid angulars.

Postcranial elements. A high diversity of ceratopsid axial and appendicular postcranial bones is documented from the Lake Diefenbaker Bonebed (Appendix III; Figures 2.9-10). First, a syncervical comprising the first three vertebrae (RSKM P3217.563, Figure 2.9A-E), a diagnostic characteristic of Ceratopsidae (Campione & Holmes 2006), was collected. The atlas arch is nearly absent save for a small process protruding dorsally from the atlas centrum (Figure 2.9A-B). Despite the poor preservation of the axis spine, this syncervical has a ventral keel that forms prominences clearly corresponding to the three vertebrae. This feature is more evident in centrosaurines than in chasmosaurines (Campione & Holmes 2006), hence supporting an assignment to cf. *Centrosaurus*. The axial and third cervical spines are in poor condition as well, with only a few centimetres of the former's dorsal ridge still preserved. The centra are in a more pristine state, displaying a nearly complete anterior cotylus to accommodate the occipital condyle (Figure 2.9D) and a nearly complete heart-shaped posterior articular surface (Figure 2.9E).

Four more vertebrae can be confidently referred to Ceratopsidae. Two neural arches belong to the anterior dorsal series, both tentatively identified as D5 (RSKM P3217.416 and RSKM P3217.374, Figure 2.9F-G) based on the overall shapes of their pre-and postzygapophyses, parapophyses and transverse processes (Holmes & Ryan 2013). Another consists of an anterior caudal with the subcircular centrum diagnostic of Ceratopsidae (RSKM P3217.561, Figure 2.9H-I), tentatively identified as Ca5 based on the combined shapes of its pre-, post- and diapophyses (Holmes & Ryan 2013).

Ceratopsid appendicular elements include three identifiable scapulae (Figure 2.10), a left ulna with spiral fractures at both extremities (RSKM P3217.465, Figure 2.9J-L), a complete left ischium (RSKM P3217.572, Figure 2.9P-R), and a near-complete right second metatarsal (RSKM P3217.566, Figure 2.9M-O). The ischium is assigned to cf. *Centrosaurus* since the ischial foot lacks the pronounced near-90° curve characteristic of chasmosaurines (Lull 1933; Dodson *et al.* 2004). It displays a fracture at mid-shaft caused by a rock hammer during its excavation in the field. A comparison of three of the scapulae reported from this locality sheds light on the size (and thus ontogenetic) variation observed among the preserved ceratopsid population. The largest specimen, found at Quarry B, is 76.5 cm long from the scapulocoracoid sutural surface to the tip of the distally widening scapular blade (RSKM P3217.560, Figure 2.10A-C). A slightly rounded distal end to the scapula suggests a closer taxonomic affinity to Centrosaurinae than to Chasmosaurinae. The large size of the specimen combined with the absence of a coracoid fused to the rugose scapulocoracoid sutural surface suggests it belonged to a subadult individual (Dodson *et al.* 2004). In contrast, another scapula from the bonebed has the same general shape but is barely more than 30 cm long (RSKM P3217.519, Figure 2.10D-F). It is only missing the last few centimetres of its distal apex and thus belongs to a juvenile. The last notable ceratopsid scapula is more difficult to identify due to its poorer preservation but has a distinct scapular ridge extending obliquely from the supraglenoid ridge to the craniodorsal blade (RSKM P3217.588, Figure 2.10G-H). The entire bone would have been nearer in size to the adult than to the juvenile scapula but the glenoid appears shorter, suggesting that this specimen did not belong to a fully grown individual either.

Hadrosaurids

The most noteworthy hadrosaurid specimen from the Lake Diefenbaker Bonebed is a near-complete left dentary found between sites A and C (RSKM P3217.506, Figure 2.11A-D). Multiple tooth rows forming a dense tooth battery, combined with an anteriorly tapering coronoid process, support the assignment of this dentary to Hadrosauridae. A relatively short anteroposterior length combined with an abrupt ventral deflection of the rostral extremity of the ventral margin mean that this dentary belongs either to a lambeosaurine or to the short-snouted hadrosaurine *Gryposaurus* (Horner *et al.* 2004; Lowi-Merri & Evans 2020), so that this individual remains an indeterminate hadrosaurid. The inner layers of a medial dentary plate covering unerupted crown rows are also visible (Figure 2.11A, B). This plate forms the dorsal margin of the neurovascular foramina.

The posterior half of a left maxilla is also reported from the bonebed, its small size suggesting it belongs to a juvenile (RSKM P3217.415, Figure 2.11E-I). In this specimen, the medial maxillary plate and neurovascular foramina row are well preserved, and unerupted crown rows are visible in a cross-section exposed by the specimen's anterior fracture (Figure 2.11H). A slightly concave dorsal margin suggests, despite being interrupted anteriorly by a fracture, that this maxilla bore an anterior maxillary process contacting the predentary. Since this character is present in all non-lambeosaurine hadrosaurids (Horner *et al.* 2004), this maxilla is referred to subfamily Hadrosaurinae.

A partial right squamosal was also collected (RSKM P3217.585, Figure 2.11J-N). It displays well-preserved features such as an anterior process for contact with the postorbital, an ellipsoidal cotyle to accommodate the dorsal head of the quadrate and an exoccipital sutural surface that contributes to the occipital crest. However, both the postquadratic process and the lobe forming the posterior half of the skull's temporal arch are broken at their respective bases.

A relatively high diversity of hadrosaurid postcranial elements has been recovered from the Lake Diefenbaker Bonebed. These include a scapula missing both extremities, with the flat medial and lateral faces characteristic of Hadrosauridae (RSKM P3217.391, Figure 2.12A-B), as well as a complete humerus of juvenile size with the long and wide deltopectoral crest characteristic of Lambeosaurinae (RSKM P3217.505, Figure 2.12C-D) (Horner *et al.* 2004). There is also a complete right ulna (RSKM P3217.525, Figure 2.12E-F) and the distal end of a right ischium, which can be assigned to Lambeosaurinae based on its distinctly hooked tip (RSKM P3217.417, Figure 2.12G-H) (Horner *et al.* 2004). A pubis of juvenile size lacking the entirety of its prepubic process, and the iliac and ischial peduncles, is assigned to Lambeosaurinae based on the sharp dorsal curve of the prepubic process (RSKM P3217.507, Figure 2.12I-J) (Horner *et al.* 2004). The Lake Diefenbaker Bonebed thus appears to contain remains of both hadrosaurid subfamilies.

Theropods

Tyrannosaurid teeth are the most common theropod elements at the Lake Diefenbaker Bonebed, as in similar Late Cretaceous North American localities (Varricchio 1995; Tumarkin-Deratzian 1997;

Ryan *et al.* 2001). This family is also represented by a near-complete posterior caudal (RSKM P3193.1, Figure 2.13A-D). The caudal has a very shallow and elongated centrum, with a barely distinguishable neural spine, complete postzygapophyses and broken prezygapophyses that would have overlapped the preceding vertebra. Its position along the tail is tentatively estimated at Ca21-23, inclusive, based on a near-complete *Gorgosaurus libratus* tail (Lambe 1917). Furthermore, the transverse span of its paired pre-and postzygapophyses relative to centrum width is far lesser than in ornithomimid tails.

A slender, hollow bone with a spiral fracture is identified as a caenagnathid right second metatarsal (RSKM P3217.481, Figure 2.13E-I). Its proximal extremity is not preserved and its distal condyle, despite being moderately eroded, is sufficiently preserved to suggest that it projected slightly anteriorly relative to the metatarsal's long axis. A facet for accommodation of a widened third metatarsal is visible in lateral view, beginning wide distally then tapering proximally while remaining visible at the fracture point (Figure 2.13G-H). This facet is typical of arctometatarsalian pedes, in which metatarsal III is pinched between metatarsals II and IV and projects forward relative to the latter (Holtz 1995). One of the best-preserved features of this specimen is a pronounced posteromedial ridge, which rises and appears to recede over a short length along the metatarsal shaft (Figure 2.13F-I). This overall morphology suggests that RSKM P3217.481 belongs to the elmisaurine subfamily within Caenagnathidae. Its most diagnostic character consists of a short posteromedial ridge so prominent that it would have protruded beyond the posterior edge of the distal condyle, a key trait distinguishing Elmisaurinae from other caenagnathids and coelurosaurs in general (Funston *et al.* 2016). Furthermore, it has an almost identical mirrored shape to RSKM P2600.1, an intact left metatarsal II from the Upper Maastrichtian Frenchman Formation of Saskatchewan referred to *Leptorhynchos* sp. (Funston *et al.* 2016: figure 10B). In both specimens the central part of the shaft, just proximal to the distal condyle, appears weakly sinusoidal in anterior and posterior view, and the shaft appears constricted just proximal to the distal condyle in medial and lateral view (caused by the sharp rise of the posteromedial ridge). This comparison suggests that ~60% of the total length of RSKM P3217.481 is preserved. The only other published specimen displaying a closely similar morphology is a second metatarsal from the Hell Creek Formation of Montana (Varricchio 2001). RSKM P3217.481 also shares its gracile proportions and very rounded, anteriorly projecting distal condyle with a left fourth metatarsal from Dinosaur Provincial Park identified as *Citipes elegans* (Funston 2020: figure 13), although the latter has a distinctly less prominent posteromedial ridge as is characteristic of that digit.

Nonetheless, the possible referral of RSKM P3217.481 to another cœlurosaur lineage sharing the arctometatarsalian pedal condition was also considered. First, it differs from troodontid second metatarsals in that it is not nearly as distally compressed in anterior view (see Wilson & Currie 1985; van der Reest & Currie 2017). Secondly, the specimen is more gracile than any ornithomimid second metatarsal or any caenagnathine caenagnathid second or fourth metatarsal (see Osborn 1917; Currie & Russell 1988; Funston *et al.* 2015; pers. obs.). Lastly, although it appears superficially similar to ornithomimid fourth metatarsals, it differs from those in that the metatarsal III facet wraps less extensively onto the central shaft's anterior face, and in that the shaft thins at a level proximal to the posteromedial ridge in medial and lateral view instead of retaining the thickness reached at the posteromedial ridge up to the proximal end of the metatarsal as seen in ornithomimids (see Osborn 1917; pers. obs.). Considering that the Lake Diefenbaker Bonebed is in the Dinosaur Park Formation, the elmisaurine second metatarsal reported here can be tentatively assigned to *Citipes elegans*, the only elmisaurine recognized from Dinosaur Provincial Park and the smallest of the three caenagnathid species reported from that locality (Funston 2020).

2.3.4 Updated diversity of the Lake Diefenbaker Bonebed

The frequency of each skeletal element per taxon recovered *in situ* from the main macrofossil bone layer of the Lake Diefenbaker Bonebed is displayed in the Appendix III and Figure 2.14A-B. The vast majority of these elements are ornithischian, whether ceratopsid, hadrosaurid or indeterminate, with approximately two ceratopsids for every hadrosaurid among identifiable elements. Some of them can be confidently identified to the subfamily level (see description above), which means that both hadrosaurid subfamilies and both ceratopsid subfamilies (accounting for the previously reported *Chasmosaurus* parietals (Sternberg 1940)) are now known from this locality. Among rarer vertebrates, a few tyrannosaurid teeth, trionychid turtle carapace fragments and potential fish elements have been recovered. Champsosaurs are represented by a high diversity of skeletal elements, most notably a complete basioccipital, two coracoids and two ilia. The most novel addition to the bonebed's overall species richness is the metatarsal referred to the small edentulous theropod family Caenagnathidae (see description above). Considering that two small ankylosaurid osteoderms were previously reported among the microfossils (Gilbert *et al.* 2018), the absence of any larger osteoderm of that family from the bonebed proved a little surprising.

A comparison of taxon abundances across all material so far collected from the Lake Diefenbaker Bonebed demonstrates how little the macrofossils contribute to overall specimen-level abundance (Figure 2.14C-F). Unsurprisingly, the two families already present in the microfossil assemblage that exhibit the highest increases in abundance due to the inclusion of macrofossils are Ceratopsidae and Hadrosauridae, and these increases are probably underestimated given the high frequency of indeterminate ornithischian and dinosaur remains. However, microfossils collected *ex situ* after 2015 were included neither in the Gilbert *et al*. (2018) census nor in this updated census, which means that macrofossil abundance relative to microfossil abundance remains overestimated.

The observed alpha diversity of the Lake Diefenbaker Bonebed increased from 42 to 43 since the analysis of Gilbert *et al*. (2018). However, the estimated alpha diversity increased twice to thrice as much relative to observed diversity, depending on the non-parametric species richness estimator used (Table 1). Considering that the Chao-1, Jackknife 2 and ACE estimators are all sensitive to the presence of singletons or doubletons, this trend is attributed to the addition of a single very rare taxon (Caenagnathidae), which suggests a higher number of theoretically missing taxa than were estimated to exist in an analysis solely including the 2018 dataset. Conversely, the increase in ceratopsid and hadrosaurid abundances (which were already >2 in the microsite) must have had a negligible effect on the estimated values. However, observed species richness has been underestimated in this analysis since identifiable centrosaurine and chasmosaurine elements were all lumped under Ceratopsidae, as were hadrosaurine and lambeosaurine elements under Hadrosauridae. Had they remained as their own respective operational taxonomic units and considering that Chasmosaurinae and Hadrosaurinae would have formed additional singletons, the estimated alpha diversity would have been inflated.

A comparison of dinosaur diversity between the Lake Diefenbaker Bonebed (LDB) and three Dinosaur Provincial Park bonebeds (*Styracosaurus*-dominated BB042, *Centrosaurus*-dominated BB043 and multigeneric BB047) is also presented in Table 1. Despite having a much smaller sample size than BB043 and BB047, the LDB has an observed taxonomic richness equal to that of BB047, as well as a higher predicted species richness according to two of the three selected species richness estimators (Chao-1 and second-order Jackknife). Only the ACE yields a higher alpha diversity estimate for BB047 than for the LDB. With the former two estimators at least, the LDB consistently displays the highest increases between observed and predicted diversity regardless of the choice of species richness estimator. This pattern is explained by the high abundance of singletons and doubletons in the LDB dataset relative to either DPP dataset, which is likely an artifact of the former's relatively small sample size. It must also be noted that none of BB042's small theropods were identified at family level and that no caenagnathids were identified in the BB047 sample studied in this analysis, despite the family being subsequently reported from the same bonebed (Funston 2020). It thus follows that the dinosaur diversity of both BB042 and BB047 is certainly underestimated in this study.

2.4 Discussion

2.4.1 An increased dinosaur diversity for Saskatchewan

Since the discovery of a partial *Chasmosaurus russelli* frill in a likely extension of the present bonebed, the dinosaur diversity of Saskatchewan Landing Provincial Park at lower taxonomic levels now also includes a centrosaurine ceratopsid referred to *Centrosaurus apertus*, indeterminate lambeosaurines and hadrosaurines and, most surprisingly, an elmisaurine caenagnathid that we refer to *Citipes elegans*. The latter represents the first caenagnathid occurrence in the Campanian of Saskatchewan, following the identifications of elmisaurines and large caenagnathines in the late Maastrichtian Frenchman Formation of Grasslands National Park (Bell *et al.* 2015; Funston *et al.* 2016). Considering that *Citipes* is so elusive, partly due to the taphonomic bias against small-bodied dinosaurs in the DPF (Brown *et al.* 2013), it is all the more extraordinary to find it within a bonebed dominated by what is arguably the single most abundant dinosaur species of the DPF metacommunity's fossil assemblage.

If the macrofossil assemblage of the Lake Diefenbaker Bonebed alone is accounted for, it is currently classified as a monodominant ceratopsid bonebed considering that this family represents about 52% of all identifiable isolated elements at the family level. This value was calculated after discarding all indeterminate turtles, fishes and dinosaurs, following the definition of Blob & Badgley (2007). It must be noted that this proportion is far lower than in Alberta's *Centrosaurus*-dominated bonebeds (Ryan *et al.* 2001; Eberth & Getty 2005; Eberth *et al.* 2010; Chiba *et al.* 2015; Eberth 2015) and is more similar to the ~57% reported from the best known *Styracosaurus* bonebed (BB042) (Visser 1986: figure 29). However, most ribs were identified as indeterminate ornithischian, so the Lake Diefenbaker Bonebed's proportion of ceratopsids is likely underestimated. Despite being classified as ceratopsid-dominated, this bonebed has a dinosaur taxonomic diversity more comparable to that of the multigeneric BB047 than to that of the other two ceratopsid-dominated bonebeds. If these localities each contained a comparable sample of specimens identifiable at the genus or species level, a beta (between-site) diversity analysis would have been warranted to further explore their similarities in faunal composition (Tuomisto 2010; Vavrek & Larsson 2010). However, the present lack of taxonomic resolution beyond the family level would cause an artificially low beta diversity for this region of the Campanian Western Interior basin. With alpha diversity alone, little can be said about patterns in dinosaur community structure along the coastal-inland palaeoenvironmental gradient between DPP and Saskatchewan Landing Provincial Park beyond the fact that raw taxonomic richness at the family level remains stable. Nevertheless, it is clear that all three dinosaurs identified at the species level in Saskatchewan Landing are also known from the DPP assemblage. This at least confirms overlap in dinosaur faunal composition regardless of proximity to the Western Interior Seaway, which leads us to predict a low beta diversity at a regional spatial scale pending more detailed species identifications.

What remains certain is that a detailed taphonomic study of this bonebed will be crucial in order to determine the respective degrees of autochthony of its macro- and microfossils, as well as the time resolution of the combined assemblage. This will lead to more accurate estimates of local alpha diversity and relative taxon abundances, which could be of great interest considering the locality's intermediate palaeogeographical position between marine and terrestrial biomes. Multigeneric macrofossil and microfossil bonebeds have long been known to represent distinct taphonomic modes, which are each divided into categories defined by their depositional settings and preservation conditions (Eberth *et al.* 1990; Eberth & Currie 2005; Rogers & Brady 2010). The Lake Diefenbaker Bonebed is an interesting case in that it contains large samples representing both taphonomic modes, although all diversity analyses so far aggregated microfossils sampled in bulk matrix from the main bone layer itself with microfossils collected at the surface of an underlying horizon with a completely different sedimentary facies (Gilbert *et al.* 2018). Additionally, the first analysis included a *Baptornis* pelvis found *in situ*, albeit about 2 metres above the main bone layer, while the present analysis now includes the *Chasmosaurus* parietals found in an unlocated quarry in the bonebed's vicinity. This implies a certain degree of spatiotemporal averaging for the DPF community of Saskatchewan Landing Provincial Park included in these estimates, which was initially acknowledged when discussing the unusually high abundance of salamander fossils for a marginal marine setting (Gilbert *et al.* 2018). Among the macrofossils, the clear separation of a lower horizon containing almost complete and intact isolated elements from an upper horizon exclusively containing heavily eroded fragments and bone pebbles suggests different taphonomic histories for these two horizons. The former assemblage (which is the source of the locality's entire macrofossil diversity) is interpreted as an attritional mix of locally-derived and transported elements, considering the apparent lack of association between any two elements and the lack of any clear pattern in long-axis orientation. This suggests greater taphonomic similarity to the less extensive section of Jack's Birthday Site, an attritional assemblage in the Two Medicine Formation of Montana dominated by isolated (including a few complete) elements (Varricchio 1995), than to the Princess Bonebed in DPP, which is interpreted to have a more allochthonous origin given the broken state of even the most complete elements from this site (Eberth *et al.* 2015). The relatively high abundance of insect borings in several macrofossils is another important aspect of the Lake Diefenbaker Bonebed's taphonomy. This damage type is very rarely reported elsewhere in the Dinosaur Park Formation and is altogether absent from Alberta's *Centrosaurus* and *Styracosaurus* bonebeds, despite the latter being represented by higher sample sizes (Visser 1986; Ryan *et al.* 2001; Eberth & Getty 2005; Chiba *et al.* 2015; Eberth 2015). Alongside weathering traces, the insect damage suggests more frequent subaerial exposure of the Lake Diefenbaker Bonebed than of comparable Alberta localities after final aggregation of the skeletal elements. The proximity of that locality to the coast further raises the possibility that this exposure was caused by tides and not just by seasonal droughts, which is in line with the current sedimentological interpretation of its depositional environment (Gilbert *et al.* 2019) and its unusual palaeogeographical location.

Crucially, the majority of the Lake Diefenbaker Bonebed's most taxonomically informative elements are among the most complete, which implies a parautochthonous origin for them at least. These observations lead us to maintain that the best-preserved dinosaur remains reported in the present study (such as those of *Centrosaurus* and *Citipes*) are unlikely to have been transported 250 km downstream from the vicinity of DPP without incurring further damage. Therefore, they are now introduced as key components of the marginal marine late Campanian community of the DPF in

Saskatchewan Landing Provincial Park and conversely expand Saskatchewan's dinosaur fossil record. These taphonomic considerations thus increase the credibility of the relatively high dinosaur diversity estimate obtained for the Lake Diefenbaker Bonebed.

2.4.2 Contributions of the geographical and stratigraphic distribution of Centrosaurus *to understanding the palaeoecology of late Campanian Laramidia*

The bonebed presented in this study does not represent the first occurrence of *Centrosaurus apertus* for Saskatchewan, considering the previous discovery of a long recurving nasal horncore referred to that species from the Muddy Lake Bonebed near Unity (Eberth *et al.* 1990; Brown *et al.* 2014). Nonetheless, the Lake Diefenbaker Bonebed has produced a partial parietal (RSKM P3217.500) that is far more diagnostic of *C. apertus* than any nasal (see Ryan *et al.* 2001). Furthermore, it represents the first occurrence of this species in such proximity to the Western Interior Seaway, which has important implications for our understanding of its habitat preferences and of the relative age of the Dinosaur Park Formation's outcrops in Saskatchewan Landing Provincial Park.

***An updated geographical distribution for* Centrosaurus apertus**

Prior to the current study, the geographical distribution of *Centrosaurus apertus* stretched from a southern extremity in the Oldman Formation (time-equivalent to the lower DPF of DPP) of the Milk River Valley (Chiba *et al.* 2015) to the northernmost outcrops of the DPF at Muddy Lake (Eberth *et al.* 1990). The occurrence of this species in the former locality demonstrated that it had a habitat range encompassing better-drained floodplains located further inland, possibly in a more xeric palaeoenvironment. The Belly River Group exposed in Dinosaur Provincial Park has been hypothesized to be composed of at least four megaherbivore assemblage zones, of which only the lowest biozone of the DPF has produced *C. apertus* remains (Ryan & Evans 2005; Mallon *et al.* 2012; Mallon 2019; Eberth *et al.* 2023). Therefore, that species has only been found in the lower half of the formation in sediments formed in fluvial/paralic environments interpreted to have a perennially wet subtropical climate (Eberth 2005; Koppelhus 2005; Bamforth & Koppelhus 2018). The report of a bonebed dominated by *C. apertus* individuals in a marginal marine setting (albeit still within a coastal floodplain) thus further expands the habitat range of this species. In no other locality did this ceratopsid co-occur with such an abundant marine fauna, most notably hesperornithiform birds and a high diversity of sharks. The most ecologically comparable unit in Dinosaur Provincial Park is in the uppermost portions of the DPF above the Lethbridge Coal Zone: it preserves a similar vertebrate microfauna to that of the Lake Diefenbaker Bonebed but was populated by a centrosaurine species more anatomically similar to *Pachyrhinosaurus* or *Achelousaurus* (Ryan *et al.* 2010). Considering evidence from vertebrate microfossil localities that ceratopsids increased in relative abundance with increasing proximity to shore (Brinkman *et al.* 1998), the occurrence of *Centrosaurus* in such a coastal setting is actually less surprising than its occurrence in a more inland setting such as the Oldman Formation of southern Alberta. The additional occurrence of *Chasmosaurus russelli* in the coastal community represented in the Lake Diefenbaker Bonebed deserves further mention since it has only been reported from far more inland Campanian Alberta localities otherwise (Campbell *et al.* 2019). Even the Unity Bonebed was located nearer the palaeoshoreline than the DPP or South Saskatchewan River bonebeds, and yet proved more similar in depositional setting and vertebrate diversity to the former than to the Lake Diefenbaker Bonebed (Eberth *et al.* 1990). The only possibly peculiar specimen at Unity is a short, thin ceratopsid nasal horncore with a faintly sinusoidal shape never reported elsewhere in the Western Interior Basin (Eberth *et al.* 1990). However, this unique anatomy might simply represent a pathology on a *Chasmosaurus* sp. individual.

Climate change has been proposed as one of the key factors driving megaherbivorous dinosaur turnover in Late Cretaceous North America since it arguably affects plant food geographical distributions (Sampson & Loewen 2010). This constitutes an example of a turnover pulse hypothesis, where abiotic factors are the main cause of rapid faunal replacement (Vrba 1993), whether that turnover involved evolution within sedentary populations, species tracking specific habitats within the Laramidian plain, or both of these mechanisms (Mallon *et al.* 2012). A habitat tracking model is best supported in the late Campanian-Maastrichtian Horseshoe Canyon Formation of central Alberta, where closely related species, particularly hadrosaurs, were proposed to migrate in and out of the region following shifts in precipitation regimes (Eberth *et al.* 2013). Assuming that the habitat tracking hypothesis is true for every detected pattern of megaherbivore turnover during the Late Cretaceous, it could be predicted that taxa found in the upper Dinosaur Park Formation preferred coastal plain environments closer to shore, while those found in the lower DPF preferred more inland environments. Reports of *Corythosaurus casuarius* from the lower DPF near Hilda (Evans 2002), a *Styracosaurus albertensis* skeleton and a *Prosaurolophus maximus* skull occurring together less than 5 m below the Lethbridge Coal Zone (LCZ) in Sage Creek (where only the upper DPF is exposed) (Evans *et al.* 2015), and a *Lambeosaurus magnicristatus* skeleton found almost within the LCZ near Manyberries (Evans & Reisz 2007), are occasionally cited as support for the habitat tracking hypothesis since they are consistently found in the same depositional environments as their DPP conspecifics. However, these occurrences also tend to fall within the range of their DPP conspecifics, as is known because their relative stratigraphic heights can be estimated from isochronous boundary horizons of the DPF found near their respective quarries (Evans *et al.* 2015). In addition, the initial report of *Centrosaurus apertus* from the Oldman Formation of southern Alberta was already recognized by Mallon *et al*. (2012) as implying a rare case of a megaherbivore that did not appear to track any particular habitat in Late Cretaceous Laramidia. The assemblage described from Saskatchewan Landing Provincial Park now provides more evidence in support of a generalist tendency for *C. apertus*. Alongside the recent report of *Corythosaurus* in the Judith River Formation of Montana (Takasaki *et al.* 2023), it further suggests that the restricted observed palaeogeographical ranges of most dinosaurs known from DPP are likely an artifact of the limited spatial extent of presently exposed strata that were deposited under conditions favourable to fossilization. More exploration is therefore warranted in less extensive outcrops of the Belly River Group outside DPP to confirm a similar pattern in less common species.

A revised age for the Dinosaur Park Formation in southwestern Saskatchewan

The DPF of Saskatchewan Landing Provincial Park was initially thought to be temporally equivalent to the uppermost DPF of DPP based on the Lake Diefenbaker Bonebed's stratigraphic position ~20 m below the local DPF-Bearpaw Formation contact as well as the occurrences of *Accuratipollis macrosolenoides* and *Mancicorpus tripodiformis* among the palynomorph assemblage sampled within the first 10 m overlying the bonebed (Braman & Sweet 2012; Gilbert *et al.* 2018). The fact that *Chasmosaurus russelli* was the only non-avian dinosaur identified at the species level in that locality (prior to this study) did not provide further biostratigraphic constraints considering its extensive temporal range from the lower DPF to the base of the Lethbridge Coal Zone in Alberta (Campbell *et al.* 2019). However, the Saskatchewan Landing palynoflora has now been found to co-occur with *Centrosaurus apertus*, a dinosaur species that is only known elsewhere from the lower half of the DPF in DPP and along the South Saskatchewan River, as well as the time-equivalent lower DPF near Unity and uppermost Oldman Formation in southernmost Alberta (Eberth *et al.* 1990, 2010; Chiba *et al.* 2015). Evidence of temporal faunal turnover among all megaherbivores throughout the Belly River Group is mounting (Mallon *et al.* 2012; Evans *et al.* 2015; Lowi-Merri & Evans 2020), with varying degrees of stratigraphic overlap even in far less sampled clades such as Chasmosaurinae (Campbell *et al.* 2019). In DPP, Centrosaurinae is arguably the clade that exhibits the most consistent faunal turnover pattern of all, where *Styracosaurus* appears to completely replace *Centrosaurus* in the upper DPF (Brown *et al.* 2020). Therefore, it is very unlikely that *Centrosaurus* persisted in the more coastal upper DPF deposits of Saskatchewan while being locally replaced by *Styracosaurus* further inland within a continuous alluvial floodplain which lacked any evidence for a palaeogeographical barrier. Additionally, the latest palynostratigraphy of southern Alberta suggests that the co-occurrence of the palynomorphs *A. macrosolenoides* and *M. tripodiformis* at Saskatchewan Landing Provincial Park is no longer a reliable age indicator since their respective ranges are now shown to overlap the boundary between the *Cranwellia rumseyensis* – *Translucentipollis plicatilis* zone (equivalent to the lower DPF) and the *Accuratipollis configuratus* – *Mancicorpus tripodiformis* zone (equivalent to the upper DPF) (Braman 2013, 2018; Eberth *et al.* 2023). The latest geochronology of DPP therefore suggests that the stratigraphic ranges of *A. macrosolenoides* and *M. tripodiformis* slightly overlap the stratigraphic range of *C. apertus* (Eberth *et al.* 2023). Furthermore, *C. rumseyensis* and *T. plicatilis* were also reported from the Saskatchewan Landing palynomorph assemblage (Gilbert *et al.* 2018: table 1). Lastly, the ceratopsid assigned to *Centrosaurus* at the Muddy Lake Bonebed was found almost 20 m below the lowest occurrence of *M. tripodiformis*, which implies stratigraphic equivalence to the lower DPF (Eberth *et al.* 1990). Considering all this evidence, we now propose that the DPF of Saskatchewan Landing Provincial Park is also correlated to the lower DPF (rather than the upper DPF) of DPP, *contra* Gilbert *et al*. (2018). This interpretation remains fully consistent with the stratigraphic distribution of *Chasmosaurus russelli* in Alberta. Similar reasoning was followed in the first report of *Corythosaurus* from Montana (Takasaki *et al.* 2023), in which the specimen's host horizon within the Judith River Formation was proposed to be contemporaneous with the lower DPF (based on the fact that *Corythosaurus* is only known from the lower DPF in Alberta). In any case, the high sensitivity of floral assemblages to climate disturbances is well documented in recent ecosystems (Bertin 2008 and references therein; Tovar *et al.* 2022), and the distribution of Late Cretaceous floras has been shown to follow similar trends (Wolfe & Upchurch 1987; Parrish & Spicer 1988; Spicer & Herman 2010). In contrast, the original interpretation of the Saskatchewan Landing palynoflora seemed to be based on the premise that floral composition almost ubiquitously reflects time and is barely influenced by sea level or local climatic trends. Consequently, the presence of *Centrosaurus apertus* in the Lake Diefenbaker Bonebed is deemed a more reliable relative age indicator for the DPF than its palynofloral composition.

This revised age estimate is also consistent with the high stratigraphic proximity of the Lake Diefenbaker Bonebed to the local DPF-Bearpaw Formation contact. The Belly River Group's formational contacts have been essential to correlating hundreds of fossil quarries and bonebeds throughout most of the exposures of this stratigraphic unit in Alberta (Currie & Russell 2005; Eberth *et al.* 2010; Chiba *et al.* 2015; Evans *et al.* 2015). The Oldman-DPF contact is isochronous throughout DPP and as far South as the South Saskatchewan River area in Alberta (Rogers *et al.* 2023; Eberth 2024). The DPF-Bearpaw contact is isochronous throughout all southeastern Alberta, including the Milk River Valley, as it records the rapid westward Bearpaw marine transgression (Eberth & Hamblin 1993). However, the DPF-Bearpaw contact is diachronous in southwestern Saskatchewan precisely because it records minor oscillations in sea level throughout the late Campanian leading to the main transgression (Caldwell 1982; Eberth 2005; Gilbert *et al.* 2019). As a result, it should have little to no influence on estimates of the relative age of the DPF in Saskatchewan Landing Provincial Park. This diachronicity was acknowledged in the palynostratigraphic analysis (Gilbert *et al.* 2018), yet the DPF-Bearpaw contact visible at that locality was still considered to be more recent than in our revised interpretation. Instead, the discovery of *Centrosaurus apertus* in the Lake Diefenbaker Bonebed leads us to propose that the marginal marine fauna of which this species formed a part was coeval with the fauna of the lower DPF in DPP, at a time when the DPP area was still located ~250 km inland from Laramidia's eastern shore.

2.5 Conclusions

The most important discoveries arising from the excavation of the Lake Diefenbaker Bonebed were the expansion of the known geographical distributions of *Centrosaurus apertus* and of *Citipes elegans* up to the eastern coast of northern Laramidia. The identification of more non-avian dinosaurs at the species level (previously known only from Alberta) in a much more coastal palaeohabitat confirms that the overlap in nonmarine community composition along the inland-coastal gradient present in the region during the late Campanian was higher than that detected from microfossil samples alone. This raises the possibility of increased connectivity between these communities in terms of the mobility of individuals, with corollary implications for increased species interactions and energy flow throughout the breadth of the Laramidian coastal plain in the region. It follows that these additions to the Campanian dinosaur fauna of Saskatchewan reinforce the hypothesis that all roughly coeval localities of the Belly River Group, from the Lake Diefenbaker Bonebed in the East to Dinosaur Provincial Park in the West at the very least, formed a metacommunity. Furthermore, what is now the best documented occurrence of *Centrosaurus apertus* from Saskatchewan strongly suggests that the Dinosaur Park Formation outcrops exposed in Saskatchewan Landing Provincial Park are more ancient than the age previously estimated from palynostratigraphy. This age also suggests that this locality was at the boundary between the eastern range edges of the local non-avian dinosaurs and the western range edges of marine vertebrates seldom found in time-equivalent deposits of the DPF of Alberta. It is hoped that this project has successfully demonstrated how evidence from multiple localities of the DPF sampled along a moderately time averaged spatial gradient (beyond the temporal gradient observed in DPP alone) helps to complete the overview of an increasingly well-understood metacommunity that evolved on a regional scale in response to a major marine transgression.

2.6 References

BAMFORTH, E. L. 2013. Paleoecology and paleoenvironmental trends immediately prior to the end-Cretaceous extinction in the latest Maastrichtian (66Ma) Frenchman Formation, Saskatchewan, Canada.Unpublished Ph.D. Thesis, McGill University, Montreal, 405pp.

———. 2022. A new, large specimen of *Prognathodon overtoni* (Squamata, Mosasauridae) from Grasslands National Park, Saskatchewan. *10th Annual Meeting Canadian Society of Vertebrate Paleontology Abstracts*, **10**, 9–10.

——— and KOPPELHUS, E. B. 2018. New absolute paleoclimate estimates from Dinosaur Provincial Park, Alberta (Campanian, Late Cretaceous): Preliminary results based on a new fossil leaf assemblage. *6th Annual Meeting Canadian Society of Vertebrate Paleontology Abstracts*, **6**, 10–11.

BÉLAND, P. and RUSSELL, D. A. 1978. Paleoecology of Dinosaur Provincial Park (Cretaceous), Alberta, interpreted from the distribution of articulated vertebrate remains. *Canadian Journal of Earth Sciences*, **15**, 1012–1024.

BELL, P. R., CURRIE, P. J. and RUSSELL, D. A. 2015. Large caenagnathids (Dinosauria, Oviraptorosauria) from the uppermost Cretaceous of western Canada. *Cretaceous Research*, **52**, 101–107.

BERTIN, R. I. 2008. Plant Phenology And Distribution In Relation To Recent Climate Change. *The Journal of the Torrey Botanical Society*, **135**, 126–146.

BLOB, R. W. and BADGLEY, C. 2007. Numerical Methods for Bonebed Analysis. *In* ROGERS, R. R., EBERT, D. A. and FIORILLO, A. R. (eds.) *Bonebeds: Genesis, Analysis, and Paleobiological Significance*, The University of Chicago Press, Chicago and London, 333–396 pp.

BRAMAN, D. R. 2013. *Triprojectate Pollen Occurrence in the Western Canada Sedimentary Basin and the Group's Global Relationships*. Royal Tyrrell Museum of Palaeontology, Drumheller, AB.

———. 2018. Terrestrial palynostratigraphy of the Upper Cretaceous (Santonian) to lowermost Paleocene of southern Alberta, Canada. *Palynology*, **42**, 102–147.

——— and SWEET, A. R. 2012. Biostratigraphically useful Late Cretaceous–Paleocene Terrestrial palynomorphs from the Canadian Western Interior Sedimentary Basin. *Palynology*, **36**, 8–35.

BRINKMAN, D. B. 1990. Paleoecology of the Judith River Formation (Campanian) of Dinosaur Provincial Park, Alberta, Canada: Evidence from vertebrate microfossil localities. *Palaeogeography, Palaeoclimatology, Palaeoecology*, **78**, 37–54.

———, RYAN, M. J. and EBERTH, D. A. 1998. The paleogeographic and stratigraphic distribution of ceratopsids (Ornithischia) in the upper Judith River Group of Western Canada. *PALAIOS*, **13**, 160–169.

———, RUSSELL, A. P., EBERTH, D. A. and PENG, J. 2004. Vertebrate palaeocommunities of the lower Judith River Group (Campanian) of southeastern Alberta, Canada, as interpreted from vertebrate microfossil assemblages. *Palaeogeography, Palaeoclimatology, Palaeoecology*, **213**, 295–313.

———, BRAMAN, D. R., NEUMAN, A. G., RALRICK, P. E. and SATO, T. 2005. A Vertebrate Assemblage from the Marine Shales of the Lethbridge Coal Zone. *In* CURRIE, P. J. and KOPPELHUS, E. B. (eds.) *Dinosaur Provincial Park: A Spectacular Ancient Ecosystem Revealed*, Indiana University Press, Bloomington, 486–500 pp.

BROWN, C. M., RUSSELL, A. P. and RYAN, M. J. 2009. Pattern and transition of surficial bone texture of the centrosaurine frill and their ontogenetic and taxonomic implications. *Journal of Vertebrate Paleontology*, **29**, 132–141.

———, RYAN, M. J. and EVANS, D. C. 2014. A census of Canadian dinosaurs: more than a century of discovery. *In* BININDA-EMONDS, O. R. P., POWELL, G. L., JAMNICZKY, H. A., BAUER, A. M. and THEODOR, J. (eds.) *All Animals Are Interesting; A Festschrift in Honour of Anthony P. Russell*, BIS-Verlag der Carl von Ossietzky Universität Oldenburg, Oldenburg, 151–208 pp.

———, HOLMES, R. and CURRIE, P. 2020. A subadult individual of *Styracosaurus albertensis* (Ornithischia: Ceratopsidae) with comments on ontogeny and intraspecific variation in Styracosaurus and Centrosaurus. *Vertebrate Anatomy Morphology Palaeontology*, **8**, 67–95.

———, EVANS, D. C., CAMPIONE, N. E., O'BRIEN, L. J. and EBERTH, D. A. 2013. Evidence for taphonomic size bias in the Dinosaur Park Formation (Campanian, Alberta), a model Mesozoic terrestrial alluvial-paralic system. *Palaeogeography, Palaeoclimatology, Palaeoecology*, **372**, 108–122.

CALDWELL, W. G. E. 1982. The Cretaceous System in the Williston Basin - a modern appraisal. *In* CHRISTOPHER, J. E. and KALDI, J. (eds.) *Fourth International Williston Basin Symposium*, Saskatchewan Geological Survey, Special Publication no 6, 295–312 pp.

CAMPBELL, J. A., RYAN, M. J., SCHRÖDER-ADAMS, C. J., EVANS, D. C. and HOLMES, R. B. 2018. New insights into chasmosaurine (Dinosauria: Ceratopsidae) skulls from the Upper Cretaceous (Campanian) of Alberta, and an update on the distribution of accessory frill fenestrae in Chasmosaurinae. *PeerJ*, **6**, e5194.

———, ———, ———, HOLMES, R. B. and EVANS, D. C. 2019. Temporal range extension and evolution of the chasmosaurine ceratopsid *'Vagaceratops' irvinensis* (Dinosauria: Ornithischia) in the Upper Cretaceous (Campanian) Dinosaur Park Formation of Alberta. *Vertebrate Anatomy Morphology Palaeontology*, **7**, 83–100.

CAMPIONE, N. E. and HOLMES, R. 2006. The anatomy and homologies of the ceratopsid syncervical. *Journal of Vertebrate Paleontology*, **26**, 1014–1017.

CHAO, A. and LEE, S.-M. 1992. Estimating the Number of Classes via Sample Coverage. *Journal of the American Statistical Association*, **87**, 210–217.

CHIBA, K., RYAN, M. J., BRAMAN, D. R., EBERTH, D. A., SCOTT, E. E., BROWN, C. M., KOBAYASHI, Y. and EVANS, D. C. 2015. Taphonomy of a monodominant *Centrosaurus* *apertus* (Dinosauria: Ceratopsia) bonebed from the Upper Oldman Formation of Southeastern Alberta. *PALAIOS*, **30**, 655–667.

CIGNONI, P., CALLIERI, M., CORSINI, M., DELLEPIANE, M., GANOVELLI, F. and RANZUGLIA, G. 2008. MeshLab: an Open-Source Mesh Processing Tool. 1–8.

COLWELL, R. K. and CODDINGTON, J. A. 1994. Estimating terrestrial biodiversity through extrapolation. *Philosophical Transactions of the Royal Society of London. Series B: Biological Sciences*, **345**, 101–118.

CULLEN, T. M. and EVANS, D. C. 2016. Palaeoenvironmental drivers of vertebrate community composition in the Belly River Group (Campanian) of Alberta, Canada, with implications for dinosaur biogeography. *BMC Ecology*, **16**, 52.

———, ZANNO, L., LARSON, D. W., TODD, E., CURRIE, P. J. and EVANS, D. C. 2021. Anatomical, morphometric, and stratigraphic analyses of theropod biodiversity in the Upper Cretaceous (Campanian) Dinosaur Park Formation. *Canadian Journal of Earth Sciences*, **58**, 870–884.

CURRIE, P. J. and RUSSELL, D. A. 1988. Osteology and relationships of *Chirostenotes pergracilis* (Saurischia, Theropoda) from the Judith River (Oldman) Formation of Alberta, Canada. *Canadian Journal of Earth Sciences*, **25**, 972–986.

——— and KOPPELHUS, E. B. 2005. *Dinosaur Provincial Park: A Spectacular Ancient Ecosystem Revealed*. Bloomington & Indianapolis.

——— and RUSSELL, D. A. 2005. The Geographic and Stratigraphic Distribution of Articulated and Associated Dinosaur Remains. *In* CURRIE, P. J. and KOPPELHUS, E. B. (eds.) *Dinosaur Provincial Park: A Spectacular Ancient Ecosystem Revealed*, Indiana University Press, Bloomington, 537–569 pp.

DAWSON, F. M., EVANS, C. G., MARSH, R. and RICHARDSON, R. 1994. Uppermost Cretaceous and Tertiary strata of the Western Canada sedimentary basin. *In* MOSSOP, G. and SHETSEN, I.

(eds.) *Geological Atlas of the Western Canada Sedimentary Basin*, Canadian Society of Petroleum Geologists and the Alberta Research Council, Edmonton, 387–407 pp.

DODSON, P. and CURRIE, P. J. 1988. The smallest ceratopsid skull–Judith River Formation of Alberta. *Canadian Journal of Earth Sciences*, **25**, 926–930.

DODSON, P., FORSTER, C. A. and SAMPSON, S. D. 2004. Ceratopsidae. *In* DODSON, P., WEISHAMPEL, D. B. and OSMÓLSKA, H. (eds.) *The Dinosauria*, University of California Press, Berkeley & Los Angeles, 494–513 pp.

EBERTH, D. A. 2005. The Geology. *In* CURRIE, P. J. and KOPPELHUS, E. B. (eds.) *Dinosaur Provincial Park: A Spectacular Ancient Ecosystem Revealed*, Indiana University Press, Bloomington, 54–82 pp.

———. 2015. Origins of dinosaur bonebeds in the Cretaceous of Alberta, Canada. *Canadian Journal of Earth Sciences*, **52**, 655–681.

———. 2024. Stratigraphic architecture of the Belly River Group (Campanian, Cretaceous) in the plains of southern Alberta: Revisions and updates to an existing model and implications for correlating dinosaur-rich strata. *PLOS ONE*, **19**, e0292318.

——— and HAMBLIN, A. P. 1993. Tectonic, stratigraphic, and sedimentologic significance of a regional discontinuity in the upper Judith River Group (Belly River wedge) of southern Alberta, Saskatchewan, and northern Montana. *Canadian Journal of Earth Sciences*, **30**, 174–200.

——— and BRINKMAN, D. B. 1997. Paleoecology of an Estuarine, Incised-Valley Fill in the Dinosaur Park Formation (Judith River Group, Upper Cretaceous) of Southern Alberta, Canada. *PALAIOS*, **12**, 43–58.

EBERTH, D. A. and GETTY, M. A. 2005. Ceratopsian Bonebeds: Occurrence, Origins, and Significance. *In* CURRIE, P. J. and KOPPELHUS, E. B. (eds.) *Dinosaur Provincial Park: A Spectacular Ancient Ecosystem Revealed*, Indiana University Press, Bloomington, 501–536 pp.

EBERTH, D. A. and CURRIE, P. J. 2005. Vertebrate Taphonomy and Taphonomic Modes. *In* CURRIE, P. J. and KOPPELHUS, E. B. (eds.) *Dinosaur Provincial Park: A Spectacular Ancient Ecosystem Revealed*, Indiana University Press, Bloomington, 453–477 pp.

———, BRAMAN, D. R. and TOKARYK, T. T. 1990. Stratigraphy, sedimentology and vertebrate paleontology of the Judith River Formation (Campanian) near Muddy Lake, west-central Saskatchewan. *Bulletin of Canadian Petroleum Geology*, **38**, 387–406.

———, BRINKMAN, D. B. and BARKAS, V. 2010. A Centrosaurine Mega-Bonebed from the Upper Cretaceous of Southern Alberta: Implications for Behavior and Death Events. *In* RYAN, M. J., CHINNERY-ALLGEIER, B. J. and EBERTH, D. A. (eds.) *New Perspectives on Horned Dinosaurs*, Indiana University Press, Bloomington & Indianapolis, 495–508 pp.

———, EVANS, D. C. and LLOYD, D. W. H. 2015. Occurrence and Taphonomy of the First Documented Hadrosaurid Bonebed from the Dinosaur Park Formation (Belly River Group, Campanian) at Dinosaur Provincial Park, Alberta, Canada. *In* EBERTH, D. A. and EVANS, D. C. (eds.) *Hadrosaurs*, Indiana University Press, Bloomington, 502–523 pp.

———, ———, BRINKMAN, D. B., THERRIEN, F., TANKE, D. H. and RUSSELL, L. S. 2013. Dinosaur biostratigraphy of the Edmonton Group (Upper Cretaceous), Alberta, Canada: evidence for climate influence. *Canadian Journal of Earth Sciences*, **50**, 701–726.

EBERTH, D. A., EVANS, D. C., RAMEZANI, J., KAMO, S. L., BROWN, C. M., CURRIE, P. J. and BRAMAN, D. R. 2023. Calibrating geologic strata, dinosaurs, and other fossils at Dinosaur Provincial Park (Alberta, Canada) using a new CA-ID-TIMS U–Pb geochronology. *Canadian Journal of Earth Sciences*, **60**, 1627–1646.

EVANS, D. C. 2002. A juvenile *Corythosaurus* skull (Ornithischia: Hadrosauridae) from the Dinosaur Park Formation, southeastern Alberta. *Canadian Paleontology Conference Proceedings and Abstracts*, **12**, 11–14.

——— and REISZ, R. R. 2007. Anatomy and Relationships of *Lambeosaurus magnicristatus*, a crested hadrosaurid dinosaur (Ornithischia) from the Dinosaur Park Formation, Alberta. *Journal of Vertebrate Paleontology*, **27**, 373–393.

———, MCGARRITY, C. T. and RYAN, M. J. 2015. A Skull of *Prosaurolophus maximus* from Southeastern Alberta and the Spatiotemporal Distribution of Faunal Zones in the Dinosaur Park Formation. *In* EBERTH, D. A. and EVANS, D. C. (eds.) *Hadrosaurs*, Indiana University Press, Bloomington, 200–207 pp.

FOX, R. C. 2005. Late Cretaceous Mammals. *In* CURRIE, P. J. and KOPPELHUS, E. B. (eds.) *Dinosaur Provincial Park: A Spectacular Ancient Ecosystem Revealed*, Indiana University Press, Bloomington, 417–449 pp.

FREDERICKSON, J. A. and TUMARKIN-DERATZIAN, A. R. 2014. Craniofacial ontogeny in *Centrosaurus apertus*. *PeerJ*, **2**, e252.

FUNSTON, G. F. 2020. Caenagnathids of the Dinosaur Park Formation (Campanian) of Alberta, Canada: anatomy, osteohistology, taxonomy, and evolution. *Vertebrate Anatomy Morphology Palaeontology*, **8**, 105–153.

———, CURRIE, P. J. and BURNS, M. E. 2016. New Elmisaurine Specimens from North America and Their Relationship to the Mongolian *Elmisaurus rarus*. *Acta Palaeontologica Polonica*, **61**, 159–173.

———, PERSONS, W. S., BRADLEY, G. J. and CURRIE, P. J. 2015. New material of the large-bodied caenagnathid *Caenagnathus collinsi* from the Dinosaur Park Formation of Alberta, Canada. *Cretaceous Research*, **54**, 179–187.

GAO, K.-Q. and FOX, R. C. 1996. Taxonomy and evolution of Late Cretaceous lizards (Reptilia: Squamata) from Western Canada. *Bulletin of Carnegie Museum of Natural History*, **33**, 1–107.

GILBERT, M. M., BUATOIS, L. A. and RENAUT, R. W. 2019. Ichnology and depositional environments of the Upper Cretaceous Dinosaur Park – Bearpaw formation transition in the

Cypress Hills region of Southwestern Saskatchewan, Canada. *Cretaceous Research*, **98**, 189–210.

———, BAMFORTH, E. L., BUATOIS, L. A. and RENAUT, R. W. 2018. Paleoecology and sedimentology of a vertebrate microfossil assemblage from the easternmost Dinosaur Park Formation (Late Cretaceous, Upper Campanian,) Saskatchewan, Canada: Reconstructing diversity in a coastal ecosystem. *Palaeogeography, Palaeoclimatology, Palaeoecology*, **495**, 227–244.

GOOGLE EARTH PRO, V. 7.3.6.9345 (64-BIT). 2022. Saskatchewan Landing Provincial Park. Coordinates 12 U 704928 m E, 5618707 m N. Eye alt. 30 km.

HAMMER, Ø. and HARPER, D. A. T. 2006. *Paleontological Data Analysis*. Blackwell Publishing, Oxford.

HAQ, B. U. 2014. Cretaceous eustasy revisited. *Global and Planetary Change*, **113**, 44–58.

HASIOTIS, S. T., FIORILLO, A. R. and HANNA, R. R. 1999. Preliminary report on borings in Jurassic dinosaur bones: evidence for invertebrate-vertebrate interactions. *In* GILLETTE, D. D. (ed.) *Vertebrate Paleontology in Utah*, Miscellaneous publication 99-1. Utah Geological Survey, 193–200 pp.

HOLMES, R. B. and RYAN, M. J. 2013. The postcranial skeleton of *Styracosaurus albertensis*. *Kirtlandia*, **58**, 5–37.

HOLTZ, T. R. 1995. The arctometatarsalian pes, an unusual structure of the metatarsus of Cretaceous Theropoda (Dinosauria: Saurischia). *Journal of Vertebrate Paleontology*, **14**, 480–519.

HORNER, J. R., WEISHAMPEL, D. B. and FORSTER, C. A. 2004. Hadrosauridae. *In* DODSON, P., WEISHAMPEL, D. B. and OSMÓLSKA, H. (eds.) *The Dinosauria*, University of California Press, Berkeley & Los Angeles, 438–463 pp.

HORTAL, J., BORGES, P. a. V. and GASPAR, C. 2006. Evaluating the performance of species richness estimators: sensitivity to sample grain size. *Journal of Animal Ecology*, **75**, 274–287.

JIMÉNEZ-HUIDOBRO, P., CALDWELL, M. W., PAPARELLA, I. and BULLARD, T. S. 2019. A new species of tylosaurine mosasaur from the upper Campanian Bearpaw Formation of Saskatchewan, Canada. *Journal of Systematic Palaeontology*, **17**, 849–864.

KOPPELHUS, E. B. 2005. Paleobotany. *In* CURRIE, P. J. and KOPPELHUS, E. B. (eds.) *Dinosaur Provincial Park: A Spectacular Ancient Ecosystem Revealed*, Indiana University Press, Bloomington, 131–138 pp.

LAMBE, L. M. 1904. On the squamoso-parietal crest of the horned dinosaurs *Centrosaurus apertus* and *Monoclonius canadensis* from the Cretaceous of Alberta. *Transactions of the Royal Society of Canada*, **2 (Sec. 4)**, 3–12.

———. 1910. Note on the parietal crest of *Centrosaurus apertus* and a proposed new generic name for *Stereocephalus tutus*. *Ottawa Naturalist*, **24**, 149–151.

———. 1917. *The Cretaceous Theropodous Dinosaur* Gorgosaurus. Geological Survey of Canada, Ottawa.

LEIBOLD, M. A., HOLYOAK, M., MOUQUET, N., AMARASEKARE, P., CHASE, J. M., HOOPES, M. F., HOLT, R. D., SHURIN, J. B., LAW, R., TILMAN, D., LOREAU, M. and GONZALEZ, A. 2004. The metacommunity concept: a framework for multi-scale community ecology. *Ecology Letters*, **7**, 601–613.

LONGRICH, N. R. 2010. *Mojoceratops perifania*, a new chasmosaurine ceratopsid from the Late Campanian of Western North America. *Journal of Paleontology*, **84**, 681–694.

LOWI-MERRI, T. M. and EVANS, D. C. 2020. Cranial variation in *Gryposaurus* and biostratigraphy of hadrosaurines (Ornithischia: Hadrosauridae) from the Dinosaur Park Formation of Alberta, Canada. *Canadian Journal of Earth Sciences*, **57**, 765–779.

LULL, R. S. 1933. A revision of the Ceratopsia or horned dinosaurs. *Memoirs of the Peabody Museum of Natural History*, **3**, 1–175.

MALLON, J. C. 2019. Competition structured a Late Cretaceous megaherbivorous dinosaur assemblage. *Scientific Reports*, **9**, 15447.

———, HOLMES, R. B. and RUFOLO, S. J. 2023. Development and homology of the medial parietal ornamentation in centrosaurine ceratopsids (Dinosauria, Ornithischia). *Journal of Vertebrate Paleontology*, **42**, e2211637.

———, EVANS, D. C., RYAN, M. J. and ANDERSON, J. S. 2012. Megaherbivorous dinosaur turnover in the Dinosaur Park Formation (upper Campanian) of Alberta, Canada. *Palaeogeography, Palaeoclimatology, Palaeoecology*, **350–352**, 124–138.

MUCCI, S., DEMERS-POTVIN, A. and LARSSON, H. C. E. 2022. An undescribed DPF outcrop in west-central Saskatchewan reveals the paleocoastline of the Western Interior Seaway. *10th Annual Meeting Canadian Society of Vertebrate Paleontology Abstracts*, **10**, 36–37.

OSBORN, H. F. 1917. Skeletal adaptations of *Ornitholestes*, *Struthiomimus*, *Tyrannosaurus*. *Bulletin of the AMNH*, **35**, 733–771, pl. XXIV–XXVII.

PARRISH, J. T. and SPICER, R. A. 1988. Late Cretaceous terrestrial vegetation: A near-polar temperature curve. *Geology*, **16**, 22–25.

R CORE TEAM. 2023. *R: A language and environment for statistical computing*. R Foundation for Statistical Computing, Vienna, Austria. Downloaded from URL https://www.R-project.org/ .

RAMEZANI, J., BEVERIDGE, T. L., ROGERS, R. R., EBERTH, D. A. and ROBERTS, E. M. 2022. Calibrating the zenith of dinosaur diversity in the Campanian of the Western Interior Basin by CA-ID-TIMS U–Pb geochronology. *Scientific Reports*, **12**, 16026.

RAY, D. C., VAN BUCHEM, F. S. P., BAINES, G., DAVIES, A., GRÉSELLE, B., SIMMONS, M. D. and ROBSON, C. 2019. The magnitude and cause of short-term eustatic Cretaceous sea-level change: A synthesis. *Earth-Science Reviews*, **197**, 102901.

VAN DER REEST, A. J. and CURRIE, P. J. 2017. Troodontids (Theropoda) from the Dinosaur Park Formation, Alberta, with a description of a unique new taxon: implications for deinonychosaur diversity in North America. *Canadian Journal of Earth Sciences*, **54**, 919–935.

ROGERS, R. R. 1992. Non-marine borings in dinosaur bones from the Upper Cretaceous Two Medicine Formation, northwestern Montana. *Journal of Vertebrate Paleontology*, **12**, 528–531.

——— and BRADY, M. E. 2010. Origins of microfossil bonebeds: insights from the Upper Cretaceous Judith River Formation of north-central Montana. *Paleobiology*, **36**, 80–112.

———, EBERTH, D. A. and RAMEZANI, J. 2023. The "Judith River−Belly River problem" revisited (Montana-Alberta-Saskatchewan): New perspectives on the correlation of Campanian dinosaur-bearing strata based on a revised stratigraphic model updated with CA-ID-TIMS U-Pb geochronology. *GSA Bulletin*.

RUSSELL, L. S. 1966. Dinosaur hunting in Western Canada. *Royal Ontario Museum Life Sciences Contributions*, **70**, 1–37.

ROYAL TYRRELL COLLECTIONS. 2024. *TMP1996.012.0433*. https://rtmp.emuseum.com/search/TMP1996.012.0433

RYAN, M. J. and EVANS, D. C. 2005. Ornithischian Dinosaurs. *In* CURRIE, P. J. and KOPPELHUS, E. B. (eds.) *Dinosaur Provincial Park: A Spectacular Ancient Ecosystem Revealed*, Indiana University Press, Bloomington, 312–348 pp.

RYAN, M. J., RUSSELL, A. P., EBERTH, D. A. and CURRIE, P. J. 2001. The Taphonomy of a *Centrosaurus* (Ornithischia: Ceratopsidae) Bone Bed from the Dinosaur Park Formation (Upper Campanian), Alberta, Canada, with Comments on Cranial Ontogeny. *Palaios*, **16**, 482–506.

———, EBERTH, D. A., BRINKMAN, D. B., CURRIE, P. J. and TANKE, D. H. 2010. A New *Pachyrhinosaurus*-Like Ceratopsid from the Upper Dinosaur Park Formation (Late Campanian) of Southern Alberta, Canada. *In* RYAN, M. J., EBERTH, D. A., CHINNERY-ALLGEIER, B. J.

and RALRICK, P. E. (eds.) *New Perspectives on Horned Dinosaurs: The Royal Tyrrell Museum Ceratopsian Symposium*, Indiana University Press, Bloomington, 141–155 pp.

SAMPSON, S. D. and LOEWEN, M. A. 2010. Unraveling a Radiation: A Review of the Diversity, Stratigraphic Distribution, Biogeography, and Evolution of Horned Dinosaurs (Ornithischia: Ceratopsidae). *In* RYAN, M. J., CHINNERY-ALLGEIER, B. J. and EBERTH, D. A. (eds.) *New Perspectives on Horned Dinosaurs*, Indiana University Press, Bloomington & Indianapolis, 405–427 pp.

———, RYAN, M. J. and TANKE, D. H. 1997. Craniofacial ontogeny in centrosaurine dinosaurs (Ornithischia: Ceratopsidae): taxonomic and behavioral implications. *Zoological Journal of the Linnean Society*, **121**, 293–337.

SATO, T. 2003. *Terminonatator ponteixensis*, a new elasmosaur (Reptilia; Sauropterygia) from the Upper Cretaceous of Saskatchewan. *Journal of Vertebrate Paleontology*, **23**, 89–103.

———. 2005. A new polycotylid plesiosaur (Reptilia: Sauropterygia) from the Upper Cretaceous Bearpaw Formation in Saskatchewan, Canada. *Journal of Paleontology*, **79**, 969–980.

SMITH, E. P. and VAN BELLE, G. 1984. Nonparametric Estimation of Species Richness. *Biometrics*, **40**, 119–129.

SPICER, R. A. and HERMAN, A. B. 2010. The Late Cretaceous environment of the Arctic: A quantitative reassessment based on plant fossils. *Palaeogeography, Palaeoclimatology, Palaeoecology*, **295**, 423–442.

STERNBERG, C. M. 1940. Ceratopsidae from Alberta. *Journal of Paleontology*, **14**, 468–480.

STREET, H. P., BAMFORTH, E. L. and GILBERT, M. M. 2019. The Formation of a Marine Bonebed at the Upper Cretaceous Dinosaur Park - Bearpaw Transition of West - Central Saskatchewan, Canada. *Frontiers in Earth Science*, **7**, 1–15.

TAKASAKI, R., CHIBA, K., FIORILLO, A. R., BRINK, K. S., EVANS, D. C., FANTI, F., SANEYOSHI, M., MALTESE, A. and ISHIGAKI, S. 2023. Description of the first definitive

Corythosaurus (Dinosauria, Hadrosauridae) specimens from the Judith River Formation in Montana, USA and their paleobiogeographical significance. *The Anatomical Record*, **306**, 1918–1938.

THOMAS, R. G., SMITH, D. G., WOOD, J. M., VISSER, J., CALVERLEY-RANGE, E. A. and KOSTER, E. H. 1987. Inclined heterolithic stratification—Terminology, description, interpretation and significance. *Sedimentary Geology*, **53**, 123–179.

TOKARYK, T. T. and HARINGTON, C. R. 1992. *Baptornis* sp. (Aves: Hesperornithiformes) from the Judith River Formation (Campanian) of Saskatchewan, Canada. *Journal of Paleontology*, **66**, 1010–1012.

TOVAR, C., CARRIL, A. F., GUTIÉRREZ, A. G., AHRENDS, A., FITA, L., ZANINELLI, P., FLOMBAUM, P., ABARZÚA, A. M., ALARCÓN, D., ASCHERO, V., BÁEZ, S., BARROS, A., CARILLA, J., FERRERO, M. E., FLANTUA, S. G. A., GONZÁLES, P., MENÉNDEZ, C. G., PÉREZ-ESCOBAR, O. A., PAUCHARD, A., RUSCICA, R. C., SÄRKINEN, T., SÖRENSSON, A. A., SRUR, A., VILLALBA, R. and HOLLINGSWORTH, P. M. 2022. Understanding climate change impacts on biome and plant distributions in the Andes: Challenges and opportunities. *Journal of Biogeography*, **49**, 1420–1442.

TUMARKIN-DERATZIAN, A. R. 1997. Sedimentology, Taphonomy, and Faunal Review of a Multigeneric Bonebed (Bonebed 47) in the Dinosaur Park Formation (Campanian) of Southern Alberta, Canada.Unpublished B.Sc. Thesis, Lafayette College, Easton, PA, 107pp.

TUOMISTO, H. 2010. A diversity of beta diversities: straightening up a concept gone awry. Part 1. Defining beta diversity as a function of alpha and gamma diversity. *Ecography*, **33**, 2–22.

VARRICCHIO, D. J. 1995. Taphonomy of Jack's Birthday Site, a diverse dinosaur bonebed from the Upper Cretaceous Two Medicine Formation of Montana. *Palaeogeography, Palaeoclimatology, Palaeoecology*, **114**, 297–323.

———. 2001. Late Cretaceous Oviraptorosaur (Theropoda) Dinosaurs from Montana. *In* TANKE, D. H. and CARPENTER, K. (eds.) *Mesozoic Vertebrate Life*, Indiana University Press, Bloomington, 42–57 pp.

VAVREK, M. J. 2010. Palaeomacroecology: Large Scale Patterns in Species Diversity Through the Fossil Record.Unpublished Ph.D. Thesis, McGill University, Montreal, 222pp.

———. 2011. *fossil*: Palaeoecological and palaeogeographical analysis tools. *Palaeontologia Electronica*, **14**, 1–16.

——— and LARSSON, H. C. E. 2010. Low beta diversity of Maastrichtian dinosaurs of North America. *Proceedings of the National Academy of Sciences of the United States of America*, **107**, 8265–8268.

VISSER, J. 1986. Sedimentology and taphonomy of a *Styracosaurus* bonebed in the Late Cretaceous Judith River Formation, Dinosaur Provincial Park, Alberta.Unpublished M.Sc. Thesis, University of Calgary, Calgary, 150pp.

VRBA, E. S. 1993. Turnover pulses, the Red Queen, and related topics. *American Journal of Science*, **293-A**, 418–452.

WHEELER, J. O., HOFFMAN, P. F., CARD, K. D., DAVIDSON, A., SANFORD, B. V., OKULITCH, A. V. and ROEST, W. R. 1996. Geological map of Canada / Carte géologique du Canada.

WILSON, M. C. and CURRIE, P. J. 1985. *Stenonychosaurus inequalis* (Saurischia: Theropoda) from the Judith River (Oldman) Formation of Alberta: new findings on metatarsal structure. *Canadian Journal of Earth Sciences*, **22**, 1813–1817.

WOLFE, J. A. and UPCHURCH, G. R. 1987. North American nonmarine climates and vegetation during the Late Cretaceous. *Palaeogeography, Palaeoclimatology, Palaeoecology*, **61**, 33–77.

2.7 Figures

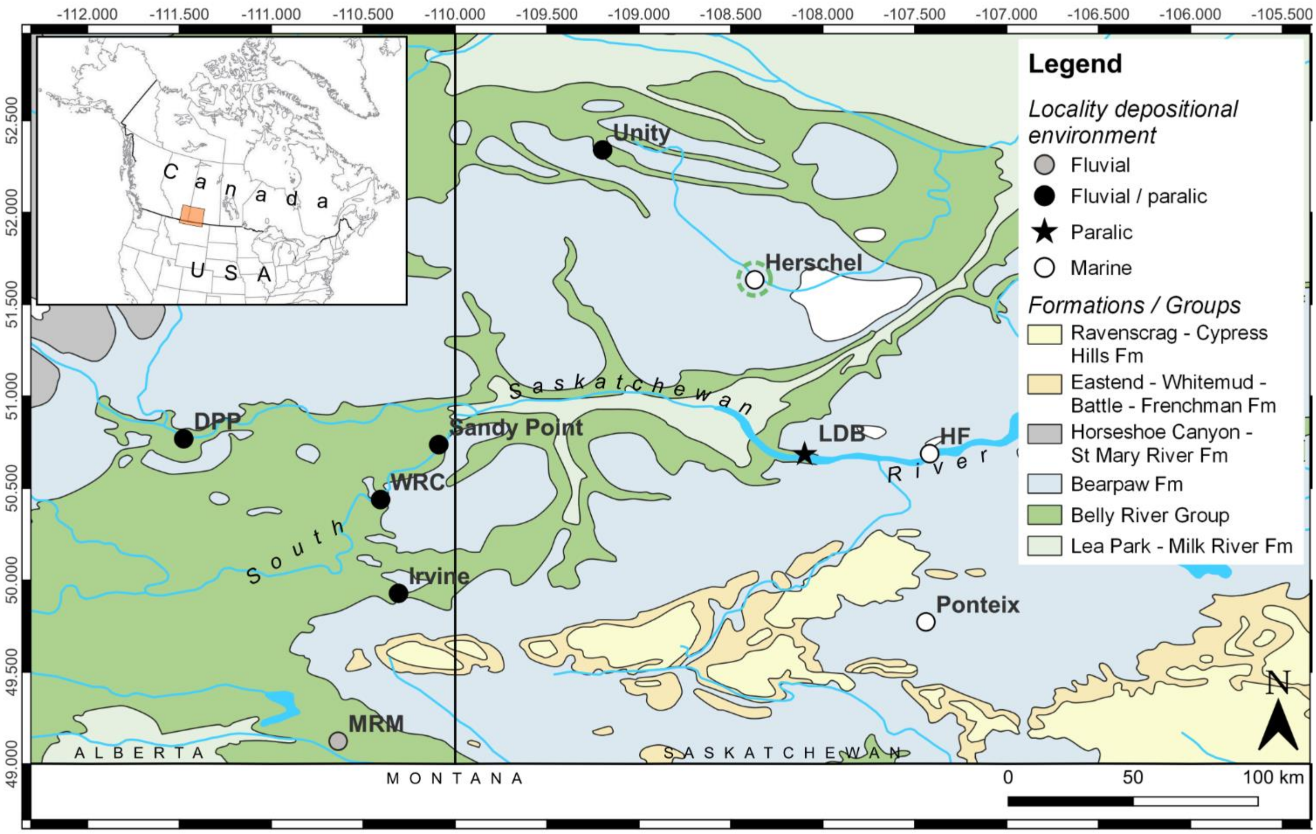

Figure 2.1. Significant late Campanian fossil localities of southwestern Saskatchewan and southeastern Alberta mapped against surficial geology (inset from map of North America, top left corner). **Abbreviations: DPP,** Dinosaur Provincial Park (Oldman, Dinosaur Park and Bearpaw formations); **HF**, Herbert Ferry, location of a tylosaurine mosasaur (Bearpaw Fm); **LDB,** Lake Diefenbaker Bonebed (DPF); **MRM,** Milk River-Manyberries area (Oldman Fm); **WRC**, White Rock Coulee (DPF). Dotted circle indicates limited Dinosaur Park Fm exposure near Herschel. Grid coordinates in WGS84 decimal degrees. Formation boundaries modified from Dawson *et al*. (1994) and Wheeler *et al*. (1996).

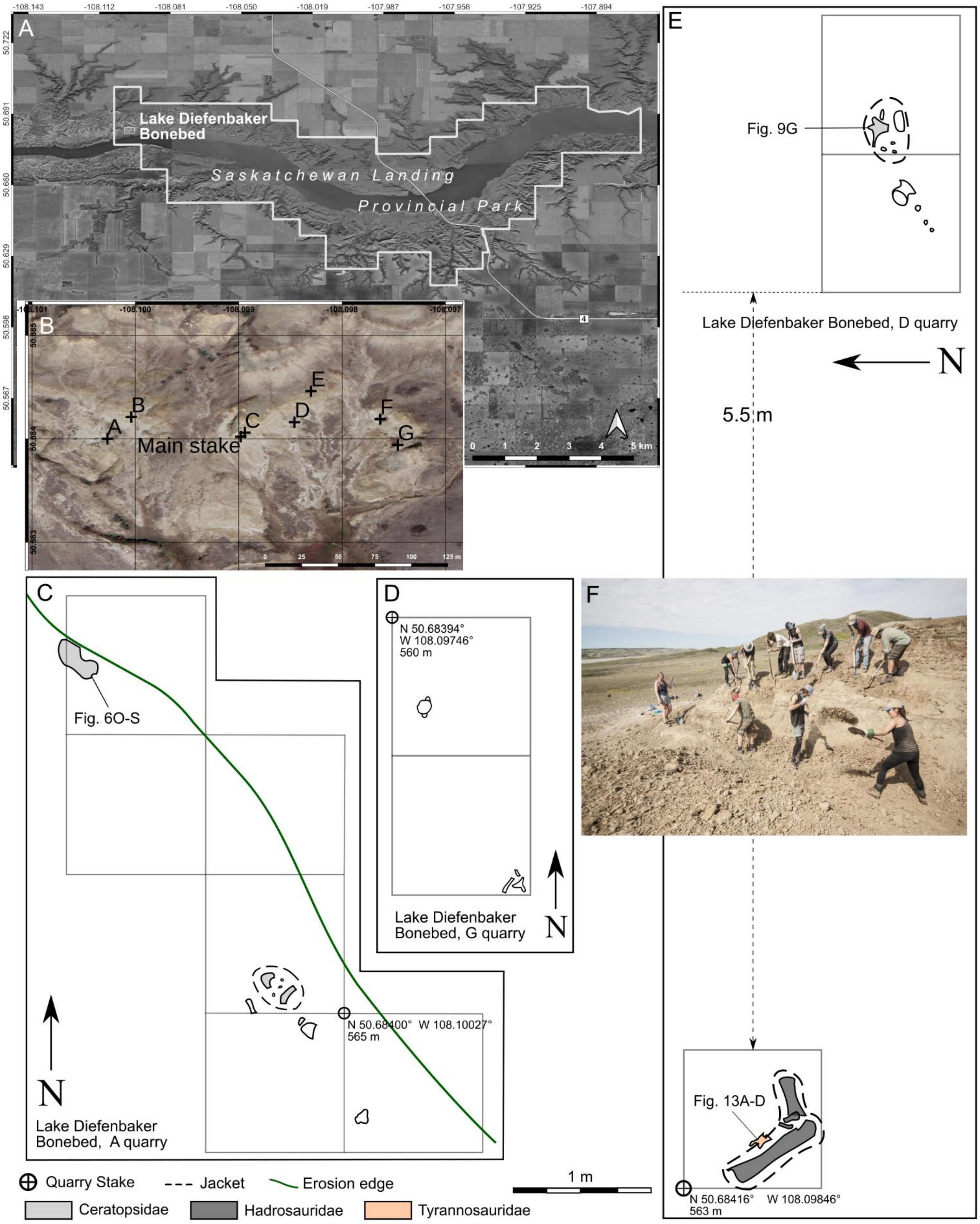
A
-108.143
-108.112
-108.081
-108.050
-108.019
-107.987
-107.956
-107.925
-107.894
50.722
50.691
50.660
50.629
50.598
50.567
Lake Diefenbaker Bonebed
Saskatchewan Landing Provincial Park
4
0 1 2 3 4 5 km
B
-108.101
-108.100
-108.099
-108.098
-108.097
50.685
50.684
50.683
A
B
C
D
E
F
G
Main stake
0 25 50 75 100 125 m
C
Fig. 6O-S
N 50.68400° W 108.10027°
565 m
N
Lake Diefenbaker Bonebed, A quarry
D
N 50.68394°
W 108.09746°
560 m
N
Lake Diefenbaker Bonebed, G quarry
E
Fig. 9G
Lake Diefenbaker Bonebed, D quarry
N
5.5 m
Fig. 13A-D
N 50.68416° W 108.09846°
563 m
F
Quarry Stake
Jacket
Erosion edge
1 m
Ceratopsidae
Hadrosauridae
Tyrannosauridae

Figure 2.2. Geographical setting of Lake Diefenbaker Bonebed (LDB) alongside small quarry maps. A, location of LDB within Saskatchewan Landing Provincial Park. B, inset of A focused on LDB, with location of each quarry stake for 2012-2018 excavations, with main stake planted near Quarry C. C-E, maps of the smaller quarries within the bonebed, all excavated in 2012. C, map of Quarry A. D, map of Quarry G. E, map of Quarry D. F, the 2017 McGill Vertebrate Palaeontology Field Course crew removing overburden along the erosional edge of Quarry C (photograph courtesy of K. Dumas, used with permission). Labels indicate figured fossil specimens. All quarry maps to scale, all coordinates in WGS84 decimal degrees. Aerial images extracted from Google Earth (Google Earth Pro, v. 7.3.6.9345 (64-bit), 2022).

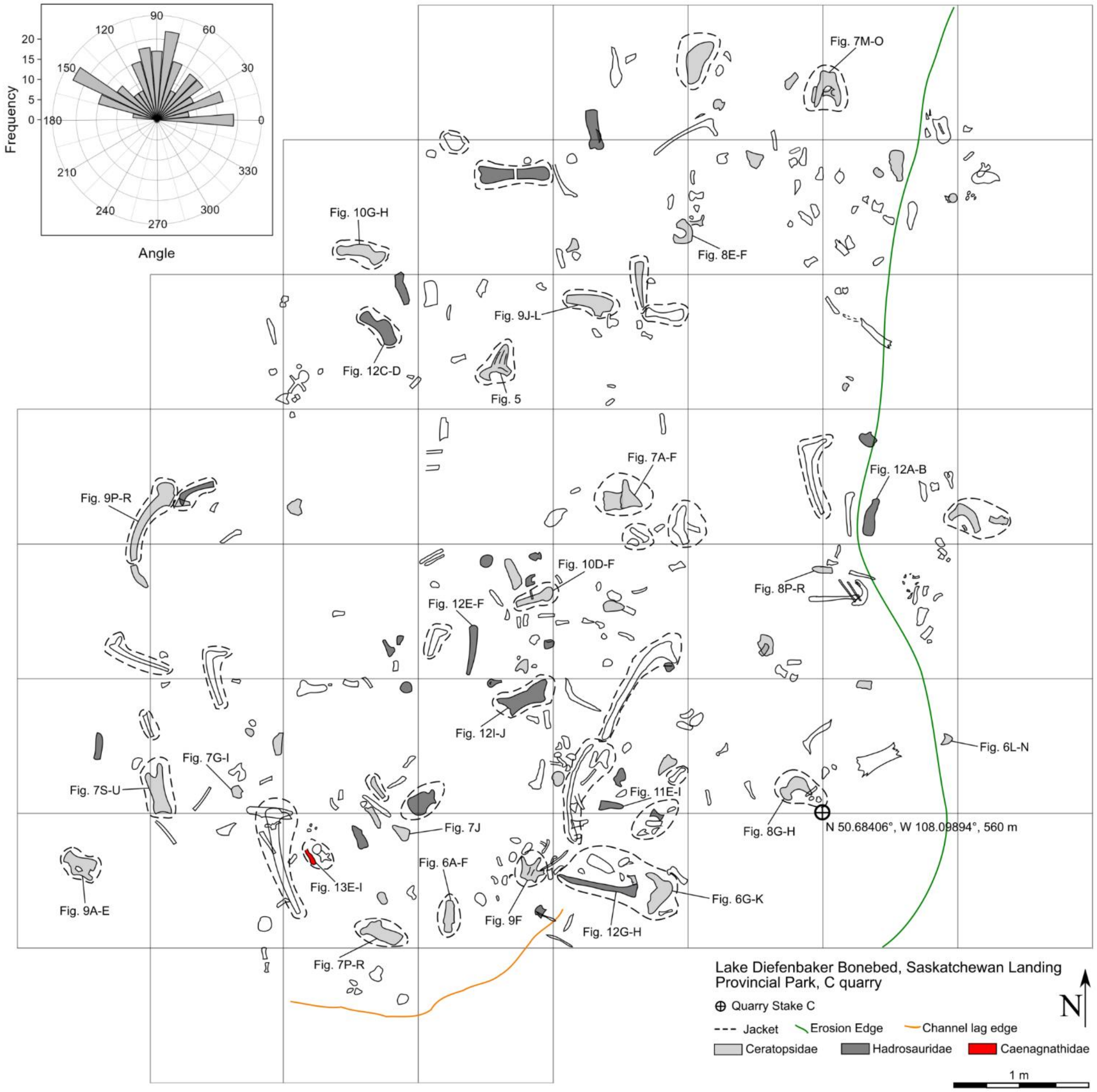

Figure 2.3. Map of Lake Diefenbaker Bonebed, Quarry C. Labels indicate figured fossil specimens. Coordinates in WGS84 decimal degrees.

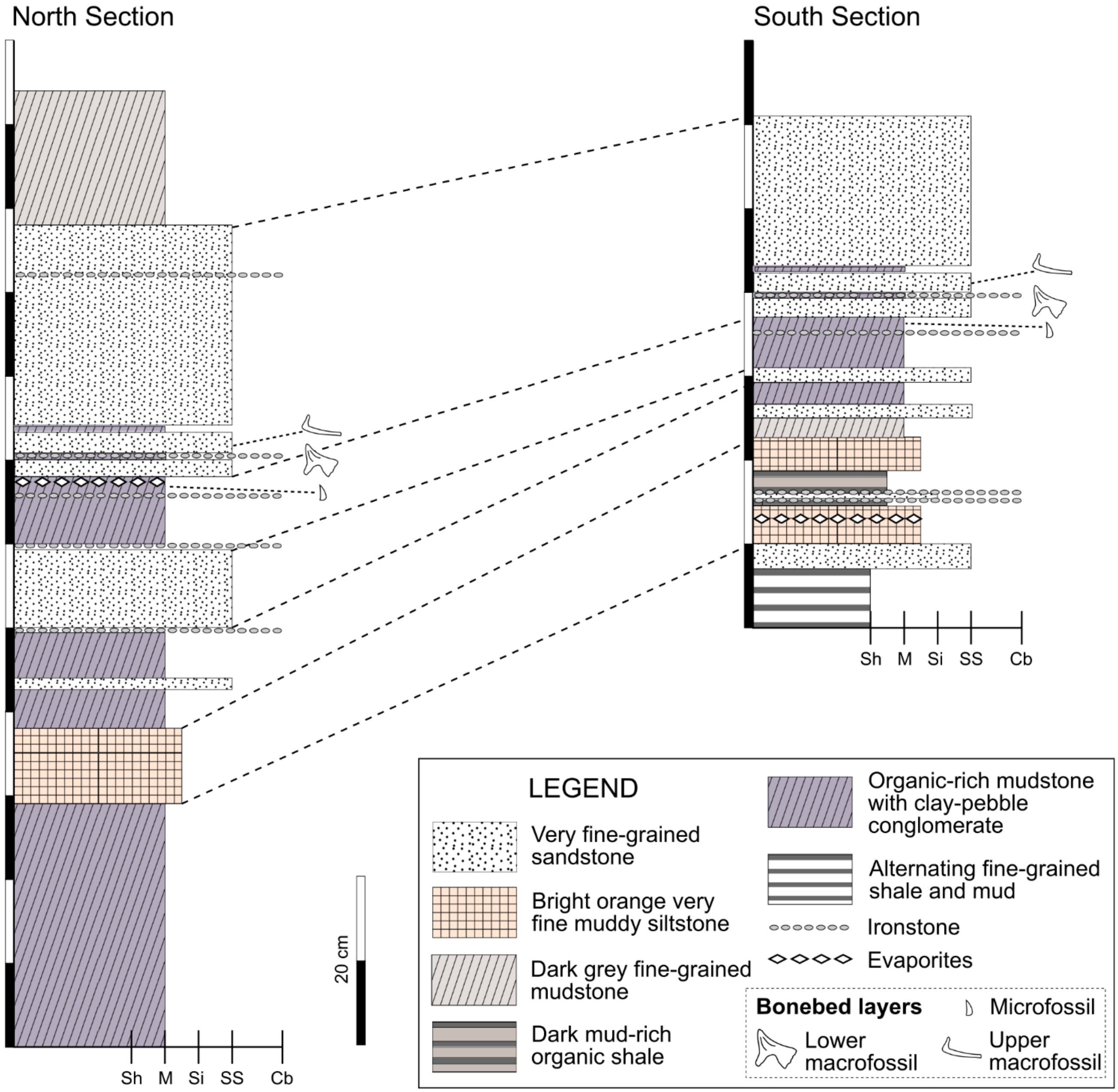

Figure 2.4. Stratigraphic sections measured at northern and southern extremities of Lake Diefenbaker Bonebed, Quarry C. **Abbreviations: Sh**, shale; **M**, mudstone; **Si**, siltstone; **SS**, sandstone; **Cb**, cobbles.

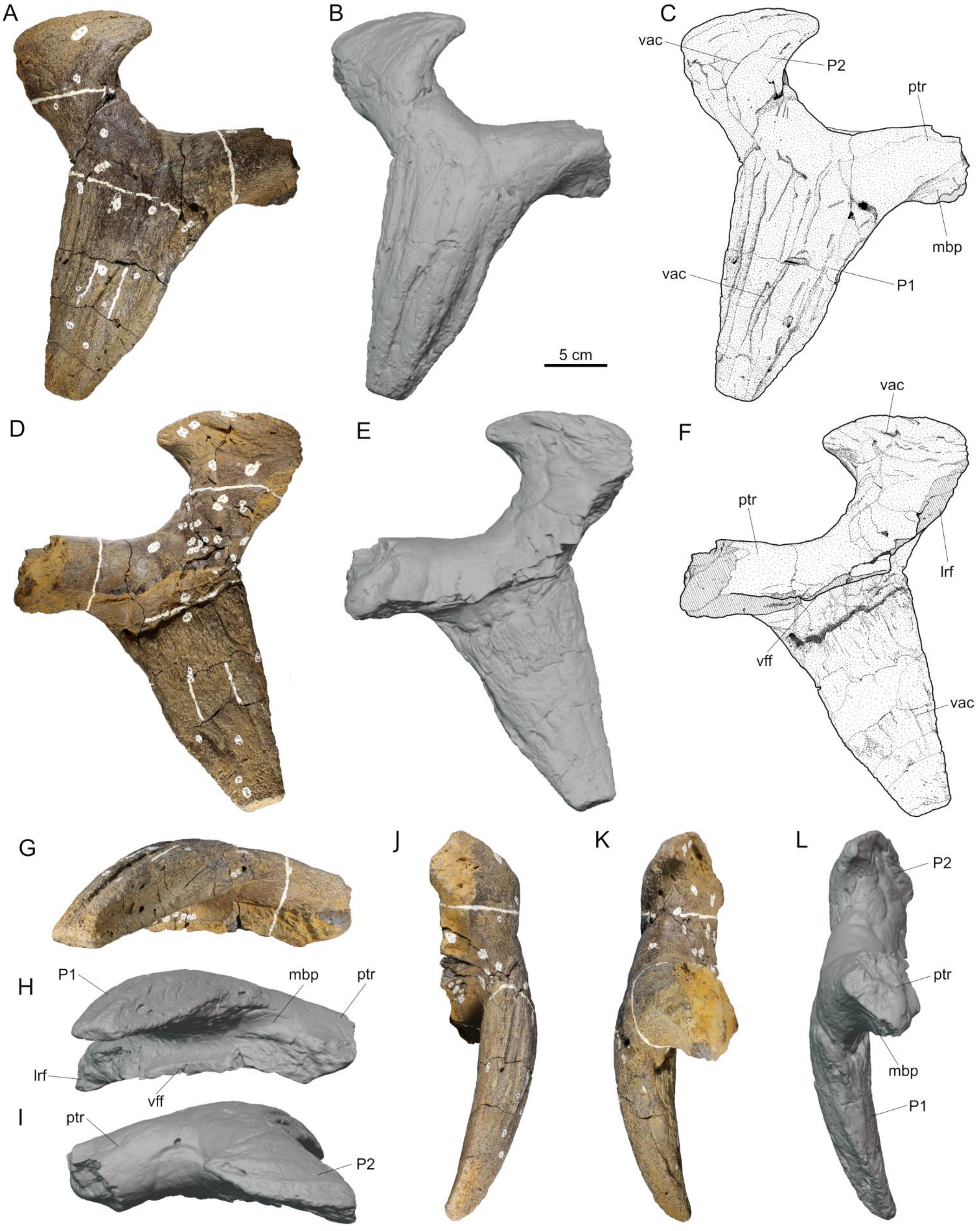
A
B
C
vac
P2
ptr
mbp
vac
P1
5 cm
D
E
F
vac
ptr
lrf
vff
vac
G
J
K
L
P2
H
P1
mbp
ptr
lrf
vff
I
ptr
P2
ptr
mbp
P1

Figure 2.5. Partial right parietal from Lake Diefenbaker Bonebed RSKM P3217.500 referred to *Centrosaurus apertus* in A-C, dorsal view; D-F, ventral view; G-H, anterior view; I, posterior view; J, lateral view; K-L, medial view. **Abbreviations: lrf**, lateral ramus facet; **mbp**, median bar posterior extremity; **ptr**, posterior transverse ramus; **P1**, first parietal process; **P2**, second parietal process; **vac**, vascular channel; **vff**, facet for ventral flange of posterior transverse ramus. All images to scale.

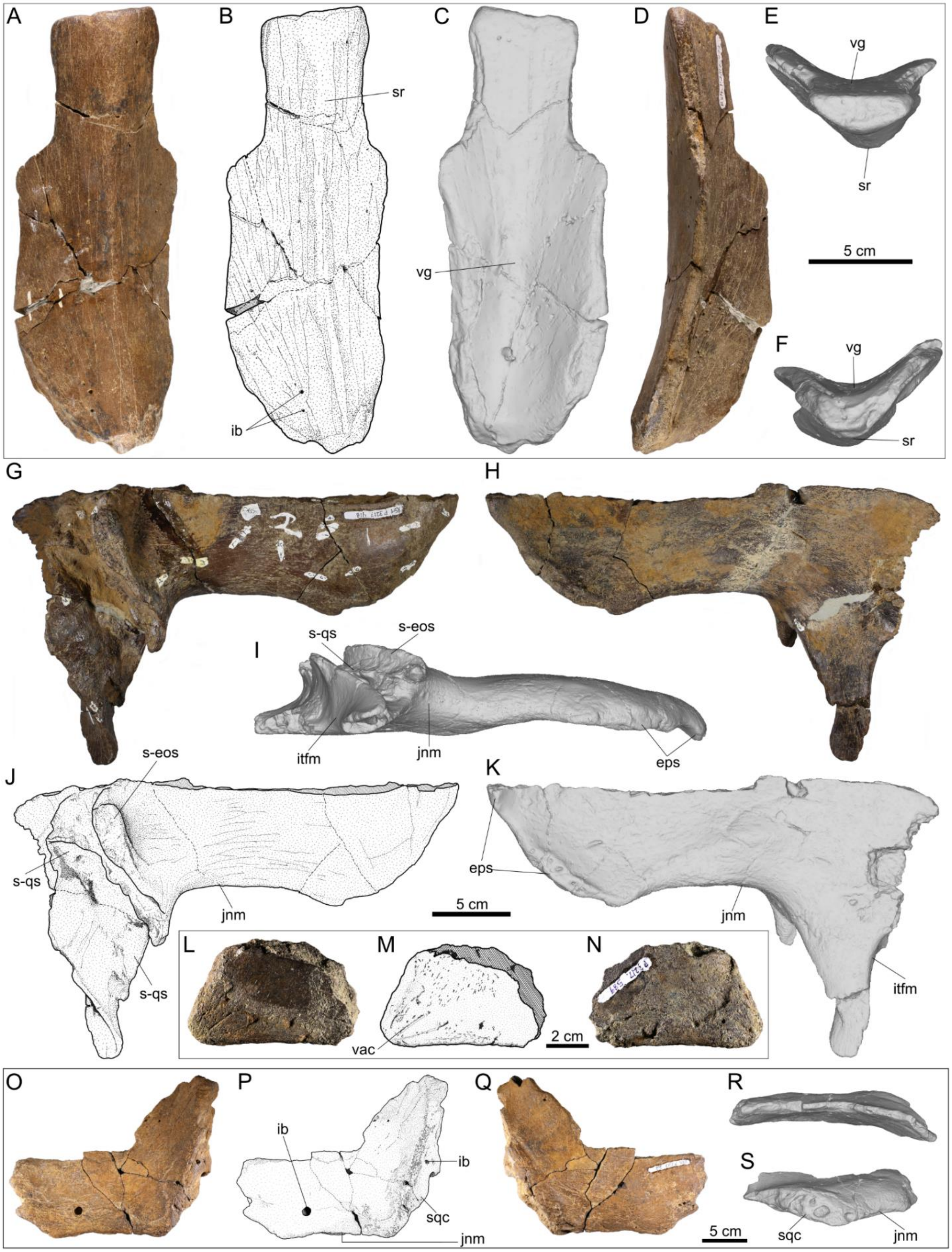
A
B
C
D
E
sr
vg
vg
sr
5 cm
F
vg
sr
ib
G
H
I
s-qs
s-eos
itfm
jnm
eps
J
s-eos
s-qs
jnm
s-qs
K
eps
jnm
itfm
5 cm
L
M
N
vac
2 cm
O
P
Q
R
S
ib
ib
sqc
jnm
5 cm
sqc
jnm

Figure 2.6. Other selected ceratopsid frill elements from Lake Diefenbaker Bonebed. A-F, juvenile centrosaurine median parietal bar RSKM P3217.473 in (A-B) dorsal view; (C) ventral view; (D) left ventrolateral view; (E) posterior view; (F) anterior view. G-K, partial centrosaurine right squamosal RSKM P3217.418 in (G, J) medial view; (H, K) lateral view; (I) ventral view. L-N, epiparietal RSKM P3217.589, orientation uncertain. O-S, partial centrosaurine left squamosal RSKM P3217.368 in (O-P) lateral view; (Q) medial view; (R) dorsal (frill cross-section) view; (S) oblique (posteromedioventral) view. **Abbreviations: eps**, episquamosal sutural surface; **ib**, insect borings; **itfm**, infratemporal fenestra margin; **jnm**, jugal notch margin; **s-eos**, squamosal-exoccipital sutural surface; **sqc**, squamosal corner; **s-qs**, squamosal-quadrate sutural surface; **sr**, sagittal ridge; **vac**, vascular channel; **vg**, ventral groove.

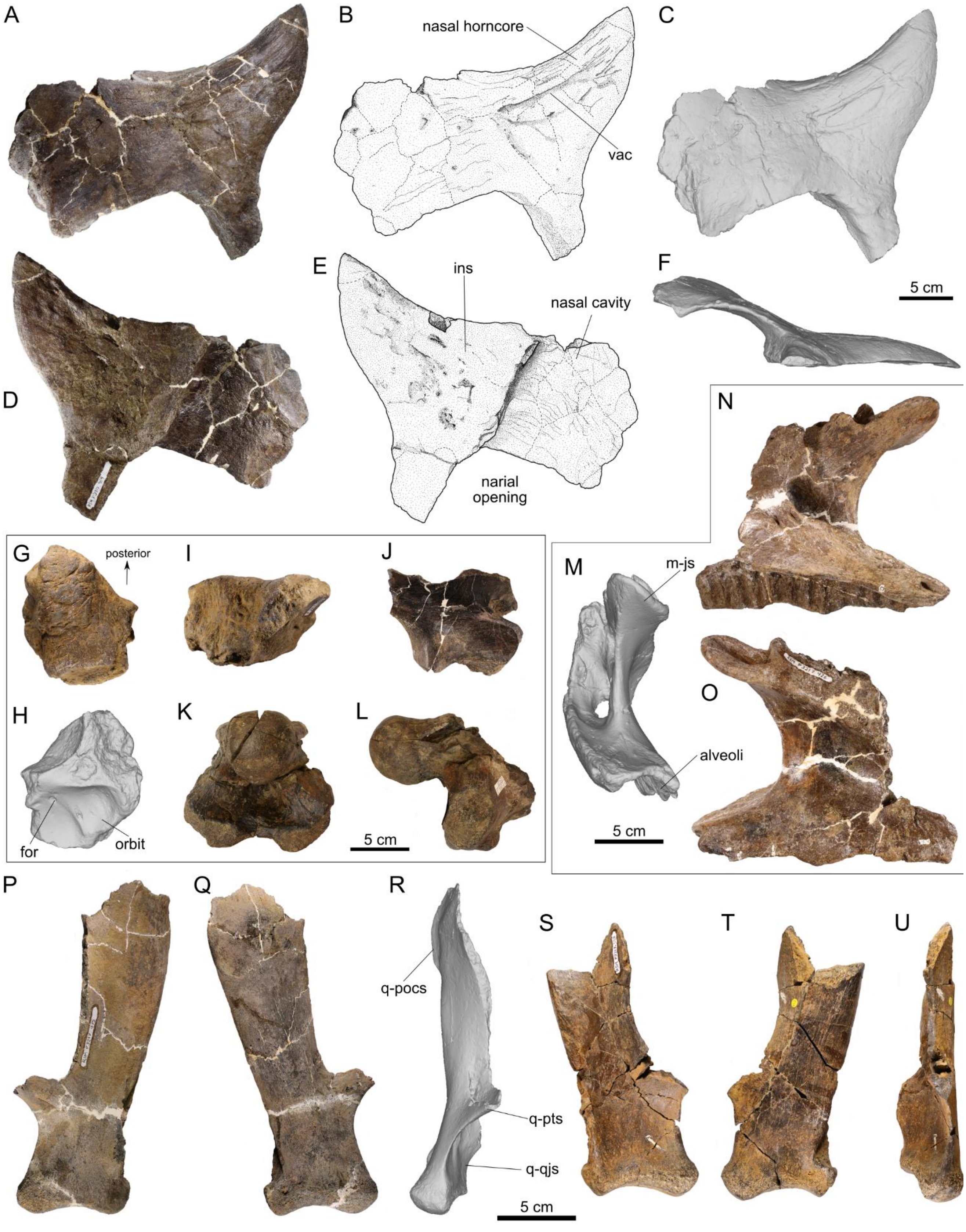
A
B
nasal horncore
vac
C
D
E
ins
nasal cavity
narial opening
F
5 cm
G
posterior
H
for
orbit
I
J
K
L
5 cm
M
m-js
alveoli
5 cm
N
O
P
Q
R
q-pocs
q-pts
q-qjs
5 cm
S
T
U

Figure 2.7. Selected ceratopsid cranial elements from Lake Diefenbaker Bonebed. A-F, centrosaurine right nasal RSKM P3217.464 in (A-C) lateral view; (D-E) medial view; (F) anteroventral view. G-I, partial left frontal component of supracranial cavity RSKM P3217.552 in (G) dorsal view; (H) ventral view; (I) medial view. J, braincase element P3217.479; K-L, basioccipital RSKM P2199.3 in (K) posterior view; (L) left lateral view. M-O, partial right maxilla RSKM P3217.426 in (M) posterior view; (N) medial view; (O) lateral view. P-R, left quadrate RSKM P3217.475 in (P) anterior view; (Q) posterior view; (R) medial view. S-U, partial right quadrate RSKM P3217.558 in (S) anterior view; (T) posterior view; (U) medial view. **Abbreviations: for**, foramina; **ins**, internasal sutural surface; **m-js**, maxilla-jugal sutural surface; **q-pocs**, quadrate-paroccipital process sutural surface; **q-pts**, quadrate-pterygoid sutural surface; **q-qjs**, quadrate-quadratojugal sutural surface; **vac**, vascular channel.

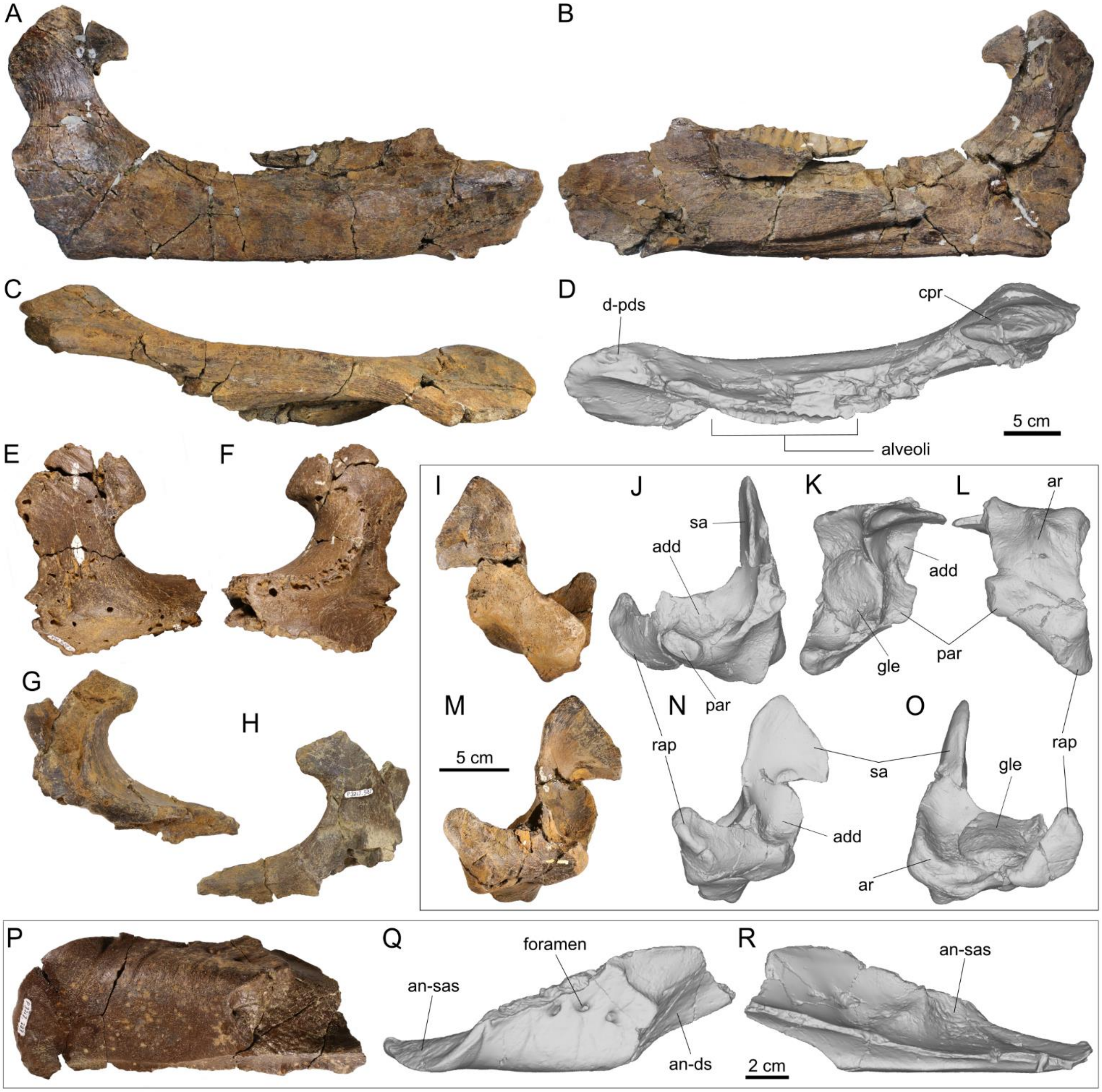
A
B
C
D
d-pds
cpr
alveoli
5 cm
E
F
G
H
I
J
K
L
sa
add
add
ar
par
gle
par
M
N
O
5 cm
rap
sa
gle
rap
add
ar
P
Q
R
foramen
an-sas
an-sas
an-ds
2 cm

Figure 2.8. Selected ceratopsid mandibular elements from Lake Diefenbaker Bonebed. A-D, right dentary RSKM P3217.586 in (A) lateral view; (B) medial view; (C) ventral view; (D) occlusal view. E-F, posterior right dentary RSKM P3217.371 in (E) lateral view; (F) medial view. G-H, posterior left dentary RSKM P3217.587 in (G) medial view; (H) lateral view. I-O, left surangular-articular complex RSKM P3217.530 in (I) lateral view; (J) anterior view; (K) dorsal view; (L) ventral view; (M-N) medial view; (O) posterior view. P-R, right angular RSKM P3217.383 in (P) anteroventral view; (Q) lateral view; (R) medial view. **Abbreviations: add**, adductor fossa; **an-ds**, angular-dentary sutural surface; **an-sas**, angular-surangular sutural surface; **ar**, articular; **cpr**, coronoid process; **d-pds**, dentary-predentary sutural surface; **gle**, glenoid fossa; **par**, prearticular; **rap**, retroarticular process; **sa**, surangular. All dentary specimens to scale.

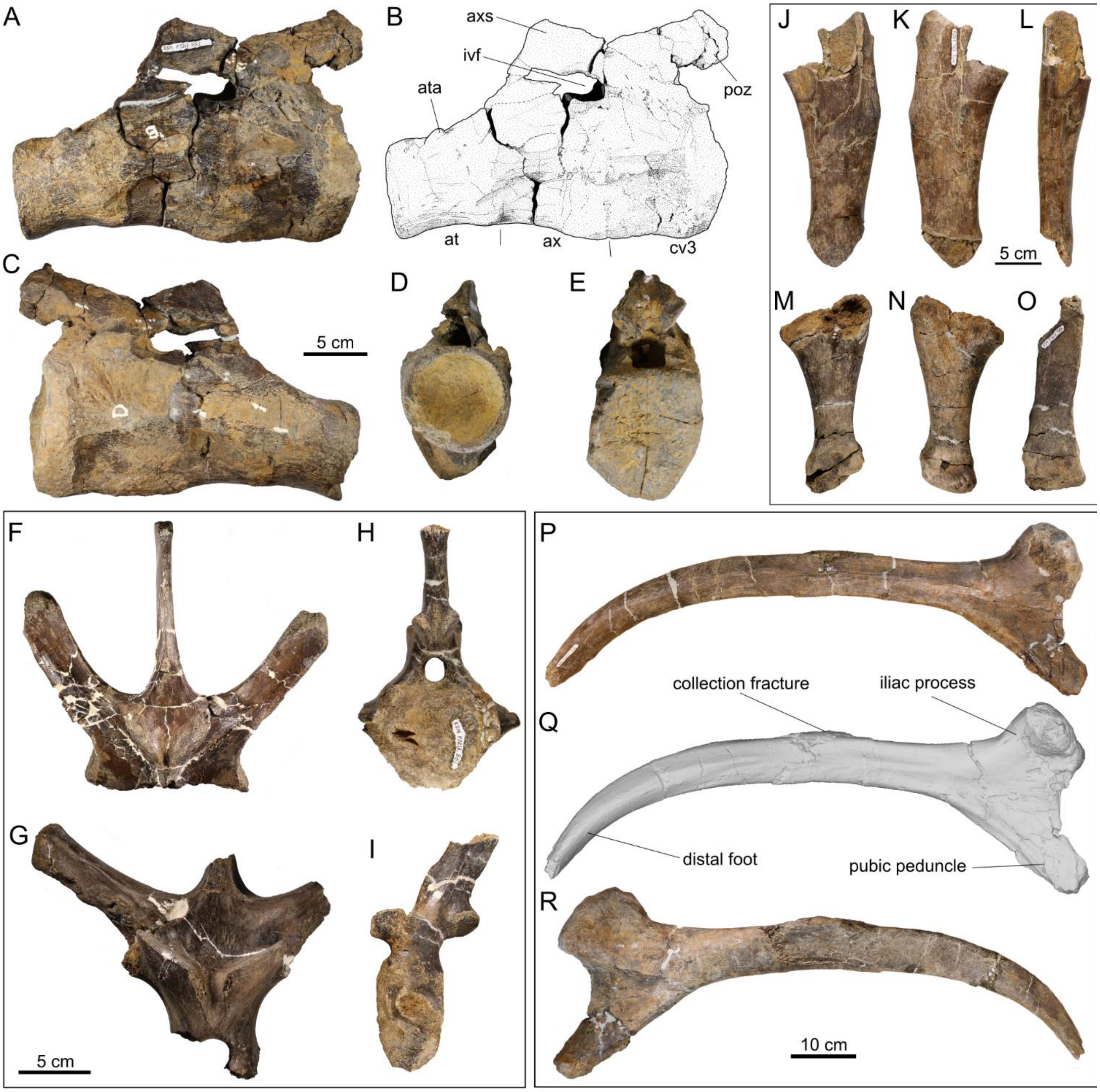
A
B
axs
ivf
ata
poz
at
ax
cv3
C
5 cm
D
E
J
K
L
5 cm
M
N
O
F
H
G
I
5 cm
P
collection fracture
iliac process
Q
distal foot
pubic peduncle
R
10 cm

Figure 2.9. Selected ceratopsid postcranial elements from Lake Diefenbaker Bonebed. A-E, centrosaurine syncervical RSKM P3217.563 in (A-B) left lateral view; (C) right lateral view; (D) anterior view; (E) posterior view. Short strokes mark each vertebral boundary. F-I, selected vertebrae: (F) anterior dorsal neural arch RSKM P3217.416 in posterior view; (G) anterior dorsal RSKM P3217.374 in anterior view; (H-I) anterior caudal RSKM P3217.561 in (H) anterior view; (I) left lateral view. J-L, left ulna RSKM P3217.465 in (J) anterior view; (K) posterior view, (L) medial view. M-O, right metatarsal II RSKM P3217.566 in (M) lateral view; (N) medial view; (O) dorsal view. P-R, centrosaurine left ischium RSKM P3217.572 in (P-Q) medial view; (R) lateral view. **Abbreviations:** **at**, atlas; **ata**, atlantal arch; **ax**, axis; **axs**, axial spine; **cv3**, third cervical; **ivf**, intervertebral foramen; **poz**, postzygapophysis.

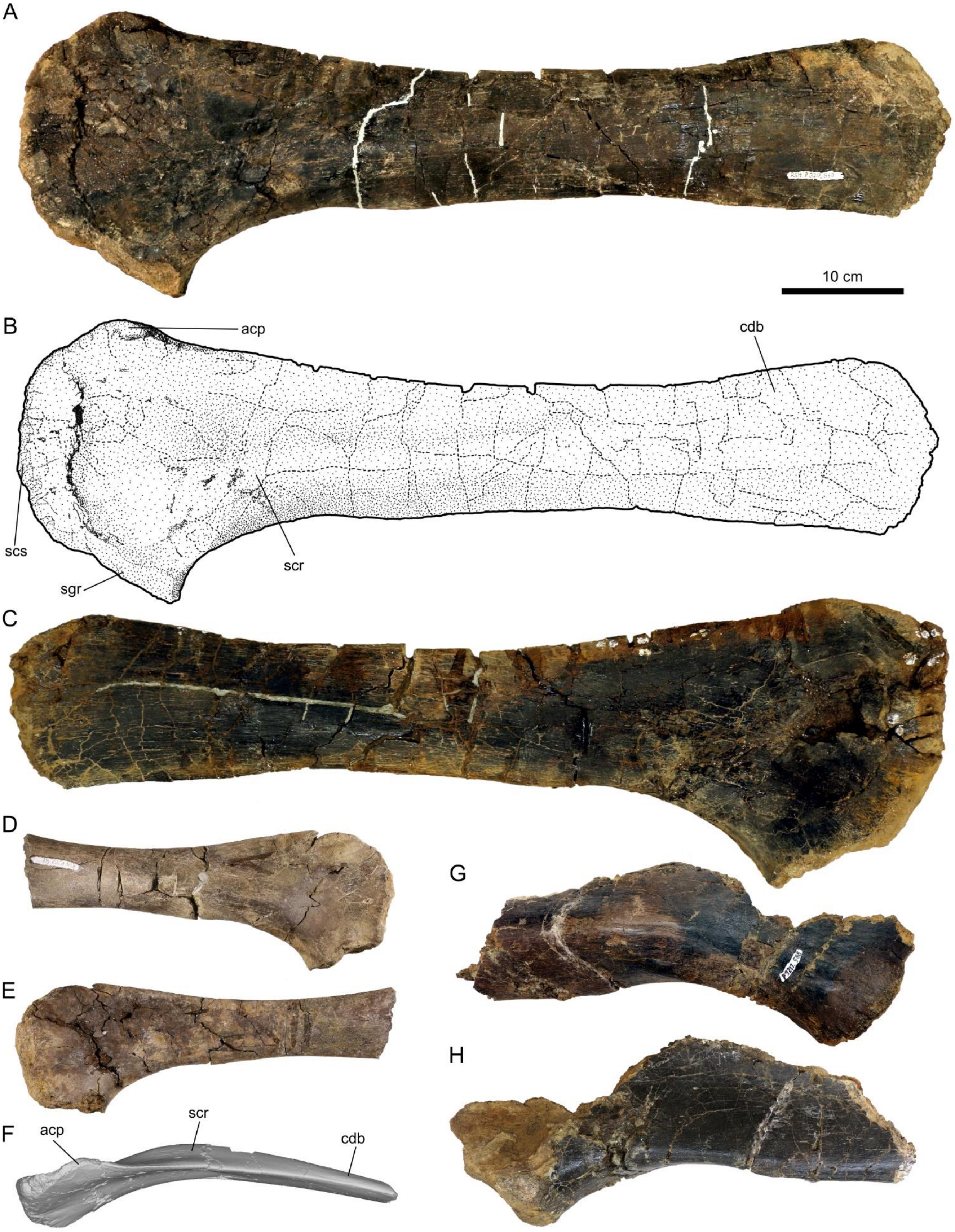
A
10 cm
B
acp
cdb
scs
scr
sgr
C
D
G
E
H
F
acp
scr
cdb

Figure 2.10. Size variation in centrosaurine scapulae from Lake Diefenbaker Bonebed. A-C, adult left scapula RSKM P3217.560 in (A-B) lateral view; (C) medial view. D-F, partial juvenile right scapula RSKM P3217.519 in (D) lateral view; (E) medial view; (F) anterior view. G-H, partial juvenile/subadult right scapula RSKM P3217.588 in (G) lateral view; (H) medial view. **Abbreviations:** **acp**, acromion process; **cdb**, craniodorsal blade; **scs**, scapulocoracoid sutural surface; **scr**, scapular ridge; **sgr**, supraglenoid ridge. All specimens to scale.

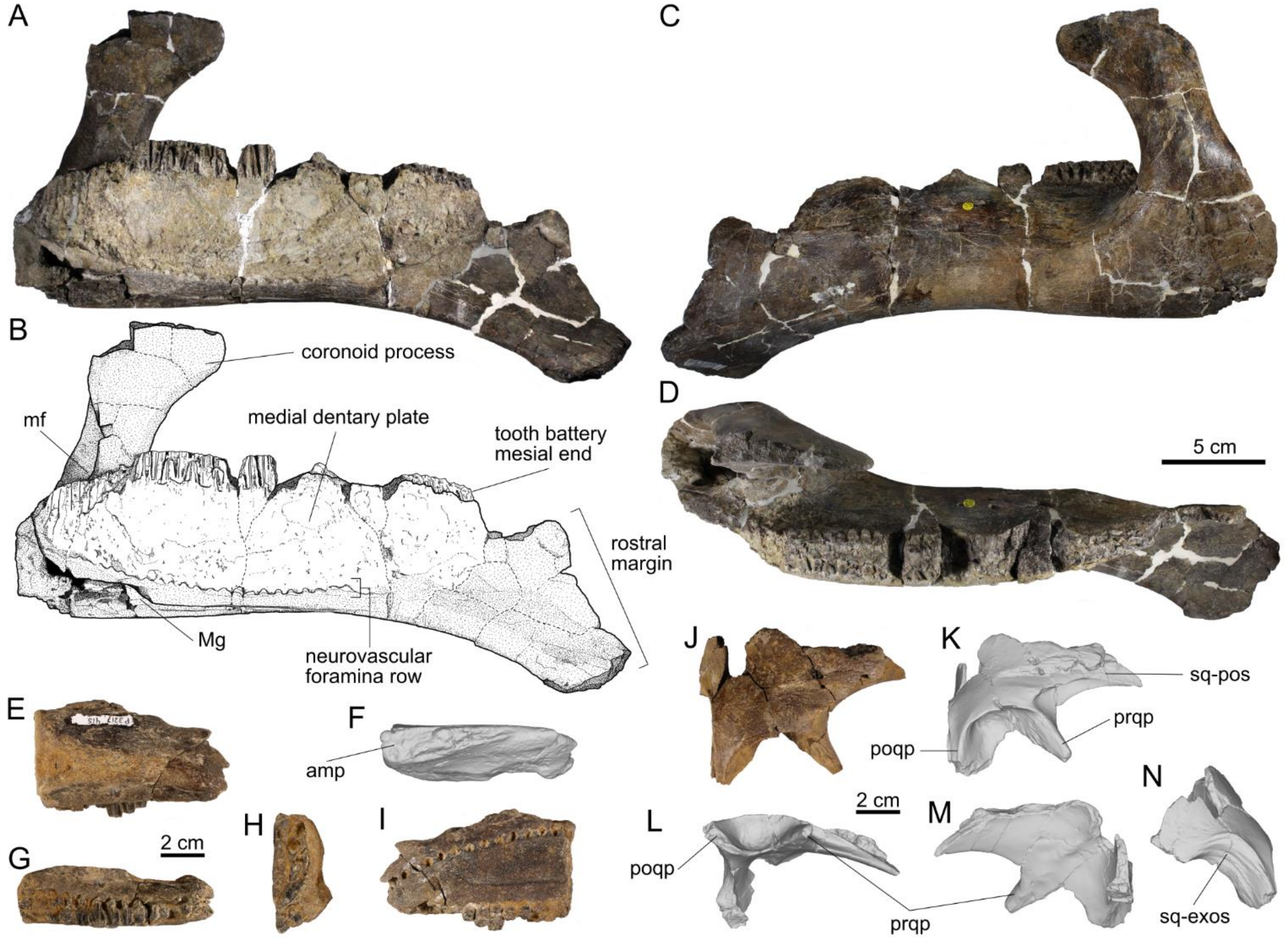

Figure 2.11. Selected hadrosaurid cranial and mandibular elements from Lake Diefenbaker Bonebed. A-D, left dentary RSKM P3217.506 in (A-B) medial view; (C) lateral view; (D) occlusal view. E-I, partial juvenile hadrosaurine left maxilla RSKM P3217.415 in (E) lateral view; (F) dorsal view; (G) occlusal view; (H) anterior view; (I) medial view. J-N, partial right squamosal RSKM P3217.585 in (J) dorsolateral view; (K) lateral view; (L) ventral view; (M) medial view; (N) posterior view. **Abbreviations: amp**, origin of anterior maxillary process; **mf**, mandibular fossa; **Mg**, Meckelian groove; **poqp**, postquadratic process; **prqp**, prequadratic process; **sq-exos**, squamosal-exoccipital sutural surface; **sq-pos**, squamosal-postorbital sutural surface.

Figure 2.12. Selected hadrosaurid postcranial elements from Lake Diefenbaker Bonebed. A-B, partial scapula RSKM P3217.391 in (A) medial view; (B) lateral view. C-D, juvenile lambeosaurine right humerus RSKM P3217.505 in (C) anterior view; (D) posterior view. E-F, right ulna RSKM P3217.525 in (E) posterior view; (F) anterior view. G-H, lambeosaurine right ischium RSKM P3217.417 in (G) medial view; (H) lateral view. I-J, juvenile lambeosaurine pubis RSKM P3217.507 in (I) medial view; (J) lateral view.

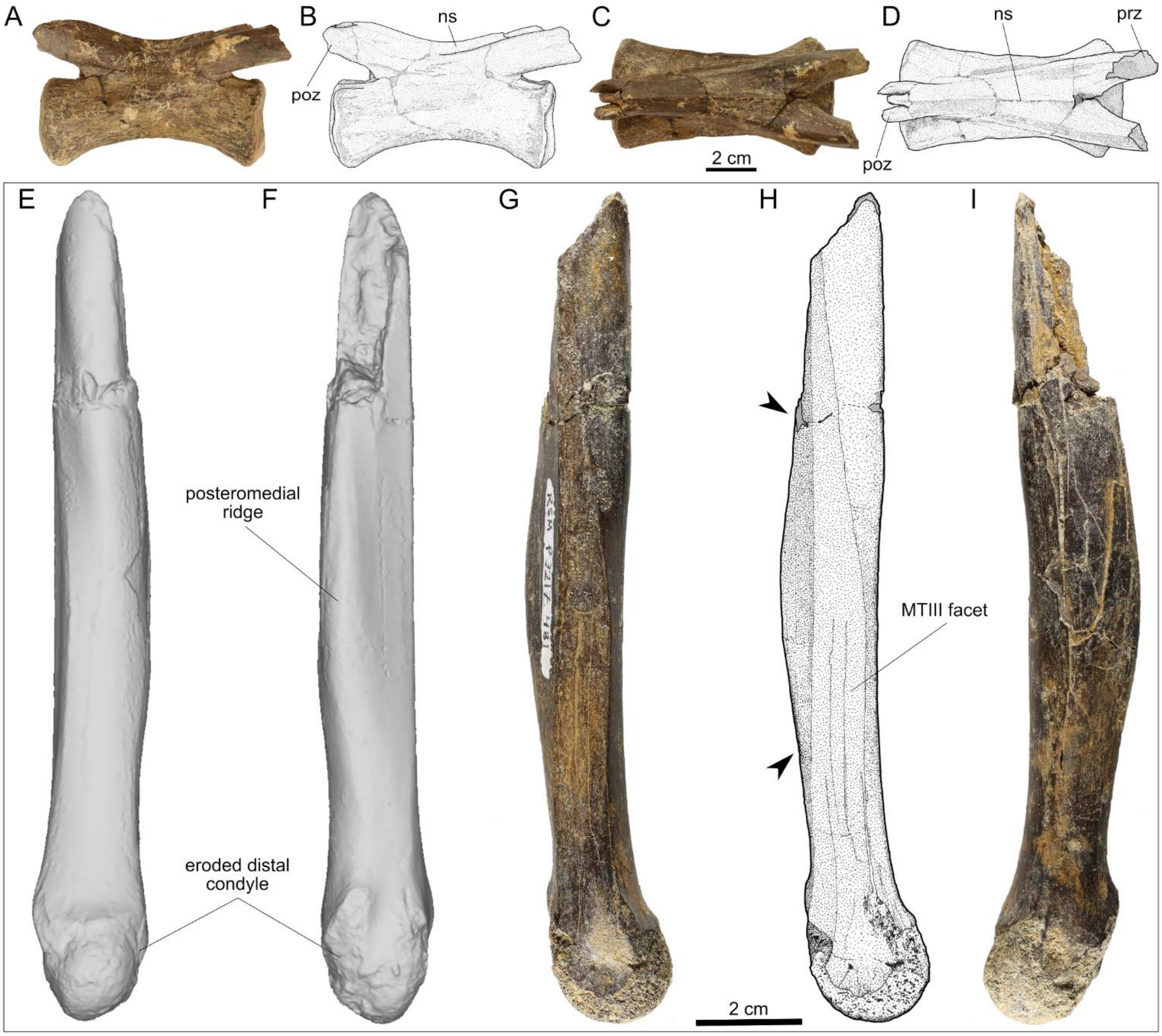

Figure 2.13. Selected theropod remains from Lake Diefenbaker Bonebed. A-D, tyrannosaurid posterior caudal RSKM P3193.1 in (A-B) right lateral view; (C-D) dorsal view. E-I, partial right second metatarsal RSKM P3217.481 of an elmisaurine caenagnathid cf. *Citipes elegans* in (E) anterior view; (F) posterior view; (G-H) lateral view; (I) medial view. **Abbreviations: MTIII**, third metatarsal; **ns**, neural spine; **poz**, postzygapophysis; **prz**, prezygapophysis.

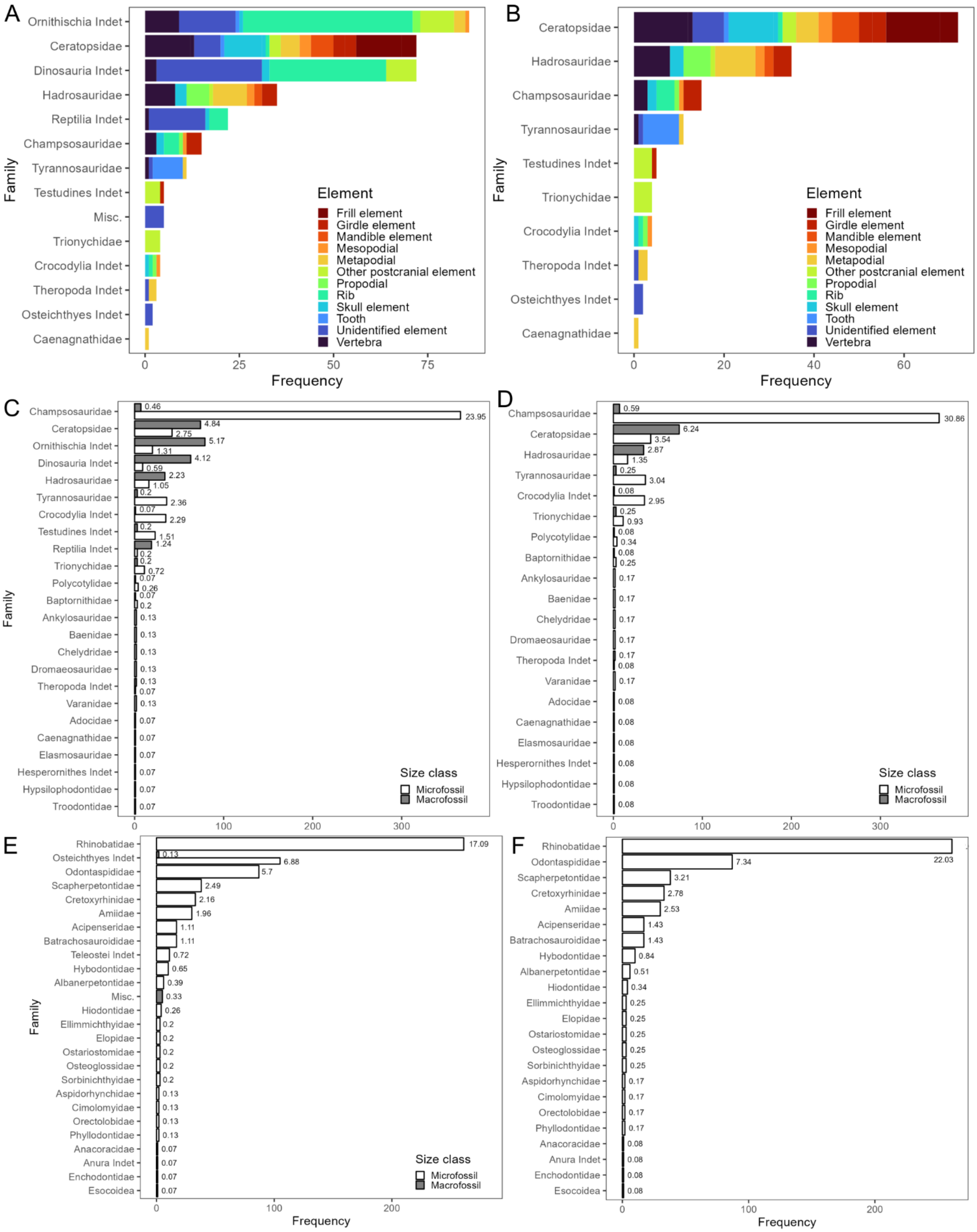
A
Ornithischia Indet
Ceratopsidae
Dinosauria Indet
Hadrosauridae
Reptilia Indet
Champsosauridae
Tyrannosauridae
Testudines Indet
Misc.
Trionychidae
Crocodylia Indet
Theropoda Indet
Osteichthyes Indet
Caenagnathidae
Family
0
25
50
75
Frequency
Element
Frill element
Girdle element
Mandible element
Mesopodial
Metapodial
Other postcranial element
Propodial
Rib
Skull element
Tooth
Unidentified element
Vertebra
B
Ceratopsidae
Hadrosauridae
Champsosauridae
Tyrannosauridae
Testudines Indet
Trionychidae
Crocodylia Indet
Theropoda Indet
Osteichthyes Indet
Caenagnathidae
Family
0
20
40
60
Frequency
Element
Frill element
Girdle element
Mandible element
Mesopodial
Metapodial
Other postcranial element
Propodial
Rib
Skull element
Tooth
Unidentified element
Vertebra
C
Champsosauridae 0.46 23.95
Ceratopsidae 4.84 2.75
Ornithischia Indet 5.17 1.31
Dinosauria Indet 4.12 0.59
Hadrosauridae 2.23 1.05
Tyrannosauridae 0.2 2.36
Crocodylia Indet 0.07 2.29
Testudines Indet 0.2 1.51
Reptilia Indet 1.24 0.2
Trionychidae 0.2 0.72
Polycotylidae 0.07 0.26
Baptornithidae 0.07 0.2
Ankylosauridae 0.13
Baenidae 0.13
Chelydridae 0.13
Dromaeosauridae 0.13
Theropoda Indet 0.13 0.07
Varanidae 0.13
Adocidae 0.07
Caenagnathidae 0.07
Elasmosauridae 0.07
Hesperornithes Indet 0.07
Hypsilophodontidae 0.07
Troodontidae 0.07
Family
0
100
200
300
Size class
Microfossil
Macrofossil
D
Champsosauridae 0.59 30.86
Ceratopsidae 6.24 3.54
Hadrosauridae 2.87 1.35
Tyrannosauridae 0.25 3.04
Crocodylia Indet 0.08 2.95
Trionychidae 0.25 0.93
Polycotylidae 0.08 0.34
Baptornithidae 0.08 0.25
Ankylosauridae 0.17
Baenidae 0.17
Chelydridae 0.17
Dromaeosauridae 0.17
Theropoda Indet 0.17 0.08
Varanidae 0.17
Adocidae 0.08
Caenagnathidae 0.08
Elasmosauridae 0.08
Hesperornithes Indet 0.08
Hypsilophodontidae 0.08
Troodontidae 0.08
0
100
200
300
Size class
Microfossil
Macrofossil
E
Rhinobatidae 17.09
Osteichthyes Indet 0.13 6.88
Odontaspididae 5.7
Scapherpetontidae 2.49
Cretoxyrhinidae 2.16
Amiidae 1.96
Acipenseridae 1.11
Batrachosauroididae 1.11
Teleostei Indet 0.72
Hybodontidae 0.65
Albanerpetontidae 0.39
Misc. 0.33
Hiodontidae 0.26
Ellimmichthyidae 0.2
Elopidae 0.2
Ostariostomidae 0.2
Osteoglossidae 0.2
Sorbinichthyidae 0.2
Aspidorhynchidae 0.13
Cimolomyidae 0.13
Orectolobidae 0.13
Phyllodontidae 0.13
Anacoracidae 0.07
Anura Indet 0.07
Enchodontidae 0.07
Esocoidea 0.07
Family
0
100
200
Frequency
Size class
Microfossil
Macrofossil
F
Rhinobatidae 22.03
Odontaspididae 7.34
Scapherpetontidae 3.21
Cretoxyrhinidae 2.78
Amiidae 2.53
Acipenseridae 1.43
Batrachosauroididae 1.43
Hybodontidae 0.84
Albanerpetontidae 0.51
Hiodontidae 0.34
Ellimmichthyidae 0.25
Elopidae 0.25
Ostariostomidae 0.25
Osteoglossidae 0.25
Sorbinichthyidae 0.25
Aspidorhynchidae 0.17
Cimolomyidae 0.17
Orectolobidae 0.17
Phyllodontidae 0.17
Anacoracidae 0.08
Anura Indet 0.08
Enchodontidae 0.08
Esocoidea 0.08
0
100
200
Frequency

Figure 2.14. Taxonomic diversity of the Lake Diefenbaker Bonebed. A-B, frequency of skeletal elements per family in the macrofossil bonebed, including (A) and excluding (B) abundant indeterminate specimens. C-D, reptile (including bird) diversity of the macrofossil bonebed and vertebrate microfossil locality combined, including (C) and excluding (D) abundant indeterminate specimens. E-F, non-reptile diversity of the macrofossil bonebed and vertebrate microfossil locality combined, including (E) and excluding (F) abundant indeterminate specimens. The posterior parietals of *Chasmosaurus russelli* (CMN 8803), as well as two indeterminate ceratopsid basioccipitals collected by T. Tokaryk *et al*. (RSKM P2199.3-4), are included in Figure 14 C-F.

2.8 Tables

Table 2.1. Comparisons of the estimated alpha (within-site) diversity within Lake Diefenbaker Bonebed, as well as dinosaur alpha diversity between Lake Diefenbaker Bonebed and three Dinosaur Provincial Park bonebeds (ceratopsid-dominant BB042 and BB043 and multigeneric BB047).

	Lake Diefenbaker Bonebed			**BB042**	**BB043**	**BB047**
	All fossils	*Microvertebrate locality only*	*Dinosaurs only*	*Dinosaurs only*	*Dinosaurs only*	*Dinosaurs only*
Number of specimens	1,182	1,036	216	112	1,434	855*
Observed taxon richness	43	42	9	5	6	9
Chao-1	50.5625	48.25	11.25	5	6	11
Jackknife-2	56.9645	53.9653	12.9444	6.9464	7.9958	11.9895
ACE	48.1563	46.0541	11.25	5.1875	6.2222	16

Vertebrate microsite locality dataset assembled from Gilbert *et al*. (2018). Dinosaur diversity data obtained from Visser (1986: figure 29) for BB042, Ryan *et al*. (2001: table 1) for BB043 and from Tumarkin-Deratzian (1997: figure 23 and appendix B) for BB047. Chao-1, Second-order Jackknife (Jackknife-2) and Abundance-based coverage estimator (ACE) are non-parametric species richness estimators. Dinosaur diversity includes specimens collected *in* and *ex situ* for all 3 bonebeds.

*Absolute abundances calculated from relative abundances in Tumarkin-Deratzian (1997: figure 23) and complemented by frequency table in Tumarkin-Deratzian (1997: appendix B).

BRIDGING TEXT

Chapter 2 contributed to our knowledge of the spatial dimension of the biodiversity of the Belly River Group (BRG) ecosystem by documenting a bonebed located to the East of Dinosaur Provincial Park. Since the latter has by far the most vertically extensive exposures of the BRG throughout western Canada, it is the best place to investigate the temporal dimension of that biodiversity knowledge. Chapter 3 therefore presents studies of the geological setting of some of the fossil quarries and bonebeds that were explored over the course of five field seasons in the Park as part of the present thesis. These surveys included ground-based observations but also, more innovatively, aerial photographs taken using unmanned aerial vehicles (UAVs) which were combined through structure-from-motion photogrammetry to create 3-D digital outcrop models and 2-D digital elevation models and orthomosaics. These models showed promise in distinguishing sedimentary architectural units that could contribute to stratigraphically correlating the Park's hundreds of quarries and thus refine the time resolution of the biotic and abiotic changes that occurred throughout the 2.5 million years of BRG exposures outcropping there. Therefore, the following chapter addresses the Gouldian shortfall on species' stratigraphic (and thus temporal) distributions in Dinosaur Provincial Park. It primarily consists of a manuscript focused on the geological setting of a multigeneric bonebed that has been intensely explored over these field seasons. The remainder includes shorter descriptions of a new fossil plant site, a new ceratopsid skull quarry, and two fossil invertebrate localities which will contribute to an estimated three additional manuscripts as part of a long-term research project on the palaeoecology of Dinosaur Provincial Park.

CHAPTER 3. Insights into the temporal resolution of the Late Cretaceous (Campanian) Dinosaur Provincial Park biota (Alberta, Canada) from 3-D stratigraphic mapping

Abstract

Time averaging of fossils in fluvio-deltaic sedimentary rocks is an important obstacle to achieving an informative relative age resolution for local palaeodiversity patterns. One of the best examples of this phenomenon is observed in the palaeobiota preserved in the Belly River Group (Late Cretaceous, Campanian) of Dinosaur Provincial Park (DPP), Alberta, Canada. Although it combines the world's most complete dinosaur chronofauna with precise and accurate *absolute* age constraints obtained from ashfall deposits, there remain significant *relative* age uncertainties between those. The biostratigraphic position of a multigeneric bonebed at a transitional period between two successive dinosaur assemblage zones, combined with its proximity to an exposure of the Oldman-Dinosaur Park Formation (OF-DPF) contact, together provide an ideal study system for such an investigation. Aerial images acquired in the field were aligned by structure-from-motion (SfM) photogrammetry to construct a 3-D digital outcrop model (DOM), a digital elevation model (DEM), and an orthomosaic of the 0.446 km^2 area surrounding the bonebed, in which the lower ~40 m of the DPF were represented. The first key result of their examination is that the absolute elevation of the OF-DPF contact varies by ~12 m locally, which causes hitherto underestimated uncertainties on any fossil locality's stratigraphic height relative to it. The second is that the lower DPF has the potential to be locally subdivided into at least three successive channel cut-and-fill rhythms, some of which are promising candidate marker beds for a more expansive correlation of DPP's fossil heritage. This chapter also presents four more DOMs for a plant locality, a new ceratopsid skull quarry, and two invertebrate localities which provide a more regional sedimentological context for the BB190 project. The rapid development of unmanned aerial vehicle (UAV) technology now raises the prospect of exploring DPP's stratigraphy on a larger scale than is possible from ground-based surveys alone to resolve this relative age conundrum.

3.1 Introduction

Over the last few decades, there has been a growing interest in earth and life sciences to investigate the potential of our planet's geological and palaeontological heritage to inform modern conservation decisions in view of the global ecological stresses we are currently facing (Willis & Birks 2006; Erwin 2009; Polly *et al.* 2011), leading to the emergence of conservation palaeobiology as an applied subdiscipline of palaeoecology (Dietl & Flessa 2011; Dietl *et al.* 2015; Barnosky *et al.* 2017). However, it is evident that climate and biodiversity patterns inferred along geological time scales (usually varying between 10^5 and 10^7 years) can only constitute relevant baselines for detecting anomalies in the rates of patterns occurring on an *ecological* time scale (10^1 to 10^2 years) if they are relatively well constrained temporally (Behrensmeyer & Hook 1992; DiMichele *et al.* 2004). In this respect, geochronological breakthroughs have been essential to our increasing understanding of the tempo of macroevolutionary and macroecological processes in deep time (Knoll & Nowak 2017; Wu *et al.* 2023). The latter are usually detected from analyses of massive databases spanning multiple continents for at least tens of millions of years and underlie a growing consensus that the present global warming and extinction rates far exceed the 'background' rates observed in the fossil record (Jablonski 1991; Barnosky *et al.* 2011; Ceballos *et al.* 2015; De Vos *et al.* 2015). That said, the temporal resolution of regional- to continental-scale fossil databases can be limited by a phenomenon known as 'analytical time averaging', defined as 'analytical errors in […] methods used in chrono-, litho-, and biostratigraphy' which, for instance, can erroneously suggest that communities known from geographically distinct fossil localities coexisted (Behrensmeyer & Hook, 1992: p.76). This may lead to overestimates of past biodiversity despite taphonomic filters that contrastingly reduce the proportion of that diversity preserved in the fossil record (Kidwell & Flessa 1995; Behrensmeyer *et al.* 2000; Kidwell & Holland 2002).

The confounding effects of analytical time averaging imply that studies of biotic responses to perturbations in deep time on a more local scale can theoretically be more informative than global-scale studies, especially with mounting evidence that biodiversity has been influenced by distinct processes at global and regional scales (Vermeij & Leighton 2003; Benson *et al.* 2021). The last two million years of Earth's history arguably remain the most urgently informative since they offer a sufficiently long-term perspective of rapid climate shifts at a very high temporal resolution combined with unmatched local community completeness which includes several species whose biology is relatively easy to interpret due to their high similarity to extant relatives (Guthrie 2006; DeSantis *et al.* 2019; Groff *et al.* 2020). Therefore, this record provides some of the most powerful evidence for the depauperate state of our present vertebrate communities (Lyons *et al.* 2016; Smith *et al.* 2016; Tóth *et al.* 2019; Fricke *et al.* 2022). Nonetheless, it can also be argued that a greater understanding of past community responses under much higher atmospheric carbon and eustatic sea levels is equally relevant considering that present perturbations are on course to exceed what has occurred throughout the glacial-interglacial cycles (IPCC 2023). This is where relatively complete fossil assemblages recording more ancient events can contribute (DiMichele *et al.* 2004; Blanco *et al.* 2021; Fraser *et al.* 2021; Roopnarine & Banker 2021), at least when the magnitude of those perturbations and responses is calibrated by a sufficiently precise and accurate geochronology (e.g. Barry *et al*., 1985). Some of the most striking evidence they can provide concerns biotic decline and recovery before and after mass extinction events (Barnes 1988; Johnson & Hickey 1990; Roopnarine *et al.* 2007; Wilson 2013; Roopnarine & Angielczyk 2015; Lyson *et al.* 2019; Dai *et al.* 2023), as well as more subtle shifts in species' geographical range and phenotypic evolution rates in response to such episodes of relatively rapid climate change as the Paleocene-Eocene Thermal Maximum (Gingerich & Gunnell 1995; Wing *et al.* 2005; Currano *et al.* 2008; Smith *et al.* 2009; Secord *et al.* 2012). However, the time calibration that constrains these patterns often only consists of a few absolute age boundaries along a given stratigraphic section, which provide age estimates with very high uncertainties for individual fossil sites located *between* them.

This persistent constraint means that rigorous palaeoecological studies with limited analytical time averaging can only be achieved in a select few fossil localities with exceptional deposition and preservation. Even the most temporally constrained of these localities are thus subject to an extent to the 'taphonomic' type of time averaging, where local palaeodiversity becomes overestimated due to sedimentary and taphonomic processes that amalgamate chronologically disparate fossil assemblages (Behrensmeyer & Hook 1992; Behrensmeyer *et al.* 2000). Although some depositional settings (such as marine and lacustrine environments) are less prone to taphonomic time averaging due to relatively constant rock accumulation rates coupled with clearly identifiable vertically successive bedding planes, the same cannot be said for fluvio-deltaic deposits, which are more prone to depositional hiatuses caused by reduced sediment supply or palaeochannel incisions into underlying strata (Behrensmeyer 1982; Behrensmeyer & Hook 1992; Kidwell & Holland 2002). The reality observed in the latter means that a channel flowing after a prolonged depositional hiatus can theoretically cut into strata that are older by as much as 10^6-10^7-year scales. This would initially result in stratigraphic positions erroneously interpreted as equivalent (prior to their corrections) between fossils formed in those heterogeneous adjacent deposits, which would initially obscure any potential eco-evolutionary change occurring at a given locality through time. In extreme cases, more recent channels may be erroneously interpreted as underlying older beds if only limited, discontinuous outcrops are available.

3.1.1 The current temporal resolution of the Dinosaur Provincial Park palaeobiota

Considering the problematic outlined above, the late Campanian exposures of the Judith River (Belly River) Group (Eberth & Hamblin 1993; Hamblin & Abrahamson 1996) cropping out along the Red Deer River in Dinosaur Provincial Park (DPP), Alberta, Canada, constitute a particularly intriguing study system. After more than a century of sustained geological and palaeontological exploration (Russell 1966; Currie 1981, 2005), DPP represents one of the most intensely studied Mesozoic ecosystems in terms of palaeoenvironment, temporal resolution and palaeodiversity. Firstly, palaeoenvironmental changes inferred from the DPP sedimentary succession are well understood: the exclusively sandy (alluvial) facies of the Oldman Formation are overlain by the alluvial, deltaic and paralic facies of the Dinosaur Park Formation (DPF) and eventually the shales of the Bearpaw Formation, thus indicating a gradually increasing proximity of an ancient floodplain on the palaeolandmass of Laramidia to the advancing Bearpaw Sea at the start of the last transgression of the Western Interior Seaway (Kauffman & Caldwell 1993; Eberth 2005). Secondly, the tempo of this environmental transition is well constrained, with 100 m of exposed stratigraphic section representing an estimated 2.429 ± 0.024 Myr based on the latest U-Pb zircon geochronology of 5 stratigraphically distinct beds of bentonite mudstone (Thomas *et al.* 1990; Ramezani *et al.* 2022; Eberth *et al.* 2023). This interval is roughly equal in duration to the Quaternary (Cohen *et al.* 2013), which represents exceptional temporal resolution for any locality more ancient than the latter period. Most importantly from a biological perspective, DPP preserves one of the most diverse nonmarine fossil assemblages on the planet across the entire Phanerozoic Eon, with an unmatched density of dinosaur and other tetrapod skeletons reported from an area of badlands covering approximately 80 km^2, thus rendering its analytical time averaging relatively insignificant (Dodson 1983; Currie & Koppelhus 2005 and papers therein; Brown *et al.* 2013*a*). Crucially, precise geographical coordinates are known for more than 650 bonebeds and individual skeleton quarries to date (Figure 3.1A; Currie & Koppelhus 2005: Supplementary CD-ROM; Currie & Russell 2005). This invaluable dataset was made possible by a foresighted quarry staking program initiated by C.M. and Levi Sternberg (Geological Survey of Canada), as well as W.A. Parks (Royal Ontario Museum), in 1935 and 1936 (Sternberg 1936, 1950; Tanke 2005), combined with differential GPS surveys conducted from 1999 to 2003 (MacDonald *et al.* 2005). Such a detailed record of stratigraphic distributions for terrestrial and aquatic vertebrates with limited analytical and taphonomic time averaging is unique among comparably well-known Mesozoic terrestrial ecosystems and has been essential to taphonomic and palaeoecological studies of the Park at least for the last 60 years (Dodson 1971; Béland & Russell 1978; Visser 1986; Wood *et al.* 1988;

Eberth 1990, 2015; Ryan *et al.* 2001; Currie & Russell 2005; Eberth & Currie 2005; Eberth & Getty 2005; Cullen *et al.* 2021). Some of the most significant advances in those fields consisted of the detection of patterns of vertebrate faunal turnover from different taphonomic modes across the Belly River Group's exposures. Firstly, relative abundances estimated from vertebrate microfossil localities revealed a shift in dominance from inland to coastal taxa in conjunction with the aforementioned habitat change (Brinkman 1990; Brinkman *et al.* 1998; Cullen & Evans 2016; but see also Oreska & Carrano 2019). Secondly, the distribution of associated and articulated dinosaur skeletons suggests the presence of 4 megaherbivore assemblage zones across the Oldman and Dinosaur Park Formations collectively forming a possible chronofauna, each of which are now known to have durations varying between ~650 and ~700 ka (Mallon 2019; Eberth *et al.* 2023). However, the respective influences of evolutionary change and ecological replacement in response to climate or habitat change on this particular turnover pattern remain far more debatable (Ryan & Evans 2005; Evans *et al.* 2009, 2015; Mallon *et al.* 2012; Lowi-Merri & Evans 2020). Together, these lines of evidence suggest that Dinosaur Provincial Park may preserve one of the world's most promising palaeobiotas in the distant geological past to investigate biotic responses to a relatively rapid sea level rise over a time interval that is short enough to have some relevance for conservation palaeobiology purposes.

The consistent detection of biodiversity patterns for several dinosaur taxa across these studies implies a high degree of confidence in the relative age of the Park's individual bonebeds and quarries. However, each of these sites' stratigraphic positions has been estimated solely from its height relative to the nearest measured location of the Oldman-Dinosaur Park Formation (OF-DPF) contact on an isopach map of the Park (Brinkman 1990; Eberth 2005; Cullen *et al.* 2021), while scarcely considering their local sedimentological setting beyond its taphonomic significance (Dodson 1971; Wood *et al.* 1988; Eberth 1990). In other words, the quarries of DPP have never been successfully correlated in any lithostratigraphic sense over large distances, a situation usually explained by the lack of consistently identifiable laterally continuous sedimentary strata (Dodson 1971). Indeed, the frequent downcutting of muddy overbank deposits by overlying sandy point bar or thalweg deposits disrupts the lateral continuity of several sedimentary layers and can introduce vertical amalgamation of successive palaeochannels even at a local scale (Wood 1985, 1989). Such vertical and lateral lithological facies variability introduces considerable challenges to mapping any outcrop in DPP, let alone sequence stratigraphic correlation attempts. Since mean and maximum offsets between specimens' observed and adjusted stratigraphic positions above the OF-DPF contact have been estimated at 3.7 and 14.5 m, respectively, quarries located at a similar stratigraphic height in the Park cannot always be assumed to have a similar relative age (Brown 2013: Ch. 4). The correction of stratigraphic heights of quarries located at the bases of palaeochannel deposits that cut into underlying sediments (which host most of the Park's best preserved skeletons) (Eberth & Getty 2005; Brown 2013: Ch. 4) has been shown to resolve their individual stratigraphic accuracies, although its benefits for a more widespread correlation across the entire Park remain limited. The current situation therefore suggests that our understanding of ecological and evolutionary trends in the DPP palaeobiota is still clouded to a certain extent by taphonomic time averaging.

The taxonomic and stratigraphic resolution available for the Belly River Group (BRG) biota of DPP is higher than in most Mesozoic groups or formations with similar depositional environments, which places this locality at the forefront of the debate on the macroecological and macroevolutionary (but also taphonomic) drivers of dinosaur diversity (Barrett *et al.* 2009; Brusatte *et al.* 2012; Gates *et al.* 2012; Chiarenza *et al.* 2019; Mallon 2019). Nevertheless, the completeness of the Park's vertebrate fossil record is such that the evolution of that palaeocommunity deserves investigation at an even finer scale. Our motivation for this paper is to determine what is the very highest temporal resolution that could be reached for the BRG in DPP. Specifically, to what extent can these exposures be subdivided into series of architectural sedimentary units? To what extent would this more resolved chronostratigraphic framework support prevailing biotic turnover hypotheses that are solely founded on biostratigraphy to date and how may they provide greater resolution of the evolving local ecosystems?

Remote sensing methods that combine unmanned aerial vehicle (UAV) flights and structure-from-motion multi-view stereo (SfM-MVS) photogrammetry with ground observations are rapidly evolving in geoscience fields (Colomina & Molina 2014; Pavlis & Mason 2017; Nesbit *et al.* 2020). Image collections acquired in the field can be processed into georeferenced 3-D digital outcrop models (DOMs), 2-D orthomosaics and 2.5-D digital elevation model (DEMs) that provide significant advantages over ground-based large-scale geological surveys, as previously noted (Bond *et al.* 2007). Most importantly, UAV-based SfM methods reduce or even negate the need for *a posteriori* interpolation between isolated sedimentary logs (i.e., measured stratigraphic sections), which is inevitable in traditional mapping methods and can be error-prone. In a way, their inherent bi-and tridimensionality can be considered to connect one-dimensional dots composed of, for instance, fossil quarry locations and stratigraphic sections on a map. Additionally, their digital outputs have far higher lateral (x, y) and vertical (z) geometrical and locational accuracy than panoramic photographs traditionally used to connect the aforementioned features (see Wood 1985, 1989; Eberth *et al.* 2015). UAV-based SfM photogrammetry has already proved highly accurate for the complex badlands landscapes of Dinosaur Provincial Park, where it was applied to decisively support a fully fluvial (as opposed to estuarine or marginal marine) depositional environment for the Dinosaur Park Formation's channel meander belts (Mayo *et al.* 2023), and to map the migration of one of these sedimentary units (Nesbit *et al.* 2018; Durkin *et al.* 2020). A similar method was applied to map the geographic and stratigraphic distributions of fossil remains in the Nemegt Formation of southern Mongolia alongside stratigraphic and taphonomic observations (Fanti *et al.* 2018, 2024). These studies have shown that lithofacies identifications and measurements obtained from a well-designed DOM are at least as accurate as ground-based measurements, with the aforementioned advantage of lateral facies continuity. Considering these promising findings for the sedimentology of DPP, we have applied UAV-based SfM photogrammetry to identify four vertically successive channel-belt sequences over a nearly

500-m^2 area that encompasses the lower half of the Dinosaur Park Formation and surrounds a multigeneric bonebed (Bonebed 190, see Figure 3.1A). The identification of the erosional contacts between each of these channel cut-and-fill rhythms also prompted an estimation of the potential surface area of BB190, as well as an investigation of the effect of local variation in the nearest exposed OF-DPF contact's absolute elevation on the relative heights of the bonebed's main areas of fossil aggregation and of its more isolated individual specimens.

Stratigraphic patterns are then investigated on a more regional scale by comparing the geological setting of the BB190 area with that of four smaller areas also reconstructed using UAV flights and SfM photogrammetry in DPP. These additional projects focus on a newly discovered fossil plant locality on a ridge with a continuous exposure of the BRG from the OF-DPF contact to prairie level, a newly excavated ceratopsid skull found near the top of the Lethbridge Coal Zone, and two invertebrate localities.

3.2 Geological setting and study area

The Red Deer River valley within the bounds of Dinosaur Provincial Park displays the largest contiguous badland landscape in Canada, which was formed by bedrock erosion largely triggered by glacial meltwater since the Wisconsinian deglaciation (~15 ka ago) during the retreat of the Laurentide ice cap (Campbell 1970; Evans 2000). The dominance of smectite-rich sandstones, siltstones, and mudstones in these outcrops combined with a seasonally semi-arid regional climate with intense wind, rainfall and fluvial runoff episodes contribute to high erosion rates of 4 mm/year on average (Campbell 1970; Eberth 2005). This erosion has produced a constantly changing mosaic of buttes, mesas, rills, coulees and hoodoos with very sparse vegetation between river and prairie levels, thus presenting ideal conditions for exposing fossils. The badlands of DPP record the upper ~100 m of the 280 m thick Belly River Group. The uppermost 10-20 m of the Oldman Formation (OF) are exposed, overlain disconformably by the ~80 m thick Dinosaur Park Formation (DPF), which is itself gradationally overlain by marine shales of the Bearpaw Formation (Eberth & Hamblin 1993; Eberth 2005; Eberth *et al.* 2023). Those bedrock exposures are broadly stacked horizontally, with a ~0.05º dip to the northwest characteristic of all Upper Cretaceous strata in the North American Great Plains (Dawson *et al.* 1994; Eberth 2005; Nesbit *et al.* 2018). Although the OF originated from a lobe of the Judith River-Belly River clastic wedge that deposited sediments in a general northeasterly direction during the Claggett marine regressive cycle, the DPF originated from a separate clastic lobe that deposited sediments in a general southeast direction into a subsiding foreland basin that was undergoing increased accommodation and sediment supply throughout the Bearpaw transgressive cycle (Cant & Stockmal 1989; Eberth & Hamblin 1993; Hamblin 1997). These formations thus represent distinct events in the broader depositional history of the Belly River Group's clastic wedges, which has been shown to be more influenced by the North American Cordillera's tectonic activity (on a regional scale) than by the eustatic sea level rise which was occurring on a global scale throughout the latest Campanian (Cant & Stockmal 1989; Eberth *et al.* 2023). The contact between the sedimentary packages deposited by these two clastic lobes in DPP represents a hiatus between their respective times of deposition, and forms an erosional discontinuity which is consistently identifiable by (1) a marked facies transition from the pale ochre iron-stained sandstones of the OF to a mosaic of pale gray (often trough cross-bedded) sandstones characteristic of the DPF, and (2) contrasting gamma-ray signatures from subsurface well logs throughout southern Alberta (Eberth & Hamblin 1993; Eberth 2005, 2024; Eberth *et al.* 2023). The latest U-Pb zircon ages reveal that the OF-DPF contact forms an isochronous datum in DPP and in north-central Montana dated at ca. 76.3 Ma (Rogers *et al.* 2023), though it still appears to be time-transgressive throughout southernmost Alberta and southwestern Saskatchewan (Eberth & Hamblin 1993; Chiba *et al.* 2015; Evans *et al.* 2015; Eberth 2024). Despite this growing chronostratigraphic significance across the Western Interior Basin, the OF-DPF contact's absolute elevation has been shown to vary by up to ~30 m across DPP alone (Eberth & Hamblin 1993; Eberth 2005; Figure 3.1B), which raises the possibility that it could vary almost as substantially on an even more local scale within the present study area around Bonebed 190.

The sedimentary layers of the Dinosaur Park Formation are interpreted as successive channel meander belts cutting into (then migrating along) a wide floodplain that stretched along the eastern shore of Laramidia, with an average palaeocurrent flowing east-southeast into the advancing Bearpaw Sea (Koster *et al.* 1987; Wood *et al.* 1988; Wood 1989; Hamblin 1997). Channel cut-and-fill cycles can be designated as 'rhythms' *sensu* Wood (1985) and consist of fining-upward sequences composed of at least two of the four major lithofacies types of the DPF. In order of grain size from the coarsest (indicating a high-energy depositional setting) to the finest (low-energy), these lithofacies are (1) trough cross-bedded sandstones (TX) interpreted as either channel lag or lower point bar deposits; (2) inclined bedding sandstones (IBS) interpreted as mid-to-upper point bar lateral accretion deposits; (3) inclined heterolithic strata (IHS) consisting of interbedded sandstone and siltstone with varying ratios, interpreted as the mid-to-upper point bar lateral accretion deposits with fluctuating hydraulic energy (Koster 1983; Thomas *et al.* 1987); and (4) siltstones and mudstones interpreted as overbank (i.e. floodplain palaeosol) deposits. The most ambitious sequence stratigraphic correlation ever achieved in DPP has been undertaken over ~1 km^2 in the Cathedral area in the Park's Core (Wood 1985; Figure 3.1A): it led to the identification of six rhythms constrained by erosional contacts, which were recognized by the presence of channel lags containing intraclasts, clay-ironstone pebbles and organic debris (including fossils). Any erosional contact is thus considered a more robust datum between different channel cut-and-fill cycles than a gradational contact between TX and IHS or TX and IBS that only reflects the lateral accretion of point bars formed by the same channel (Wood 1989). Furthermore, sandstone ribbons less than 10 cm thick (interpreted as ephemeral channels pinching out at their lateral extremities) were distinguished from deeper and more laterally continuous sandstone members. Overall, these initial studies of the alluvial architecture of the DPF exposed in DPP have laid the groundwork for a correlation of individual fossil localities at a greater spatial scale. The sedimentological principles they established have now been applied to identify equivalent architectural units in a different region of the Park with a similar order of magnitude in surface area, in this case as a means to achieve chronostratigraphic research objectives with palaeoecological implications.

Bonebed 190 is situated in the Iddesleigh area of DPP, which includes approximately the eastern third of the Red Deer River's right bank within the Park's boundaries (Figure 3.1A). Although this region has been historically less explored than the Core or the Steveville badlands due to its relative isolation, it has still produced unique and spectacular vertebrate specimens, such as the near-complete holotypes of the centrosaurine ceratopsid *Styracosaurus albertensis* (Quarry 16) and the ankylosaurid *Scolosaurus cutleri* (Q080) (Lambe 1913; Nopcsa 1928) as well as an unnamed pachyrhinosaur similar to *Achelousaurus* recovered much more recently from the Lethbridge Coal Zone (Q240) (Ryan *et al.* 2010). It also contains a dense *Centrosaurus*-dominated bonebed (BB180) whose exploration led to the Park's most recently discovered bentonite, which provided additional radioisotopic dates for the local Belly River Group (Brown *et al.* 2020; Ramezani *et al.* 2022; Eberth *et al.* 2023). BB190 itself is located near the summit of a plateau that includes the upper Oldman Formation and the lower half (~40 m) of the Dinosaur Park Formation. It was first discovered on July 19, 2002, during fieldwork led by Mike Archer and Henk Godthelp (Australian Museum) (Philip Currie, personal communication, 2022) and classified as a multigeneric bonebed due to its considerable vertebrate macro- and microfossil diversity (see Eberth & Currie (2005)). One of the most significant specimens of the initial BB190 collection consists of centrosaurine partial parietals (TMP2005.009.0069) that cannot be identified at a lower taxonomic level due to their lack of preserved diagnostic characters, although they appear more similar to *Centrosaurus* than *Styracosaurus* (Royal Tyrrell Collections, 2023). Considering that these two species seem to be key members of successive megaherbivore assemblage zones in the DPF (Ryan & Evans 2005; Mallon *et al.* 2012), the high apparent stratigraphic proximity of BB190 to the hypothetical boundary between these two biozones deserved further attention.

BB190 was not explored again until mid-June 2018, when a crew of McGill University's Vertebrate Palaeontology field course found new potential outcrops of that locality in collaboration with the University of Alberta. The combination of high observed diversity with high preservation quality in BB190 initiated a long-term project aiming to estimate that locality's species richness and taxon abundances. Furthermore, an extensive Oldman-Dinosaur Park Formation contact was identified along a wide coulee located far closer to BB190 than the nearest previously identified contacts (marked as Contact 160 and Contact 162, see Currie & Koppelhus (2005: Supplementary CD-ROM)). This discovery therefore laid an additional foundation for the following study of the bonebed's geological setting since it provided an opportunity to quantify uncertainties in the stratigraphic position of BB190 while simultaneously identifying architectural units with potential stratigraphic relevance that extend beyond the study area.

The relevance of the channel rhythm succession observed at BB190 to the rest of the eastern reaches of Dinosaur Provincial Park will be assessed by comparing its observed patterns with those of four other localities surveyed by UAV during the same fieldwork program. The least extensive projects presented in this study aim to trace different horizons rich in bivalves in the Happy Jack's area of the Park (Clam04 and Clam06) as supplementary demonstrations of the potential of UAV flights and SfM photogrammetry to trace fossil beds. Another of these projects presents the geological setting of a ceratopsid skull uncovered from the Dinosaur Park Formation's Lethbridge Coal Zone in the Iddesleigh area during the 2023 field season. Lastly, the most extensive project resulting from these additional surveys presents the geological setting of a fossil plant locality in the Happy Jack's Area that was only discovered during the 2022 field season by McGill University undergraduates André Mueller and Louis-Philippe Bateman. The location of this particular site on a ridge rising from the Oldman-Dinosaur Park Formation contact to prairie level with continuous outcrop exposures creates a perfect opportunity to map a near-complete section of the Belly River Group exposed in Dinosaur Provincial Park. This creates further opportunities to compare the lower half of the plant site's section with the lower Dinosaur Park Formation preserved around BB190, and to compare the Lethbridge Coal Zone (LCZ) of the plant site's section with the LCZ succession leading to the new ceratopsid skull.

3.3 Material and methods

3.3.1 Field data acquisition

Bonebed 190 – aerial data acquisition. UAV flights were conducted around BB190 during two separate field seasons. The first two flights were conducted on August 21, 2021, and covered the entire extent of the flight area (~0.5 km^2) in overcast weather in order to minimize the presence of shadows on steeper exposures. A third flight occurred on August 14, 2022, covering a more restricted area around the most continuous outcrop exposure of the Oldman-Dinosaur Park Formation contact near the bonebed. The weather was sunnier during the 2022 flight, but the studied contact was not obscured by any shadows since it is located on a southwest-facing slope and the UAV was flown during the early afternoon.

Two multirotor UAVs were selected to capture images of the study area: a DJI Mavic 2 Pro equipped with a Hasselblad L1D-20c 16.8 megapixel (MP) digital camera with a 10.26 mm focal length and pixel size of 2.53 x 2.53 µm, and a smaller DJI Mavic Air2S equipped with a DJI FC3411 20 MP digital camera with a 8.38 mm focal length and pixel size of 2.51 x 2.51 µm. Both cameras have a 72 dpi vertical and horizontal resolution. All flights were manually piloted to avoid crashing the drone into the complex terrain, using multiple camera pitch angles. As a result, image overlap and sidelap were both estimated at 60-80% throughout each flight instead of being automated. For the 2021 flights, the DJI Mavic 2 Pro covered the entire mapped area and was flown ~80 m above the BB190 host layer in generally parallel flight lines, capturing 669 images at a 0˚ pitch angle off-nadir (with a camera exposure time of 1/400 second, F-stop of 2.8 and ISO speed of 200), while the DJI Mavic

Air2S was flown solely over the sandstone horizon hosting BB190 at ~50 m above ground level along a relatively free flight path, capturing 99 images at a 0˚ pitch angle (with a camera exposure time of 1/500 second, F-stop of 2.8 and ISO speed of 240) (Figure 3.2A-D). The 2022 flight only involved the DJI Mavic 2 Pro UAV and its path followed generally parallel flight lines, with a camera exposure time of 1/400 second, F-stop of 4 and ISO speed of 100. Its first 285 images were captured ~50 m above the top of the escarpment bearing the OF-DPF contact at a 0˚ pitch angle. Two subsequent flights were taken at a ~20 m lower elevation for the last 67 images at a 45˚ camera pitch angle to enhance coverage of the contact's subvertical surface (Figure 3.2C). A total of 1,122 images were thus recorded and processed from these flights. The flight and camera parameters for the BB190 mapping project are compared with those of less extensive projects for other localities in Table 3.1.

Considering that each UAV camera's GPS/GNSS (global navigation satellite system) receiver has a Z accuracy of ±10 m, it was deemed necessary to measure ground control points (GCPs) across the study area before each flight to increase the project's georeferencing accuracy during subsequent image processing. Six GCPs were distributed around the BB190 host horizon for the 2021 flights and six more around the exposures displaying the OF-DPF contact (three along the top of the coulee and three along the bottom) for the 2022 flight (Table 3.2; Figure 3.2E-F). GCP coordinates were recorded with a SXBlue II + GNSS GPS receiver (Geneq. Inc., Montréal, Québec, Canada). This model contains a Space Based Augmentation System (SBAS) that improves positional accuracy by using real-time differential corrections (Joyce & Moen 2018). Each of the flights lasted 60-120 minutes, with much of that time spent laying and subsequently removing GCPs.

Bonebed 190 – ground data acquisition. Fossils and stratigraphic measurements were collected at BB190 from the 2018 to the 2023 field seasons. As fossil specimens were collected from the BB190 host horizon, their coordinates were recorded (either with commercial-grade GPS receivers or the SX Blue GPS receiver) to locate them on eventual mapping projects resulting from aerial surveys (Table

3.3). As the lateral extent of BB190 was expanded, some of these specimen locations became reference points for newly identified outcrops of the bonebed, which were assigned quarry numbers BB190A-D. Stratigraphic sections were also measured on foot during the 2022 field season to establish the bonebed's geological setting using a more traditional method, using Jacob's staffs and Brunton compasses to establish bedding thicknesses. The most extensive section was measured along a footpath leading to the bonebed's northwest corner, from one of the nearest identified Oldman-DPF contacts to a hoodoo representing the highest available point of the BB190 host horizon, located between quarries BB190A, B and C (Figure 3.2E). The deeper and wider coulee lying immediately to the north has a far more continuous exposed Oldman-DPF contact and was initially considered for the stratigraphic section, yet its slopes proved too steep for the field crew to be able to take measurements. A far more constrained section was measured immediately above and below an overbank deposit marked as BB303 due to its unusual lithology compared with other outcrops of the bonebed (Figure 3.2E).

Mapping other DPP localities. Four other aerial surveys were conducted over DPP fossil localities: the HCEL Plant 2022 locality was mapped on August 17, 2023, the ceratopsid quarry on August 15, 2023, and both invertebrate localities Clam06 and Clam04 on August 20, 2022. Each of these projects necessitated a single flight along perpendicular flight lines and solely involved the DJI Mavic 2 Pro UAV, with the camera lens always oriented at a 0˚ pitch angle off-nadir. Other flight and camera parameters are compared between these projects (alongside BB190) in Table 3.1. Stratigraphic sections were measured at all four localities. The most extensive of these was measured at the plant site since it is located along a rill that bears continuous outcrop exposures from the Oldman-Dinosaur Park Formation contact (at its base) to just below the Dinosaur Park-Bearpaw Formation contact (near prairie level). The stratigraphic section for the ceratopsid quarry only extended downslope as far as the base of the underlying Lethbridge Coal Zone and the sections for the invertebrate localities only constrained to the immediate over- and underlying sedimentary layers.

3.3.2 UAV data processing

The UAV images were processed through structure-from-motion photogrammetry (SfM), an emerging 3-D modeling method based on overlapping 2-D images captured from a device in motion (see Nesbit *et al.* 2018 and references therein). SfM was performed using Agisoft Metashape Professional version 2.0.2, build 16404 (commercial software, Agisoft LLC, St. Petersburg, Russia), and a high-performance workstation (Intel® Core^{TM} i7-7820X central processing unit (CPU) at 3.60 GHz with 127.68 GB of random-access memory (RAM) and an NVIDIA GeForce GTX 1080 Ti graphics card).

The SfM photogrammetry workflow was applied through the following steps. First, all 1,122 images were imported into the same project and aligned at the highest possible accuracy through detection of automatic tie points shared by overlapping images (Figure 3.2A-D). Since the 2022 flight area completely overlapped with the 2021 flight area, the alignment of images captured during these two different field seasons was performed seamlessly without any elevation offset between the two image collections. Image alignment resulted in a sparse 3D point cloud that was already georeferenced at this stage (due to the geotags from the UAVs' GPS receivers). However, georeferencing was only completed by importing GCP data to optimize geolocation accuracy. The X, Y and Z errors for GCP and camera locations were calculated at that stage (see Appendix IV). The point cloud was then densified at ultra high quality using depth maps as source data and point confidence calculated alongside point colours in the Advanced options (Figure 3.2D). The dense point cloud was converted in two parallel workflows: (1) a 2.5-D digital elevation model (DEM, see Figure 3.2E) leading to a 2-D orthomosaic and (2) an interpolated 3-D mesh.

By classifying points into Ground and High vegetation categories and discarding the latter from the source data for DEM generation, a digital terrain model (DTM, a DEM category which only accounts for ground surface with as little high vegetation as possible) was produced. The DEM ensured accurate pixel geolocation during the removal of distortions caused by perspective from the original

UAV images, thus enabling the creation of an orthomosaic, a 2-D image preserving equal horizontal and vertical distances. A 3-D mesh was also generated with a high face count at ultra high quality to obtain a Digital Outcrop Model (DOM) aimed at improving observations of the study area's steeper terrain alongside the DEM and orthomosaic. Mesh surface resolution was improved by building texture obtained from the original UAV images. The most detailed texture was obtained through the creation of a version of the DOM that consisted of an Agisoft tiled model (.tls Agisoft proprietary file).

3.3.3 Geospatial data analysis

2-D, 2.5-D and 3-D data visualization. The DEM and orthomosaic were exported from Agisoft and imported into QGIS 3.24.1 'Tisler', an open-source geographical information system software (QGIS: http://www.qgis.org), to visually represent possible contacts between sedimentary architectural units and to quantify their elevation variation. These SfM photogrammetry output files were imported in a QGIS project alongside .csv files containing the coordinates of fossil specimens collected from BB190 in the course of this study, as well as .csv files containing all other known fossil and formational contact localities known from DPP (updated from Currie & Koppelhus 2005: Supplementary CD-ROM). Furthermore, a DEM of the entire Park curated at (and obtained from) the Royal Tyrrell Museum of Palaeontology (TMP) was imported into the same project (see Figure 3.1) to compare elevation measurements within the mapped BB190 Amphitheatre area with localities elsewhere in DPP. The tiled model version of the DOM was solely visualized in the Agisoft interface, from which 2-D renders were extracted (at a resolution of 10,000 pixels for images' horizontal axis) to create figures, and from which channel rhythm depths were measured along 20 digital vertical sections across the study area. As for the plant, ceratopsid and invertebrate sites, DOM visualization and render generation were experimented in Blender, an open-source 3-D analysis and film editing software (Community 2018). Contacts between architectural units were traced in Blender using the Grease Pencil tool while ensuring that the strokes were tied to mesh surface. Renders of the DOMs were produced by setting the camera in Orthographic mode while adjusting its orthographic scale. The location and rotation of the camera for each render were saved along the X, Y and Z axes of Blender's user interface as keyframes displayed along a timeline, from which 3-D animations can be produced. The resolution of each render was adjusted in the Render output parameters, with the compression of exported images set to 10% (instead of the usual 15%).

Digital lithofacies identification**.** The succession of sedimentary facies was carefully examined on the orthomosaic, complemented by surveys of the DOM in Agisoft. The resolution of the DOM and orthomosaic texture enabled the identification of three main facies, which broadly correspond to the 'digital facies' (dF) of Nesbit *et al.* (2018). Coarse-grained facies were identified as sandstone (dF1), which include massive, cross-bedded and ripple-laminated sandstones. It was not possible to distinguish trough cross-bedded sandstones (TX) from inclined bedding sandstones (IBS), although the former lithofacies was identified far more often in the stratigraphic section and is far more widespread in the Park (Wood 1985, 1989). Facies displaying interbedded sandstones and siltstones were identified as inclined heterolithic strata (IHS, corresponding to dF2 and dF3). Thick fine-grained facies were digitally identified as mudstones (broadly corresponding to dF4). In this study, mudstone is used as an umbrella term that also includes siltstones and claystones and is synonymous with the shales of Wood (1985, 1989). Since the main architectural units that we were aiming to identify consisted of entire rhythms initiating as coarse-grained sandstones then fining upward into massive mudstones, a more subdivided facies classification (as in Durkin *et al.* (2020)) was not deemed necessary.

Facies identification led to tracing polylines (i.e., sets of consecutive points connected by straight line segments) along continuous contacts identified between architectural units, as well as correcting the identity of some lithological units which were erroneously identified in ground-based stratigraphic sections. Elevation contour lines were extracted in QGIS from the BB190 DEM (one set at 5 m intervals and another at 1 m intervals) and saved in a layer overlying the orthomosaic surface to rapidly assess elevation variation within and among neighbouring contacts during the polyline tracing process.

Horizontal and vertical distance measurements. The horizontal length of each of the BB190 Amphitheatre area's architectural unit contacts was measured as the sum of the distances calculated for each polyline traced along the orthomosaic in QGIS. This is also where the bonebed's minimum surface area was calculated by connecting its most distant fossil localities with a polygon. The *Sample raster values* algorithm (found in the QGIS processing toolbox) was used to obtain the elevation of fossil localities and of architectural unit contacts estimated from the DEM. The GPS readings recorded for the most significant collected fossils enabled comparisons of absolute and relative elevations between field-based and DEM-derived estimates. For each of the continuous contacts exposed throughout the BB190 mapped area, series of points were produced from their corresponding polylines at a 5 m interval using the *Points along geometry* sampling algorithm (also in the QGIS processing toolbox). Once the DEM-generated coordinate data was obtained from QGIS, it was exported into .csv files that were processed for graphical and statistical analyses on elevations of fossils and architectural unit contacts in R v 2024.04.0 Build 735 (R Core Team 2023).

The elevation of the Oldman-Dinosaur Park Formation (OF-DPF) contact identified around BB190 was compared with those of 10 previously identified contacts located east and west of that locality along the Red Deer River's right bank (in the Iddesleigh area of the Park). This necessitated extracting coordinates from the DEM covering the entire Park (beyond the immediate BB190 Amphitheatre area). With this data, the variability in the elevation of the OF-DPF contact could be compared between a region where that contact was measured repeatedly at a very high spatial density (within the BB190 Amphitheatre area) and a more extensive region where it was measured at a much lower density (i.e., previously identified contact locations). The mean, variance and standard deviation of the contact's elevation were thus compared between these two groups of sampled points. Before statistically comparing the means, a Levene's test was undertaken and produced a *p*-value of 0.7205 (F value = 0.1284, df = 1), which indicates that the null hypothesis of variance homogeneity between the two groups cannot be rejected. Therefore, the means were compared using a 2-sample *t*-test assuming equal variances. The same statistical tests were used to compare the mean elevation of the contact points sampled around BB190 with the mean elevation of 48 contact locations measured along the Park's public loop road (see Figure 3.1B), since the latter is the area of the Park where the OF-DPF contact was measured at the highest spatial density prior to this study.

Additionally, mean heights and standard deviations above the OF-DPF contact for the main quarries identified across BB190 (obtained from the DEM generated in this study) were compared between three groups of selected contacts: (1) Contacts 160 and 162; (2) 10 contacts sampled within a very localized area, at 15-20 m intervals along the north slope of the coulee with the most continuous OF-DPF contact exposures; (3) 11 contacts sampled across the entire extent of the BB190 DEM (including Contacts 160 and 162). Each of these groups included the highest and lowest possible points to obtain the entire range of relative heights. To test whether mean relative height was significantly different for at least one of these groups of contacts, a one-way analysis of variance (ANOVA) was performed. The ANOVA was chosen because Levene's tests confirmed the statistical homogeneity of each group's variance.

To quantify the elevation uncertainty of the DEM, the root mean square error (RMSE) of elevation readings of the most accurately measured sites located in the study area and not used for DEM georeferencing was calculated. The selected check points were as follows: four individual specimen locations recorded with the more accurate GPS receiver during their excavation, the original BB190 quarry stake and the locations of Oldman-DPF contacts 160 and 162. The latter three were recorded with a differential GPS receiver during the early 2000s, so must be similarly suitable check points (Currie & Koppelhus 2005: Supplementary CD-ROM; MacDonald *et al.* 2005). GCPs were not considered as check points since they had already been used to calibrate the entire mapping project.

RMSE was thus calculated as the square root of the mean of all squared differences in elevation between the GPS readings and the predicted elevations extracted from the DEM in QGIS. Since the variation in elevation of the local Oldman-DPF contact measured on the BB190 DEM will eventually be compared with the variation in that contact's elevation across the entire Park, the RMSE of the DEM provided by the TMP was also calculated based on the observed and predicted elevations of almost all skeleton quarries and bonebeds previously measured with the differential GPS (Currie & Koppelhus 2005: Supplementary CD-ROM; MacDonald *et al.* 2005). After the removal of outliers (with elevation difference > ±10 m), the elevation RMSE of the DEM covering the entirety of DPP was ±2.18 m. If collected skeleton quarries alone (minus outliers) were considered, the RMSE was decreased to ±1.72 m. Considering that the first individual skeleton quarries to be relocated were marked with quarry stakes by C.M. Sternberg (Currie 2005; Tanke 2005), unlike other sites such as bonebeds, the RMSE derived from quarries alone is likely derived from more accurate GPS readings and is thus selected over the more conservative RMSE.

3.4 Results

3.4.1 Bonebed 190 – description of architectural units

The mapping project of the BB190 Area produced through SfM photogrammetry covered 0.446 km^2 of Dinosaur Provincial Park, at a ground resolution of 1.91 cm/pixel, with a GCP elevation RMSE of 0.42 m and a DEM elevation RMSE of ±1.09 m (Table 3.1). A summary examination of the orthomosaic reveals that BB190 is located at the summit of a plateau that widens between two primary coulees flowing to the northwest (Figure 3.3). The plateau displays crenellated northern and western margins created by alternating rills and coulees. The bonebed's host horizon is a thick sandstone preserved in an almost semi-circular shape with lower horizons dipping towards the circle's centroid, hence the designation of this entire plateau as the BB190 Amphitheatre area. Almost all the fossils found within the orthomosaic's extent during this study have been uncovered along the lower contact of this sandstone unit. The minimal surface area of BB190 has been estimated at ~91,200 m^2 by connecting its most distant fossil localities into a polygon on QGIS. The Dinosaur Park Formation in the BB190 Amphitheatre area is interpreted to contain four architectural units representing a channel rhythm succession through time (above the Oldman Formation). They were identified by examining the entire extent of the DOM and orthomosaic and were all found at the site of the main stratigraphic section as well (Figure 3.4A-B).

The Oldman-Dinosaur Park Formation contact. The coulee that forms the northern margin of the BB190 Amphitheatre area has the longest continuous exposures of the Oldman-Dinosaur Park Formation (OF-DPF) contact in the study area (Figure 3.3). These exposures lie further away from the river than the two contact points that were previously measured in the vicinity (Contacts 160, 162). They display a sedimentary transition which is always indicative of the presence of this formational contact, from the massive ochre coarse-grained sandstones of the Oldman Formation to the pale grey, often trough cross-bedded, sandstones of the Dinosaur Park Formation (Figure 3.5A-C). The OF-DPF contact is also detected, albeit less extensively, in a secondary coulee along which the stratigraphic section was measured (Figures 3.4A-B, 3.6A), as well as a butte located West of the BB190 Amphitheatre area along which Contact 162 was located (Figure 3.3). The ochre to grey sandstone succession is often broken by a massive silty ironstone whose upper margin is level with the contact (Figure 3.5A-B). This facies is commonly found across the Park at this level (Eberth *et al.* 2023: figure 2), although it is replaced by a clay-ironstone intraclast table at the lowest point of the stratigraphic section (measured at 658 ±1 m, Figure 3.4A-B).

The OF-DPF contact had variable elevations that were quantified across the BB190 mapped area (Figure 3.7A-B). Across both northern and southern slopes of the aforementioned coulee, the contact's absolute elevation fluctuated significantly since the root mean square error (RMSE) of 1.09 m derived from the DEM is far lower than the observed elevation range of 8.36 ± 2.18 m (Table 3.4;

Figure 3.7A). The northern slope's contact (shown on Figure 3.5A-B) has a mean height of 659.79 m with a standard deviation of 1.52 m. That same contact was selected to sample points as references for the relative height of BB190 quarries and fossils. The southern slope's contact has a mean height of 660.38 m with a standard deviation of 2.22 m. The elevation range of all 182 OF-DPF contacts within the BB190 mapped area (including less extensive contact exposures) was then compared to that of the 10 nearest contact localities known prior to this study, distributed along the entire eastern third of the Red Deer River's right bank within DPP (Figures 3.1A-B, 3.7B). In this dataset (based on the DEM covering the entire Park), the BB190 contact series is shown to have an elevation range of 11.52 ± 3.44 m and a mean elevation of 658.64 m with a standard deviation of 2.47 m (Table 3.4). The 10 other contacts have an elevation range of 7.92 ± 3.44 m, with a mean elevation of 659.46 m and a standard deviation of 2.66 m. The high density of points sampled from the BB190 contact series also reveals frequent fluctuations in absolute elevation, with at least 3 apparent peaks over an east-west transect of barely 600 m. That local variability is higher than in the 10 other contact points (likely due to a higher sample size covering a smaller geographical area), yet a 2-sample *t*-test revealed that the means between the two groups do not differ significantly ($t = -1.0237$, $df = 190$, p-value $= 0.3073$). Considering the small size of the latter sample, the BB190 OF-DPF contact was then compared with one of the OF-DPF contact exposures with the highest density of measured points prior to this study, the ~2 km^2 area that includes the Royal Tyrrell Museum field station and the Park's public loop road (Figure 3.1A-B). Those 48 sampled points have an elevation range of 11.51 ± 3.44 m, with a mean elevation of 654.28 m and a standard deviation of 2.88 m (Table 3.4). A Levene's test confirms that the variances are homogeneous between the 'public loop road' and the BB190 groups of points sampled along the OF-DPF contact (F value $= 1.3146$, $df = 1$, p-value $= 0.2528$). Therefore, a 2-sample *t*-test was performed between these two groups and showed that the contact around the public loop road has a significantly lower mean elevation than the contact in the BB190 Amphitheatre area ($t = 10.5$, $df = 228$, *p*-value = $2.2e^{-16}$). The Oldman Formation is exposed for 12-15 m depths below the OF-DPF contact in the BB190 Amphitheatre area, which is consistent with analogous outcrops throughout the Park.

Rhythm 1. The OF-DPF contact is considered a reliable datum for the base of Rhythm 1. It is confidently identified for 821 of the 1,595 m traced on the entire orthomosaic for Rhythm 1's lower contact, and tentatively identified for the remaining distance. The only feature indicative of the contact for the remainder of that distance is the massive silty ironstone cap that often crops out at this level (Figure 3.4A). The depth of Rhythm 1 varies between 5.6 and 11.5 m across the 11 digital sections along which it was measured (Table 3.5). This variation is attributed to exposures where its channel base dips significantly (Figure 3.5C) combined with exposures where it is downcut by the overlying Rhythm 2 (Figure 3.6B). The first trough cross-bedded sandstone (TX1) outcrops at the base of the section for 1.78 m above the OF-DPF contact. TX1 is cut by a siltstone drape reaching a ~2-m thickness in the section's trajectory. The drape then pinches out either side of its maximum depth and is capped by a clay-ironstone intraclast table before being overlain by two more metres of sandstone. TX1 has a gradational contact with IHS1, which extends upwards for 1.25 m. MUD1 is not clearly visible on the northern outcrop of the coulee where the field section was measured, but it is on the southern one (Figure 3.4B). The points sampled along Rhythm 1 (including those sampled from the clearly defined Oldman-Dinosaur Park Formation contact) have a mean elevation of ~660 m (Table 3.4; Figure 3.7C).

Rhythm 2. Rhythms 1 and 2 were initially considered as a single indivisible architectural unit in the field, but closer examination of the entire DOM revealed that they were distinct. A few outcrops bear a laterally continuous clay-ironstone table that separates a thin underlying mudstone unit (interpreted as MUD1) from an overlying sandstone often laterally accreting into IHS (interpreted as TX2/IHS2) (Figure 3.6A-B). This suggests an erosional contact where a new channel cut into MUD1, thus initiating a new channel cut-and-fill sequence. Where vertical amalgamation of channel deposits prevents the use of a mudstone bed as a datum (e.g. Figure 3.5C), changes in direction of lateral accretion can be the only line of evidence for the presence of an erosional contact during digital observations (Figure 3.6A). Along the stratigraphic section, TX2 has an erosional contact with IHS1 marked by the same clay-ironstone intraclast table found throughout the study area (Figures 3.4A, 3.5A-B, 3.6B). On the northern rill of the coulee, TX2 is only 0.8 m thick before being overlain by MUD2. On the rill forming the southern edge of the stratigraphic section's coulee, TX2 is much deeper and displays extensive lateral accretion into IHS as Rhythm 2 downcuts Rhythm 1 (Figure 3.6A). MUD2 extends for a total of ~4.3 m along the section and is cut by two channel ribbons: a deeper 1-m thick trough cross-bedded sandstone unit (visible on both sides of the coulee) and a shallower ~0.8-m thick IHS that appears to accrete laterally into IBS. Such sandstone ribbons are deceptively common within MUD2 along several outcrops of the mapped area: they often appear to represent the base of a new rhythm, yet they often pinch out laterally (Figures 3.5A-B, 3.6A). Across the study area, Rhythm 2 has a lower contact traced for 1,558 m at a mean elevation of ~666 m (Table 3.4; Figure 3.7C), with depths ranging from 5.0 to 10.7 m (Table 3.5).

***Rhythm 3*.** This architectural unit displays the stratigraphic section's most straightforward fining-upward sequence, with a 1.43-m thick TX3 overlain by a ~2.25-m thick IHS3 and then a massive 5.75-m thick MUD3 unit (Figure 3.4). The contacts between these units are all gradational despite the odd clay-ironstone intraclast table at the TX3-IHS3 contact. Across the study area, Rhythm 3 has a lower contact traced for ~2,004 m at a mean elevation of ~674 m (Table 3.4; Figure 3.7C), with depths ranging from 9.9 to 14.9 m (Table 3.5). MUD3 is thicker, with depths ranging from 3.8 to 6.9 m (Table 3.5) and is more continuous than the other mudstone units within the mapped area (Figures 3.3-3.6). Its lower contact (estimated due to its oft-gradational nature with underlying IHS) is traced for 3,122 m at a mean elevation of ~681 m (Table 3.4; Figure 3.7C). Its upper contact (with Rhythm 4, which hosts BB190) has been traced for 3,463 m, at a mean elevation of ~686 m (Table 3.4; Figure 3.7C). Since this contact is consistently present across the mapped area and is relatively easy to identify, it constitutes a reliable datum (in addition to the OF-DPF contact) for estimating the relative heights of the fossil quarries explored throughout this project.

Rhythm 4 – the Bonebed 190 host horizon. This unit caps the plateau at the summit of the Bonebed 190 Amphitheatre area, but its entire depth is not preserved in the immediate vicinity of the bonebed due to postglacial erosion (Figure 3.4B). A closer examination of the sediments hosting BB190 in the vicinity of the main stratigraphic section reveals that a very shallow clay-pebble conglomerate marks the erosional edge between the MUD3 and TX4 units (Figure 3.4C). This conglomerate is characteristic of a paleochannel base lag and the most fossil-rich horizon of BB190 lies just above it, at the base of a trough cross-bedded sandstone (TX4) extending for ~7.1 m until a coarse cemented sandstone cap that marks the end of the stratigraphic section. The clay-pebble conglomerate appears to grade into a clay-ironstone table composed of larger nodules at more eastern exposures of the base of Rhythm 4, as seen near the collection sites of fused tyrannosaur nasals and of a tyrannosaur dentary near the original BB190 quarry stake (Figure 3.8A). The entire depth of Rhythm 4 can only be measured at the eastern extremity of the mapped area, where absolute elevation increases again beyond the BB190 plateau. This is where TX4 fines eastward into IHS4 until it appears to be erosionally overlain by a rhythm that does not sufficiently extend into the mapped area to be traced continuously (Figure 3.6C). Rhythm 4 has a depth ranging from 13.1 to 14.5 m below this possible contact (Table 3.5). This places the highest reaches of the mapped area at an absolute elevation of ~702 m, around 44 m above the local OF-DPF contact's mean elevation.

All identified BB190 quarries are traced to the same horizon at the base of TX4: these include the original BB190 locality, which hosts a highly productive vertebrate microsite, as well as the BB190A-C extensions (Figure 3.8A-G). BB190A, the most extensive macrofossil quarry of the area so far, is notable for its high abundance of ankylosaur remains and its map has been successfully overlain on the orthomosaic to demonstrate that the latter has a sufficiently high resolution for displaying fossil collecting data (Figure 3.9A-C). BB190B and C have the greatest proximity to the trajectory of the stratigraphic section (Figure 3.4B), with the latter yielding one of the most impressive specimens of the entire area in the form of a centrosaurine ceratopsid nasal horncore (Figures 3.8F). BB190C was initially thought to be in a higher horizon than the other quarries since it had a GPS reading ~1.5 m higher than the bonebed horizon base measured a few metres away (Figure 3.4A-B). However, an observation of its depositional setting confirms that it was formed in the same horizon. An uncollected articulated hadrosaur skeleton consisting of a heavily eroded vertebral series locked in ironstone is also reported just east of BB190's main localities in the same horizon (U197, see Figure 3.3).

Most of the upper horizons of TX4 do not display any fossil aggregations qualifying as bonebeds, although they have yielded well preserved isolated specimens such as a centrosaurine squamosal, a complete toothless hadrosaur dentary and fused tyrannosaur nasals (Figure 3.8A-G). The only exception consists of a low-density hadrosaur-dominated bonebed in a narrow coulee, ~1.5 m above the BB190 horizon (BB303, Figure 3.9D-F). Instead of lying in a channel base lag, most of the bones of BB303 are associated with a sandstone that coarsens upwards into a 20-cm thick clay-ironstone intraclast table extending for around 10 m^2. A few of them were even found within the ironstone lens itself (Figure 3.9E). This lithological setting is indicative of a very local overbank levee deposit formed during the migration of the TX4 paleochannel across the surrounding floodplain.

Estimating the stratigraphic position of Bonebeds 190 and 303. A total of 7 bonebed and 24 individual fossil specimen localities had their coordinates recorded during the exploration of BB190 (Table 3.3). Together, they constitute an ideal dataset to investigate the effect of the variation in absolute elevation of architectural unit contacts on the measured stratigraphic positions of individual specimens and bonebeds. First, the effect of the local variability in elevation of the local Oldman-Dinosaur Park Formation contact was assessed by comparing the means and standard deviations of the heights of each marked specimen relative to three different groups of sampled points (Table 3.3, Figure 3.10A). Overall, mean heights measured from Contacts 160 and 162 alone were consistently lower than heights based on the 10 points sampled along the same exposure, as well as heights based on 11 more distant points distributed across the entire traced contact (Figure 3.10B). On the other hand, mean heights obtained from the latter two groups were almost identical (within ~7 cm). For instance, the BB190A quarry had a mean height of 25.45 m above the groups consisting of Contacts 160 and 162, but mean heights of 28.06 and 27.99 m above the groups consisting of the 10 close contacts and the 11 distant contacts, respectively. However, the standard deviations displayed a different pattern between these three groups: for each locality, the 'Contact 160 and 162' group had a range of ~2.7 m and a standard deviation of 1.89 m; the group of 10 close contacts had a range of ~6.3 m and a standard deviation of 1.94 m; and the group of 10 more distant contacts had a range of ~8.9 m and a standard deviation of 2.95 m. Therefore, the group of 10 OF-DPF contact points sampled along the same coulee had a lower variability in elevation than the group with a similar sample size assembled from scattered exposures of the contact, because the former were far more clustered around their mean (Figure 3.10B). In fact, the variability of the group restricted to that coulee was more comparable to that observed in the group solely consisting of Contacts 160 and 162, despite having a ~3m difference between their means. The one-way ANOVA between the three groups produced an F-value of 0.9674 (df = 2, *p*-value = 0.3972), therefore the null hypothesis of statistically homogeneous means between the three groups was not rejected.

The heights of those same fossil specimens were also compared relative to the base of their host horizon, i.e. the MUD3-Rhythm 4 contact, using field-based and DEM-derived absolute elevations (Figure 3.10C). For the DEM-derived data, each specimen's height was measured relative to the nearest point sampled along the Rhythm 4 contact. Since those contacts were not always measured in the field, several field-based heights were measured based on the contact that was recorded along the stratigraphic section, which explains occasional negative values for specimens located far from that contact. The use of this alternative datum shows that BB190C falls well within the first 50 cm above the base of Rhythm 4. It means that this quarry was likely part of the same specimen accumulation event as the other BB190 quarries. Nonetheless, the DEM-derived heights suggest the presence of a second, far less productive, bone horizon since BB303 and several more isolated specimens fall 1-1.5 m above the channel base (Figure 3.10C). However, it must be noted that none of the heights reported between the lowest horizon and the proposed slightly upper horizon are statistically significant due to the propagation of absolute elevation errors for each specimen-contact pair. Unsurprisingly, the only two specimens significantly higher than the others are a hadrosaur dentary and a fragmentary maxilla that were collected east of all main quarries of the bonebed.

3.4.2 Alluvial architecture of other DPP localities

HCEL Plant 2022. The mapping project for the 2022 plant site was based on 279 images and covered 0.09 km^2 of Dinosaur Provincial Park, at a ground resolution of 1.85 cm/pixel, with GCP elevation RMSE of 5.2 cm and a DEM elevation RMSE of 1.47 m (Table 3.1; Figure 3.11). The lower portion of the stratigraphic section is presented in Figure 3.12 and its upper half in Figure 3.13 alongside orthographic elevation renders of the corresponding outcrops. A massive 46-cm thick silty ironstone with a distinctive dark orange colour marks the Oldman-Dinosaur Park Formation contact at the base of the section. That unit is overlain by a 63-cm thick compact, tabular, almost white siltstone, then an olive gray mudstone for the next 2.6 m. The next 8.16 m of the section consist of a thick trough cross-bedded sandstone capped by a ~7-cm thick clay-ironstone intraclast table, which is overlain by another olive gray mudstone with a depth of 2.76 m this time. The sandstone becomes substantially pinched out along both northeast and southwest sides of the rill, and conversely the overlying mudstone thickens so much in those same directions that it appears to merge with the lower siltstone. The only other place where the sandstone thickens again is along a smaller rill located ~100 m due north of the base of the stratigraphic section (Figure 3.11). This architecture, combined with an apparent lack of lateral fining into inclined heterolithic strata or inclined bedding strata, suggests that this TX represents a channel ribbon that ephemerally cut into a single massive mudstone, and not the base of an additional rhythm. The mudstone is erosionally overlain by an 8.6-m thick trough cross-bedded sandstone with rare silt and mud stripes and a coarser cemented sandstone unit halfway up. Above that massive unit lies yet another mudstone for 1.75 m, which is locally cut by a shallow sandstone ribbon ~60 cm thick. The latter is the host unit of Bonebed 234. The next unit consists of a 4.6-m thick series of inclined heterolithic strata (IHS) that grade vertically and laterally into inclined bedding and trough cross-bedded sandstones, which form a butte that rises in isolation from the main slope of the rill leading to prairie level. The lower 3.7 m of the IHS contain five horizons in fine-grained sandstone to coarse-grained siltstone containing varying abundances of fossil angiosperm and gymnosperm leaves, plant hash and fragmentary invertebrate fossils, as well as Bonebed 233. The lowest fossil plant horizon's elevation is measured at 688.0 ± 0.8 m, which is 26.4 ± 1.8 m above the Oldman-Dinosaur Park Formation contact measured at the base of the ridge. A headless hadrosaur skeleton quarry (Q053) located north-northwest of the butte also appears to be from one of the same horizons and is also used as a check point (Figure 3.11). The GPS readings obtained for that skeleton, along with the main fossil plant layer, were used as check points to measure the RMSE of the DEM covering the entire ridge (Table 3.6). The contact between the IHS and the overlying sandstone is at the same elevation on both southeastern and northwestern extremities of the butte and is locally marked by a clay-ironstone intraclast table. An eroding hadrosaur scapula is reported at the base of that sandstone up-section from Q053. The sandstone has a very shallow cemented interval midsection and has a few mud drapes near its gradational contact with a 1.35-m thick mudstone that thickens laterally in both directions. Another thick TX follows for 7.71 m and completely downcuts the aforementioned mudstone ~100 m due west of the point of the section where its base was measured. This sandstone contains occasional ironstone and silt/mud drapes before fining upward into a gradational contact with the last mudstone (which is 1.45 m thick) before the Lethbridge Coal Zone's lower contact. The LCZ's main coal unit is 65 cm thick along the section's trajectory, then is overlain by a 5.75-m pale gray mudstone. The latter unit fines into a silt-claystone marl with some coal for 43 cm just below its midsection. A finer-grained marl with more coal completely overlies that last thick claystone unit for ~1.2 m before being overlain by a ~3.5-m thick TX and a ~2-m thick pale gray mudstone before prairie level. There is no trace of the Dinosaur Park-Bearpaw Formation contact in the section, which likely means that the LCZ is not fully preserved here. The last sandstone pinches out laterally (east and west of the section, see Figure 3.11) into a ribbon so that the uppermost horizon of the LCZ is usually dominated by the gray mudstone, in contrast to the pattern observed at the stratigraphic section.

Lethbridge Coal Zone ceratopsid quarry (Q300). The mapping project for Quarry 300 was based on 286 images and covered 0.034 km^2 of Dinosaur Provincial Park, at a ground resolution of 1.11 cm/pixel, with a GCP elevation RMSE of 11.7 cm and a DEM elevation RMSE of 64 cm (Figure 3.14; Table 3.1). The stratigraphic section was measured from the quarry in which the ceratopsid skull was excavated (elevation ~743 m) to the upper boundary of the Lethbridge Coal Zone's deepest coal unit (elevation ~728 m) (Figure 3.15). Lateral tracing of the identified lithological units revealed that the section was measured across a local slump in the LCZ's sedimentary succession (e.g. Figure 3.15E). The LCZ lower contact has an estimated elevation ranging between 722 and 723 m along the log. The uppermost coal horizon of the LCZ's main coal unit has a colour closer to jet black than the underlying coal, which is dark brown to russet instead. The LCZ's main coal unit is overlain by a 1.8-m thick pale gray siltstone, which is then capped by a clay-ironstone intraclast table. A silt-claystone marl follows for 1 m, then gives way to a tan shale with minor silt for 1 m. This unit is overlain by 6 m of dense olive gray mudstone, which hosts two clay-ironstone intraclast tables (each 10 cm thick, elevation ~740 m) near its upper boundary. The claystone then coarsens into a 70-cm thick pale grey siltstone ledge, this time containing a 2-cm thick strip of very coarse-grained silty ironstone 20 cm below its upper boundary. Above that lies a black shale strip barely a few centimetres thick, followed by 1.2 m of tan shale with minor silt leading to the quarry's erosional edge less than 1 m below prairie level. The black shale was likely deposited during an anoxic event relatively high above the LCZ lower contact, but is unlikely to represent a contact between the Dinosaur Park and Bearpaw Formations because the overlying tan siltstone is more indicative of non-marine floodplain deposits (Brinkman *et al.* 2005). Since the latter is not fully preserved above Q300, the DPF-Bearpaw Formation contact (sensu Eberth & Hamblin 1993) is not exposed there either. The ceratopsid quarry's elevation is measured at 743.26 ± 0.48 m, which is 15 ± 0.82 m above the nearest coal layer of the LCZ (Table 3.6).

Invertebrate localities. The mapping project for Clam04 was based on 339 images and covered 0.023 km^2 of Dinosaur Provincial Park, at a ground resolution of 0.715 cm/pixel, with a GCP elevation RMSE of 60.8 cm (Table 3.1). The mapping project for Clam06 was based on 265 images and covered 0.01 km^2 of Dinosaur Provincial Park, at a ground resolution of 0.815 cm/pixel, with a GCP elevation RMSE of 52.12 cm (Table 3.1). No DEM RMSE is available for either of these projects since no sites were measured as check points. These two invertebrate localities were revealed to have marked differences in their lithology and stratigraphic position. Clam06 lies within the Oldman Formation since its horizon with the highest bivalve density is in a massive ~30-cm thick silty ironstone bed at an elevation of 657.3 m, which is ~2.5 m below the Oldman-Dinosaur Park Formation contact (Figure 3.16). The shells in this horizon are often complete and appear to have been open before burial. The OF-DPF contact is highly visible at this locality since it consists of a boundary between the ochre siltstone of the Oldman Formation and the olive gray sandstone of the DPF, which occasionally coarsens laterally into a thick silty ironstone ledge with a similar lithology to the main bivalve bed (Figure 3.16D). This unit is underlain by an olive-gray siltstone for ~3 m and is overlain by a ~1-m thick ochre mudstone containing bivalve shells that are cracked almost to a powdery state (Figure 3.16E). Along the overlying ~1 m, there is an alternating pattern of unstructured sandstone and ochre silt- and mudstone horizons, followed by a clay-ironstone intraclast table. The latter is situated around two thirds of the way up from the sandy ironstone that forms the main bivalve horizon and the sandy ironstone that forms part of the local OF-DPF contact.

In contrast to Clam06, Clam04 lies much higher above the OF-DPF contact, although this can only be inferred from absolute elevation (663 m) since the contact is not clearly exposed at this locality (Figure 3.17). The mapping of the Clam04 locality revealed that it laterally extended across the coulee from which it was initially located (Figure 3.17A, D). Its uppermost bivalve host horizon consists of a 10-cm thick clay-ironstone intraclast table containing complete shells and sparse dinosaur bones along its lateral extent. It overlies a ~30-cm thick cemented sandstone with broken shells, some of which can be viewed in cross-section on the outcrop. Below that lies a succession of olive green to pale gray siltstone and mudstone beds, the uppermost of which having a ~1 m thickness with more broken shells and the occasional dinosaur bone (Figure 3.17B).

3.5 Discussion

In this project, the BB190 Amphitheatre area and nearby fossil localities in the Happy Jack's and Iddesleigh areas proved an ideal palaeoecological study system to investigate three questions concurrently. First, we assessed the impact of the local Oldman-Dinosaur Park Formation contact's absolute elevation variability on the measured stratigraphic position of BB190, along with its biostratigraphic implications for Dinosaur Provincial Park as a whole. Second, we assessed the potential of some architectural units along BB190's stratigraphic succession as marker beds that could be identified along the Park's Belly River Group exposures. Third, we assessed the efficiency of UAV-SfM mapping methods to digitally expand the reconstruction of stratigraphic architecture laterally throughout a relatively broad and complex study area.

3.5.1 The impact of the Oldman-Dinosaur Park Formation contact's elevation variability on stratigraphic distributions

The presence of laterally continuous exposures of the Oldman-Dinosaur Park Formation (OF-DPF) contact at the base of a stratigraphic succession with a mixed faunal bonebed created an opportunity to investigate the extent to which a fossil locality's elevation (and therefore stratigraphic position) relative to that ubiquitous datum can vary in Dinosaur Provincial Park. The OF-DPF contact's elevation was already known to vary by as much as ~30 m over the ~20 km east-west transect of Dinosaur Provincial Park, despite forming an isochronous datum within that same transect. In this respect, one of the key results of the present study is that the OF-DPF contact is now shown to vary substantially by ~10 m (including RMSE) through a single coulee stretching for barely 300 m near Bonebed 190. Relative height estimates for the bonebed's quarries also suggest that the standard deviation associated with the contact's mean elevation increases if that mean is calculated from a high sample size, and that this increase in variability can be tempered if the sample of measurements is located within a single slope of badlands instead of being located across different coulees and buttes. When RMSE is accounted for, the OF-DPF contact's elevation mean and variance (from a ~11.5 m elevation range) observed over a ~600 m east-west transect across the area mapped around that bonebed were not significantly different from the elevation mean and variance (from a ~8 m elevation range) observed across the 10 nearest contacts spread over a ~4.5 km east-west transect along the Red Deer River.

The admittedly low sample size of the latter series prompted us to quantify that elevation variation elsewhere in the Park, this time around the field station and public loop road where the OF-DPF contact was measured at the highest spatial density prior to this study. The elevation range and variance obtained for that sample over a ~2 km east-west transect was found to be very similar to those observed across the BB190 area, which suggests that the important fluctuations in local elevation observed around BB190 are in no way restricted to the eastern reaches of DPP. However, the detection of a statistically lower mean elevation for the contact around the public loop road compared to the BB190 Amphitheatre area (the former being located 8-9 km to the west) was not very surprising, since it confirms previous observations of a structural dip of the Belly River Group's strata to the northwest (Eberth & Hamblin 1993; Eberth 2005). These results altogether demonstrate that the OF-DPF contact in the Park can have a similar elevation range on a very local scale to an exposure of the same datum extending on a different spatial order of magnitude. In this way, they confirm a hypothesis that was widely accepted in the geoscience community due to the clear erosional nature of the discontinuity the contact represents (Eberth & Hamblin 1993; Eberth 2005; Rogers *et al.* 2023), but crucially never tested quantitatively until this study. Furthermore, we predict that the frequent peaks and troughs revealed by the detailed tracing of the contact around BB190 will also be detected across the longer transects to which it was compared once the latter are examined in greater detail with a higher density of sampled points and that this pattern will become ubiquitous across Dinosaur Provincial Park. The UAV-SfM photogrammetry method applied in this study has been shown to be a highly promising means of achieving that particular objective. The fact that the OF-DPF contact's elevation can vary by ~10 m along a single coulee among outcrops exhibiting ~0.05º structural dip implies important palaeorelief on the contact's erosional surface. In turn, this means that the oldest channel rhythms ever deposited in the Dinosaur Park Formation may well have been completely downcut by more recent ones.

It is understandable that the previous research focused on the OF-DPF contact so rarely led to a quantification of its local elevation variation because it was conducted with chronostratigraphic objectives in mind, and such variation remains irrelevant at the temporal scale of the geological drivers of the Judith River-Belly River clastic wedge. The only attempt to visualize that pattern occurred as part of an investigation of the geographical and stratigraphic distribution of the Park's dinosaur skeletons (Currie & Russell 2005). Now, the present study shows that this variation is worth understanding quantitatively among the outcrop locations of this contact in the Western Interior Basin from a palaeontological perspective. This is especially relevant for a system such as DPP that presents such a complete fossil record with strong evidence of turnover in community structure and composition occurring on 10^5-10^6 yr temporal scales, where the currently accepted stratigraphic distributions of species at the foundation of this evidence have been universally derived from individual fossil specimens' heights relative to the OF-DPF contact itself (Brinkman 1990; Ryan & Evans 2005; Mallon *et al.* 2012; Cullen & Evans 2016; Mallon 2019; Eberth *et al.* 2023). A visualization of the maximum possible range in the height of BB190 relative to its nearby OF-DPF exposures in the context of DPP's general stratigraphy shows that this range (including root mean square error propagation) represents ~15% of the Park's entire average outcrop depth and ~20% of the average depth of the Dinosaur Park Formation alone (Figure 3.18). This indicates that the estimated relative height of a given skeleton or bonebed is highly dependent on the location of its referred OF-DPF contact even within a few hundred metres, and so that several reference points along that contact are ideally recommended to quantify that height uncertainty. It therefore introduces an additional source of error on the stratigraphic position accuracy of any fossil in the Park, which is in the same order of magnitude as the maximum error (14.5 m) calculated from the location of several *Centrosaurus apertus* specimens at the bottom of palaeochannels that downcut underlying sediments (Brown 2013: Ch. 4). It was already acknowledged that the latter source of error could exceed the entire vertical distance of the Park's more constrained observed stratigraphic distributions, such as that of *Styracosaurus albertensis* (Brown 2013: Ch. 4). Now, results from BB190 suggest that these very distributions may not be estimated from the OF-DPF contact as accurately as was previously assumed, even after correcting the stratigraphic heights of palaeochannel-hosted specimens. Furthermore, the position error arising from the OF-DPF contact's heterogeneous elevation differs from the error derived from palaeochannel host horizons in two important respects. The first (and more important) one is that the latter error can be corrected by identifying the elevation of the upper boundary of a given fossil's host rhythm (which can also vary locally depending on its erosional or gradational nature, see Wood (1989)), while no such simple correction exists regarding the OF-DPF contact. The calculation of descriptive statistics (i.e., mean and standard deviations and errors) for relative height as demonstrated for BB190 may represent the most accurate possible correction in that case, although the uncertainties that linger around it render it unsatisfactory at the temporal scale of the DPF's apparent biotic patterns. Secondly, corrections for channel-hosted specimens will (by definition) always shift their stratigraphic position up-section, while the proposed correction relative to the OF-DPF contact can shift those same positions in either direction, thus being far less predictable.

Contributions of the BB190 survey to DPF biostratigraphy. The resulting uncertainties on the accuracy of stratigraphic distributions in DPP become especially problematic for localities that may be near boundaries of temporal zones defined by biostratigraphy, which sometimes lack any referrable lithostratigraphic datum. BB190 represents an ideal case study to illustrate this additional issue since it was always suspected to lie very close to the proposed boundary between two of the Park's megaherbivorous dinosaur assemblage zones (MAZ-1 and MAZ-2 following Mallon *et al*. (2012)). However, it has only yielded two dinosaur fossils possibly identifiable at species level to date: the first (found before this study) consists of partial parietals tentatively assigned to *Centrosaurus apertus* based on their overall anatomy but lacking any potentially diagnostic character due to broken parietal processes at both parietal process P1 loci (Sampson *et al.* 1997; Royal Tyrrell Collections 2023). The other is a very short parietal fragment that appears to preserve the bases of two large parietal processes very close together (Figure 3.8G), which is a diagnostic character of *Styracosaurus albertensis*, the centrosaurine ceratopsid consistently hypothesized to succeed *Centrosaurus* in the Park's chronofauna (Ryan & Evans 2005; Sampson & Loewen 2010; Mallon *et al.* 2012; Mallon 2019; Eberth *et al.* 2023). However, the latter specimen was surface collected at the level of the BB190 horizon, which means it could have been washed out of a higher horizon, while the more complete parietals were clearly collected *in situ* from the BB190 original quarry. The discovery of a complete nasal horn core from the bonebed (Figure 3.8F) only indicates that it belongs to a ceratopsid of the centrosaurine subfamily due to its considerable elongation, but its recurved shape is reported in osteologically mature individuals of both *Centrosaurus* and *Styracosaurus* and therefore provides no information that would be diagnostic at lower taxonomic levels (Sampson *et al.* 1997; Ryan *et al.* 2001, 2007). The lack of available biostratigraphic evidence to settle BB190's position between MAZ-1 and MAZ-2 provided an added incentive to estimate it based on the local OF-DPF contact instead. Regardless of the combination of referred points sampled along the contact, the bonebed consistently had an ambiguous position since it always landed within the absolute age uncertainty of the estimated MAZ-1-MAZ-2 boundary (Figure 3.18). Relative height estimates based on a larger sample size of points selected along the contact only shifted the mean closer to the MAZ-1-MAZ-2 boundary compared to the height estimated solely from the only 2 points measured before this study. The original quarry of BB190 was selected over the newly discovered ones for Figure 3.18 since it had the mean relative height with the greatest vertical distance from the MAZ-1-MAZ-2 boundary, and so its elevation range would have been the likeliest to fall within one of these two biozones.

Such lingering uncertainty over the biostratigraphic position of BB190 implies that it (or at least its host horizon) is ideally located to test the megaherbivore turnover hypothesis. The high preservation quality (by bonebed standards) observed in its most complete specimens combined with the high lateral continuity of its host channel horizon raises the possibility of future discoveries, including skeletons preserving more diagnostic features. Indeed, the observed lithology can be interpreted as a channel lag-channel point bar complex, which is the ideal depositional setting for vertebrate skeletons in DPP (Dodson 1971; Wood *et al.* 1988; Eberth & Currie 2005). If future explorations eventually revealed the stratigraphic co-occurrence of species currently assumed to have non-overlapping stratigraphic distributions (e.g. a co-occurrence of *Centrosaurus* and *Styracosaurus* in the same horizon), it would lay the first significant challenge to a paradigm that has prevailed since C. M. Sternberg began investigating geographical and stratigraphic distributions throughout the area nearly 75 years ago

(Sternberg 1950). It might also offer insight into the mode of evolution of those species due to competing hypotheses between cladogenesis (i.e. speciation arising from lineages splitting from a common ancestor) and anagenesis (i.e. speciation occurring along the same lineage), especially in ceratopsians where evidence for anagenesis is more widely reported than in other taxa (Sampson & Loewen 2010; Scannella *et al.* 2014; Campbell *et al.* 2019; Fowler & Fowler 2020; Wilson *et al.* 2020). Factors supporting a hypothesis of phyletic evolution (whatever its mode) independent of abiotic conditions as a key driver of megaherbivore turnover in the Belly River Group community (and at least in coeval biotas throughout late Campanian Laramidia) are (1) a high degree of biogeographical provinciality unparalleled in the Mesozoic Era (despite a relatively equable climate across Laramidia's latitudinal gradient), as well as (2) a stupendously high turnover rate in the DPF largely driven by variation in cranial ornamentation instead of any ecomorphologically relevant characters (Sampson 1995; Lehman 2001; Sampson *et al.* 2010; Mallon & Anderson 2014; Fowler 2017; Mallon 2019). On the other hand, the locations of those biogeographical provinces may well have shifted subtly along that same latitudinal gradient, with each megaherbivore fauna tracking a specific climate and habitat into regions where the Belly River Group is not as well exposed as in DPP. In any case, centrosaurines constitute a textbook example of this biotic turnover pattern since the only characters that are diagnostic of chronologically successive species throughout most of the Belly River Group in that subfamily (i.e. *Coronosaurus brinkmani*, *Centrosaurus apertus* and *Styracosaurus albertensis*) reside in their parietal frill ornamentation, which is likely to be driven by sexual selection far more than natural selection (Sampson *et al.* 1997; Ryan & Russell 2005; Ryan *et al.* 2007; Frederickson & Tumarkin-Deratzian 2014). In contrast, the latest Campanian – early Maastrichtian Horseshoe Canyon Formation has three tentative biozones (like the DPF), yet they are spread over at least twice the DPF's duration and appear more reflective of major fluctuations in abiotic conditions (Eberth *et al.* 2013; Eberth & Kamo 2020). Furthermore, there is growing evidence that a few DPP species at least have a wider geographical (and likely habitat) range than previously assumed following more sustained exploration of nearby coeval localities, although these range expansions remain on a far lesser spatial scale than prevailing late Campanian dinosaur biogeographical provinces (Chiba *et al.* 2015; Takasaki *et al.* 2023; Demers-Potvin & Larsson 2024). Discussions of the respective influences of ecological and evolutionary drivers on non-avialan dinosaur diversity are especially relevant to the MAZ-1 – MAZ -2 transition (of all faunal assemblage zone boundaries in DPP) since it has even less convincing lithological evidence of a palaeohabitat shift to support ecological replacement, rather than phyletic evolution, as the driver of biotic turnover. The dominant lithology of the Dinosaur Park Formation broadly shifts from a sandy zone in the lower half of the formation to a muddy zone in its upper half (Eberth 2005; Eberth *et al.* 2023), yet that transition roughly postdates the MAZ-1 – MAZ -2 boundary by at least 10 m (Mallon *et al.* 2012). In any case, this shift in lithology is more accurately indicative of decreased accommodation and corresponding sediment supply over time, which offers very little information on more relevant factors of animal distributions such as floral composition and its classically derived ecological niche and ecospace predictions.

3.5.2 Contributions of the BB190 survey to the lithostratigraphy of the DPF

In light of the concerns outlined in the previous section regarding the accuracy of any fossil's height relative to the Oldman-Dinosaur Park Formation contact as a reliable proxy of its stratigraphic position, what else can be done to correct the time averaging of the Dinosaur Provincial Park biota(s) more accurately? Could a more qualitative stratigraphic correlation model be a solution, whereby each quarry is assigned to a sedimentary architectural unit of varying depth regardless of its quantitative relative height? This would undoubtedly reduce the high apparent temporal resolution suggested by height above the OF-DPF contact since fossils found at vertical distances of as much as 14-15 m would realistically be assigned to the same time zone. This would render possible time differences between two bonebeds separated by ~1.5 m irrelevant, as in the case of BB303 compared to BB190 in this study. Additionally, this could imply even more acceptance of time averaging since these units should necessarily contain at least two of the three major lithofacies types that compose each of the DPF's channel cut-and-fill rhythms (i.e. mudstones, siltstones and trough cross-bedded sandstones) to minimize the risk of taphonomic bias (Wood *et al.* 1988; Eberth 1990; Eberth & Currie 2005; Brown *et al.* 2013; Eberth 2015). Nonetheless, this alternative relative age scale would certainly not be as misleading since it would nullify two of the major sources of stratigraphic position error identified in the Belly River Group, i.e. the variability in OF-DPF contact elevation (this study) *and* the palaeochannel downcutting effect (Eberth & Getty 2005; Brown 2013: Ch. 4). Additionally, it would further integrate information on each quarry's depositional environment with information on its stratigraphic position. These are the theoretical benefits of such an alternative correlation approach, but they would only be attainable if several of these rhythms could be traced individually over a sufficiently long lateral distance to correlate a statistically significant number of quarries, bonebeds and microfossil localities. Considering the lack of lateral continuity that defines any fluvial deposit as opposed to marine or lacustrine deposits (see Introduction), this is a tall order indeed. In any case, there remains the intriguing possibility that the duration of deposition represented by each channel cut-and-fill rhythm is actually insignificant on a geological scale, so that the great depths reached by some of them represent little time averaging after all. When a stratigraphic section is constrained by two bentonite beds that have yielded reliable radioisotopic dates (as is the case of several fluvial deposits across the Western Interior Basin), mean rock accumulation rates can be estimated (Ramezani *et al.* 2022; Eberth *et al.* 2023). However, these fail to account for relatively high sedimentation rates observed in individual fluvial/deltaic deposits (Behrensmeyer 1982), including some Late Cretaceous palaeochannels located near DPP (Eberth 1996). If those rates were estimated for some rhythms in DPP (based on palaeocurrent direction and bankfull depths in analogous modern fluvio-deltaic systems), they would likely have a $10^3 – 10^5$ yr time resolution for a given depth (Behrensmeyer 1982), which would be far shorter than the duration obtained by geochronology for a stratigraphic interval of similar depth. This would imply frequent and long-lasting depositional hiatuses throughout the Park's lithostratigraphic succession.

The present study, as well as others (Wood 1985, 1989; Nesbit *et al.* 2018), shows that the identification of the Park's main lithofacies (and of the rhythms they compose) can be an effective way of subdividing the Belly River Group's lithostratigraphic succession, at least on a scale of 10^2-10^3 m^2. For example, the sequence stratigraphic correlation of the Cathedral area covered around twice the surface area mapped around BB190, and still led to the identification of six successive rhythms over a vertical distance of 60 m roughly corresponding to the upper two thirds of the DPF (Wood 1985). That correlation was achieved despite occasional interruptions in some units' lateral continuity caused by the vertical amalgamation of stacked trough cross-bedded sandstones that completely eroded underlying abandoned channel fill mudstone deposits. This complicating factor was observed far less often in the BB190 Amphitheatre area, which led to the identification of four successive rhythms subdividing the lower half of the DPF in that region (Figure 3.18). Considering that this interval has yielded approximately 80% of all vertebrate fossils known from the DPF in the Park (Eberth & Currie 2005; Henderson & Tanke 2010; Brown *et al.* 2013), an exploration of the lateral continuity of at least some of these units beyond the current study area is recommended in hope of reducing the magnitude of current taphonomic time averaging. We acknowledge that Rhythm 2 is not as promising a candidate as the other identified units since its contact with the underlying Rhythm 1 was so erosive that it often completely eroded more heterogeneous lithofacies such as MUD1 and could often be detected solely by thin clay-ironstone intraclast layers characteristic of erosional contacts (Wood 1985). It is likely that Rhythm 2 will eventually be merged with Rhythm 1, which would likely assign the vast majority of the lower DPF's fossil quarries to the same time zone and thus stall potential time averaging reduction efforts (Eberth & Currie 2005). In any case, the validity of any of these individual rhythms as regionally significant architectural units would be nullified if a new rhythm that completely downcuts

Rhythm 1 all the way to the OF-DPF contact is identified up- or downstream. Under this scenario, the most realistic time zones will likely be composed of stacked palaeochannel deposits.

The most promising candidate marker bed identified in the BB190 Amphitheatre area may not actually be a sandstone, but rather a massive mudstone (MUD3, see Results; Figure 3.18). It is true that the local elevation of its lower contact is more variable than that of the OF-DPF contact around the bonebed (Table 3.4), but it is still hypothesized that the location of its upper and lower contacts should be more constant over long distances than that of downcutting palaeochannel deposits. Furthermore, there is already tentative evidence that it can be correlated in very distant localities of the Park. First, one of the deepest massive mudstone beds identified in the Dinosaur Park Formation type section (measured at the eastern edge of the Park boundaries in the Iddesleigh area) is located 21-23 m above the OF-DPF contact within the same relative height interval as MUD3, although it is roughly 2-3 times thinner in section (Eberth *et al.* 2023: figure 2). Second, the 'massive shale SH1', which caps the lowest 'channel rhythm' identified in the Cathedral area, might be at the same relative height as MUD3 when accounting for structural dip (Wood 1985), although this line of evidence is less promising because it is around four times further away from BB190.

Assuming that Rhythms 1 and 2 should form a single time zone and that MUD3 represents a significant marker bed for the DPF of Dinosaur Provincial Park, the ~700 ka of MAZ-1 (*Corythosaurus*-*Centrosaurus apertus*) could still be subdivided into 3 sequential time intervals, which represents a resolution unparalleled for fluvial deposits in deep time. Interestingly, the stratigraphic position of massive mudstone MUD3 tentatively coincides with the replacement of *Corythosaurus casuarius* with *Corythosaurus intermedius*, although the latter is very rarely found and thus likely has an underestimated stratigraphic range (Parks 1923; Mallon 2019). The sheer depth of MUD3 around BB190 (compared to other mudstones) might simply be explained by a relative lack of local erosion from the overlying coarse member. That said, if it was traced across the entire Park's exposures, it might indicate a period of decreased accommodation and sediment supply in this region of Laramidia's foreland basin and may provide evidence in support of environmental change at the MAZ-1 – MAZ-2 boundary. However, one potential constraint to the correlation of this particular mudstone bed on a more regional scale is that the ratio in vertical proportion of coarse-grained to fine-grained sedimentary members is not consistent within Dinosaur Provincial Park (Wood 1989): while that ratio oscillates around 3.0 in the Park's south-central area and can be as high as 7.0 in the Cathedral area due to extreme vertical channel amalgamation (Wood 1985; Visser 1986), it drops to 0.42 in the Steveville badlands (Koster 1983: 99, 103). This means that MUD3 might be almost impossible to distinguish from similar lithofacies in the latter region, as is already apparent from recent geological surveys (Nesbit *et al.* 2018; Durkin *et al.* 2020). Therefore, a broader examination of the sedimentary succession in DPP might still lead us to conclude that the local succession observed in the BB190 Amphitheatre area happens to be easier to interpret than in almost any other region.

3.5.3 Connecting the lithostratigraphic and palaeoecological dots with other DPP localities

When all five orthomosaics generated for this study are overlain simultaneously on a map of Dinosaur Provincial Park, they provide an overview of the total surface area that has been mapped around specific fossil localities in the Happy Jack's and Iddesleigh areas to date (Figure 3.19A). The BB190 project renders around one fifth of the area of the lower Dinosaur Park Formation (DPF) visible in the Iddesleigh area, including a substantial stretch of the Oldman-Dinosaur Park Formation (OF-DPF) contact. The project focused on the HCEL Plant 2022 locality renders a transect displaying the entire sedimentary succession of the DPF from its contact with the Oldman Formation to the upper horizons of the Lethbridge Coal Zone (LCZ). The other three projects were less stratigraphically extensive, although the excavation of the ceratopsid skull prompted a survey of the local facies succession through most of the LCZ and the Clam06 locality area displayed yet another clear exposure of the OF-DPF contact. Given the current coverage, to what extent can the architectural units identified around BB190 be found in the other localities, at least at the plant site? One way to initiate this investigation is to plot the absolute elevation of some of the most significant lithological contacts across the east-west axis of the Happy Jack's and Iddesleigh areas. The elevation data presented in Figure 3.19B has been generated from the same giant DEM encompassing the entire Park (instead of separate DEMs created for each local project) while accounting for the ~0.05º average structural dip to the northwest observed throughout the Belly River Group in DPP.

The only contact selected for this preliminary analysis which is widely accepted to be correlated across the entire Park is the OF-DPF contact. The high fluctuation in elevation *within* each locality first observed around BB190 is still observed: even over the 0.01 km^2 area of the Clam06 project, the OF-DPF contact has an elevation range of around 4 m! Displaying the elevations of the OF-DPF contact over a much longer transect by comparing those obtained from the original differential GPS survey of the Park alongside the far more densely sampled elevations obtained during the present study illustrates even more effectively how much of the local elevation variation was not previously detected. Otherwise, there is no clear increase or decrease in its elevation along the ~2 km between the three mapped localities where it is visible (BB190, Clam06 and HCEL Plant 2022). The only conspicuous peak in elevation comes from three contacts that were measured by differential GPS away from the Red Deer River along Jackson Coulee. Overall, the elevation variability of the OF-DPF contact offers a baseline to assess the extent of more controversial marker beds higher in the DPF.

During the UAV surveys and digital reconstructions of the outcrops around BB190 and the HCEL Plant 2022 site, it was noted that these two localities had a very similar geological setting at the same elevation. As previously mentioned, the host horizons of both BB190 (Rhythm 4 at this locality) and the plant site (Rhythm 2 at that locality) are at a similar elevation (687 and 688 m respectively), and each of them overlies a relatively thick mudstone unit (MUD3 in BB190). The considerable lateral extent of Rhythm 4 and MUD3 around BB190 raises the hypothesis that those same architectural units can be correlated at the plant site. As it stands, supporting evidence from the preliminary plot presented in Figure 3.19B is mixed. On one hand, the elevations of lower contacts for the mudstone and overlying rhythm at the plant site are similar to their proposed counterparts at BB190. On the other hand, their mean elevation seems a little higher than predicted from the ~0.05º average structural dip. One evident way to resolve this debate would be to image the totality of the Belly River Group's exposures in DPP using the same UAF-SfM photogrammetry method applied to the five isolated projects presented in this study. Such a reconstruction has already been started for the entire Happy Jack's area of the Park and its preliminary examination does suggest that the HCEL Plant 2022 site's 'Rhythm 2 mudstone' has a remarkable lateral continuity, even several kilometres away from that plant site (see Appendix IV). However, its height relative to MUD3 (accounting for structural dip) has yet to be estimated due to relative geolocation inaccuracies and imprecision arising from that preliminary UAV flight protocol. This is because we attempted to combine point clouds of distinct overlapping transects of the badlands produced from images that were acquired from two different UAV models whose built-in GPS receivers had different positional accuracies. The correction of each image's geographical location with GCPs solved this issue only partially. In the future, we highly recommend attempting such a project using a single UAV equipped with Real-time kinematics (RTK) or a Post-processing kinematics (PPK) module.

The other mapping projects presented in this chapter could serve in the future as good starting points to test the potential of a few other lithological units as chronostratigraphically significant marker beds. For instance, a ~75-cm thick carbonate shale layer that appears to split the middle DPF hosting the *Prosaurolophus-Styracosaurus* zone into two diachronous units has reportedly been traced from the Plateau Tuff (in the Cathedral area) eastwards for ~7 km (Eberth 2005; Eberth *et al.* 2023). Considering that the digital reconstruction and stratigraphic section of the entire ridge hosting the HCEL Plant 2022 site includes the same time interval, a closer look at the local lithology is certainly warranted. If the rhythms discussed above prove insufficiently continuous and this marker bed is shown to have a far more constant variation in elevation than the OF-DPF contact, it could become a very promising alternative datum for estimating stratigraphic distributions. Furthermore, it would evidently be nearer to upper DPF quarries than the OF-DPF contact, which would reduce the propagation of errors derived from ground-based vertical section measurements. Of course, it is entirely possible that such a thin layer may have been locally eroded by one of those infamously downcutting palaeochannels. In this way, the expansion of the project currently underway in the Happy Jack's area should increase the probability of detecting this marker bed (Appendix IV).

The Iddesleigh area is known to have the most complete stratigraphic bedrock section in Dinosaur Provincial Park, including the only significant exposures of the Bearpaw Formation in the region (Eberth 2005). A 3-D or even 2-D reconstruction of the region would therefore enable testing of the consistency of the transition from one of the higher marine shale deposits to the highest underlying tan siltstone bed as a proposed contact between the Lethbridge Coal Zone and the Bearpaw Formation (Brinkman *et al.* 2005; Eberth *et al.* 2023). The LCZ also appears to be the host horizon of the ceratopsid uncovered at Quarry 300, although its contact with the Bearpaw Formation does not seem to be preserved there. The thin black shale immediately underlying that siltstone is strongly indicative of an anoxic marine environment, but may simply represent a temporary landward incursion of the Bearpaw Sea, and many such incursions are recorded throughout the LCZ by bioturbated muds and silts that cut underlying channel deposits (Beavan & Russell 1999). It must also be noted that ammonites have been reported from similar levels elsewhere in the Park (Philip Currie, personal communication, 2022; personal observation, 2023). However, we caution that they should not be automatically treated as biostratigraphic indicators of the Bearpaw Formation (in the absence of any lithostratigraphic evidence) since they may simply be indicative of similar marine incursions. In any case, the few vertebrate microfossil localities known from the LCZ present the highest shark diversity of the entire DPF by far (Beavan & Russell 1999; Brinkman *et al.* 2005), which is indicative of brackish to saltwater environments that would have been highly suitable for ammonites as well. In that case, the mapped area should likely be expanded eastwards, towards the DPF type section, where absolute elevation at prairie level is highest and the DPF-Bearpaw Formation contact is most consistently exposed (Eberth 2005; Eberth *et al.* 2023). It must also be noted that the facies composition of the LCZ (above the main coal units at least) differed markedly between Q300 and the plant site: while the former displayed the interbedding among clays, silts and shales that is characteristic of that member, the latter displayed a massive sandstone in the LCZ's mid-section, which indicates local persistence of palaeochannels. It is far from surprising that the LCZ depositional environment was not as homogenous as is often depicted and should still preserve evidence of the odd river or estuary given its very high proximity to the Western Interior Seaway. This is yet another example of the power of digital outcrop reconstructions of entire landscapes to 'connect the dots' between otherwise isolated fossil quarries and stratigraphic sections.

As for the ceratopsid skull whose discovery was the real incentive for the mapping of a small segment of the LCZ, little can be concluded about its lower-level taxonomy until it gets prepared in the lab. Its location in the LCZ means that it should likely be assigned either to *Chasmosaurus irvinensis* or to an unnamed pachyrhinosaur tentatively assigned to *Achelousaurus* (Ryan *et al.* 2010). However, its nasal horn core is very elongated and it therefore shares a greater affinity with the *Centrosaurus-Styracosaurus* lineage than the Pachyrhinosaurini 'tribe', even though the former should have gone locally extinct by the time of the LCZ according to our present understanding of ceratopsid species turnover in Dinosaur Provincial Park (Figure 3.18). In fact, that nasal horn core seems to be procurving so much more than in any *Centrosaurus* specimen that it is slightly reminiscent of osteologically mature individuals of *Einiosaurus procurvicornis* (Sampson 1995). The latter species is only known from the Two Medicine Formation near the Alberta-Montana border, and the latest radioisotopic dates confirm that that formation completely overlapped with the DPF in time (Ramezani *et al.* 2022). In conclusion, it remains to be seen whether the intriguing ceratopsid uncovered at the Park's Q300 represents a geographical (or even stratigraphic) range expansion of an already known species or a new species altogether.

Final considerations should be given to the bivalve assemblages whose host horizons were mapped at the Clam04 and Clam06 localities. While their respective projects had less stratigraphic significance, they did provide an interesting taphonomic insight considering the high density of bivalves fossilized in a clayey or silty ironstone matrix. Dense fossil mollusc aggregations in Dinosaur Provincial Park have previously been hypothesized to have formed during mass drowning events (Johnston & Hendy 2005). However, the dark orange colour of the ironstone that hosts most of the bivalves we came across is usually associated with oxidation and therefore subaerial exposure. That, along with the observation that several of the shells were open in the matrix, leads us to hypothesize that those aggregations were formed by mass drought events instead. This is supported by a geochemical analysis of mollusc shells similarly preserved in ironstone in the Hell Creek and Fort Union Formations of North Dakota that revealed varying amounts of goethite and siderite, with the former being a common oxidation product of the latter when exposed to air (Justham 2008). Considering the frequent association of vertebrate fossils with ironstone in the Park and considering the abundant evidence for drought events in the contemporaneous Two Medicine Formation in nearby north-central Montana (Rogers 1990; Varricchio & Horner 1993; Varricchio 1995), we further hypothesize that several of the Park's bonebeds were drought-induced attritional assemblages and not flood-induced catastrophic assemblages, *contra* what has been accepted for the last 40 years (Currie & Dodson 1984; Eberth & Getty 2005; Eberth 2015). This in turn leads to an alternative interpretation of the significance of the wildfires that must have occurred frequently in the Park as shown by abundant charcoal deposits reported throughout the Oldman and Dinosaur Park Formations (Brown *et al.* 2012). The high concentration of charcoal detected in bonebeds relative to other taphonomic modes in the Park was initially hypothesized to reflect the significant role of fire-induced vegetation loss in accelerating local erosion, thus facilitating flash floods leading to mass death events (Brown *et al.* 2012). However, the drought hypothesis outlined above leads us to suggest that the prevalence of those fires in the Dinosaur Provincial Park ecosystem may equally be interpreted as evidence of periodic dry episodes that could have been a more likely cause of some death assemblages. In any case, the prevalence of charcoal in the DPF's sediments is very characteristic of terrestrial ecosystems throughout the Cretaceous, likely due to higher atmospheric oxygen concentrations than in the present (Bond & Scott 2010; Brown *et al.* 2012; Bamforth *et al.* 2014).

Even if the ironstone around some bones may reflect a drought that occurred long after the death of their original owner (and thus may not be their cause of death), it suggests at least that they were exposed subaerially after their initial burial. Furthermore, bones hosted in ironstone often show more signs of abrasion or weathering than those found in sandstone channel bases, and these characteristics are often indicative of dry conditions. Lastly, the paradox between the duration of the time intervals inferred from radioisotopic dating in the Park and the (likely smaller) proportion of that geological time actually preserved in the Park's exposures may also support the hypothesis of more frequent droughts in the region during the late Campanian since those events would necessarily equate to reduced or interrupted fluvial sediment supply. It is interesting in this respect to note that the OF-DPF contact is widely accepted to represent a depositional hiatus between two clastic wedges (Rogers *et al.* 2023) and that the same massive ironstone facies which characterizes that contact also hosts invertebrate shells and bones throughout the Belly River Group, whether in the OF (as in Clam06) or the DPF (as in Clam04).

If the hypothesis that ironstone is an indicator of local drought events eventually fails to be rejected by geochemical evidence, it could fundamentally shift the prevailing paradigm that the DPF ecosystem had an equably wet warm temperate climate for its entire duration. Our current understanding of the DPF's palaeoclimate is largely influenced by its palynological and palaeobotanical record (Bell 1965; Ramanujam 1972; Jarzen 1982; Braman 2005; Koppelhus 2005), as well as a rare case of palaeotemperature measurements derived from oxygen isotopes sampled from freshwater turtle fossil remains (Barrick *et al.* 1999). However, in one of the very first modern palaeoecological studies of DPP, Dodson already noted the presence of growth rings in petrified wood samples and

Champsosaurus vertebrae as suggestive of some form of seasonality as part of the region's palaeoclimate (Dodson 1971). The advent of quantitative methods to estimate palaeoclimate parameters such as temperature and precipitation from physiognomic characters in well preserved fossil leaves now raises the possibility of integrating palaeobotanical data with other climate proxies in a more objective way (Wolfe & Upchurch 1987; Greenwood 2007; Spicer *et al.* 2021). A preliminary analysis of the Park's past climate, based on an angiosperm-dominated leaf assemblage discovered by the McGill University vertebrate palaeontology field course's 2017 crew, already suggests a mild seasonal cycle in temperature, although precipitation still appears high year-round (Bamforth & Koppelhus 2018). However, these estimates are from a single bed, so it cannot be assumed that they reflect all ~2 Myr of the DPF's climate. In this regard, the discovery of the new fossil plant locality whose geological setting was presented as part of this chapter will provide invaluable information to characterize the DPF's climatic variability – and its implications for observed palaeodiversity patterns – in greater detail (Mueller *et al.* in prep). Furthermore, palaeoclimate patterns will be detected at a higher temporal resolution if the ongoing large-scale mapping project bears fruit.

3.5.4 Can Dinosaur Provincial Park's time resolution conundrum be solved from the air?

The preceding discussion outlines the necessity to detect common architectural units (or at least marker beds) across the entirety of Dinosaur Provincial Park's exposures as possible solutions to characterize the DPP biota in even greater temporal detail. Considering the huge spatial scale of this exploration and the steep badlands terrain for intensive ground-based excursions, we remain convinced that the future lies in the air, by acquiring images with UAVs in the field, processing them in the lab through SfM photogrammetry, and verifying digital lithofacies identifications with ground-based stratigraphic sections. The aerial survey of the BB190 Amphitheatre area presented in this paper has provided an additional proof of concept for this method, albeit with a slightly different workflow from similar studies in the Park (Nesbit *et al.* 2018, 2020; Nesbit & Hugenholtz 2019; Durkin *et al.* 2020;

Mayo *et al.* 2023). Importantly, we corroborate the results of that previous research showing that UAV flight protocols applied in the field led to reconstructions that had a sufficiently high resolution to digitally identify the DPF's main lithofacies types. An exhaustive exploration of the 3-D digital outcrop model (DOM) and orthomosaic in tandem also provided an efficient assessment of the relevance of each of the lithological units measured in the stratigraphic section to the surrounding alluvial architecture. As an example, some sandstone ribbons would have been indistinguishable from more significant sandstone rhythms using the stratigraphic section alone, but their examination in their entirety from contiguous imaged 2-D and 3-D outcrop surfaces greatly facilitated that task. We acknowledge that more sections should have been measured around the bonebed to explore the full potential of ground-based sequence stratigraphic correlation, but that was due to our decision to focus efforts on fossil collection towards a more palaeoecological objective. In addition, the precision of the elevation measurements derived from the root mean square error (RMSE) of the digital elevation model (DEM) obtained from SfM photogrammetry is likely lower than that of measuring staffs used in ground-based stratigraphic mapping, but the latter method has a key precision disadvantage. Its precision may indeed be higher than any remote-sensing approach if a given datum (e.g. the OF-DPF contact) is in close vertical proximity to a given quarry due to a relative lack of measurement error propagation, but that can change quickly if the quarry is located higher in section since those errors will accumulate due to an increasing number of individual measurements with growing vertical distance from the OF-DPF contact. In contrast, the DEM RMSE is (by definition) consistent across the entire mapped area.

From a palaeontological perspective, the identification of the host horizon of BB190 over a relatively large area enabled by SfM photogrammetry constitutes an exciting development in itself. The surface area of the bonebed was estimated at almost 0.1 km^2 from the most distant locations of its known exposed fossils alone. Considering that the same sandstone outcrop extends for considerable distances up- and downriver, BB190 may originally have covered a substantially larger area. In comparison, the Park's classic *Centrosaurus*-dominated bonebed (BB043) only covers ~13 km^2 (Ryan *et al.* 2001) and the Park's only other well-described multigeneric bonebed to date (BB047) was sampled for fossils over 190 m^2 despite having a more laterally extensive host horizon (Tumarkin-Deratzian 1997). However, BB190 might not quite have reached the estimated 2.3 km^2 of the Hilda *Centrosaurus* mega-bonebed from the DPF of the South Saskatchewan River (Eberth *et al.* 2010). Nonetheless, an exhaustive aerial coverage of the Park's exposures combined with accurate GPS readings might provide key evidence to test the lateral extent of several of its bonebeds. This leads us to predict that a remote-sensing approach, combined with a sustained collection of taphonomic data on the ground for individual fossil aggregations (see Brown *et al.* 2020), will reveal that several localities currently assigned distinct quarry numbers in the Park are in fact part of the same gigantic bonebeds, and so that the Hilda mega-bonebed is not as unusual in its extent. It follows that these bonebeds would constitute valuable additional marker beds for the stratigraphy of the Belly River Group exposed in DPP.

The takeaways from the remote sensing of BB190 are promising, yet there is room for improvement. For instance, incorporating more oblique images on the steep slopes of DPP is shown to increase model accuracy (Nesbit & Hugenholtz 2019). The lack of oblique images for most of the mapped area, with the exception of the OF-DPF contact, may have contributed to difficulties in identifying individual bedding planes within the same rhythm, as has been shown elsewhere (Nesbit *et al.* 2018). A detailed sedimentological study of the bonebed's host horizon would admittedly have offered more insight than relative height measurements alone into the status of fossiliferous layers proposed to represent distinct depositional events from BB190, most notably BB303. It would certainly have reduced the reliance on the tracing of a polyline along an erosional contact that was detected digitally on the orthomosaic, but it is deemed beyond the scope of the present paper. Additionally, some taphonomically relevant facies are simply undetectable from the air (even with a 20 MP camera) and must still be inspected from the ground, as was the case of the clay-pebble conglomerate that confirmed the formation of BB190 along a palaeochannel lag. It should be noted that several of these thin units are less than 10 cm thick, which reveals a lower resolution limit to the maps produced by UAV-SfM photogrammetry in this study. Ashfall-derived bentonites are yet another lithological facies that can only be distinguished from other mudstones by ground-based observations for now: in fact, it is worth noting that two of the five bentonites currently known from DPP were found by pure serendipity, during sequence stratigraphic correlation of the Cathedral area in the case of the Plateau Tuff (Wood 1985; Thomas *et al.* 1990) and during the relatively recent excavation of BB180 in the case of the Jackson Coulee bentonite (Brown *et al.* 2020). In any case, considerable sedimentological expertise is required to recognize that several of the DPF's erosional contacts might actually be part of the same channel meander belt migration (Nesbit *et al.* 2018; Durkin *et al.* 2020). All these caveats show that even the UAV camera with the highest available resolution cannot completely replace ground-based observations, which often provide the context needed to interpret large-scale patterns detected from aerial geological mapping.

Finally, we stress that the data visualization method outlined in this paper is not as practical as it should be. This can partly be explained by our initial emphasis on the orthomosaic as the primary source of digital facies identification due to its efficient integration to 2-D maps in QGIS. However, closer examinations of the outcrops' 3-D structure proved more and more necessary as our understanding of the local stratigraphy increased. For instance, the erosional contact marking Rhythm 2 was only identified once the DOM was inspected in tandem with the orthomosaic. Moreover, channel rhythm depth measurements proved more efficient to obtain by placing manual tie points on the DOM's surface instead of calculating those depths from absolute heights extracted from two series of points sampled along two successive erosional contacts. The acquisition of outcrop data from the DOM, not just from the DEM and orthomosaic (as was initially planned), may therefore create logistical challenges in terms of geospatial data availability. In future work, we recommend all the vector data be measured from the DOM, and subsequently plotted on the same surface in an online repository (e.g. Nesbit *et al.* 2020), to make the study more interactive and reproducible for viewers and workers who are not as familiar with the terrain of Dinosaur Provincial Park. The outcrop annotation workflow attempted in Blender for some of the projects (such as the plant and ceratopsid sites) may also prove a useful alternative once it is combined with the movie editing available in the same program, which can enable sharing high-resolution video files of lesser size than the usual file types associated with meshes or point clouds.

The experience acquired during the entire BB190 survey process, from image acquisition and facies observation in the field to digital facies identification from resulting landscape reconstructions, has offered key insights into the best practices to follow as our team currently begins the creation of a base map covering the entire Park through a similar workflow to the one outlined in this paper, albeit adapted to a far greater spatial scale. In this way, BB190 is strategically located as a starting point for this project due to its well-exposed local OF-DPF contact but also due to its proximity to other potential marker beds. These include the massive mudstone at the base of BB190 (which is possibly equivalent to the mudstone at the base of the plant site), as well as the carbonate shale layer and the last tan siltstone layer below the Lethbridge Coal Zone-Bearpaw Formation contact. Considering that the Horseshoe Canyon Formation exposed upstream of DPP displays a more regular succession of visually distinctive coal zones forming laterally extensive marker beds with less vertical mixing of non-contemporaneous strata than in DPP, combined with five distinct bentonites (Quinney *et al.* 2013; Eberth & Kamo 2020), a similar UAV mapping project for that sedimentary unit would more likely yield a successful correlation of its fossil localities (Eberth *et al.* 2013). However, the diversity of the DPP fossil assemblage is so exceptional that it provides a sufficient incentive to persist in our current long-term geological mapping project as we strive to further understand the tempo of its ecological (and possibly evolutionary) patterns.

3.6 Conclusions

What began as an essentially exploratory project with the main objective of assessing the geographical extent and palaeodiversity of a mixed faunal bonebed in Dinosaur Provincial Park eventually evolved into a deeper investigation of the Park's entire geological setting through a combination of emerging and enduring technologies. The high fossil discovery rate of the BB190 Amphitheatre area since the renewal of prospection in 2018 suggests that it remains a highly promising study system to investigate the palaeoecology of the Dinosaur Park Formation during a very constrained time span. The present study forms the stratigraphic context for this ongoing project and has concurrently provided two key insights into the temporal resolution of the DPP biota suggesting that (1) stratigraphic positions solely based on the OF-DPF contact contain major uncertainties even on a local scale and (2) at least some of the channel cut-and-fill rhythms detected in our survey deserve investigation on a broader scale to subdivide the DPF into more lithostratigraphically significant units than the current biostratigraphic frameworks. Together, they represent significant contributions to our understanding of DPP's evolutionary palaeoecology. This project has led to a greater understanding of the benefits and pitfalls of 3-D stratigraphic mapping based on UAV-SfM photogrammetry. It leads to the prediction that the greater spatial overview of the Belly River Group exposed in Dinosaur Provincial Park afforded by the parallel exploration of digital outcrop models (DOMs), digital elevation models (DEMs) and orthomosaics will lead to the distinction of more laterally continuous units as potential marker beds from local units that have hindered solely ground-based stratigraphic correlation attempts. This emerging technology therefore represents one of the most promising solutions to the conundrum surrounding the temporal resolution of the Park's biodiversity patterns.

3.7 References

BAMFORTH, E. L. and KOPPELHUS, E. B. 2018. New absolute paleoclimate estimates from Dinosaur Provincial Park, Alberta (Campanian, Late Cretaceous): Preliminary results based on a new fossil leaf assemblage. *6th Annual Meeting Canadian Society of Vertebrate Paleontology Abstracts*, **6**, 10–11.

BAMFORTH, E. L., BUTTON, C. L. and LARSSON, H. C. E. 2014. Paleoclimate estimates and fire ecology immediately prior to the end-Cretaceous mass extinction in the Frenchman Formation (66Ma), Saskatchewan, Canada. *Palaeogeography, Palaeoclimatology, Palaeoecology*, **401**, 96–110.

BARNES, C. R. 1988. Stratigraphy and Palaeontology of the Ordovician-Silurian boundary interval, Anticosti. *Bulletin of the British Museum, Natural History, Geology Series*, **43**, 195–219.

BARNOSKY, A. D., MATZKE, N., TOMIYA, S., WOGAN, G. O. U., SWARTZ, B., QUENTAL, T. B., MARSHALL, C., MCGUIRE, J. L., LINDSEY, E. L., MAGUIRE, K. C., MERSEY, B. and FERRER, E. A. 2011. Has the Earth's sixth mass extinction already arrived? *Nature*, **471**, 51–57.

———, HADLY, E. A., GONZALEZ, P., HEAD, J., POLLY, P. D., LAWING, A. M., ERONEN, J. T., ACKERLY, D. D., ALEX, K., BIBER, E., BLOIS, J., BRASHARES, J., CEBALLOS, G., DAVIS, E., DIETL, G. P., DIRZO, R., DOREMUS, H., FORTELIUS, M., GREENE, H. W., HELLMANN, J., HICKLER, T., JACKSON, S. T., KEMP, M., KOCH, P. L., KREMEN, C., LINDSEY, E. L., LOOY, C., MARSHALL, C. R., MENDENHALL, C., MULCH, A., MYCHAJLIW, A. M., NOWAK, C., RAMAKRISHNAN, U., SCHNITZLER, J., SHRESTHA, K. D., SOLARI, K., STEGNER, L., STEGNER, M. A., STENSETH, N. C., WAKE, M. H. and ZHANG, Z. 2017. Merging paleobiology with conservation biology to guide the future of terrestrial ecosystems. *Science*, **355**, eaah4787.

BARRETT, P. M., MCGOWAN, A. J. and PAGE, V. 2009. Dinosaur diversity and the rock record. *Proceedings of the Royal Society B: Biological Sciences*, **276**, 2667–2674.

BARRICK, R. E., FISCHER, A. G. and SHOWERS, W. J. 1999. Oxygen Isotopes from Turtle Bone: Applications for Terrestrial Paleoclimates? *PALAIOS*, **14**, 186–191.

BARRY, J. C., JOHNSON, N. M., RAZA, S. M. and JACOBS, L. L. 1985. Neogene mammalian faunal change in southern Asia: Correlations with climatic, tectonic, and eustatic events. *Geology*, **13**, 637–640.

BEAVAN, N. R. and RUSSELL, A. P. 1999. An elasmobranch assemblage from the terrestrial-marine transitional Lethbridge Coal Zone (Dinosaur Park Formation: Upper Campanian), Alberta, Canada. *Journal of Paleontology*, **73**, 494–503.

BEHRENSMEYER, A. K. 1982. Time Resolution in Fluvial Vertebrate Assemblages. *Paleobiology*, **8**, 211–227.

BEHRENSMEYER, A. K. and HOOK, R. W. 1992. Paleoenvironmental Contexts and Taphonomic Modes. *In* BEHRENSMEYER, A. K., DAMUTH, J. D., DIMICHELE, W. A., POTTS, R., SUES, H.-D. and WING, S. L. (eds.) *Terrestrial Ecosystems through Time*, The University of Chicago Press, Chicago, 15–136 pp.

BEHRENSMEYER, A. K., KIDWELL, S. M. and GASTALDO, R. A. 2000. Taphonomy and paleobiology. *Paleobiology*, **26**, 103–147.

BÉLAND, P. and RUSSELL, D. A. 1978. Paleoecology of Dinosaur Provincial Park (Cretaceous), Alberta, interpreted from the distribution of articulated vertebrate remains. *Canadian Journal of Earth Sciences*, **15**, 1012–1024.

BELL, W. A. 1965. *Uppermost Cretaceous and Paleocene Plants of Western Canada*. Geological Survey of Canada, Paper 65-35, Ottawa.

BENSON, R. B. J., BUTLER, R., CLOSE, R. A., SAUPE, E. and RABOSKY, D. L. 2021. Biodiversity across space and time in the fossil record. *Current Biology*, **31**, R1225–R1236.

BLANCO, F., CALATAYUD, J., MARTÍN-PEREA, D. M., DOMINGO, M. S., MENÉNDEZ, I., MÜLLER, J., FERNÁNDEZ, M. H. and CANTALAPIEDRA, J. L. 2021. Punctuated ecological equilibrium in mammal communities over evolutionary time scales. *Science*, **372**, 300–303.

BOND, C. E., SHIPTON, Z. K., JONES, R. R., BUTLER, R. W. H. and GIBBS, A. D. 2007. Knowledge transfer in a digital world: Field data acquisition, uncertainty, visualization, and data management. *Geosphere*, **3**, 568–576.

BOND, W. J. and SCOTT, A. C. 2010. Fire and the spread of flowering plants in the Cretaceous. *The New Phytologist*, **188**, 1137–1150.

BRAMAN, D. R. 2005. Campanian Palynomorphs. *In* CURRIE, P. J. and KOPPELHUS, E. B. (eds.) *Dinosaur Provincial Park: A Spectacular Ancient Ecosystem Revealed*, Indiana University Press, Bloomington, 101–130 pp.

BRINKMAN, D. B. 1990. Paleoecology of the Judith River Formation (Campanian) of Dinosaur Provincial Park, Alberta, Canada: Evidence from vertebrate microfossil localities. *Palaeogeography, Palaeoclimatology, Palaeoecology*, **78**, 37–54.

———, RYAN, M. J. and EBERTH, D. A. 1998. The paleogeographic and stratigraphic distribution of ceratopsids (Ornithischia) in the upper Judith River Group of Western Canada. *PALAIOS*, **13**, 160–169.

———, BRAMAN, D. R., NEUMAN, A. G., RALRICK, P. E. and SATO, T. 2005. A Vertebrate Assemblage from the Marine Shales of the Lethbridge Coal Zone. *In* CURRIE, P. J. and KOPPELHUS, E. B. (eds.) *Dinosaur Provincial Park: A Spectacular Ancient Ecosystem Revealed*, Indiana University Press, Bloomington, 486–500 pp.

BROWN, C. M. 2013. Advances in Quantitative Methods in Dinosaur Palaeobiology: A Case Study in Horned Dinosaur Evolution.Unpublished Ph.D. Thesis, University of Toronto, Toronto, 443pp.

———, EVANS, D. C., CAMPIONE, N. E., O'BRIEN, L. J. and EBERTH, D. A. 2013. Evidence for taphonomic size bias in the Dinosaur Park Formation (Campanian, Alberta), a model Mesozoic terrestrial alluvial-paralic system. *Palaeogeography, Palaeoclimatology, Palaeoecology*, **372**, 108–122.

———, HERRIDGE-BERRY, S., CHIBA, K., VITKUS, A. and EBERTH, D. A. 2020. High-resolution (centimetre-scale) GPS/GIS-based 3D mapping and spatial analysis of in situ fossils in two horned-dinosaur bonebeds in the Dinosaur Park Formation (Upper Cretaceous) at Dinosaur Provincial Park, Alberta, Canada. *Canadian Journal of Earth Sciences*, **58**, 225–246.

BROWN, S. A. E., SCOTT, A. C., GLASSPOOL, I. J. and COLLINSON, M. E. 2012. Cretaceous wildfires and their impact on the Earth system. *Cretaceous Research*, **36**, 162–190.

BRUSATTE, S. L., BUTLER, R. J., PRIETO-MARQUEZ, A. and NORELL, M. A. 2012. Dinosaur morphological diversity and the end-Cretaceous extinction. *Nature Communications*, **3**, 8.

CAMPBELL, I. A. 1970. Erosion Rates in the Steveville Badlands, Alberta. *Canadian Geographies / Géographies canadiennes*, **14**, 202–216.

CAMPBELL, J. A., RYAN, M. J., SCHRÖDER-ADAMS, C. J., HOLMES, R. B. and EVANS, D. C. 2019. Temporal range extension and evolution of the chasmosaurine ceratopsid *'Vagaceratops' irvinensis* (Dinosauria: Ornithischia) in the Upper Cretaceous (Campanian) Dinosaur Park Formation of Alberta. *Vertebrate Anatomy Morphology Palaeontology*, **7**, 83–100.

CANT, D. J. and STOCKMAL, G. S. 1989. The Alberta foreland basin: relationship between stratigraphy and Cordilleran terrane-accretion events. *Canadian Journal of Earth Sciences*, **26**, 1964–1975.

CEBALLOS, G., EHRLICH, P. R., BARNOSKY, A. D., GARCÍA, A., PRINGLE, R. M. and PALMER, T. M. 2015. Accelerated modern human–induced species losses: Entering the sixth mass extinction. *Science Advances*, **1**, e1400253.

CHIARENZA, A. A., MANNION, P. D., LUNT, D. J., FARNSWORTH, A., JONES, L. A., KELLAND, S.-J. and ALLISON, P. A. 2019. Ecological niche modelling does not support climatically-driven dinosaur diversity decline before the Cretaceous/Paleogene mass extinction. *Nature Communications*, **10**, 1091.

CHIBA, K., RYAN, M. J., BRAMAN, D. R., EBERTH, D. A., SCOTT, E. E., BROWN, C. M., KOBAYASHI, Y. and EVANS, D. C. 2015. Taphonomy of a monodominant *Centrosaurus apertus* (Dinosauria: Ceratopsia) bonebed from the Upper Oldman Formation of Southeastern Alberta. *PALAIOS*, **30**, 655–667.

COHEN, K. M., FINNEY, S. C., GIBBARD, P. L. and FAN, J. X. 2013. The ICS International Chronostratigraphic Chart. *Episodes*, **36**, 199–204.

COLOMINA, I. and MOLINA, P. 2014. Unmanned aerial systems for photogrammetry and remote sensing: A review. *ISPRS Journal of Photogrammetry and Remote Sensing*, **92**, 79–97.

COMMUNITY, B. O. 2018. Blender - a 3D modelling and rendering package. .

CULLEN, T. M. and EVANS, D. C. 2016. Palaeoenvironmental drivers of vertebrate community composition in the Belly River Group (Campanian) of Alberta, Canada, with implications for dinosaur biogeography. *BMC Ecology*, **16**, 52.

———, ZANNO, L., LARSON, D. W., TODD, E., CURRIE, P. J. and EVANS, D. C. 2021. Anatomical, morphometric, and stratigraphic analyses of theropod biodiversity in the Upper Cretaceous (Campanian) Dinosaur Park Formation. *Canadian Journal of Earth Sciences*, **58**, 870–884.

CURRANO, E. D., WILF, P., WING, S. L., LABANDEIRA, C. C., LOVELOCK, E. C. and ROYER, D. L. 2008. Sharply increased insect herbivory during the Paleocene-Eocene Thermal Maximum. *Proceedings of the National Academy of Sciences*, **105**, 1960–1964.

CURRIE, P. J. 1981. Hunting dinosaurs in Alberta’s great bonebed. *Canadian Geographic*, **101**, 34–39.

———. 2005. History of Research. *In* CURRIE, P. J. and KOPPELHUS, E. B. (eds.) *Dinosaur Provincial Park: A Spectacular Ancient Ecosystem Revealed*, Indiana University Press, Bloomington, 3–33 pp.

——— and DODSON, P. 1984. Mass death of a herd of ceratopsian dinosaurs. *Third Symposium on Mesozoic Terrestrial Ecosystems*, 61–66.

——— and KOPPELHUS, E. B. 2005. *Dinosaur Provincial Park: A Spectacular Ancient Ecosystem Revealed*. Bloomington & Indianapolis.

——— and RUSSELL, D. A. 2005. The Geographic and Stratigraphic Distribution of Articulated and Associated Dinosaur Remains. *In* CURRIE, P. J. and KOPPELHUS, E. B. (eds.) *Dinosaur Provincial Park: A Spectacular Ancient Ecosystem Revealed*, Indiana University Press, Bloomington, 537–569 pp.

DAI, X., DAVIES, J. H. F. L., YUAN, Z., BRAYARD, A., OVTCHAROVA, M., XU, G., LIU, X., SMITH, C. P. A., SCHWEITZER, C. E., LI, M., PERROT, M. G., JIANG, S., MIAO, L., CAO, Y., YAN, J., BAI, R., WANG, F., GUO, W., SONG, H., TIAN, L., DAL CORSO, J., LIU, Y., CHU, D. and SONG, H. 2023. A Mesozoic fossil lagerstätte from 250.8 million years ago shows a modern-type marine ecosystem. *Science*, **379**, 567–572.

DAWSON, F. M., EVANS, C. G., MARSH, R. and RICHARDSON, R. 1994. Uppermost Cretaceous and Tertiary strata of the Western Canada sedimentary basin. *In* MOSSOP, G. and SHETSEN, I. (eds.) *Geological Atlas of the Western Canada Sedimentary Basin*, Canadian Society of Petroleum Geologists and the Alberta Research Council, Edmonton, 387–407 pp.

DE VOS, J. M., JOPPA, L. N., GITTLEMAN, J. L., STEPHENS, P. R. and PIMM, S. L. 2015. Estimating the normal background rate of species extinction. *Conservation Biology*, **29**, 452–462.

DEMERS-POTVIN, A. V. and LARSSON, H. C. E. 2024. Occurrence of *Centrosaurus apertus* (Ceratopsidae: Centrosaurinae) in Saskatchewan, Canada, and expanded dinosaur diversity in the easternmost exposure of the Late Cretaceous (Campanian) Dinosaur Park Formation. *Canadian Journal of Earth Sciences*, **in press**, 1-29, dx.doi.org/10.1139/cjes-2023-0125.

DESANTIS, L. R. G., CRITES, J. M., FERANEC, R. S., FOX-DOBBS, K., FARRELL, A. B., HARRIS, J. M., TAKEUCHI, G. T. and CERLING, T. E. 2019. Causes and Consequences of Pleistocene Megafaunal Extinctions as Revealed from Rancho La Brea Mammals. *Current Biology*, **29**, 2488-2495.e2.

DIETL, G. P. and FLESSA, K. W. 2011. Conservation paleobiology: putting the dead to work. *Trends in Ecology & Evolution*, **26**, 30–37.

———, KIDWELL, S. M., BRENNER, M., BURNEY, D. A., FLESSA, K. W., JACKSON, S. T. and KOCH, P. L. 2015. Conservation Paleobiology: Leveraging Knowledge of the Past to Inform Conservation and Restoration. *Annual Review of Earth and Planetary Sciences*, **43**, 79–103.

DIMICHELE, W. A., BEHRENSMEYER, A. k., OLSZEWSKI, T. d., LABANDEIRA, C. c., PANDOLFI, J. m., WING, S. l. and BOBE, R. 2004. Long-Term Stasis in Ecological Assemblages: Evidence from the Fossil Record. *Annual Review of Ecology, Evolution, and Systematics*, **35**, 285–322.

DODSON, P. 1971. Sedimentology and taphonomy of the Oldman Formation (Campanian), Dinosaur Provincial Park, Alberta (Canada). *Palaeogeography, Palaeoclimatology, Palaeoecology*, **10**, 21–74.

———. 1983. A Faunal Review of the Judith River (Oldman) Formation, Dinosaur Provincial Park, Alberta, Canada. *The Mosasaur*, **1**, 89–118.

DURKIN, P. R., HUBBARD, S. M., HOLBROOK, J., WELESCHUK, Z., NESBIT, P., HUGENHOLTZ, C., LYONS, T. and SMITH, D. G. 2020. Recognizing the product of concave-bank sedimentary processes in fluvial meander-belt strata. *Sedimentology*, **67**, 2819–2849.

EBERTH, D. A. 1990. Stratigraphy and sedimentology of vertebrate microfossil sites in the uppermost Judith River Formation (Campanian), Dinosaur Provincial Park, Alberta, Canada. *Palaeogeography, Palaeoclimatology, Palaeoecology*, **78**, 1–36.

———. 1996. Origin and significance of mud-filled incised valleys (Upper Cretaceous) in southern Alberta, Canada. *Sedimentology*, **43**, 459–477.

———. 2005. The Geology. *In* CURRIE, P. J. and KOPPELHUS, E. B. (eds.) *Dinosaur Provincial Park: A Spectacular Ancient Ecosystem Revealed*, Indiana University Press, Bloomington, 54–82 pp.

———. 2015. Origins of dinosaur bonebeds in the Cretaceous of Alberta, Canada. *Canadian Journal of Earth Sciences*, **52**, 655–681.

———. 2024. Stratigraphic architecture of the Belly River Group (Campanian, Cretaceous) in the plains of southern Alberta: Revisions and updates to an existing model and implications for correlating dinosaur-rich strata. *PLOS ONE*, **19**, e0292318.

——— and HAMBLIN, A. P. 1993. Tectonic, stratigraphic, and sedimentologic significance of a regional discontinuity in the upper Judith River Group (Belly River wedge) of southern Alberta, Saskatchewan, and northern Montana. *Canadian Journal of Earth Sciences*, **30**, 174–200.

——— and CURRIE, P. J. 2005. Vertebrate Taphonomy and Taphonomic Modes. *In* CURRIE, P. J. and KOPPELHUS, E. B. (eds.) *Dinosaur Provincial Park: A Spectacular Ancient Ecosystem Revealed*, Indiana University Press, Bloomington, 453–477 pp.

——— and GETTY, M. A. 2005. Ceratopsian Bonebeds: Occurrence, Origins, and Significance. *In* CURRIE, P. J. and KOPPELHUS, E. B. (eds.) *Dinosaur Provincial Park: A Spectacular Ancient Ecosystem Revealed*, Indiana University Press, Bloomington, 501–536 pp.

——— and KAMO, S. L. 2020. High-precision U–Pb CA–ID–TIMS dating and chronostratigraphy of the dinosaur-rich Horseshoe Canyon Formation (Upper Cretaceous, Campanian–Maastrichtian), Red Deer River valley, Alberta, Canada. *Canadian Journal of Earth Sciences*, **57**, 1220–1237.

———, BRINKMAN, D. B. and BARKAS, V. 2010. A Centrosaurine Mega-Bonebed from the Upper Cretaceous of Southern Alberta: Implications for Behavior and Death Events. *In* RYAN, M. J., CHINNERY-ALLGEIER, B. J. and EBERTH, D. A. (eds.) *New Perspectives on Horned Dinosaurs*, Indiana University Press, Bloomington & Indianapolis, 495–508 pp.

———, EVANS, D. C. and LLOYD, D. W. H. 2015. Occurrence and Taphonomy of the First Documented Hadrosaurid Bonebed from the Dinosaur Park Formation (Belly River Group, Campanian) at Dinosaur Provincial Park, Alberta, Canada. *In* EBERTH, D. A. and EVANS, D. C. (eds.) *Hadrosaurs*, Indiana University Press, Bloomington, 502–523 pp.

———, ———, BRINKMAN, D. B., THERRIEN, F., TANKE, D. H. and RUSSELL, L. S. 2013. Dinosaur biostratigraphy of the Edmonton Group (Upper Cretaceous), Alberta, Canada: evidence for climate influence. *Canadian Journal of Earth Sciences*, **50**, 701–726.

EBERTH, D. A., EVANS, D. C., RAMEZANI, J., KAMO, S. L., BROWN, C. M., CURRIE, P. J. and BRAMAN, D. R. 2023. Calibrating geologic strata, dinosaurs, and other fossils at Dinosaur Provincial Park (Alberta, Canada) using a new CA-ID-TIMS U–Pb geochronology. *Canadian Journal of Earth Sciences*, **60**, 1627–1646.

ERWIN, D. H. 2009. A call to the custodians of deep time. *Nature*, **462**, 282–283.

EVANS, D. C., BAVINGTON, R. and CAMPIONE, N. E. 2009. An unusual hadrosaurid braincase from the Dinosaur Park Formation and the biostratigraphy of *Parasaurolophus* (Ornithischia: Lambeosaurinae) from southern Alberta. *Canadian Journal of Earth Sciences*, **46**, 791–800.

———, MCGARRITY, C. T. and RYAN, M. J. 2015. A Skull of *Prosaurolophus maximus* from Southeastern Alberta and the Spatiotemporal Distribution of Faunal Zones in the Dinosaur Park Formation. *In* EBERTH, D. A. and EVANS, D. C. (eds.) *Hadrosaurs*, Indiana University Press, Bloomington, 200–207 pp.

EVANS, D. J. A. 2000. Quaternary geology and geomorphology of the Dinosaur Provincial Park area and surrounding plains, Alberta, Canada: the identification of former glacial lobes, drainage diversions and meltwater flood tracks. *Quaternary Science Reviews*, **19**, 931–958.

FANTI, F., CANTELLI, L. and ANGELICOLA, L. 2018. High-resolution maps of Khulsan and Nemegt localities (Nemegt Basin, southern Mongolia): Stratigraphic implications. *Palaeogeography, Palaeoclimatology, Palaeoecology*, **494**, 14–28.

———, ———, CURRIE, P. J., FUNSTON, G. F., CENNI, N., CATELLANI, S., CHINZORIG, T., TSOGTBAATAR, K. H. and BARSBOLD, R. 2024. High-resolution UAV maps of the Gobi Desert provide new insights into the Upper Cretaceous of Mongolia. *Cretaceous Research*, **161**, 105916.

FOWLER, D. W. 2017. Revised geochronology, correlation, and dinosaur stratigraphic ranges of the Santonian-Maastrichtian (Late Cretaceous) formations of the Western Interior of North America. *PLOS ONE*, **12**, e0188426.

FOWLER, D. W. and FOWLER, E. A. F. 2020. Transitional evolutionary forms in chasmosaurine ceratopsid dinosaurs: evidence from the Campanian of New Mexico. *PeerJ*, **8**, e9251.

FRASER, D., SOUL, L. C., TÓTH, A. B., BALK, M. A., ERONEN, J. T., PINEDA-MUNOZ, S., SHUPINSKI, A. B., VILLASEÑOR, A., BARR, W. A., BEHRENSMEYER, A. K., DU, A., FAITH, J. T., GOTELLI, N. J., GRAVES, G. R., JUKAR, A. M., LOOY, C. V., MILLER, J. H., POTTS, R. and LYONS, S. K. 2021. Investigating Biotic Interactions in Deep Time. *Trends in Ecology & Evolution*, **36**, 61–75.

FREDERICKSON, J. A. and TUMARKIN-DERATZIAN, A. R. 2014. Craniofacial ontogeny in *Centrosaurus apertus*. *PeerJ*, **2**, e252.

FRICKE, E. C., HSIEH, C., MIDDLETON, O., GORCZYNSKI, D., CAPPELLO, C. D., SANISIDRO, O., ROWAN, J., SVENNING, J.-C. and BEAUDROT, L. 2022. Collapse of terrestrial mammal food webs since the Late Pleistocene. *Science*, **377**, 1008–1011.

GATES, T. A., PRIETO-MÁRQUEZ, A. and ZANNO, L. E. 2012. Mountain Building Triggered Late Cretaceous North American Megaherbivore Dinosaur Radiation. *PLOS ONE*, **7**, e42135.

GINGERICH, P. D. and GUNNELL, G. F. 1995. Rates of evolution in Paleocene-Eocene mammals of the Clarks Fork Basin, Wyoming, and a comparison with Neogene Siwalik lineages of Pakistan. *Palaeogeography, Palaeoclimatology, Palaeoecology*, **115**, 227–247.

GREENWOOD, D. R. 2007. Fossil angiosperm leaves and climate: from Wolfe and Dilcher to Burnham and Wilf. *Courier Forschungsinstitut Senckenberg*, **258**, 95–108.

GROFF, D. V., HAMLEY, K. M., LESSARD, T. J. R., GREENAWALT, K. E., YASUHARA, M., BRICKLE, P. and GILL, J. L. 2020. Seabird establishment during regional cooling drove a terrestrial ecosystem shift 5000 years ago. *Science Advances*, **6**, eabb2788.

GUTHRIE, R. D. 2006. New carbon dates link climatic change with human colonization and Pleistocene extinctions. *Nature*, **441**, 207–209.

HAMBLIN, A. P. 1997. Regional distribution and dispersal of the Dinosaur Park Formation, Belly River Group, surface and subsurface of southern Alberta. *Bulletin of Canadian Petroleum Geology*, **45**, 377–399.

——— and ABRAHAMSON, B. W. 1996. Stratigraphic architecture of 'basal Belly River' cycles, Foremost Formation, Belly River Group, subsurface of southern Alberta and southwestern Saskatchewan I. *Bulletin of Canadian Petroleum Geology*, **44**, 654–673.

HENDERSON, D. M. and TANKE, D. H. 2010. Estimating past and future dinosaur skeletal abundances in Dinosaur Provincial Park, Alberta, Canada. *Canadian Journal of Earth Sciences*, **47**, 1291–1304.

INTERGOVERNMENTAL PANEL ON CLIMATE CHANGE (IPCC). 2023. Climate Change 2021—The Physical Science Basis: Working Group I Contribution to the Sixth Assessment Report of the Intergovernmental Panel on Climate Change. Cambridge University Press, Cambridge, UK. https://doi.org/10.1017/9781009157896

JABLONSKI, D. 1991. Extinctions: A Paleontological Perspective. *Science*, **253**, 754–757.

JARZEN, D. M. 1982. Palynology of Dinosaur Provincial Park (Campanian) Alberta. *Syllogeus*, **38**, 1–69.

JOHNSON, K. R. and HICKEY, L. J. 1990. Megafloral change across the Cretaceous/Tertiary boundary in the northern Great Plains and Rocky Mountains, U.S.A. *In Geological Society of America Special Papers*, Vol. 247. Geological Society of America, 433–444 pp.

JOHNSTON, P. A. and HENDY, A. J. W. 2005. Paleoecology of Mollusks from the Upper Cretaceous Belly River Group. *In Dinosaur Provincial Park: A Spectacular Ancient Ecosystem Revealed*, Indiana University Press, Bloomington, 139–166 pp.

JOYCE, M. and MOEN, R. 2018. *Accuracy of a modular GPS/GLONASS receiver*. National Resources Research Institute, University of Minnesota, Duluth, Minnesota, 23 pp.

JUSTHAM, T. 2008. Geochemical Analysis of Ironstone Preserved Molluscan Fossils of the Hell Creek Formation (Cretaceous) and Ludlow Member of the Fort Union Formation (Paleogene) of Southwestern North Dakota.University of North Dakotapp.

KAUFFMAN, E. G. and CALDWELL, W. G. E. 1993. The Western Interior Basin in space and time. *In* CALDWELL, W. G. E. and KAUFFMAN, E. G. (eds.) *Evolution of the Western Interior Basin*, Geological Association of Canada, St. John’s, Newfoundland, 1–30 pp.

KIDWELL, S. M. and FLESSA, K. W. 1995. The quality of the fossil record: Populations, Species, and Communities. *Annual Review of Ecology and Systematics*, **26**, 269–299.

——— and HOLLAND, S. M. 2002. The Quality of the Fossil Record: Implications for Evolutionary Analyses. *Annual Review of Ecology and Systematics*, **33**, 561–588.

KNOLL, A. H. and NOWAK, M. A. 2017. The timetable of evolution. *Science Advances*, **3**, e1603076.

KOPPELHUS, E. B. 2005. Paleobotany. *In* CURRIE, P. J. and KOPPELHUS, E. B. (eds.) *Dinosaur Provincial Park: A Spectacular Ancient Ecosystem Revealed*, Indiana University Press, Bloomington, 131–138 pp.

KOSTER, E. H. 1983. *Sedimentology of the Upper Cretaceous Judith River (Belly River) Formation, Dinosaur Provincial Park, Alberta*. *The Mesozoic of Middle North America*. Canadian Society of Petroleum Geologists Conference, Calgary.

———, CURRIE, P. J., EBERTH, D. A., BRINKMAN, D. B., JOHNSTON, P. A. and BRAMAN, D. R. 1987. *Sedimentology and Palaeontology of the Upper Cretaceous Judith River/Bearpaw Formations at Dinosaur Provincial Park, Alberta*. Geological Association of Canada, Mineralogical Association of Canada, Joint Annual Meeting, Saskatoon, Saskatchewan.

LAMBE, L. M. 1913. A new genus and species of Ceratopsia from the Belly River Formation of Alberta. *The Ottawa Naturalist*, **27**, 109–116.

LEHMAN, T. M. 2001. Late Cretaceous Dinosaur Provinciality. *In* TANKE, D. H. and CARPENTER, K. (eds.) *Mesozoic Vertebrate Life*, Indiana University Press, Bloomington, 310–328 pp.

LOWI-MERRI, T. M. and EVANS, D. C. 2020. Cranial variation in *Gryposaurus* and biostratigraphy of hadrosaurines (Ornithischia: Hadrosauridae) from the Dinosaur Park Formation of Alberta, Canada. *Canadian Journal of Earth Sciences*, **57**, 765–779.

LYONS, S. K., AMATANGELO, K. L., BEHRENSMEYER, A. K., BERCOVICI, A., BLOIS, J. L., DAVIS, M., DIMICHELE, W. A., DU, A., ERONEN, J. T., TYLER FAITH, J., GRAVES, G. R., JUD, N., LABANDEIRA, C., LOOY, C. V., MCGILL, B., MILLER, J. H., PATTERSON, D., PINEDA-MUNOZ, S., POTTS, R., RIDDLE, B., TERRY, R., TÓTH, A., ULRICH, W., VILLASEÑOR, A., WING, S., ANDERSON, H., ANDERSON, J., WALLER, D. and GOTELLI, N. J. 2016. Holocene shifts in the assembly of plant and animal communities implicate human impacts. *Nature*, **529**, 80–83.

LYSON, T. R., MILLER, I. M., BERCOVICI, A. D., WEISSENBURGER, K., FUENTES, A. J., CLYDE, W. C., HAGADORN, J. W., BUTRIM, M. J., JOHNSON, K. R., FLEMING, R. F., BARCLAY, R. S., MACCRACKEN, S. A., LLOYD, B., WILSON, G. P., KRAUSE, D. W. and CHESTER, S. G. B. 2019. Exceptional continental record of biotic recovery after the Cretaceous–Paleogene mass extinction. *Science*, **366**, 977–983.

MACDONALD, M., CURRIE, P. J. and SPENCER, W. A. 2005. Precise Mapping of Fossil Sites in the Park Using Survey Grade GPS Technology. *In* CURRIE, P. J. and KOPPELHUS, E. B. (eds.) *Dinosaur Provincial Park: A Spectacular Ancient Ecosystem Revealed*, Indiana University Press, Bloomington, 478–485 pp.

MALLON, J. C. 2019. Competition structured a Late Cretaceous megaherbivorous dinosaur assemblage. *Scientific Reports*, **9**, 15447.

——— and ANDERSON, J. S. 2014. Implications of beak morphology for the evolutionary paleoecology of the megaherbivorous dinosaurs from the Dinosaur Park Formation (upper Campanian) of Alberta, Canada. *Palaeogeography, Palaeoclimatology, Palaeoecology*, **394**, 29–41.

———, EVANS, D. C., RYAN, M. J. and ANDERSON, J. S. 2012. Megaherbivorous dinosaur turnover in the Dinosaur Park Formation (upper Campanian) of Alberta, Canada. *Palaeogeography, Palaeoclimatology, Palaeoecology*, **350–352**, 124–138.

MAYO, K., SILVA, R. L. and DURKIN, P. R. 2023. Paleoenvironmental reconstruction of Late Cretaceous rivers, Dinosaur Park Formation, Alberta, Canada. *Sedimentary Geology*, **457**, 106499.

NESBIT, P. R. and HUGENHOLTZ, C. H. 2019. Enhancing UAV–SfM 3D Model Accuracy in High-Relief Landscapes by Incorporating Oblique Images. *Remote Sensing*, **11**, 239.

———, DURKIN, P. R., HUGENHOLTZ, C. H., HUBBARD, S. M. and KUCHARCZYK, M. 2018. 3-D stratigraphic mapping using a digital outcrop model derived from UAV images and structure-from-motion photogrammetry. *Geosphere*, **14**, 2469–2486.

———, BOULDING, A., HUGENHOLTZ, C., DURKIN, P. and HUBBARD, S. 2020. Visualization and Sharing of 3D Digital Outcrop Models to Promote Open Science. *GSA Today*, **30**, 4–10.

NOPCSA, F. 1928. Palaeontological notes on reptiles. *Geologica Hungarica, Seria Palaeontologica*, **1**, 1–84.

ORESKA, M. P. J. and CARRANO, M. T. 2019. Paleocommunity mixing increases with marine transgression in Dinosaur Park Formation (Upper Cretaceous) vertebrate microfossil assemblages. *Paleobiology*, **45**, 136–153.

PARKS, W. A. 1923. Corythosaurus intermedius*, a New Species of Trachodont Dinosaur*. University Library, Toronto.

Parks Division, Alberta Tourism, Parks and Recreation. 2013. Dinosaur Provincial Park World Heritage Site. Scale 1:30,000.

PAVLIS, T. L. and MASON, K. A. 2017. The New World of 3D Geologic Mapping. *GSA Today*, 4–10.

POLLY, P. D., ERONEN, J. T., FRED, M., DIETL, G. P., MOSBRUGGER, V., SCHEIDEGGER, C., FRANK, D. C., DAMUTH, J., STENSETH, N. C. and FORTELIUS, M. 2011. History matters: ecometrics and integrative climate change biology. *Proceedings of the Royal Society B: Biological Sciences*, **278**, 1131–1140.

QUINNEY, A., THERRIEN, F., ZELENITSKY, D. K. and EBERTH, D. A. 2013. Palaeoenvironmental and palaeoclimatic reconstruction of the Upper Cretaceous (late Campanian–early Maastrichtian) Horseshoe Canyon Formation, Alberta, Canada. *Palaeogeography, Palaeoclimatology, Palaeoecology*, **371**, 26–44.

R CORE TEAM. 2023. *R: A language and environment for statistical computing*. R Foundation for Statistical Computing, Vienna, Austria. Downloaded from URL https://www.R-project.org/.

RAMANUJAM, C. G. K. 1972. Fossil coniferous woods from the Oldman Formation (Upper Cretaceous) of Alberta. *Canadian Journal of Botany*, **50**, 595–602.

RAMEZANI, J., BEVERIDGE, T. L., ROGERS, R. R., EBERTH, D. A. and ROBERTS, E. M. 2022. Calibrating the zenith of dinosaur diversity in the Campanian of the Western Interior Basin by CA-ID-TIMS U–Pb geochronology. *Scientific Reports*, **12**, 16026.

ROGERS, R. R. 1990. Taphonomy of Three Dinosaur Bone Beds in the Upper Cretaceous Two Medicine Formation of Northwestern Montana: Evidence for Drought-Related Mortality. *PALAIOS*, **5**, 394–413.

———, EBERTH, D. A. and RAMEZANI, J. 2023. The "Judith River−Belly River problem" revisited (Montana-Alberta-Saskatchewan): New perspectives on the correlation of Campanian dinosaur-bearing strata based on a revised stratigraphic model updated with CA-ID-TIMS U-Pb geochronology. *GSA Bulletin*.

ROOPNARINE, P. D. and ANGIELCZYK, K. D. 2015. Community stability and selective extinction during the Permian-Triassic mass extinction. *Science*, **350**, 90–93.

——— and BANKER, R. M. W. 2021. Ecological stasis on geological time scales. *Science*, **372**, 237–238.

ROOPNARINE, P. D., ANGIELCZYK, K. D., WANG, S. C. and HERTOG, R. 2007. Trophic network models explain instability of Early Triassic terrestrial communities. *Proceedings of the Royal Society B: Biological Sciences*, **274**, 2077–2086.

ROYAL TYRRELL COLLECTIONS. 2023. *TMP2005.009.0069*. Downloaded from https://rtmp.emuseum.com/objects/141713/tmp20050090069 on 8 December 2023.

RUSSELL, L. S. 1966. Dinosaur hunting in Western Canada. *Royal Ontario Museum Life Sciences Contributions*, **70**, 1–37.

RYAN, M. J. and EVANS, D. C. 2005. Ornithischian Dinosaurs. *In Dinosaur Provincial Park: A Spectacular Ancient Ecosystem Revealed*, Indiana University Press, Bloomington, 312–348 pp.

RYAN, M. J. and RUSSELL, A. P. 2005. A new centrosaurine ceratopsid from the Oldman Formation of Alberta and its implications for centrosaurine taxonomy and systematics. *Canadian Journal of Earth Sciences*, **42**, 1369–1387.

———, HOLMES, R. and RUSSELL, A. P. 2007. A revision of the late campanian centrosaurine ceratopsid genus *Styracosaurus* from the Western Interior of North America. *Journal of Vertebrate Paleontology*, **27**, 944–962.

RYAN, M. J., RUSSELL, A. P., EBERTH, D. A. and CURRIE, P. J. 2001. The Taphonomy of a *Centrosaurus* (Ornithischia: Ceratopsidae) Bone Bed from the Dinosaur Park Formation (Upper Campanian), Alberta, Canada, with Comments on Cranial Ontogeny. *Palaios*, **16**, 482–506.

———, EBERTH, D. A., BRINKMAN, D. B., CURRIE, P. J. and TANKE, D. H. 2010. A New *Pachyrhinosaurus*-Like Ceratopsid from the Upper Dinosaur Park Formation (Late Campanian) of Southern Alberta, Canada. *In* RYAN, M. J., EBERTH, D. A., CHINNERY-ALLGEIER, B. J. and RALRICK, P. E. (eds.) *New Perspectives on Horned Dinosaurs: The Royal Tyrrell Museum Ceratopsian Symposium*, Indiana University Press, Bloomington, 141–155 pp.

SAMPSON, S. D. 1995. Two new horned dinosaurs from the upper Cretaceous Two Medicine Formation of Montana; with a phylogenetic analysis of the Centrosaurinae (Ornithischia: Ceratopsidae). *Journal of Vertebrate Paleontology*, **15**, 743–760.

——— and LOEWEN, M. A. 2010. Unraveling a Radiation: A Review of the Diversity, Stratigraphic Distribution, Biogeography, and Evolution of Horned Dinosaurs (Ornithischia: Ceratopsidae). *In* RYAN, M. J., CHINNERY-ALLGEIER, B. J. and EBERTH, D. A. (eds.) *New Perspectives on Horned Dinosaurs*, Indiana University Press, Bloomington & Indianapolis, 405–427 pp.

———, RYAN, M. J. and TANKE, D. H. 1997. Craniofacial ontogeny in centrosaurine dinosaurs (Ornithischia: Ceratopsidae): taxonomic and behavioral implications. *Zoological Journal of the Linnean Society*, **121**, 293–337.

———, LOEWEN, M. A., FARKE, A. A., ROBERTS, E. M., FORSTER, C. A., SMITH, J. A. and TITUS, A. L. 2010. New Horned Dinosaurs from Utah Provide Evidence for Intracontinental Dinosaur Endemism. *PLOS ONE*, **5**, e12292.

SCANNELLA, J. B., FOWLER, D. W., GOODWIN, M. B. and HORNER, J. R. 2014. Evolutionary trends in *Triceratops* from the Hell Creek Formation, Montana. *Proceedings of the National Academy of Sciences*, **111**, 10245–10250.

SECORD, R., BLOCH, J. I., CHESTER, S. G. B., BOYER, D. M., WOOD, A. R., WING, S. L., KRAUS, M. J., MCINERNEY, F. A. and KRIGBAUM, J. 2012. Evolution of the Earliest Horses Driven by Climate Change in the Paleocene-Eocene Thermal Maximum. *Science*, **335**, 959–962.

SMITH, F. A., TOMÉ, C. P., ELLIOTT SMITH, E. A., LYONS, S. K., NEWSOME, S. D. and STAFFORD, T. W. 2016. Unraveling the consequences of the terminal Pleistocene megafauna extinction on mammal community assembly. *Ecography*, **39**, 223–239.

SMITH, J. J., HASIOTIS, S. T., KRAUS, M. J. and WOODY, D. T. 2009. Transient dwarfism of soil fauna during the Paleocene–Eocene Thermal Maximum. *Proceedings of the National Academy of Sciences*, **106**, 17655–17660.

SPICER, R. A., YANG, J., SPICER, T. E. V. and FARNSWORTH, A. 2021. Woody dicot leaf traits as a palaeoclimate proxy: 100 years of development and application. *Palaeogeography, Palaeoclimatology, Palaeoecology*, **562**, 110138.

STERNBERG, C. M. 1936. Preliminary map 969A, Steveville sheet, Alberta. .

———. 1950. Steveville west of the 4th meridian, with notes on fossil localities. .

TAKASAKI, R., CHIBA, K., FIORILLO, A. R., BRINK, K. S., EVANS, D. C., FANTI, F., SANEYOSHI, M., MALTESE, A. and ISHIGAKI, S. 2023. Description of the first definitive *Corythosaurus* (Dinosauria, Hadrosauridae) specimens from the Judith River Formation in

Montana, USA and their paleobiogeographical significance. *The Anatomical Record*, **306**, 1918–1938.

TANKE, D. H. 2005. Identifying Lost Quarries. *In* CURRIE, P. J. and KOPPELHUS, E. B. (eds.) *Dinosaur Provincial Park: A Spectacular Ancient Ecosystem Revealed*, Indiana University Press, Bloomington, 34–53 pp.

THOMAS, R. G., EBERTH, D. A., DEINO, A. L. and ROBINSON, D. 1990. Composition, radioisotopic ages, and potential significance of an altered volcanic ash (bentonite) from the Upper Cretaceous Judith River Formation, Dinosaur Provincial Park, southern Alberta, Canada. *Cretaceous Research*, **11**, 125–162.

———, SMITH, D. G., WOOD, J. M., VISSER, J., CALVERLEY-RANGE, E. A. and KOSTER, E. H. 1987. Inclined heterolithic stratification—Terminology, description, interpretation and significance. *Sedimentary Geology*, **53**, 123–179.

TÓTH, A. B., LYONS, S. K., BARR, W. A., BEHRENSMEYER, A. K., BLOIS, J. L., BOBE, R., DAVIS, M., DU, A., ERONEN, J. T., FAITH, J. T., FRASER, D., GOTELLI, N. J., GRAVES, G. R., JUKAR, A. M., MILLER, J. H., PINEDA-MUNOZ, S., SOUL, L. C., VILLASEÑOR, A. and ALROY, J. 2019. Reorganization of surviving mammal communities after the end-Pleistocene megafaunal extinction. *Science*, **365**, 1305–1308.

TUMARKIN-DERATZIAN, A. R. 1997. Sedimentology, Taphonomy, and Faunal Review of a Multigeneric Bonebed (Bonebed 47) in the Dinosaur Park Formation (Campanian) of Southern Alberta, Canada.Unpublished B.Sc. Thesis, Lafayette College, Easton, PA, 107pp.

VARRICCHIO, D. J. 1995. Taphonomy of Jack's Birthday Site, a diverse dinosaur bonebed from the Upper Cretaceous Two Medicine Formation of Montana. *Palaeogeography, Palaeoclimatology, Palaeoecology*, **114**, 297–323.

——— and HORNER, J. R. 1993. Hadrosaurid and lambeosaurid bone beds from the Upper Cretaceous Two Medicine Formation of Montana: taphonomic and biologic implications. *Canadian Journal of Earth Sciences*, **30**, 997–1006.

VERMEIJ, G. J. and LEIGHTON, L. R. 2003. Does global diversity mean anything? *Paleobiology*, **29**, 3–7.

VISSER, J. 1986. Sedimentology and taphonomy of a *Styracosaurus* bonebed in the Late Cretaceous Judith River Formation, Dinosaur Provincial Park, Alberta.Unpublished M.Sc. Thesis, University of Calgary, Calgary, 150pp.

WILLIS, K. J. and BIRKS, H. J. B. 2006. What Is Natural? The Need for a Long-Term Perspective in Biodiversity Conservation. *Science*, **314**, 1261–1265.

WILSON, G. P. 2013. Mammals across the K/Pg boundary in northeastern Montana, U.S.A.: dental morphology and body-size patterns reveal extinction selectivity and immigrant-fueled ecospace filling. *Paleobiology*, **39**, 429–469.

WILSON, J. P., RYAN, M. J. and EVANS, D. C. 2020. A new, transitional centrosaurine ceratopsid from the Upper Cretaceous Two Medicine Formation of Montana and the evolution of the '*Styracosaurus*-line' dinosaurs. *Royal Society Open Science*, **7**, 200284.

WING, S. L., HARRINGTON, G. J., SMITH, F. A., BLOCH, J. I., BOYER, D. M. and FREEMAN, K. H. 2005. Transient Floral Change and Rapid Global Warming at the Paleocene-Eocene Boundary. *Science*, **310**, 993–996.

WOLFE, J. A. and UPCHURCH, G. R. 1987. North American nonmarine climates and vegetation during the Late Cretaceous. *Palaeogeography, Palaeoclimatology, Palaeoecology*, **61**, 33–77.

WOOD, J. M. 1985. Sedimentology of the Late Cretaceous Judith River Formation, 'Cathedral' area, Dinosaur Provincial Park, Alberta.Unpublished M.Sc. Thesis, University of Calgary, 215pp.

———. 1989. Alluvial architecture of the Upper Cretaceous Judith River Formation, Dinosaur Provincial Park, Alberta, Canada. *Bulletin of Canadian Petroleum Geology*, **37**, 169–181.

———, THOMAS, R. G. and VISSER, J. 1988. Fluvial processes and vertebrate taphonomy: the Upper Cretaceous Judith River formation, South-Central dinosaur Provincial Park, Alberta, Canada. *Palaeogeography, Palaeoclimatology, Palaeoecology*, **66**, 127–143.

WU, Y., FANG, X. and JI, J. 2023. A global zircon U–Th–Pb geochronological database. *Earth System Science Data*, **15**, 5171–5181.

3.8 Figures

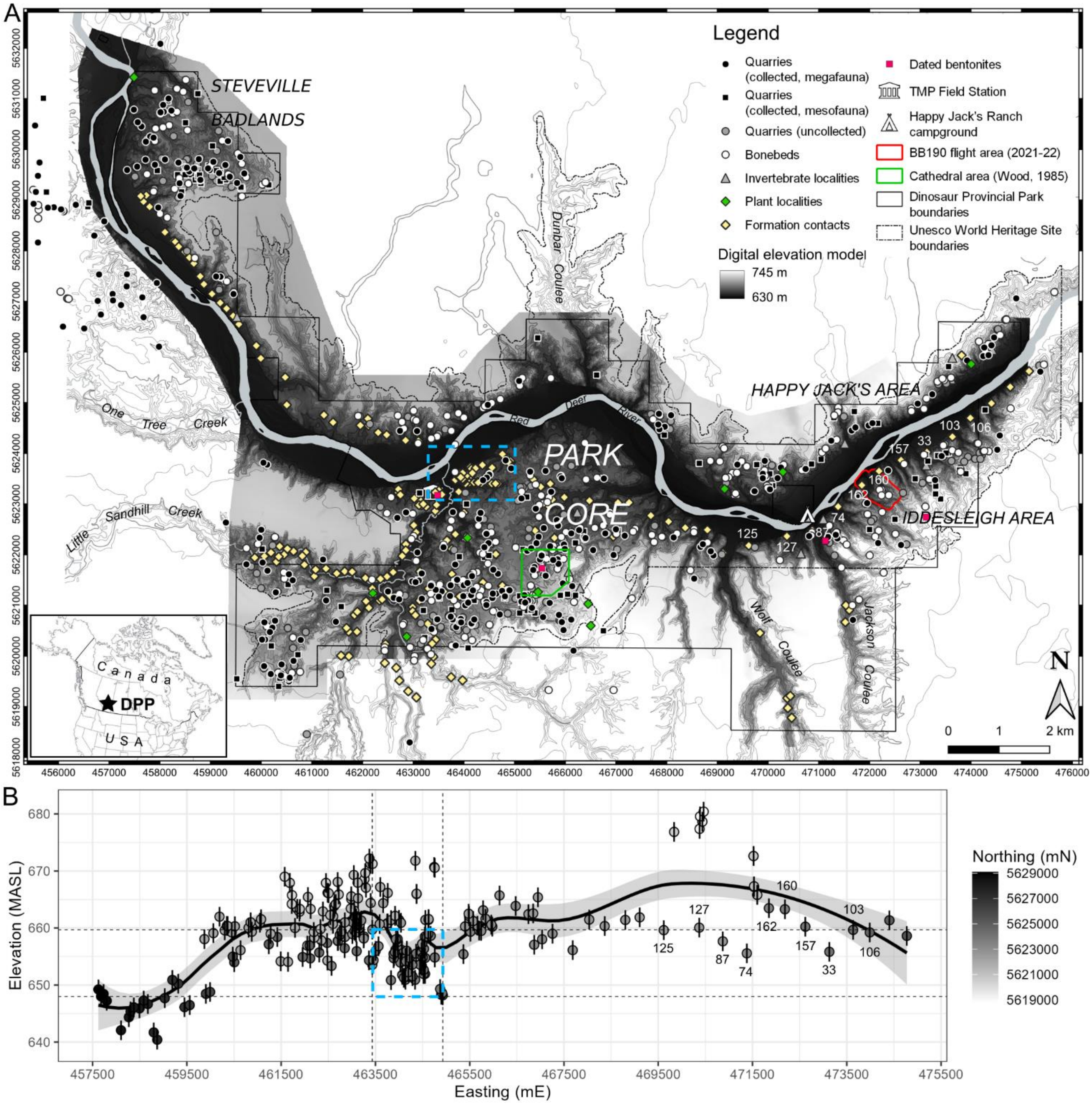
A
Legend
Quarries (collected, megafauna)
Quarries (collected, mesofauna)
Quarries (uncollected)
Bonebeds
Invertebrate localities
Plant localities
Formation contacts
Dated bentonites
TMP Field Station
Happy Jack's Ranch campground
BB190 flight area (2021-22)
Cathedral area (Wood, 1985)
Dinosaur Provincial Park boundaries
Unesco World Heritage Site boundaries
Digital elevation model
745 m
630 m
STEVEVILLE BADLANDS
PARK CORE
HAPPY JACK'S AREA
IDDESLEIGH AREA
Dunbar Coulee
Red Deer River
One Tree Creek
Little Sandhill Creek
Wolf Coulee
Jackson Coulee
Canada
DPP
USA
N
0
1
2 km
103
106
157
33
160
162
74
87
125
127
5632000
5631000
5630000
5629000
5628000
5627000
5626000
5625000
5624000
5623000
5622000
5621000
5620000
5619000
5618000
456000
457000
458000
459000
460000
461000
462000
463000
464000
465000
466000
467000
468000
469000
470000
471000
472000
473000
474000
475000
476000
B
Elevation (MASL)
680
670
660
650
640
Easting (mE)
457500
459500
461500
463500
465500
467500
469500
471500
473500
475500
127
160
162
103
125
87
74
157
33
106
Northing (mN)
5629000
5627000
5625000
5623000
5621000
5619000

Figure 3.1. Overview of the geological and palaeontological heritage of Dinosaur Provincial Park in the context of a digital elevation model (DEM). A, location of drone flight area covering Bonebed 190 among significant fossil quarries and other geological features within Dinosaur Provincial Park (DPP). Quarry and formational contact locations available from database assembled by first author, updated from Currie & Koppelhus (2005: Supplementary CD-ROM), see Appendix II. bentonite locations available from Ramezani *et al*. (2022). Numbers indicate Oldman-Dinosaur Park Formation contacts that are compared with OF-DPF contact measured in the present study. DEM assembled by aerial Lidar scanning in 2015, provided courtesy of Royal Tyrrell Museum of Palaeontology (TMP). Elevation contour lines redrawn from topographic map of DPP (2013) georeferenced on QGIS. B, absolute elevation extracted from TMP DEM for all points measured along OF-DPF contact during a differential GPS survey occurring from 1999 to 2003 along an east-west axis. Coordinates in WGS84 / Universal Transverse Mercator zone 12N, EGM96 geoid. Dashed light blue rectangles indicate same series of points measured around TMP field station and DPP public loop road.

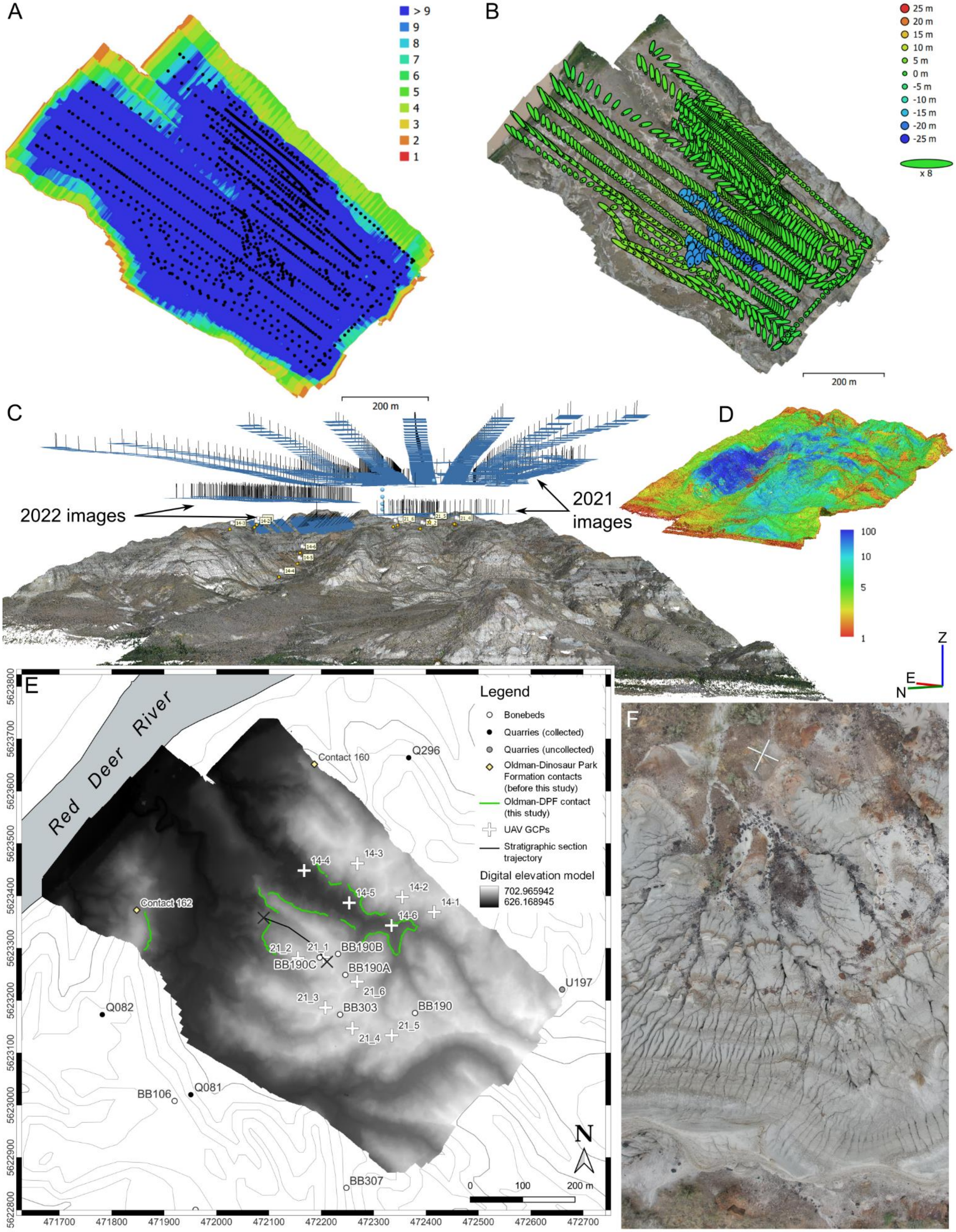
A
> 9
9
8
7
6
5
4
3
2
1
B
25 m
20 m
15 m
10 m
5 m
0 m
-5 m
-10 m
-15 m
-20 m
-25 m
x 8
200 m
C
200 m
2022 images
2021 images
D
100
10
5
1
Z
E
N
E
Red Deer River
Legend
Bonebeds
Quarries (collected)
Quarries (uncollected)
Oldman-Dinosaur Park Formation contacts (before this study)
Oldman-DPF contact (this study)
UAV GCPs
Stratigraphic section trajectory
Digital elevation model
702.965942
626.168945
Contact 160
Q296
Contact 162
14-4
14-3
14-5
14-2
14-1
14-6
21_2
21_1
BB190B
BB190C
BB190A
21_6
21_3
BB303
BB190
21_5
21_4
U197
Q082
BB106
Q081
BB307
N
0
100
200 m
5623800
5623700
5623600
5623500
5623400
5623300
5623200
5623100
5623000
5622900
5622800
471700
471800
471900
472000
472100
472200
472300
472400
472500
472600
472700
F

Figure 3.2. Overview of unmanned aerial vehicle (UAV) structure-from-motion (SfM) photogrammetry process leading to creation of digital outcrop model (DOM), digital elevation model (DEM) and orthomosaic of Bonebed 190 Amphitheatre area; survey area 0.446 km^2. A, UAV camera locations and image overlap obtained from Agisoft Metashape processing report: colour palette indicates number of overlapping images per grid cell. B, UAV camera location error estimates along flight paths obtained from Agisoft Metashape processing report: Z error represented by ellipse colour; X, Y errors represented by ellipse shape; estimated camera locations marked with black dot. C, perspective render of dense 3-D point cloud generated from UAV image alignment followed by geolocation optimization with ground control points (GCPs, marked with flags). Image dataset combined from 2021 and 2022 flights; 2022 images (including some taken at 45˚ pitch angle) cover well-exposed Oldman-Dinosaur Park Formation contact. D, orthographic render of dense 3-D point cloud coloured by point confidence; blue represents highest point confidence, as seen on the outcrop photographed at oblique angles (see Figure 3.2C). E, DEM with GCP locations, significant fossil quarries and measured Oldman-Dinosaur Park Formation contacts. Coordinates in WGS84 / Universal Transverse Mercator zone 12N, EGM96 geoid. Quarry and formational contact locations available from database assembled by first author, updated from Currie and Koppelhus (2005: Supplementary CD-ROM). Black crosses mark start and end points of main stratigraphic section measured during 2022 field season. F, inset of image captured during 2021 flight at low elevation over BB190 host horizon; note GCP made of two white Jacob staffs (GCP 21_3 in Figure 3.2E).

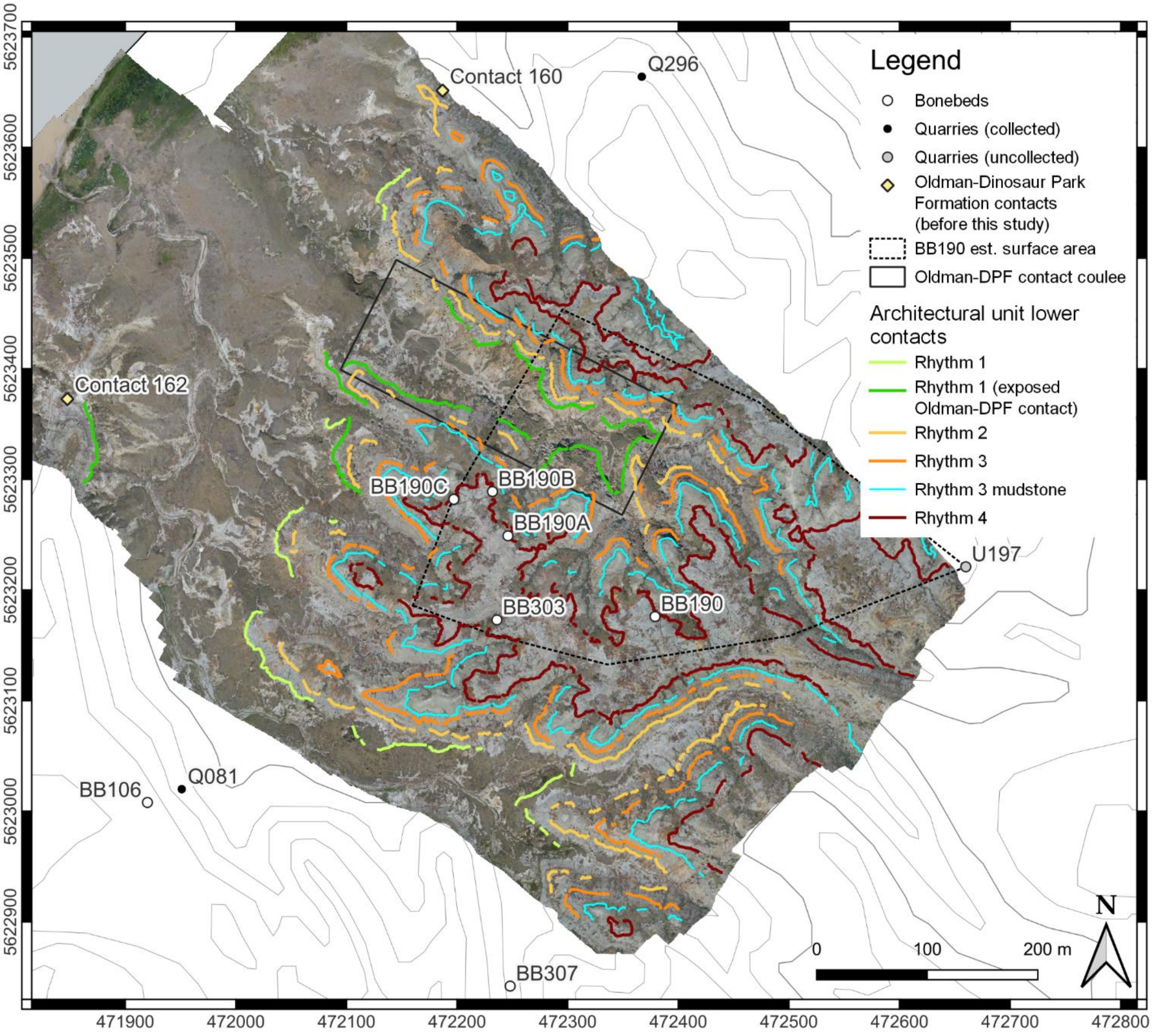

Figure 3.3. Identification of architectural sedimentary units across Bonebed 190 Amphitheatre area using orthomosaic highlighting contacts between identified architectural sedimentary units. 'BB190' point marks original quarry stake marked in 2002; 'BB190A-C' and 'BB303' points mark fossil-rich localities discovered during this study. Note semi-circular shape formed by ridge marked by dark red contact between Rhythm 3 mudstone and Rhythm 4, hence the proposed 'Amphitheatre' toponym. Coordinates in WGS84 / Universal Transverse Mercator zone 12N. Quarry and formational contact locations available from database assembled by first author, updated from Currie and Koppelhus (2005: Supplementary CD-ROM).

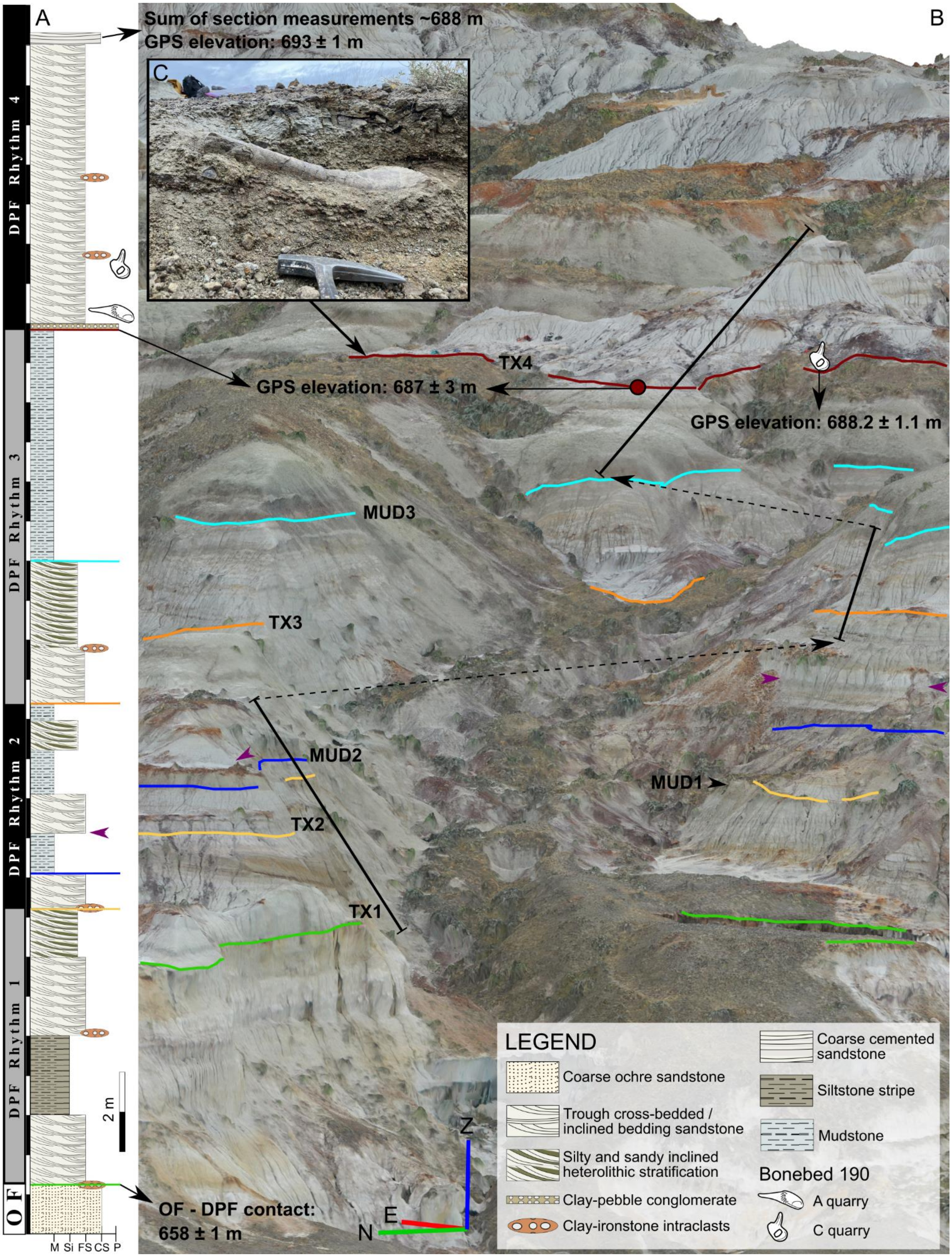
A
B
C
Sum of section measurements ~688 m
GPS elevation: 693 ± 1 m
DPF Rhythm 4
DPF Rhythm 3
DPF Rhythm 2
DPF Rhythm 1
OF
TX4
GPS elevation: 687 ± 3 m
GPS elevation: 688.2 ± 1.1 m
MUD3
TX3
MUD2
MUD1
TX2
TX1
OF - DPF contact:
658 ± 1 m
2 m
M Si FS CS P
Z
E
N
LEGEND
Coarse ochre sandstone
Trough cross-bedded / inclined bedding sandstone
Silty and sandy inclined heterolithic stratification
Clay-pebble conglomerate
Clay-ironstone intraclasts
Coarse cemented sandstone
Siltstone stripe
Mudstone
Bonebed 190
A quarry
C quarry

Figure 3.4. Visualization of architectural units of BB190 Amphitheatre area using stratigraphic section and digital outcrop model (DOM). A, stratigraphic section measured along secondary coulee leading to BB190. B, orthographic render of DOM displaying outcrop exposures measured for stratigraphic section. C, cross-sectional photograph of clay-pebble conglomerate forming erosional contact between MUD3 and TX4, hosting ceratopsid pubis collected from BB190B quarry. Colour code for lower contacts of architectural sedimentary units identified across entire mapped area same as in Figure 3.3; burgundy arrowheads mark sandstone ribbon cutting into MUD2. Black strokes indicate extent of measured outcrops, dashed arrows indicate interruptions in continuous sequence measurements. Lower half of section corrected during examination of DOM after fieldwork. **Abbreviations: M** and **MUD,** mudstone; **Si,** siltstone; **FS,** fine-grained sandstone; **CS,** coarse-grained sandstone; **P,** pebbles; **TX,** trough cross-bedded sandstone; **DPF,** Dinosaur Park Formation; **OF,** Oldman Formation.

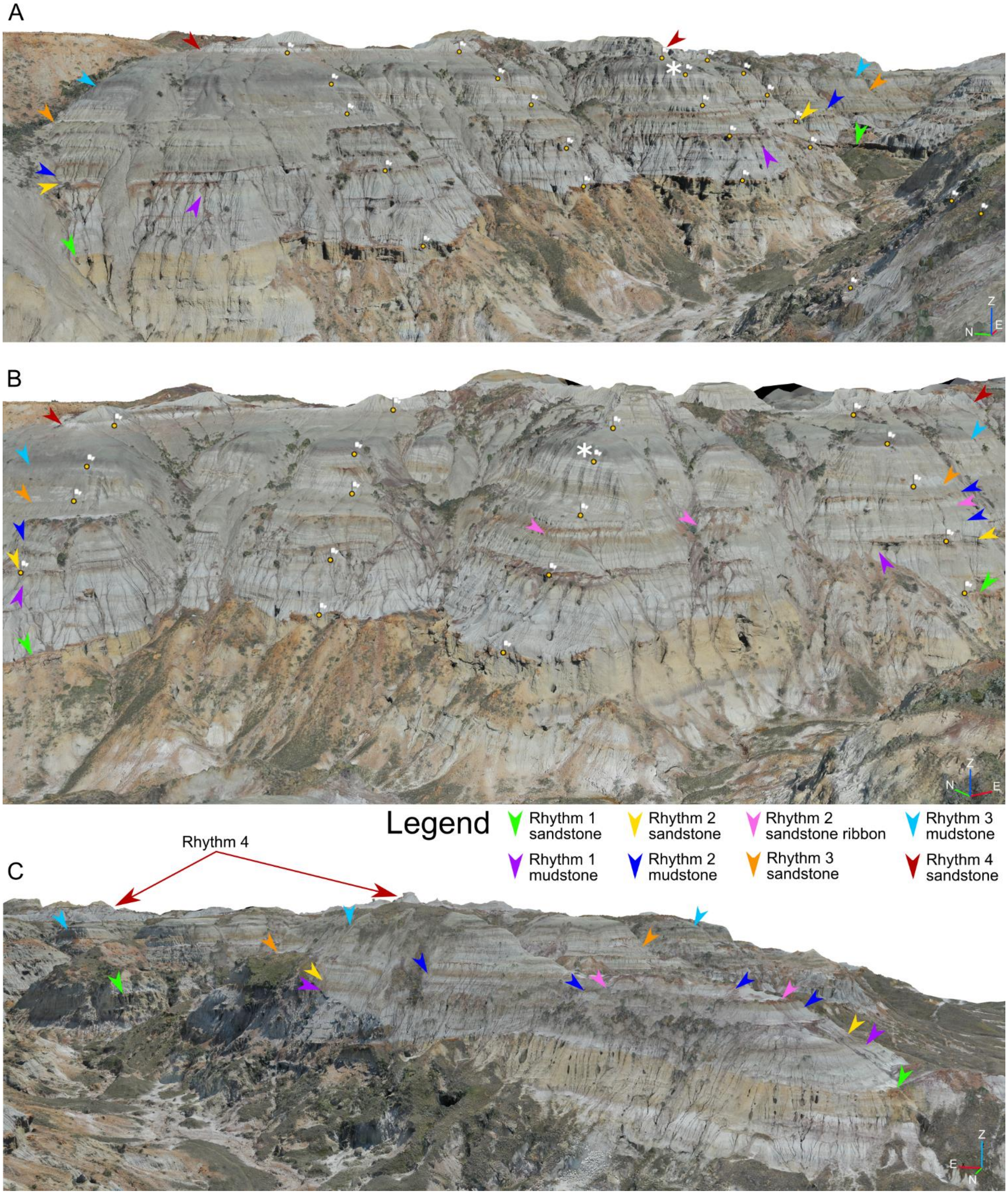
A
Z
N
E
B
Z
N
E
Legend
Rhythm 1 sandstone
Rhythm 1 mudstone
Rhythm 2 sandstone
Rhythm 2 mudstone
Rhythm 2 sandstone ribbon
Rhythm 3 sandstone
Rhythm 3 mudstone
Rhythm 4 sandstone
C
Rhythm 4
Z
E
N

Figure 3.5. Perspective renders of digital outcrop model (DOM) highlighting channel cut-and-fill succession above a continuously exposed Oldman-Dinosaur Park Formation (OF-DPF) contact extending along both flanks of the coulee located along the northern margin of the BB190 Amphitheatre area. OF-DPF contact marks base of Rhythm 1 sandstone. A, exposure on northern slope of the coulee. B, close-up of A from a different viewing angle; note occasional thick blocks of silty ironstone at the OF-DPF contact, dark red clay-ironstone table at base of Rhythm 2 sandstone and laterally discontinuous sandstone ribbon cutting within Rhythm 2 mudstone. C, exposure on southern flank of the coulee; note southeastward slump in OF-DPF contact and vertical amalgamation of sandstone units pinching out mudstone units to the southeast. Ticks mark bases of each identified lithological unit, points marked with flags indicate digital sections traced to measure local rhythm depths in Agisoft, white asterisk indicates same location in A and B.

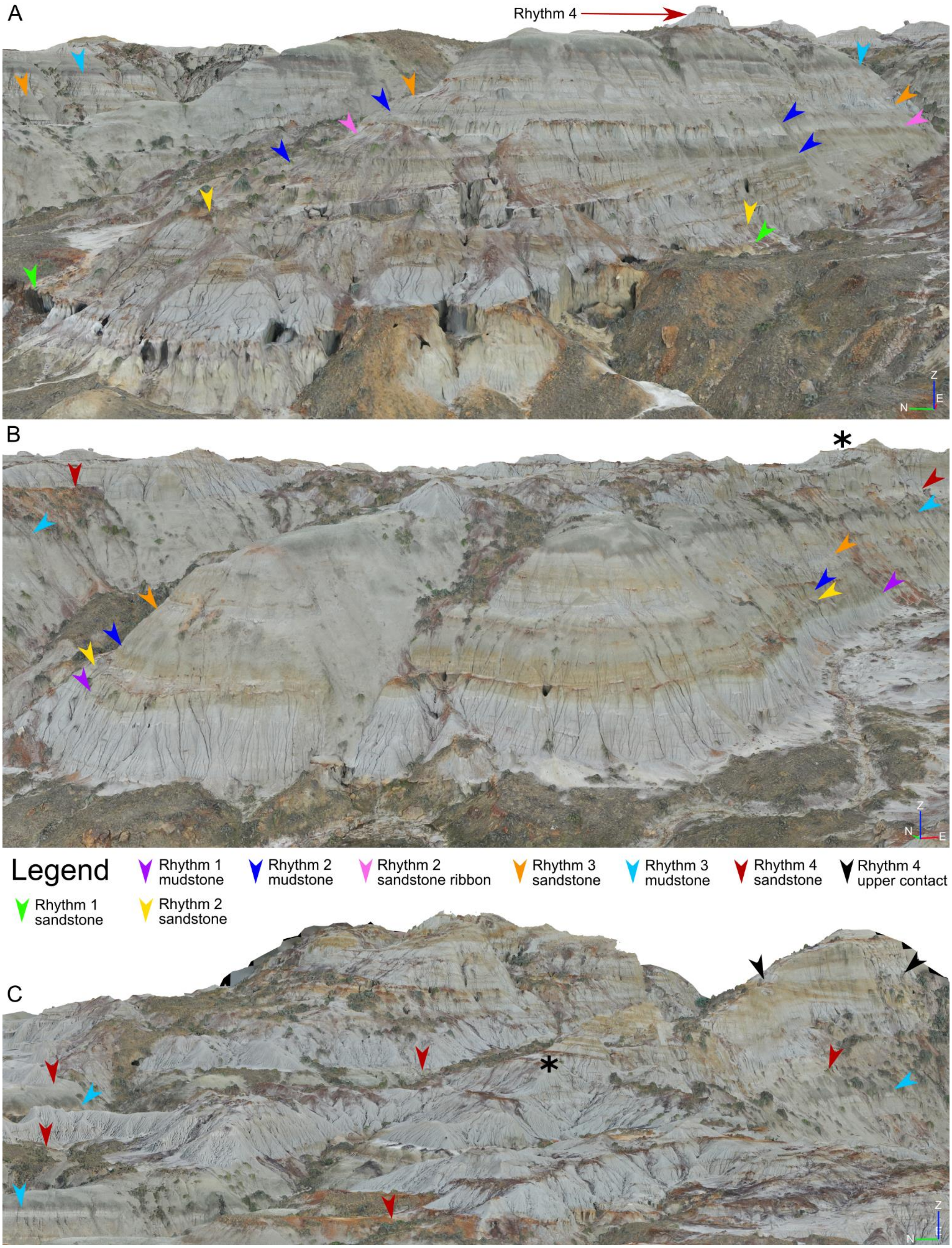
A
Rhythm 4
Z
N
E
B
*
Z
N
E
Legend
Rhythm 1 mudstone
Rhythm 2 mudstone
Rhythm 2 sandstone ribbon
Rhythm 3 sandstone
Rhythm 3 mudstone
Rhythm 4 sandstone
Rhythm 4 upper contact
Rhythm 1 sandstone
Rhythm 2 sandstone
C
*
Z
N

Figure 3.6. Additional renders of digital outcrop model (DOM) highlighting channel cut-and-fill succession in the BB190 Amphitheatre area. A, perspective render of exposure of rill forming southern margin of secondary coulee along which the main stratigraphic section was measured (see Figure 3.4). Oldman-Dinosaur Park Formation contact marks base of Rhythm 1 sandstone; note change in direction of lateral accretion of ochre siltstone ribbons above and below contact with Rhythm 2 sandstone, as well as laterally discontinuous sandstone ribbon cutting within Rhythm 2 mudstone. B, perspective render of exposure on southern margin of BB190 Amphitheatre area highlighting subtle contact between Rhythms 1 and 2; note Rhythm 2 sandstone downcutting Rhythm 1 mudstone at contact marked by dark red clay-ironstone table. C, orthographic render of uppermost exposures of the Dinosaur Park Formation located upstream from Figure 3.6B, where the plateau hosting the bonebed narrows into a ridge stretching to the southeast beyond the reaches of the DOM; note possible initiation of a new rhythm at the top of Rhythm 4 with different directions of lateral accretion above and below the proposed contact. Ticks mark bases of each identified lithological unit; black asterisk marks same location in B and C.

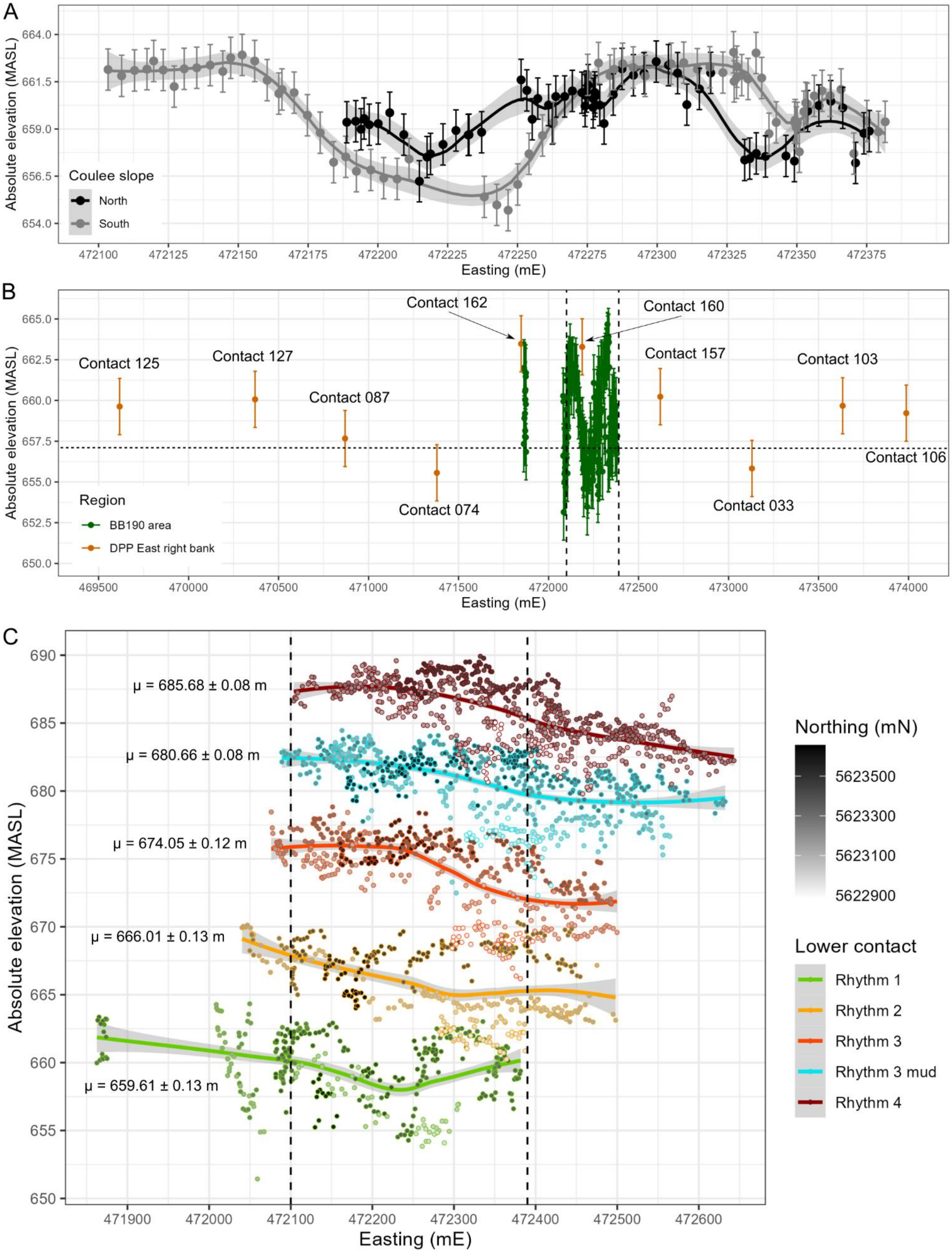
A
Absolute elevation (MASL)
664.0
661.5
659.0
656.5
654.0
Coulee slope
North
South
472100
472125
472150
472175
472200
472225
472250
472275
472300
472325
472350
472375
Easting (mE)
B
Absolute elevation (MASL)
665.0
662.5
660.0
657.5
655.0
652.5
650.0
Contact 162
Contact 160
Contact 125
Contact 127
Contact 157
Contact 103
Contact 087
Contact 106
Contact 074
Contact 033
Region
BB190 area
DPP East right bank
469500
470000
470500
471000
471500
472000
472500
473000
473500
474000
Easting (mE)
C
Absolute elevation (MASL)
690
685
680
675
670
665
660
655
650
μ = 685.68 ± 0.08 m
μ = 680.66 ± 0.08 m
μ = 674.05 ± 0.12 m
μ = 666.01 ± 0.13 m
μ = 659.61 ± 0.13 m
471900
472000
472100
472200
472300
472400
472500
472600
Easting (mE)
Northing (mN)
5623500
5623300
5623100
5622900
Lower contact
Rhythm 1
Rhythm 2
Rhythm 3
Rhythm 3 mud
Rhythm 4

Figure 3.7. Measurement of architectural unit contacts within and beyond BB190 Amphitheatre area. A, measurement of Oldman-Dinosaur Park Formation (OF-DPF) contact elevation solely within a wide coulee forming northern margin of Amphitheatre area; elevation extracted from digital elevation model (DEM) generated during this study and 95% confidence interval of trend curves. B, comparison of OF-DPF contact elevations between aforementioned coulee and all contacts measured along Dinosaur Provincial Park (DPP) eastern right bank during DGPS survey in the early 2000s; elevation for both groups extracted from DEM generated during aerial Lidar survey of DPP. Mean contact elevations with standard errors are as follows: 658.64 ± 0.18 m (BB190 area), 659.46 ± 0.84 m (DPP East right bank). Vertical dashed lines indicate extent of region studied in Figure 3.7A; horizontal dotted line indicates ~0.05˚ average structural dip of DPP exposures to the northwest. C, comparison of architectural unit lower contacts across BB190 Amphitheatre area. Elevation extracted from DEM generated during this study, with 95% confidence interval of trend curves; vertical dashed lines indicate extent of region studied in Figure 3.7A; error bars omitted to improve point visibility; standard error provided with mean elevation for each contact.

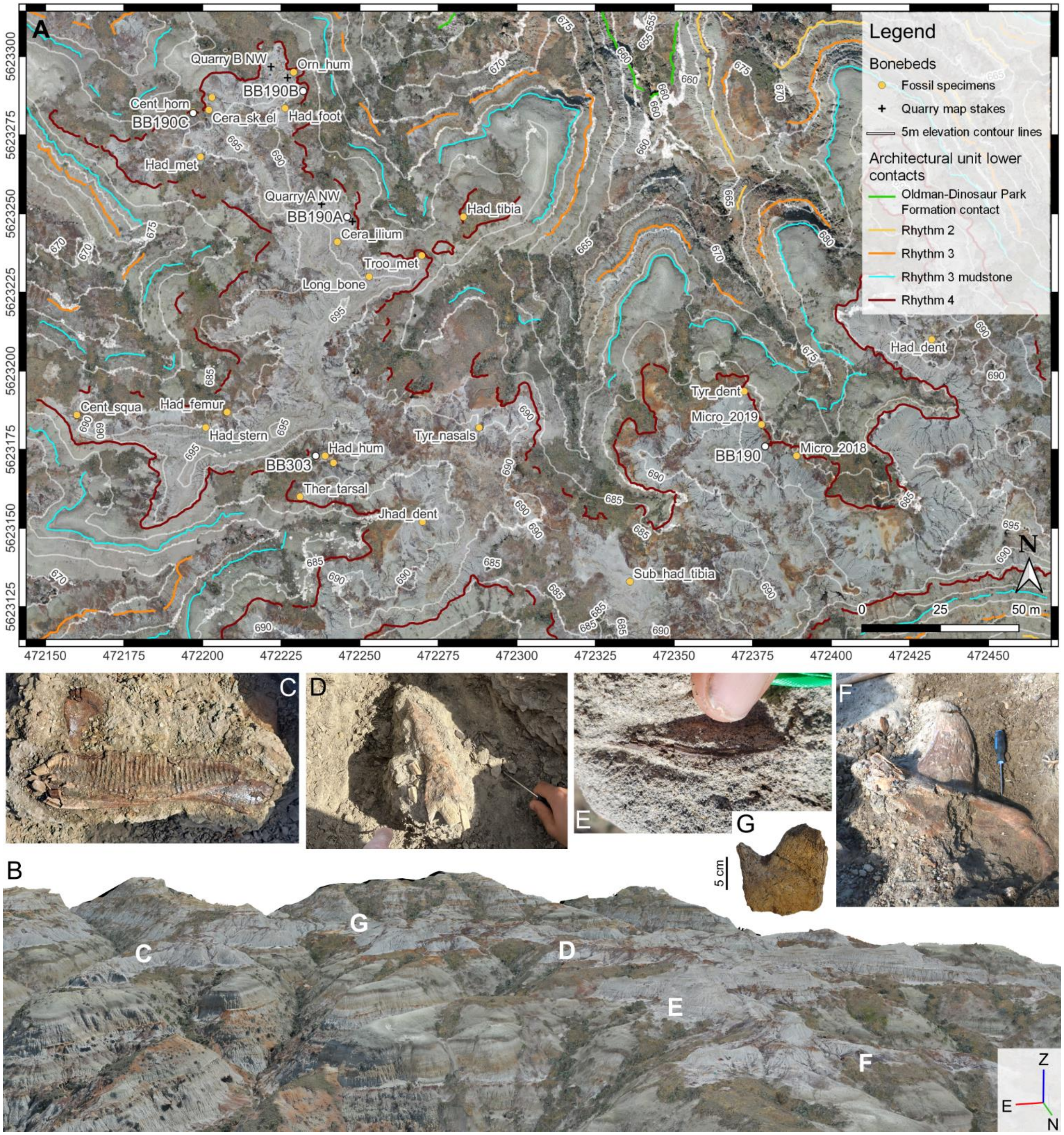
A
Legend
Bonebeds
Fossil specimens
Quarry map stakes
5m elevation contour lines
Architectural unit lower contacts
Oldman-Dinosaur Park Formation contact
Rhythm 2
Rhythm 3
Rhythm 3 mudstone
Rhythm 4
Quarry B NW
Orn_hum
BB190B
Cent_horn
BB190C
Cera_sk_el
Had_foot
Had_met
Quarry A NW
BB190A
Cera_ilium
Had_tibia
Troo_met
Long_bone
Had_dent
Tyr_dent
Micro_2019
BB190
Micro_2018
Cent_squa
Had_femur
Had_stern
Tyr_nasals
BB303
Had_hum
Ther_tarsal
Jhad_dent
Sub_had_tibia
N
0
25
50 m
5623300
5623275
5623250
5623225
5623200
5623175
5623150
5623125
472150
472175
472200
472225
472250
472275
472300
472325
472350
472375
472400
472425
472450
C
D
E
F
G
5 cm
B
Z
E
N

Figure 3.8. Location of significant fossil specimens collected within Bonebed 190 horizon. A, overview of BB190 host horizon within Rhythm 4; 'BB190' point marks original quarry stake for the bonebed identified in 2003; 'BB190' point marks original quarry stake marked in 2002; 'BB190A-C' and 'BB303' points mark fossil-rich localities discovered during this study. Coordinates in WGS84 / Universal Transverse Mercator zone 12N, EGM96 geoid. B, location of significant fossil specimens along BB190 horizon at base of Rhythm 4, projected on perspective render of digital outcrop model. C, complete left hadrosaur dentary collected in 2023 near eastern edge of Amphitheatre, ~8m above main BB190 horizon; photo courtesy of Andre Mueller. D, fused tyrannosaur nasals collected in 2023 about halfway between BB190 original quarry height and BB303 quarry height. E, bowfin (family Amiidae) dentary collected in 2022 at BB190A quarry, 10 cm above main bonebed horizon; photo courtesy of Hans Larsson. F, centrosaurine ceratopsid nasal horn core with premaxilla collected in 2018 at BB190C quarry, at northwestern edge of Amphitheatre. G, ceratopsid (cf. *Styracosaurus*) parietal fragment collected *ex situ* in 2019 near BB190 microsite.

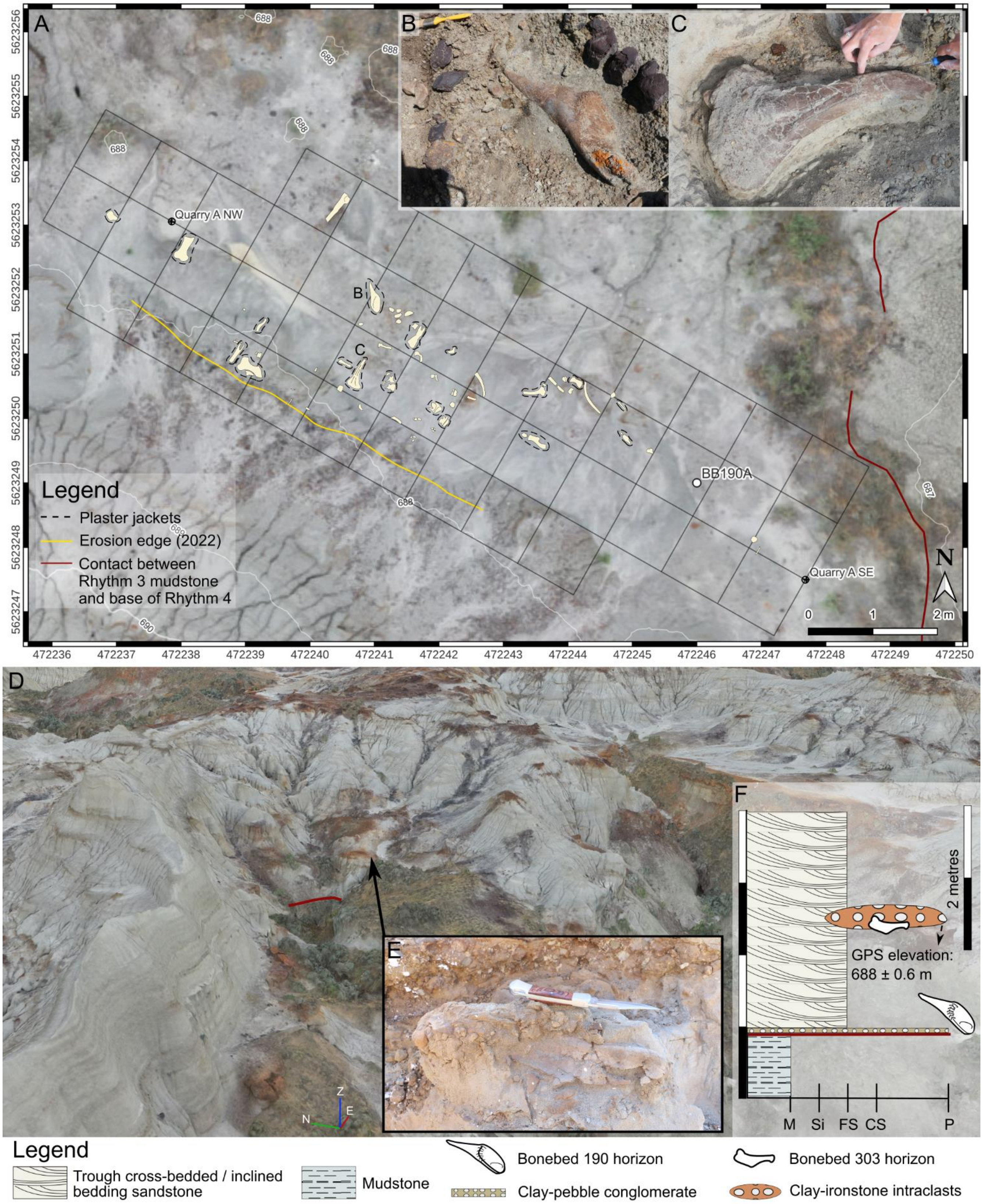
A
B
C
D
E
F
5623256
5623255
5623254
5623253
5623252
5623251
5623250
5623249
5623248
5623247
472236
472237
472238
472239
472240
472241
472242
472243
472244
472245
472246
472247
472248
472249
472250
688
687
689
690
Quarry A NW
Quarry A SE
BB190A
Legend
Plaster jackets
Erosion edge (2022)
Contact between Rhythm 3 mudstone and base of Rhythm 4
N
0
1
2 m
Z
E
N
2 metres
GPS elevation: 688 ± 0.6 m
M
Si
FS
CS
P
Legend
Trough cross-bedded / inclined bedding sandstone
Mudstone
Bonebed 190 horizon
Clay-pebble conglomerate
Bonebed 303 horizon
Clay-ironstone intraclasts

Figure 3.9. Examination of BB190A and BB303 localities. A, BB190A quarry map overlain on orthomosaic. BB190A point represents location of stake for original 2019 quarry map; NW and SE stakes mark corrected 2022 quarry map. B, nodosaurid parascapular spine uncovered from BB190A quarry in 2018. C, nodosaurid left ischium uncovered from BB190A in 2019. Coordinates in WGS84 / Universal Transverse Mercator zone 12N, EGM96 geoid. Quarry and formational contact locations available from database assembled by first author, updated from Currie and Koppelhus (2005: Supplementary CD-ROM; Appendix II). D, perspective render of narrow coulee hosting BB303 locality. E, possible hadrosaur maxilla found in coarsening upward sandstone at base of clay-ironstone intraclast lens. F, short sedimentary log of BB303; burgundy stroke marks same contact (between MUD3 and Rhythm 4) as in Figure 3.9D. **Abbreviations: M,** mudstone; **Si,** siltstone; **FS,** fine-grained sandstone; **CS,** coarse-grained sandstone; **P,** pebbles.

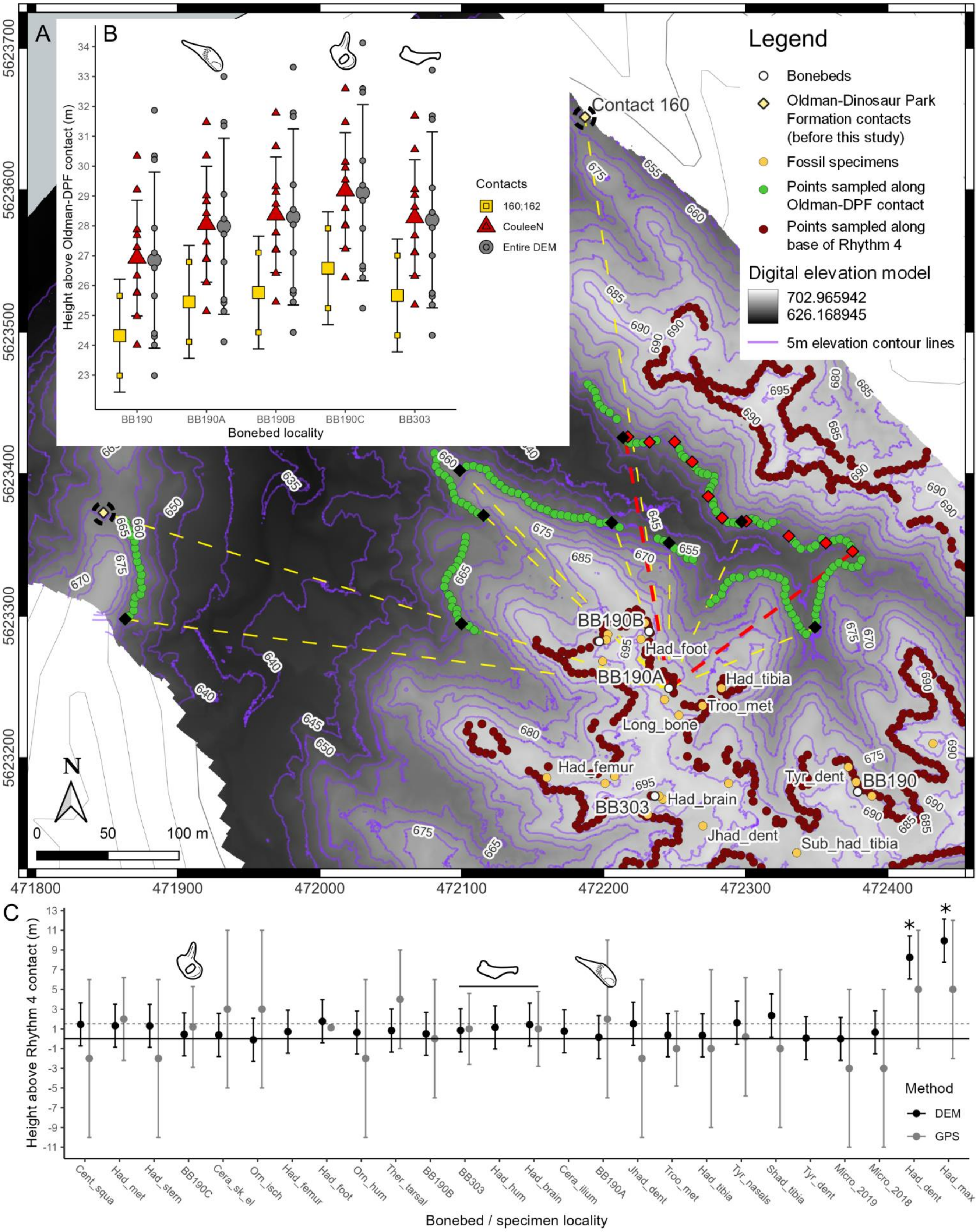

A
B
Height above Oldman-DPF contact (m)
Bonebed locality
BB190
BB190A
BB190B
BB190C
BB303
Contacts
160;162
CouleeN
Entire DEM
Legend
Bonebeds
Oldman-Dinosaur Park Formation contacts (before this study)
Fossil specimens
Points sampled along Oldman-DPF contact
Points sampled along base of Rhythm 4
Digital elevation model
702.965942
626.168945
5m elevation contour lines
Contact 160
BB190B
Had_foot
BB190A
Had_tibia
Troo_met
Long_bone
Had_femur
Had_brain
BB303
Jhad_dent
Tyr_dent
BB190
Sub_had_tibia
N
0
50
100 m
5623700
5623600
5623500
5623400
5623300
5623200
471800
471900
472000
472100
472200
472300
472400
C
Height above Rhythm 4 contact (m)
Bonebed / specimen locality
Cent_squa
Had_met
Had_stern
BB190C
Cera_sk_el
Orn_isch
Had_femur
Had_foot
Orn_hum
Ther_tarsal
BB190B
BB303
Had_hum
Had_brain
Cera_ilium
BB190A
Jhad_dent
Troo_met
Had_tibia
Tyr_nasals
Shad_tibia
Tyr_dent
Micro_2019
Micro_2018
Had_dent
Had_max
Method
DEM
GPS
*
*

Figure 3.10. Heights of main bonebed quarries and individual fossil specimens above significant architectural unit contacts identified across the BB190 Amphitheatre area. A, location of selected Oldman-Dinosaur Park Formation (OF-DPF) contacts for estimating average specimen/bonebed relative height overlain on digital elevation model (DEM) of study area. Dashed lines connect BB190A (used as example) to all selected contacts; points highlighted in red and yellow represent contacts sampled along point series generated from DEM. Coordinates in WGS84 / Universal Transverse Mercator zone 12N, EGM96 geoid. B, average heights above OF-DPF contact estimated from DEM for the five main BB190 quarries identified in this study, based on (1) Contacts 160 and 162 (available from Currie and Koppelhus (2005: Supplementary CD-ROM)); (2) 10 points selected along northern slope of coulee with longest continually preserved OF-DPF contact (red in Figure 3.10A); (3) 11 contacts selected across entire study area (including Contacts 160 and 162 and additional yellow points in Figure 3.10A). Larger points correspond to group means, and error bars are their standard deviations. Point colours in A and B refer to the same groups. C, heights above Rhythm 4 contact for significant bonebed quarries and collected fossil specimens, compared between heights measured with GPS in the field and heights extracted from DEM at nearest point(s) to each specimen along contact polyline traced in QGIS. Dotted line 1.5 m above Rhythm 4 contact marks hypothetical second bonebed layer. Localities ranked by longitude, with the westernmost on the left; notable specimens recovered from BB190A (nodosaurid parascapular spine) and BB190C (centrosaurine nasal horn core) overlie their respective quarry heights; asterisks mark specimens located significantly higher than all others. Note that the same coordinates obtained along the stratigraphic section were used to measure several heights obtained from GPS readings due to lack of raw data, which explains negative values.

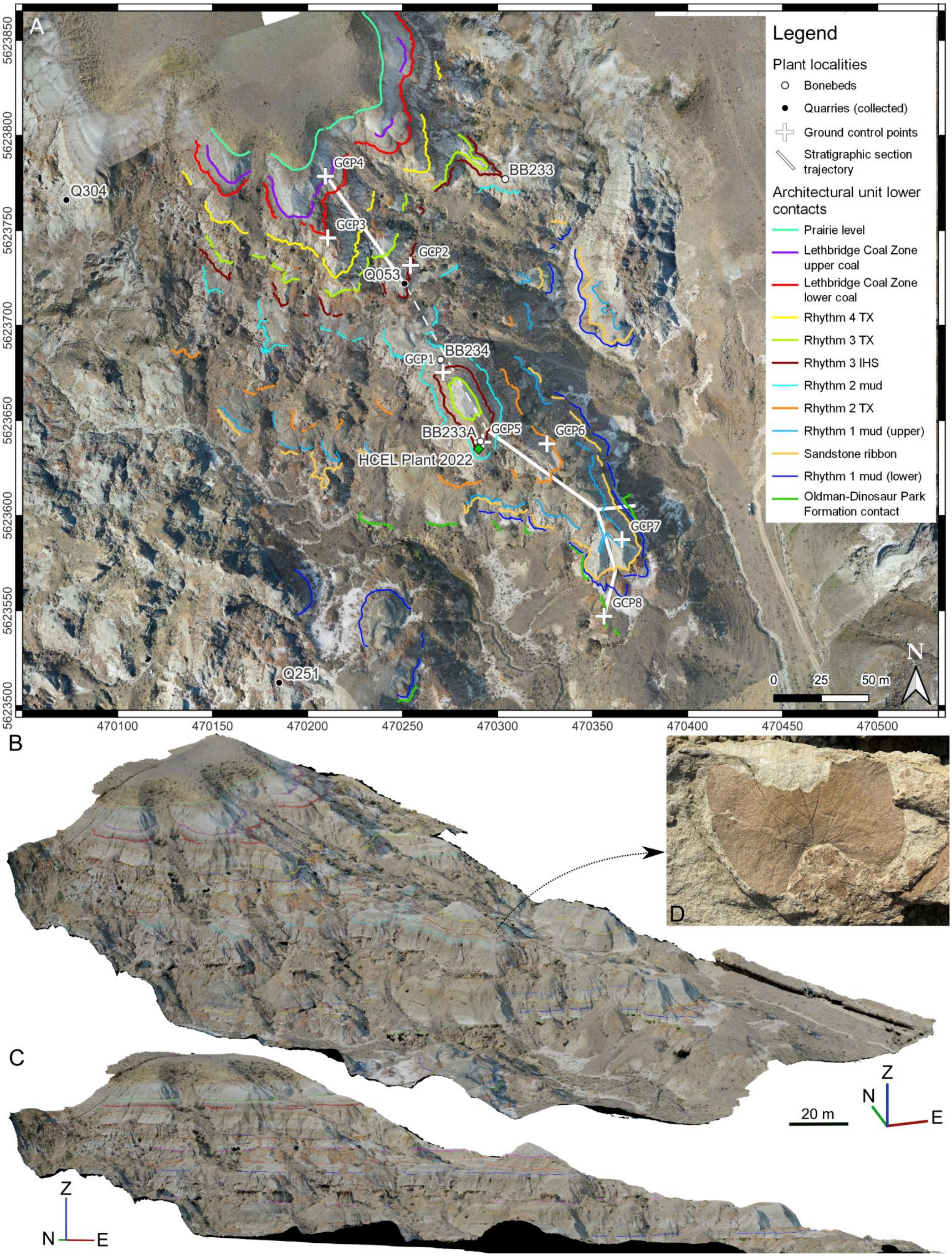
A
Legend
Plant localities
Bonebeds
Quarries (collected)
Ground control points
Stratigraphic section trajectory
Architectural unit lower contacts
Prairie level
Lethbridge Coal Zone upper coal
Lethbridge Coal Zone lower coal
Rhythm 4 TX
Rhythm 3 TX
Rhythm 3 IHS
Rhythm 2 mud
Rhythm 2 TX
Rhythm 1 mud (upper)
Sandstone ribbon
Rhythm 1 mud (lower)
Oldman-Dinosaur Park Formation contact
Q304
GCP4
GCP3
GCP2
Q053
BB233
GCP1
BB234
BB233A
GCP5
GCP6
HCEL Plant 2022
GCP7
GCP8
Q251
N
0
25
50 m
5623850
5623800
5623750
5623700
5623650
5623600
5623550
5623500
470100
470150
470200
470250
470300
470350
470400
470450
470500
B
C
D
Z
N
E
20 m
Z
N
E

Figure 3.11. Identification of architectural sedimentary units across vicinity of HCEL Plant 2022 quarry. A, Orthomosaic highlighting contacts between identified architectural sedimentary units; intraformational contacts named after their respective overlying unit, overlying separate preliminary orthomosaic produced in 2021 covering larger surface area (see Appendix IV). White dashed line indicates interruption in continuous stratigraphic section measurements. B, C, orthographic renders generated in Blender of digital outcrop model (DOM), highlighting succession of architectural sedimentary units following same colour code as in Figure 3.11A. D, fossil angiosperm leaf collected at HCEL Plant 2022 site during 2023 field season. Coordinates in WGS84 / Universal Transverse Mercator zone 12N. Quarry and formational contact locations available from database assembled by first author, updated from Currie and Koppelhus (2005: Supplementary CD-ROM).

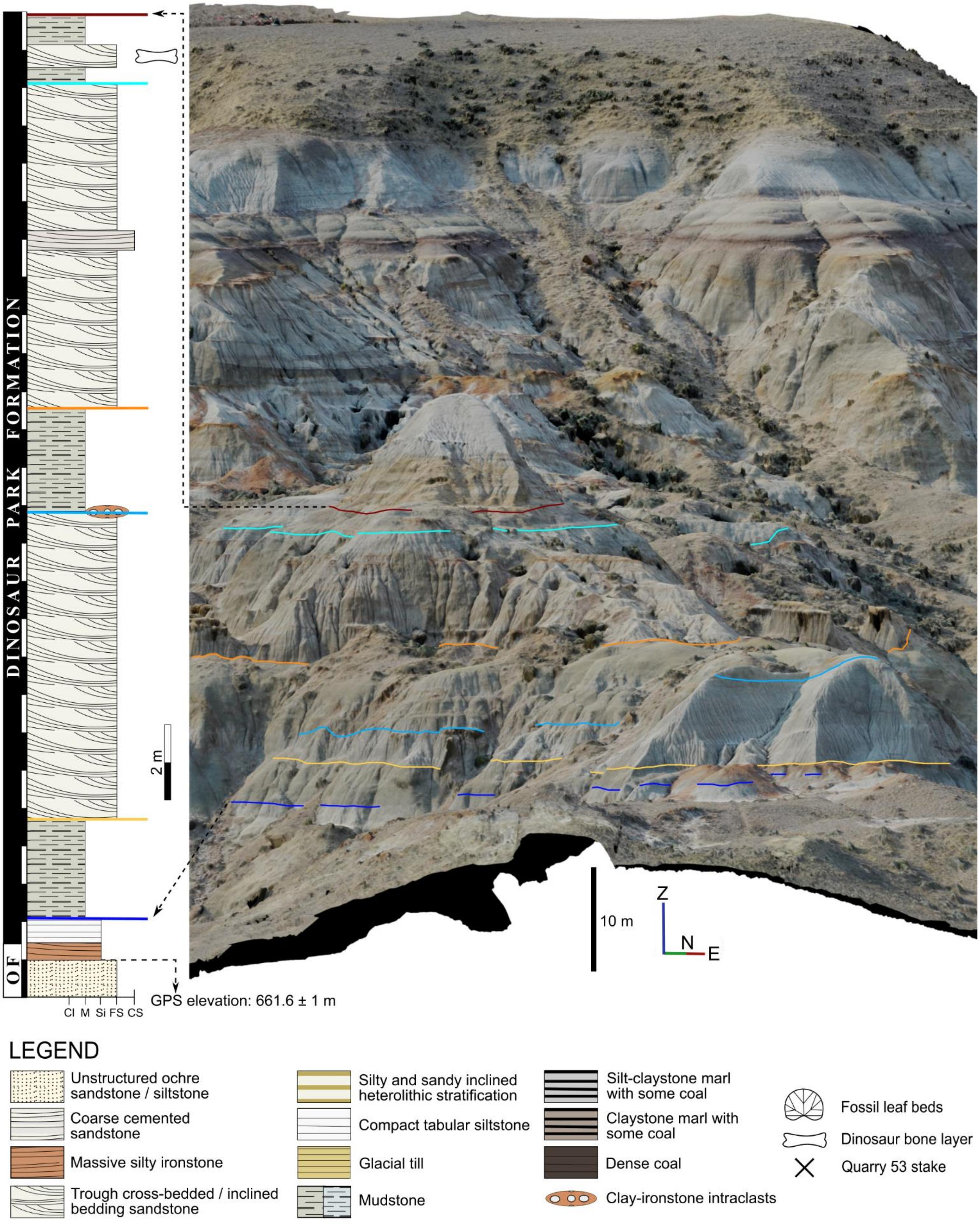
DINOSAUR PARK FORMATION
OF
2 m
Cl M Si FS CS
GPS elevation: 661.6 ± 1 m
10 m
Z
N
E
LEGEND
Unstructured ochre sandstone / siltstone
Coarse cemented sandstone
Massive silty ironstone
Trough cross-bedded / inclined bedding sandstone
Silty and sandy inclined heterolithic stratification
Compact tabular siltstone
Glacial till
Mudstone
Silt-claystone marl with some coal
Claystone marl with some coal
Dense coal
Clay-ironstone intraclasts
Fossil leaf beds
Dinosaur bone layer
Quarry 53 stake

Figure 3.12. Stratigraphic section (lower half) of HCEL Plant 2022 quarry displayed against orthographic render (generated in Blender) of its corresponding digital outcrop model (DOM). Colour code for bases of architectural sedimentary units same as in Figure 3.11, connected between render and stratigraphic section by dashed arrows. **Abbreviations: Cl,** claystone; **M,** mudstone; **Si,** siltstone; **FS,** fine-grained sandstone; **CS,** coarse-grained sandstone; **OF,** Oldman Formation.

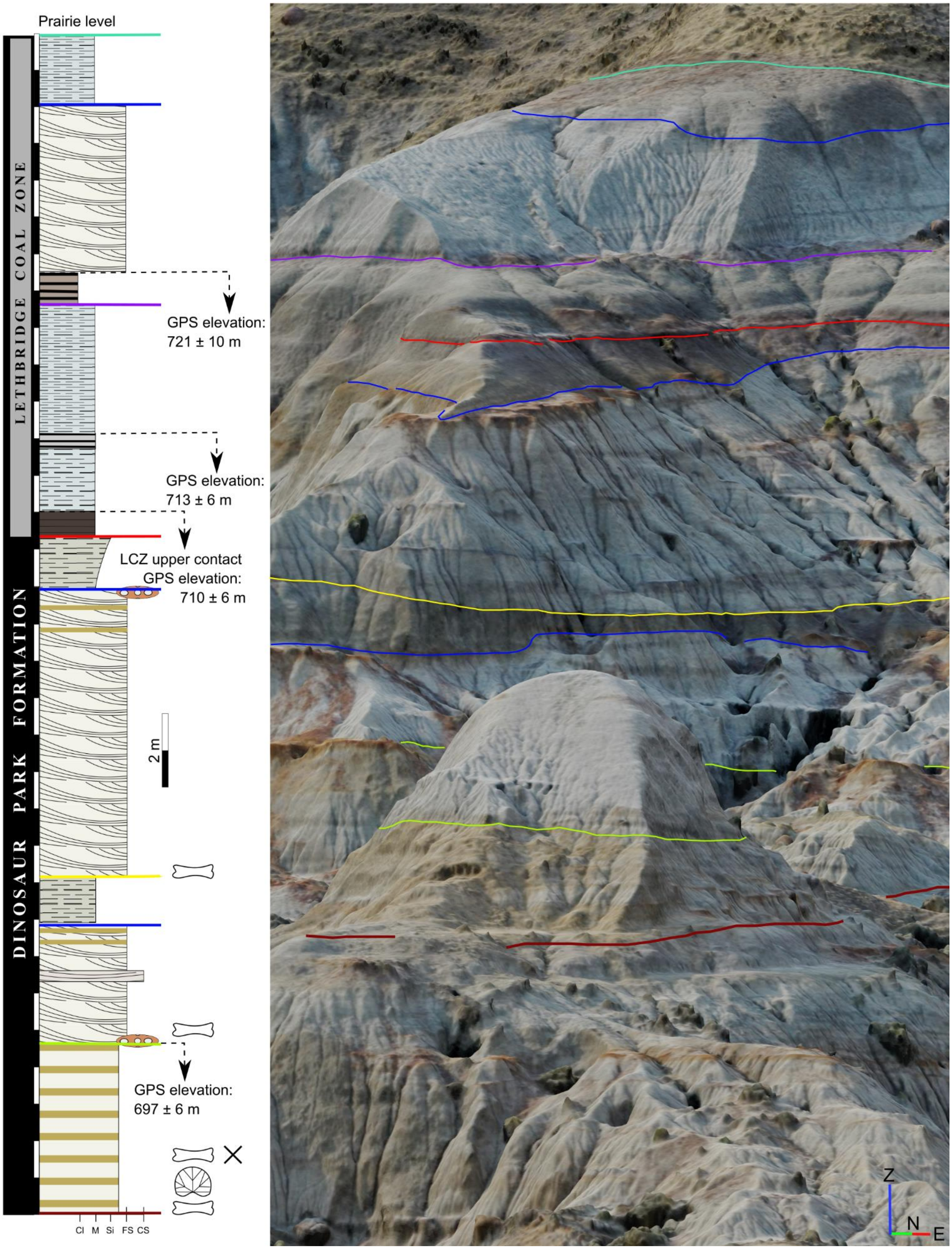
Prairie level
LETHBRIDGE COAL ZONE
DINOSAUR PARK FORMATION
GPS elevation:
721 ± 10 m
GPS elevation:
713 ± 6 m
LCZ upper contact
GPS elevation:
710 ± 6 m
2 m
GPS elevation:
697 ± 6 m
Cl
M
Si
FS
CS
Z
N
E

Figure 3.13. Stratigraphic section (upper half) of HCEL Plant 2022 quarry displayed against orthographic render (generated in Blender) of its corresponding digital outcrop model (DOM). Colour code for bases of architectural sedimentary units same as in Figure 3.11. Portion of section overlying uppermost GPS measurement corrected during examination of DOM, digital elevation model (DEM) and orthomosaic after fieldwork. **Abbreviations: Cl,** claystone; **M,** mudstone; **Si,** siltstone; **FS,** fine-grained sandstone; **CS,** coarse-grained sandstone. See Figure 3.12 for symbol legend.

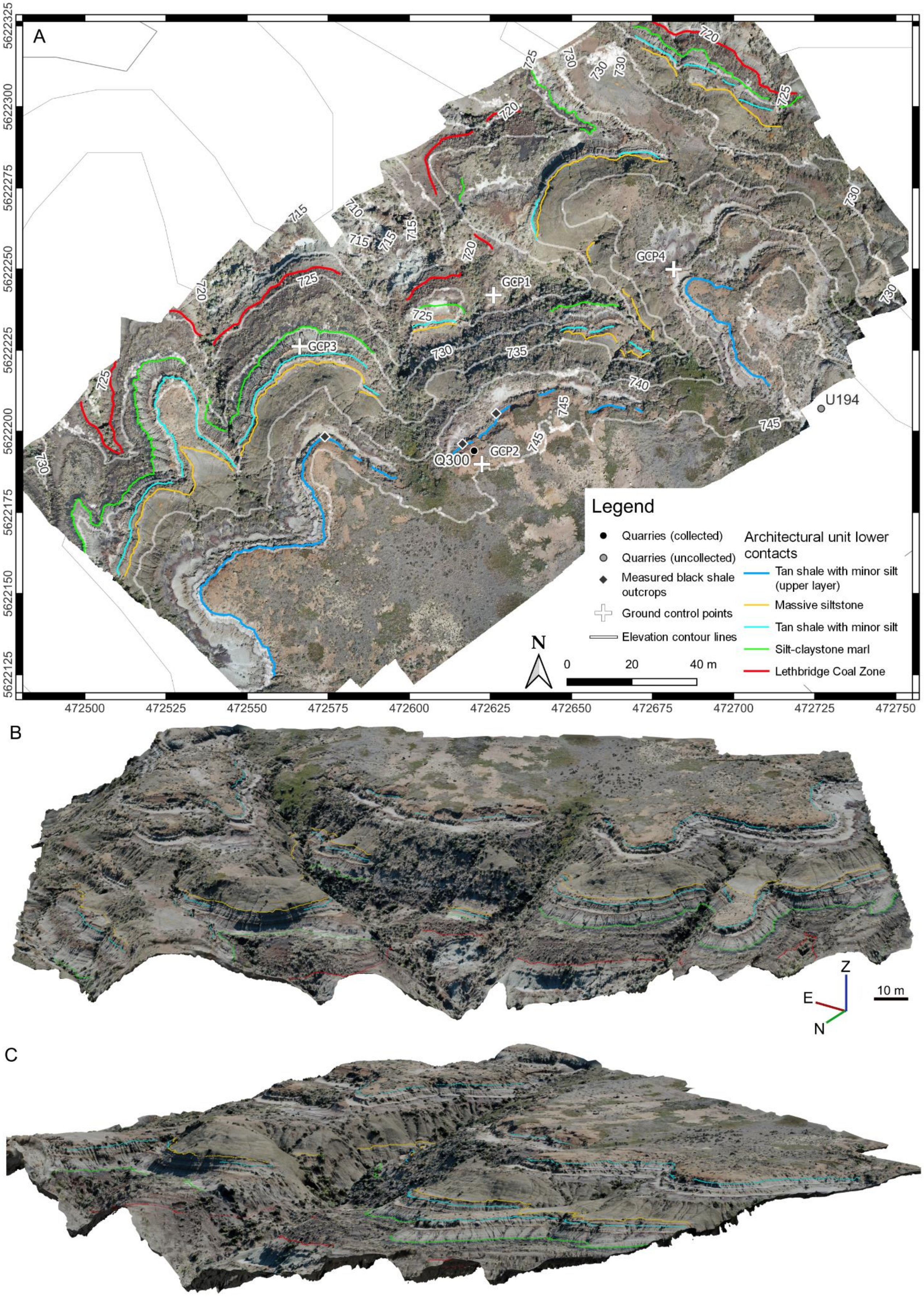A
Legend
Quarries (collected)
Quarries (uncollected)
Measured black shale outcrops
Ground control points
Elevation contour lines
Architectural unit lower contacts
Tan shale with minor silt (upper layer)
Massive siltstone
Tan shale with minor silt
Silt-claystone marl
Lethbridge Coal Zone
N
0
20
40 m
GCP1
GCP2
GCP3
GCP4
Q300
U194
715
710
720
725
730
735
740
745
5622325
5622300
5622275
5622250
5622225
5622200
5622175
5622150
5622125
472500
472525
472550
472575
472600
472625
472650
472675
472700
472725
472750
B
Z
E
N
10 m
C

Figure 3.14. Identification of architectural sedimentary units across vicinity of new ceratopsid skull quarry in the Lethbridge Coal Zone (Quarry 300). A, orthomosaic highlighting contacts between identified architectural sedimentary units. Intraformational contacts named after their respective overlying unit. B, orthographic render of digital outcrop model (DOM) highlighting succession of architectural sedimentary units following same colour code as in Figure 3.14A. C, orthographic render generated in Blender of same DOM. Coordinates in WGS84 / Universal Transverse Mercator zone 12N, EGM96 geoid. Quarry and formational contact locations available from database assembled by first author, updated from Currie and Koppelhus (2005: Supplementary CD-ROM).

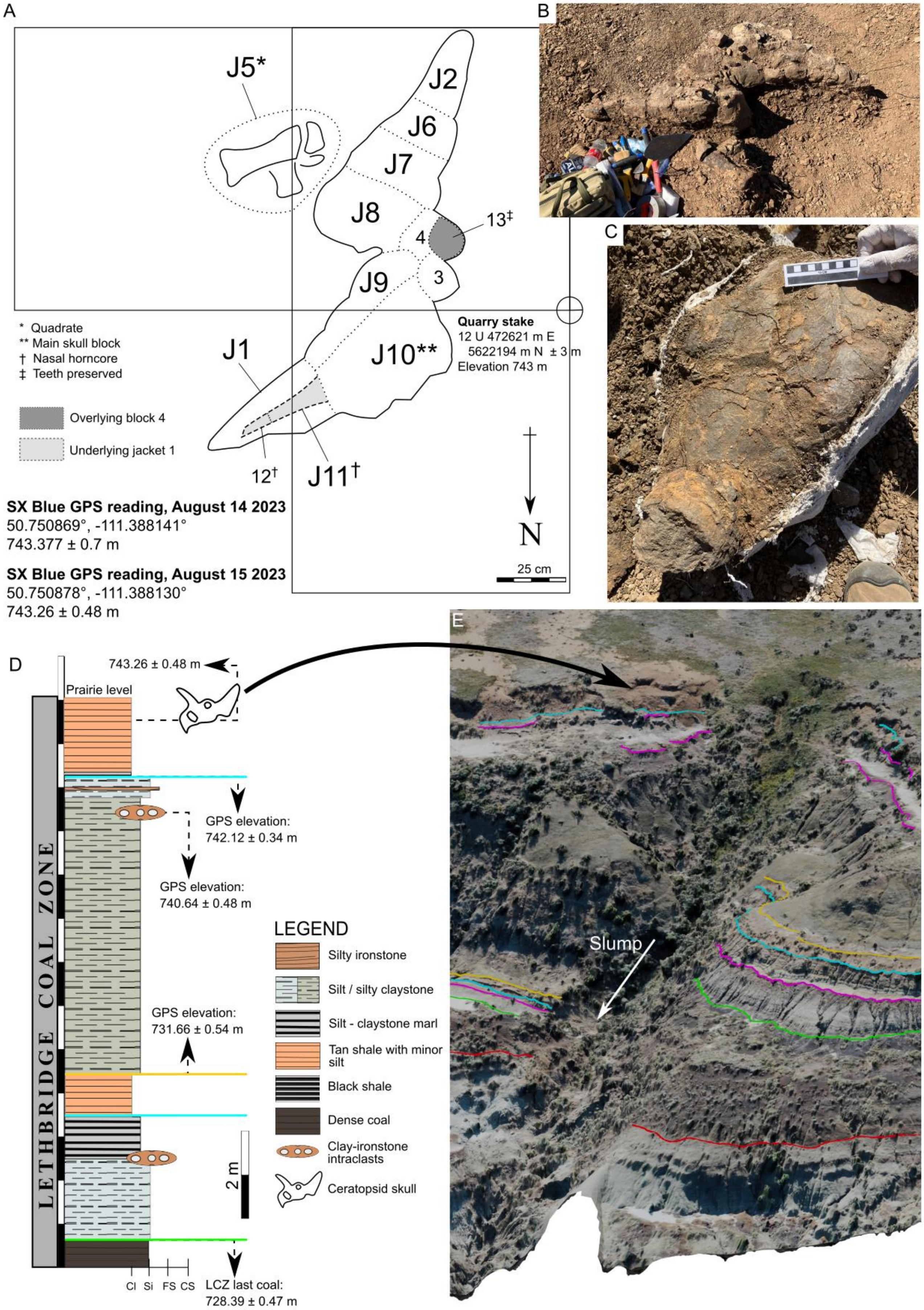
A
B
C
D
E
J5*
J2
J6
J7
J8
4
13‡
J9
3
J1
J10**
12†
J11†
* Quadrate
** Main skull block
† Nasal horncore
‡ Teeth preserved
Overlying block 4
Underlying jacket 1
Quarry stake
12 U 472621 m E
5622194 m N ± 3 m
Elevation 743 m
SX Blue GPS reading, August 14 2023
50.750869°, -111.388141°
743.377 ± 0.7 m
SX Blue GPS reading, August 15 2023
50.750878°, -111.388130°
743.26 ± 0.48 m
N
25 cm
743.26 ± 0.48 m
Prairie level
GPS elevation:
742.12 ± 0.34 m
GPS elevation:
740.64 ± 0.48 m
GPS elevation:
731.66 ± 0.54 m
LETHBRIDGE COAL ZONE
2 m
Cl Si FS CS
LCZ last coal:
728.39 ± 0.47 m
LEGEND
Silty ironstone
Silt / silty claystone
Silt - claystone marl
Tan shale with minor silt
Black shale
Dense coal
Clay-ironstone intraclasts
Ceratopsid skull
Slump

Figure 3.15. Quarry map and geological setting of new ceratopsid skull quarry in the Lethbridge Coal Zone (Quarry 300). A, quarry map indicating division of skull into individual collected blocks. B, photograph (taken from southeast) of ceratopsid skull exposed during excavation; note tan colour of host shale sedimentary unit. C, photograph of anterior skull roof revealed after flipping block J10; note postorbitals visible on each side and broken surface at base of nasal horncore. D, stratigraphic section measured from upper bound of deepest coal interval of Lethbridge Coal Zone to sub-prairie level. E, orthographic render generated in Blender in oblique northwest view of digital outcrop model (DOM) surveyed for section leading to quarry; note slump on left side of image (immediately below quarry) compared to right side. Strokes of same colour mark same contact; pink strokes in E mark ironstone beds. **Abbreviations: Cl,** claystone; **J,** plaster jacket; **Si,** siltstone; **FS,** fine-grained sandstone; **CS,** coarse-grained sandstone.

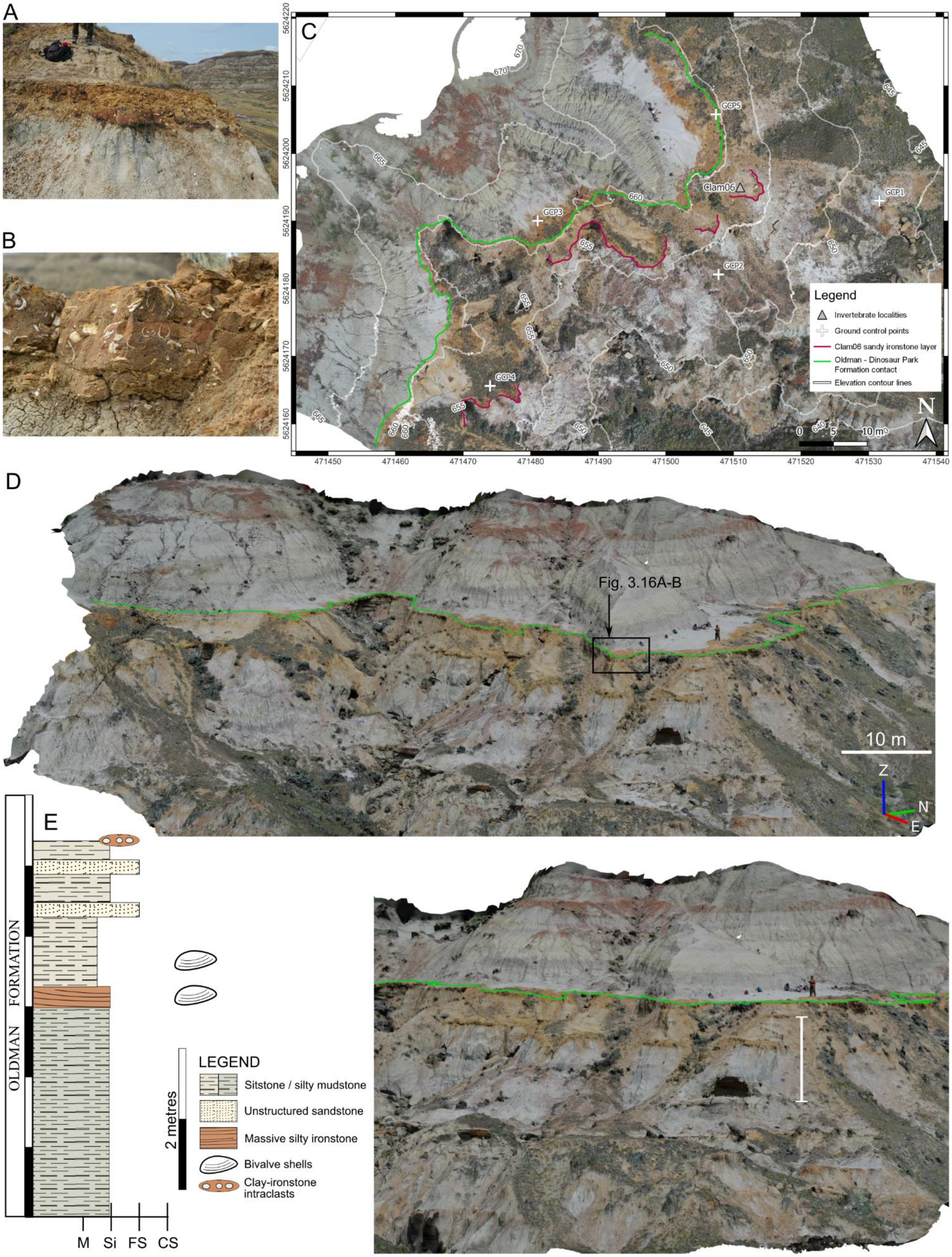
A
B
C
D
E
5624220
5624210
5624200
5624190
5624180
5624170
5624160
471450
471460
471470
471480
471490
471500
471510
471520
471530
471540
670
665
660
655
650
645
640
GCP1
GCP2
GCP3
GCP4
GCP5
Clam06
Legend
Invertebrate localities
Ground control points
Clam06 sandy ironstone layer
Oldman - Dinosaur Park Formation contact
Elevation contour lines
0
5
10 m
N
Fig. 3.16A-B
10 m
Z
N
E
OLDMAN FORMATION
LEGEND
Sitstone / silty mudstone
Unstructured sandstone
Massive silty ironstone
Bivalve shells
Clay-ironstone intraclasts
2 metres
M
Si
FS
CS

Figure 3.16. Geological setting of Clam06 invertebrate locality, Oldman Formation. A, B, detailed photographs of sandy ironstone hosting densest bivalve beds of Clam06. C, orthomosaic with topographic contour lines extracted from corresponding digital elevation model (DEM). D, orthographic render generated in Blender of digital outcrop model (DOM) highlighting Oldman Formation - Dinosaur Park Formation contact. E, constrained stratigraphic section of Clam06 (left) displayed against orthographic lateral east view of its corresponding outcrops (right); white stroke indicates vertical extent of section. Coordinates in WGS84 / Universal Transverse Mercator zone 12N, EGM96 geoid. Quarry and formational contact locations available from database assembled by first author, updated from Currie and Koppelhus (2005: Supplementary CD-ROM). **Abbreviations: M,** mudstone; **Si,** siltstone; **FS,** fine-grained sandstone; **CS,** coarse-grained sandstone.

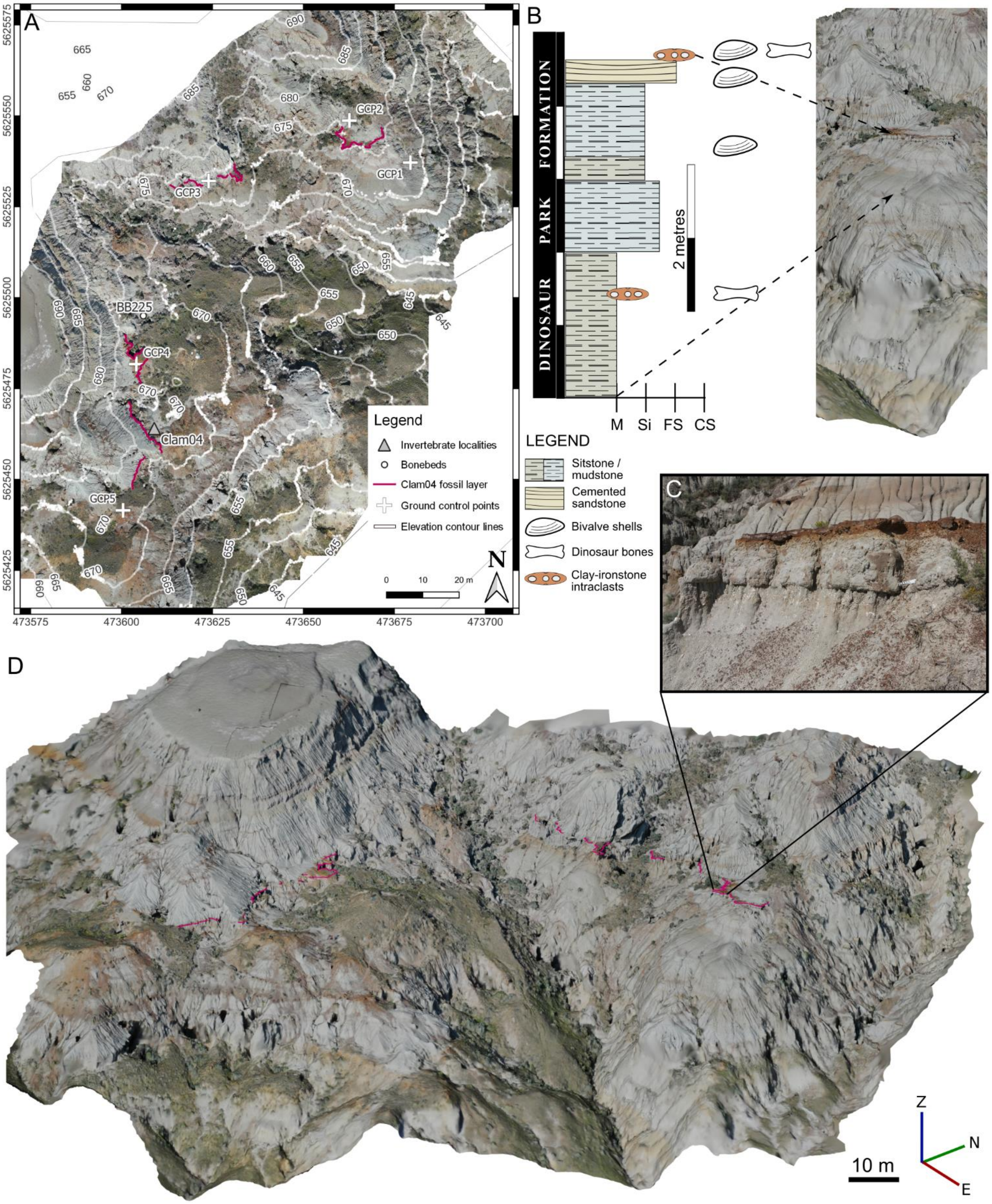
A
B
C
D
Legend
Invertebrate localities
Bonebeds
Clam04 fossil layer
Ground control points
Elevation contour lines
BB225
Clam04
GCP1
GCP2
GCP3
GCP4
GCP5
0 10 20 m
N
5625575
5625550
5625525
5625500
5625475
5625450
5625425
473575
473600
473625
473650
473675
473700
DINOSAUR PARK FORMATION
2 metres
M
Si
FS
CS
LEGEND
Sitstone / mudstone
Cemented sandstone
Bivalve shells
Dinosaur bones
Clay-ironstone intraclasts
Z
N
E
10 m

Figure 3.17. Geological setting of Clam04 invertebrate locality, Dinosaur Park Formation. A, orthomosaic with topographic contour lines extracted from corresponding digital elevation model (DEM); ‘Clam04’ indicates original point of quarry logging, burgundy stroke indicates extent of bivalve-rich horizon traced during mapping. B, constrained stratigraphic section of Clam04 displayed against orthographic near-lateral southeast view of its corresponding outcrops. C, detailed photograph of bivalve beds in successive lithological units: clay-ironstone intraclasts (on top), then cemented sandstone with sharp overhang above siltstone, scale bar 10 cm. D, orthographic render, generated in Blender, of digital outcrop model (DOM), with same colour code indicating uppermost bivalve-rich horizon. Coordinates in WGS84 / Universal Transverse Mercator zone 12N, EGM96 geoid. Quarry and formational contact locations available from database assembled by first author, updated from Currie and Koppelhus (2005: Supplementary CD-ROM). **Abbreviations: M,** mudstone; **Si,** siltstone; **FS,** fine-grained sandstone; **CS,** coarse-grained sandstone.

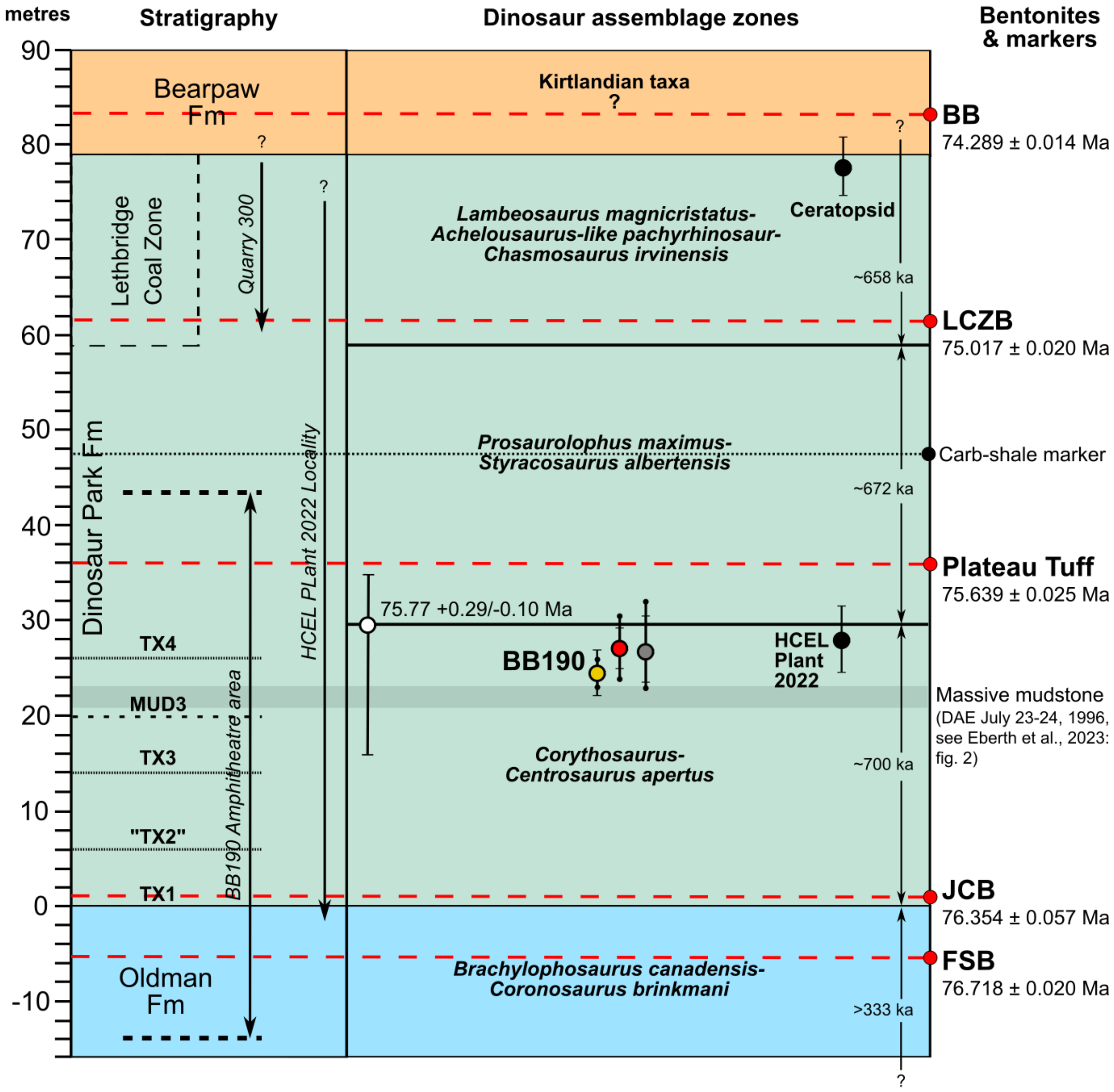
metres
Stratigraphy
Dinosaur assemblage zones
Bentonites & markers
90
80
70
60
50
40
30
20
10
0
-10
Bearpaw Fm
Kirtlandian taxa
?
BB
74.289 ± 0.014 Ma
?
Lethbridge Coal Zone
Quarry 300
?
Ceratopsid
Lambeosaurus magnicristatus-
Achelousaurus-like pachyrhinosaur-
Chasmosaurus irvinensis
~658 ka
LCZB
75.017 ± 0.020 Ma
Dinosaur Park Fm
HCEL PLant 2022 Locality
Prosaurolophus maximus-
Styracosaurus albertensis
Carb-shale marker
~672 ka
Plateau Tuff
75.639 ± 0.025 Ma
75.77 +0.29/-0.10 Ma
TX4
BB190
HCEL Plant 2022
MUD3
Massive mudstone
(DAE July 23-24, 1996, see Eberth et al., 2023: fig. 2)
TX3
Corythosaurus-
Centrosaurus apertus
~700 ka
"TX2"
BB190 Amphitheatre area
TX1
JCB
76.354 ± 0.057 Ma
FSB
76.718 ± 0.020 Ma
Oldman Fm
Brachylophosaurus canadensis-
Coronosaurus brinkmani
>333 ka
?

Figure 3.18. Bonebed 190, HCEL Plant 2022 quarry and Quarry 300 placed in the litho- and biostratigraphic context of Dinosaur Provincial Park, modified from Eberth *et al*. (2023). BB190 (original quarry) height above Oldman-Dinosaur Park Formation contact based on 3 groups of points sampled along contact as in Figure 3.10B, with mean, minimum and maximum height (as well as error bars representing standard deviations) on display for each group; note that those heights were not corrected for channel downcutting (see main text). Thick dashed black lines indicate approximate upper and lower relative height boundaries of mapped area; thinner dashed black lines indicate mean height of lower contact for each architectural unit identified in BB190 Amphitheatre area, MUD3 highlighted among other units' mudstones due to greater potential as a marker bed, TX2 bracketed due to less certain validity as distinct architectural unit (see Discussion). Radioisotopic age uncertainty of biozone boundary projected on relative height axis based on latest published rock accumulation rates between each bentonite (Eberth *et al.* 2023). **Abbreviations: BB,** Bearpaw bentonite; **FSB,** Field Station bentonite; **JCB,** Jackson Coulee bentonite; **LCZB,** Lethbridge Coal Zone bentonite; **MUD,** massive mudstone; **TX,** trough cross-bedded sandstone.

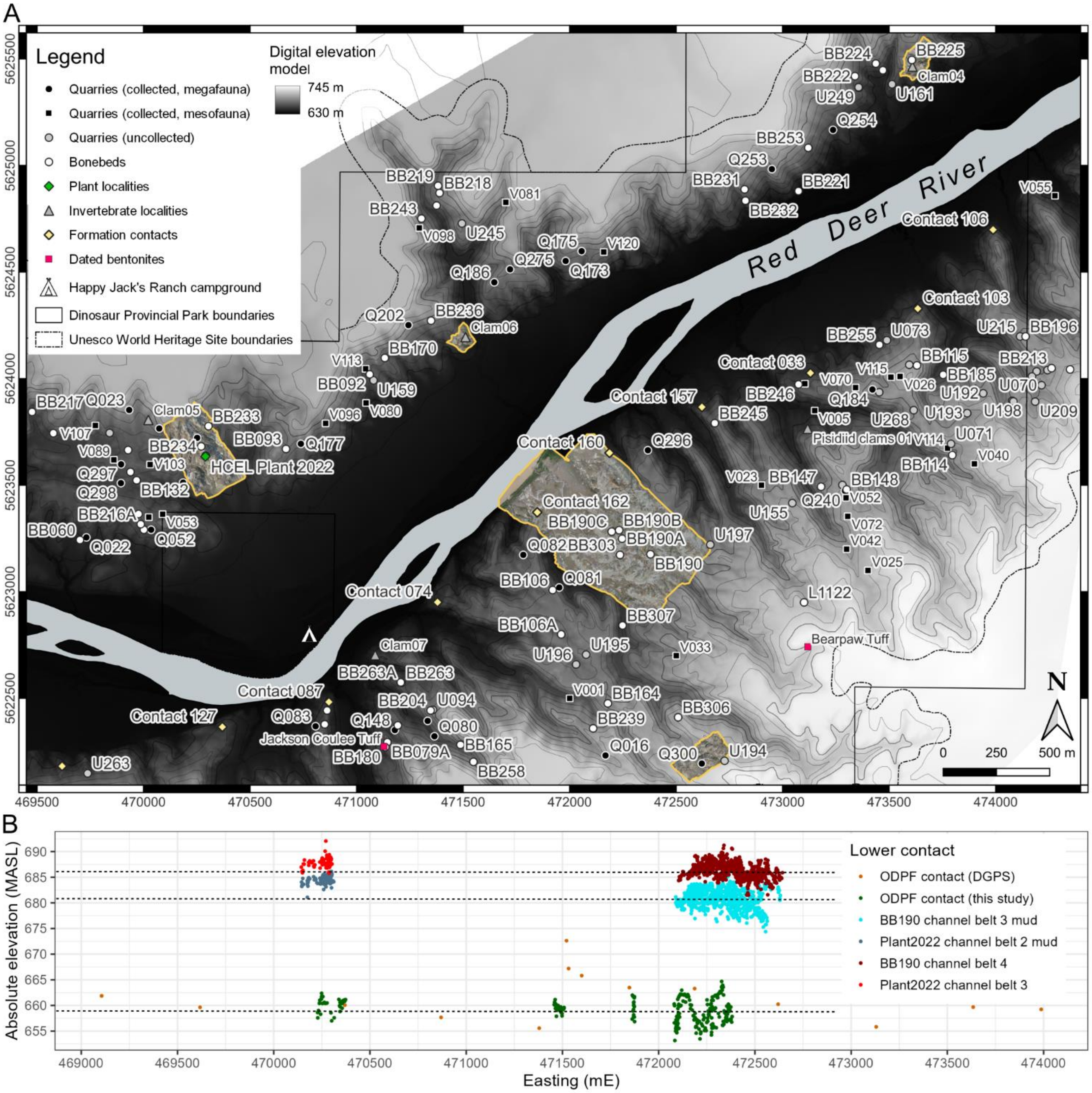
A
Legend
Quarries (collected, megafauna)
Quarries (collected, mesofauna)
Quarries (uncollected)
Bonebeds
Plant localities
Invertebrate localities
Formation contacts
Dated bentonites
Happy Jack's Ranch campground
Dinosaur Provincial Park boundaries
Unesco World Heritage Site boundaries
Digital elevation model
745 m
630 m
Red Deer River
N
0
250
500 m
BB225
BB224
BB222
Clam04
U249
U161
Q254
BB253
Q253
BB231
BB221
BB232
V055
Contact 106
BB219
BB218
V081
BB243
V098
U245
Q175
V120
Q275
Q173
Q186
Q202
BB236
Clam06
BB170
V113
BB092
U159
V096
V080
BB217
Q023
Clam05
BB233
V107
V089
BB234
BB093
Q177
V103
HCEL Plant 2022
Q297
Q298
BB132
BB216A
V053
BB060
Q052
Q022
Contact 103
U215
BB196
BB255
U073
Contact 033
V115
BB115
BB213
V070
V026
BB185
U070
BB246
Q184
U192
Contact 157
U268
U193
U198
U209
BB245
V005
Pisidiid clams 01
V114
U071
Contact 160
Q296
V040
BB114
V023
BB147
BB148
Contact 162
Q240
V052
U155
BB190C
BB190B
V072
Q082
BB303
BB190A
U197
V042
BB190
V025
BB106
Q081
Contact 074
L1122
BB307
BB106A
Bearpaw Tuff
U195
U196
V033
Clam07
BB263A
BB263
Contact 087
V001
BB164
BB204
U094
Contact 127
Q083
Q148
Q080
BB239
BB306
Jackson Coulee Tuff
BB165
BB180
BB079A
Q016
Q300
U194
BB258
U263
5625500
5625000
5624500
5624000
5623500
5623000
5622500
469500
470000
470500
471000
471500
472000
472500
473000
473500
474000
B
Absolute elevation (MASL)
690
685
680
675
670
665
660
655
Easting (mE)
469000
469500
470000
470500
471000
471500
472000
472500
473000
473500
474000
Lower contact
ODPF contact (DGPS)
ODPF contact (this study)
BB190 channel belt 3 mud
Plant2022 channel belt 2 mud
BB190 channel belt 4
Plant2022 channel belt 3

Figure 3.19. Geographical distribution of Dinosaur Provincial Park mapping projects presented in this chapter, along with stratigraphic distribution of their more significant marker beds. A, location of the five orthomosaics documenting the geological setting of DPP fossil localities explored during McGill University Vertebrate Palaeontology Field Course program (as of 2023): Bonebed 190 (multigeneric bonebed explored since 2018), HCEL Plant 2022 (fossil leaf locality discovered in 2022), Quarry 300 (disarticulated ceratopsid skull uncovered from Lethbridge Coal Zone in 2023) and invertebrate localities Clam04 and Clam06 (first visited in 2021). Quarry and formational contact locations available from database assembled by first author, updated from Currie and Koppelhus (2005: Supplementary CD-ROM; Appendix II). Bentonite tuff locations available from Ramezani *et al.* (2022). Digital elevation model (DEM) ranges from ~630 m (black) to ~745 m (white), created via Lidar coverage achieved in 2015, provided courtesy of the Royal Tyrrell Museum of Palaeontology (TMP). B, comparison of absolute elevation of potential marker beds between BB190, HCEL Plant 2022 and Clam06. Elevation extracted from TMP DEM, coordinates in WGS84 / Universal Transverse Mercator zone 12N, EGM96 geoid. Elevation contour lines redrawn from topographic map of DPP (2013) georeferenced on QGIS. Horizontal dotted lines indicate ~0.05˚ average structural dip of DPP exposures to the northwest.

3.9 Tables

Table 3.1. Metadata for Dinosaur Provincial Park mapping projects presented in Chapter 3. Abbreviations: **DEM,** digital elevation model; **GCP,** ground control point; **RMSE,** root mean square error; UAV, unmanned aerial vehicle.

	BB190	HCEL Plant 2022	Quarry 300	Clam04	Clam06
UAV flight metadata					
No. flights	3	1	1	1	1
No. images processed	1,122	279	286	339	265
Coverage area (km^2)	0.446	0.0907	0.0339	0.0225	0.00951
Ground resolution (cm/pixel)	1.91	1.85	1.11	0.715	0.815
Height above ground (m)*	~30; ~50; ~80	~40	~40	~10	~10
Georeferencing					
No. GCPs	12	8	4	5	5
GCP X RMSE (m)	0.442273	0.108745	0.126819	0.152086	0.402442
GCP Y RMSE (m)	0.761722	0.258947	0.411113	0.257562	0.307524
GCP Z RMSE (m)	0.420918	0.0521228	0.116586	0.521197	0.607853
DEM Z RMSE (m)	1.092980	1.470666	0.642941	5.997729**	0.207263**
Camera parameters					
Exposure time (second)	1/500-1/400	1/400	1/400	1/400	1/400
F-stop	2.8; 4	2.8	2.8	4	2.8
ISO speed	100; 200; 240	120	160	100	100

*Defined as above BB190 host horizon for BB190 project and above highest point in other projects.

**RMSE calculated solely from points measured before this study.

Table 3.2. Ground control point measurements for Dinosaur Provincial Park mapping projects presented in Chapter 3. All coordinates in WGS84 horizontal datum, EGM96 geoid.

Project	Year	GCP No.	Latitude	Longitude	Elevation (m)	Z error (m)
BB190	2021	21-1	50.76065238	-111.3940977	688.68	1.2
BB190	2021	21-2	50.7606319	-111.3947881	688.38	1.2
BB190	2021	21-3	50.75978285	-111.3940391	689.56	1.2
BB190	2021	21-4	50.75942865	-111.3933062	686.38	1.2
BB190	2021	21-5	50.75931225	-111.39224	687.28	1.2
BB190	2021	21-6	50.76023237	-111.3931835	688.35	1.2
BB190	2022	14-1	50.761436	-111.391109	688.0	1.171
BB190	2022	14-2	50.761691	-111.391974	687.2	0.981
BB190	2022	14-3	50.762264	-111.393195	689.753	1.003
BB190	2022	14-4	50.762137	-111.394635	643.533	1.024
BB190	2022	14-5	50.761586	-111.39341	646.526	1.085
BB190	2022	14-6	50.761201	-111.392262	652.601	1.264
Plant 2022	2023	GCP1	50.764083	-111.421536	690.056	0.656
Plant 2022	2023	GCP2	50.764589	-111.421785	689.556	0.861
Plant 2022	2023	GCP3	50.764716	-111.422403	711.343	1.04
Plant 2022	2023	GCP4	50.765008	-111.422423	714.263	0.951
Plant 2022	2023	GCP5	50.763754	-111.421238	689.829	1.044
Plant 2022	2023	GCP6	50.763748	-111.420758	677.772	0.631
Plant 2022	2023	GCP7	50.763297	-111.420194	676.755	1.041
Plant 2022	2023	GCP8	50.762934	-111.420325	663.749	0.424
Quarry 300	2023	GCP1	50.75131	-111.388042	723.75	0.59
Quarry 300	2023	GCP2	50.750841	-111.388089	744.515	0.63

Quarry 300	2023	GCP3	50.751165	-111.388888	733.0	0.74
Quarry 300	2023	GCP4	50.751384	-111.387255	740.05	0.56
Clam04	2022	GCP1	50.780991	-111.403706	672.0	0.5
Clam04	2022	GCP2	50.781094	-111.404043	675.0	0.8
Clam04	2022	GCP3	50.780943	-111.404423	674.4	0.8
Clam04	2022	GCP4	50.780489	-111.404521	673.0	0.8
Clam04	2022	GCP5	50.780127	-111.40405	672.2	0.8
Clam06	2022	GCP1	50.768802	-111.403706	647.3	0.8
Clam06	2022	GCP2	50.768703	-111.404043	653.2	0.8
Clam06	2022	GCP3	50.768773	-111.404423	659.9	1
Clam06	2022	GCP4	50.768553	-111.404521	659.1	1.1
Clam06	2022	GCP5	50.768916	-111.40405	661.8	0.85

Table 3.3. BB190 fossil specimen, quarry stake and nearby formational contact coordinates. Coordinates recorded with WGS84 / UTM zone 12N projected coordinate system, except if recorded with SX Blue GPS receiver (originally in decimal degrees then transformed to facilitate comparisons here); vertical coordinates using EGM96 geoid. Ortho relocation means that specimen location was never recorded with GPS, instead its quarry was relocated on the orthomosaic. **Abbreviations: DEM,** digital elevation model; **DGPS,** differential GPS receiver; **MASL,** metres above sea level; **OF-DPF,** Oldman-Dinosaur Park Formation contact; **SD,** standard deviation. All relative elevations (heights) calculated from Z coordinates extracted from DEM generated for this study; features marked in bold used as check points to measure root mean square error of BB190 DEM generated for this study. This table is split in two due to its size constraints.

Table 3.3A. Metadata for relative heights.

Feature	Locality	Measurement year; method	Easting (mE)	Northing (mN)	GPS elev. ± Z error (MASL)
BB190	BB190 (Original)	2002; DGPS	472379	5623176	687.7 ± 0.1
BB190A stake	BB190A	2018; Garmin	472246	5623249	689 ± 5
Ceratopsid pubis	BB190B (stake)	2023; Garmin	472232	5623289	687 ± 3
Centrosaurine nasal horn core	BB190C (stake)	2022; SX Blue	472197	5623282	688.2 ± 1.1
Hadrosaurid maxilla	BB303 (stake)	2022; SX Blue	472236	5623173	688 ± 0.6
Microsite 2018	BB190 (Original)	2018; Garmin	472389	5623173	684 ± 5
Microsite 2019	BB190 (Original)	2019; Garmin	472378	5623183	684 ± 5
Quarry A NW stake	BB190A	2023; ortho	472237.85	5623253.05	NA
Quarry A SE stake	BB190A	2023; ortho	472247.7	5623247.5	NA
Quarry B NW stake	BB190B	2021; Garmin	472221.8	5623296.8	682.25 ± 5
Quarry B SE stake	BB190B	2021; Garmin	472227	5623293.2	NA
Centrosaurine squamosal	BB190 (other)	2018; Garmin	472160	5623186	685 ± 5
Ceratopsid ilium	BB190A	2021; Garmin	472242.89	5623241.03	681.64 ± 5
Ceratopsid skull element	BB190C	2019; Garmin	472202	5623283	690 ± 5
Hadrosaurid humerus	BB303	2022; ortho; Garmin	472239	5623173	NA
Hadrosaurid maxilla fragment	BB190 (other)	2023; Garmin	472500	5623158	695 ± 4
Hadrosaurid braincase	BB303	2022; SX Blue	472242	5623171	688 ± 0.8
Hadrosaurid left dentary	BB190 (other)	2023; Garmin	472432	5623210	695 ± 3
Hadrosaurid sternal plate	BB190 (other)	2018; Garmin	472201	5623182	685 ± 5
Hadrosaurid femur	BB190 (other)	2019; ortho; Garmin	472207.8	5623186.9	NA
Hadrosaurid tibia	BB190A	2022; Garmin	472283	5623249	686 ± 5
Subadult hadrosaurid tibia	BB190 (other)	2019; Garmin	472336	5623133	686 ± 5
Hadrosaurid foot bones	BB190B	2021; Garmin	472226.2	5623283.5	688.12 ± 5
Hadrosaurid metatarsal	BB190C	2022; SX Blue	472199	5623268	689 ± 1.2
Juvenile hadrosaurid dentary	BB190 (other)	2018; Garmin	472270	5623152	685 ± 5
Ornithomimid ischium	BB190C	2019; Garmin	472203	5623287	690 ± 5
Ornithomimid humerus	BB190B	2022; Garmin	472229	5623295	685 ± 5
Tyrannosaurid nasals	BB190 (other)	2023; Garmin	472288	5623182	688 ± 3
Tyrannosaurid dentary	BB190 (Original)	2022; ortho	472372.4	5623193.5	NA
Troodontid metatarsal	BB190A	2022; SX Blue	472270	5623237	686 ± 0.8
Theropod tarsal element	BB190 (other)	2023; Garmin	472231	5623160	691 ± 2
Ornithischian long bone fragment (not collected)	BB190 (other)	2018; Garmin	472253	5623230	NA
Contact 160	NA	2002; DGPS	472186.859	5623651.467	663. ± 0.1
Contact 162	NA	2002; DGPS	471847.626	5623372.669	663.2 ± 0.1

Table 3.3B. Relative heights of fossil specimens.

Feature	BB190 DEM elev ± 1.092 (MASL)	Mean height Contacts 160;162 ± SD 1.89 (m)	Mean height 10 nearby OF-DPF contacts ± SD 1.94 (m)	Mean height 11 distant OF-DPF contacts ± SD 2.95 (m)	Height Rhythm 4 ± 2.18 (m)
BB190	686.6	24.32	26.92	26.85	NA
BB190A stake	687.7	25.45	28.06	27.99	0.16
Ceratopsid pubis	688.0	25.77	28.37	28.30	0.50
Centrosaurine nasal horn core	688.8	26.58	29.18	29.11	0.44
Hadrosaurid maxilla	687.9	25.67	28.27	28.20	0.85
Microsite 2018	685.9	23.67	26.27	26.20	0.66
Microsite 2019	685.8	23.51	26.11	26.05	-0.01
Quarry A NW stake	687.9	25.65	28.25	28.18	NA
Quarry A SE stake	687.6	25.35	27.95	27.88	NA
Quarry B NW stake	688.8	26.55	29.15	29.08	NA
Quarry B SE stake	688.7	26.45	29.05	28.98	NA
Centrosaurine squamosal	688.4	26.15	28.75	28.68	1.45
Ceratopsid ilium	688.2	25.92	28.52	28.45	0.76
Ceratopsid skull element	688.6	26.33	28.93	28.86	0.38
Hadrosaurid humerus	688.2	25.97	28.57	28.50	1.15
Hadrosaurid maxilla fragment	692.1	29.82	32.43	32.36	9.94
Hadrosaurid braincase	688.5	26.25	28.85	28.79	1.43
Hadrosaurid left dentary	691.7	29.43	32.03	31.96	8.24
Hadrosaurid sternal plate	690.0	27.78	30.38	30.31	1.31
Hadrosaurid femur	688.7	26.49	29.09	29.02	0.72
Hadrosaurid tibia	688.1	25.84	28.44	28.37	0.34
Subadult hadrosaurid tibia	687.2	24.97	27.57	27.50	2.35
Hadrosaurid foot bones	689.3	27.04	29.64	29.57	1.77
Hadrosaurid metatarsal	689.7	27.40	30.01	29.94	1.32
Juvenile hadrosaurid dentary	687.6	25.37	27.97	27.90	1.52
Ornithomimid ischium	689.0	25.84	28.44	28.37	-0.10
Ornithomimid humerus	688.3	26.01	28.61	28.54	0.63
Tyrannosaurid nasals	689.9	27.62	30.22	30.15	1.62
Tyrannosaurid dentary	686.5	24.25	26.85	26.78	0.06
Troodontid metatarsal	687.6	25.33	27.93	27.86	0.36
Theropod tarsal element	688.5	26.31	28.90	28.83	0.83
Ornithischian long bone fragment (not collected)	689.9	27.64	30.24	30.17	NA
Contact 160	660.9	NA	NA	NA	NA
Contact 162	663.6	NA	NA	NA	NA

Table 3.4. Descriptive statistics including standard deviation (σ) and variance (σ^2) for elevation of Oldman-Dinosaur Park Formation (ODPF) contact and of other architectural unit contacts identified in and around Bonebed 190 Amphitheatre area. Contacts marked in bold were analyzed with digital elevation model (DEM) including entire extent of Dinosaur Provincial Park, provided by Royal Tyrrell Museum of Palaeontology (RMSE ±1.72 m); other contacts analyzed with DEM generated during this study (RMSE ±1.09 m). Elevation range uncertainties are 2*RMSE.

Contact	N sampled points	Elevation (m)					
		Min	Max	Range	Mean	σ	σ^2
OF-DPF (BB190 area coulee)	132	654.70	663.06	8.36 ± 2.18	660.12	1.95	3.81
OF-DPF (BB190 coulee, N slope)	59	656.23	662.56	6.33 ± 2.18	659.79	1.52	2.30
OF-DPF (BB190 coulee, S slope)	73	654.70	663.06	8.36 ± 2.18	660.38	2.22	4.92
OF-DPF (entire BB190 area)	182	653.15	664.67	11.52 ± 3.44	658.64	2.47	6.08
OF-DPF (DPP right bank)	10	655.56	663.48	7.92 ± 3.44	659.46	2.66	7.05
OF-DPF (public loop road)	48	648.21	659.72	11.51 ± 3.44	654.28	2.88	8.31
Rhythm 1 (incl. OF-DPF)	359	651.44	664.33	12.89 ± 2.18	659.61	2.40	5.75
Rhythm 2	366	660.25	670.33	10.08 ± 2.18	666.01	2.49	6.20
Rhythm 3	468	666.18	678.83	12.65 ± 2.18	674.05	2.68	7.19
Rhythm 3 (MUD3)	690	672.29	684.46	12.17 ± 2.18	680.66	2.22	4.91
Rhythm 4	753	679.79	689.92	10.13 ± 2.18	685.68	2.24	5.00

*BB190 area coulee corresponds to area within black inset in Figure 3.3.

Table 3.5. Architectural unit depths digitally measured at 20 sections of the BB190 Amphitheatre area based on digital outcrop model (DOM) generated through structure-from-motion (SfM) photogrammetry. Numbers marked in bold indicate minimum and maximum depths measured.

Section	Channel cut-and-fill rhythm depth ± error (m)				
	Rhythm 1	Rhythm 2	Rhythm 3	Mudstone 3	Rhythm 4
1	8.44 ± 0.58	7.00 ± 0.44	11.65 ± 0.08	4.24 ± 0.08	NA
2	10.33 ± 0.42	8.70 ± 0.05	10.80 ± 0.11	5.69 ± 0.11	NA
3	7.55 ± 0.03	8.80 ± 0.02	12.24 ± 0.05	6.49 ± 0.06	NA
4	8.04 ± 0.05	8.05 ± 0.08	11.00 ± 0.06	4.26 ± 0.03	NA
5	**11.54 ± 0.59**	9.13 ± 0.06	11.62 ± 0.09	5.68 ± 0.07	NA
6	**5.60 ± 0.02**	**10.71 ± 0.01**	12.82 ± 0.05	5.93 ± 0.07	NA
7	5.80 ± 0.06	8.44 ± 0.32	12.18 ± 0.31	5.52 ± 0.06	NA
8	6.45 ± 0.02	10.23 ± 0.04	**9.90 ± 0.03**	4.57 ± 0.07	NA
9	10.02 ± 0.05	6.03 ± 0.41	13.58 ± 0.43	5.48 ± 0.39	NA
	7.22 ± 0.07	5.20 ± 0.42			
10	7.55 ± 0.03	8.95 ± 0.59	**14.94 ± 0.64**	**6.93 ± 0.93**	NA
11	NA	7.52 ± 0.10	10.97 ± 0.003	**3.78 ± 0.06**	NA
12	NA	7.50 ± 0.11	11.53 ± 0.11	4.37 ± 0.05	NA
13	NA	8.18 ± 0.96	10.73 ± 0.82	4.35 ± 0.32	NA
14	NA	5.94 ± 0.40	12.45 ± 1.09	5.55 ± 0.71	NA
15	NA	6.95 ± 0.14	14.37 ± 0.13	5.54 ± 0.12	NA
16	NA	7.90 ± 0.04	11.78 ± 0.04	4.99 ± 0.03	NA
17	NA	NA	NA	4.14 ± 0.04	**14.49 ± 0.08**
18	NA	NA	NA	4.55 ± 0.18	14.29 ± 0.09
19	NA	NA	NA	NA	**13.09 ± 0.28**
20	10.24 ± 0.03	**4.99 ± 0.04**	12.23 ± 0.08	4.09 ± 0.09	NA

Table 3.6. Coordinates for locations of fossil and lithological contacts measured at the HCEL Plant 2022 site and ceratopsid quarry (Q300), used as check points to calculate their respective DEMs' elevation errors. All coordinates in WGS84 horizontal datum, elevation in orthometric height (above mean global sea level). **Abbreviations: DEM,** digital elevation model; **GCP,** ground control point; **MASL,** metres above sea level; **UAV,** unmanned aerial vehicle.

Feature	Latitude	Longitude	GPS elev. ± Z error (MASL)	DEM elevation (MASL)
HCEL Plant 2022	50.763724	-111.421269	688.0 ± 0.8	689.69
Quarry 053*	50.764547	-111.421888	688.6 ± 1.2	689.81
Quarry 300	50.750878	-111.388130	743.26 ± 0.48	743.76
Black shale below Quarry 300	50.750897	-111.388174	742.12 ± 0.34	742.06
Black shale West of Quarry 300	50.750915	-111.388776	742.2 ± 0.8	741.75
Black shale East of Quarry 300	50.750982	-111.388028	741.1 ± 0.53	743.00

*Located with HCEL Plant 2022 DEM, initially measured for a GCP in a separate UAV survey (see Appendix IV).

BRIDGING TEXT

The last two chapters have investigated aspects of the biodiversity of the Dinosaur Provincial Park biota – and of nearby coeval localities – through space and time, two dimensions which are (understandably) frequently addressed in palaeontology. However, energy transfer via species interactions, which can be modeled in ecological networks such as food webs, is one dimension of biodiversity which is only beginning to be investigated in that field with any consistency. It can be argued that the fundamental impossibility to observe interactions within and among extinct species makes any food webs for palaeocommunities futile, yet advances in functional morphology, palaeoecology and modern community ecology now enable more realistic dietary interpretations of fossil remains than ever before. Bearing that in mind, the exceptional fossil record of Dinosaur Provincial Park is now put to work to create the first trophic network ever attempted for a nonmarine Mesozoic community dominated by non-avialan dinosaurs. This network is intended to contain a series of food webs representing different time intervals of the Belly River Group and will eventually warrant a thorough description of its nodes (species/clades) and of the links (trophic interactions) connecting them. For the immediate purpose of this thesis, the DPP food web is applied to ask more direct questions on the variation in the trophic position of one of the most iconic predators ever to walk on Earth, the tyrannosaurid theropod dinosaur *Gorgosaurus libratus*. Therefore, the following chapter addresses the Eltonian shortfall on species' interactions in the Dinosaur Provincial Park ecosystem.

Chapter 4 Tyrannosaurs were dragons, not lions: food webs reveal the ecological role of apex predators in the Dinosaur Provincial Park biota

Abstract

Functional traits of keystone predators can predict aspects of community structure. Consequently, lions and Komodo dragons represent two extant terrestrial apex predators with contrasting trophic ontogenies, associated predator-prey biomass, and diversity distributions in low to mid-latitude ecosystems. Considering the persistence of the trophic function of apex predators over deep time, to what extent would large theropod dinosaurs, an iconic group of extinct carnivores, have any extant analogue? Using the exceptional vertebrate fossil record of the Late Cretaceous Dinosaur Provincial Park biota, we show that the tyrannosaurid *Gorgosaurus libratus* had a more similar trophic role to the Komodo dragon than to lions in two ways. We created the first quantitative site-specific food web ever achieved for any non-avialan dinosaur palaeocommunity demonstrating that *G. libratus* underwent a shift in its trophic position through its ontogeny, comparable to Komodo dragons. Additionally, biomass density ratios estimated between *G. libratus* and its prey species are consistently higher than predator-prey ratios of mammal-dominated faunas and more comparable to those observed on Komodo Island. Our results demonstrate how including ontogenetic intraspecific variation in ecological networks adds a new dimension to characterize the trophic role of extinct species with a sufficiently complete fossil record.

4.1 Introduction

Ecosystem communities consist of species, their ecological roles, and the interactions connecting them (Banker *et al.* 2022). Within those structures, apex predators have a keystone role as indicators of their respective communities' stability and resilience to perturbations. Indeed, several predators at the top of their communities' food chains are known to exert top-down control on the biomass and density of primary and secondary consumer species at lower trophic levels, with their local extirpation or extinction often triggering trophic cascades (Ritchie & Johnson 2009; Estes *et al.* 2011; Ripple *et al.* 2014). Consequently, understanding the factors that determine the extent of top-down control from, and bottom-up control on, apex predators is key to understanding their patterns of prey selection, the distribution of biomass and energy flux across their community's trophic levels, and their extinction risk. These factors consist of traits pertaining to morphology (such as body size, locomotion, and craniomandibular and dental anatomy), metabolic requirements (such as energetic constraints and related territory size), and growth and reproductive strategies (Peters & Wassenberg 1983; Carbone *et al.* 1999, 2010; Brose *et al.* 2006, 2019). Moreover, these traits can be examined throughout animals' life history to define their ecological role in greater detail.

During the Holocene and Anthropocene epochs, nearly every landmass on Earth has had large carnivoran mammals as apex predators characterized by high metabolic requirements due to endothermy, as well as a *K*-selected reproductive strategy involving slow life histories and parental care, which collectively result in a relatively uniform selection of prey species throughout ontogeny and low population densities (Carbone *et al.* 1999; Hatton *et al.* 2015; Jessop *et al.* 2020). At the other extreme of the extant terrestrial apex predator trait spectrum lies the Komodo dragon *Varanus komodoensis*, which is now restricted to the Lesser Sunda Islands of Indonesia and is characterized by an almost completely opposite suite of traits: low metabolic requirements due to ectothermy, and an *R*-selected reproductive strategy lacking parental care. These traits result in significant dietary shifts observed throughout ontogeny at relatively high population densities (Imansyah *et al.* 2008; Laver *et* *al.* 2012; Purwandana *et al.* 2016; Jessop *et al.* 2020). Consequently, the Komodo dragon is one of the only extant reptiles to reach a sufficiently high adult body size to hunt large mammal prey, albeit via a completely different strategy from large felids or canids reflecting its lower metabolic rate (Auffenberg 1981; Purwandana *et al.* 2016). Conversely, the relatively low food requirements of ectotherms likely explain the lack of evidence for top-down control by the Komodo dragon on its resources (Ripple *et al.* 2014; Jessop *et al.* 2020). This paradigm suggests that the structure of relatively stable extant terrestrial communities is influenced by apex predators that fit one of only two highly contrasting functional trait suites.

Considering the extremely high disparity of recent terrestrial apex predator life histories, did this paradigm persist throughout our planet's history (at least since the origin of a simple vertebrate trophic structure), or does it simply reflect the dominance of most extant non-marine ecosystems by mammals? This is where palaeontology can contribute to this debate by describing extinct apex predator clades from fossil remains, which in turn provide the original evidence for proposing (and occasionally testing) hypotheses on their function within ancient ecosystems (Damuth 1992). In this regard, tyrannosaurid dinosaurs of the latest Cretaceous Period (Campanian to Maastrichtian stages) constitute a particularly promising case study as extinct apex predators, since their spectacular fossil record (relative to other theropods) has stimulated particularly intensive research on their palaeobiology (Russell 1970; Hutchinson & Garcia 2002; Erickson *et al.* 2004, 2006; Brusatte *et al.* 2010; Brusatte & Carr 2016; Carr 2020; Dececchi *et al.* 2020, Brown *et al.* 2022*a*). Of particular interest to the present study is the growing evidence for juvenile tyrannosaurs occupying multiple entire trophic guilds in their communities, as seen today in Komodo dragons but not in a single large extant fully terrestrial carnivoran mammal (Holtz 2021; Schroeder *et al.* 2021). One juvenile *Gorgosaurus libratus* skeleton with an estimated body mass of ~300 kg was even fossilized with two skeletons of the ~18 kg theropod *Citipes elegans* among its stomach contents (Therrien *et al.* 2023), thus demonstrating that these predators consumed small prey relative to their body size. Now that ecomorphological hypotheses arising from these studies have been proposed, how can we test them further to assess whether tyrannosaurs were trophic analogues of ‘lions’ or ‘dragons’ in their ecosystem?

We now propose that quantitative trophic networks composed of consumer-resource interactions (i.e. food webs) provide answers to this question. Indeed, these networks define the ecological role of species relative to their entire community (beyond assessing their functional traits in isolation from other co-occurring species), by revealing the effects of their functional traits and inferred biotic interactions on their trophic position along food chains (Williams & Martinez 2000, 2004; Eklöf *et al*. 2013; Poisot *et al.* 2016; Delmas *et al.* 2019; Banker *et al.* 2022). While quantitative food webs are now a mainstay of extant community ecology (Yodzis 1998; Cohen *et al.* 2003; Roopnarine & Dineen 2018; Brose *et al.* 2019; Rossi *et al.* 2019; O’Connor *et al.* 2020; Caron *et al.* 2024), they have been used to measure the structure of palaeocommunities across only seven different deep time intervals so far across Earth’s history (Dunne *et al.* 2008, 2014; Mitchell *et al.* 2012; Roopnarine & Angielczyk 2015; Roopnarine *et al.* 2017; Kempf *et al.* 2020; Fricke *et al.* 2022; García-Girón *et al.* 2022; Cortés & Larsson 2023; Huang *et al.* 2023).

The ecomorphological inferences on tyrannosaurid feeding behaviour outlined above are now sufficiently developed to lay a foundation for inferring trophic interactions with co-occurring species and assemble them in a trophic network to test broader hypotheses on the ecological role of these apex predators at the community level of biological organization. In light of these conditions, we argue that the Late Cretaceous (Campanian) exposures of the Belly River Group (BRG) in Dinosaur Provincial Park (DPP), Alberta, Canada, are an ideal system to investigate the role of tyrannosaurids in their ecosystem. The remarkable anatomical fossil record of DPP has already enabled one of the most thorough descriptions of dinosaur community structure on Earth, at least in terms of taxonomic and functional diversity (Figures 4.1-4.3; Béland & Russell 1978; Dodson 1983; Brinkman 1990; Currie & Koppelhus 2005, Brown *et al.* 2013*b*; Mallon 2019). Importantly for this study, the Park’s most abundant apex predator, the albertosaurine *Gorgosaurus libratus*, is represented by a relatively complete ontogenetic series (Currie 2003*a*; Therrien *et al.* 2021; Voris *et al.* 2022). Moreover, the likely prey composition of this species is well known (compared to other predatory dinosaurs) since the high completeness of the DPP fossil assemblage makes its dinosaur size distribution fairly comparable to the mammal size distribution of a relatively pristine terrestrial ecosystem such as the Serengeti, at least for body masses above ~20 kg (Figure 4.3A). Therefore, the DPP palaeobiota has strong foundations for combining its species and their inferred interactions into the first ecological networks ever attempted for a Mesozoic non-marine community at the highest possible taxonomic resolution. Furthermore, well constrained stratigraphic distributions for those constituent taxa now raise the possibility of estimating abundance (and by extension biomass) at distinct trophic levels obtained from such a network across stratigraphic (and potentially temporal) intervals (Figure 4.1B; Currie & Russell 2005; Mallon *et al.* 2012; Ramezani *et al.* 2022; Eberth *et al.* 2023).

In the following study, we ask two main questions, using the uniquely detailed fossil record of Dinosaur Provincial Park as a model system for a Late Cretaceous community with one of the best-known tyrannosaurid dinosaurs (*Gorgosaurus libratus*) among its apex predators. First, what will the creation of a highly resolved trophic network for DPP with quantifiable properties reveal about the stability of the trophic position of *G. libratus* throughout its ontogeny? Second, what will dinosaur biomass estimates reveal about the abundance of predators relative to their likely prey in the DPP community, of which *G. libratus* was almost certainly a key component? For each of these questions, *G. libratus* will be compared with two groups of hypothetical extant analogues that exhibit highly contrasting metabolic and life history strategies outlined above: the lion *Panthera leo* in Serengeti National Park, Tanzania, and the Komodo dragon *Varanus komodoensis*, the undisputed native apex predator of Komodo and of neighbouring islands. These predators were also selected because they both inhabit terrestrial ecosystems which have potentially analogous abiotic conditions to the Late Cretaceous of Alberta, i.e., a subtropical climate with low temperature seasonality and a mosaic of woodlands and open plains. Cenograms and histograms of the DPP, Komodo and Serengeti communities (limited to clades of potential ecological analogues) already suggest that these apex predators each have a different ecological impact (Figure 4.3A-B): the DPP community displays a wide body size gap between two large tyrannosaurids (*Gorgosaurus* and *Daspletosaurus*) and the next largest carnivorous dinosaur (a niche partially filled by juvenile tyrannosaurids, as shown by Schroeder *et al*. (2021)), while the Serengeti lacks any comparable gap and various Komodo dragon life stages occupy nearly the entire size range of niches for mammals weighing >1 kg. These size distributions now set the stage to reconstruct ecological networks for each of these communities. Therefore, we hypothesize that variation in trophic links leading to *G. libratus* at different life stages will result in significant shifts in trophic position similar to those seen in *V. komodoensis*. Wexxx also hypothesize that the predator-prey ratio of the DPP community was more similar to that of an extant community with more abundant megafauna, such as African savanna localities, than to that of the Lesser Sunda Islands.

4.1.1 Study area: Dinosaur Provincial Park, a model system for tyrannosaur palaeoecology

Dinosaur Provincial Park (DPP) is particularly famous for displaying a very high fossil diversity of dinosaurs and other Mesozoic vertebrates as a result of more than 120 years of palaeontological exploration (Russell 1966; Béland & Russell 1978; Dodson 1983; Ryan & Russell 2001; Currie 2005; Eberth & Currie 2005, Brown *et al.* 2013*b*). Around 50 of the 166 vertebrate species described from its badlands outcrops are dinosaurs, which constitutes around 7% of all non-avian dinosaur species known on Earth (Wang & Dodson 2006; Benton 2008), with a less complete plant and invertebrate record representing indispensable additional ecospaces and trophic levels for an eventual food web (Braman 2005; Johnston & Hendy 2005; Koppelhus 2005). Crucially, several of DPP's vertebrate species have extremely well-preserved skulls and skeletons, which provide invaluable anatomical evidence for life history traits such as possible trophic interactions (e.g. Brinkman 2005;

Mallon & Anderson 2013; Mallon *et al.* 2013). For the purposes of this study, apex predators in that ecosystem are represented by three tyrannosaurid dinosaur species, two of which coexisted at any time interval of the BRG. The *Daspletosaurus* lineage is very rarely represented among the Park's skeletons and seems to have split into *D. torosus*, which is restricted to the Oldman Formation, and a likely distinct species restricted to the overlying Dinosaur Park Formation (Currie 2003*a*; Loewen *et al.* 2013). In contrast, *Gorgosaurus libratus* persisted throughout the entire BRG as the most abundant of the Park's tyrannosaurids, with a relatively complete skeletal record that has made it a model species for tyrannosaurid biology (Lambe 1914, 1917; Russell 1970, Currie 2003*a, b*; Erickson *et al.* 2004; Currie & Russell 2005). Of high relevance to the present study is the fact that the recent description of two rare juvenile *G. libratus* skeletons from DPP has probably provided the strongest evidence to date in support of ontogenetic dietary shifts in tyrannosaurids (Therrien *et al.* 2021, 2023; Voris *et al.* 2022). Considering that *G. libratus* has a much more complete fossil record and genuinely appeared more abundant in its community, it was selected instead of *Daspletosaurus* for this study.

While other Mesozoic sedimentary units around the globe have a vertebrate diversity on a similar scale, DPP preserves an extinct community at a uniquely high spatial fidelity and temporal resolution. First, an estimated 50% of the Park's individual fossil quarries (around 600 collected and uncollected associated and/or articulated skeletons and more than 300 bonebeds) have been (re)located with highly precise GPS coordinates in an unprecedented effort to document their geographical and stratigraphic distribution (Currie 2005; MacDonald *et al.* 2005; Tanke 2005). Almost all of these quarries are located within an ~80 km^2 area of badlands along the Red Deer River (Figure 4.1A; Béland & Russell 1978; Currie & Russell 2005), making the DPP fossil assemblage far more spatially constrained than ones of comparable size known from other famous dinosaur-bearing strata such as the Hell Creek, Morrison and Nemegt Formations (Dodson *et al.* 1980; Hartman *et al.* 2002; Eberth 2018). Furthermore, the 100 m thick succession of sedimentary horizons hosting these quarries is well calibrated in geological time since it is known to represent ~2.43 Ma due to precise radioisotopic dating of four beds of bentonite claystone ranging across nearly the entire stratigraphic breadth of the BRG in the Park (Thomas *et al.* 1990; Ramezani *et al.* 2022; Eberth *et al.* 2023). As a whole, this geological and palaeontological record has revealed patterns of vertebrate species turnover, through variation in alpha diversity and relative abundance, at a geological time scale rarely achieved for non-marine fluvial channel sedimentary deposits (Brinkman 1990; Mallon *et al.* 2012; Cullen & Evans 2016; Cullen *et al.* 2021). Admittedly, the DPP fossil record has a well documented taphonomic size bias in which small-bodied animals are underrepresented (Brown *et al.* 2013*b, a*). This results in a left-skewed terrestrial vertebrate body size distribution, even when juveniles of large dinosaur species likely undergoing ontogenetic dietary shifts (or at least expansions) are considered distinct operational units from the adults (Figures 4.2, 4.3A-B). However, this limitation is characteristic of almost every terrestrial fossil vertebrate assemblage (Damuth 1982; Benson 2018, Brown *et al.* 2022*b*), and is arguably outweighed in DPP by the uniquely high geographical and stratigraphic control achieved for that locality.

4.2 Material and methods

4.2.1 Assembly of consumer-resource matrices

The raw datasets for creating empirical food webs in this study consist of series of pairwise consumer-resource interactions displayed as matrices, with rows representing resources and columns representing consumers. Each cell in the matrix contains either number 1 (indicating presence of a trophic interaction, i.e. a link between two nodes) or 0 (absence). This binary approach meant that each trophic link had the same weight in all food webs. This decision was made because of the understandable lack of reliable estimates of relative abundance of each resource in the dietary composition of extinct animals from Dinosaur Provincial Park (DPP) as an indicator of link strength. An alternative indicator of link strength based on the number of lines of evidence for trophic interactions in fossil species was considered (see Dunne *et al.* 2014), yet it did not prove sufficiently comparable to the extant food webs which are also part of this study. The evidence for all links included in the matrix comes from a literature review of observed and inferred dietary preferences for all its consumer nodes. This review was particularly intensive for DPP because of the reliance on fossil material to infer feasible links (see below). The Serengeti food web analyzed in this study combined two already published food webs with overlapping nodes (Baskerville *et al.* 2011; de Visser *et al.* 2011), and the Komodo food web was assembled from observed trophic interactions published in the literature. More details on the creation of the extant food webs are provided below. We elected to present trophic links between nodes in a matrix instead of an edge list, even though the latter format has often been adopted in previous studies (see de Visser *et al.* 2011; Dunne *et al.* 2014; Cortés & Larsson 2023). This is because the software we used to generate food webs accommodates both raw data formats, and because matrices are far more convenient to edit than edge lists in terms of adding/removing nodes and links.

Some general rules regarding node and link selection were retained for all food webs: first, carrion was retained as a distinct node to account for more specialized scavengers. Since this node has a trophic level of 1 (because carrion does not consume any resources), and most predators are assumed to consume carrion unless specified otherwise in the literature, the retention of this node results in lowering most predators' trophic level, although not to a significant extent given the large number of alternate resources available to them. Second, eggs were not included among resources. Third, juveniles and adults of the same species were usually collapsed into the same node, even in well-documented cases of ontogenetic dietary shifts (such as frogs and crocodilians). This means that the diets of nymphs and larvae were included among trophic links for insects. Only for tyrannosaurids, hadrosaurids, ceratopsids and the Komodo dragon were distinct nodes assigned to different ontogenetic stages because of the particular focus of this study on these clades (see below). As for general trophic link rules, cannibalistic and plant-pollinator links were excluded from all datasets by default. The following paragraphs explain the methodology behind the assemblage of fossil and extant community datasets in greater detail.

Dinosaur Provincial Park datasets

Node selection. Nodes for Dinosaur Provincial Park were selected at the highest possible taxonomic resolution that the fossil record could offer for different clades. This resulted in most tetrapod nodes representing individual species, while several fish and invertebrate nodes were resolved at the family or order level. Considering that the Park's entire fossil record is distributed over a period of almost 2.5 million years and that some of its species did not co-occur, the DPP consumer-resource matrix had different versions, which each represented a distinct stratigraphic interval with a distinct dinosaur megafaunal composition: (1) the Oldman Formation; (2) the Dinosaur Park Formation's Megaherbivore Assemblage Zone (MAZ) 1a; the DPF MAZ-1b; the DPF MAZ-2a; the DPF MAZ-2b (corresponding to the Lethbridge Coal Zone); and finally a fully time averaged version which included every single dinosaur species known, even those which likely never co-occurred (e.g., *Centrosaurus apertus* and *Styracosaurus albertensis*), to compare its node and network properties with the more time-constrained versions. In total, 49 nodes (excluding juvenile megafauna) have been attributed to non-avialan dinosaurs at the genus or species level across DPP's biozones. In this respect, thescelosaurids constitute a notable exception since they can only be resolved to the subfamily level (Orodrominae) due to a relative lack of diagnostic characters among their very fragmentary remains (Brown *et al.* 2013*a*). This alpha diversity is slightly lower than the ~51 species counted elsewhere (Wang & Dodson 2006) since we elected to exclude likely junior synonyms such as *Chasmosaurus canadensis*. On the other hand, *Corythosaurus intermedius* and *Lambeosaurus clavinitialis* are included in DPF MAZ-1b due to their relatively diagnostic head crests (Mallon 2019), and so are the rare ceratopsids *Spinops sternbergorum* and *Mercuriceratops gemini* based on sufficiently distinctive frill characters (Farke *et al.* 2011; Ryan *et al.* 2014). Our dataset also has a node for *Sphaerotholus lyonsi*, a recently described pachycephalosaur that significantly increases the small ornithischian species richness from the Park (Woodruff *et al.* 2023). Distinct nodes are also assigned to potentially problematic small theropods such as

Richardoestesia isosceles, cf. *R. gilmorei*, cf. *Paronychodon*, cf. *Pectinodon*, as well as *Rativates evadens*, cf. *Qiupalong* and an elusive large unnamed ornithomimid, due to sufficient diagnostic characters being present in teeth and isolated postcranial elements (Sankey *et al.* 2002; Longrich 2008; Larson & Currie 2013; McFeeters *et al.* 2016, 2017). Concerning tyrannosaurids, we considered *Daspletosaurus torosus* to be a distinct species (therefore a distinct node) from an undescribed *Daspletosaurus* species found in the Dinosaur Park Formation and time-equivalent Oldman Formation of the Manyberries area in southeastern Alberta, based on recent taxonomic studies (Paulina Carabajal *et al.* 2021; Scherer & Voiculescu-Holvad 2024).

Since complete turnover in species' occurrence has only been convincingly demonstrated for tyrannosaurids, hadrosaurids, ceratopsids and some ankylosaurs (Currie & Russell 2005; Mallon *et al.* 2012; Arbour & Currie 2013), almost every other taxon included among the nodes was assumed to persist throughout the Belly River Group in DPP, with taxa represented by very rare specimens likely to be vastly undersampled (e.g. leptoceratopsids, see Ryan *et al*. (2012)). The only exceptions were made for clades whose absence from a certain time interval seemed to represent a true negative signal due to the influence of changing environmental conditions combined with a fairly reliable fossil sample size. This was the case of the shark *Hybodus montanensis*, whose teeth are consistently absent from all vertebrate microfossil localities in the lower DPF before appearing in upper DPF localities, likely due to the ongoing transgression of the Bearpaw Sea (Brinkman 1990). The DPF MAZ-1a and DPF MAZ-1b versions were deemed to have the most complete faunal assemblage (with minimal time averaging) because they represent the two biozones encountered in the lower DPF, the most intensely sampled interval of the Belly River Group in the Park (Currie & Russell 2005). Therefore, they were selected to be compared to extant food webs in this study. Moreover, the fact that megaherbivore species richness varies slightly between each of these food webs raised the opportunity to obtain a range of feasible trophic levels for the predators that feed on them at different stratigraphic intervals (instead of a single time averaged value).

Ontogenetic dietary shifts in dinosaurs were accounted for in the DPP food webs by assigning distinct nodes for adults and juveniles of all tyrannosaurid, hadrosaurid and ceratopsid species included in each consumer-resource matrix, for a total of 22 of the Park's 49 dinosaur taxa recognized in this study. It must be noted that hadrosaurids and ceratopsids are considered to have undergone dietary expansion through ontogeny, instead of true dietary shifts involving replacement of one suite of resources by another. Each tyrannosaurid had a third node for young juveniles considering indirect anatomical evidence that they fed on even smaller prey than mid-sized juveniles (Therrien *et al.* 2021). To investigate an alternative suite of trophic links for tyrannosaurids at each ontogenetic stage, additional versions of the DPF MAZ-1a and DPF MAZ-1b consumer-resource matrices were produced in which all aquatic and semiaquatic nodes (including potential prey such as turtles and champsosaurs) were excluded, adults' diets were almost strictly limited to megaherbivores, and pack hunting was accounted for. The latter condition implied that juveniles, not just adults, also had trophic links to adult megaherbivores since they would cooperate with adults in bringing down prey. To investigate the effect of the exclusion of juvenile megaherbivores from tyrannosaur prey, two more versions of the matrices were produced: one of the DPF MAZ-1a (not accounting for pack hunting) and one of the DPF MAZ-1b (accounting for pack hunting).

While large vertebrates are well represented in the fossil record on which the DPP food web rests, almost every other clade is underrepresented due to taphonomic biases. This meant that some nodes were added to the DPP food web despite representing taxa whose fossils have not yet been found there. For example, a minority of fishes and small tetrapods included among the network's nodes are not known from the local DPP fossil assemblage but are reported from neighbouring coeval localities such as the Irvine and Onefour vertebrate microfossil localities. These include the large sirenid salamander *Habrosaurus prodilatus* (Gardner 2005), as well as anguid, scincid and teiid lizards (Caldwell 2005), some ornithurine birds (Longrich 2009), and a tetra-like teleost assigned to order Characiformes (Newbrey *et al.* 2009). Considering that small-bodied vertebrates are underrepresented in the DPP fossil assemblage, the local absence of these species likely reflects sampling error more than a genuine ecological signal. Likewise, arthropods are probably the most elusive hard-bodied organisms in the DPP terrestrial fossil assemblage, with the only published occurrences consisting of a millipede and an aphid in amber (family Cretamyzidae) (Johnston & Hendy 2005; McKellar *et al.* 2019). Therefore, several nodes each representing an arthropod order were erected from the faunal list of nearby Grassy Lake Amber, which is located in the slightly older Foremost Formation (Pike 1994; McKellar *et al.* 2008). More insect orders are now represented in DPP following recent discoveries of the first insect compression and impression fossils from this locality after more than a century of exploration (Mueller *et al.* in prep.). Plants are yet another underrepresented key component of the DPP community, with only three conifer families known from the fossil wood and leaf record, and only ten angiosperm species known from the fossil macroflora (Koppelhus 2005). Most of the plant diversity from the Park currently resides in the palynoflora, where bryophytes, lycopods, cycads, eight fern families, and seventeen angiosperm families are currently recognized (Jarzen 1982; Braman 2005). This limitation ultimately proved irrelevant since we elected to define plant nodes by higher-level taxonomy (e.g. angiosperms, conifers) instead of the species level, in order to make trophic levels more comparable to those of the extant food webs included in this study. Nonetheless, angiosperms were assigned three nodes defined by a distinct plant part within a single tree, i.e. leaves, shoots, and seeds/fruit, to reflect the fact that some consumers only eat select parts of a given tree or shrub species. The more highly resolved version of this food web (Demers-Potvin & Larsson in prep.) has distinct nodes for each plant family identified in the Park's palaeobotanical record. Lastly, bacteria were included among the primary producers following the Messel food web (Dunne *et al.* 2014), despite their evident absence from the DPP fossil record. This decision was made to reflect the diets of invertebrate consumers (such as bivalves) as realistically as possible. In this way, the DPP community was sufficiently represented in key ecological niches to measure trophic levels reliably in the resulting food web.

Link selection. Several lines of evidence were drawn from the literature to infer feasible trophic links in the Dinosaur Provincial Park community. These lines of evidence can be classified as direct or indirect: the former offer a clear identification of the consumer and of the resource (often at the species level), either as direct observations of an interaction between extant relatives (which can only apply to modern communities), or as stomach contents in extant or fossil organisms, and thus provide evidence for realized trophic interactions in a community. In contrast, the latter are a series of traits that predict feasible interactions without confirming the resource's exact identity, such as functional morphology, body size, spatiotemporal co-occurrence, tooth wear, and stable isotope ratios extracted from tissue. The relevance of these lines of evidence was highly variable between the nodes included in each network based on two factors: (1) the completeness of the fossil material; (2) the existence of phylogenetically close extant relatives allowing uniformitarian assumptions. Based on these taphonomic and evolutionary criteria, the consumers of the DPP community were classified into four categories defined by different combinations of evidence for their trophic links (Table 4.1).

The first category contains species represented by complete skulls and/or skeletons while having (or being anatomically similar to) close extant relatives. It mostly includes aquatic and semiaquatic species, notably the Park's turtles and crocodilians (Brinkman 2005; Wu 2005), as well as a few fish species such as the ray *Myledaphus bipartitus*, the large elopomorph *Paratarpon apogerontus* and the sturgeon *Anchiacipenser acanthaspis* (Bardack 1970; Neuman & Brinkman 2005; Sato *et al.* 2018). This is the category for which trophic links were assigned with the highest degree of confidence since most of their supporting evidence came from the literature on the feeding ecology of close extant relatives following the principle of taxonomic uniformity. Most of the proposed resources for this group of consumers also have very close extant relatives, yet a few additional links were assigned to more evolutionarily distant prey species (such as multituberculates and some ornithurines) based on anatomical traits, particularly body size estimates. It must be noted that several of the Park's turtles belong to extinct families lacking relatively close extant relatives (e.g. Baenidae and

Nanhsiungchelyidae), yet their ecomorphology suggests that they all filled similar ecospaces to extant freshwater and terrestrial turtles (Brinkman 2005).

The second category contains species represented by complete skulls and/or skeletons but lacking any near extant relative. As is expected, it includes most of the dinosaurs known from DPP, especially large-bodied species (Brown *et al.* 2013*b*). This is the group for which indirect evidence (such as the aforementioned anatomical traits) obtained from the fossil record has been investigated most intensively to infer species' ecomorphology due to its high level of preservation. For instance, DPP's unparalleled megaherbivore fossil assemblage provides the core evidence for hypotheses of dietary niche partitioning between hadrosaurids, ceratopsids and ankylosaurs (Mallon & Anderson 2013, 2014*a*, *b;* Mallon *et al.* 2013; Mallon 2019), which have profoundly influenced our understanding of Late Cretaceous dinosaur community structure. As another example, the detection of cranial and limb allometric growth from anatomical traits observed in growth series from DPP constitute the most abundant lines of evidence for ontogenetic dietary shifts in tyrannosaurids, hadrosaurids and ceratopsids (Therrien *et al.* 2021; Wyenberg-Henzler *et al.* 2021, 2022). In very rare cases, direct evidence was available as stomach contents preserved among skeletons, such as a juvenile *Gorgosaurus libratus* containing the two most complete known specimens of the small caenagnathid *Citipes elegans* (Therrien *et al.* 2023), or a more ancient relative of the Park's nodosaurids revealing a fern-dominated plant diet in its cololites (Brown *et al.* 2020). Finally, it must be noted that some of these well-preserved species have a few close relatives (within the same family or even subfamily) in the DPP fauna known from more fragmentary remains. In these cases, very closely related species were assumed to have the same trophic link distribution regardless of their completeness level in the absence of alternate evidence. For instance, the centrosaurine *Coronosaurus brinkmani* is solely known from isolated cranial elements recovered from bonebeds in the Oldman Formation (Ryan & Russell 2005), yet they do not provide any evidence that it had a significantly different dietary habit from its more recent (and far more completely known) relatives, such as *Centrosaurus apertus* and *Styracosaurus albertensis*.

The third category contains species represented by fragmentary remains and having (or being anatomically similar to) close extant relatives. It includes lizards, amphibians, and most of the fishes, known from isolated teeth, mandibles, scales and centra collected from vertebrate microfossil localities. Therefore, almost all the evidence for their trophic links comes from direct observations of their nearest extant relatives. Although most of the Park's salamanders are classified in now-extinct families (Gardner 2005), better preserved fossil relatives from other localities suggest that they all fell within the ecomorphospace occupied by extant salamanders (e.g. Estes 1975). Therefore, they were considered a better fit in the third category than in the fourth (see below).

The final category contains species represented by fragmentary remains but lacking any near extant relative. It includes almost every small-bodied dinosaur species known from the Park (including birds) as well as all mammals and the azhdarchid pterosaur *Cryodrakon boreas*. This is the category for which dietary interpretations based on morphology were most problematic because the most informative fossil specimens consist of isolated mandibles or incomplete postcranial skeletons, as in the case of caenagnathids for instance (Funston & Currie 2014; Funston 2020). Other taxa are almost solely known from teeth in the Park, such as multituberculates and the enigmatic cf. *Richardoestesia* theropods (Sankey *et al.* 2002; Fox 2005). Additionally, the lack of associated postcranial material for some taxa prevented any confident characterization of their ecospace. For instance, there is no way to know whether some of the Park's mammals were more scansorial or fossorial than others (Fox 2005), and the only bird that seems to present the faintest evidence of a distinct ecospace is an ornithurine known from a coracoid which exhibits pachyostosis, likely indicative of a diving habit (Longrich 2006, 2009). Furthermore, the relative lack of ecomorphological evidence in this category meant that stable isotope ratios extracted from teeth proved particularly valuable to provide further clues on diet. As an example, one study based on a coeval vertebrate microfossil locality from southern Alberta revealed that troodontids were more omnivorous, and that at least one multituberculate family was leaning more towards prey-dominated (rather than plant-dominated) omnivory, than their respective tooth anatomy alone would suggest (Cullen & Cousens 2023). Considering all these limitations, this was the category for which the literature on better preserved fossil relatives found outside DPP and neighbouring coeval localities was most essential.

Since body size is one of the most consistently predictive traits of trophic interactions across biomes and phylogeny (Brose *et al.* 2006; Caron *et al.* 2024), it was often used to make a final decision on animal prey species for a given consumer when other anatomical lines of evidence remained equivocal. To simplify these decisions, the maximum body size of a given species at maturity was considered here, the only exceptions being made for species that had separate nodes for adults and juveniles. Body mass estimates were already available from the literature for most of the Park's terrestrial fauna, particularly dinosaurs (Brown *et al.* 2013*b*; Benson *et al.* 2018; Campione & Evans 2020; Schroeder *et al.* 2021), while body length was more readily available for the aquatic fauna. Some body sizes were estimated as part of this study based on published scaling laws for specific taxa, such as turtles (Pough 1980), crocodilians (O'Brien *et al.* 2019) and lizards (Longrich *et al.* 2012). An attempt was made to quantify maximum and minimum prey body mass thresholds more objectively for dinosaurs, mammals, squamates and crocodilians based on a published dataset (Therrien *et al*., 2023: Supplementary data). However, the resulting regressions' confidence and prediction intervals proved too exclusive and inclusive, respectively, to statistically provide any realistic prey size range.

Appendix V presents a more comprehensive justification for all nodes and links included in a more highly resolved version of the DPP food webs (Demers-Potvin & Larsson in prep.), where nodes are assigned to each plant family identified from the macro- or palynoflora. The references are organized in a more concise table in Appendix VI.

Extant community datasets. The Serengeti food web was the easiest to assemble because it simply combined two already published food webs. The first of these has a wider taxonomic span since it includes some birds, reptiles, amphibians and small mammals alongside the megafauna, but most of its nodes represent a group of trophic species sharing a similar diet instead of individual species (de Visser *et al.* 2011). This dataset was combined with a dataset more focused on mammals and plants from the Serengeti (Baskerville *et al.* 2011), in which each node represents a distinct species in order to increase the taxonomic resolution of the final food web and thus make it more comparable to the Dinosaur Provincial Park and Komodo food webs. Edge lists available from the supplementary data for both aforementioned publications were then converted into consumer-resource matrices. Juvenile and young juvenile nodes were also added for the lion (*Panthera leo*) to compare ontogenetic trends in this species' trophic position to those for *Gorgosaurus libratus* and *Varanus komodoensis*. Young juvenile body masses were estimated at their weaning age (8 months) while juvenile body masses were estimated at their age of independence from their pride (18 months) based on a least-squares regression between female lions' age and body size (Smuts *et al.* 1980; Kingdon 2015). Trophic link distributions were also modified from the two original datasets for some lion life stages. For example, the spotted hyena (*Crocuta crocuta*) is known to prey on lion cubs (Harrington 2004), thus a link was added between this node and the young juvenile lion node. Another link was added between adult and young juvenile lions to account for rare cases of cannibalism, even if it results from infanticide rather than a habitual foraging activity (Bothma & Walker 1999). Lastly, the 'decaying material' node in the Serengeti food web was defined as carcasses not killed by adult lions in order for weaned young juveniles to have a series of trophic links more comparable to those of more mature life stages due to the restriction of their diet to prey which they did not kill themselves.

The creation of the Komodo food web required a more thorough literature review because no prior attempt was ever made to assemble trophic interactions from that community in a similar manner to the Serengeti. The most comprehensive reference for the diet of the Komodo dragon consisted of an ambitious field study of the behavioural ecology of this species, conducted from 1969 to 1972 (Auffenberg 1981). Prey species were mostly identified from examinations of fecal pellets corroborated by observations and accounts of predation from local witnesses. This reference contains additional information on trophic links that complete the Komodo food web, including the predators of juvenile Komodo dragons, the plant food of the community's most common herbivores, and even scavenging (mostly bird and insect) species that compete with Komodo dragons for carrion. To account for observed ontogenetic dietary shifts in the Komodo dragon, this species was divided into four nodes in the food web, each of which corresponds to a distinct body size class (correlated with age) based on stomach contents and the aforementioned data combined in Purwandana *et al*. (2016): young juvenile (hatchling), juvenile, subadult and adult. In contrast with the more recent study, Auffenberg (1981) never explicitly mentioned the concept of ontogenetic niche shifts, yet crucially divided his fecal pellet samples into size categories that reflect the body size of the predator and are thus likely correlated with age. Therefore, Purwandana *et al*. (2016) proved the most authoritative reference for establishing broad dietary preferences at each ontogenetic stage, while Auffenberg (1981) contained more detailed species lists for each major prey group (e.g. the lizard and cricket species consumed at juvenile stages). Together, these two references lay the foundation for a food web for Komodo Island resolved at the species level, in which the trophic level of the Komodo dragon at each ontogenetic dietary shift could be measured. Cannibalistic links were generally excluded from all consumer-resource matrices in this study, but they were exceptionally included in a second version of the Komodo consumer-resource matrix considering the discovery of small Komodo dragon individuals in some fecal pellets (Auffenberg 1981) and the division of this species into nodes defined by size classes. This allowed us to test the effect of the inclusion of cannibalism on the trophic levels of the Komodo dragon's three older ontogenetic nodes.

Plants could be resolved at the species level for both the Serengeti and Komodo food webs based on the available references, However, their nodes were collapsed into the same categories defined for the Dinosaur Provincial Park food webs to make all trophic levels among secondary consumers more comparable between datasets. References for all nodes and links that together form the Serengeti and Komodo food webs are available alongside the Dinosaur Provincial Park food web references in Appendix VI.

4.2.2 Food web generation, visualization, and analysis

Consumer-resource matrices were opened in the Network3D software to generate, visualize, and quantitatively analyze each food web (Yoon *et al.* 2004; Williams 2010). Network3D was written by R. J. Williams and provided by J. Dunne (Santa Fe Institute). The raw versions of each consumer-resource matrix were stored as separate sheets in an Excel file, and each of them was converted into a .txt file that was opened into Network3D for analysis. Most of the network and node properties of each food web were calculated with Network3D, of which Prey-averaged trophic level (PATL) was considered the most important indicator of trophic position for the food webs' apex predators at different ontogenetic stages. PATL was calculated as 1 + the average trophic level of each predator's prey (see Williams and Martinez (2004)). Mean food chain length (also known as 'Chain-averaged trophic level', see Williams and Martinez (2004)) was an alternative measurement of trophic position selected for this study. It could not be obtained from Network3D, so it was calculated from the 'cheddar' R package instead (Hudson *et al.* 2013). This package necessitated the transformation of each consumer-resource matrix into an edge list, from which a table of the frequency of each chain length for each node was produced using the 'TrophicChainStats' function. Mean chain lengths (as well as their median, variance and standard deviation) were subsequently calculated using R statistical software v 2024.04.0 Build 735 (R Core Team 2023).

Chain length measurements are far more difficult to compare than trophic level measurements between food webs of distinct communities because the former's value is much more sensitive to links connecting consumers located at a similar prey-averaged (or short/long-weighted) trophic level. This means that trophic analogues which have a similar PATL in distinct food webs can have highly different mean chain lengths if some taxa or ecological niches are not represented sufficiently equally between them. Consequently, the node and link distributions of all three communities' food webs (especially DPP) were edited to ensure that their respective chain lengths were sufficiently comparable. First, all aquatic and semiaquatic nodes were excluded from the DPP food web, otherwise the chains of all terrestrial predators feeding on some of these nodes (e.g. a tyrannosaurid consuming a trionychid turtle) would have been much longer relative to Serengeti and Komodo chains. Second, we ensured that taxa represented by likely trophic analogues in each food web (e.g. coleopterans or insectivorous lizards) had very similar trophic link suites to prevent them from having a confounding effect on the trophic position of nodes higher up the food chain. Third, several nodes with nearly identical suites of links were collapsed into nodes at a lower taxonomic resolution representing 'trophic species'. For instance, nearly every multituberculate mammal species in the DPP food web was collapsed into a single 'Multituberculata' node. Additionally, some of the trophic species in the DPP food web aggregated nodes with slightly different link combinations, otherwise this network would have had longer chains relative to the others. As an example, DPP's largest lizard (the varanoid *Palaeosaniwa canadensis*) was hypothesized to consume the two smaller varanoid species in the unconstrained version of that food web. However, retaining all these nodes would have added steps which lack any analogue in the extant food webs' chains (at least with their current node and link distribution), and thus all three species were lumped into the 'Varanoidea' trophic species node. Chain lengths were thus obtained for 'trophic species' versions of the DPP food web with and without pack hunting in tyrannosaurids, of the Serengeti food web with adult lion trophic links including and excluding prey weighing less than 20 kg, and of the Komodo food web with and without cannibalism between Komodo dragon life stages. PATL had already been calculated for the food webs' fully resolved versions, but it was calculated again for the 'trophic species' versions to obtain values that were directly comparable to obtained mean chain lengths. It must be noted that DPP food webs resolved to ‘trophic species’ had the exact same node composition regardless of their biostratigraphic zone since their megaherbivorous dinosaurs were not resolved to the species level. Therefore, their results can apply to any zone of the Dinosaur Park Formation, whether MAZ-1a, MAZ-1b, or MAZ-2.

4.2.3 Predator and prey biomass density estimates

The second major analysis of this study consisted of a comparison of the biomass of apex predators in extinct and extant communities with that of their prey. This required access to body mass and density estimates for each species included in the analysis. Biomass densities for most mammals >5 kg in communities from various African, Asian and North American protected areas and wildernesses were available from a published database (Hatton *et al.* 2015). Biomass densities for the Komodo dragon and its prey were obtained from more focused studies based on different census methods (Auffenberg 1981; Jessop *et al.* 2020). Biomass densities for Dinosaur Provincial Park were understandably more challenging to obtain due to reliance on fossil datasets affected by taphonomy. To estimate biomass density, body mass, abundance and surface area estimates were required. Body mass estimates for each included species were readily available from the literature (see previous section on trophic node and link selection). To remain consistent with the taxon and body mass range selections of Hatton *et al*. (2015), only dinosaurs weighing more than 5 kg were selected from the DPP community. As for surface area, two different scenarios were tested: one in which the area was restricted to the badlands where the Belly River Group is exposed in and around DPP (which amounts to ~120 km^2), and a much larger area (~1,950 km^2) delineated by a circle with a diameter approximately equal to the distance between the westernmost and easternmost quarries of the Dinosaur Park Formation located in DPP’s immediate vicinity (Figure 4.4E). While the smaller area might yield more realistic densities since it only includes fossil-bearing outcrops, the larger area is also worth investigating in case the density estimated from the badlands area alone is overestimated due to time averaging and the fact that every single individual preserved as a fossil specimen had a much larger spatial range that would have extended beyond the badlands area during its lifetime.

Dinosaur species abundance data was obtained from a database of DPP's individual fossil quarries and skeletal specimens initiated by Philip Currie (Currie & Russell 2005), and now expanded through the inclusion of recently discovered specimens as part of this study (Appendix II). The horizontal and vertical GPS coordinates of the quarries listed in this database enabled the selection of subsets of the data corresponding to estimate biomass at more constrained stratigraphic intervals and thus increase the time resolution of the DPP biomass estimates to make them more comparable to the extant ones. Skeletons which were uncollected and/or unidentifiable at the species level (most of which are indeterminate hadrosaurs) were also included to reduce collection bias favouring rarer specimens. Ceratopsid-dominated bonebeds were counted as a single occurrence (i.e. weighed equally to an isolated skeleton) due to their distinct taphonomic history (Eberth & Currie 2005; Eberth & Getty 2005). Considering that small theropods and small ornithischians are rarely preserved as skeletons due to the size taphonomic bias operating against them, isolated elements were also included in the uncorrected version of the dataset (e.g. isolated ornithomimid metatarsals). Therefore, with abundance, surface area and body mass, biomass densities for dinosaur predators and prey were estimated for DPP using different versions of the dataset.

In terms of time resolution, biomass densities were estimated for three versions: one which includes the entire time averaged DPP fossil assemblage (including skeletons with unknown locality data), one which includes the fossils found only in the lowermost 10 m of the Dinosaur Park Formation (MAZ-1a, see Figure 4.1B), one constrained to the 10-30 m interval (MAZ-1b), and one which is limited to the upper half of the DPF (MAZ-2, 25 to 50 m above the Oldman-Dinosaur Park Formation contact). The assemblage for the lowermost DPF had an almost equal biomass to the assemblage for the upper DPF despite representing a far thinner stratigraphic interval, which simply reflects a gradual decrease in skeleton fossilization potential from the base to the top of the DPF, attributed to a decrease in the proportion of sandstone-dominated point bar deposits (Currie & Russell 2005).

Biomass density corrections for Dinosaur Provincial Park. Considering the overrepresentation of large dinosaur skeletons in the DPP fossil assemblage, the biomass estimates for the two most constrained stratigraphic intervals were corrected by estimating more realistic abundances for all dinosaur species weighing less than 1,000 kg at maturity and for tyrannosaurid, hadrosaurid and ceratopsid juveniles due to the distinct trophic niche they likely occupied relative to the adults. Small-bodied species' abundances were corrected using regressions obtained from Damuth's law, a series of negative correlations between body mass and density that are consistent across biomes and phylogeny (Damuth 1981, 1987, 2007). The sample from the lowermost 10 m of the DPF was selected to make these corrections because it is by far the most complete for any stratigraphic interval in the Park. Abundances for small ornithischians and ornithomimids were corrected with the regression obtained from the mammal primary consumer dataset of Damuth (1987); this dataset seemed to yield reliable density estimates because the densities of the three most frequently found herbivores of the lower DPF (*Corythosaurus casuarius*, *Centrosaurus apertus* and *Gryposaurus notabilis*, based on the 120 km^2 surface area) all fell well within the regression's 95% confidence interval (Figure 4.4C). An extra step was required to estimate small carnivorous and omnivorous theropod densities based on the mammal secondary consumer dataset because the density of the most frequently found predator in the Park (*Gorgosaurus libratus*) fell far above the regression's confidence interval (Figure 4.4A). Therefore, the mammal dataset was combined with an extant reptile mass-density dataset from the same study, with all extant densities corrected for metabolic rate by dividing reptile densities by 20 and multiplying mammal densities by 10 (Figure 4.4B). This correction brought the density of *G. libratus* comfortably within the regression's confidence interval and confirmed that the small theropods were likely undersampled in the DPP fossil assemblage. To obtain conservative estimates of predator biomass relative to prey, corrected herbivore densities were obtained directly from their regression's mean while predator densities were obtained from the lower bound of their regression's confidence interval. Additionally, taxa that appear significantly rarer than very close relatives had their abundances corrected downwards after the initial correction. For instance, teeth of *Dromaeosaurus albertensis* are consistently less abundant than teeth of *Saurornitholestes langstoni* in vertebrate microfossil localities (Brinkman, unpublished data), so the former had a lower estimated density than the latter in this study despite the mass-density scaling law predicting a higher density due to its lesser body size. The abundances of other underrepresented terrestrial tetrapods in the Park's fossil skeleton assemblage (lizards and mammals) were also estimated using this method based on the appropriate dataset (Damuth 1987) to obtain a terrestrial trophic biomass pyramid for the lowermost DPF of DPP.

The abundances of juvenile megafauna were estimated using published survivorship curves. Juvenile hadrosaurid and ceratopsid mean body masses and biomass proportions were obtained from curves aggregated in Wyenberg-Henzler *et al*. (2021). Biomass proportions for tyrannosaurids were obtained from Schroeder *et al*. (2021) and estimated mean body masses at each age obtained from Erickson *et al*. (2004, corrected 2016). Together, these two datasets enabled the calculation of a mean body mass for the young juvenile and juvenile stages defined in the DPP trophic network (see previous section on trophic node and link selection). The age thresholds for each ontogenetic niche shift (young juvenile to juvenile and juvenile to subadult/adult) were obtained from Therrien *et al*. (2021). With these parameters, the mean estimated body mass of a mid-sized juvenile *Gorgosaurus libratus* was 307 kg (Figure 4.4D), which is almost identical to the 335 kg estimated for a real specimen which died at that life stage (Therrien *et al.* 2023). With these biomass corrections, the biomass density of the largest dinosaur predators and prey of DPP could be compared with extant datasets under different alternate parameters, whether time resolution, surface area, inclusion of juveniles or correction of underrepresented species' abundances, thus accounting for uncertainties that arise with the characterization of any extinct community.

For each version of the biomass density datasets, total prey biomass was compared to total predator biomass and the biomass of the apex predator that contributes most to that overall predator biomass. In this way, the contribution of *Gorgosaurus libratus* to the biomass of DPP predators could be compared with the contribution of *Panthera leo* in Africa and of *P. tigris* in India, while *Canis lupus* and *Varanus komodoensis* were the only predators included in their respective datasets. Caenagnathids were not included among the predator biomass due to recent research suggesting they were plant-dominated omnivores (Funston, pers. comm.).

4.3 Results

4.3.1 Food web visualization and analysis

Food webs for the Dinosaur Park Formation's Megaherbivore Assemblage Zone (MAZ) 1a are presented in Figure 4.5A-B. Its most inclusive version contains terrestrial and aquatic taxa and assumes very strict ontogenetic dietary shifts for tyrannosaurids (Figure 4.5A), while the other version only contains fully terrestrial taxa and accounts for cooperative hunting in tyrannosaurids, with adult prey preferences restricted to megaherbivores to show the lowest possible trophic level they could feasibly reach (Figure 4.5B). Food webs for the Serengeti and Komodo Island are presented in Figure 4.5C-D. Apex predator nodes are highlighted in each graph. Basic network statistics are presented in Table 4.2, including alternate versions of each DPP food web which exclude all aquatic and semiaquatic organisms. The communities representing each time interval of the lower DPF have slightly different numbers of nodes and links solely due to different megaherbivore dinosaur assemblage compositions. MAZ-1a has two ankylosaurids (*Euoplocephalus tutus* and *Dyoplosaurus acutosquameus*) and a single nodosaurid (*Edmontonia rugosidens*), while MAZ-1b has a single ankylosaurid (*E. tutus*) but two nodosaurids (*E. rugosidens* and *Panoplosaurus mirus*), as well as two more lambeosaurine hadrosaurids than MAZ-1a. These two faunal zones were selected in preference to the Oldman Formation or Lethbridge Coal Zone since they have the most complete fossil assemblages across each of the Belly River Group's stratigraphic units. Since DPP is no exception to the general rule that dinosaur communities exhibit a left-skewed body size distribution (Brown *et al.* 2013*b*; Benson 2018), the proportion of terrestrial megafauna above different size thresholds (45 and 1,000 kg) was compared between all food webs in this study (Table 4.2). The proportion of DPP megafauna >1,000 kg (which only includes tyrannosaurids and megaherbivores) is considerably higher than in the Serengeti, as was expected given its high diversity (Figure 4.3). Interestingly, the proportion of megafauna >45 kg is almost equal between DPP and the Serengeti, while it is (unsurprisingly) much lower in the Komodo community due to its insular location.

The frequency distribution of prey-averaged trophic levels (PATL) was compared between each figured food web (Figure 4.5; Table 4.2). It is worth noting here that mean PATL was almost equal in all networks, regardless of their very different taxonomic compositions, thus making their trophic level properties fairly comparable. The relatively high number of primary producer nodes (PATL = 1) in the DPP food webs is explained by the inclusion of bacteria for this community alone (see Material and methods). Despite this slight inconsistency with the extant food webs, we argue that they have little effect on dinosaur trophic levels because (1) they each have very few consumers, and (2) these are largely restricted to invertebrate clades. One of the more interesting patterns observed in PATL distribution lies in the high abundance of nodes at level 4 and above in DPP compared to the Serengeti in particular, even when aquatic and semiaquatic animals are excluded. The additional exclusion of all juvenile megafauna nodes from the DPP food webs would not significantly change this pattern since the level 4 bin would only lose between 2 and 4 juvenile tyrannosaurid nodes depending on the version.

4.3.2 Apex predator trophic levels through ontogeny

Ontogenetic shifts in trophic level were measured among the dominant apex predators of Dinosaur Provincial Park (*Gorgosaurus libratus*), of the Serengeti (*Panthera leo*), and of Komodo (*Varanus komodoensis*). To ensure that they were reasonably comparable, the mean chain lengths of likely trophic analogues were controlled between each food web in the ‘trophic species’ versions (Table 4.3; Figure 4.6A). Since there was no significant difference in mean chain length within any of these groups (e.g. spiders or scincid lizards), we can be confident at least that discrepancies observed between each community’s apex predator in this study are not simply explained by exceedingly long or short chains leading to trophic analogues at lower levels. Moreover, the mean chain lengths of some of the stagodontid marsupials and varanoid lizard species in the fully resolved DPP food web were compared to the mean chain lengths of their respective trophic species (Table 4.3; Figure 4.6A). As was expected, some of the species that compose these trophic groups had mean chain length differences exceeding 1 (particularly among varanoids), which added at least one step to DPP chains leading to apex predators, thus inflating their mean chain lengths compared to predators in extant food webs.

Since trophic level was entirely determined by prey composition regardless of its method of measurement, simplified networks were displayed to indicate different link distributions to key trophic guilds among apex predators depending on the nodes and links selected for each food web version (Figure 4.7A-C). In the main version of the DPP food webs, ontogenetic dietary shifts were hypothesized to be very pronounced, with relatively little dietary overlap between each stage (Figure 4.7A). This implied that young juveniles consumed all lizards, all semiaquatic amphibians, all non-avialan dinosaurs weighing less than 20 kg (except *Dromaeosaurus*), all mammals, and all birds weighing more than 1 kg. Mid-sized juveniles consumed larger prey on average, including all lizards, mammals and birds weighing more than 1 kg, all non-avian dinosaurs weighing less than 500 kg (including juvenile megaherbivores), and all semiaquatic tetrapods. In contrast, adults and subadults were proposed to consume all other non-avialan dinosaurs (including juvenile megaherbivores), as well as crocodilians, choristoderes and turtles weighing more than 5 kg. In the alternate version of the DPP food webs, only fully terrestrial taxa were retained, link selection for *G. libratus* accounted for pack hunting, and prey for adult *G. libratus* was restricted to megaherbivores (Figure 4.7A). Since pack hunting possibly involved cooperation between individuals at different ontogenetic stages to take down large prey, all megaherbivore nodes (whether adult or juvenile) were linked to nodes at all tyrannosaurid growth stages. Therefore, this model allowed far more dietary overlap between each life stage.

Since *P. leo* was split into three ontogenetic nodes in the Serengeti food web (partly to compare with *G. libratus*), each life stage had a slightly different trophic link composition (Figure 4.7B). First, links to young juveniles were restricted to prey species weighing between 20 kg and 1 tonne since social lions must hunt relatively large prey to sustain their prides (Bothma & Walker 1999; Owen-Smith & Mills 2008; Clements *et al.* 2014), and weaned (but still dependent) young juveniles feed on kills provided by mature members of those prides. Second, the main version of the Serengeti food web only accounted for pack hunting and thus constrained juvenile and adult lion trophic links to the same prey size range as the young juveniles. An alternate version accounted for solitary lifestyles in some juvenile and adult lions, which are particularly common in males (Packer & Pusey 1987): here, links to all small-bodied species were retained from the original dataset since solitary lions are more opportunistic hunters (de Visser *et al.* 2011; Kingdon 2015), and links to the largest prey species (and the spotted hyena *Crocuta crocuta*) were removed for juveniles.

The Komodo food web differed from the other two food webs since *V. komodoensis* seems to have an additional ontogenetic dietary shift relative to *G. libratus*, with individuals of intermediate body size (corresponding to a subadult growth stage) having a distinct prey composition from larger adults and smaller juveniles (Purwandana *et al.* 2016). Young juveniles (around hatchling stage) almost exclusively feed on insects and geckos; larger juveniles mostly feed on lizards, small rodents, and snakes; subadults feed on rodents, snakes, birds, and occasionally large ungulates; and adults feed almost exclusively on large ungulates with a minor bird component (Figure 4.7C). An alternate version of the Komodo food web included size-dependent cannibalistic links between each ontogenetic stage of *V. komodoensis* while retaining all other links.

These alternate trophic link distributions resulted in some variation in trophic position for each predator's ontogenetic stage in the 'trophic species' food web versions, whether prey-averaged trophic level (PATL, Figure 4.7D) or mean chain length (CL, Figure 4.7E). PATL barely changed for *P. leo*, remaining stable slightly between ~3.1 and ~3.3. This was expected considering the very high dietary overlap between adults and juveniles as a result of ontogenetic dietary expansion from the young juvenile stage instead of a genuine ontogenetic dietary shift. In the main version of the Serengeti food web, PATL increased even less for adults relative to young juveniles, the only difference being due to the occurrence of lion cubs in adults' diet as a product of infanticide. Interestingly, shifts in CL were far more pronounced between the young juvenile and juvenile lion stages. This is because weaned young juveniles were assigned a higher proportion of medium-to-large herbivores (which all have CL = 1 by definition) among their links, while independent juveniles and adults occasionally have solitary lifestyles, thus a higher proportion of small prey with longer CL due to omnivorous or carnivorous diets. The slightly higher CL of juvenile lions relative to adults is simply due to the inclusion of omnivorous mice among their trophic links in one version of the food web (Figure 4.7B). The CL and PATL trends observed for the lion illustrate well how the former measurement is far more sensitive than the latter to variation in trophic link distribution between distinct nodes of the same network.

In comparison, the true ontogenetic niche shifts proposed for *G. libratus* and observed in *V. komodoensis* were reflected in more consistent trophic level variation. In *V. komodoensis*, hatchlings had a PATL of 3.68, which increased to nearly 4.0 in juveniles and reached as much as ~4.08 in subadults, followed by a sharp decrease to slightly under 3.6 in adults (Table 4.4; Figure 4.7D). This trend is explained by the high proportion of herbivorous crickets in the hatchlings' diet, the increasing proportion of omnivores, carnivores and insectivores in the diets of the juveniles and subadults, and the high proportion of herbivorous ungulates in the adults' diet. When cannibalism among *V. komodoensis* was included, the trophic levels of every stage except the hatchlings slightly increased to account for additional secondary consumers among trophic links, but it also resulted in lower overall ontogenetic variation in PATL. Considering that the adult *V. komodoensis* got three more links, this was the node that had the highest increase in PATL (by around 0.4) due to cannibalism. While PATL rose and then fell through ontogeny in *V. komodoensis*, CL increased fairly constantly, from ~4.5 in hatchlings to more than 7 in adults, and nearly 9 in cannibalistic adults (Table 4.4; Figure 4.7E). This trend is explained by the relatively high number of short chains for hatchlings, which are usually composed of detritus or carrion consumed by an insect and eventually consumed by a hatchling. This was in stark contrast with the adults, which have a narrower dietary breadth than juveniles and subadults, meaning that each prey occupies a higher proportion of their total dietary breadth. One of these resources is the wild boar *Sus scrofa*, whose omnivorous diet includes some snakes and even *V. komodoensis* hatchlings (Figure 4.7C). This resulted in a much higher CL for this species than for obligate herbivores hunted by large dragons such as the Rusa deer *Cervus timorensis* and the water buffalo *Bubalis bubalis* and was the main cause of the relatively high CL observed in adult and subadult *V. komodoensis*. CL increased slightly for each of the three larger size categories in the cannibalistic version of the Komodo food web due to their predation on one to three additional secondary consumer nodes.

In *Gorgosaurus libratus*, PATL generally decreased constantly through ontogeny: using the DPF 'trophic species' food web (without pack hunting) as an example, it decreased from ~4.1 in young juveniles to ~3.9 in juveniles, until it reached ~3.7 in adults (Table 4.4; Figure 4.7D). This trend is explained by the higher proportion of herbivores at low trophic levels in the adults' link distribution, while both juvenile stages have largely omnivorous and carnivorous mammals in their diet, and the smallest juveniles' diet is further supplemented by carnivorous or insectivorous lizards located at even higher trophic levels. In the pack hunting version, the inclusion of megaherbivorous dinosaurs as prey for all ontogenetic stages led to decreases of 0.25-0.35 for each juvenile PATL, and the more exclusive link distribution for adults resulted in a sharper decrease in PATL worth nearly an entire trophic level, which became even lower than the lowest PATL recovered for *P. leo* in the Serengeti (Table 4.4). Additionally, the effect of the exclusion of juvenile megaherbivores from prey on tyrannosaur trophic level was investigated to obtain trophic level measurements consistent with food webs that do not track trophic properties through ontogeny. As expected, the version of the MAZ-1a food web that lacked any juveniles but still retained aquatic taxa produced the highest possible trophic levels for juveniles and adults (PATL = ~4.15 and ~3.8 respectively). Trends in PATL obtained from the fully resolved food web versions were also plotted through ontogeny yet were not significantly different from trends observed in the 'trophic species' food webs (Figure 4.6B). It is still worth noting that young juvenile Komodo dragons always had a lower PATL in these versions than young juvenile *G. libratus*, and that adult *G. libratus* reached a higher PATL than the adult Komodo dragon even when cannibalism is accounted for in the latter. Elsewhere, the higher number of megaherbivores in the DPF MAZ-1b food web (compared to the DPF MAZ-1a food web) resulted in consistently lower, yet insignificant, PATL values in the former. Interestingly, it must be noted that most of the PATL variation observed in *G. libratus* and *V. komodoensis* occurred almost one trophic level higher than in *P. leo*. This is best explained by the fact that the former had a greater proportion of omnivorous and carnivorous prey than the latter, with the marked exception of the DPP food web versions in which tyrannosaurids were megaherbivore specialists.

The measurement of CL through ontogeny produced a very different pattern for *G. libratus* for the pack hunting version of the DPP food web compared to extant predators. While CL gradually increased for *P. leo* and *V. komodoensis*, it faintly increased for *G. libratus* between young juvenile and juvenile stages (from 7.43 to 8.325) before significantly decreasing for adults ($CL = 2.15 \pm \sigma = 0.395$) (Table 4.4; Figure 4.7E). This was due to the fact that trophic links for adult *G. libratus* were restricted to megaherbivores (and their respective juveniles), while juvenile *G. libratus* had several trophic links leading to omnivores and carnivores (such as small theropods and mammals) in contrast. Obligate herbivores almost solely consumed resources at PATL = 1, thus the chains leading to adult *G. libratus* were far shorter on average than the chains leading to earlier ontogenetic stages of that species. When adult *G. libratus* were not specialist megaherbivore consumers, the mean chain length ontogenetic pattern of that species mirrored that of the extant predators, albeit at the top of chains which were 2-3 steps longer on average. If mean chain lengths of trophic analogues had not been controlled between each 'trophic species' food web version, juvenile tyrannosaurids' mean chain length would have been as high as 13. However, that result was best explained by an excessive number of steps among arthropod nodes compared to the extant food webs, and thus was more likely the effect of inconsistent trophic link assignments between each food web's original version.

4.3.3 Predator-prey biomass densities

Dinosaur biomass densities estimated for Dinosaur Provincial Park were compared to more recent communities under alternate combinations of spatial area, temporal resolution and taxon abundance (Figures 4.8A, 4.9A). When all DPP predators were included in biomass estimates, predator biomass densities usually fell within the range of variation observed on Komodo Island, whose sole native apex predator is *Varanus komodoensis*. All extant mammal-dominated localities had predator biomasses around one order of magnitude lower than those of DPP samples with similar prey biomasses. The only DPP samples that had a higher predator biomass than any extant locality pooled fossils from all stratigraphic intervals of the Belly River Group for a relatively small surface area of 120 km^2 (Figures 4.8A, 4.9A, top right corner). The corrections of small dinosaur abundances (including juvenile megafauna) did not significantly affect the position of the DPP samples on a log scale due to the relatively small body size of each of these groups. For instance, the DPF MAZ-1a sample had uncorrected predator and prey biomasses of ~254 and ~2,865 kg/km^2 respectively, for a predator/prey biomass ratio of ~0.090. With the addition of juvenile megafauna, predator and prey biomass increased to ~300 and ~3,430 kg/km^2 respectively, for a predator/prey biomass ratio of ~0.088. After correcting for small-bodied dinosaur abundances and counting caenagnathids and troodontids as predators (as in the uncorrected versions), predator and prey biomass further increased to ~520 and ~4,834 kg/km^2 respectively, for a predator/prey biomass ratio of ~0.11. When caenagnathids and troodontids counted as prey instead, predator biomass decreased to ~335 kg/km^2 and prey biomass increased to more than 5,000 kg/km^2, for a ratio of 0.067. In comparison, Komodo predator/prey biomass ratios varied between 0.01 and ~0.4 across all studied localities, and all DPP biomass ratios were included within this range. In contrast, extant large mammal communities had ratios varying between 0.002 and 0.025, almost within an entire order of magnitude below the variation observed on Komodo.

Biomass pyramids for the terrestrial animals of DPF MAZ-1a, MAZ-1b and MAZ-2 were produced by combining estimated biomass (for the smaller 120 km^2 area) with trophic levels obtained from the food web (Figures 4.8B, 4.9B). These versions included biomasses corrected with Damuth's mass-density scaling law for small-bodied taxa which are underrepresented in the Park's fossil record, such as small ornithischians, small theropods and mammals. Birds were not included in the total paravian biomass because a mass-density regression was unavailable for this particularly derived clade (Damuth 1987). Juvenile megafauna biomass was not included in this version either. Overall, the biomass pyramid of Dinosaur Provincial Park is markedly bottom-heavy, as is expected for modern terrestrial communities (Trebilco *et al.* 2013; Perkins *et al.* 2022). However, the skew towards lower trophic levels would not be as pronounced if semiaquatic predators such as turtles, champsosaurs and crocodilians were included, given that they likely consumed some terrestrial prey.

When only the most important contributor to predator biomass was included in each community, the pattern remained the same: even if *Gorgosaurus libratus* was the only predator included for DPP, its biomass density remained far more comparable to that of *Varanus komodoensis* than to that of *Panthera leo* or *P. tigris* (Figure 4.10A). A closer examination of the relative biomass distribution of each predator in the most diverse predator communities (excluding juveniles tyrannosaurids) provided additional information on their structure. When small predatory dinosaur abundances were not corrected in the DPP MAZ-1a sample, *G. libratus* occupied almost 80% of predator biomass, with the rarer *Daspletosaurus* sp. occupying another 19% (Figure 4.10B). This overwhelming tyrannosaurid dominance is much more reminiscent of the predator distribution of Komodo Island than of that of mammal-dominated communities. When small predatory dinosaur abundances were corrected, the relative biomass of *G. libratus* fell to ~60%, which remained much higher than the mean biomass density observed in the African savanna for *P. leo* (Figure 4.10C). Overall, the predator biomass of Dinosaur Provincial Park's dinosaur community displayed a curious pattern where its dinosaur predator species richness is comparable to that of the most complex remaining extant land mammal communities, but where its predator biomass distribution is somehow more comparable to that of *Varanus komodoensis* in the much more species-poor Komodo Island community.

4.4 Discussion

This study aimed to assess the ecological impact of tyrannosaurids on their community, and to compare it with possible extant analogues, using *Gorgosaurus libratus* in the Dinosaur Provincial Park (DPP) biota as a model system. This was achieved by independently measuring trophic level through ontogeny and predator-prey biomass density ratios, two ecological properties on which hypotheses could be tested relatively rigorously considering available fossil evidence. It resulted in the first ecological networks ever attempted at a high taxonomic resolution for a non-avialan dinosaur community and for Komodo Island. Moreover, these networks are now among the most complex ever modeled for any terrestrial community while accounting for dietary variation through ontogeny. Combined with biomass density estimates, they now suggest that tyrannosaurids had a trophic impact more similar to that of the Komodo dragon *Varanus komodoensis* than to that of a large carnivoran (in this case the lion *Panthera leo*) among extant terrestrial apex predators.

First, the food webs created for DPP demonstrate that ontogenetic dietary shifts proposed for tyrannosaurids are translated into significant ontogenetic shifts in trophic position, whether as prey-averaged trophic level or mean chain length, in a pattern that is generally more similar to the Komodo dragon than to the lion. However, the magnitude of this shift in trophic position is not exactly identical to that of the former: while the PATL of *V. komodoensis* increases then decreases through ontogeny, it appears to gradually decrease in *G. libratus*, with young juveniles of the latter potentially reaching a level unmatched at any dragon ontogenetic stage. The one scenario where *G. libratus* has a completely different shift in mean chain length from the two extant predators is explained by an extremely specialized diet focused on large herbivores. The latter metric in particular suggests that the paths through which energy was transferred to large tyrannosaurids was more variable throughout their growth than for any potentially analogous extant apex predator. Second, biomass densities estimated for predatory dinosaurs in DPP suggest that they were on par with those of the Komodo dragon relative to their prey, even when *G. libratus* alone was accounted for. This study also produced the first biomass pyramid obtained from trophic level measurements for any palaeocommunity. At first glance, the pyramid produced for the best-known time interval of the Dinosaur Park Formation is heavily skewed towards primary consumers and does not suggest a markedly different biomass distribution between predators and prey compared with extant carnivoran-dominated communities. However, closer examination reveals that its predator-prey biomass density ratio was at least one order of magnitude higher than typical mammalian predator-prey biomass density ratios.

We acknowledge that taphonomic biases inherent to the fossil record impose clear limitations on both of the major analyses performed in this study. Concerning the food webs, the relative lack of direct evidence of trophic interactions in the DPP fossil record caused a near-total reliance on feasible (instead of realized) interactions to create links in the network. This means that the complexity of the DPP food webs is likely overestimated compared to the extant food webs. Furthermore, the fossil assemblage of the DPP community has a clear taphonomic size bias in favor of large-bodied terrestrial vertebrate remains (Brown *et al.* 2013*b*), which means that the number of nodes (and thus links) involving smaller vertebrates, invertebrates and plants was almost certainly underestimated. It is thus possible that these two limitations together altered the distribution of trophic links in the DPP food webs. Nevertheless, we maintain that the DPP, Komodo and Serengeti food webs remain fairly comparable for trophic level measurements since we have ensured control on mean chain lengths between each of them (see Material and methods). It can also be argued that some circular reasoning was involved in our hypotheses since trophic levels and food chain lengths for species at different growth stages can be reasonably predicted from their feasible trophic links. However, we dispute this position because one cannot always assume that a different combination of resources at each of these stages will always result in clear shifts in trophic position. Trophic omnivory has long been known to cause long chains in food webs (Williams & Martinez 2004; Banker *et al.* 2022), but mean chain length remains particularly difficult to predict compared to other node properties due to the necessity to compute all possible paths leading to a consumer, especially in highly resolved networks such as those presented in this study.

We also show that the biomass densities estimated for the Park's most commonly preserved dinosaur species within a well-constrained stratigraphic interval are still realistic compared to analogous data on extant large predators and prey, despite the reliance on a fossil assemblage affected by a taphonomic bias at a low spatiotemporal resolution relative to extant communities. Therefore, it is possible that the lowermost 10 m of the Dinosaur Park Formation's fossil assemblage are at an equilibrium between skeleton preservation rate and stratigraphic resolution, and thus can be deemed sufficiently representative of standing crops. Lastly, we acknowledge that the depauperate state of extant ecosystems may have slightly skewed some predator biomass density estimates, especially for the large carnivorans, thus making their comparison with a dinosaur community even more problematic. To have a more pristine mammal-dominated community in the study, we thus considered estimating biomass densities for the Rancho La Brea fauna of southern California, one of the world's best known Pleistocene localities (Spencer *et al.* 2003; DeSantis *et al.* 2019; O'Keefe *et al.* 2023). However, due to the well documented overrepresentation of predators in its fossil assemblage

(McHorse *et al.* 2012), and the lack of any reliable density estimates caused by the preservation of carcasses in asphalt deposits, we elected not to retain this analysis in the final results.

4.4.1 Evaluating the accuracy of the Dinosaur Provincial Park community reconstruction

The impact of network node and link selection on trophic levels. Considering that the creation of any food web at a high taxonomical resolution necessitates far more time and effort than the creation of a simplified one, it is deemed necessary to justify the decision to pursue the former approach for this study. At least one of the reasons proposed earlier was vindicated here through the detection of trophic interactions between taxa that likely occupied a very similar ecospace. For instance, if all lizard species known from DPP had been collapsed into a single 'trophic species' for all PATL measurements, several feasible links (such as *Palaeosaniwa* preying on small teiids) would not have been accounted for. Consequently, the relatively high variability in lizard trophic levels (from ~3.45 in the teiid *Glyptogenys ornata* to ~4.2 in *Palaeosaniwa*) would not have been appreciated, which in turn would have affected all of their predators' trophic levels (including juvenile tyrannosaurids) and thus skewed our perception of the average number of nodes in the community's food chains.

However, it must be acknowledged that the DPP food webs may not be entirely comparable to the Serengeti and Komodo food webs. First, the DPP food webs include all vertebrate taxa known from this locality, while that is not the case of the extant datasets. For instance, the small mammals, reptiles, amphibians and birds of the Serengeti food web remain largely collapsed into trophic species nodes (de Visser *et al.* 2011: appendix S1). Second, the extinct state of the DPP community, combined with a relative lack of direct evidence for trophic interactions among its fossils, necessitates a near total reliance on feasible (as opposed to realized) interactions to assemble its food web. Even when only a single megaherbivore assemblage zone is included in each version of the DPP food web, this means that its complexity is likely overestimated relative to the extant food webs, especially between its primary and secondary consumers. Conversely, the most evident limitation of the current node and link selection lies in the low taxonomic resolution of the primary producers (especially plants) relative to their consumers. Together, the underestimation of link frequency from producers to consumers combined with the overestimation of link frequency between primary and secondary consumers could pull the trophic levels of several omnivores and carnivores away from their true position. For instance, if the six smallest lizards (mass < 0.3 kg) were excluded from the inferred diets of young juvenile tyrannosaurids, the latter's PATL would decrease to such an extent that it would become lower than that of mid-sized juveniles and nearly equal to that of Komodo dragon hatchlings due to the relatively high PATLs of those largely insectivorous predators. This would make ontogenetic PATL shifts in tyrannosaurids nearly identical to those observed in Komodo dragons. What is certain is that the PATL of several omnivores, such as troodontids and caenagnathids in DPP (Funston & Currie 2014; Lamanna *et al.* 2014; Cullen & Cousens 2023), would be much lower if plants were resolved to the same level as animals: this is because those omnivores would have a greater proportion of links emerging from the lowest trophic level (to calculate their PATL), as well as a greater proportion of the shortest possible food chains (to calculate their mean chain length). Likewise, all wild pigs in the fully resolved versions of the extant food webs have PATLs closer to 3 than to 2: ~2.6 in the warthog *Phacochoerus aethiopicus*, ~2.7 in the bushpig *Potamochoerus porcus*, and ~3.2 in the wild boar *Sus scrofa*, the latter being driven by predation on snakes in Komodo (Auffenberg 1981). If the plants consumed by these omnivores were all resolved at the species level, their PATLs would fall significantly. Considering that omnivorous theropods were likely highly diverse in DPP and that they were certainly prey for large juvenile tyrannosaurids (Therrien *et al.* 2023), this alternate node and link selection would result in a far less pronounced trophic level decrease between juvenile and adult/subadult tyrannosaurid stages. Therefore, these caveats can affect our conclusions on the similarity of the ecological network node properties of tyrannosaurids relative to either of the two major types of extant terrestrial apex predator.

Nonetheless, there is reason to believe that the caveats outlined above have few negative effects on the accuracy of network and especially individual node property measurements. Concerning node selection, it could be argued that the underrepresentation of small-bodied animals among the selected nodes of the Serengeti and Komodo food webs would actually make their body size distribution more comparable to that of the DPP fossil assemblage considering the taphonomic size bias detected in the latter (Brown *et al.* 2013*b*). However, this hypothesis has yet to be tested statistically and is deemed to be beyond the scope of this paper. Furthermore, trait-based models of pairwise trophic interactions trained on empirical food webs have been shown to predict individual trophic interactions fairly accurately, even in biotas with highly contrasting environmental conditions (Caron *et al.* 2024). This suggests that more derived individual node metrics, such as trophic levels, can be more transferable and comparable between disparate communities than network-wide metrics such as connectance and modularity when rules based on traits are applied consistently to an extinct food web, as was achieved here. Ultimately, the most convincing way to make the DPP networks more comparable to the extant networks would be to adopt a ‘metanetwork’ approach (Roopnarine *et al.* 2007; Mitchell *et al.* 2012; Roopnarine & Dineen 2018; Huang *et al.* 2023): individual species would be assigned to guilds (equivalent to trophic species) and links assigned based on species’ traits to form a ‘metanetwork’ where each node represents a guild, from which a range of feasible species-level networks would be stochastically generated. In this way, the exact same node and link selection rules would apply to each food web, whether it represents an extant or extinct community.

The lack of diet fractions (i.e. the proportion of each resource in a given consumer’s diet) as an indicator of the relative strength of each trophic link (e.g. Saigo *et al.* 2015) is another important limitation of this study. These are available for extant species whose behavioural ecology has been most thoroughly investigated in the field: for example, kill counts for large African carnivores reveal a narrow body size range of preferred prey within a broader diet range (Sinclair *et al.* 2003; Hayward & Kerley 2005; Hayward 2006; Owen-Smith & Mills 2008), and Komodo dragons based on identification of prey remains in fecal pellets (Auffenberg 1981). Even DPP taxa with close extant relatives such as crocodilians, frogs, fishes and turtles could have realistic linkage strengths estimated from relative prey abundances in stomach contents (Stewart & Sandison 1972; Scott & Crossman 1973; Williams & Christiansen 1981; Magnusson *et al.* 1987; Aresco & Gunzburger 2007; Saalfeld *et al.* 2011). However, their diet fractions would always have higher uncertainties than those obtained for extant relatives because of the need to account for totally extinct taxa (e.g. multituberculate mammals or scapherpetontid salamanders) among their feasible prey composition. Understandably, such detailed information may never be available at a low taxonomic level for non-avian dinosaurs, with the nearest equivalent consisting of stable isotope ratios extracted from teeth as coarse indicators of trophic level (Fricke & Pearson 2008; Cullen *et al.* 2020; Cullen & Cousens 2023).

Consequently, the lack of comparable data for almost every extinct consumer (and several extant ones) forced the assumption that each consumer obtained an equal quantity of energy from each of its resources in this study. It follows that this assumption has likely reduced the accuracy of several measured trophic levels in every food web. For example, the Hawksbill sea turtle *Eretmochelys imbricata* has the same weight as deer or wild boar in Komodo dragon trophic levels, yet the former constitutes a minor fraction of the predator's diet compared to the latter (Auffenberg 1981). Considering that the sea turtle has a PATL of ~3.33 (which is higher than any ungulate in the community), it led to an overestimated PATL for the Komodo dragon. In any case, this slight discrepancy would not change the overall pattern of ontogenetic trophic level shift in this species.

While an index of relative link strength based on diet fraction would have great potential to detect dietary niche partitioning through ontogeny to an even greater extent *within* a species, it could also be applied to reflect patterns of dietary niche partitioning *between* morphologically similar taxa. For instance, two sympatric softshell turtle species have the same prey composition in terms of taxic diversity (at varying taxonomic levels), yet that composition is very different in terms of abundance (Williams & Christiansen 1981). This pattern is explained by slight spatial segregation between the two species within the same river systems and could not have been detected from their morphology alone.

Because such detailed ecological characterization is understandably unavailable from taxa solely represented by fossils (notably dinosaurs in this study), several morphologically similar species in the DPP food web have identical trophic link distributions which only coarsely reflect dietary niche partitioning at the family level among hadrosaurids, ceratopsids, nodosaurids and ankylosaurids (Mallon & Anderson 2013, 2014*a, b*; Mallon *et al.* 2013; Mallon 2019). However, studies of potentially analogous herbivore assemblages such as those of the African savanna reveal far more specialized food preferences for several species (Grange & Duncan 2006; Pansu *et al.* 2019). In this respect, the creation of distinct nodes for leaves, shoots, and seeds/fruit for angiosperms (instead of a single node) in the DPP food web constitutes a partial attempt to differentiate herbivore trophic link distributions, until an updated version with every angiosperm resolved at the family level at least is completed (Demers-Potvin & Larsson in prep). Near the top of the DPP network's food chains, the dromaeosaurids *Dromaeosaurus* and *Saurornitholestes* may have had slightly different prey preferences due to their diverging estimated body masses (15 kg for the former and nearly 22 kg for the latter). However, the remaining ecomorphological traits available from their (admittedly rare) fossil remains are so similar that they could not reasonably justify distinctive trophic link distributions in this current version of the food web. The same situation prevails at the very top between the tyrannosaurids *Gorgosaurus* and *Daspletosaurus*, which arguably display even greater overlap in maximum body size, feeding apparatus and postcranial morphology (Farlow & Pianka 2002). The (likely) very high dietary niche overlap speculated for *Gorgosaurus* and *Daspletosaurus* is particularly surprising when compared to extant terrestrial predator communities, where it is generally at its lowest among the largest constituent species (Farlow & Pianka 2002). This led the latter authors to speculate that these two tyrannosaurids had slightly different habitat preferences in the Laramidian coastal plain, and/or that DPP was located around the northern range limit of *Daspletosaurus* (due to its rarity relative to *Gorgosaurus*), to explain their coexistence with minimal interspecific competition. This is yet another case in the DPP community where future palaeoecological research could eventually justify the inference of diet fractions (and thus slightly different trophic positions) between morphologically similar species to refine their trophic positions within a food web.

The accuracy of biomass density estimates between predators and prey. The other major analysis conducted in this study to evaluate the impact of tyrannosaurids on their community consisted of biomass density estimates between predators and prey in Dinosaur Provincial Park. However, its results are arguably more problematic to interpret than the results derived from the ecological networks such as food webs because the former require accurate fossil abundance data, while the latter only require the occurrence of at least one (or a few) well preserved specimens to infer trophic links regardless of their abundance. If the food web of the Dinosaur Park Formation's MAZ-1a is taken as an example, we are reasonably certain that its dinosaur species richness (which affects the number of nodes and links) is not overestimated because it only includes one megaherbivore assemblage zone. However, it is possible that the abundance of each of these species varied through that same stratigraphic interval without leaving any fossil evidence. Therefore, the biomass density analysis is far more sensitive to the taphonomic biases and variable time resolution that affect the fidelity of the composition of any fossil assemblage relative to its original community (Behrensmeyer & Hook 1992; Kidwell & Flessa 1995; Behrensmeyer *et al.* 2000).

In this regard, the first major limitation that can be addressed for DPP biomass density estimates lies in their relatively low spatiotemporal resolution, where (a) the surface area used to calculate these densities is open for debate, and (b) the densities estimated for specific stratigraphic intervals (even the lowermost DPF) are averages of several successive standing populations distributed over relatively short geological time intervals. While several of the biomass counts sampled from African and Indian localities are means calculated from different censuses, they are separated by a few decades at the most (Hatton *et al.* 2015). In contrast, the individual skeleton quarries and bonebeds of DPP are separated by durations that were likely on the order of 10^5-10^6 years based on estimated rock accumulation rates

(Eberth 2005; Eberth *et al.* 2023). Even the lowest ~30 m of the Dinosaur Park Formation, which correspond to DPF MAZ-1, could represent as much as ~700,000 years (Mallon *et al.* 2012; Eberth *et al.* 2023). This means that the lowermost 10 m of the DPF, which have historically yielded the highest abundance of fossil material, could represent (at most) 200-250 ka. That said, the near totality of DPP's fossils were preserved in fluvial and deltaic environments (Wood *et al.* 1988; Wood 1989; Durkin *et al.* 2020), which typically have a time resolution varying between 10^0 – 10^4 years (for floodplains and channel fills) and 10^3 – 10^5 years (for channel lags) (Behrensmeyer 1982; Behrensmeyer & Hook 1992). This means that some palaeochannels have a depth equal to the stratigraphic height of the entire lowermost DPF (Brown 2013: Ch. 4), yet likely represent only a few tens of thousands of years of rock accumulation at the most instead of a temporal order of magnitude ten times higher. Therefore, it is possible that the actual sedimentary horizons that form the Park's stratigraphic succession were collectively deposited over far shorter time intervals than the time ranges bracketed by each of its radioisotopically dated bentonites (see Ramezani *et al.* 2022; Eberth *et al.* 2023). This would imply that the average densities obtained from the most constrained DPF stratigraphic intervals represent durations that are relatively comparable to an ecological time scale available from modern ecosystems. However, this hypothesis must still be tested through a more detailed survey of the entire area of fossil-bearing badlands exposed in the Park (see Chapter 3). In terms of spatial fidelity, we concede that we did not attempt to make a more elaborate analysis based on estimates of total dinosaur fossil abundances per unit volume, which accounted for skeletons lost to erosion, as well as skeletons remaining in unexposed beds of the Belly River Group (Henderson & Tanke 2010).

It is also worth reiterating that the sample of fossil specimens included in biomass estimates for any chosen stratigraphic interval is only a fraction of the total known fossil abundance of any given taxon in DPP. While associated skeletons were included (whether articulated or disarticulated), other taphonomic modes such as bonebeds and vertebrate microfossil localities were excluded due to their distinct taphonomic histories combined with uncertainties about the true number of individuals they represent (Dodson 1983; Eberth & Currie 2005; Eberth & Getty 2005). Additionally, the fossil skeleton densities calculated for constrained stratigraphic intervals (DPF MAZ-1a and DPF MAZ-2) strictly include the specimens whose stratigraphic height could be measured, i.e. those whose quarry GPS coordinates were available. This means that around 100 specimens lacking precise and accurate locality data could not be included in these samples, and thus that skeletal densities for each of these intervals should be higher by around 1/3 (Tanke 2005; Henderson & Tanke 2010). At least, the sample that included the skeletons known from all of the Park's horizons (whether from known or lost quarries) did not have a markedly different predator/prey biomass ratio (~0.09) than any of the more stratigraphically constrained samples (MAZ-1a: ~0.090; MAZ-1b: ~0.1; MAZ-2: ~0.074) and remained within the orders of magnitude of predator and prey biomass densities observed in the Komodo community.

Indeed, the large dinosaur densities obtained solely from the abundance of skeletons with precise and accurate locality data remained realistic compared to extant animal densities, regardless of the chosen DPP time interval. Moreover, the fact that the DPF's MAZ-1a (which seems particularly rich in fossils) displays a very high similarity between the observed skeletal densities of the Park's most abundant large dinosaur species to densities predicted by Damuth's law suggests that the fossilization and collection rates of its dinosaur megafauna skeleton assemblage is at an equilibrium with its (presently available) time resolution. Even if each of its dinosaur species' abundances were increased by around 1/3 to account for lost quarry localities, they would remain unlikely to fall outside the range of density variation observed in extant mammals (Damuth 1987). Considering that herbivorous dinosaurs (especially ornithischians) likely had a slower metabolic rate than mammals of equal size (Grady *et al.* 2014), yet that no attempt was made to correct Damuth's mammalian herbivore densities to compare them with dinosaurs, such corrected densities might actually be more realistic since they would reflect dinosaurs' hypothetically lower energy requirements. This caveat aside, the flaws of Damuth's law become more apparent when it comes to predicting the densities of DPP's less well-preserved taxa. Since body mass is the only variable that is accounted for in this model, it ignores other ecological variables that determine population densities, not least interactions between some of these species such as competition. This may not be so problematic when the dataset is used to estimate the abundance of a single species' population, as was recently done with *Tyrannosaurus rex* (Marshall *et al.* 2021), or of species that never co-occurred in the same habitat. However, as the food web in the present study suggests, several taxa in DPP likely had considerable ecospace overlap in terms of diet or habitat use, thus their densities ideally should not be estimated independently from each other. This limitation resulted in very homogeneous densities for DPP species of similar metabolic rate and body size (e.g. small mammals and lizards), which is completely unrealistic given the prevalence of competitive exclusion in extant communities, notably the African savanna (Hatton *et al.* 2015; Périquet *et al.* 2015). That said, the inclusion of competition in density predictions is unlikely to alter total densities significantly from our current results, and the corrections of small-bodied species' biomasses in the DPP community did not markedly increase total biomass in any case.

Considering the high predator-prey biomass ratio in the DPP community relative to extant communities with large mammalian apex predators, it remains possible that predator densities were overestimated in DPP. On one hand, the fact that they fall within the Komodo predator-prey biomass range suggests that they are not wildly overestimated, at least compared to some extant communities. On the other hand, the fact that the DPP ecosystem could support a much higher predator biomass relative to, say, the African savanna (despite having a similar relative biomass density distribution among its predator species) deserves further investigation. First, it could be argued that corrected densities for juvenile tyrannosaurids and small-bodied predators (dromaeosaurids, troodontids and close relatives) were overestimated, even considering that the latter were corrected to the lower bound of the predator mass-density regression line's confidence interval while small-bodied herbivore densities were raised up to the regression line itself. For instance, the corrected densities of dromaeosaurids and troodontids combined for the Dinosaur Park Formation's Megaherbivore Assemblage Zone 1a were just above 3.3 km^{-2} while those of tyrannosaurids (including juveniles) only reached 0.33 km^{-2}. This produces a density ratio of nearly 10 between small and large predators, which is much higher than the ratios of 2-3 estimated for African savanna communities such as the Serengeti (Sinclair *et al.* 2003). However, even when these groups were excluded from biomass density counts, predator densities based on adult tyrannosaurids alone remained very high. For example, *Gorgosaurus* alone (without juveniles) had a biomass density of nearly 12 kg/km^2 in DPF MAZ-1a (for a 1,950 km^2 area), which is more than twice the entire large predator biomass of the African savanna community with the most similar prey biomass density (5 kg/km^2). Therefore, this pattern suggests that the dinosaur *megafauna* biomass estimates are the key factors to examine here: to show that predator biomasses are overestimated in the Park, it should be demonstrated that tyrannosaurids had a higher fossilization, discovery, and/or collection probability than megaherbivores. So far, this evidence is conspicuously lacking (Béland & Russell 1978; Currie & Russell 2005), and instead the hollow structure of tyrannosaurid bones (as theropods) should make them less likely to fossilize than large ornithischian bones. A collection bias can be confidently ruled out because the skeleton counts include specimens that were found but not collected, since hadrosaurid abundances would be underestimated otherwise.

Alternatively, it is possible that ankylosaurs are underrepresented in the Park's skeletal assemblage (instead of tyrannosaurids being overrepresented). Indeed, ankylosaur skeletons are rare in the Park's fossil assemblage compared to hadrosaurids and ceratopsians (Béland & Russell 1978; Arbour & Currie 2013), and there is little reason to believe that their elements (excluding perhaps osteoderms) would be more prone to pre-burial reworking. Since ankylosaurs appear to have had physiological adaptations to cool hot dry air in their nasal cavity (Bourke *et al.* 2018), they have been proposed to prefer drier inland habitats than other megaherbivores. This might imply that ankylosaurs had genuinely low population sizes in the paralic to coastal sections of the Laramidian floodplain, especially considering the consistent lack of evidence for gregarious behaviour from monodominant bonebeds in this clade compared to hadrosaurids and ceratopsians (Ryan *et al.* 2001; Eberth & Getty

2005; Eberth *et al.* 2015; Bell *et al.* 2018). Alternatively, they might have had more local habitat preferences along that floodplain: if they did not venture near fresh water as often as other dinosaurs, their fossilization potential in point bar deposits, which are the ideal setting for articulated skeleton preservation in the Park, would be reduced (Dodson 1971; Wood *et al.* 1988). However, this hypothesis might be extremely difficult to test with our current knowledge. In any case, ankylosaurs were likely very infrequent prey even for the largest tyrannosaurids due to their imposing natural armour and (in the case of ankylosaurids) weaponized tails (Arbour & Currie 2015; Arbour & Zanno 2018). Therefore, it could be argued that they should not even be included among the definite dinosaur prey biomass densities if energy flux between trophic levels were shown to be distributed more accurately. What is more certain is that similar reasons can be invoked to exclude the very largest adult megaherbivores (i.e. elephants, giraffes and rhinoceroses) from African savanna prey biomass densities, as was done previously (Hatton *et al.* 2015), since individuals that reach full size lack any natural enemies except in a few localities (John Power & Shem Compion 2009).

4.4.2 Palaeoecological evidence suggests tyrannosaurids were more analogous to dragons than to lions

The food webs and biomass distributions presented in this study contribute to a longstanding debate on non-avialan dinosaur (particularly tyrannosaurid) palaeobiology. Considering available palaeontological evidence, one of the strongest cases for ontogenetic niche shifts in extinct apex predators has been made for tyrannosaurids from the latest Cretaceous of Asia and North America. First, some of the species with the most extensive skeletal records display clear evidence of allometric growth through their ontogeny, suggesting significant shifts in bite force, cursorial ability, and thus likely prey composition (Dececchi *et al.* 2020; Therrien *et al.* 2021; Voris *et al.* 2022). Second, some of these hypotheses are confirmed by rare direct evidence of predation by large juvenile tyrannosaurs on small-bodied dinosaurs as stomach contents (Therrien *et al.* 2023), which is particularly convenient for the present study considering that this evidence comes from Dinosaur Provincial Park. Third, the theropod body size distribution of every well-known biota dominated by tyrannosaurids during the latest Cretaceous is highly unusual compared to that of modern carnivoran mammals and even to that of more ancient dinosaur communities (Farlow & Pianka 2002; Schroeder *et al.* 2021): indeed, the former consistently lack any predator weighing between 100 and 1,000 kg while the latter have far more continuous body size distributions, yet juvenile tyrannosaurids would have occupied this body size range (therefore a likely distinct ecological niche) instead of ceratosaurs and abelisaurs which were part of more ancient theropod communities. Therefore, evidence of niche assimilation, ontogenetic niche shifts and high growth rates in tyrannosaurids already suggested that Komodo dragons were their nearest analogues among modern terrestrial apex predators.

In contrast, evidence of bipedality, pneumaticity for an advanced respiratory system involving air sacs, and feathery integument suggests that tyrannosaurids, along with other bipedal dinosaurs, had high metabolic requirements more comparable to birds and mammals than to other reptiles, with an endothermic, or at least mesothermic, body temperature control strategy (Xu *et al.* 2004, 2012; Sereno *et al.* 2008; Grady *et al.* 2014). Additionally, the close phylogenetic relationship of non-avian theropods to birds, along with evidence from nesting sites, suggests a certain degree of parental care, which would imply that the diets of juveniles (at least hatchlings) were not very different from those of adults (Norell *et al.* 1995; Varricchio *et al.* 2008). One last line of evidence specifically concerning tyrannosaurids consists of bonebeds and trackways containing individuals of different sizes and (likely) growth stages, which can be interpreted as evidence of cooperative hunting comparable to extant social carnivores (Currie & Eberth 2010; McCrea *et al.* 2014; Titus *et al.* 2021). Alternatively, these bonebeds might simply represent a temporary aggregation of opportunistic individuals around a kill site rather than a coordinated pack hunting strategy, which would be more similar to Komodo dragon feeding behaviour (Auffenberg 1981).

Altogether, these independent palaeobiological lines of evidence could not fully settle the debate on the ecological role of Late Cretaceous tyrannosaurids. We now propose that the ecological networks and biomass distributions produced for the Dinosaur Provincial Park biota in this study decisively shift the balance towards Komodo dragons as the nearest extant trophic analogues for these extinct predators. As in previous research (Banker *et al.* 2022; Amiraux *et al.* 2023), this case study demonstrates the utility of quantitative ecological networks to establish the function of a species in its community beyond its functional traits alone, with the potential to highlight hitherto undetected similarities and differences in the respective trophic positions of potential analogues that evolved as part of vastly different faunas which evolved under disparate biotic and abiotic conditions. Furthermore, we show that the novel attribution of distinct nodes defined by ontogenetic dietary shifts in these networks is a promising way to complete the comparison of these species when fossil growth series are available.

Implications of the predator-prey biomass distribution of Dinosaur Provincial Park. The relationship between predator and prey biomass observed in DPP has a similar slope to the scaling law detected in extant communities (Hatton *et al.* 2015), regardless of the clades and life stages included in the DPP predator and prey categories. While the proportion of biomass between predator and prey categories (and between distinct trophic levels) proved highly variable depending on the ecosystem, the rate of increase in predator and prey biomass density appeared very similar regardless. These results alone are noteworthy since they suggest that a predator-prey power law was broadly consistent across terrestrial tetrapod communities not only through space, as was previously shown (Hatton *et al.* 2015; Perkins *et al.* 2022), but also throughout geological time. Furthermore, our results remain consistent with a previous estimate of megafauna biomass in DPP based on a smaller sample size, which found a similarly high predator biomass in that Cretaceous biota relative to the modern African savanna (Béland & Russell 1978). Our study now has the added novelty of showing that the DPP predator biomass is actually comparable to that of at least one extant community, albeit one dominated by an ectothermic apex predator. Considering that lower metabolic rates could explain such high population densities, the high biomass estimated by the previous authors was initially cited as support for ectothermy in non-avian dinosaurs (and by extension close ecological affinity to other reptiles such as the Komodo dragon). Since then, new discoveries suggest that even dinosaur species in the lineages most distantly related to birds had a higher metabolic rate than any other extant reptile (Grady *et al.* 2014). This implies that energetic constraints alone are insufficient to explain the high predator biomass of the DPP fossil assemblage, and that other environmental factors (yet to be determined) result in a surprisingly similar biomass distribution to that observed in a community with very different abiotic conditions and evolutionary histories. Juvenile tyrannosaurids and megaherbivores were included in some versions of biomass density estimates for the Park, yet this did not result in any significant decrease in predator-prey biomass density ratios. In this respect, the influence of climate conditions characteristic of much of the Cretaceous Period (but alien to the present) on primary and secondary productivity in dinosaur ecosystems may eventually prove a fertile ground to resolve this conundrum (Wolfe & Upchurch 1987; Brown *et al.* 2012; Herman *et al.* 2016). Unfortunately, our current state of knowledge on the DPP palaeoflora is vastly lagging behind that of its vertebrate consumers, which conversely raises great uncertainties on the palaeoclimate inferences that can be drawn from it and thus limits inferences about the influence of prevailing climate conditions on the DPP palaeobiota's primary productivity.

4.4.3 Future directions

Curiously, not a single site-specific and highly resolved quantitative food web has ever been produced for a Mesozoic dinosaur community until this study. Latest Cretaceous and early Paleogene communities of the Western Interior of North America were already investigated using a similar approach, yet they were highly simplified due to the fact that their individual nodes represented ‘trophic species’ or ecological guilds (Mitchell *et al.* 2012; García-Girón *et al.* 2022). Conversely, energetic requirements derived from biomass and population density estimates have been hypothesized in non-avian dinosaurs more than in any other extinct animal group (Farlow 1993; Farlow *et al.* 2010; Carbone *et al.* 2011; Kane *et al.* 2016), in part due to a longstanding debate on their metabolic rate relative to birds, mammals and other diapsids (Bakker 1975; Grady *et al.* 2014). Some of these studies traced energy flow along food chains, yet the food webs they formed were assembled in a qualitative way, thus lacking the potential to compute node and network properties (Matsukawa *et al.* 2006, 2014). The Dinosaur Provincial Park fauna has proven a particularly popular study system in this regard due to its exceptional dinosaur fossil record (Farlow 1976; Farlow & Pianka 2002; Farlow *et al.* 2022), and this study now provides a detailed quantitative food web that can form a framework to map the hypothetical distribution of that community’s energy flux.

Ontogenetic niche shifts in diet are usually driven by variation in body size and energy requirements throughout an animal’s life history (Werner & Gilliam 1984). While they are prevalent in large semiaquatic predators such as crocodilians (Dodson 1975; Tucker *et al.* 1996; Erickson *et al.* 2003; Platt *et al.* 2006; Gignac & Erickson 2016), they are conspicuously rare in fully terrestrial extant apex predators with the exception of *V. komodoensis* (Purwandana *et al.* 2016). While past research was more focused on the effect of the inclusion of several life stages for the same species on food web complexity in aquatic environments (Clegg *et al.* 2018), the present study is the first to directly test the effect of ontogenetic dietary shifts in animals on their trophic position in a food web, whether extant or extinct. The assimilation of trophic niches for small-bodied terrestrial tetrapods by juveniles of larger species is gaining support as one of the main drivers of the peculiar body size distribution of non-avian dinosaur faunas relative to that of more recent mammals (Codron *et al.* 2012; Holtz 2021; Schroeder *et al.* 2021). This hypothesis is supported by mounting anatomical evidence suggesting that ontogenetic dietary shifts were common in non-avian dinosaurs (Wang *et al.* 2017; Woodruff *et al.* 2018; Therrien *et al.* 2021, 2023; Wyenberg-Henzler *et al.* 2021). Therefore, the present study is predicted to create a precedent for comparing terrestrial community structure between the Mesozoic and Cenozoic eras by accounting for variation in ecological niche occupancy through ontogeny.

4.5 Conclusions

Decades of research on tyrannosaurid dinosaur biology have laid strong foundations to test hypotheses on the impact of those apex predators on their community using ecological metrics. These questions have now been investigated in this study through the creation of the first site-specific ecological network and resulting trophic biomass pyramid ever attempted at a high taxonomic resolution for a terrestrial Mesozoic community containing non-avialan dinosaurs. This study now decisively suggests that one of the best-known tyrannosaurids (*Gorgosaurus libratus*) had an ecological role more similar to Komodo dragons than to lions among extant terrestrial apex predators inhabiting potentially analogous ecosystems to the Dinosaur Provincial Park palaeobiota, by revealing marked ontogenetic shifts in trophic position based on evidence for ontogenetic shifts in dietary preferences, as well as revealing an estimated predator biomass well within the range observed on Komodo. If other ecological traits could be investigated as rigorously for tyrannosaurs in the future, they could yet reveal more affinity to large carnivorans in contrast to the current results, but that will likely require further palaeobiological advances. We argue that this study now introduces a promising avenue of research to compare the ecological role of extinct species with that of possible extant analogues by accounting for ontogenetic intraspecific variation throughout their life history.

4.6 References

AMIRAUX, R., YURKOWSKI, D. J., ARCHAMBAULT, P., PIERREJEAN, M. and MUNDY, C. J. 2023. Top predator sea stars are the benthic equivalent to polar bears of the pelagic realm. *Proceedings of the National Academy of Sciences*, **120**, e2216701120.

ARBOUR, V. M. and CURRIE, P. J. 2013. *Euoplocephalus tutus* and the Diversity of Ankylosaurid Dinosaurs in the Late Cretaceous of Alberta, Canada, and Montana, USA. *PLOS ONE*, **8**, e62421.

——— and ———. 2015. Ankylosaurid dinosaur tail clubs evolved through stepwise acquisition of key features. *Journal of Anatomy*, **227**, 514–523.

——— and ZANNO, L. E. 2018. The evolution of tail weaponization in amniotes. *Proceedings of the Royal Society B: Biological Sciences*, **285**, 20172299.

ARESCO, M. J. and GUNZBURGER, M. S. 2007. Ecology and Morphology of *Chelydra serpentina* in Northwestern Florida. *Southeastern Naturalist*, **6**, 435–448.

AUFFENBERG, W. 1981. *The Behavioral Ecology of the Komodo Monitor*. University Presses of Florida, Gainesville.

BAKKER, R. T. 1975. Dinosaur Renaissance. *Scientific American*, **232**, 58–79.

BANKER, R. M. W., DINEEN, A. A., SORMAN, M. G., TYLER, C. L. and ROOPNARINE, P. D. 2022. Beyond functional diversity: The importance of trophic position to understanding functional processes in community evolution. *Frontiers in Ecology and Evolution*, **10**, 983374.

BARDACK, D. 1970. *A New Teleost from the Oldman Formation (Cretaceous) of Alberta*. Publications in Palaeontology 3. National Museums of Canada, 1–20 pp.

BASKERVILLE, E. B., DOBSON, A. P., BEDFORD, T., ALLESINA, S., ANDERSON, T. M. and PASCUAL, M. 2011. Spatial Guilds in the Serengeti Food Web Revealed by a Bayesian Group Model. *PLOS Computational Biology*, **7**, e1002321.

BEHRENSMEYER, A. K. 1982. Time Resolution in Fluvial Vertebrate Assemblages. *Paleobiology*, **8**, 211–227.

BEHRENSMEYER, A. K. and HOOK, R. W. 1992. Paleoenvironmental Contexts and Taphonomic Modes. *In* BEHRENSMEYER, A. K., DAMUTH, J. D., DIMICHELE, W. A., POTTS, R., SUES, H.-D. and WING, S. L. (eds.) *Terrestrial Ecosystems through Time*, The University of Chicago Press, Chicago, 15–136 pp.

BEHRENSMEYER, A. K., KIDWELL, S. M. and GASTALDO, R. A. 2000. Taphonomy and paleobiology. *Paleobiology*, **26**, 103–147.

BÉLAND, P. and RUSSELL, D. A. 1978. Paleoecology of Dinosaur Provincial Park (Cretaceous), Alberta, interpreted from the distribution of articulated vertebrate remains. *Canadian Journal of Earth Sciences*, **15**, 1012–1024.

BELL, P. R., EVANS, D. C., EBERTH, D. A., FANTI, F., TSOGTBAATAR, Kh. and RYAN, M. J. 2018. Sedimentological and taphonomic observations on the “Dragon’s Tomb” Saurolophus (Hadrosauridae) bonebed, Nemegt Formation (Upper Cretaceous), Mongolia. *Palaeogeography, Palaeoclimatology, Palaeoecology*, **494**, 75–90.

BENSON, R. B. J. 2018. Dinosaur Macroevolution and Macroecology. *Annual Review of Ecology, Evolution, and Systematics*, **49**, 379–408.

BENSON, R. B. J., HUNT, G., CARRANO, M. T. and CAMPIONE, N. 2018. Cope’s rule and the adaptive landscape of dinosaur body size evolution. *Palaeontology*, **61**, 13–48.

BENTON, M. J. 2008. How to find a dinosaur, and the role of synonymy in biodiversity studies. *Paleobiology*, **34**, 516–533.

BOTHMA, J. d. P. and WALKER, C. 1999. The African lion. *In Larger Carnivores of the African Savannas*, Springer, Berlin, Heidelberg, 23–59 pp.

BOURKE, J. M., PORTER, W. R. and WITMER, L. M. 2018. Convoluted nasal passages function as efficient heat exchangers in ankylosaurs (Dinosauria: Ornithischia: Thyreophora). *PLOS ONE*, **13**, e0207381.

BRAMAN, D. R. 2005. Campanian Palynomorphs. *In* CURRIE, P. J. and KOPPELHUS, E. B. (eds.) *Dinosaur Provincial Park: A Spectacular Ancient Ecosystem Revealed*, Indiana University Press, Bloomington, 101–130 pp.

BRINKMAN, D. B. 1990. Paleoecology of the Judith River Formation (Campanian) of Dinosaur Provincial Park, Alberta, Canada: Evidence from vertebrate microfossil localities. *Palaeogeography, Palaeoclimatology, Palaeoecology*, **78**, 37–54.

———. 2005. Turtles: Diversity, Paleoecology, and Distribution. *In* CURRIE, P. J. and KOPPELHUS, E. B. (eds.) *Dinosaur Provincial Park: A Spectacular Ancient Ecosystem Revealed*, Indiana University Press, Bloomington, 202–220 pp.

BROSE, U., JONSSON, T., BERLOW, E. L., WARREN, P., BANASEK-RICHTER, C., BERSIER, L.-F., BLANCHARD, J. L., BREY, T., CARPENTER, S. R., BLANDENIER, M.-F. C., CUSHING, L., DAWAH, H. A., DELL, T., EDWARDS, F., HARPER-SMITH, S., JACOB, U., LEDGER, M. E., MARTINEZ, N. D., MEMMOTT, J., MINTENBECK, K., PINNEGAR, J. K., RALL, B. C., RAYNER, T. S., REUMAN, D. C., RUESS, L., ULRICH, W., WILLIAMS, R. J., WOODWARD, G. and COHEN, J. E. 2006. Consumer–Resource Body-Size Relationships in Natural Food Webs. *Ecology*, **87**, 2411–2417.

———, ARCHAMBAULT, P., BARNES, A. D., BERSIER, L.-F., BOY, T., CANNING-CLODE, J., CONTI, E., DIAS, M., DIGEL, C., DISSANAYAKE, A., FLORES, A. A. V., FUSSMANN, K., GAUZENS, B., GRAY, C., HÄUSSLER, J., HIRT, M. R., JACOB, U., JOCHUM, M., KÉFI, S., MCLAUGHLIN, O., MACPHERSON, M. M., LATZ, E., LAYER-DOBRA, K., LEGAGNEUX, P., LI, Y., MADEIRA, C., MARTINEZ, N. D., MENDONÇA, V., MULDER, C., NAVARRETE, S. A., O'GORMAN, E. J., OTT, D., PAULA, J., PERKINS, D., PIECHNIK,

D., POKROVSKY, I., RAFFAELLI, D., RALL, B. C., ROSENBAUM, B., RYSER, R., SILVA, A., SOHLSTRÖM, E. H., SOKOLOVA, N., THOMPSON, M. S. A., THOMPSON, R. M., VERMANDELE, F., VINAGRE, C., WANG, S., WEFER, J. M., WILLIAMS, R. J., WIETERS, E., WOODWARD, G. and ILES, A. C. 2019. Predator traits determine food-web architecture across ecosystems. *Nature Ecology & Evolution*, **3**, 919–927.

BROWN, C. M. 2013. Advances in Quantitative Methods in Dinosaur Palaeobiology: A Case Study in Horned Dinosaur Evolution.Unpublished Ph.D. Thesis, University of Toronto, Toronto, 443pp.

———, CURRIE, P. J. and THERRIEN, F. 2022*a*. Intraspecific facial bite marks in tyrannosaurids provide insight into sexual maturity and evolution of bird-like intersexual display. *Paleobiology*, **48**, 12–43.

———, EVANS, D. C., RYAN, M. J. and RUSSELL, A. P. 2013*a*. New data on the diversity and abundance of small-bodied ornithopods (Dinosauria, Ornithischia) from the Belly River Group (Campanian) of Alberta. *Journal of Vertebrate Paleontology*, **33**, 495–520.

BROWN, C. M., CAMPIONE, N. E., MANTILLA, G. P. W. and EVANS, D. C. 2022*b*. Size-driven preservational and macroecological biases in the latest Maastrichtian terrestrial vertebrate assemblages of North America. *Paleobiology*, **48**, 210–238.

BROWN, C. M., EVANS, D. C., CAMPIONE, N. E., O'BRIEN, L. J. and EBERTH, D. A. 2013*b*. Evidence for taphonomic size bias in the Dinosaur Park Formation (Campanian, Alberta), a model Mesozoic terrestrial alluvial-paralic system. *Palaeogeography, Palaeoclimatology, Palaeoecology*, **372**, 108–122.

BROWN, C. M., GREENWOOD, D. R., KALYNIUK, J. E., BRAMAN, D. R., HENDERSON, D. M., GREENWOOD, C. L. and BASINGER, J. F. 2020. Dietary palaeoecology of an Early Cretaceous armoured dinosaur (Ornithischia; Nodosauridae) based on floral analysis of stomach contents. *Royal Society Open Science*, **7**, 200305.

BROWN, S. A. E., SCOTT, A. C., GLASSPOOL, I. J. and COLLINSON, M. E. 2012. Cretaceous wildfires and their impact on the Earth system. *Cretaceous Research*, **36**, 162–190.

BRUSATTE, S. L. and CARR, T. D. 2016. The phylogeny and evolutionary history of tyrannosauroid dinosaurs. *Scientific Reports*, **6**, 20252.

———, NORELL, M. A., CARR, T. D., ERICKSON, G. M., HUTCHINSON, J. R., BALANOFF, A. M., BEVER, G. S., CHOINIERE, J. N., MAKOVICKY, P. J. and XU, X. 2010. Tyrannosaur paleobiology: new research on ancient exemplar organisms. *Science*, **329**, 1481–5.

CALDWELL, M. W. 2005. The Squamates: Origins, Phylogeny, and Paleoecology. *In* CURRIE, P. J. and KOPPELHUS, E. B. (eds.) *Dinosaur Provincial Park: A Spectacular Ancient Ecosystem Revealed*, Indiana University Press, Bloomington, 235–248 pp.

CAMPIONE, N. E. and EVANS, D. C. 2020. The accuracy and precision of body mass estimation in non-avian dinosaurs. *Biological Reviews*, **95**, 1759–1797.

CARBONE, C., PETTORELLI, N. and STEPHENS, P. A. 2010. The bigger they come, the harder they fall: body size and prey abundance influence predator–prey ratios. *Biology Letters*, **7**, 312–315.

———, TURVEY, S. T. and BIELBY, J. 2011. Intra-guild competition and its implications for one of the biggest terrestrial predators, *Tyrannosaurus rex*. *Proceedings of the Royal Society B: Biological Sciences*, **278**, 2682–2690.

———, MACE, G. M., ROBERTS, S. C. and MACDONALD, D. W. 1999. Energetic constraints on the diet of terrestrial carnivores. *Nature*, **402**, 286–288.

CARON, D., BROSE, U., LURGI, M., BLANCHET, F. G., GRAVEL, D. and POLLOCK, L. J. 2024. Trait-matching models predict pairwise interactions across regions, not food web properties. *Global Ecology and Biogeography*, **33**, e13807.

CARPENTER, K. 2010. Species concept in North American stegosaurs. *Swiss Journal of Geosciences*, **103**, 155–162.

CARR, T. D. 2020. A high-resolution growth series of *Tyrannosaurus rex* obtained from multiple lines of evidence. *PeerJ*, **8**, e9192.

CLEGG, T., ALI, M. and BECKERMAN, A. P. 2018. The impact of intraspecific variation on food web structure. *Ecology*, **99**, 2712–2720.

CLEMENTS, H. S., TAMBLING, C. J., HAYWARD, M. W. and KERLEY, G. I. H. 2014. An Objective Approach to Determining the Weight Ranges of Prey Preferred by and Accessible to the Five Large African Carnivores. *PLOS ONE*, **9**, e101054.

CODRON, D., CARBONE, C., MÜLLER, D. W. H. and CLAUSS, M. 2012. Ontogenetic niche shifts in dinosaurs influenced size, diversity and extinction in terrestrial vertebrates. *Biology Letters*, **8**, 620–623.

COHEN, J. E., JONSSON, T. and CARPENTER, S. R. 2003. Ecological community description using the food web, species abundance, and body size. *Proceedings of the National Academy of Sciences*, **100**, 1781–1786.

CORTÉS, D. and LARSSON, H. C. E. 2023. Top of the food chains: an ecological network of the marine Paja Formation biota from the Early Cretaceous of Colombia reveals the highest trophic levels ever estimated. *Zoological Journal of the Linnean Society*, zlad092.

CULLEN, T. M. and EVANS, D. C. 2016. Palaeoenvironmental drivers of vertebrate community composition in the Belly River Group (Campanian) of Alberta, Canada, with implications for dinosaur biogeography. *BMC Ecology*, **16**, 52.

——— and COUSENS, B. L. 2023. New biogeochemical insights into Mesozoic terrestrial paleoecology and evidence for omnivory in troodontid dinosaurs. *GSA Bulletin*.

———, ZANNO, L., LARSON, D. W., TODD, E., CURRIE, P. J. and EVANS, D. C. 2021. Anatomical, morphometric, and stratigraphic analyses of theropod biodiversity in the Upper Cretaceous (Campanian) Dinosaur Park Formation. *Canadian Journal of Earth Sciences*, **58**, 870–884.

CULLEN, T. M., LONGSTAFFE, F. J., WORTMANN, U. G., HUANG, L., FANTI, F., GOODWIN, M. B., RYAN, M. J. and EVANS, D. C. 2020. Large-scale stable isotope characterization of a Late Cretaceous dinosaur-dominated ecosystem. *Geology*, **48**, 546–551.

CURRIE, P. J. 2003*a*. Cranial anatomy of tyrannosaurid dinosaurs from the Late Cretaceous of Alberta,Canada. *Acta Palaeontologica Polonica*, **48**, 191–226.

———. 2003*b*. Allometric growth in tyrannosaurids (Dinosauria: Theropoda) from the Upper Cretaceous of North America and Asia. *Canadian Journal of Earth Sciences*, **40**, 651–665.

———. 2005. History of Research. *In* CURRIE, P. J. and KOPPELHUS, E. B. (eds.) *Dinosaur Provincial Park: A Spectacular Ancient Ecosystem Revealed*, Indiana University Press, Bloomington, 3–33 pp.

——— and KOPPELHUS, E. B. 2005. *Dinosaur Provincial Park: A Spectacular Ancient Ecosystem Revealed*. Bloomington & Indianapolis.

——— and RUSSELL, D. A. 2005. The Geographic and Stratigraphic Distribution of Articulated and Associated Dinosaur Remains. *In* CURRIE, P. J. and KOPPELHUS, E. B. (eds.) *Dinosaur Provincial Park: A Spectacular Ancient Ecosystem Revealed*, Indiana University Press, Bloomington, 537–569 pp.

CURRIE, P. J. and EBERTH, D. A. 2010. On gregarious behavior in *Albertosaurus*. *Canadian Journal of Earth Sciences*, **47**, 1277–1289.

CURRIE, P. J., HOLMES, R. B., RYAN, M. J. and COY, C. 2016. A juvenile chasmosaurine ceratopsid (Dinosauria, Ornithischia) from the Dinosaur Park Formation, Alberta, Canada. *Journal of Vertebrate Paleontology*, **36**, e1048348.

DAMUTH, J. D. 1981. Population density and body size in mammals. *Nature*, **290**, 699–700.

———. 1982. Analysis of the preservation of community structure in assemblages of fossil mammals. *Paleobiology*, **8**, 434–446.

———. 1987. Interspecific allometry of population density in mammals and other animals: the independence of body mass and population energy-use. *Biological Journal of the Linnean Society*, **31**, 193–246.

———. 1992. Taxon-free characterization of animal communities. *In Terrestrial Ecosystems Through Time*, The University of Chicago Press, Chicago, 183–203 pp.

———. 2007. A Macroevolutionary Explanation for Energy Equivalence in the Scaling of Body Size and Population Density. *The American Naturalist*, **169**, 621–631.

DECECCHI, T. A., MLOSZEWSKA, A. M., JR, T. R. H., HABIB, M. B. and LARSSON, H. C. E. 2020. The fast and the frugal: Divergent locomotory strategies drive limb lengthening in theropod dinosaurs. *PLOS ONE*, **15**, e0223698.

DELMAS, E., BESSON, M., BRICE, M.-H., BURKLE, L. A., DALLA RIVA, G. V., FORTIN, M.-J., GRAVEL, D., GUIMARÃES JR., P. R., HEMBRY, D. H., NEWMAN, E. A., OLESEN, J. M., PIRES, M. M., YEAKEL, J. D. and POISOT, T. 2019. Analysing ecological networks of species interactions. *Biological Reviews*, **94**, 16–36.

DESANTIS, L. R. G., CRITES, J. M., FERANEC, R. S., FOX-DOBBS, K., FARRELL, A. B., HARRIS, J. M., TAKEUCHI, G. T. and CERLING, T. E. 2019. Causes and Consequences of Pleistocene Megafaunal Extinctions as Revealed from Rancho La Brea Mammals. *Current Biology*, **29**, 2488-2495.e2.

DODSON, P. 1971. Sedimentology and taphonomy of the Oldman Formation (Campanian), Dinosaur Provincial Park, Alberta (Canada). *Palaeogeography, Palaeoclimatology, Palaeoecology*, **10**, 21–74.

———. 1975. Functional and ecological significance of relative growth in *Alligator*. *Journal of Zoology*, **175**, 315–355.

———. 1983. A Faunal Review of the Judith River (Oldman) Formation, Dinosaur Provincial Park, Alberta, Canada. *The Mosasaur*, **1**, 89–118.

DODSON, P., BEHRENSMEYER, A. K., BAKKER, R. T. and MCINTOSH, J. S. 1980. Taphonomy and Paleoecology of the Dinosaur Beds of the Jurassic Morrison Formation. *Paleobiology*, **6**, 208–232.

DUNNE, J. A., LABANDEIRA, C. C. and WILLIAMS, R. J. 2014. Highly resolved early Eocene food webs show development of modern trophic structure after the end-Cretaceous extinction. *Proceedings of the Royal Society B: Biological Sciences*, **281**, 20133280.

———, WILLIAMS, R. J., MARTINEZ, N. D., WOOD, R. A. and ERWIN, D. H. 2008. Compilation and Network Analyses of Cambrian Food Webs. *PLOS Biology*, **6**, e102.

DURKIN, P. R., HUBBARD, S. M., HOLBROOK, J., WELESCHUK, Z., NESBIT, P., HUGENHOLTZ, C., LYONS, T. and SMITH, D. G. 2020. Recognizing the product of concave-bank sedimentary processes in fluvial meander-belt strata. *Sedimentology*, **67**, 2819–2849.

EBERTH, D. A. 2005. The Geology. *In* CURRIE, P. J. and KOPPELHUS, E. B. (eds.) *Dinosaur Provincial Park: A Spectacular Ancient Ecosystem Revealed*, Indiana University Press, Bloomington, 54–82 pp.

EBERTH, D. A. 2018. Stratigraphy and paleoenvironmental evolution of the dinosaur-rich Baruungoyot-Nemegt succession (Upper Cretaceous), Nemegt Basin, southern Mongolia. *Palaeogeography, Palaeoclimatology, Palaeoecology*, **494**, 29–50.

EBERTH, D. A. and CURRIE, P. J. 2005. Vertebrate Taphonomy and Taphonomic Modes. *In* CURRIE, P. J. and KOPPELHUS, E. B. (eds.) *Dinosaur Provincial Park: A Spectacular Ancient Ecosystem Revealed*, Indiana University Press, Bloomington, 453–477 pp.

EBERTH, D. A. and GETTY, M. A. 2005. Ceratopsian Bonebeds: Occurrence, Origins, and Significance. *In* CURRIE, P. J. and KOPPELHUS, E. B. (eds.) *Dinosaur Provincial Park: A Spectacular Ancient Ecosystem Revealed*, Indiana University Press, Bloomington, 501–536 pp.

EBERTH, D. A., EVANS, D. C. and LLOYD, D. W. H. 2015. Occurrence and Taphonomy of the First Documented Hadrosaurid Bonebed from the Dinosaur Park Formation (Belly River Group, Campanian) at Dinosaur Provincial Park, Alberta, Canada. *In* EBERTH, D. A. and EVANS, D. C. (eds.) *Hadrosaurs*, Indiana University Press, Bloomington, 502–523 pp.

EBERTH, D. A., EVANS, D. C., RAMEZANI, J., KAMO, S. L., BROWN, C. M., CURRIE, P. J. and BRAMAN, D. R. 2023. Calibrating geologic strata, dinosaurs, and other fossils at Dinosaur Provincial Park (Alberta, Canada) using a new CA-ID-TIMS U–Pb geochronology. *Canadian Journal of Earth Sciences*, **60**, 1627–1646.

EKLÖF, A., JACOB, U., KOPP, J., BOSCH, J., CASTRO-URGAL, R., CHACOFF, N. P., DALSGAARD, B., DE SASSI, C., GALETTI, M., GUMARÃES, P. R., LOMÁSCOLO, S. B., MARTÍN GONZÁLEZ, A. M., PIZO, M. A., RADER, R., RODRIGO, A., TYLIANAKIS, J. M., VÁZQUEZ, D. P. and ALLESINA, S. 2013. The dimensionality of ecological networks. *Ecology Letters*, **16**, 577-583.

ERICKSON, G. M., LAPPIN, A. K. and VLIET, K. A. 2003. The ontogeny of bite-force performance in American alligator (*Alligator mississippiensis*). *Journal of Zoology*, **260**, 317–327.

———, CURRIE, P. J., INOUYE, B. D. and WINN, A. A. 2006. Tyrannosaur Life Tables: An Example of Nonavian Dinosaur Population Biology. *Science*, **313**, 213–217.

———, MAKOVICKY, P. J., CURRIE, P. J., NORELL, M. A., YERBY, S. A. and BROCHU, C. A. 2004. Gigantism and comparative life-history parameters of tyrannosaurid dinosaurs. *Nature*, **430**, 772.

———, ———, ———, ———, ——— and ———. 2016. Correction: Corrigendum: Gigantism and comparative life-history parameters of tyrannosaurid dinosaurs. *Nature*, **531**, 538–538.

ESTES, J. A., TERBORGH, J., BRASHARES, J. S., POWER, M. E., BERGER, J., BOND, W. J., CARPENTER, S. R., ESSINGTON, T. E., HOLT, R. D., JACKSON, J. B. C., MARQUIS, R. J., OKSANEN, L., OKSANEN, T., PAINE, R. T., PIKITCH, E. K., RIPPLE, W. J., SANDIN, S. A., SCHEFFER, M., SCHOENER, T. W., SHURIN, J. B., SINCLAIR, A. R. E., SOULÉ, M. E., VIRTANEN, R. and WARDLE, D. A. 2011. Trophic Downgrading of Planet Earth. *Science*, **333**, 301–306.

ESTES, R. 1975. Lower Vertebrates from the Fort Union Formation, Late Paleocene, Big Horn Basin, Wyoming. *Herpetologica*, **31**, 365–385.

FARKE, A. A., RYAN, M. J., BARRETT, P. M., TANKE, D. H., BRAMAN, D. R., LOEWEN, M. A. and GRAHAM, M. R. 2011. A New Centrosaurine from the Late Cretaceous of Alberta, Canada, and the Evolution of Parietal Ornamentation in Horned Dinosaurs. *Acta Palaeontologica Polonica*, **56**, 691–702.

FARLOW, J. O. 1976. A Consideration of the Trophic Dynamics of a Late Cretaceous Large-Dinosaur Community (Oldman Formation). *Ecology*, **57**, 841–857.

———. 1993. On the rareness of big, fierce animals: speculations about the body sizes, population densities, and geographic ranges of predatory mammals and large carnivorous dinosaurs. *American Journal of Science*, **293-A**, 167–199.

——— and PIANKA, E. R. 2002. Body Size Overlap, Habitat Partitioning and Living Space Requirements of Terrestrial Vertebrate Predators: Implications for the Paleoecology of Large Theropod Dinosaurs. *Historical Biology*, **16**, 21–40.

———, COROIAN, I. D. and FOSTER, J. R. 2010. Giants on the landscape: modelling the abundance of megaherbivorous dinosaurs of the Morrison Formation (Late Jurassic, western USA). *Historical Biology*, **22**, 403–429.

———, COROIAN, D., CURRIE, P. J., FOSTER, J. R., MALLON, J. C. and THERRIEN, F. 2022. “Dragons” on the landscape: Modeling the abundance of large carnivorous dinosaurs of the Upper Jurassic Morrison Formation (USA) and the Upper Cretaceous Dinosaur Park Formation (Canada). *The Anatomical Record*, **306**, 1669–1696.

FOX, R. C. 2005. Late Cretaceous Mammals. *In* CURRIE, P. J. and KOPPELHUS, E. B. (eds.) *Dinosaur Provincial Park: A Spectacular Ancient Ecosystem Revealed*, Indiana University Press, Bloomington, 417–449 pp.

FRICKE, E. C., HSIEH, C., MIDDLETON, O., GORCZYNSKI, D., CAPPELLO, C. D., SANISIDRO, O., ROWAN, J., SVENNING, J.-C. and BEAUDROT, L. 2022. Collapse of terrestrial mammal food webs since the Late Pleistocene. *Science*, **377**, 1008–1011.

FRICKE, H. C. and PEARSON, D. A. 2008. Stable isotope evidence for changes in dietary niche partitioning among hadrosaurian and ceratopsian dinosaurs of the Hell Creek Formation, North Dakota. *Paleobiology*, **34**, 534–552.

FUNSTON, G. F. 2020. Caenagnathids of the Dinosaur Park Formation (Campanian) of Alberta, Canada: anatomy, osteohistology, taxonomy, and evolution. *Vertebrate Anatomy Morphology Palaeontology*, **8**, 105–153.

FUNSTON, G. F. and CURRIE, P. J. 2014. A previously undescribed caenagnathid mandible from the late Campanian of Alberta, and insights into the diet of *Chirostenotes pergracilis* (Dinosauria: Oviraptorosauria). *Canadian Journal of Earth Sciences*, **51**, 156–165.

GARCÍA-GIRÓN, J., CHIARENZA, A. A., ALAHUHTA, J., DEMAR, D. G., HEINO, J., MANNION, P. D., WILLIAMSON, T. E., WILSON MANTILLA, G. P. and BRUSATTE, S. L. 2022. Shifts in food webs and niche stability shaped survivorship and extinction at the end-Cretaceous. *Science Advances*, **8**, eadd5040.

GARDNER, J. D. 2005. Lissamphibians. *In* CURRIE, P. J. and KOPPELHUS, E. B. (eds.) *Dinosaur Provincial Park: A Spectacular Ancient Ecosystem Revealed*, Indiana University Press, Bloomington, 186–201 pp.

GIGNAC, P. M. and ERICKSON, G. M. 2016. Ontogenetic bite-force modeling of *Alligator mississippiensis*: implications for dietary transitions in a large-bodied vertebrate and the evolution of crocodylian feeding. *Journal of Zoology*, **299**, 229–238.

GRADY, J. M., ENQUIST, B. J., DETTWEILER-ROBINSON, E., WRIGHT, N. A. and SMITH, F. A. 2014. Evidence for mesothermy in dinosaurs. *Science*, **344**, 1268.

GRANGE, S. and DUNCAN, P. 2006. Bottom-up and top-down processes in African ungulate communities: resources and predation acting on the relative abundance of zebra and grazing bovids. *Ecography*, **29**, 899–907.

HARRINGTON, E. 2004. Panthera leo *(lion)*. Animal Diversity Web. Downloaded from https://animaldiversity.org/accounts/Panthera_leo/ on 1 August 2024.

HARTMAN, J. H., JOHNSON, K. R. and NICHOLS, D. J. 2002. *The Hell Creek Formation and the Cretaceous-Tertiary Boundary in the Northern Great Plains: An Integrated Continental Record of the End of the Cretaceous*. Geological Society of America.

HATTON, I. A., MCCANN, K. S., FRYXELL, J. M., DAVIES, T. J., SMERLAK, M., SINCLAIR, A. R. E. and LOREAU, M. 2015. The predator-prey power law: Biomass scaling across terrestrial and aquatic biomes. *Science*, **349**, aac6284.

HAYWARD, M. W. 2006. Prey preferences of the spotted hyaena (*Crocuta crocuta*) and degree of dietary overlap with the lion (*Panthera leo*). *Journal of Zoology*, **270**, 606–614.

HAYWARD, M. W. and KERLEY, G. I. H. 2005. Prey preferences of the lion (*Panthera leo*). *Journal of Zoology*, **267**, 309–322.

HENDERSON, D. M. and TANKE, D. H. 2010. Estimating past and future dinosaur skeletal abundances in Dinosaur Provincial Park, Alberta, Canada. *Canadian Journal of Earth Sciences*, **47**, 1291–1304.

HERMAN, A. B., SPICER, R. A. and SPICER, T. E. V. 2016. Environmental constraints on terrestrial vertebrate behaviour and reproduction in the high Arctic of the Late Cretaceous. *Palaeogeography, Palaeoclimatology, Palaeoecology*, **441**, 317–338.

HOLTZ, T. R. 2021. Theropod guild structure and the tyrannosaurid niche assimilation hypothesis: implications for predatory dinosaur macroecology and ontogeny in later Late Cretaceous Asiamerica. *Canadian Journal of Earth Sciences*, **58**, 778–795.

HUANG, Y., CHEN, Z.-Q., ROOPNARINE, P. D., BENTON, M. J., ZHAO, L., FENG, X. and LI, Z. 2023. The stability and collapse of marine ecosystems during the Permian-Triassic mass extinction. *Current Biology*, **33**, 1059-1070.e4.

HUDSON, L. N., EMERSON, R., JENKINS, G. B., LAYER, K., LEDGER, M. E., PICHLER, D. E., THOMPSON, M. S. A., O'GORMAN, E. J., WOODWARD, G. and REUMAN, D. C. 2013. Cheddar: analysis and visualisation of ecological communities in R. *Methods in Ecology and Evolution*, **4**, 99–104.

HUTCHINSON, J. R. and GARCIA, M. 2002. *Tyrannosaurus* was not a fast runner. *Nature*, **415**, 1018.

IMANSYAH, M. J., JESSOP, T. S., CIOFI, C. and AKBAR, Z. 2008. Ontogenetic differences in the spatial ecology of immature Komodo dragons. *Journal of Zoology*, **274**, 107–115.

JARZEN, D. M. 1982. Palynology of Dinosaur Provincial Park (Campanian) Alberta. *Syllogeus*, **38**, 1–69.

JESSOP, T. S., ARIEFIANDY, A., FORSYTH, D. M., PURWANDANA, D., WHITE, C. R., BENU, Y. J., MADSEN, T., HARLOW, H. J. and LETNIC, M. 2020. Komodo dragons are not ecological analogs of apex mammalian predators. *Ecology*, **101**, e02970.

JOHN POWER, R. and SHEM COMPION, R. X. 2009. Lion predation on elephants in the Savuti, Chobe National Park, Botswana. *African Zoology*, **44**, 36–44.

JOHNSTON, P. A. and HENDY, A. J. W. 2005. Paleoecology of Mollusks from the Upper Cretaceous Belly River Group. *In Dinosaur Provincial Park: A Spectacular Ancient Ecosystem Revealed*, Indiana University Press, Bloomington, 139–166 pp.

KANE, A., HEALY, K., RUXTON, G. D. and JACKSON, A. L. 2016. Body Size as a Driver of Scavenging in Theropod Dinosaurs. *The American Naturalist*, **187**, 706–716.

KEMPF, H. L., CASTRO, I. O., DINEEN, A. A., TYLER, C. L. and ROOPNARINE, P. D. 2020. Comparisons of Late Ordovician ecosystem dynamics before and after the Richmondian invasion reveal consequences of invasive species in benthic marine paleocommunities. *Paleobiology*, **46**, 320–336.

KIDWELL, S. M. and FLESSA, K. W. 1995. The quality of the fossil record: Populations, Species, and Communities. *Annual Review of Ecology and Systematics*, **26**, 269–299.

KINGDON, J. 2015. *The Kingdon field guide to African mammals*. Princeton University Press, Princeton, NJ.

KOPPELHUS, E. 2005. Paleobotany. *In* CURRIE, P. J. and KOPPELHUS, E. B. (eds.) *Dinosaur Provincial Park: A Spectacular Ancient Ecosystem Revealed*, Indiana University Press, Bloomington, 131–138 pp.

LAMANNA, M. C., SUES, H. D., SCHACHNER, E. R. and LYSON, T. R. 2014. A new large-bodied oviraptorosaurian theropod dinosaur from the latest Cretaceous of western North America. *Plos One*, **9**.

LAMBE, L. M. 1914. On the fore-limb of a carnivorous dinosaur from the Belly River Formation of Alberta, and a new genus of Ceratopsia from the same horizon, with remarks on the integument of some Cretaceous herbivorous dinosaurs. *The Ottawa Naturalist*, **27**, 129–135.

———. 1917. *The Cretaceous Theropodous Dinosaur* Gorgosaurus. Geological Survey of Canada, Ottawa.

LARSON, D. W. and CURRIE, P. J. 2013. Multivariate Analyses of Small Theropod Dinosaur Teeth and Implications for Paleoecological Turnover through Time. *PLOS ONE*, **8**, e54329.

LAVER, R. J., PURWANDANA, D., ARIEFIANDY, A., IMANSYAH, J., FORSYTH, D., CIOFI, C. and JESSOP, T. S. 2012. Life-History and Spatial Determinants of Somatic Growth Dynamics in Komodo Dragon Populations. *PLOS ONE*, **7**, e45398.

LOEWEN, M. A., IRMIS, R. B., SERTICH, J. J. W., CURRIE, P. J. and SAMPSON, S. D. 2013. Tyrant Dinosaur Evolution Tracks the Rise and Fall of Late Cretaceous Oceans. *PLOS ONE*, **8**, e79420.

LONGRICH, N. R. 2006. An ornithurine bird from the Late Cretaceous of Alberta, Canada. *Canadian Journal of Earth Sciences*, **43**, 1-7.

———. 2008. A New, Large Ornithomimid from the Cretaceous Dinosaur Park Formation of Alberta, Canada: Implications for the Study of Dissociated Dinosaur Remains. *Palaeontology*, **51**, 983–997.

———. 2009. An ornithurine-dominated avifauna from the Belly River Group (Campanian, Upper Cretaceous) of Alberta, Canada. *Cretaceous Research*, **30**, 161–177.

———, BHULLAR, B.-A. S. and GAUTHIER, J. A. 2012. Mass extinction of lizards and snakes at the Cretaceous–Paleogene boundary. *Proceedings of the National Academy of Sciences*, **109**, 21396–21401.

MACDONALD, M., CURRIE, P. J. and SPENCER, W. A. 2005. Precise Mapping of Fossil Sites in the Park Using Survey Grade GPS Technology. *In* CURRIE, P. J. and KOPPELHUS, E. B. (eds.) *Dinosaur Provincial Park: A Spectacular Ancient Ecosystem Revealed*, Indiana University Press, Bloomington, 478–485 pp.

MAGNUSSON, W. E., DA SILVA, E. V. and LIMA, A. P. 1987. Diets of Amazonian Crocodilians. *Journal of Herpetology*, **21**, 85–95.

MALLON, J. C. 2019. Competition structured a Late Cretaceous megaherbivorous dinosaur assemblage. *Scientific Reports*, **9**, 15447.

——— and ANDERSON, J. S. 2013. Skull Ecomorphology of Megaherbivorous Dinosaurs from the Dinosaur Park Formation (Upper Campanian) of Alberta, Canada. *PLoS ONE*, **8**, e67182.

——— and ———. 2014*a*. Implications of beak morphology for the evolutionary paleoecology of the megaherbivorous dinosaurs from the Dinosaur Park Formation (upper Campanian) of Alberta, Canada. *Palaeogeography, Palaeoclimatology, Palaeoecology*, **394**, 29–41.

——— and ———. 2014*b*. The Functional and Palaeoecological Implications of Tooth Morphology and Wear for the Megaherbivorous Dinosaurs from the Dinosaur Park Formation (Upper Campanian) of Alberta, Canada. *PLOS ONE*, **9**, e98605.

———, EVANS, D. C., RYAN, M. J. and ANDERSON, J. S. 2012. Megaherbivorous dinosaur turnover in the Dinosaur Park Formation (upper Campanian) of Alberta, Canada. *Palaeogeography, Palaeoclimatology, Palaeoecology*, **350–352**, 124–138.

———, ———, ——— and ———. 2013. Feeding height stratification among the herbivorous dinosaurs from the Dinosaur Park Formation (upper Campanian) of Alberta, Canada. *BMC Ecology*, **13**, 14.

MARSHALL, C. R., LATORRE, D. V., WILSON, C. J., FRANK, T. M., MAGOULICK, K. M., ZIMMT, J. B. and POUST, A. W. 2021. Absolute abundance and preservation rate of Tyrannosaurus rex. *Science*, **372**, 284–287.

MATSUKAWA, M., SHIBATA, K., SATO, K., XING, X. and LOCKLEY, M. G. 2014. The Early Cretaceous terrestrial ecosystems of the Jehol Biota based on food-web and energy-flow models. *Biological Journal of the Linnean Society*, **113**, 836–853.

———, SAIKI, K., ITO, M., OBATA, I., NICHOLS, D. J., LOCKLEY, M. G., KUKIHARA, R. and SHIBATA, K. 2006. Early Cretaceous terrestrial ecosystems in East Asia based on food-web and energy-flow models. *Cretaceous Research*, **27**, 285–307.

MCCREA, R. T., BUCKLEY, L. G., FARLOW, J. O., LOCKLEY, M. G., CURRIE, P. J., MATTHEWS, N. A. and PEMBERTON, S. G. 2014. A ‘terror of tyrannosaurs’: the first trackways of tyrannosaurids and evidence of gregariousness and pathology in Tyrannosauridae. *Plos ONE*, **9**, e103613.

MCFEETERS, B., RYAN, M. J., SCHRÖDER-ADAMS, C. and CULLEN, T. M. 2016. A new ornithomimid theropod from the Dinosaur Park Formation of Alberta, Canada. *Journal of Vertebrate Paleontology*, **36**, e1221415.

———, ———, ——— and CURRIE, P. J. 2017. First North American occurrences of *Qiupalong* (Theropoda: Ornithomimidae) and the palaeobiogeography of derived ornithomimids. *FACETS*, **2**, 355–373.

MCHORSE, B. K., ORCUTT, J. D. and DAVIS, E. B. 2012. The carnivoran fauna of Rancho La Brea: Average or aberrant? *Palaeogeography, Palaeoclimatology, Palaeoecology*, **329–330**, 118–123.

MCKELLAR, R. C., WOLFE, A. P., TAPPERT, R. and MUEHLENBACHS, K. 2008. Correlation of Grassy Lake and Cedar Lake ambers using infrared spectroscopy, stable isotopes, and palaeoentomology. *Canadian Journal of Earth Sciences*, **45**, 1061–1082.

———, JONES, E., ENGEL, M. S., TAPPERT, R., WOLFE, A. P., MUEHLENBACHS, K., COCKX, P., KOPPELHUS, E. B. and CURRIE, P. J. 2019. A direct association between amber and dinosaur remains provides paleoecological insights. *Scientific Reports*, **9**, 17916.

MITCHELL, J. S., ROOPNARINE, P. D. and ANGIELCZYK, K. D. 2012. Late Cretaceous restructuring of terrestrial communities facilitated the end-Cretaceous mass extinction in North America. *Proceedings of the National Academy of Sciences*, **109**, 18857–18861.

NEUMAN, A. G. and BRINKMAN, D. B. 2005. Fishes of the Fluvial Beds. *In* CURRIE, P. J. and KOPPELHUS, E. B. (eds.) *Dinosaur Provincial Park: A Spectacular Ancient Ecosystem Revealed*, Indiana University Press, Bloomington, 167–185 pp.

NEWBREY, M. G., MURRAY, A. M., WILSON, M. V. H., BRINKMAN, D. B. and NEUMAN, A. G. 2009. Seventy-five-million-year-old tropical tetra-like fish from Canada tracks Cretaceous global warming. *Proceedings of the Royal Society B: Biological Sciences*, **276**, 3829–3833.

NORELL, M. A., CLARK, J. M., CHIAPPE, L. M. and DASHZEVEG, D. 1995. A nesting dinosaur. *Nature*, **378**, 774–776.

O'BRIEN, H. D., LYNCH, L. M., VLIET, K. A., BRUEGGEN, J., ERICKSON, G. M. and GIGNAC, P. M. 2019. Crocodylian Head Width Allometry and Phylogenetic Prediction of Body Size in Extinct Crocodyliforms. *Integrative Organismal Biology*, **1**, 1–15.

O'CONNOR, L. M. J., POLLOCK, L. J., BRAGA, J., FICETOLA, G. F., MAIORANO, L., MARTINEZ-ALMOYNA, C., MONTEMAGGIORI, A., OHLMANN, M. and THUILLER, W. 2020. Unveiling the food webs of tetrapods across Europe through the prism of the Eltonian niche. *Journal of Biogeography*, **47**, 181–192.

O'KEEFE, F. R., DUNN, R. E., WEITZEL, E. M., WATERS, M. R., MARTINEZ, L. N., BINDER, W. J., SOUTHON, J. R., COHEN, J. E., MEACHEN, J. A., DESANTIS, L. R. G., KIRBY, M. E., GHEZZO, E., COLTRAIN, J. B., FULLER, B. T., FARRELL, A. B., TAKEUCHI, G. T., MACDONALD, G., DAVIS, E. B. and LINDSEY, E. L. 2023. Pre–Younger Dryas megafaunal extirpation at Rancho La Brea linked to fire-driven state shift. *Science*, **381**, eabo3594.

OWEN-SMITH, N. and MILLS, M. G. L. 2008. Predator–prey size relationships in an African large-mammal food web. *Journal of Animal Ecology*, **77**, 173–183.

PACKER, C. and PUSEY, A. E. 1987. Intrasexual Cooperation and the Sex Ratio in African Lions. *The American Naturalist*, **130**, 636–642.

PANSU, J., GUYTON, J. A., POTTER, A. B., ATKINS, J. L., DASKIN, J. H., WURSTEN, B., KARTZINEL, T. R. and PRINGLE, R. M. 2019. Trophic ecology of large herbivores in a reassembling African ecosystem. *Journal of Ecology*, **107**, 1355–1376.

Parks Division, Alberta Tourism, Parks and Recreation. 2013. Dinosaur Provincial Park World Heritage Site. Scale 1:30,000.

PAULINA CARABAJAL, A., CURRIE, P. J., DUDGEON, T. W., LARSSON, H. C. E. and MIYASHITA, T. 2021. Two braincases of *Daspletosaurus* (Theropoda: Tyrannosauridae): anatomy and comparison1. *Canadian Journal of Earth Sciences*, **58**, 885–910.

PÉRIQUET, S., FRITZ, H. and REVILLA, E. 2015. The Lion King and the Hyaena Queen: large carnivore interactions and coexistence. *Biological Reviews*, **90**, 1197–1214.

PERKINS, D. M., HATTON, I. A., GAUZENS, B., BARNES, A. D., OTT, D., ROSENBAUM, B., VINAGRE, C. and BROSE, U. 2022. Consistent predator-prey biomass scaling in complex food webs. *Nature Communications*, **13**, 4990.

PETERS, R. H. and WASSENBERG, K. 1983. The effect of body size on animal abundance. *Oecologia*, **60**, 89–96.

PIKE, E. M. 1994. Historical changes in insect community structure as indicated by hexapods of Upper Cretaceous Alberta (Grassy Lake) amber. *The Canadian Entomologist*, **126**, 695–702.

PLATT, S. G., RAINWATER, T. R., FINGER, A. G., THORBJARNARSON, J. B., ANDERSON, T. A. and MCMURRY, S. T. 2006. Food habits, ontogenetic dietary partitioning and observations of foraging behaviour of Morelet's crocodile (*Crocodylus moreletii*) in northern Belize. *Herpetological Journal*, **16**, 281–290.

POISOT, T., STOUFFER, D. B. and KÉFI, S. 2016. Describe, understand and predict: why do we need networks in ecology? *Functional Ecology*, **30**, 1878–1882.

POUGH, F. H. 1980. The Advantages of Ectothermy for Tetrapods. *The American Naturalist*, **115**, 92–112.

PURWANDANA, D., ARIEFIANDY, A., IMANSYAH, M. J., SENO, A., CIOFI, C., LETNIC, M. and JESSOP, T. S. 2016. Ecological allometries and niche use dynamics across Komodo dragon ontogeny. *The Science of Nature*, **103**, 27.

R CORE TEAM. 2023. *R: A language and environment for statistical computing*. R Foundation for Statistical Computing, Vienna, Austria. Downloaded from URL https://www.R-project.org/ .

RAMEZANI, J., BEVERIDGE, T. L., ROGERS, R. R., EBERTH, D. A. and ROBERTS, E. M. 2022. Calibrating the zenith of dinosaur diversity in the Campanian of the Western Interior Basin by CA-ID-TIMS U–Pb geochronology. *Scientific Reports*, **12**, 16026.

RIPPLE, W. J., ESTES, J. A., BESCHTA, R. L., WILMERS, C. C., RITCHIE, E. G., HEBBLEWHITE, M., BERGER, J., ELMHAGEN, B., LETNIC, M., NELSON, M. P., SCHMITZ, O. J., SMITH, D. W., WALLACH, A. D. and WIRSING, A. J. 2014. Status and Ecological Effects of the World's Largest Carnivores. *Science*, **343**, 1241484.

RITCHIE, E. G. and JOHNSON, C. N. 2009. Predator interactions, mesopredator release and biodiversity conservation. *Ecology Letters*, **12**, 982–998.

ROOPNARINE, P. D. and ANGIELCZYK, K. D. 2015. Community stability and selective extinction during the Permian-Triassic mass extinction. *Science*, **350**, 90–93.

——— and DINEEN, A. A. 2018. Coral Reefs in Crisis: The Reliability of Deep-Time Food Web Reconstructions as Analogs for the Present. *In* TYLER, C. L. and SCHNEIDER, C. L. (eds.) *Marine Conservation Paleobiology*, Springer International Publishing, Cham, 105–141 pp.

ROOPNARINE, P. D., ANGIELCZYK, K. D., WANG, S. C. and HERTOG, R. 2007. Trophic network models explain instability of Early Triassic terrestrial communities. *Proceedings of the Royal Society B: Biological Sciences*, **274**, 2077–2086.

ROOPNARINE, P. D., ANGIELCZYK, K. D., OLROYD, S. L., NESBITT, S. J., BOTHA-BRINK, J., PEECOOK, B. R., DAY, M. O. and SMITH, R. M. H. 2017. Comparative ecological dynamics of Permian-Triassic communities from the Karoo, Luangwa, and Ruhuhu Basins of southern Africa. *Journal of Vertebrate Paleontology*, **37**, 254–272.

ROSSI, L., SPORTA CAPUTI, S., CALIZZA, E., CAREDDU, G., OLIVERIO, M., SCHIAPARELLI, S. and COSTANTINI, M. L. 2019. Antarctic food web architecture under varying dynamics of sea ice cover. *Scientific Reports*, **9**, 12454.

RUSSELL, D. A. 1970. *Tyrannosaurs From the Late Cretaceous of Western Canada*. National Museums of Canada, Ottawa.

RUSSELL, L. S. 1966. Dinosaur hunting in Western Canada. *Royal Ontario Museum Life Sciences Contributions*, **70**, 1–37.

RYAN, M. J. and RUSSELL, A. P. 2001. Dinosaurs of Alberta (exclusive of Aves). *In* TANKE, D. H. and CARPENTER, K. (eds.) *Mesozoic Vertebrate Life*, Indiana University Press, Bloomington, 279–297 pp.

RYAN, M. J. and RUSSELL, A. P. 2005. A new centrosaurine ceratopsid from the Oldman Formation of Alberta and its implications for centrosaurine taxonomy and systematics. *Canadian Journal of Earth Sciences*, **42**, 1369–1387.

RYAN, M. J., RUSSELL, A. P., EBERTH, D. A. and CURRIE, P. J. 2001. The Taphonomy of a *Centrosaurus* (Ornithischia: Ceratopsidae) Bone Bed from the Dinosaur Park Formation (Upper Campanian), Alberta, Canada, with Comments on Cranial Ontogeny. *Palaios*, **16**, 482–506.

RYAN, M. J., EVANS, D. C., CURRIE, P. J. and LOEWEN, M. A. 2014. A new chasmosaurine from northern Laramidia expands frill disparity in ceratopsid dinosaurs. *Naturwissenschaften*, **101**, 505–512.

———, ———, ———, BROWN, C. M. and BRINKMAN, D. 2012. New leptoceratopsids from the Upper Cretaceous of Alberta, Canada. *Cretaceous Research*, **35**, 69–80.

SAALFELD, D. T., CONWAY, W. C. and CALKINS, G. E. 2011. Food Habits of American Alligators (*Alligator mississippiensis*) in East Texas. *Southeastern Naturalist*, **10**, 659–672.

SAIGO, M., ZILLI, F. L., MARCHESE, M. R. and DEMONTE, D. 2015. Trophic level, food chain length and omnivory in the Paraná River: a food web model approach in a floodplain river system. *Ecological Research*, **30**, 843–852.

SANKEY, J. T., BRINKMAN, D. B., GUENTHER, M. and CURRIE, P. J. 2002. Small theropod and bird teeth from the late Cretaceous (late Campanian) Judith River Group, Alberta. *Journal of Paleontology*, **76**, 751–763.

SATO, H., MURRAY, A. M., VERNYGORA, O. and CURRIE, P. J. 2018. A rare, articulated sturgeon (Chondrostei: Acipenseriformes) from the Upper Cretaceous of Dinosaur Provincial Park, Alberta, Canada. *Journal of Vertebrate Paleontology*, **38**, (1)-(15).

SCHERER, C. R. and VOICULESCU-HOLVAD, C. 2024. Reanalysis of a dataset refutes claims of anagenesis within *Tyrannosaurus*-line tyrannosaurines (Theropoda, Tyrannosauridae). *Cretaceous Research*, **155**, 105780.

SCHROEDER, K., LYONS, S. K. and SMITH, F. A. 2021. The influence of juvenile dinosaurs on community structure and diversity. *Science*, **371**, 941–944.

SCOTT, W. B. and CROSSMAN, E. J. 1973. *Freshwater fishes of Canada*. Bulletin, Fisheries Board of Canada.

SERENO, P. C., MARTINEZ, R. N., WILSON, J. A., VARRICCHIO, D. J., ALCOBER, O. A. and LARSSON, H. C. E. 2008. Evidence for avian intrathoracic air sacs in a new predatory dinosaur from Argentina. *Plos ONE*, **3**, e3303.

SINCLAIR, A. R. E., MDUMA, S. and BRASHARES, J. S. 2003. Patterns of predation in a diverse predator–prey system. *Nature*, **425**, 288–290.

SMUTS, G. L., ROBINSON, G. A. and WHYTE, I. J. 1980. Comparative growth of wild male and female lions (*Panthera leo*). *Journal of Zoology*, **190**, 365–373.

SPENCER, L. M., VALKENBURGH, B. V. and HARRIS, J. M. 2003. Taphonomic analysis of large mammals recovered from the Pleistocene Rancho La Brea tar seeps. *Paleobiology*, **29**, 561–575.

STEWART, M. M. and SANDISON, P. 1972. Comparative Food Habits of Sympatric Mink Frogs, Bullfrogs, and Green Frogs. *Journal of Herpetology*, **6**, 241–244.

TANKE, D. H. 2005. Identifying Lost Quarries. *In* CURRIE, P. J. and KOPPELHUS, E. B. (eds.) *Dinosaur Provincial Park: A Spectacular Ancient Ecosystem Revealed*, Indiana University Press, Bloomington, 34–53 pp.

THERRIEN, F., ZELENITSKY, D. K., VORIS, J. T. and TANAKA, K. 2021. Mandibular force profiles and tooth morphology in growth series of *Albertosaurus sarcophagus* and *Gorgosaurus libratus*

(Tyrannosauridae: Albertosaurinae) provide evidence for an ontogenetic dietary shift in tyrannosaurids. *Canadian Journal of Earth Sciences*, **58**, 812–828.

———, ———, TANAKA, K., VORIS, J. T., ERICKSON, G. M., CURRIE, P. J., DEBUHR, C. L. and KOBAYASHI, Y. 2023. Exceptionally preserved stomach contents of a young tyrannosaurid reveal an ontogenetic dietary shift in an iconic extinct predator. *Science Advances*, **9**, eadi0505.

THOMAS, R. G., EBERTH, D. A., DEINO, A. L. and ROBINSON, D. 1990. Composition, radioisotopic ages, and potential significance of an altered volcanic ash (bentonite) from the Upper Cretaceous Judith River Formation, Dinosaur Provincial Park, southern Alberta, Canada. *Cretaceous Research*, **11**, 125–162.

TITUS, A. L., KNOLL, K., SERTICH, J. J. W., YAMAMURA, D., SUAREZ, C. A., GLASSPOOL, I. J., GINOUVES, J. E., LUKACIC, A. K. and ROBERTS, E. M. 2021. Geology and taphonomy of a unique tyrannosaurid bonebed from the upper Campanian Kaiparowits Formation of southern Utah: implications for tyrannosaurid gregariousness. *PeerJ*, **9**, e11013.

TREBILCO, R., BAUM, J. K., SALOMON, A. K. and DULVY, N. K. 2013. Ecosystem ecology: size-based constraints on the pyramids of life. *Trends in Ecology & Evolution*, **28**, 423–431.

TUCKER, A. D., LIMPUS, C. J., MCCALLUM, H. I. and MCDONALD, K. R. 1996. Ontogenetic Dietary Partitioning by *Crocodylus johnstoni* during the Dry Season. *Copeia*, **1996**, 978–988.

VARRICCHIO, D. J., MOORE, J. R., ERICKSON, G. M., NORELL, M. A., JACKSON, F. D. and BORKOWSKI, J. J. 2008. Avian Paternal Care Had Dinosaur Origin. *Science*, **322**, 1826–1828.

DE VISSER, S. N., FREYMANN, B. P. and OLFF, H. 2011. The Serengeti food web: empirical quantification and analysis of topological changes under increasing human impact. *Journal of Animal Ecology*, **80**, 484–494.

VORIS, J. T., ZELENITSKY, D. K., THERRIEN, F., RIDGELY, R. C., CURRIE, P. J. and WITMER, L. M. 2022. Two exceptionally preserved juvenile specimens of *Gorgosaurus libratus*

(Tyrannosauridae, Albertosaurinae) provide new insight into the timing of ontogenetic changes in tyrannosaurids. *Journal of Vertebrate Paleontology*, **41**, e2041651.

WANG, S., STIEGLER, J., AMIOT, R., WANG, X., DU, G., CLARK, J. M. and XU, X. 2017. Extreme Ontogenetic Changes in a Ceratosaurian Theropod. *Current Biology*, **27**, 144–148.

WANG, S. C. and DODSON, P. 2006. Estimating the diversity of dinosaurs. *Proceedings of the National Academy of Sciences*, **103**, 13601–13605.

WERNER, E. E. and GILLIAM, J. F. 1984. The Ontogenetic Niche and Species Interactions in Size-Structured Populations. *Annual Review of Ecology, Evolution, and Systematics*, **15**, 393–425.

WILLIAMS, R. J. 2010. Network3D Software. .

WILLIAMS, R. J. and MARTINEZ, N. D. 2000. Simple rules yield complex food webs. *Nature*, **404**, 180–183.

WILLIAMS, R. J. and MARTINEZ, N. D. 2004. Limits to Trophic Levels and Omnivory in Complex Food Webs: Theory and Data. *The American Naturalist*, **163**, 458–468.

WILLIAMS, T. A. and CHRISTIANSEN, J. L. 1981. The Niches of Two Sympatric Softshell Turtles, *Trionyx muticus* and *Trionyx spiniferus*, in Iowa. *Journal of Herpetology*, **15**, 303–308.

WOLFE, J. A. and UPCHURCH, G. R. 1987. North American nonmarine climates and vegetation during the Late Cretaceous. *Palaeogeography, Palaeoclimatology, Palaeoecology*, **61**, 33–77.

WOOD, J. M. 1989. Alluvial architecture of the Upper Cretaceous Judith River Formation, Dinosaur Provincial Park, Alberta, Canada. *Bulletin of Canadian Petroleum Geology*, **37**, 169–181.

———, THOMAS, R. G. and VISSER, J. 1988. Fluvial processes and vertebrate taphonomy: the Upper Cretaceous Judith River formation, South-Central dinosaur Provincial Park, Alberta, Canada. *Palaeogeography, Palaeoclimatology, Palaeoecology*, **66**, 127–143.

WOODRUFF, D. C., SCHOTT, R. K. and EVANS, D. C. 2023. Two new species of small-bodied pachycephalosaurine (Dinosauria, Marginocephalia) from the uppermost Cretaceous of North

America suggest hidden diversity in well-sampled formations. *Papers in Palaeontology*, **9**, e1535.

———, CARR, T. D., STORRS, G. W., WASKOW, K., SCANNELLA, J. B., NORDÉN, K. K. and WILSON, J. P. 2018. The Smallest Diplodocid Skull Reveals Cranial Ontogeny and Growth-Related Dietary Changes in the Largest Dinosaurs. *Scientific Reports*, **8**, 14341.

WU, X.-C. 2005. Crocodylians. *In* CURRIE, P. J. and KOPPELHUS, E. B. (eds.) *Dinosaur Provincial Park: A Spectacular Ancient Ecosystem Revealed*, Indiana University Press, Bloomington, 277–291 pp.

WYENBERG-HENZLER, T., PATTERSON, R. T. and MALLON, J. C. 2021. Size-mediated competition and community structure in a Late Cretaceous herbivorous dinosaur assemblage. *Historical Biology*, **34**, 2230–2240.

———, ——— and ———. 2022. Ontogenetic dietary shifts in North American hadrosaurids (Dinosauria: Ornithischia). *Cretaceous Research*, **135**, 105177.

XU, X., NORELL, M. A., KUANG, X., WANG, X., ZHAO, Q. and JIA, C. 2004. Basal tyrannosauroids from China and evidence for protofeathers in tyrannosauroids. *Nature*, **431**, 680–4.

———, WANG, K., ZHANG, K., MA, Q., XING, L., SULLIVAN, C., HU, D., CHENG, S. and WANG, S. 2012. A gigantic feathered dinosaur from the Lower Cretaceous of China. *Nature*, **484**, 92–95.

YODZIS, P. 1998. Local trophodynamics and the interaction of marine mammals and fisheries in the Benguela ecosystem. *Journal of Animal Ecology*, **67**, 635–658.

YOON, I., WILLIAMS, R. J., LEVINE, E., YOON, S., DUNNE, J. A. and MARTINEZ, N. D. 2004. Webs on the Web (WOW): 3D visualization of ecological networks on the WWW for collaborative research and education. *Visualization and Data Analysis*, **5295**, 124–132.

4.7 Figures

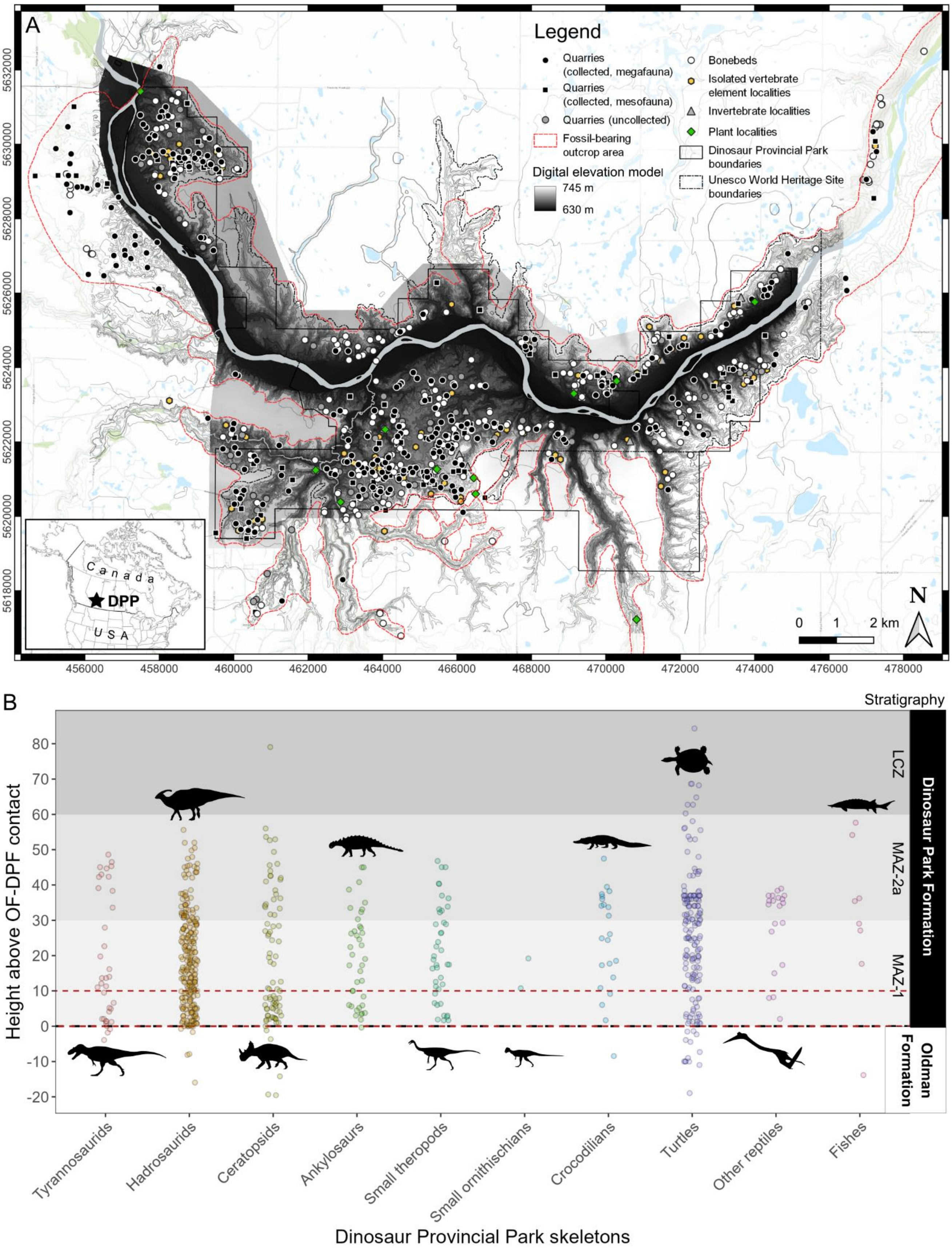
A
Legend
Quarries (collected, megafauna)
Quarries (collected, mesofauna)
Quarries (uncollected)
Fossil-bearing outcrop area
Digital elevation model
745 m
630 m
Bonebeds
Isolated vertebrate element localities
Invertebrate localities
Plant localities
Dinosaur Provincial Park boundaries
Unesco World Heritage Site boundaries
Canada
DPP
USA
N
0 1 2 km
5632000
5630000
5628000
5626000
5624000
5622000
5620000
5618000
456000
458000
460000
462000
464000
466000
468000
470000
472000
474000
476000
478000
B
Stratigraphy
LCZ
MAZ-2a
MAZ-1
Dinosaur Park Formation
Oldman Formation
Height above OF-DPF contact
80
70
60
50
40
30
20
10
0
-10
-20
Tyrannosaurids
Hadrosaurids
Ceratopsids
Ankylosaurs
Small theropods
Small ornithischians
Crocodilians
Turtles
Other reptiles
Fishes
Dinosaur Provincial Park skeletons

Figure 4.1. Geographical and stratigraphic location of main fossil quarries and outcropping areas of the Belly River Group (BRG) in Dinosaur Provincial Park (DPP) and vicinity, Alberta, Canada. A, geographical location of quarries within and immediately outside DPP. Coordinates in WGS84 / Universal Transverse Mercator zone 12N, EGM96 geoid. Digital elevation model created via Lidar coverage achieved in 2015, provided courtesy of the Royal Tyrrell Museum of Palaeontology (TMP). Elevation contour lines redrawn from topographic map of DPP (2013) georeferenced on QGIS. B, stratigraphic distribution of all associated fossil vertebrate skeletons collected from DPP area with known locality coordinates. Quarry and formational contact locations available from database assembled by first author, updated from Currie and Koppelhus (2005: Supplementary CD-ROM; Appendix II); dotted red lines denote Dinosaur Park Formation Megaherbivore Assemblage Zone 1a (DPF MAZ-1a), the stratigraphic interval used as main reference for time-constrained biomass density estimates.

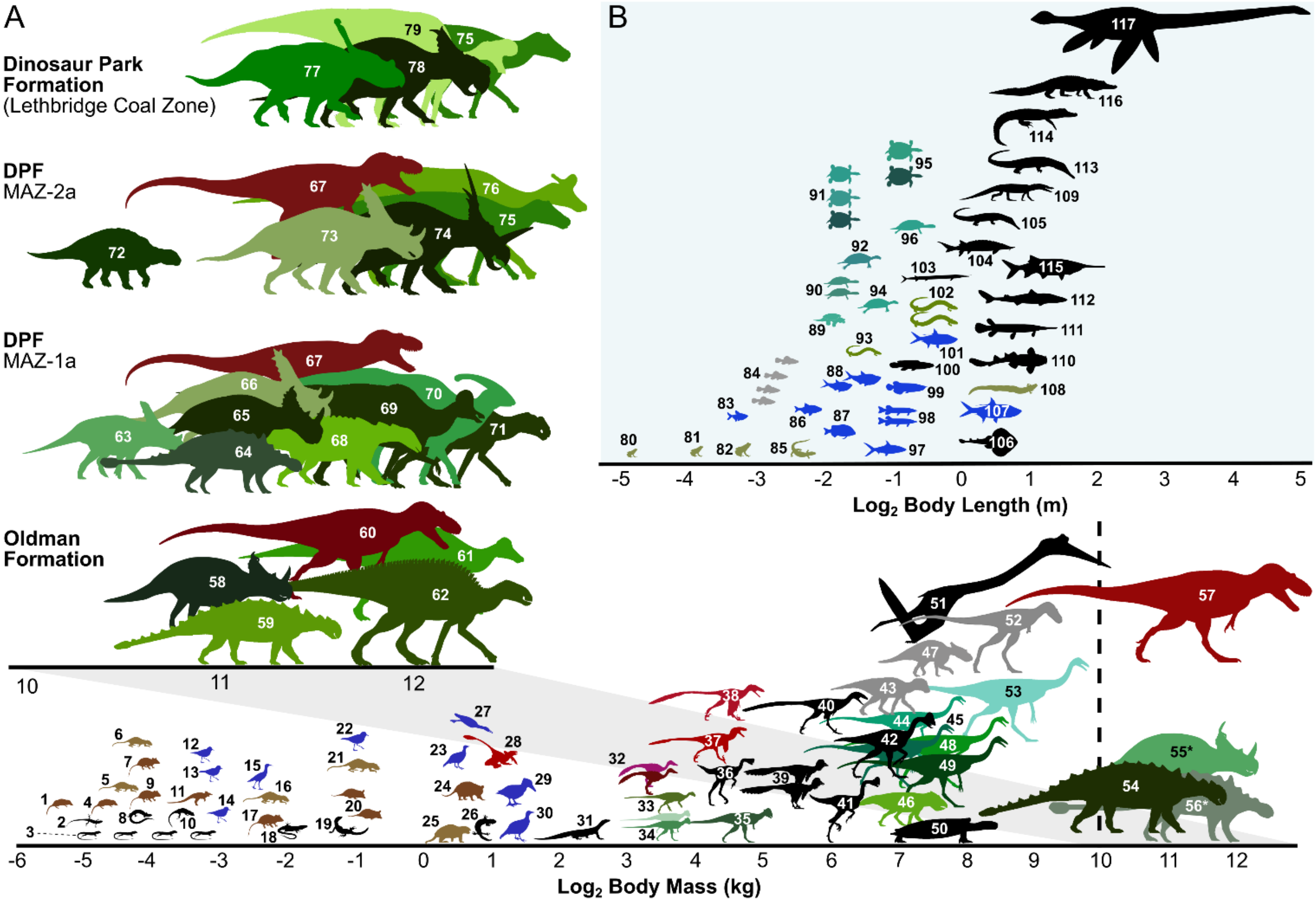

1 *Paranyctoides sternbergi*
2 *Orthrioscincus mixtus*
3 Small teiid lizards (4)
4 Cimolestidae
5 *Cimexomys* spp.
6 *Mesodma primaeva*
7 *Pediomys* spp.
8 *Odaxosaurus priscus*
9 *Alphadon halleyi*
10 ?*Exostinus* sp.
11 *Gypsonictops lewisi*
12 Ornithurine B
13 Ornithurine F
14 Ornithurine C
15 Ornithurine E
16 *Cimolodon* spp.
17 *Turgidodon praesagus*
18 *Socognathus unicuspis*
19 *Parasaniwa* sp.
20 *Eodelphis browni* and *Eodelphis cutleri*
21 *Cimolomys clarki*
22 Ornithurine D
23 *Palintropus* sp. B
24 *Didelphodon* sp.
25 *Meniscoessus major*
26 *Labrodioctes* cf. *montanensis*
27 Ornithurine A
28 *Hesperonychus elizabethae*
29 Ornithurine G
30 *Palintropus* sp. A
31 *Palaeosaniwa canadensis*
32 cf. *Richardoestesia gilmorei* and cf. *R. isosceles*
33 Orodrominae
34 *Foraminacephale brevis* and *Sphaerotholus lyonsi*
35 *Stegoceras validum*
36 *Citipes elegans*
37 *Dromaeosaurus albertensis*
38 *Saurornitholestes langstoni*
39 cf. *Paronychodon* and cf. *Pectinodon*
40 *Stenonychosaurus inequalis*
41 *Chirostenotes pergracilis*
42 *Caenagnathus collinsi*
43 Juvenile hadrosaurid
44 cf. *Qiupalong* sp.
45 *Rativates evadens*
46 *Unescoceratops koppelhusae*
47 Juvenile ceratopsid
48 *Struthiomimus altus*
49 *Ornithomimius edmontonicus*
50 *Basilemys variolosa*
51 *Cryodrakon boreas*
52 Juvenile tyrannosaurid
53 Large unnamed ornithomimid
54 *Euoplocephalus tutus*
55 *Spinops sternbergorum*
56 *Anodontosaurus lambei*
57 *Gorgosaurus libratus*
58 *Coronosaurus brinkmani*
59 *Scolosaurus cutleri*
60 *Daspletosaurus torosus*
61 cf *Hypacrosaurus*
62 *Brachylophosaurus canadensis*
63 *Mercuriceratops gemini*
64 *Dyoplosaurus acutosquameus*
65 *Centrosaurus apertus*
66 *Chasmosaurus russelli*
67 *Daspletosaurus* sp.
68 *Edmontonia rugosidens*
69 *Corythosaurus casuarius*
70 *Parasaurolophus walkeri*
71 *Gryposaurus notabilis*
72 *Panoplosaurus mirus*
73 *Chasmosaurus belli*
74 *Styracosaurus albertensis*
75 *Prosaurolophus maximus*
76 *Lambeosaurus lambei*
77 *Chasmosaurus irvinensis*
78 cf. *Achelousaurus*
79 *Lambeosaurus magnicristatus*

80 *Tyrrellbatrachus brinkmani*
81 Anura indet.
82 *Hensonbatrachus kermiti*
83 Characiformes
84 Acanthomorpha (4)
85 *Albanerpeton* spp.
86 Hiodontidae
87 *Cretophareodus alberticus*
88 *Horseshoeichthys* sp. and *Diplomystus* sp.
89 Chelydridae
90 *Plesiobaena antiqua* and *Boremys pulchra*
91 *Axestemys foveatus*, *A. allani* and "*Apalone*" *latus*
92 *Adocus* sp.
93 *Opisthotriton kayi*
94 *Judithemys sukhanovi*
95 *Axestemys splendida* and Trionychidae gen. et sp. indet
96 *Neurankylus eximius*
97 *Notogoneus* sp.
98 *Oldmanesox canadensis* and *Estesesox foxi*
99 *Coriops amnicolus*
100 Amiidae
101 *Paralbula casei*
102 *Scapherpeton tectum* and *Lisserpeton bairdi*
103 *Belonostomus longirostris*
104 *Anchiacipenser acanthaspis*
105 *Champsosaurus lindoei*
106 *Myledaphus bipartitus*
107 *Paratarpon apogerontus*
108 *Habrosaurus prodilatus*
109 cf. *Stangerochampsa*
110 Orectolobidae
111 *Lepisosteus*
112 *Hybodus montanensis*
113 *Champsosaurus natator*
114 *Albertochampsa langstoni*
115 Polyodontidae
116 *Leidyosuchus canadensis*
117 *Fluvionectes sloanae*

Figure 4.2. Body size distribution of vertebrate taxa known from Dinosaur Provincial Park and nearby localities of the Belly River Group in Alberta. A, terrestrial tetrapods distributed along body mass axis: taxa found throughout the Oldman and Dinosaur Park Formations (DPF) presented along main axis (exception: *Anodontosaurus lambei* and *Spinops sternbergorum* based solely on specimens lacking stratigraphic locality data, thus marked with asterisk); taxa found in distinct megafaunal assemblage zones presented along secondary axis constrained to higher body masses; dashed line indicates taphonomic size bias threshold (~1,000 kg), on the right of which species are usually known from far more complete fossil material (Brown *et al.* 2013*b*). DPF MAZ-1b megafauna not on display due to redundant overlaps in faunal composition with MAZ-1a and MAZ-2a. Silhouette colours are as follows: dark to pale green for herbivorous dinosaurs, red to dark pink for hypercarnivorous dinosaurs, blue for birds, pale brown for multituberculates, dark brown for therians, grey for juvenile megafauna. B, aquatic and semiaquatic vertebrates known from upper DPF distributed along body length axis. Silhouette colours are as follows: turquoise for turtles, olive green for amphibians, blue for teleosts (except acanthomorphs in grey due to lack of body length estimates). Silhouettes of smaller animals not to scale. Silhouette references: juvenile tyrannosaurid from Therrien *et al*. (2023), juvenile ceratopsid from Currie *et al*. (2016), *Caenagnathus*, *Chirostenotes* and *Citipes* from Funston (2020), *Corythosaurus* from G. Paul in Carpenter (2010), see Appendix V for acknowledgements for other silhouettes.

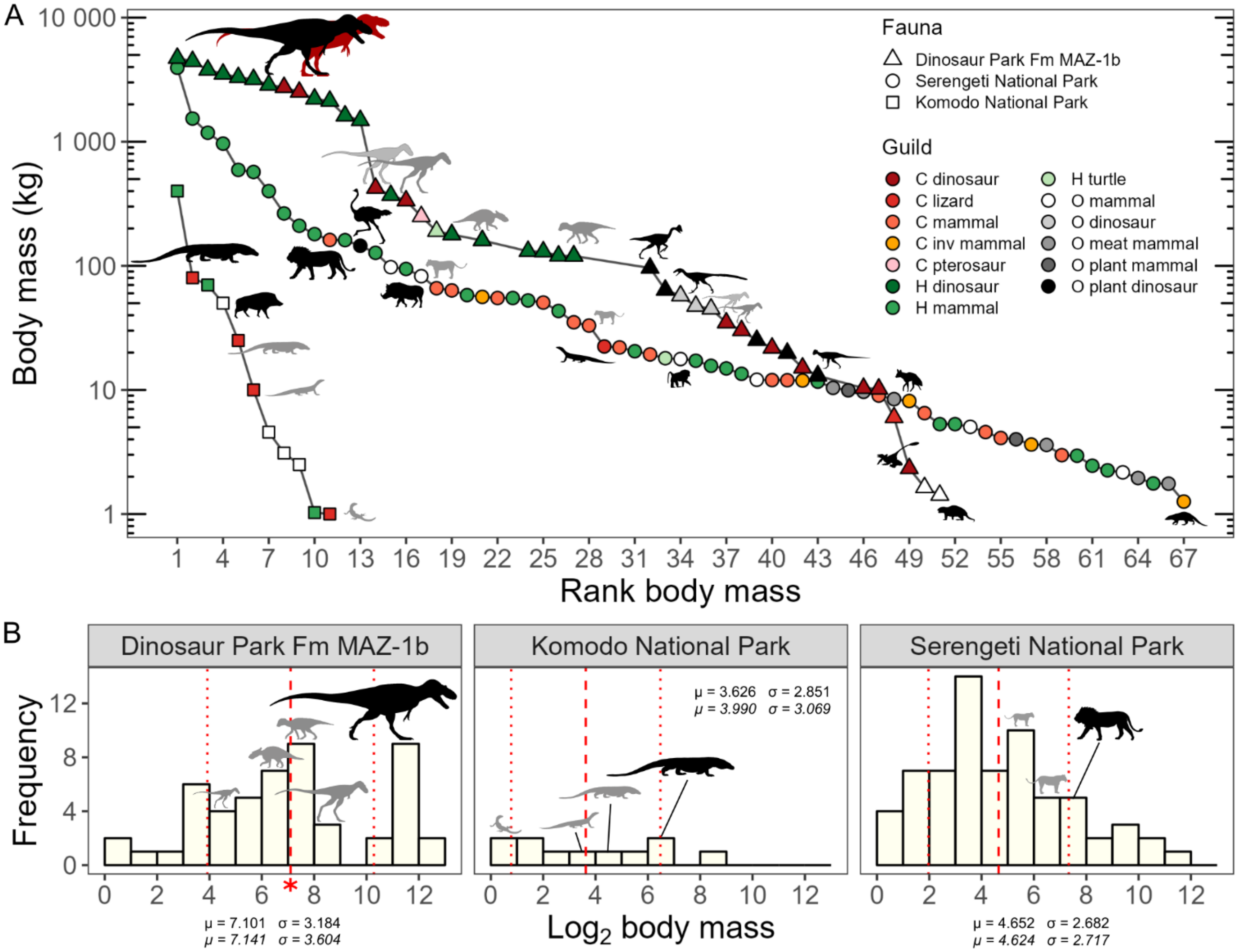
A
10 000
1 000
100
10
1
Body mass (kg)
1
4
7
10
13
16
19
22
25
28
31
34
37
40
43
46
49
52
55
58
61
64
67
Rank body mass
Fauna
Dinosaur Park Fm MAZ-1b
Serengeti National Park
Komodo National Park
Guild
C dinosaur
C lizard
C mammal
C inv mammal
C pterosaur
H dinosaur
H mammal
H turtle
O mammal
O dinosaur
O meat mammal
O plant mammal
O plant dinosaur
B
Dinosaur Park Fm MAZ-1b
Komodo National Park
Serengeti National Park
Frequency
12
8
4
0
0
2
4
6
8
10
12
*
μ = 7.101 σ = 3.184
μ = 7.141 σ = 3.604
μ = 3.626 σ = 2.851
μ = 3.990 σ = 3.069
Log2 body mass
μ = 4.652 σ = 2.682
μ = 4.624 σ = 2.717

Figure 4.3. Body size distributions of the Komodo, Serengeti, and Dinosaur Park Formation (DPF) MAZ-1b terrestrial communities. All native mammals >1 kg are included; DPF dataset contains all non-avialan dinosaurs, including juvenile tyrannosaurids, hadrosaurids, and ceratopsids (in grey, see Material and methods), and largest pterosaur, turtle and lizard; extant datasets include lion and Komodo dragon juvenile stages (in grey, see Material and methods); Serengeti dataset includes largest bird, turtle and lizard. A, cenograms highlighting distribution of feeding guilds (C, carnivore; H, herbivore; O, omnivore, including plant- or meat-dominated diets). B, histograms including aforementioned juveniles; mean body mass in DPF differs significantly from Serengeti (*p*-value = 9.7e^{-05} with juveniles; 0.0012 without) and from Komodo only when juveniles included (*p*-value = 0.008; 0.1288 without juveniles) (see asterisk), means and standard deviations in italics for versions excluding juveniles. Silhouette references: juvenile tyrannosaurid from Therrien *et al*. (2023), juvenile ceratopsid from Currie *et al*. (2016), see Appendix V for acknowledgements for other silhouettes.

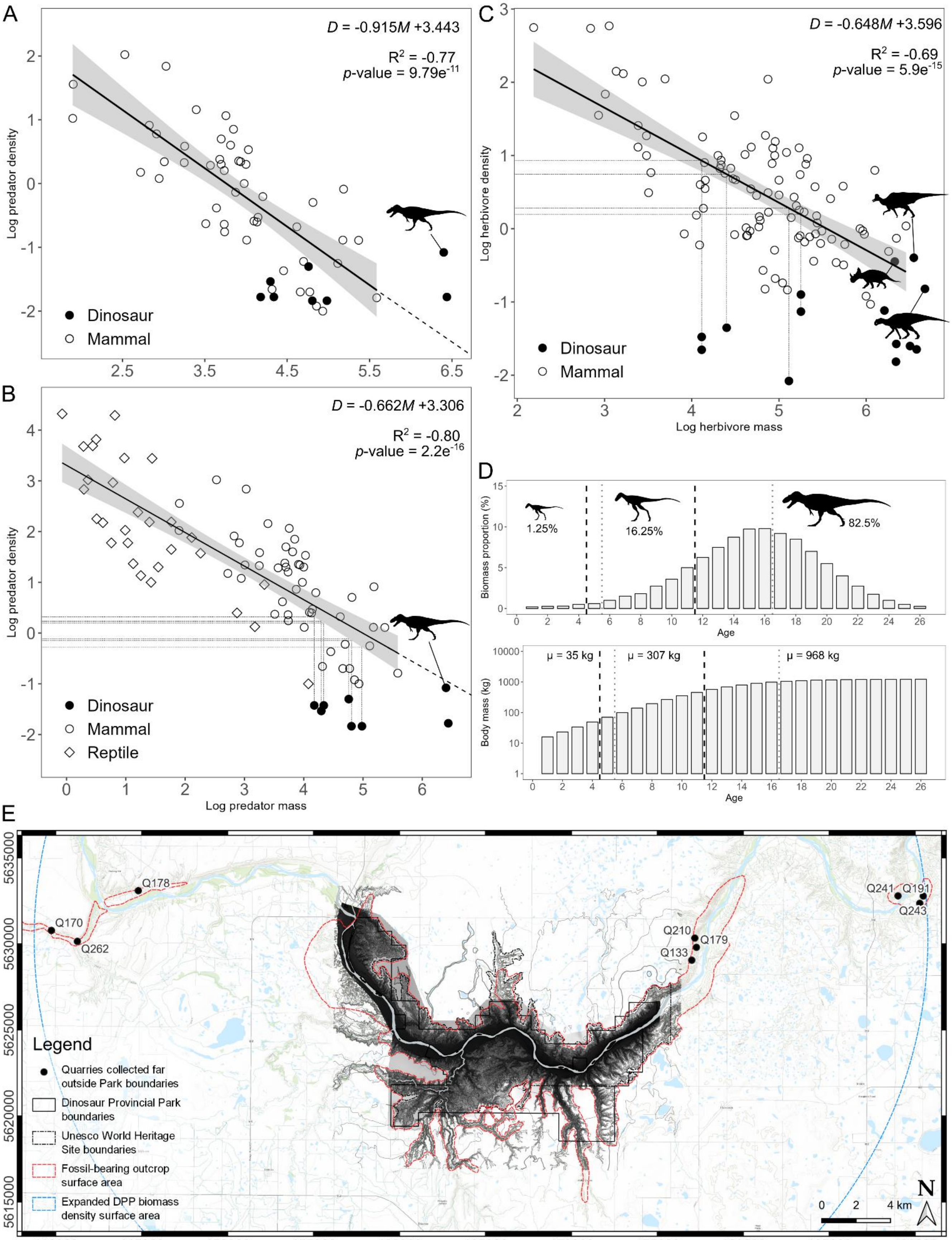
A
D = -0.915M +3.443
R² = -0.77
p-value = 9.79e-11
Log predator density
Dinosaur
Mammal
2.5
3.5
4.5
5.5
6.5
B
D = -0.662M +3.306
R² = -0.80
p-value = 2.2e-16
Log predator density
Log predator mass
Dinosaur
Mammal
Reptile
C
D = -0.648M +3.596
R² = -0.69
p-value = 5.9e-15
Log herbivore density
Log herbivore mass
Dinosaur
Mammal
D
Biomass proportion (%)
1.25%
16.25%
82.5%
Age
Body mass (kg)
μ = 35 kg
μ = 307 kg
μ = 968 kg
Age
E
Q178
Q170
Q262
Q210
Q179
Q133
Q241
Q191
Q243
Legend
Quarries collected far outside Park boundaries
Dinosaur Provincial Park boundaries
Unesco World Heritage Site boundaries
Fossil-bearing outcrop surface area
Expanded DPP biomass density surface area
N
0
2
4 km
5635000
5630000
5625000
5620000
5615000
440000
445000
450000
455000
460000
465000
470000
475000
480000
485000
490000

Figure 4.4. Body mass and density corrections for Dinosaur Provincial Park (DPP) dinosaurs. A, DPP predatory dinosaur densities observed from fossil skeleton record against body mass, compared to mammal vertebrate consumer dataset of Damuth (1987); *Gorgosaurus libratus* highlighted with silhouette. B, same dinosaur body mass-density plot compared to dataset from Damuth (1987) now including reptile and mammal vertebrate consumers, with densities corrected for metabolic rate (see Material and methods). C, DPP (Dinosaur Park Formation MAZ-1a) herbivorous dinosaur densities observed from fossil skeleton record against body mass, compared to herbivorous mammal dataset of Damuth (1987); *Centrosaurus apertus*, *Corythosaurus casuarius* and *Gryposaurus notabilis* highlighted with silhouettes. Each species' density includes proportion of skeletons unidentified at the species level based on respective frequencies of identifiable specimens; DPP densities in A-C assume 120 km^2 surface area. D, distributions of biomass proportions and body mass by age class for *Gorgosaurus libratus*. Biomass proportions obtained from Schroeder *et al*. (2021); body masses obtained from survivorship curve of Erickson *et al*. (2004, corr. 2016); black dashed lines delineate age classes defined in Therrien *et al*. (2021) (followed in this study, with corresponding total biomass proportions per age class), grey dotted lines delineate age classes defined in Schroeder *et al*. (2021); mean body mass for each age class accounts for biomass proportions. E, large-scale overview of region surrounding DPP, highlighting fossil quarries located beyond protected area boundaries yet still within Belly River Group; coloured margins correspond to 120 and 1,950 km^2 surface areas used to estimate biomass densities, the latter of which is defined by the maximum distance between two quarries. Silhouette references: juvenile tyrannosaurid from Therrien *et al*. (2023), juvenile ceratopsid from Currie *et al*. (2016), *Corythosaurus* from G. Paul in Carpenter (2010), see Appendix V for acknowledgements for other silhouettes.

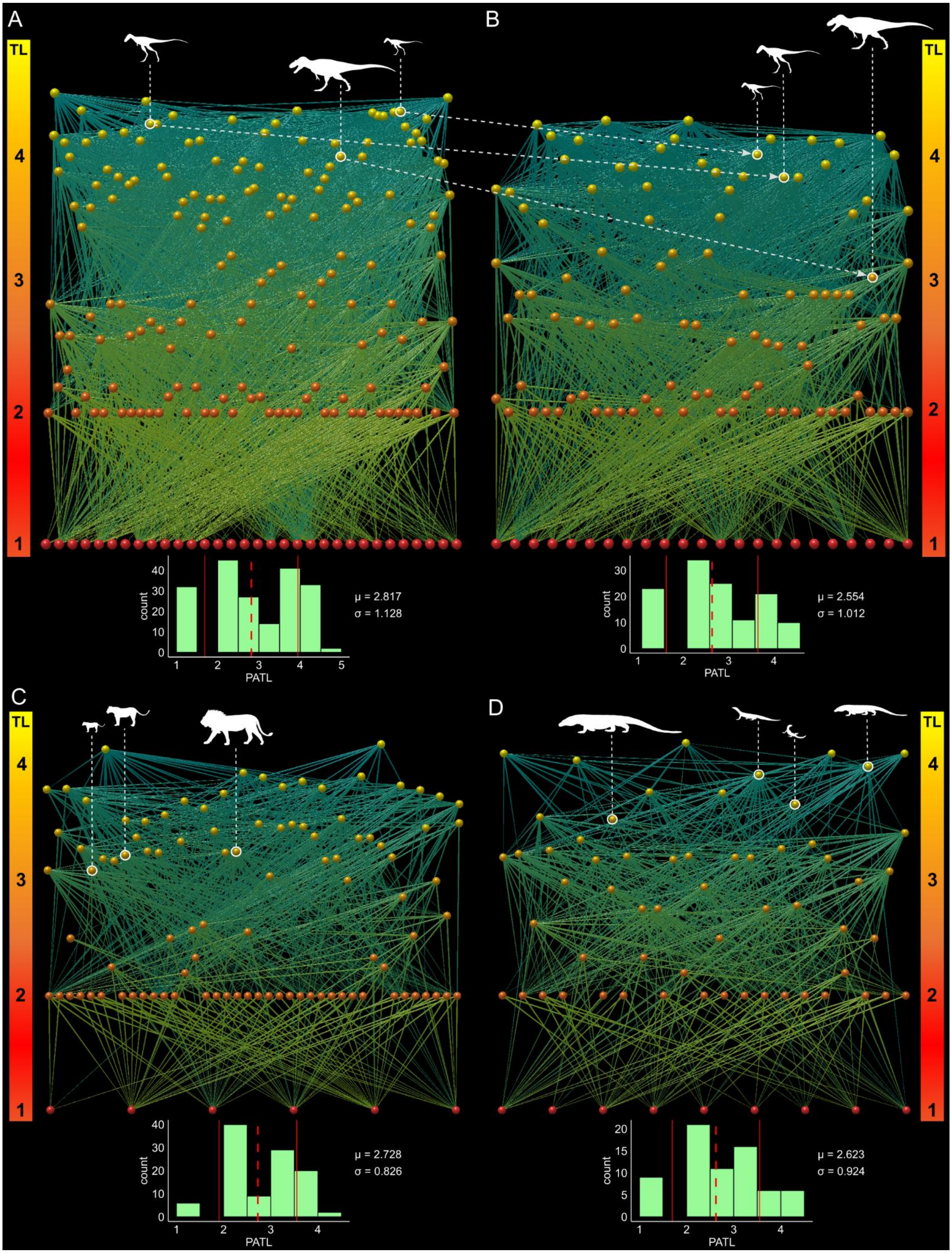
A
TL
4
3
2
1
count
40
30
20
10
0
1
2
3
4
5
PATL
μ = 2.817
σ = 1.128
B
TL
4
3
2
1
count
30
20
10
0
1
2
3
4
PATL
μ = 2.554
σ = 1.012
C
TL
4
3
2
1
count
40
30
20
10
0
1
2
3
4
PATL
μ = 2.728
σ = 0.826
D
TL
4
3
2
1
count
20
15
10
5
0
1
2
3
4
PATL
μ = 2.623
σ = 0.924

Figure 4.5. Ecological networks displaying food webs at full taxonomic resolution and prey-averaged trophic level (PATL) frequency distributions (with mean μ and standard deviation σ) for each community in this study, highlighting trophic positions of apex predators compared between them. A, B, Dinosaur Park Formation (DPF) Megaherbivore Assemblage Zone 1a (MAZ-1a) network highlighting *Gorgosaurus libratus* at young juvenile, juvenile, and subadult/adult stages in a version including terrestrial, aquatic and semiaquatic nodes (A), and a version only including terrestrial nodes with tyrannosaurid links accounting for cooperative hunting between ontogenetic stages and adults exclusively feeding on megaherbivores (B). C, Serengeti network assembled from two published food webs (Baskerville *et al.* 2011; de Visser *et al.* 2011), highlighting lion *Panthera leo* at weaned cub (young juvenile), juvenile and adult stages. D, Komodo network created from primary literature on feeding behaviour (Auffenberg 1981; Purwandana *et al.* 2016), highlighting Komodo dragon *Varanus komodoensis* at young juvenile, juvenile, subadult and adult stages. Silhouette references: juvenile tyrannosaurid from Therrien *et al*. (2023), adult male lion from G. Paola-Munoz, adult and subadult Komodo dragon modified from M. Hodiono (see Acknowledgements).

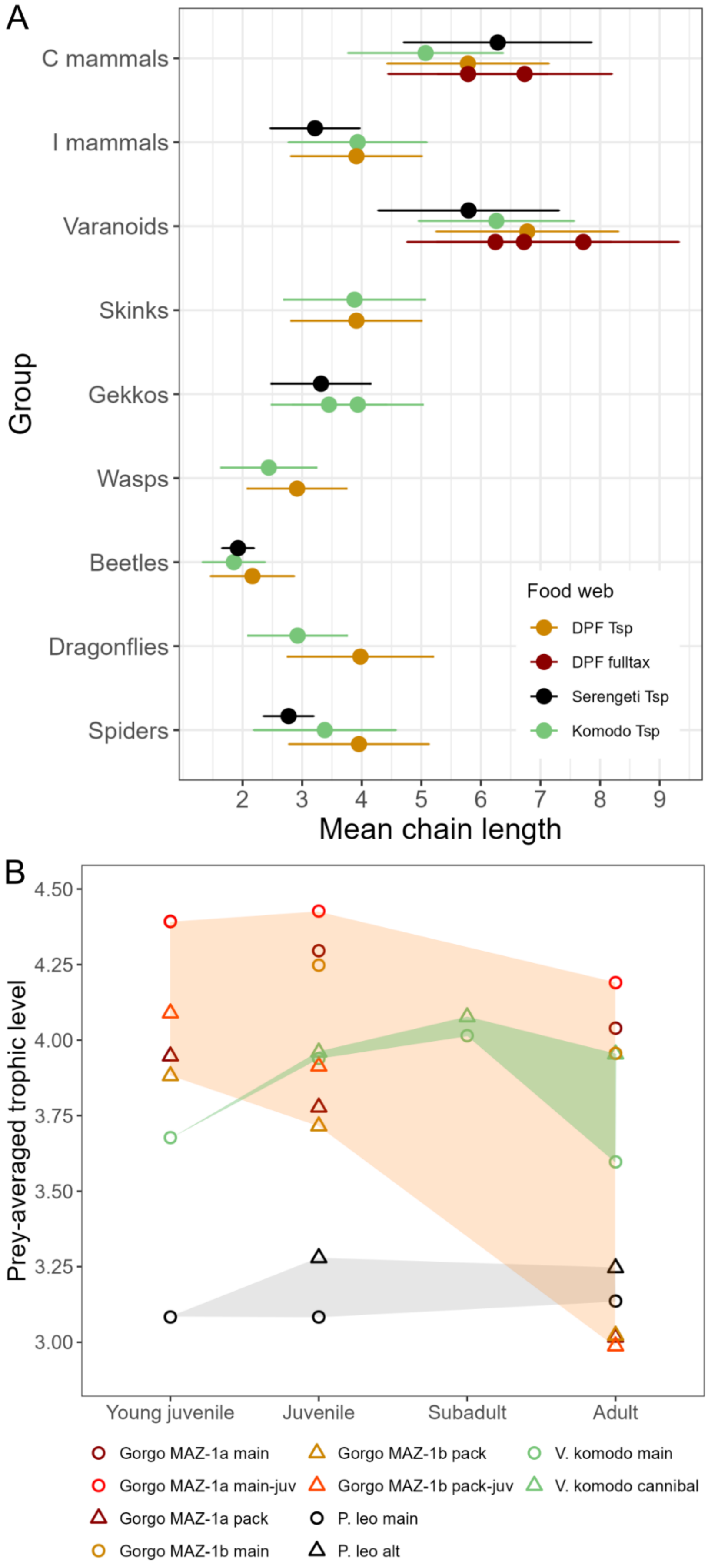
A
Group
C mammals
I mammals
Varanoids
Skinks
Gekkos
Wasps
Beetles
Dragonflies
Spiders
2
3
4
5
6
7
8
9
Mean chain length
Food web
DPF Tsp
DPF fulltax
Serengeti Tsp
Komodo Tsp
B
Prey-averaged trophic level
4.50
4.25
4.00
3.75
3.50
3.25
3.00
Young juvenile
Juvenile
Subadult
Adult
Gorgo MAZ-1a main
Gorgo MAZ-1a main-juv
Gorgo MAZ-1a pack
Gorgo MAZ-1b main
Gorgo MAZ-1b pack
Gorgo MAZ-1b pack-juv
P. leo main
P. leo alt
V. komodo main
V. komodo cannibal

Figure 4.6. Trophic positions in extinct and extant food webs. A, mean chain lengths (with standard deviations) compared between possible trophic analogues of Dinosaur Park Formation (DPF), Serengeti and Komodo food webs (see Table 4.3). Komodo varanoid is subadult *V. komodoensis*; I mammals corresponds to insectivores; C mammals correspond to meat-dominated omnivores. B, prey-averaged trophic level through ontogeny compared between DPF (*G. libratus*), Serengeti (*Panthera leo*) and Komodo (*V. komodoensis*) apex predators based on fully resolved food webs; DPF versions accounting for pack hunting also exclude aquatic and semiaquatic taxa, trophospaces illustrated by convex hulls, variances not shown for clarity. **Abbreviations: Tsp,** food web composed of trophic species; **fulltax,** food web at highest possible taxonomic resolution (with trophic species nodes split into individual species nodes).

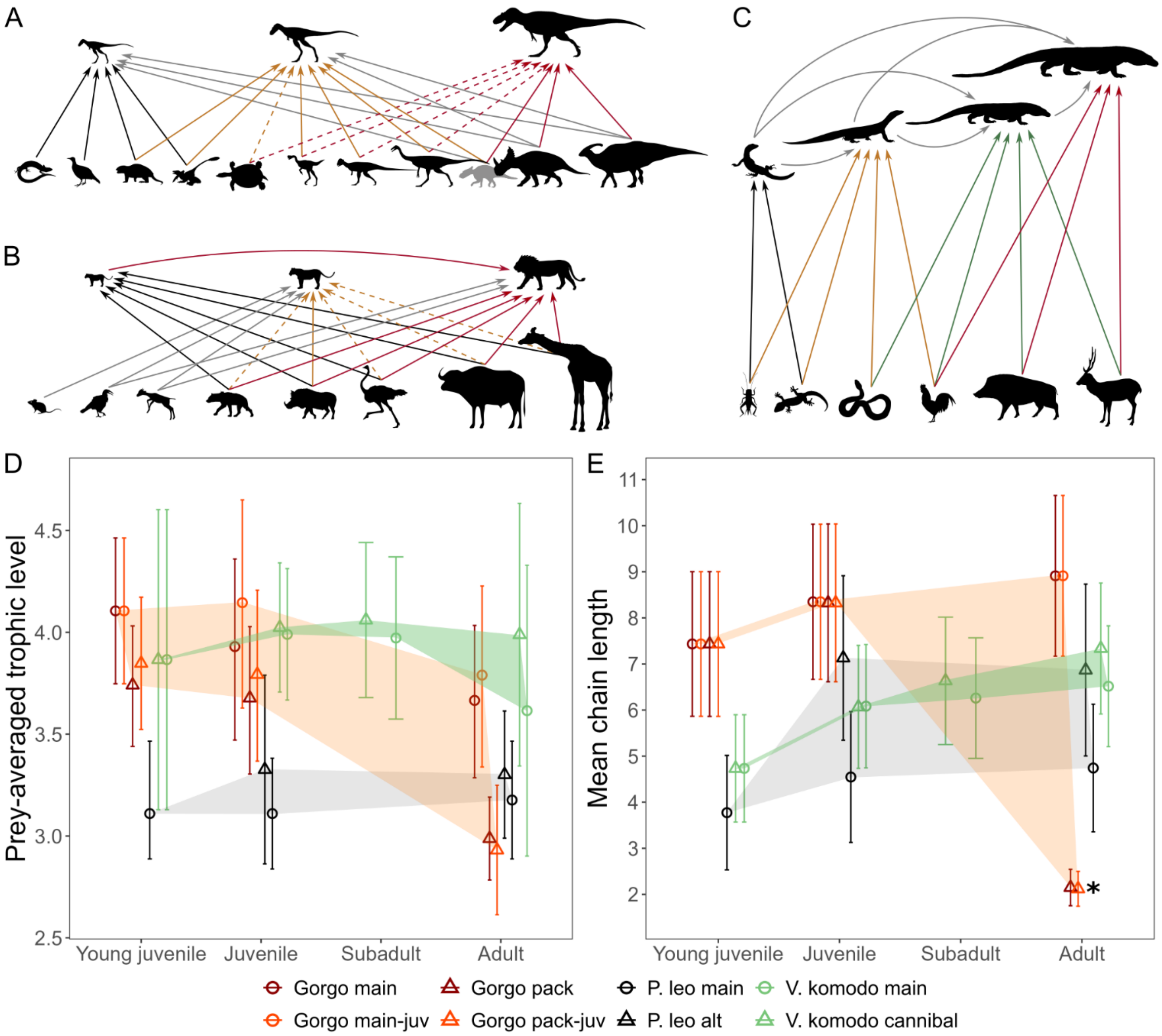
A
B
C
D
E
Prey-averaged trophic level
4.5
4.0
3.5
3.0
2.5
Mean chain length
11
10
9
8
7
6
5
4
3
2
*
Young juvenile
Juvenile
Subadult
Adult
Gorgo main
Gorgo main-juv
Gorgo pack
Gorgo pack-juv
P. leo main
P. leo alt
V. komodo main
V. komodo cannibal

Figure 4.7. Trophic position through ontogeny in extinct and extant apex predators. A, trophic links at each life stage in *Gorgosaurus libratus* (young juvenile, juvenile and subadult/adult): food webs accounting for pack hunting have links added (grey arrows) and removed (dashed arrows) compared to versions with less dietary overlap between tyrannosaurid life stages; grey silhouette indicates juvenile megaherbivore. B, trophic links at each life stage in *Panthera leo* (weaned cub, juvenile and adult): food webs including solitary hunters have links added (grey arrows) and removed (dashed arrows). C, trophic links at each life stage in *Varanus komodoensis* (young juvenile, juvenile, subadult and adult): grey arrows indicate cannibalism. D and E, shifts in trophic position through ontogeny compared between apex predators of Dinosaur Park Formation (*G. libratus*), Serengeti (*P. leo*) and Komodo (*V. komodoensis*), measured with (D) prey-averaged trophic level (with 95% confidence interval of mean) and (E) mean chain length (with standard deviation) based on trophic species food web versions. Trophospaces illustrated with convex hulls, asterisk in E indicates significantly different mean chain length for adult *G. libratus*. Silhouette references: juvenile tyrannosaurid from Therrien *et al*. (2023), juvenile ceratopsid from Currie *et al*. (2016), *Citipes* from Funston (2020), adult and subadult Komodo dragon modified from M. Hodiono, see Appendix V for acknowledgements for other silhouettes.

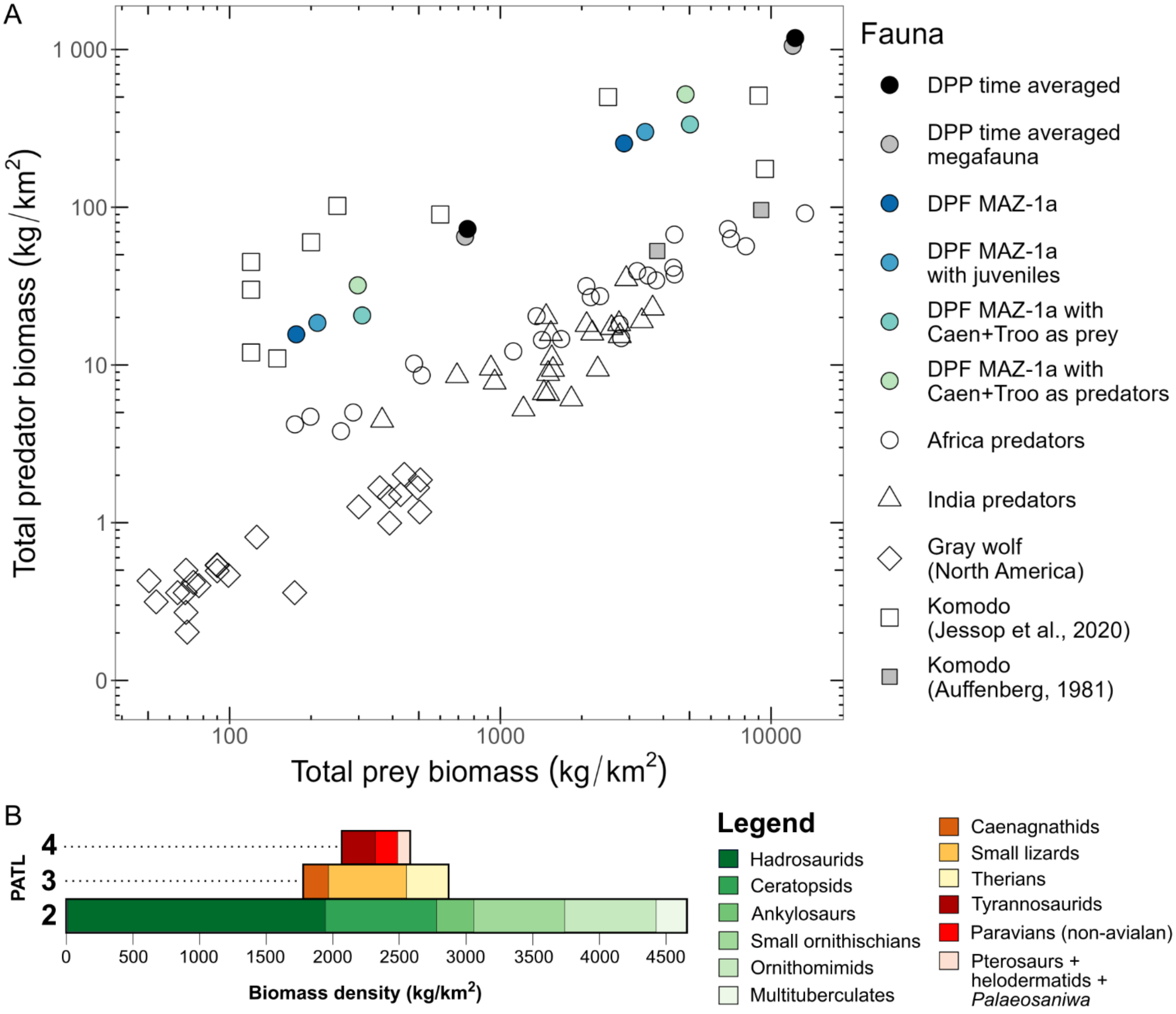
A
Total predator biomass (kg/km^2)
1 000
100
10
1
0
100
1000
10000
Total prey biomass (kg/km^2)
Fauna
DPP time averaged
DPP time averaged megafauna
DPF MAZ-1a
DPF MAZ-1a with juveniles
DPF MAZ-1a with Caen+Troo as prey
DPF MAZ-1a with Caen+Troo as predators
Africa predators
India predators
Gray wolf (North America)
Komodo (Jessop et al., 2020)
Komodo (Auffenberg, 1981)
B
PATL
4
3
2
0
500
1000
1500
2000
2500
3000
3500
4000
4500
Biomass density (kg/km^2)
Legend
Hadrosaurids
Ceratopsids
Ankylosaurs
Small ornithischians
Ornithomimids
Multituberculates
Caenagnathids
Small lizards
Therians
Tyrannosaurids
Paravians (non-avialan)
Pterosaurs + helodermatids + *Palaeosaniwa*

Figure 4.8. Biomass density estimates for Dinosaur Provincial Park (DPP) biota focused on Dinosaur Park Formation Megaherbivore Assemblage Zone 1a (MAZ-1a). A, total predator biomass density plotted against total prey biomass density, compared between DPP and extant communities, only including dinosaur/mammal predators and prey >5kg. DPP cluster on the left represents biomass densities calculated for 1,950 km^2 surface area, DPP cluster on the right represents biomass densities calculated for 120 km^2 surface area. Data for Africa, India and gray wolf obtained from Hatton *et al*. (2015). B, trophic biomass density pyramid for DPF MAZ-1a using prey-averaged trophic level (PATL) of fully resolved food web, assuming 120 km^2 surface area, not including juvenile megafauna. Hadrosaurid, ceratopsid, ankylosaur, tyrannosaurid and pterosaur densities estimated from quarry locality database assembled by first author, updated from Currie and Koppelhus (2005: Supplementary CD-ROM; Appendix II); other densities corrected with mass-density regressions (Damuth 1987), see Material and methods and Figure 4.4.

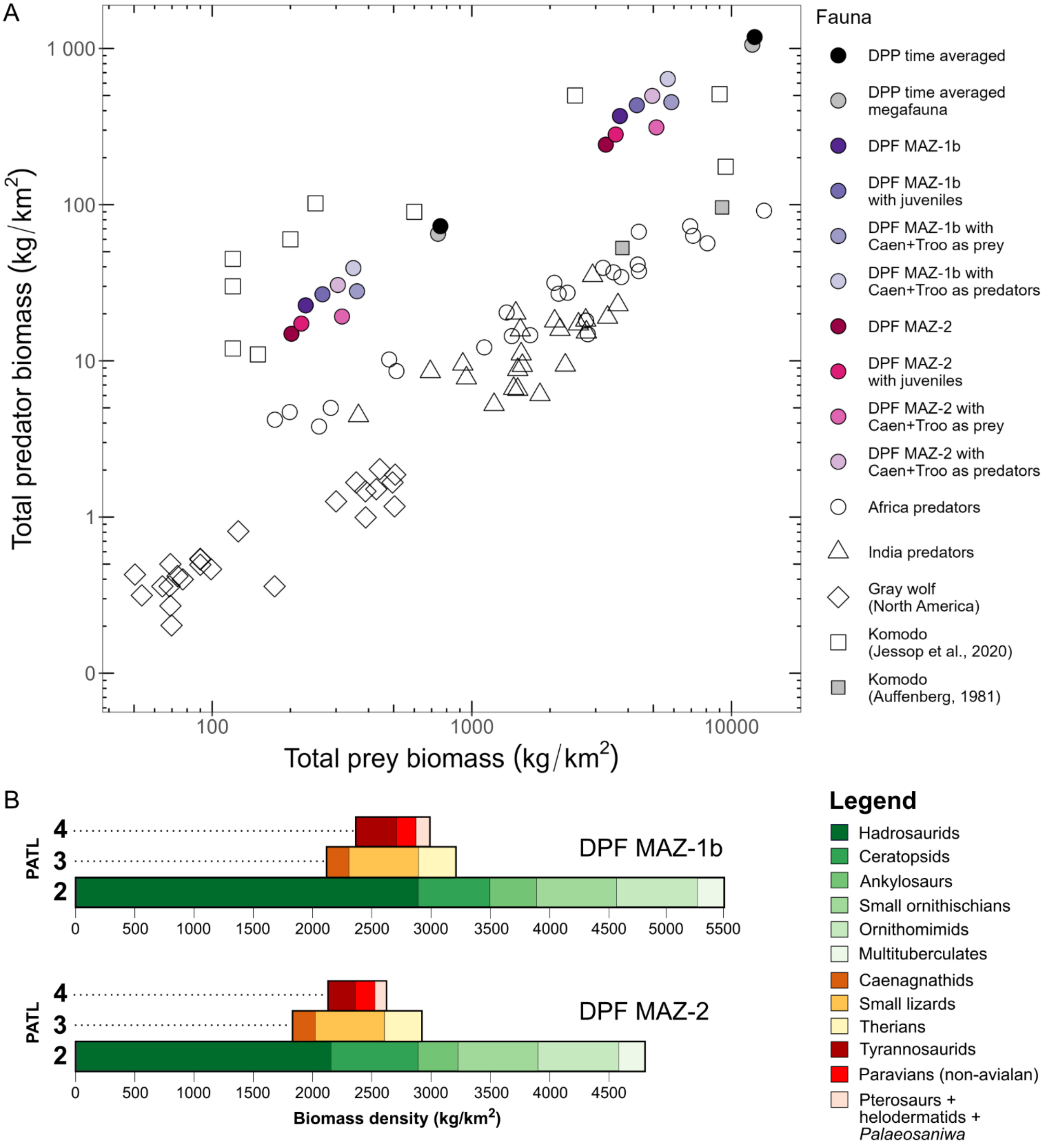
A
Total predator biomass (kg/km^2)
1 000
100
10
1
0
Total prey biomass (kg/km^2)
100
1000
10000
Fauna
DPP time averaged
DPP time averaged megafauna
DPF MAZ-1b
DPF MAZ-1b with juveniles
DPF MAZ-1b with Caen+Troo as prey
DPF MAZ-1b with Caen+Troo as predators
DPF MAZ-2
DPF MAZ-2 with juveniles
DPF MAZ-2 with Caen+Troo as prey
DPF MAZ-2 with Caen+Troo as predators
Africa predators
India predators
Gray wolf (North America)
Komodo (Jessop et al., 2020)
Komodo (Auffenberg, 1981)
B
PATL
4
3
2
DPF MAZ-1b
0
500
1000
1500
2000
2500
3000
3500
4000
4500
5000
5500
PATL
4
3
2
DPF MAZ-2
0
500
1000
1500
2000
2500
3000
3500
4000
4500
Biomass density (kg/km^2)
Legend
Hadrosaurids
Ceratopsids
Ankylosaurs
Small ornithischians
Ornithomimids
Multituberculates
Caenagnathids
Small lizards
Therians
Tyrannosaurids
Paravians (non-avialan)
Pterosaurs + helodermatids + *Palaeosaniwa*

Figure 4.9. Biomass density estimates for Dinosaur Provincial Park (DPP) biota focused on Dinosaur Park Formation Megaherbivore Assemblage Zones 1b and 2 (MAZ-1b, MAZ-2). A, total predator biomass density plotted against total prey biomass density, compared between DPP and extant communities, only including dinosaur/mammal predators and prey >5kg. DPP cluster on the left represents biomass densities calculated for 1,950 km^2 surface area, DPP cluster on the right represents biomass densities calculated for 120 km^2 surface area. Data for Africa, India and gray wolf obtained from Hatton *et al*. (2015). B, trophic biomass density pyramids for DPF MAZ-1b and MAZ-2 using prey-averaged trophic level (PATL) of fully resolved food web, assuming 120 km^2 surface area, not including juvenile megafauna. Hadrosaurid, ceratopsid, ankylosaur, tyrannosaurid and pterosaur densities estimated from quarry locality database assembled by first author, updated from Currie and Koppelhus (2005: Supplementary CD-ROM; Appendix II); other densities corrected with mass-density regressions (Damuth 1987), see Material and methods and Figure 4.4.

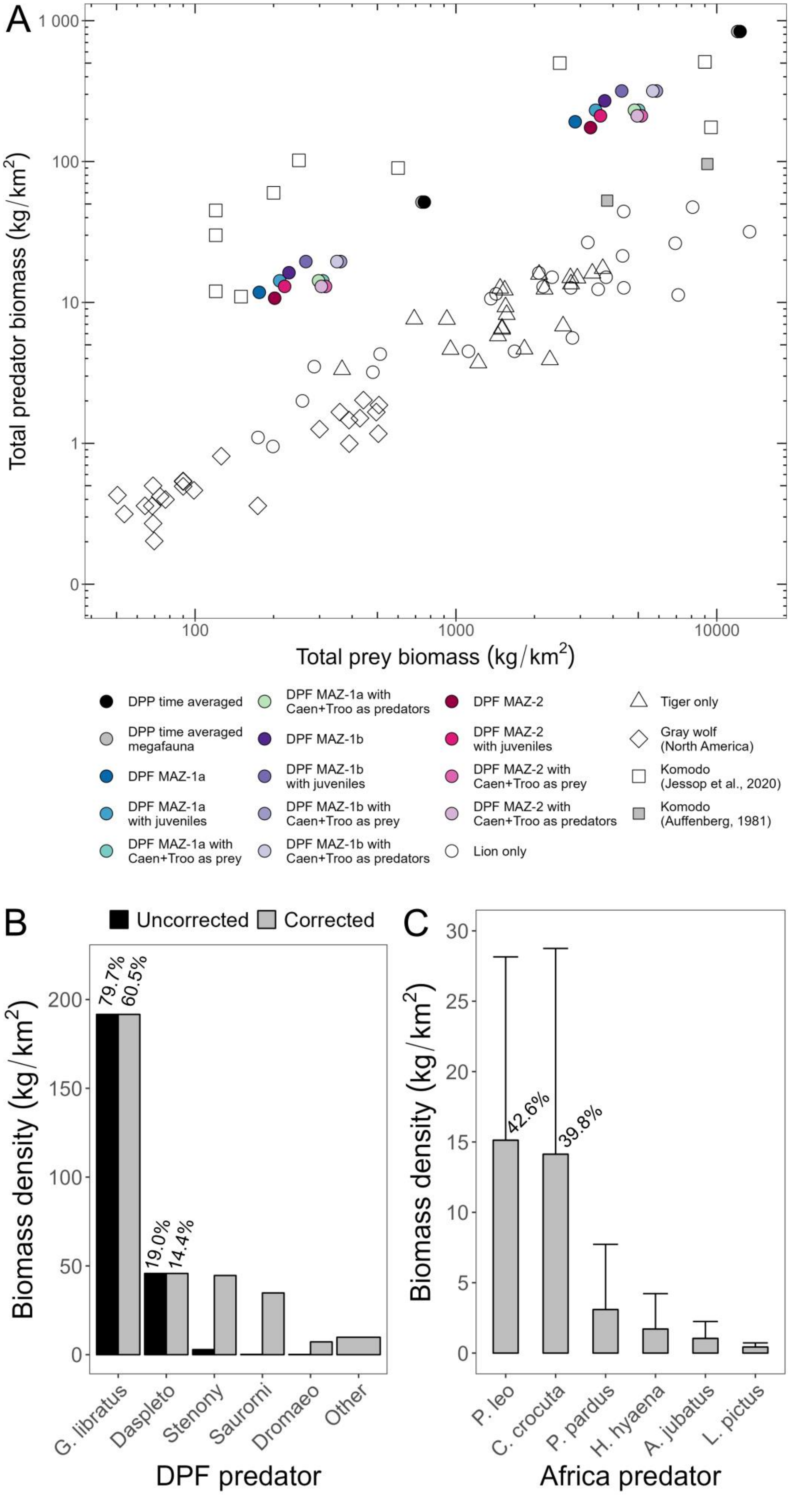
A
1 000
100
10
1
0
Total predator biomass (kg/km^2)
100
1000
10000
Total prey biomass (kg/km^2)
DPP time averaged
DPP time averaged megafauna
DPF MAZ-1a
DPF MAZ-1a with juveniles
DPF MAZ-1a with Caen+Troo as prey
DPF MAZ-1a with Caen+Troo as predators
DPF MAZ-1b
DPF MAZ-1b with juveniles
DPF MAZ-1b with Caen+Troo as prey
DPF MAZ-1b with Caen+Troo as predators
DPF MAZ-2
DPF MAZ-2 with juveniles
DPF MAZ-2 with Caen+Troo as prey
DPF MAZ-2 with Caen+Troo as predators
Lion only
Tiger only
Gray wolf (North America)
Komodo (Jessop et al., 2020)
Komodo (Auffenberg, 1981)
B
Uncorrected
Corrected
Biomass density (kg/km^2)
200
150
100
50
0
79.7%
60.5%
19.0%
14.4%
G. libratus
Daspleto
Stenony
Saurorni
Dromaeo
Other
DPF predator
C
Biomass density (kg/km^2)
30
25
20
15
10
5
0
42.6%
39.8%
P. leo
C. crocuta
P. pardus
H. hyaena
A. jubatus
L. pictus
Africa predator

Figure 4.10. Comparison of biomass of *Gorgosaurus libratus* with biomass of extant apex predators. A, dominant apex predator biomass density plotted against total prey biomass density, compared between Dinosaur Provincial Park (DPP) and extant communities, only including dinosaur/mammal predators and prey >5kg. DPP cluster on the left represents biomass densities calculated for a 1,950 km^2 surface area, DPP cluster on the right represents biomass densities calculated for a 120 km^2 surface area. B, relative dinosaur predator biomass densities in Dinosaur Park Formation Megaherbivore Assemblage Zone 1a (MAZ-1a), assuming 120 km^2 surface area; tyrannosaurid biomass does not include juveniles. C, mean and variance of large mammal relative predator biomass densities in 23 African savanna communities; percentages in African dataset refer to mean. Extinct biomass densities corrected with Damuth (1987) (see Material and methods, Figure 4.4); data for Africa, India and gray wolf obtained from Hatton *et al*. (2015).

4.8 Tables

Table 4.1. Categories of trophic link attribution for the Dinosaur Provincial Park community defined by taphonomic mode and phylogenetic relatedness to extant relatives.

Category	Lines of evidence for trophic links (in order of importance)	Taxa included
Complete fossils Near extant relatives present	**Stomach contents, direct interaction observations** (taxonomic uniformity) Functional morphology, body size	Testudines, Crocodilia, *Myledaphus bipartitus, Paratarpon apogerontus*, *Anchiacipenser acanthaspis*
Complete fossils Near extant relatives absent	**Functional morphology, body size** Stomach contents, tooth wear, stable isotope ratios	Tyrannosauridae, Hadrosauridae, Ceratopsidae, Ornithomimidae, Dromaeosauridae, Plesiosauria, Champsosauridae
Fragmentary fossils Near extant relatives present	**Stomach contents, direct interaction observations** (taxonomic uniformity) Functional morphology, body size	Remaining fishes, Caudata, Anura, Squamata
Fragmentary fossils Near extant relatives absent	**Functional morphology, body size**, tooth wear, stable isotope ratios	Pterosauria, Orodrominae, Pachycephalosauridae, Leptoceratopsidae, Caenagnathidae, Troodontidae, problematic theropods, Ornithurae, Mammalia

Table 4.2. Network statistics of food webs for Dinosaur Provincial Park (Dinosaur Park Formation Megaherbivore Assemblage Zone (MAZ) 1a and MAZ-1b), Serengeti and Komodo. Statistics include juvenile megafauna nodes unless indicated otherwise.

Abbreviations: S, number of nodes; **L,** number of links; **L/S,** linkage density; **L/S^2,** connectance; **FracB,** fraction of basal nodes (TL = 1); **FracH,** fraction of herbivore nodes (TL = 2); **FracO,** fraction of omnivore nodes; **FracTop,** fraction of apex predator nodes; **FracAqua**, fraction of aquatic and semiaquatic nodes; **FracTerr>45kg,** fraction of terrestrial megafauna >45 kg; **FracTerr>1T,** fraction of terrestrial megafauna >1,000 kg; **FracPATL>4**, fraction of nodes with prey-averaged trophic level > 4; **Terr+pack-juv**, food web version excluding aquatic, semiaquatic and juvenile nodes, with tyrannosaurid links accounting for cooperative hunting.

Network statistics	**DPF MAZ-1a**		**DPF MAZ-1b**		**DPF - Trophic species**		**Serengeti**	**Komodo**
	Main	*Main-juv*	*Main*	*Terr+pack-juv*	*Terrestrial only*	*Terrestrial pack-hunting*		
S	194	188	198	120	87	87	106	69
L	3,376	3,309	3,428	1,669	745	747	765	577
L/S	17.402	17.601	17.313	13.908	8.563	8.586	7.217	8.362
L/S^2	0.0897	0.0936	0.0874	0.1159	0.0984	0.0987	0.0690	0.1212
FracB	0.165	0.170	0.162	0.192	0.264	0.264	0.057	0.130
FracH	0.144	0.133	0.152	0.158	0.195	0.195	0.330	0.246
FracO	0.691	0.697	0.687	0.667	0.552	0.552	0.604	0.623
FracTop	0.021	0.048	0.020	0.067	0.023	0.034	0.151	0.058
FracAqua	0.366	0.378	0.359	0	0	0	0.057	0.087
*FracTerr>45kg**	0.268	0.214	0.205	0.217	0.230	0.230	0.240	0.063
*FracTerr>1T**	0.089	0.094	0.102	0.108	0.080	0.080	0.040	0
FracPATL>4	0.180	0.186	0.168	0.1	0.023	0.011	0.019	0.087

*Excluding aquatic and semiaquatic nodes.

Table 4.3. Trophic properties of likely trophic analogues in Dinosaur Park Formation (DPF), Serengeti and Komodo food webs (trophic species versions unless specified otherwise). **Abbreviations: PATL,** prey-averaged trophic level; **CL,** chain length (mean, median, variance and standard deviation); **Tsp,** food web version with trophic species; **fulltax,** full taxonomic resolution (species level).

Predator group	**Food web**	**PATL**	**Mean CL**	**Med CL**	**Var CL**	**SD CL**
Araneidae	DPF Tsp	3.275	3.953	4	1.376	1.173
	Serengeti	3.514	2.772	3	0.176	0.420
	Komodo	3.314	3.379	3	1.417	1.190
Anisoptera	DPF Tsp	3.228	3.976	4	1.487	1.219
	Komodo	3.189	2.923	3	0.686	0.829
Coleoptera	DPF Tsp	2.460	2.165	2	0.491	0.701
	Serengeti	2.857	1.923	2	0.071	0.266
	Komodo	2.488	1.852	2	0.274	0.524
Hymenoptera	DPF Tsp	2.520	2.914	3	0.688	0.829
	Serengeti	2.465	2.439	3	0.637	0.798
Lygodactylus capensis	Serengeti	3.369	3.316	4	0.690	0.831
Gekko gekko	Komodo	3.293	3.449	3	0.922	0.960
Hemidactylus spp.	Komodo	3.266	3.934	4	1.187	1.089
Orthrioscincus mixtus	DPF Tsp	3.350	3.910	4	1.193	1.092
Sphenomorphus florensis	Komodo	3.283	3.879	4	1.400	1.183
Varanoidea	DPF Tsp	3.671	6.777	7	2.341	1.530
Palaeosaniwa	DPF fulltax	4.204	7.719	8	2.576	1.605
Parasaniwa	DPF fulltax	3.947	6.243	6	2.201	1.484
Labrodioctes	DPF fulltax	4.142	6.722	7	2.163	1.471
Varanus niloticus	Serengeti	3.720	5.793	6	2.304	1.518
V. komodoensis (subadult)	Komodo	3.972	6.259	6	1.709	1.307
Eutheria (other)	DPF Tsp	3.051	3.910	4	1.207	1.099
Crocidura sp.	Serengeti	3.451	3.216	3	0.562	0.750
Crocidura sp.	Komodo	3.333	3.930	4	1.345	1.160
Stagodontidae	DPF Tsp	3.404	5.782	6	1.847	1.359
Eodelphis browni	DPF fulltax	3.774	5.784	6	1.806	1.344
Didelphodon sp.	DPF fulltax	3.992	6.733	7	2.149	1.466
Helogale parvula	Serengeti	3.681	6.281	6	2.489	1.578
Paradoxurus musangus	Komodo	3.444	5.071	5	1.696	1.302

Table 4.4. Trophic properties of apex predators at each ontogenetic stage in Dinosaur Park Formation (DPF), Serengeti and Komodo food webs. **Abbreviations: PATL,** prey-averaged trophic level; **CL,** chain length (mean, median, variance and standard deviation).

Predator	Food web version	Ontogenetic stage	PATL	Var PATL	Mean CL	Var CL	SD CL
Gorgosaurus libratus	DPF MAZ-1a main	Young juvenile	4.393	NA	NA	NA	NA
		Juvenile	4.296	NA	NA	NA	NA
		Subadult/adult	4.039	NA	NA	NA	NA
	DPF MAZ-1a main – juv prey	Young juvenile	4.393	NA	NA	NA	NA
		Juvenile	4.430	NA	NA	NA	NA
		Subadult/adult	4.190	NA	NA	NA	NA
	DPF MAZ-1a pack	Young juvenile	3.947	NA	NA	NA	NA
		Juvenile	3.778	NA	NA	NA	NA
		Subadult/adult	3.016	NA	NA	NA	NA
	DPF MAZ-1b main	Young juvenile	4.393	NA	NA	NA	NA
		Juvenile	4.248	NA	NA	NA	NA
		Subadult/adult	3.956	NA	NA	NA	NA
	DPF MAZ-1b pack	Young juvenile	3.882	NA	NA	NA	NA
		Juvenile	3.716	NA	NA	NA	NA
		Subadult/adult	3.023	NA	NA	NA	NA
	DPF MAZ-1b pack – juv prey	Young juvenile	4.089	NA	NA	NA	NA
		Juvenile	3.913	NA	NA	NA	NA
		Subadult/adult	2.988	NA	NA	NA	NA
	DPF trophic sp. terr	Young juvenile	4.105	0.518	7.434	2.461	1.569
		Juvenile	3.930	0.817	8.348	2.831	1.682
		Subadult/adult	3.666	0.821	8.912	3.038	1.743
	DPF trophsp. terr – juv prey	Young juvenile	4.105	0.518	7.434	2.461	1.569
		Juvenile	4.146	0.893	8.348	2.831	1.683
		Subadult/adult	3.790	0.952	8.912	3.038	1.743
	DPF trophsp. terr + pack	Young juvenile	3.741	0.591	7.433	2.465	1.570
		Juvenile	3.677	0.768	8.325	2.929	1.711
		Subadult/adult	2.988	0.103	2.149	0.156	0.395
	DPF trophsp. terr + pack – juv prey	Young juvenile	3.848	0.591	7.433	2.464	1.570
		Juvenile	3.794	0.850	8.326	2.928	1.711
		Subadult/adult	2.931	0.145	2.121	0.143	0.378
Panthera leo	Trophic sp.	Young juvenile	3.110	0.222	3.773	1.543	1.242
		Juvenile	3.110	0.222	4.546	2.014	1.419
		Adult	3.177	0.273	4.743	1.916	1.384
Varanus komodoensis	Trophic sp. Main	Young juvenile	3.866	0.352	4.734	1.355	1.164
		Juvenile	3.990	0.611	6.084	1.791	1.338
		Subadult	3.972	0.724	6.259	1.709	1.307
		Adult	3.615	0.729	6.516	1.719	1.311
		Young juvenile	3.866	0.352	4.734	1.355	1.164

	Trophic sp. (cannibalism included)	Juvenile	4.024	0.616	6.069	1.778	1.333
		Subadult	4.061	0.738	6.633	1.912	1.383
		Adult	3.988	0.921	7.335	2.020	1.421

CHAPTER 5 – COMPREHENSIVE DISCUSSION

The three preceding chapters together addressed the Wallacean, Gouldian, and Eltonian shortfalls on the biodiversity of the Belly River Group palaeobiotas in the late Campanian of southern Alberta and Saskatchewan. As emerging technology and community ecology methods are beginning to be applied to palaeontology, how does this thesis propel research on Dinosaur Provincial Park into the second quarter of the twenty-first century? Of all the fundamental questions that can be asked about this unique locality, one may be particularly outstanding in light of the necessity to pursue palaeontology at a 'shallow' deep time scale (see Chapter 1): to what extent can biologists use biodiversity patterns tracked through deep time (and evidently unaffected by human activities) in the DPP ecosystem as a baseline for contemporary biodiversity change? This question can arguably be addressed on at least four fronts, on which some progress has been made over the course of my thesis. First, what is the highest time resolution that can be reached to track biotic and abiotic change in the DPP ecosystem through time? This is a question I have started to answer in Chapter 3, with implications that I discuss further (see Section 5.1). Second, how equable was the palaeoclimate of DPP throughout the duration of the Belly River Group? This was originally planned to be one of the main questions of my thesis, yet I still initiated some research on that front in Chapter 3. Third, to what extent can we track phenotypic evolution in DPP's vertebrate (particularly hadrosaurid, ceratopsid and tyrannosaurid) fossil assemblage? I started investigating this question with centrosaurine ceratopsids following the discovery of *Centrosaurus apertus* in Saskatchewan Landing Provincial Park (see Chapter 2; Section 5.1). This question is highly inspired from groundbreaking work on Paleocene-Eocene mammals of Wyoming which demonstrated a macroevolutionary trend in response to climate change (Gingerich & Gunnell 1995; Secord *et al.* 2012). Finally, how much of the biodiversity of DPP preserved in its fossil assemblage remains to be discovered? More precisely, which new species or life stages (e.g. juvenile dinosaurs) could be revealed with prospecting efforts targeted at stratigraphic horizons which have historically been overlooked in the Park? For instance, the Lethbridge Coal Zone is vastly underrepresented in the dinosaur chronofauna due to its lack of palaeochannel deposits, yet it appears to have a very distinct dinosaur assemblage which will only be better understood with additional discoveries. Likewise, fine-grained facies may have been neglected in the past by vertebrate palaeontologists, yet they have great potential to reveal new plant and invertebrate species. In this regard, I will briefly mention some exciting discoveries arising from this renewed focus by the field crews of which I was a part in the final conclusion of this thesis. I can also assert that the ecological network produced in Chapter 4 now lays a foundation to integrate every potential new species into updated diversity analyses of the DPP community that account for interspecific interactions.

5.1 An updated geological map to track ecology and macroevolution through time in the Dinosaur Provincial Park palaeobiota

The geological mapping project of DPP was always one of the very first and most important ideas behind this thesis, since a correlation of all fossil quarries in that locality will have a significant impact on any ecological and evolutionary pattern detected from climate, biodiversity or morphological analyses. The results shown in Chapter 3 now provide a proof of concept for identifying sedimentary architectural units on a local scale in DPP's badlands outcrops based on structure-from-motion (SfM) photogrammetry and aerial images. Together, they offer ample reason to complete an aerial mapping project across the entire Park on a subregional scale to identify and trace potential marker beds among these units using a combination of 2-D digital elevation models and orthomosaics and 3-D digital outcrop models (see Appendix IV).

Considering the entirety of the results of this thesis, the expansion of the DPP mapping project is considered to have at least three main outcomes in terms of tracking ecology and evolution in this fossil assemblage. First, a correlation of the Park's quarries based on their sedimentological setting could provide a more robust constraint on the stratigraphic distributions of several vertebrate clades than what the Oldman Formation – Dinosaur Park Formation contact alone currently offers, especially since I now demonstrate the important limitations of the latter datum in Chapter 3. Before attempting to trace marker beds throughout the DPF, a simple intermediate step would consist of measuring the height of fossil quarries and bonebeds below the lower contact of the Lethbridge Coal Zone, which is possibly the single most identifiable sedimentary unit in the entire Belly River Group. The LCZ is less accessible from the ground than the lower BRG outcrops, but the availability of unmanned aerial vehicles (UAVs) and SfM photogrammetry to digitally reconstruct entire landscapes has now enabled me to begin this particular project (manuscript in preparation). The improved stratigraphic and temporal resolution resulting from such endeavours could evidently develop the palaeoecology of the Park's chronofauna by revising currently recognized dinosaur assemblage zones as well as changes in faunal composition observed in vertebrate microfossil localities (Brinkman 1990; Mallon *et al.* 2012; Eberth *et al.* 2023). In turn, they could validate the node composition of trophic networks representing each major stratigraphic interval of the BRG, thus building on the initial food webs presented in Chapter 4. It might even be possible to estimate confidence intervals on the true temporal ranges of some species by going beyond their first and last fossil appearance data, as has occasionally been achieved in invertebrate palaeontology (Strauss & Sadler 1989; Marshall 1990, 1994, 1997). However, it must be acknowledged that the marine invertebrate fossil record is far more reliable than that of any terrestrial vertebrate group due to contrasting taphonomic filters (Kidwell & Flessa 1995; Kidwell & Holland 2002), therefore associations between distinct sedimentary facies and taphonomic modes and signatures must absolutely be accounted for to predict stratigraphic ranges in the Park (Eberth & Currie 2005; Eberth 2015).

These refined stratigraphic distributions lead to the second main outcome, where questions on the speciation mode of several dinosaur lineages represented in the DPP chronofauna could be addressed with clear macroevolutionary implications. Hadrosaurs, ceratopsians and tyrannosaurs in particular have been at the center of an enduring debate between cladogenesis (speciation by lineage divergence from a common ancestor) and anagenesis (evolution of the same population within the same lineage without divergence) (Horner *et al.* 1992; Carr *et al.* 2017; Campbell *et al.* 2019; Fowler & Fowler 2020; Lowi-Merri & Evans 2020; Wilson *et al.* 2020; Scherer & Voiculescu-Holvad 2024). If some species proposed to evolve by anagenesis were unequivocally shown to co-occur in the same stratigraphic unit (and not solely based on a similar height above a datum of highly variable elevation), anagenesis would be strongly challenged (or even altogether rejected) as a hypothetical speciation mode. I have begun such a study by quantifying the intraspecific variation of parietal anatomy in the centrosaurines *Centrosaurus apertus* and *Styracosaurus albertensis* (manuscript in preparation). Once the stratigraphic position of each studied specimen is corrected with the map, it will allow me to test whether some linear or geometric morphometric measurements of frill ornamentation are correlated with stratigraphy, which would fail to refute the anagenesis hypothesis according to which some *Centrosaurus* individuals belonged to populations which evolved into *Styracosaurus*. This study was initiated by the discovery of a partial ceratopsid parietal from Saskatchewan Landing Provincial Park eventually assigned to *Centrosaurus apertus* (see Chapter 2). Considering how far that specimen was found from the more established Albertan *Centrosaurus* localities, I began to test whether it fell within the range of anatomical variation known for that species, or whether it could belong to a different ceratopsid species (Figures 5.1, 5.2). Considering how variable the parietal processes at the P1 and P2 loci alone are in *C. apertus* (partly due to a large specimen sample size), it is little surprise that the Saskatchewan Landing specimen appears indistinguishable from its likely conspecifics.

Lastly, a more robust stratigraphic correlation based on marker beds would show which individual fossil quarries and bonebeds were formed in the same depositional event and would shed more light on the abiotic conditions of the DPP biota, on which little is currently known (see Chapter 3). For example, it could reveal that scattered individual bonebeds bearing a similar taphonomic signature (e.g. a catastrophic assemblage interpreted as mass drowning of a herd of ceratopsian dinosaurs) have the exact same host horizon and were thus formed during the same event, thus supporting the ‘mega-bonebed’ hypothesis (Eberth *et al.* 2010). Likewise, the identification of ironstone layers bearing mass mollusc death assemblages that could be laterally traced for great distances across the Park would support a hypothesis according to which droughts were far more frequent in that environment than is currently appreciated (see Chapter 3). Ultimately, this mapping project could be expanded beyond DPP to cover other fossil-rich formations in the Canadian Western Interior Basin, from the Horseshoe Canyon Formation around Drumheller to the late Maastrichtian Frenchman Formation of south-central Saskatchewan and the Wapiti Formation of northwestern Alberta (Bamforth 2013; Eberth *et al.* 2013; Bamforth *et al.* 2014; Fanti *et al.* 2015). It would be an ambitious task, but its great potential to track ecological and evolutionary changes in that region throughout the Late Cretaceous Epoch is only beginning to be fully understood.

5.2 The significance of mixed faunal bonebeds for the palaeoecology of Dinosaur Provincial Park

Two chapters in this thesis revolved around bonebeds preserving a high biodiversity: the Lake Diefenbaker Bonebed in Saskatchewan Landing Provincial Park (see Chapter 2) and Bonebed 190 in Dinosaur Provincial Park (see Chapter 3). However, mixed faunal bonebeds with dense macrofossil aggregations remain rarely studied in the Oldman and Dinosaur Park Formations compared to isolated skeletons, vertebrate microfossil localities and monodominant (usually ceratopsid) bonebeds (Eberth & Currie 2005). While some multigeneric bonebeds have yielded important fossil specimens collected in isolation, notably Bonebeds 010, 216 and 102 (personal observation), only one was ever systematically excavated with thorough taphonomic and diversity analyses (Tumarkin-Deratzian 1997). This situation is now about to change as myself and my McGill University field crew have assembled a sizeable collection from Bonebed 190, a locality which has at least one fairly dense macrofossil quarry as well as a vertebrate microsite with a high species richness. While Chapter 3 is mostly focused on the sedimentological setting of BB190, the fossils we have collected over five field seasons in that locality can now form the basis for local biodiversity estimates (manuscript in preparation). Vertebrate microfossil localities have long been known to provide invaluable snapshots of biodiversity at the highest available time resolution in fluvial channel deposits (Brinkman 1990; Bamforth 2013; Cullen & Evans 2016). Following the work conducted on BB047 as well as my own thesis, I am becoming more and more convinced that macrofossil assemblages can also reach a high species richness while preserving taxa that might be underrepresented in microfossil assemblages, notably toothless tetrapods such as ornithomimids, caenagnathids and pterosaurs. Therefore, these sites could also be key to study biodiversity at a high time resolution in the Park. Looking further afield, the biodiversity of the Lake Diefenbaker Bonebed is certainly worthy of more thorough comparisons with that of approximately coeval DPP bonebeds since it has now been shown to contain a faunal assemblage never previously encountered in the Park due to its proximity to the Bearpaw Sea. Finally, the ecological network modeling methods developed in Chapter 4 could certainly be applied to compare food web structures in different fossil communities preserved in these bonebeds, and to potentially highlight associations between taphonomic biases and the trophic guilds actually represented in those assemblages.

5.3 The macroeco-evolutionary significance of the Dinosaur Provincial Park food web

The following lines are additional thoughts which were originally intended for Chapter 4, but which will now be integrated into a more detailed study of the Dinosaur Provincial Park food web currently in preparation (Larsson & Demers-Potvin 2024; Appendix V). This study aims to examine variation in food web structure at different time intervals throughout the Belly River Group considering the profound environmental changes in the region throughout the late Campanian, from the inland/freshwater ecosystem of the Oldman Formation to the coastal/brackish-water ecosystem of the Lethbridge Coal Zone.

Ecological networks describe biotic interactions that co-occur in a community, where taxa (or groups of taxa) are represented by nodes and interactions are represented by links (Poisot *et al.* 2016;

Delmas *et al.* 2019). While interspecific competition, mutualism and parasitism have occasionally been studied with a network approach (Bascompte *et al.* 2006; Poisot *et al.* 2012; Eklöf *et al*. 2013; Kéfi *et al.* 2015; Gravel *et al.* 2019), the most frequently modeled ecological networks are food webs composed of trophic interactions where each node is a consumer (i.e. a predator) and/or a resource (i.e. a prey) (Williams & Martinez 2000, 2004). Food webs therefore constitute a very integrative way of measuring diversity in an ecosystem by revealing patterns of biomass (and therefore energy) flow from primary producers to primary and secondary consumers, which in turn can explain patterns of relative abundance, species richness and body mass distribution in a community (Cohen *et al.* 2003). Another key advantage of food webs as descriptors of community structure lies in their power to further investigate functional diversity since they enable the role of an ecological function for a given species to be established relative to the rest of its community (Banker *et al.* 2022), which is highly informative for immediate conservation objectives given the decreasing stability of several of these communities. These inherent properties of ecological networks thus likely explain their widespread use in modern characterizations of extant biotas (Yodzis 1998; Gravel *et al.* 2013; Saigo *et al.* 2015; Rossi *et al.* 2019; O'Connor *et al.* 2020; Caron *et al.* 2022, 2024; Steenweg *et al.* 2023).

By modeling the addition and removal of nodes (therefore creating or disrupting food chains), quantitative food webs also constitute a robust framework to test the complexity and impact of extinctions on the stability of a given community, which explains the increasing recognition of their value to palaeontology over the last two decades (Roopnarine 2006, 2010; Dunne *et al.* 2008, 2014; Roopnarine & Angielczyk 2015; Kempf *et al.* 2020; Fraser *et al.* 2021; Huang *et al.* 2021; Fricke *et al.* 2022). Consequently, several published ecological networks on ancient biotas revolve around one central question: how persistent has the structure of marine and/or terrestrial communities been throughout our planet's history (see Chapter 1)? Most palaeoecological studies that integrated these methods can be considered to fall in one of two categories around this question: the first one is characterized by a focus on the stability of successive communities located in the same geographical area in response to environmental perturbations over relatively constrained geological time intervals (Roopnarine & Banker 2021). In the case of moderate biotic turnover, this approach thus enables the testing of longstanding hypotheses proposing that successive communities form ‘chronofaunas’ (e.g. Olson, 1952). In contrast, this is also where major events of biotic turnover are usually investigated, such as the Permian-Triassic and Cretaceous-Paleogene mass extinction events (Mitchell *et al.* 2012; Roopnarine & Angielczyk 2015; Roopnarine *et al.* 2017, 2019; Huang *et al.* 2021, 2023; García-Girón *et al.* 2022), the Late Ordovician Richmondian invasion (Kempf *et al.* 2020), and the end-Pleistocene megafaunal extinctions (Pires *et al.* 2020; Fricke *et al.* 2022). All these studies quantify community structure by measuring trophic network (i.e. food web) properties, yet in some cases they measure functional diversity without accounting for interspecific interactions (Blanco *et al.* 2021).

A second category is characterized by the search for consistent ecological patterns between extant and extinct communities separated by immense geographical and temporal distances, usually on a macroevolutionary time scale, with less power to track community persistence over continuous time intervals. For example, the network structure of food webs assembled at a very high taxonomic resolution for the Cambrian Chengjiang and Burgess Shale biotas (Dunne *et al.* 2008) and the early Eocene Messel Shale (Dunne *et al.* 2014) has been compared to that of extant communities. In terms of individual node properties, food webs provide a framework to test whether taxa that have a similar ecological function in disparate communities have a similar effect on their energy flux by measuring their trophic position (Banker *et al.* 2022). For example, a food web of the Early Cretaceous Paja biota of Colombia revealed that its marine reptile apex predators reached higher trophic levels than any possible extant functional analogue (Cortés & Larsson 2023). The latter is particularly relevant to the present study since the trophic level of any taxon within a community reflects the frequency at which energy is transferred to it along food chains which combine into the entire web (Hall & Raffaelli 1991; Cohen & Łuczak 1992; Williams & Martinez 2004; Thompson *et al.* 2007). Therefore, questions within this category can still revolve around broad predictions of species extinctions (Dunne & Yeakel

2015), but often aim to test directly for the presence of ecological analogues to extant species (or to entire extant communities and ecosystems) throughout deep time. In this respect, the main research question of Chapter 4 on the role of tyrannosaurids as Late Cretaceous terrestrial apex predators compared to that of hypothetical extant analogues arguably falls within the second major category of palaeoecological network analysis. Admittedly, the major limitation of any trophic comparison between extant and extinct species or communities lies in uneven preservation potential between taxa during fossilization, which can introduce major uncertainties to inferences of ancient community structure (Behrensmeyer & Hook 1992; Kidwell & Flessa 1995; Behrensmeyer *et al.* 2000). Nonetheless, ecological network analysis has recently been adapted in a promising direction by disentangling ecological from taphonomic signals in fossil community composition through its ability to recreate an ancient community structure that includes 'missing' species and thus accounts for preservation biases (Roopnarine & Dineen 2018; Shaw *et al.* 2021; Swain *et al.* 2021; Cortés & Larsson 2023).

While a simplified food web for Dinosaur Provincial Park would likely produce very similar trophic levels to a more detailed one, the latter version has potential for a far greater depth of analysis on other network properties such as centrality, modularity, or dietary redundancy/partitioning, as well as incorporating body size distributions, abundance and biomass data at the species level, as seen in extant systems (see Cohen *et al.* 2003; Delmas *et al.* 2019). For instance, the detection of trophic redundancy among certain species could highlight alternative chains for energy flow if one or more of these went extinct, thus providing an indicator of the community's resilience. Additionally, some omnivorous and fully faunivorous assemblages collapsed into a single node (e.g. 'fossorial mammals') might contain predator-prey interactions among themselves, which would likely produce less accurate measurements of trophic levels and broader network properties compared to highly resolved extant food webs.

The next two paragraphs outline more general background on predator ecology (past and present) for the investigation of tyrannosaur trophic position presented in Chapter 4. Terrestrial apex predators have repeatedly evolved within evolutionarily separate tetrapod lineages since the early Permian, essentially carnivorous pelycosaurian synapsids, gorgonopsian therapsids, some squamates and crocodylomorphs, and a multitude of theropod dinosaurs (including 'terror birds') and therian mammals (Van Valkenburgh & Molnar 2002; Head *et al.* 2009; Zanno *et al.* 2015; Van Valkenburgh *et al.* 2016; Dececchi *et al.* 2020; Degrange 2020; Montefeltro *et al.* 2020; Kammerer *et al.* 2023; Singh *et al.* 2024). Apex predators thus exhibited a much higher morphological disparity through time, and also during specific geological periods, than in the present and recent past. Therefore, sufficiently detailed fossil evidence could lay foundations to investigate whether these extinct animals had significantly distinct life history strategies from extant ones, which would imply that they, and likely their entire palaeocommunity structure, lack any modern analogue. Consequently, this could suggest that energy was transferred through communities in distinct alternate stable states compared to the present day.

Unfortunately, we might never be able to obtain the ultimate characterization of the influence of these ancient predators on energy transfer through their community since that would require testing for top-down control on the abundance and species richness of their resources. In extant ecosystems, seven large carnivore species have been shown to have such a keystone role, with stabilizing effects on primary productivity, nutrient cycling and atmospheric composition (Ripple *et al.* 2014 and references therein). However, no such evidence was found for the Komodo dragon since its population energy use was shown to have no effect on the growth rate of its prey populations (Jessop *et al.* 2020). At first, this pattern may appear counterintuitive due to the overwhelming biomass of Komodo dragons relative to their prey, but their low per-capita metabolic requirements combined with solitary hunting tactics arguably reduce their kill probability at each potential prey encounter (Jessop *et al.* 2020). In this respect, the results of Chapter 4 are understandably insufficient to test whether large tyrannosaurs such as *Gorgosaurus libratus* exerted top-down control on their prey back in the Late Cretaceous. The energetic constraints of these animals have been modeled previously (Farlow 1976; Farlow *et al.* 2022), yet always remained equivocal due to lingering uncertainties about non-avialan dinosaur metabolism. Nonetheless, this question may well be worth investigating in the future, especially considering that the megaherbivore diversity of the Dinosaur Park biota is currently proposed to be controlled solely from the bottom up, at least in the published literature (Mallon 2019). The latter hypothesis is largely driven by evidence from the modern African savanna for a herbivore body size threshold, where the abundance of species weighing >150 kg is controlled by resource abundance (bottom-up) while the abundance of species below that mass is controlled by predator pressure (top-down) instead (Sinclair *et al.* 2003; Grange & Duncan 2006). However, the two tyrannosaurid species that co-occurred at any time of the Belly River Group in DPP (*G. libratus* and *Daspletosaurus* spp.) both reached considerably higher body sizes relative to their prey than in any fully terrestrial extant ecosystem, meaning that adult individuals may well have been able to tackle a fully grown hadrosaurid or ceratopsid dinosaur, particularly if some form of cooperative hunting was involved (Farlow 1993; Farlow & Pianka 2002). Furthermore, the palaeoclimate and floral composition of DPP remain poorly known relative to the vertebrate record, which means that far more research is recommended on these fronts before a bottom-up control hypothesis can be supported by evidence of resource limitations for herbivores. Ultimately, more direct evidence of feeding behaviour from fossils (whether tooth marks on bone or stomach contents) combined with more objective estimation methods for metabolic rates and dinosaur survivorship curves may at least fail to reject a hypothesis according to which tyrannosaurs exerted top-down control on all their prey by hunting fully-grown individuals as well as juveniles. The ichnofossil record of large theropod bite marks currently suggests that juveniles were preferentially consumed over adults of any dinosaur prey species (Hone & Rauhut 2010), which lent further credence to the bottom-up control hypothesis for DPP (Mallon 2019). However, this record still has a very low sample size that might not be representative of the true body size distribution of dinosaur individuals bearing tooth marks, hence the recommendation to pay more attention to this type of palaeopathology.

Beyond the immediate questions on apex predator ecology addressed in Chapter 4, the introduction of a highly resolved food web to the field of dinosaur palaeoecology has potential to stoke a debate on the similarities and differences between the structures of communities dominated by Cenozoic mammals and non-avialan dinosaurs. Several dinosaur ecomorphological traits tentatively suggest that dinosaur-dominated communities had a fundamentally different structure from the mammal-dominated communities that succeeded them after the Cretaceous-Paleogene mass extinction event (Codron *et al.* 2012; Schroeder *et al.* 2021). One of the main lines of evidence for the latter hypothesis (that dinosaur communities functioned differently from mammal communities) lies in the consistent underrepresentation of small-bodied dinosaur species in nearly every major Mesozoic biota relative to modern mammal faunas (Benson 2018). While this unusual body size distribution may reflect a consistent size-driven taphonomic bias in these fossil assemblages (Brown *et al.* 2013*c*, *b*, 2022*b*), anatomical evidence of ontogenetic niche shifts for large dinosaurs driven by extreme changes in body size and proportions through high rates of allometric growth alternatively suggests that it represents a genuine biological signal (Erickson *et al.* 2004; Woodward *et al.* 2015; Woodruff *et al.* 2018; Therrien *et al.* 2021; Wyenberg-Henzler *et al.* 2021, 2022). In turn, this evidence supports the concept of 'niche assimilation' according to which the multiple orders of magnitude of body size that large dinosaur species reached during their growth made each of their main ontogenetic stages functionally equivalent to successive niches occupied by separate mammal species (Brett-Surman 1997; Holtz 2021). Therefore, this would support the hypothesis according to which dinosaur diversity was truly limited at small body sizes due to competitive exclusion by juvenile megafauna (Codron *et al.* 2012). In turn, this line of evidence would also imply that latest Cretaceous dinosaur communities with tyrannosaurids as their apex predators existed in an alternate stable state from any modern terrestrial community, which could ultimately update fundamental current paradigms on the persistence of community structure through deep time.

5.4 Figures

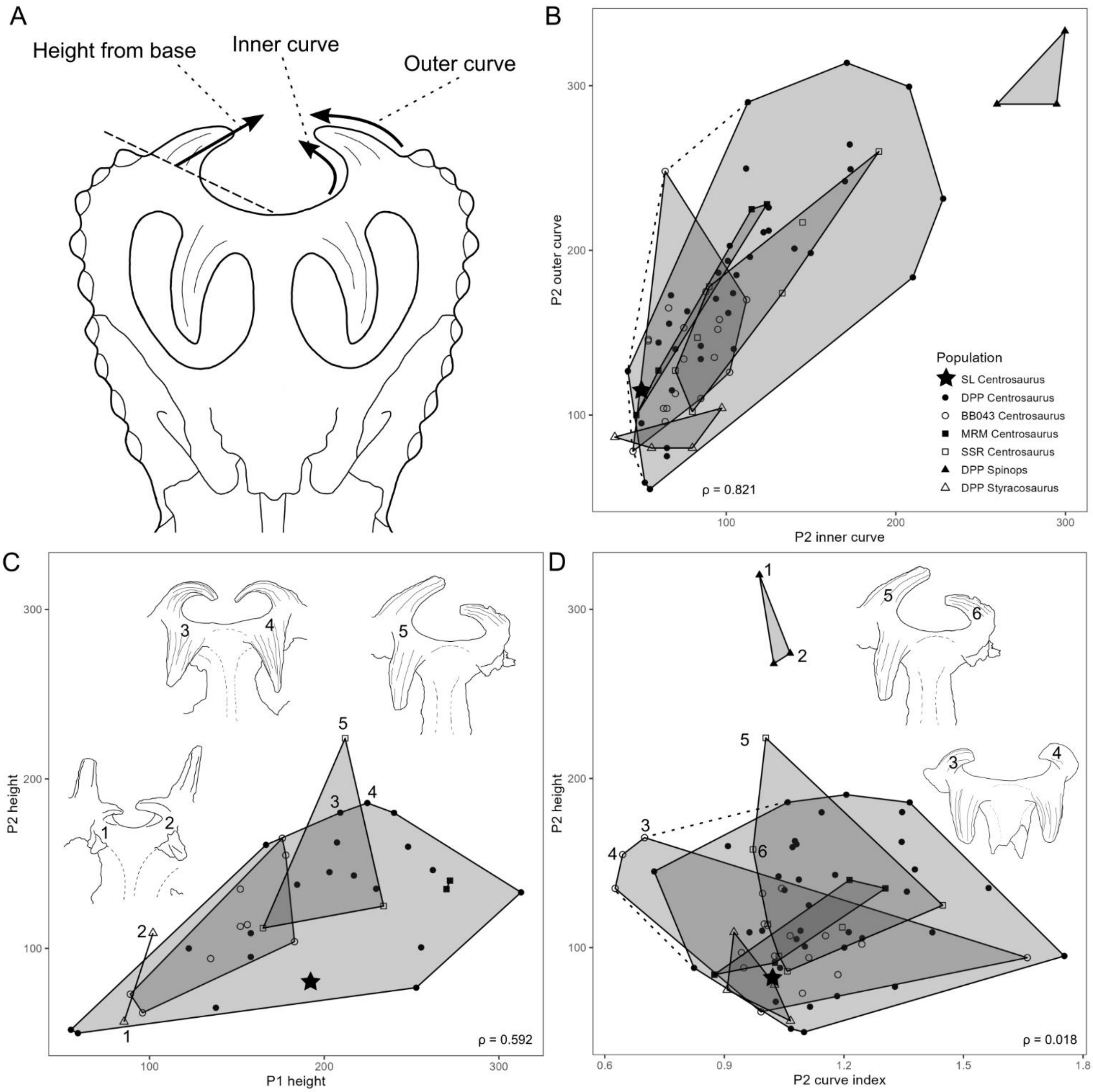
A
Height from base
Inner curve
Outer curve
B
P2 outer curve
P2 inner curve
300
200
100
100
200
300
ρ = 0.821
Population
SL Centrosaurus
DPP Centrosaurus
BB043 Centrosaurus
MRM Centrosaurus
SSR Centrosaurus
DPP Spinops
DPP Styracosaurus
C
P2 height
P1 height
300
200
100
100
200
300
1
2
3
4
5
ρ = 0.592
D
P2 height
P2 curve index
300
200
100
0.6
0.9
1.2
1.5
1.8
1
2
3
4
5
6
ρ = 0.018

Figure 5.1. Comparisons of epiparietal dimensions between various *Centrosaurus apertus*, *Styracosaurus albertensis* and *Spinops sternbergorum* populations across the Belly River Group of Alberta and Saskatchewan. A, schematic drawing (redrawn from C. M. Brown, 2013) illustrating parietal process (P*n*) measurements. B, P2 inner curve against P2 outer curve (mm). C, P1 length against P2 length (mm). D, P2 index of curvature against P2 height. Dotted lines along convex hulls show total DPP morphospace (including BB043 population). Line drawings of specimens showcasing variability in parietal process morphology are as follows: *S. albertensis* UALVP 55900 (C: 1, 2); *C. apertus* UALVP 11735 (C: 3, 4); *C. apertus* TMP 1978.006.0001 (C: 5; D: 5, 6); *S. sternbergorum* NHMUK R13607 (D: 1, 2); *C. apertus* TMP 1982.018.0079 (D: 3, 4). **Abbreviations: BB043**, Bonebed 043; **DPP**, Dinosaur Provincial Park; **MRM**, Milk River-Manyberries; **NHMUK**, Natural History Museum, London; **SL**, Saskatchewan Landing Provincial Park; **SSR**, South Saskatchewan River (including Sandy Point and White Rock Coulee); **TMP**, Royal Tyrrell Museum of Palaeontology; **UALVP**, University of Alberta Laboratory of Vertebrate Palaeontology. Spearman’s rank correlation coefficient marked as ρ. Line drawings not to scale.

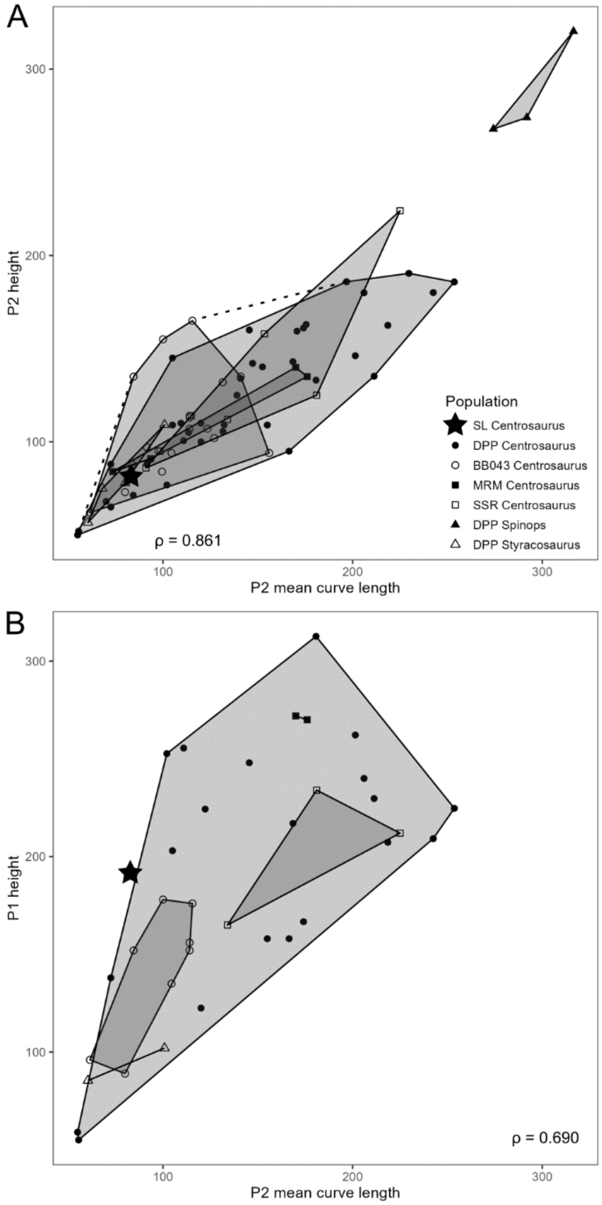

Figure 5.2. Supplementary comparisons of epiparietal dimensions between various *Centrosaurus apertus*, *Styracosaurus albertensis* and *Spinops sternbergorum* populations across the Belly River Group of Alberta and Saskatchewan. A, P2 height against P2 mean curve length (mm). B, P1 height against P2 height (mm). Dotted lines along convex hulls show total DPP morphospace (including BB043 population). **Abbreviations: BB043**, Bonebed 043; **DPP**, Dinosaur Provincial Park; **MRM**, Milk River-Manyberries; **SL**, Saskatchewan Landing Provincial Park; **SSR**, South Saskatchewan River (including Sandy Point and White Rock Coulee). Spearman’s rank correlation coefficient marked as ρ.

FINAL CONCLUSION AND SUMMARY

As I was preparing my doctoral qualifying examination three and a half years ago, I landed upon a quote from the late Wann Langston, Jr. (1965) specifically addressed at Dinosaur Provincial Park, later cited by Currie and Russell (2005), which became hugely inspirational for the remainder of my thesis research:

> New techniques of collecting and somewhat different approaches to investigation should now be employed, especially in regard to the non-dinosaurian element of the fauna. Older work needs revision in the light of contemporary knowledge from related fields of science. Additional data on the occurrence of the early collections must be gathered. Faunal studies from a biological viewpoint should be emphasized and coordinated with similar work on the associated floras and fossil invertebrates.

Nearly 60 years later, I believe that my thesis has significantly increased the potential of Dinosaur Provincial Park (DPP) to become a model system to study macroevolution and changes in terrestrial ecosystems over a relatively constrained geological time scale based on an exceptionally complete fossil assemblage. First, I have contributed to our knowledge of the spatial variation in the biodiversity of western Canada during the Late Cretaceous by documenting the rare co-occurrence of dinosaurs identified at the species level within a coastal fauna from Saskatchewan. Second, I have contributed to our knowledge of the temporal variation in the biodiversity of the DPP chronofauna by introducing a promising method for measuring species' stratigraphic distributions through digital outcrop reconstructions. Finally, I have contributed to our knowledge of the biodiversity of DPP measured through interspecific trophic interactions inferred from fossils that together form the first food web ever created to study any Mesozoic dinosaur community. In the process, I integrated new methods and technology to my research, thus further connecting palaeontology to distantly related scientific and technical disciplines such as geospatial analysis and community ecology.

Even after more than a century of exploration in Dinosaur Provincial Park, the experience I have acquired in the field and in the lab has convinced me that many more fossil discoveries are still warranted to understand how the diversity of this ancient ecosystem changed over time, especially for components of the fauna and flora that remain underrepresented due to taphonomic biases. Fortunately, I am honoured to have contributed to major discoveries on all these fronts as part of successive field crews of the McGill Vertebrate Palaeontology Field Course as I completed this thesis. First, I contributed to the discovery and excavation of a rare new fossil plant site which has produced the very first insect impression fossils ever found in the Park, thus unveiling entire clades and ecological guilds previously thought to be lost from that ancient community. Descriptions of the flora and entomofauna of that locality, as well as the information they provide on local palaeoclimate, are currently underway (Mueller *et al.*, in prep.). Second, the ceratopsid skull which I also contributed to collecting in the uppermost reaches of the Lethbridge Coal Zone is currently the single stratigraphically highest dinosaur found in the entire Park and may well belong to a new species from a time when terrestrial vertebrate fossils were rarely preserved in the region. Other highlights of these field seasons include the discoveries of the most complete soft-shelled turtle skeleton (family Trionychidae) currently known from the Park, a very rare nodosaur skull, and potentially the first juvenile centrosaurine ceratopsid associated skeleton ever found in the Park. I believe that these are the kinds of finds that inspire me to return there as often as I can to explore more of this truly unique ancient ecosystem.

Appendix I

Historical timeline of research in Dinosaur Provincial Park

This appendix is largely adapted from more detailed accounts of the history of research in Dinosaur Provincial Park (DPP) (Russell 1966; Currie 2005). The first of those two references lists all field parties that worked in the DPP region until 2004. Milestones in quarry stake installation are also reported from Tanke (2005). Since the publication of these chapters almost 20 years ago, new discoveries have been made and new technologies applied to the exploration of the Park. Therefore, the following table presents an updated summary of key events that have marked the scientific research and outreach history of this unique locality.

Institutional abbreviations: AMNH, American Museum of Natural History; GSC, Geological Survey of Canada (later NMC); NHMUK, Natural History Museum (London); NMC, National Museum of Canada; PMA, Provincial Museum of Alberta; RM, Redpath Museum; ROM, Royal Ontario Museum; TMP, Royal Tyrrell Museum of Palaeontology; UofA, University of Alberta (later UALVP); UALVP, University of Alberta Laboratory for Vertebrate Palaeontology

Table 1. Timeline of significant landmarks in history of research in Dinosaur Provincial Park

Time period	Historical event(s)
Sometime before 1871	Jesuit priest Jean-Baptiste L'Heureux writes first account of fossils from the badlands now within the Park; fossil bones evocatively identified by the Peigan people he lived with as "the grandfather of the buffalo"
1874	Fossils found by George Mercer Dawson in Wood Mountain area, southern Saskatchewan, are first official report of dinosaur bones in Western Canada
1882	Dinosaur bones found at Scabby Butte, SW of the Park area, by Richard George McConnell
1884	Joseph Burr Tyrrell finds theropod skull in Horseshoe Canyon Formation outcrops near present-day Drumheller, the holotype of *Albertosaurus sarcophagus* (Osborn 1905)
1889	Thomas Weston drifts down Red Deer River from Horseshoe Canyon Fm outcrops, finds rich fossil beds at Berry Creek and Deadlodge Canyon now within and around what would become DPP (Weston 1899)
1897, 1898, 1901	Lawrence M. Lambe, scientific illustrator at the GSC, is the first to undertake fieldwork in and to publish research on the fossils of DPP, including the first known specimens of *Centrosaurus apertus* (Lambe 1902, 1904; Osborn & Lambe 1902)
1911-1915	Barnum Brown and Peter Kaisen lead successive collecting expeditions for AMNH, discover *Corythosaurus casuarius* (Brown 1914*a*, 1916*a*) and *Prosaurolophus maximus* (Brown 1916*b*) holotypes as well as at least 15 individual *Centrosaurus* specimens in what would become known as BB043
1913-1915	Charles H. Sternberg and his sons Charles M., George F. and Levi, as well as Gustav Lindblad, collect for GSC in competition with AMNH expeditions; discoveries of the holotypes of *Gorgosaurus libratus* (Lambe 1914*a*, 1917) and *Styracosaurus albertensis* (Lambe 1913)
1914	William Cutler collects *Centrosaurus* skull and ankylosaur skeleton (*Scolosaurus cutleri* holotype), and sells them to NHMUK
1917	C. M. Sternberg discovers *Panoplosaurus mirus* holotype (Lambe 1919) as remaining Sternbergs are contracted at other museums, notably AMNH
1918-1921	ROM organizes expeditions to the Park area, led by William A. Parks (1918, 1919) and Levi Sternberg (1919, 1920, 1921), leading to discoveries of *Parasaurolophus walkeri*, *Gryposaurus* '*Kritosaurus*' *incurvimanus* and *Dyoplosaurus acutosquameus* holotypes (Parks 1919, 1920, 1922, 1923, 1924); George Sternberg leads UofA expedition to the Park in 1920, creating first collection from this locality for a western North American museum including *Stegoceras validum* holotype (Lambe 1918, Gilmore 1924*a*)
1935	Levi Sternberg leads first installation of metal stakes on completed quarries in the Park
1936	C. M. Sternberg and his son Ray relocate 90 historical quarries, mark 95 quarry stakes (including new sites); publication of a preliminary quarry map (Sternberg 1936)
1950	Publication of C. M. Sternberg's final topographic map of the Park's exposures,

	plotting 111 quarries and one formational contact (Sternberg 1950)
1954	ROM crew directs last quarry staking operation in the Park before 27-year hiatus
1955	Creation of Dinosaur Provincial Park
1959	Dinosaur Provincial Park opens to the public
1966-1967	Don Taylor leads fieldwork in the Park to create exhibit for newly established PMA
1968-1969	Dale Russell (NMC) conducts fieldwork in the Park, leading to important theropod discoveries (Russell 1969); Peter Dodson relocates more quarries and conducts first sedimentological and taphonomic analyses of the Park (Dodson 1971, 1983)
1978	John Walper rediscovers *Centrosaurus* quarry previously found by Barnum Brown (Q143), now identified as a bonebed by Philip J. Currie and crew (PMA)
1979	Designation of Dinosaur Provincial Park as UNESCO World Heritage Site; start of first systematic excavation of a bonebed in the Park, Q143 renamed (Currie 1981)
1981-1985	Quarry staking resumes in DPP; construction of TMP in Drumheller; first fossil collections in the Park for TMP (1982)
1986	First joint expedition of the Canada-China Dinosaur Project takes place in DPP (Currie 1991)
1987	Inauguration of TMP satellite field station near Dinosaur Provincial Park entrance
1994	First proposal of the 'single-event mass-death' hypothesis based on occurrence of all known *Centrosaurus* bonebeds at similar stratigraphic level
1995	New *Centrosaurus* bonebed discoveries suggest at least two mass-death events; rare discovery of complete ornithomimid skeleton among fossil plant locality
1996	After focus on ceratopsian-dominated bonebeds, TMP leads first excavation of a mixed faunal bonebed in the Park (Tumarkin-Deratzian 1997)
1997	Darren Tanke (TMP) begins annual quarry relocation and identification efforts
1999-2003	Identification of more than 650 quarries in DPP using differential GPS (MacDonald *et al.* 2005)
2005	TMP hosts Dinosaur Park Symposium, resulting in publication of first complete palaeontological review of DPP on 50th anniversary of the Park's foundation (Currie & Koppelhus 2005)
2010	Rare discovery of baby chasmosaurine skeleton, the most complete very young juvenile dinosaur specimen known from DPP to date (Currie *et al.* 2016)
2014	Rare discovery of nearly complete *Saurornitholestes* skeleton, one of the most complete small-bodied dinosaur specimens from the Park (Currie & Evans 2020)
2015	Lidar survey of DPP leads to creation of first DEM and detailed photomosaic of the Park's exposures, now deposited at TMP
2016-present	Annual RM crews led by Hans C. E. Larsson begin fieldwork in the Park, in collaboration with Philip J. Currie and Eva B. Koppelhus (UALVP); new fossil plant localities discovered in 2017 and 2022, new series of aerial surveys begins in 2021

Appendix II

Summarized database of fossil quarries and Oldman-Dinosaur Park Formation contacts in Dinosaur Provincial Park

Following significant new discoveries in DPP since 2005, this appendix constitutes an updated dataset of all georeferenced palaeontological and sedimentological features. Most of these quarries were known by the time of the publication of *Dinosaur Provincial Park: A Spectacular Ancient Ecosystem Revealed* (Currie & Koppelhus, 2005: Supplementary CD-ROM). This dataset now includes quarries discovered since 2005, as well as updated GPS measurements recorded over the last 15 years of fieldwork organized at UALVP (Currie, pers. comm., 2021-07-17). The complete version of the current database, which includes accession numbers and other additional attributes, is available from the author as .csv files. Horizontal (Easting and Northing) coordinates were measured in the NAD83 coordinate system (UTM zone 12N). Vertical coordinates (absolute elevation) were measured along the EGM96 geoid. A few quarries lacking geographical coordinates are also included to help direct future relocation efforts.

Institutional abbreviations: GSC, Geological Survey of Canada

Table 1. Marked quarries in which articulated or associated skeletons were collected in Dinosaur Provincial Park

Quarry Number	**UTM East**	**UTM North**	**Elevation (MASL)**	**Identification**	**Elements**	**Discovered/Collected by**	**Year collected**	**References**
Q001	466997	5622503	671.4	*Centrosaurus apertus*	Skull & skeleton	W.A. Parks	1919	Parks, 1921
Q002	466787	5622421	669.7	*Dyoplosaurus acutosquameus*	Holotype; partial skull & skeleton	L. Sternberg	1919	Arbour et al., 2009; Parks, 1924
Q003	466547	5622092	700	*Lambeosaurus lambei*	Partial skeleton	L. Sternberg	1919	L. S. Russell, 1966
Q004a	465133	5621075	694.6	*Prosaurolophus maximus*		L. Sternberg	1921	
Q005	462501	5621276	668	*Corythosaurus casuarius*	Complete skeleton	C.H. Sternberg / L. Sternberg	1921	Lull & Wright, 1942
Q006	462664	5621145	668.9	*Gorgosaurus libratus*	Complete skeleton; juvenile	C.H. Sternberg	1917	Matthew & Brown, 1923; D. A. Russell, 1970
Q007	463168	5621132	672.2	Lambeosaurinae		L. Sternberg	1921	Dodson, 1971
Q008	463937	5620734	688.9	*Panoplosaurus mirus*	Holotype; skull & partial skeleton	C.M. Sternberg	1917	Coombs, 1978; Lambe, 1919
Q009	464445	5621068	680.5	*Edmontonia rugosidens*	Skull & skeleton	C.H. Sternberg	1917	Coombs, 1978
Q010	465526	5622006	675.9	*Chasmosaurus russelli*	Skull & skeleton	C.M. Sternberg	1914	Godfrey & Holmes, 1995; Lambe, 1915
Q011	465473	5622355	664.1	*Corythosaurus casuarius*	4 skeletons	L. Sternberg / L. & C.M. Sternberg	1920 1936	
Q012	465574	5622527	663.2	*Parasaurolophus walkeri*	Holotype; Skull & skeleton	L. Sternberg	1920	Parks, 1922
Q013	465845	5621911	683.3	*Corythosaurus intermedius*	Skull & jaws	L. Sternberg	1920	Parks, 1923
Q014	468666	5622156	683.4	*Corythosaurus intermedius*	Scattered skull & skeleton	L. Sternberg	1919	Parks, 1923
Q015	468711	5622208	681.7	*Corythosaurus intermedius*	Skull	W.A. Parks	1919	Parks, 1923
Q016	472168	5622232	708.8	*Styracosaurus albertensis*	Holotype; complete skull & skeleton	C.H. Sternberg / L. Sternberg	1913; 1935	Holmes & Ryan, 2013; Lambe, 1913
Q017	458390	5629332	670.3	Hadrosauridae	Skeleton lost at sea	C.H. Sternberg	1916	C. H. Sternberg, 1917
Q018	458580	5629566	675.2	Hadrosauridae	Skeleton lost at sea	C.H. Sternberg	1916	C. H. Sternberg, 1917
Q019	458799	5629388	682.4	*Chasmosaurus belli*	Complete skeleton	L. Sternberg	1926	Lull, 1933
Q020	457969	5628854	682.9	*Ornithomimus*	Skull & skeleton	L. Sternberg	1926	Parks, 1928
Q021	456906	5628584	650	*Aspideretes foveatus*	Skeleton & shell	L. Sternberg	1934	
Q022	469731	5623255	651.3	*Centrosaurus apertus*	Skull	L. Sternberg	1934	
Q023	469932	5623853	705.3	*Lambeosaurus lambei*	Skull	L. Sternberg	1920	Lull & Wright, 1942
Q024	457488	5630785	650.3	*Corythosaurus casuarius*; Baenidae	Holotype. skull & skeleton; juvenile turtle skeleton	B. Brown	1912	B. Brown, 1914, 1916b
Q025	455597	5628163	683.8	*Chasmosaurus belli*	Skull & skeleton	L. Sternberg	1926	Lull, 1933

Q026	456074	5628792	654.7	*Corythosaurus casuarius*	Pelvis & tail	L. Sternberg	1933	Gilmore, 1946
Q027	456053	5628817	652.2	*Corythosaurus casuarius*	Skull & jaws	L. Sternberg	1934	Parks, 1935
Q028	455910	5628858	652.2	*Rativates evadens*	Partial skull & skeleton	L. Sternberg	1934	McFeeters et al., 2016; D. A. Russell, 1972
Q029	456343	5628907	647.1	*Gorgosaurus libratus*	Skull & skeleton	L. Sternberg	1933	D. A. Russell, 1970
Q030	456708	5628299	658.2	*Corythosaurus casuarius*	Skull	L. Sternberg	1934	
Q031	456904	5628581	649.4	*Gorgosaurus libratus*	Scattered skull	L. Sternberg	1934	D. A. Russell, 1970
Q032	457069	5627147	672.5	*Lambeosaurus lambei*	Skull & jaws	L. Sternberg	1934	Parks, 1935
Q033	456776	5627010	675.4	*Centrosaurus apertus*	Skull	L. Sternberg	1926	C. M. Sternberg, 1950
Q034	457352	5627537	648.1	*Gryposaurus notabilis*	Skull	L. Sternberg	1934	Ostrom, 1961
Q035	457942	5627365	658.7	*Gryposaurus notabilis*	Complete skull & partial skeleton	C.H. Sternberg	1913	Horner, 1992; Lambe, 1914b
Q036	457680	5626688	685.1	*Gorgosaurus libratus*	Holotype; partial skull & skeleton	C.M. Sternberg / C.H. Sternberg	1913	Lambe, 1914c, 1914a, 1917
Q037	457984	5626107	691.9	*Chasmosaurus belli*	Paratype; most of skeleton	C.H. Sternberg	1913	Lambe, 1914b
Q038	456509	5626466	668.8	Lambeosaurinae	Headless skeleton	C.H. Sternberg	1913	
Q039	456090	5626503	660.6	Lambeosaurinae	Headless skeleton	C.H. Sternberg	1915	
Q040	455793	5628850	650.2	*Corythosaurus casuarius*	Skull & jaws	L. Sternberg	1933	Parks, 1935
Q041	474519	5624073	699.6	*Euoplocephalus tutus*	Scattered skeleton	C.H. Sternberg	1914	
Q042	464148	5620622	690.1	*Centrosaurus apertus*	Skull	C.H. Sternberg	1917	
Q043	464148	5620646	690.4	*Panoplosaurus mirus*	Skull & skeleton	L. Sternberg	1935	L. S. Russell, 1940
Q044	467170	5622375	672.3	*Centrosaurus apertus*	Skull & partial skeleton	L. Sternberg	1930	
Q045	465611	5621585	699.6	*Lambeosaurus lambei*	Skull & partial skeleton; juvenile	L. Sternberg	1930	Parks, 1931
Q046	460117	5623780	690.3	*Prosaurolophus maximus*	Skull & arm	L. Sternberg	1930	Dodson, 1971
Q047	460044	5623818	683.2	*Champsosaurus natator*	Holotype; skull & partial skeleton	L. Sternberg	1930	Parks, 1933
Q048	461280	5621099	661.8	*Gorgosaurus libratus*	Skull & partial skeleton	G.F. Sternberg	1921	
Q049	460063	5620667	702.7	*Chasmosaurus belli*	Skull	L. Sternberg	1930	
Q050	455540	5630471	672.7	*Lambeosaurus lambei*	Skull	L. Sternberg	1926	Lull & Wright, 1942
Q051	455597	5629479	684.1	Lambeosaurinae	Hind leg & foot	L. Sternberg	1934	C. M. Sternberg, 1950
Q052	470035	5623291	664.5	*Euoplocephalus tutus*	Partial skeleton	L. Sternberg	1920	Penkalski, 2018
Q053	470251	5623722	685.5	Lambeosaurinae	Headless skeleton	C.H. Sternberg	1914	
Q054	467960	5624526	653.2	Hadrosauridae	Skull & partial skeleton	C.M. Sternberg	1921	
Q055	468084	5624754	690.3	Lambeosaurinae	Headless skeleton	L. Sternberg	1927	
Q056	455218	5629884	680.4	*Aspideretes foveatus*	Complete skeleton; juvenile	L. Sternberg	1934	
Q057	457638	5630453	652.4	*Centrosaurus apertus*	Complete skull	B. Brown	1912	B. Brown, 1914a; Lull,

								1933
Q058	458102	5629801	667.5	*Stegoceras validum*	Skull & partial skeleton	G.F. Sternberg	1921	Gilmore, 1924; Lambe, 1918
Q059	458172	5631005	681.6	*Euoplocephalus tutus*	Skull & partial skeleton	G.F. Sternberg	1921	Arbour & Currie, 2013; Dodson, 1971
Q060	460001	5622493	692.2	Lambeosaurinae	Posterior skeleton	C.M. Sternberg	1919	Dodson, 1971
Q061	455547	5629180	678.1	*Chirostenotes pergracilis*	Holotype; right foot	C.M. Sternberg	1928	C. M. Sternberg, 1932
Q062	464326	5622826	675.1	*Lambeosaurus lambei*	Skull & skeleton	C.M. Sternberg	1928	Lull & Wright, 1942; C. M. Sternberg, 1935
Q063	457077	5627020	670	*Chasmosaurus* sp.	Skull & skeleton	H.D.R. Lowe / C.M. Sternberg	1928	C. M. Sternberg, 1940
Q064	456802	5627532	652.9	*Leidyosuchus canadensis*	Pelvis & tail	C.M. Sternberg	1928	
Q065	457346	5627296	675.7	*Lambeosaurus lambei*	Skull & neck	C.M. Sternberg	1928	Lull & Wright, 1942; C. M. Sternberg, 1935
Q066	457235	5626929	670.3	*Leidyosuchus canadensis*	Skull	C.M. Sternberg	1928	
Q067	463848	5620574	692.5	*Corythosaurus casuarius*	Scattered skull & skeleton	C.M. Sternberg	1919	Ostrom, 1961
Q068	463777	5620723	687	*Corythosaurus intermedius*	Skull & partial skeleton	C.M. Sternberg	1919	Dodson, 1975
Q069	464637	5621233	669.7	Lambeosaurinae	Field photos	G.F. Sternberg	1922	
Q070	463913	5620667	693.9	Chasmosaurinae	Partial skull & skeleton	C.M. Sternberg	1919	Lull, 1933
Q071	463943	5620666	693.5	*Lambeosaurus lambei*	Partial skull	C.M. Sternberg	1919	Lull & Wright, 1942
Q072	465832	5622683	657.9	*Daspletosaurus torosus*	Holotype; skull & skeleton	C.M. Sternberg	1921	D. A. Russell, 1970
Q073	460547	5619502	701.4	Not identified				
Q074	460189	5619646	708.4	*Gorgosaurus libratus*	Partial skeleton	C.M. Sternberg	1917	Dodson, 1971
Q075	473815	5625936	728.4	Dinosaur Park / Bearpaw formational contact				
Q076	474404	5626134	699.6	*Prosaurolophus maximus*	Partial skull & skeleton	C.M. Sternberg	1921	
Q077	474456	5626288	668.9	*Gryposaurus notabilis*	Partial skull & skeleton	C.M. Sternberg	1921	
Q078	457810	5630254	669.1	*Centrosaurus apertus*	Skull	W.E. Cutler	1914-15	Dodson, 1971
Q079	457725	5630153	667.3	Not identified			1914-15	
Q080	471365	5622322	664.5	*Scolosaurus cutleri*	Holotype; partial headless skeleton; location disputed by D. Tanke	W.E. Cutler	1914	Nopcsa, 1928; Penkalski & Blows, 2013
Q081	471951	5623020	664.5	*Centrosaurus apertus*	Skull & partial skeleton	C.M. Sternberg	1921	
Q082	471782	5623173	675.9	*Corythosaurus casuarius*	Skull	C.M. Sternberg	1921	
Q083	470807	5622369	660	*Centrosaurus apertus*	Skull & jaws	C.H. Sternberg	1913	Lull, 1933
Q084	460124	5621686	688.5	*Parasaurolophus walkeri*	Headless skeleton	G.F. Sternberg	1921	Dodson, 1971
Q085	465498	5621907	681.3	Lambeosaurinae	Partial skull	C.H. Sternberg	1914	
Q086	465389	5621759	693.7	*Prosaurolophus maximus*	Skull & partial skeleton	C.H. Sternberg	1914	Dodson, 1971; Horner,

								1992
Q087	461473	5620678	704.8	*Lambeosaurus lambei*	Partial skeleton	C.M. Sternberg	1917	Dodson, 1975
Q088	462615	5621151	669.6	Not identified				
Q089	464502	5623591	655.2	*Scolosaurus cutleri*	Partial skeleton	B. Brown / B. Brown. P. Kaisen	1913	Dodson, 1971
Q090	464498	5623579	656.1	*Gorgosaurus libratus*	Partial skull & skeleton	B. Brown	1913	Matthew & Brown, 1923
Q091	463596	5622148	662.7	*Centrosaurus apertus*	Skull & partial skeleton	C.M. Sternberg	1917	C. M. Sternberg, 1940
Q092	464294	5622712	672.2	Not identified				
Q093	464427	5622152	681.3	Not identified				
Q094	464560	5621147	691.8	Not identified				
Q095	464751	5621288	677.9	Hadrosauridae	Tail	G.F. Sternberg	1922	
Q096	465609	5623655	662.1	Not identified				
Q097	465720	5623243	664.5	Hadrosauridae	Maxilla & quadrate			
Q098	465949	5621434	699.4	Ceratopsidae	Articulated skeleton			C. M. Sternberg, 1950
Q099	466382	5622312	677	*Gryposaurus* sp.			2010	
Q099A	466367	5622346	674.5	Not identified			2010	
Q100	457355	5629594	652.3	*Euoplocephalus tutus*	Sacrum	B. Brown	1913	Arbour et al., 2009
Q101	460288	5621258	686.3	*Panoplosaurus mirus*	Skull & partial skeleton	B. Brown	1915	
Q102	463827	5621807	676.7	*Centrosaurus apertus*	Skull	C.M. Sternberg	1917	Dodson, 1971
Q103	463780	5622842	659.4	*Brachylophosaurus canadensis*	Skull & partial skeleton	C.M. Sternberg	1936	Horner, 1992; C. M. Sternberg, 1953
Q104	464326	5622826	675.2	Lambeosaurinae	Scattered skull	C.M. Sternberg	1936	Dodson, 1971
Q105	460124	5621686	688.7	*Centrosaurus apertus*	Complete skeleton	B. Brown	1914	B. Brown, 1917
Q106	462978	5621473	665.7	*Gorgosaurus libratus*	Partial skeleton & skull	W.E. Cutler? / B. Brown	1913	Matthew & Brown, 1923
Q107	463110	5621491	670.1	Lambeosaurinae	Skull; stake not found	C.M. Sternberg		Dodson, 1971
Q108	460547	5621615	706.7	*Lambeosaurus magnicristatus*	Holotype; skull & partial skeleton	C.M. Sternberg	1919	Evans & Reisz, 2007; C. M. Sternberg, 1935
Q109	460027	5621847	684.6	*Centrosaurus apertus*	Skull & partial skeleton	C.M. Sternberg	1919	Lull, 1933
Q110	459708	5621812	684.5	*Chasmosaurus* sp.	Skull	C.M. Sternberg	1919	Campbell et al., 2019
Q111	465248	5622078	667.3	*Corythosaurus casuarius*	Skull & skeleton	B. Brown	1914	Dodson, 1971; Ostrom, 1961
Q112	463732	5621394	666.1	*Caenagnathus collinsi*	Holotype; complete lower jaw	C.M. Sternberg / R.M. Sternberg	1936	C. M. Sternberg, 1940
Q113	463045	5621460	666.1	*Leidyosuchus canadensis*	Skull & lower jaws	R.R. Hornell / L. Sternberg	1954	

Q114	465873	5620814	714.6	*Prosaurolophus maximus*	Skull & partial skeleton	R.R. Hornell / L. Sternberg	1954	Ostrom, 1961
Q115	463358	5620535	687.6	*Corythosaurus casuarius*	Skull & partial skeleton with skin impressions	R.R. Hornell / L. Sternberg	1954	Dodson, 1975
Q116	466950	5621996	707.3	*Prosaurolophus maximus*	Small skull	G. Edmund / L. Sternberg	1954	Ostrom, 1961
Q117	466396	5622330	673.5	*Corythosaurus casuarius*	Skull	R.R. Hornell / L. Sternberg	1954	Ostrom, 1961
Q118	463358	5621412	673.1	*Gryposaurus notabilis*	Partial skull	R.R. Hornell / L. Sternberg	1954	Dodson, 1975
Q119	460541	5619554	708.1	*Champsosaurus lindoei*	Skull	G.E. Lindblad	1953	Gao & Fox, 1998; L. S. Russell, 1956
Q120	460638	5619906	680	Hadrosauridae	Skull & skeleton	G.E. Lindblad	1953	
Q124	459453	5627146	669.8	*Styracosaurus albertensis*; Pachycephalosauridae	Skull & partial skeleton; pachycephalosaur skull remains	C.H. Sternberg	1916	Wall & Galton, 1979
Q125	464445	5622421	665	Hadrosauridae	Headless skeleton	C.M. Sternberg	1981-82	
Q126	464930	5623705	657.5	Hadrosauridae	Headless skeleton	C.M. Sternberg	1961	
Q127	464823	5623864	645.7	Ceratopsidae	Headless skeleton	C.M. Sternberg	1961	
Q128	464568	5621234	689.1	*Corythosaurus intermedius*	Skull & skeleton	R. Fowler / C.M. Sternberg	1964	
Q129	465086	5625431	663.3	*Champsosaurus lindoei*	Holotype; skull & skeleton	A. Lindoe	1962	Gao & Fox, 1998
Q130	455543	5629177	678	*Alphadon praesagus*	Left dentary	J.C. Danis	1966	Fox, 1979
Q131	456838	5626741	683.5	*Leidyosuchus canadensis*	Skull	J.C. Danis	1967	
Q132	458769	5629808	666	Hadrosauridae; Theropoda	Skull	D. Brinkman / D. Brinkman. M. Vickaryous	1998	
Q133	477001	5629056	699.9	*Latenivenatrix mcmasterae*	Holotype; partial skull & skeleton	I. Vanderloh	1968	D. A. Russell, 1969; van der Reest & Currie, 2017
Q134	463995	5621398	673.5	Hadrosauridae	Skull in ironstone	J. McCabe	1990	
Q135	465429	5622229	665.3	*Centrosaurus apertus*	Skull in ironstone	R.C. Fox	1969	
Q136	459170	5629533	668.1	*Centrosaurus apertus*	Skull	R.C. Fox	1969	
Q137	463736	5621397	665	*Gryposaurus notabilis*	Skull & skeleton	E. Riggs. G.F. Sternberg	1922	
Q138	463559	5621278	669.6	*Gorgosaurus libratus*	Partial postcarnial skeleton; small individual	E. Riggs. G.F. Sternberg	1922	
Q139	465530	5621984	679.5	Pterosauria	Phalanx	H. Johnson		D. A. Russell, 1972a

Q140	457904	5629698	666.1	*Saurornitholestes langstoni*	Holotype	I. Vanderloh	1974	Sues, 1978
Q141	460077	5620327	688.1	*Leidyosuchus canadensis*	Skull	L.J. Strong	1974	
Q142	458011	5632085	655	*Neurankylus*	Carapace & plastron	L.J. Strong	1975	
Q143	465855	5622575	673.3	*Centrosaurus apertus*	Partial skeleton in BB043	B. Brown / P.J. Currie	1979	
Q144	455566	5629167	678.1	*Latenivenatrix mcmasterae*	Frontals & parietals	J. Acorn / J. Acorn. P.J. Currie	1979	van der Reest & Currie, 2017
Q145	465530	5621737	699.2	*Chirostenotes pergracilis*	Partial skeleton	G.L.P. Danis	1979	Currie & Russell, 1988
Q146	462685	5622729	686.5	Lambeosaurinae	Partial skeleton	J. Hancharuk	1979	
Q147	465365	5621701	691.9	Pterosauria	Tibia distal end	D. Ost	1979	Currie & Padian, 1983
Q148	471179	5622351	667.4	*Centrosaurus apertus*	Skull	P. Béland / P.J. Currie	1980	
Q149	466270	5622486	670.3	*Gryposaurus notabilis*	Skeleton	G. Naylor / G. Maier	1980	Horner, 1992
Q150	464669	5621625	678.6	*Corythosaurus casuarius*	Skull & skeleton	G. Forsen? / G.L.P. Danis	1980-81	Currie et al., 1995
Q151	465972	5622203	677.6	*Saurornitholestes langstoni*	Left frontal	P. Dodson	1980	
Q152	455555	5629161	677.1	Pterosauria	Pubes	P.J. Currie	1979	
Q153	458408	5629082	680.3	*Champsosaurus lindoei*	Partial skull	L.J. Strong	1980	Gao & Fox, 1998
Q154	455628	5629741	659.7	Ornithomimidae	Partial skeleton	G.L.P. Danis	1980	
Q155	465912	5623557	662	Theropoda	Footprints	P.J. Currie / L.J. Strong et al.	1981	
Q155A	465904	5623548	662.1		Footprints			
Q155B	465928	5623510	656.9		Footprint	D. Tanke		
Q156	466116	5622422	668.2		Egg shell	P.J. Currie	1980	
Q157	457655	5627080	658	*Latenivenatrix mcmasterae*	Skull cap	D.A. Russell	1980	Currie, 1985; van der Reest & Currie, 2017
Q158	459588	5629851	679.5	*Cryodrakon boreas*	Partial femur	D.A. Russell / P.J. Currie	1980	Currie & Russell, 1982; Hone et al., 2019
Q159	465864	5621821	699	Plesiosauria	Partial skeleton	P.J. Currie / G. Maier	1981	
Q160	461219	5621906	669	Hadrosauridae	Partial skeleton	G.L.P. Danis	1981	
Q161	459293	5629693	664.3	*Aspideretoides foveatus*	Partial skull & skeleton	L.J. Strong	1981	Brinkman, 2005
Q162	464577	5621706	678.3	Hadrosauridae	Partial skeleton	P.J. Currie / C. Coy	1981; 1998-99	
Q163	459344	5630165	673.6	*Lambeosaurus lambei*	Skull & partial skeleton	L.J. Strong / J. McCabe	1981	

Q164	459201	5627476	659.5	*Chasmosaurus russelli*	Skull	P.J. Currie	1981	Godfrey & Holmes, 1995
Q165	465699	5622168	669.7	Hadrosauridae	Partial skeleton in BB016	G. Maier	1981-82	
Q166	463836	5620210	706	*Latenivenatrix mcmasterae*	Partial skull	L.J. Strong	1982	Currie, 1985; van der Reest & Currie, 2017
Q167	459196	5627488	660.1	Hadrosauridae	Headless skeleton	L.J. Strong / J. Shultis	1982	
Q168	465989	5622114	687.7	*Saurornitholestes langstoni*	Partial skeleton	M. Klassen	1982	
Q169	459111	5627492	663.3	Hadrosauridae	Partial skeleton	L.J. Strong / G.L.P. Danis. T. Tokaryk	1982	
Q170	439751	5630781	664.5	Ceratopsidae	Partial skeleton	L. Lund et al. / D. Tanke	1982	
Q171	464706	5620822	719.3	Hadrosauridae	Partial skeleton	J. Walper / G.L.P. Danis	1982	
Q172	467855	5624477	653.9	Hadrosauridae	Partial skeleton	G.L.P. Danis. J. Shultis / A. Mather	1982-85	
Q173	471981	5624552	675.4	Hadrosauridae	Partial skeleton	P. Harrop / S. Andrews. G. Maier	1982	
Q174	467844	5624783	678.8	*Corythosaurus casuarius*	Skull & partial skeleton	P.J. Currie / K. Aulenback	1982	
Q175	472056	5624598	683.6	*Lambeosaurus lambei*	Skull & partial skeleton	P. Dodson / J. Shultis	1982	
Q176	439753	5630784	665.3	*Champsosaurus* sp.	Partial skeleton	D. Tanke	1982	
Q177	470738	5623694	684.5	Hadrosauridae	Skull & skeleton	L.D. Watson / J. McCabe	1984	
Q178	444805	5633095	662.4	*Daspletosaurus* sp.	Skull & skeleton	P.J. Currie / M. Klassen	1985	
Q179	477273	5629803	700.3	*Styracosaurus albertensis*	Partial skull & skeleton	C.D. Switzer. J. Bancroft / P. May. K. Aulenback	1986	Ryan et al., 2007
Q180	464483	5622229	666.4	*Leidyosuchus canadensis*	Skull	J. Walper / K. Aulenback	1986	
Q181	464439	5622418	665.8	*Centrosaurus apertus*	Partial skull; juvenile	T. Tokaryk	1982	Dodson & Currie, 1988
Q182	465263	5621096	704.6	*Leidyosuchus canadensis*	Complete skull	K. Kucher / H. Larsson. R. Coria	1999	

Q183	459304	5622637	696	*Styracosaurus albertensis*	Nearly complete skull	J. McCabe / J. McCabe. C. Coy	1987	
Q184	473421	5623949	712.4	*Chasmosaurus irvinensis*	Partial skull	L.J. Strong / M. Fisk	1987	Holmes et al., 2001
Q185	466760	5623505	664	Hadrosauridae	Partial skeleton	G. Naylor? / M. Klassen. C. Coy	1986	
Q186	471646	5624452	682.5	Hadrosauridae	Partial skeleton	D. Brinkman / C. Coy. D. Fisk	1986	
Q187	464402	5622149	669.4	*Stenonychosaurus inequalis*	Braincase	T. Zhilu	1986	Currie & Zhao, 1993
Q188	459968	5622336	678	Ornithomimidae	Partial skeleton	J. McCabe / K. Kucher. C. Coy	1987	
Q189	460057	5619802	698.3	*Champsosaurus lindoei*	Skull & partial skeleton	L.J. Strong / J. McCabe	1987	
Q190	460221	5620561	694.4	Ornithomimidae	Limb elements	D. Brinkman / D. Fisk	1987	
Q191	490467	5632786	668.6	*Struthiomimus altus*	Partial skeleton	B. Nicholls	1980	Nicholls & Russell, 1981
Q192	476445	5626396	700.5	*Prosaurolophus maximus*	Skull & skeleton	J. Nicholls / B. Nicholls	1981	
Q193	476475	5626068	762.5	*Tylosaurus* sp.	Partial skeleton	G. Stonely	1983	
Q194	474568	5624354	692.7	Hadrosauridae	Partial skeleton	D. Seburn / G.L.P. Danis	1988	
Q195	463074	5624441	661.3	*Euoplocephalus tutus*	Skull & cervical ring	D. Brinkman	1998	
Q196	458985	5629593	674.6	cf. *Parasaurolophus*	Skeleton; sunk at sea?	C.H. Sternberg	1916	
Q197	460402	5619836	692.8	Lambeosaurinae	Skeleton used in IMAX film	J. McCabe / G.L.P. Danis	1988; 1991	
Q198	457877	5630232	666.1	*Euoplocephalus tutus*	Skull	W. Sloboda / P.J. Currie	1991	
Q199	460273	5620699	693.3	Ornithomimidae	Skeleton	P.J. Currie	1991	
Q200	460401	5619654	697.2	*Gorgosaurus libratus*	Skull & skeleton	P.J. Currie. D. Tanke / P.J. Currie	1991	
Q201	464202	5620723	694	*Edmontonia rugosidens*	Skull	T. Zhilu	1991	
Q202	471243	5624251	695.1	*Basilemys variolosa*	Carapace	K. Kucher	1991	
Q203	458229	5630767	671.5	*Euoplocephalus tutus*	Skull	W. Sloboda	1992	
Q204	458066	5630879	659.8	*Centrosaurus apertus*	Skull	R. Stiller / H. Larsson	1992	
Q205	464448	5623523	655.2	Lambeosaurinae	Skull		1992	

Q206	464070	5621444	686	cf. *Parasaurolophus*	Skeleton	D. Tanke	1992-96	
Q207	463442	5621309	667.9	*Cryodrakon boreas*	Holotype; partial skeleton	W. Sloboda	1992	Hone et al., 2019
Q208	460389	5619620	700.5	*Prosaurolophus maximus*	Skull	D. Tanke	1992	
Q209	463738	5620779	687.4	Ornithomimidae	Partial skeleton	W. Sloboda / K. Wallis	1992	
Q210	477179	5630340	695.3	*Daspletosaurus* sp.	Skull & partial skeleton	W. Marshall / P.J. Currie	1993	
Q211	465559	5620770	693.2	Ornithomimidae	Partial skeleton	S. Currie. K. Wallis / P.J. Currie	1993	
Q212	465963	5620514	713	*Chasmosaurus* sp.	Skull	W. Sloboda	1993	
Q213	465464	5621262	696.1	*Prosaurolophus maximus*	Skull & skeleton	D. Tanke	1993	
Q214	463475	5620725	681.9	Ornithomimidae	Partial skeleton	P.J. Currie	1994	
Q215	463503	5621173	680.8	*Daspletosaurus* sp.	Skull & partial skeleton	P.J. Currie	1994	
Q216	463082	5622047	663.2	Lambeosaurinae	Skull & partial skeleton	N. Beavan	1994	
Q217	462721	5621120	669.6	*Centrosaurus apertus*	Skull	K. Routley / W. Sloboda	1994	
Q218	466160	5620108	723.8	*Gorgosaurus libratus*	Partial skull; immature	J. McCabe / P.J. Currie	1994	
Q219	462857	5622836	657.3	*Gorgosaurus libratus*	Skull & partial skeleton	C. Manz / P.J. Currie	1995	
Q220	462202	5621241	660.2	*Gorgosaurus libratus*	Skeleton	W. Sloboda / P.J. Currie	1996-97	
Q221	464070	5622334	663.7	*Ornithomimus edmontonicus*	Skull & skeleton	P.J. Currie. C. Coy	1995	Norell et al., 2001; Zelenitsky et al., 2012
Q222	459523	5629339	682.7	*Unescoceratops koppelhusae*	Jaw with teeth; in BB055	P.J. Currie	1995	Ryan et al., 2012
Q223	464025	5621002	682	*Daspletosaurus torosus*	Skull & skeleton	B. Brown	1914	Matthew & Brown, 1923
Q224	458014	5630713	654.7	*Centrosaurus apertus*	Skull	P. Druckenmiller / K. Kucher	1997	
Q225	458709	5629623	667	Hadrosauridae	Skeleton	E. Stefanuk / M. Vickaryous. K. Kucher	1998	
Q226	459057	5629756	666.4	*Myledaphus bipartitus*	Skeleton	D. Brinkman / K. Kucher	1998	Neuman & Brinkman, 2005
Q227	458504	5629650	679.5	Nodosauridae	Skull	K. Kucher / M. Vickaryous. K. Kucher	1998	

Q228	458533	5629640	680	*Panoplosaurus mirus*	Skull & partial skeleton	M. Getty / M. Vickaryous. K. Kucher	1998	
Q229	458368	5629740	667.7	*Edmontonia*	Skull	D. Brinkman / M. Vickaryous. K. Kucher	1998	
Q230	462737	5624446	661.2	*Edmontonia rugosidens*	Skull & partial skeleton	P.J. Currie / M. Vickaryous. K. Kucher	1998	
Q231	463348	5621390	674.2	*Centrosaurus apertus*	Skull; in BB152	L. Sternberg	1927	
Q232	463166	5621632	668.2	Hadrosauridae	Disarticulated skeleton	E. Riggs. G.F. Sternberg	1922	
Q233	459381	5629460	679.9	*Basilemys variolosa*	2 specimens with skulls & limbs	D. Kazmaier / D. Brinkman	2000	
Q234	457553	5629660	665.7	*Gorgosaurus* sp.	Partial skull & jaws	D. Wagoner / P.J. Currie	2000	
Q235	464898	5621299	682.2	Ankylosauridae	Distorted skull	D. Tanke	2000	
Q236	465690	5621050	709	Tyrannosauridae	Hind leg	C.H. Sternberg	1914	D. A. Russell, 1970
Q237	464081	5621055	680.2	*Chasmosaurus* sp.	Skull & partial skeleton	G.F. Sternberg	1920	Tyson, 1977
Q238	466115	5620720	717.1	*Gorgosaurus libratus*	Skull & skeleton	E. Stefanuk / K. Kucher	1999	
Q239	465305	5623641	665.4	Hadrosauridae	Partial skeleton	E. Koppelhus / K. Kruger.G. Harding	2002	
Q240	473292	5623474	714.6	*Pachyrhinosaurus* sp.	Partial skeleton	G. Johnson / K. Kruger	2000-03	Ryan et al., 2010
Q241	489000	5632795	662.4	*Euoplocephalus tutus*	Partial skeleton	G.F. Sternberg	1915	C. H. Sternberg, 1917
Q242	490260	5632357	678.6	Hadrosauridae	Headless skeleton	C.H. Sternberg	1915	
Q243	490268	5632360	680.6	*Corythosaurus casuarius*	Skeleton	C.H. Sternberg	1915	C. H. Sternberg, 1917
Q244	465416	5622908	672	Ornithomimidae	Skeleton	P. Bell	2005	
Q245	455510	5628927	677.8	?Crocodylia		J.C. Danis		
Q246	458680	5629627	673	*Basilemys variolosa*		G.F. Sternberg / C.H. Sternberg. L. Lambe	1914	
Q247	465133	5623111	667.1	*Corythosaurus casuarius*	Skeleton in BB189	W. Sloboda	2002	
Q248	460563	5619573	700.2	*Styracosaurus albertensis*	Partial skull	D. Tanke	2004-05	C. M. Brown et al., 2020
Q249	463864	5621507	670.5	*Centrosaurus apertus*				

Q250	460621	5621497	693.1	*Styracosaurus albertensis*	Partial skull	B. Brown	1912?; 2006; 2015	B. Brown & Schlaikjer, 1937; C. M. Brown et al., 2020
Q251	470185	5623512	661.8	*Edmontonia rugosidens*				
Q252	464376	5623471		*Gryposaurus*				
Q253	472949	5624983	697.8	*Gorgosaurus libratus*				
Q254	473236	5625167	651.2	Ornithomimidae	Skeleton with feathers	D. Larson, P.J. Currie et al.	2009?	van der Reest et al., 2016
Q255	474242	5625921	669	*Chasmosaurus belli*	Nearly complete skull & skeleton; juvenile	P.J. Currie	2010	Currie et al., 2016
Q256	473923	5625833	712	*Styracosaurus albertensis*	Partial skull & skeleton			C. M. Brown et al., 2020
Q257	466135	5621380	691.3	*Gorgosaurus libratus*				
Q258	474346	5625939	650	*Gorgosaurus libratus*				
Q259	464159	5621579	688.7	*Corythosaurus casuarius*		D. Trexler		
Q260	457565	5630537	650.4	*Saurornitholestes langstoni*	Nearly complete skull & skeleton	C. Coy / C. Coy. P.J. Currie	2014	Currie & Evans, 2020
Q261	458078	5630742	658	Nodosauridae	Skull		2015	
Q262	441261	5630148	668	*Styracosaurus albertensis*	Complete skull & skeleton	S. Persons et al.	2015-18	Holmes et al., 2020
Q263	468921	5621986	698.3	*?*			2016	
Q264	469392	5623780	698	*Prosaurolophus maximus*	Skeleton; originally labeled U258	H. Larsson et al.	2016	
Q265	468867	5622069	666.8	Ankylosauridae			2015/06/15	
Q266	465207	5621056		*Anchiacipenser acanthaspis*	Skeleton	H. Sato / H. Sato et al.	2016	Sato et al., 2018
Q267	474261	5626091	701.4	*Chasmosaurus* sp.				
Q268	461295	5617724	695.75	*Styracosaurus albertensis*	Complete skull & partial skeleton	J. Wood / D. Tanke et al.	2009	C. M. Brown et al., 2020; Holmes & Ryan, 2013
Q269	465930	5620672	692.5	*Lambeosaurus lambei*				
Q270	474892	5627060	694	Crocodylia	Skull			
Q271	462928	5618297	692	*Gorgosaurus libratus*				
Q272	468540	5621530	685	*Chirostenotes pergracilis*	Jaw & partial skeleton	E. Bamforth / P.J. Currie et al.	2016	Funston & Currie, 2020
Q273	464140	5621204	671	*Euoplocephalus tutus*	Holotype; complete skull & partial skeleton	B. Brown	1912-15; 2019	Penkalski, 2018
Q274	463725	5621188	668.68	*Gorgosaurus libratus*	Skull & skeleton	B. Brown	1912-15	Matthew & Brown, 1923

Q275	471720	5624514	691.2	Lambeosaurinae	Partial postcranial skeleton	P.J. Currie et al. / H. Larsson et al.	2018	
Q276	470825	5617226		*Styracosaurus albertensis*	Partial skull		2010	C. M. Brown et al., 2020
Q277	469893	5623511	663.8	Hadrosauridae indet.	Disarticulated skull	B. Spencer / H. Larsson et al.	2019	
Q278	464444	5622412	660.2	Hadrosauridae indet.	Arm and hand	C. Coy		
Q279	468135	5622341	**676.8**	Tyrannosauridae	Disarticulated skeleton	A. Lindsay	Fall 2019	
Q280	465326	5622126	**674.1**	Hadrosauridae indet.	Near-complete skeleton	T. Kaskie	Summer 2021	
Q281	464807	5621179	**676.2**	Tyrannosauridae indet.	Maxilla and lacrimal	J. Blacklaws	Summer 2020	
Q282	464442	5621009	**683.9**	Tyrannosauridae indet.	Partial skeleton	D. Tanke	Summer 2018	
Q283	463987	5621184	**668.3**	*Centrosaurus apertus*	Partial skeleton			
Q284	458014	5630733	657.3	*Centrosaurus apertus*	Partial skull	P.J. Currie	2023-06-22	
Q285	464177	5621297	**671.8**	*Foraminacephale brevis*	Partial skull dome	P. Bell		
Q286	460016	5620326	**660.8**	*Euoplocephalus tutus*	Tail club knob	C.M. Brown et al.	2023-07-19	
Q287	460171	5620475	**660.8**	Ornithomimidae	Articulated skeleton	L. Liboiron		
Q288	458800	5629400	**648.4**	Hadrosauridae and *Plesiobaena*	Skull and carapace		1998	
Q289	475367	5625614	**655.7**	cf. *Styracosaurus albertensis*	Partial skull		2003	
Q290	464470	5624959	**654.8**	*Corythosaurus casuarius*	Partial skull	D. Tanke	2007	
Q291	471671	5620714	**672.7**	Hadrosaurinae	Skull	C. Coy	2014-05-27	
Q292	465191	5621202	695.3	Ornithomimidae	Sacrum	J. Liu; G. Funston	2015	
Q293	458951	5629626	**648.4**	*Basilemys variolosa*	Partial skeleton		2016	
Q294	460780	5620319	**669**	Ornithomimidae	Partial skeleton		2016	
Q295	465340	5620953	**670.6**	*Lambeosaurus lambei*	Skull		2017	

Q296	472367	5623664	682	*Corythosaurus* sp.	Skull	A. van der Reest	2018-06-17	
Q297	469894	5623598	**660.1**	Ankylosauridae	Tail handle segment	M. Rhodes et al.	2019-06-21	
Q298	469893	5623509	664	Lambeosaurinae cf. *Parasaurolophus*	Skull roof	B. Spencer	2000-10-18	Formerly U167
Q299	467832	5624571	654	*Axestemys allani*	Complete skeleton	H. Larsson et al.	2021-08-23	
Q300	472620	5622194	743	Ceratopsidae indet.	Partial skull	H. Larsson et al.	2018-06-17	
Q301	465759	5621896	689	Hadrosauridae	Disarticulated skull	D. Tanke	1990s	Formerly U190
Q302	459666	5629526	677	cf. *Panoplosaurus mirus*	Complete skull	A. Mueller; L.-P. Bateman	2023-08-23	
Q303	465171	5622330	670	cf. *Brachylophosaurus canadensis*	Partial skull and skeleton	P.J. Currie; C. Sullivan	2024-06-11	
Q304	470073	5623766	687.1	*Lambeosaurus lambei*	Articulated skull and skeleton	G. Funston	2018-06-05	Formerly U272
Q305	473211	5623434	700	cf. *Styracosaurus albertensis*	Disarticulated skeleton; juvenile	W. Sloboda / H. Larsson et al.	2001-07-30	Formerly U172

Elevation in bold indicates elevation estimated solely from TMP DEM.

Table 2. Monodominant, mixed faunal bonebeds and vertebrate microfossil localities marked in Dinosaur Provincial Park

Quarry Number	UTM East	UTM North	Elevation (MASL)	Identification	Discovered by	Date discovered	References / Remarks
BB001	465540	5621829	695.29	Mixed faunal		1984-08-06	
BB002	465517	5621808	690.87	Mixed faunal	J.C. Danis	1984-08-06	
BB003	465479	5621731	695.13	Mixed faunal	P.J. Currie	1984-08-02	
BB004	465393	5621781	693.94	Mixed faunal	P.J. Currie	1984-08-06	
BB005	465504	5621984	673.99	Mixed faunal	P.J. Currie	1984-08-31	
BB005A	465520	5622009	673.18	Mixed faunal	P. Dodson	1984-08-01	
BB006	466694	5623521	670.54	Microsite (Class D BB)	P.J. Currie	1984-08-07	
BB007	466623	5623521	663.88	Microsite (Class D BB)	J.C. Danis		
BB008	459539	5629922	680.36	Mixed faunal	P.J. Currie	1984-08-17	
BB009	465316	5621392	690.44	Mixed faunal	D. Tanke	1984-08-02	
BB010	465380	5621627	692.04	Mixed faunal	P.J. Currie	1984-08-18	Includes Q147
BB011	466009	5622447	669.92	Mixed faunal	P.J. Currie	1984-08-18	
BB012	465972	5622197	676.88	Mixed faunal	P. Dodson	1984-08-01	
BB013	465899	5622120	673.92	Mixed faunal	P.J. Currie	1984-08-18	
BB014	465852	5621821	698.33	Mixed faunal	P.J. Currie	1984-08-02	
BB015	465627	5621922	689.5	Mixed faunal	S. Andrews	1984-08-21	
BB016	465720	5622170	667.85	Monodominant, Hadrosauridae	P.J. Currie	1984-08-21	
BB017	469927	5623665	674.62	Mixed faunal	P.J. Currie	1984-08-22	
BB018	465149	5625489	660.81	Mixed faunal	P.J. Currie	1984-08-22	
BB020	460459	5619614	700.11	Mixed faunal	D. Tanke	1984-07-02	
BB020A	460334	5619676	693.61	Mixed faunal	P. Dodson	1986-08-03	
BB024	465490	5621892	681.95	Mixed faunal	P. Dodson	1984-08-01	
BB025	465145	5621069	695.3	Mixed faunal	P. Dodson; L.J. Strong; P.J. Currie	1985-08-01	Brinkman, 1990; Eberth, 1990
BB026	460110	5620589	703.74	Mixed faunal	P. Dodson	1984-08-01	
BB028	463804	5621495	656.33	Mixed faunal	P. Dodson	1984-08-01	
BB028A	463746	5621381	665.26	Mixed faunal	P.J. Currie	2003-07-21	
BB029	464640	5621653	680	Mixed faunal	P.J. Currie	1984-08-28	
BB030	464259	5621656	671.25	Monodominant, *Centrosaurus apertus*	D.A. Russell	1984-08-02	Eberth & Getty, 2005
BB031	466116	5622422	668.2	Mixed faunal Class D	R.A. Mussieux; D. Tanke	1980-08-27	Brinkman, 1990; Eberth, 1990
BB032	465964	5621919	706.13	Microsite (Class D BB)	P.J. Currie	1984-08-29	
BB033	457748	5629510	659.03	Mixed faunal	P.J. Currie	1984-08-29	
BB034	458003	5628730	667.11	Mixed faunal	P.J. Currie	1984-08-30	

BB035	458146	5628655	681.31	Mixed faunal	P.J. Currie	1984-08-30	
BB036	465746	5622097	679.19	Mixed faunal	P.J. Currie	1984-08-31	
BB037	464339	5621297	670.99	Mixed faunal	J. Walper		
BB038	464248	5621365	669.78	Mixed faunal	P.J. Currie	1984-09-01	
BB038A	464180	5621193	672.36	Mixed faunal	P.J. Currie	1984-09-01	
BB039	465305	5623567	662.41	Mixed faunal	P.J. Currie	1984-09-02	
BB041	470001	5623291	660.91	Monodominant, *Centrosaurus apertus*	L.J. Strong	1985-08-20	Eberth & Getty, 2005
BB041A	469292	5623613	660.84	Monodominant, *Centrosaurus apertus*	P.J. Currie	1996-08-27	Eberth & Getty, 2005
BB041AA	469221	5623530	676.69	Monodominant, *Centrosaurus apertus*	P.J. Currie	1996-08-27	
BB041AB	469158	5623518	662.6	Monodominant, *Centrosaurus apertus*		2013-05-29	
BB042	465174	5620973	698.9	Mixed faunal	D. Taylor	Summer 1966	Visser, 1986; 40% *Styracosaurus albertensis*
BB043	465855	5622575	663.76	Monodominant, *Centrosaurus apertus*	B. Brown	2009-05-31; orig. 1912?	Currie & Dodson, 1984; Ryan et al., 2001; includes Q143
BB044	458514	5631373	682.07	Mixed faunal	L.J. Strong	1985-06-03	
BB044A	458338	5631198	680.62	Mixed faunal	L.J. Strong	1985-06-03	
BB044B	458463	5631139	683.92	Mixed faunal	L.J. Strong	1985-06-03	
BB045	459232	5630175	669.77	Mixed faunal	R. Solkoski	1985-06-06	
BB046	464400	5621074	678.59	Mixed faunal	L.J. Strong	1985-06-09	
BB047ABC	463777	5620773	689.08	Mixed faunal	L.J. Strong	1985-06-13	Tumarkin-Deratzian, 1997
BB048	459003	5629683	667.68	Mixed faunal	L.J. Strong	1985-06-05	
BB049	464307	5621186	677.53	Microsite (Class D BB)	L.J. Strong	1985-06-29	
BB050	464120	5621586	685.95	Mixed faunal	L.J. Strong	1985-06-29	
BB051	464062	5622340	661.86	Mixed faunal	L.J. Strong	1985-08-31	Brinkman, 1990; Eberth, 1990
BB052	465522	5623170		Mixed faunal	J. Proudfoot	1985-06-01	
BB053	464311	5622042	668.35	Mixed faunal	L.J. Strong	1985-08-31	
BB054	459354	5629457	678.34	fish; frog; hadrosaur tooth	L.J. Strong	1985-06-05	Brinkman, 1990; Eberth, 1990
BB054A	459350	5629507	676.04	fish; frog; hadrosaur tooth	L.J. Strong	1985-06-05	Brinkman, 1990; Eberth, 1990
BB055	459531	5629357	682.33	Mixed faunal	M. Hirsch; B. Hirsch	1985-07-13	Includes *Unescoceratops koppelhusae* holotype
BB056	459702	5629452	684.42		L.J. Strong	1985-07-18	
BB057X	477035	5629053	694.29	Microsite (Class D BB)	P. Dodson	2007-06-16	
BB057Y	477072	5628982	673.8	Microsite (Class D BB)			
BB057Z	477058	5629031	686.18	Microsite (Class D BB)	P. Dodson	2007-06-16	
BB058	456202	5627052	672	Mixed faunal	P. Dodson	1985-08-11	
BB059	463803	5620572	697.77	Mixed faunal	L.J. Strong	1985-08-12	
BB060	469701	5623243	648.12	Mixed faunal	L.J. Strong	1985-08-20	

BB061	466580	5622530	673.87	*Centrosaurus apertus* plus mixed faunal	P.J. Currie; L.J. Strong; D. Tanke	1985-08-22	Eberth & Getty, 2005
BB061A	466746	5622578	664.41	*Centrosaurus apertus* plus mixed faunal	P.J. Currie; L.J. Strong; D. Tanke	1985-08-22	Eberth & Getty, 2005
BB062	466875	5622846	659.62	*Centrosaurus apertus* plus mixed faunal	D.A. Russell		
BB062A	466877	5622794	666.41	Mixed faunal	P.J. Currie; L.J. Strong	1985-08-22	
BB063	466996	5622407	671.54	Mixed faunal	P.J. Currie	1985-08-22	
BB063A	467006	5622413	679.23	Mixed faunal	P.J. Currie		
BB064	459219	5627460	658.85	Mixed faunal	L.J. Strong et al.	1985-08-08	
BB065	463865	5621001	670.83	Hadrosauridae; Tyrannosauridae	L.J. Strong	1985-08-31	
BB066	463597	5622201	662.49	Mixed faunal	L.J. Strong	1985-08-31	
BB067	464014	5617123	707.04	Mixed faunal	L.J. Strong	1986-06-11	
BB068	463928	5617389	707.13	Mixed faunal	L.J. Strong	1986-06-11	
BB069	463761	5620207	698.44	Mixed faunal	L.J. Strong	1986-06-02	
BB070	463751	5624446	664.01	Mixed faunal	L.J. Strong	1986-06-16	Brinkman, 1990; Eberth, 1990
BB071	471196	5622243	690.98	Mixed faunal	P.J. Currie; L.J. Strong	1986-06-10	
BB072	464503	5620619	699.08	Mixed faunal	K. Aulenback	1986-06-19	
BB073	464621	5620893	698.4	Mixed faunal	P.J. Currie; L.J. Strong	1986-06-19	
BB074	464575	5620884	694.73	Mixed faunal	P.J. Currie; L.J. Strong	1986-06-19	
BB075	465337	5621092	704.24	Mixed faunal	P. Dodson	1986-08-21	Brinkman, 1990; Eberth, 1990
BB076	467847	5624453	652.4	Mixed faunal	L.J. Strong	1986-07-22	
BB077	467867	5624746	674.04	Mixed faunal	P.J. Currie	1986-07-22	
BB078	467729	5624673	675.48	Mixed faunal	P.J. Currie	1986-07-23	Brinkman, 1990; Eberth, 1990
BB079	471193	5622373	679.49	Microsite (Class D BB)	P. Dodson	1986-08-03	
BB081A	460456	5621529	704.26	Microsite (Class D BB)	P. Dodson	1986-08-03	
BB081B	460447	5621652	702.85	Microsite (Class D BB)	P. Dodson	1986-08-02	
BB084	465911	5620699	703.71	Mixed faunal	E. Koster; B. Buoy	1986-08-06	
BB085	464598	5622253	714.61	Mixed faunal	L.J. Strong	1986-08-09	Incorporates BB040
BB086	464624	5622256	666.43	Mixed faunal	L.J. Strong	1986-08-02	Brinkman, 1990; Eberth, 1990
BB086A	466978	5621962	661.84	Mixed faunal	L.J. Strong	1986-08-02	Brinkman, 1990; Eberth, 1990
BB087	465911	5620699	697.33	Mixed faunal	L.J. Strong	1986-08-20	
BB088	467750	5622250	709	Microsite Class D			Eberth, 1990
BB089	464493	5616783	735.7	Fish; Ceratopsidae; tree and plant	L.J. Strong	1986-06-10	
BB090	462812	5620653	679.49	Mixed faunal	J. Walper; P.J. Currie et al.	1988-06-02	
BB091	462794	5620616	672.9	Monodominant, *Centrosaurus apertus*	R. Ens; J. Walper	1988-05-02	Eberth & Getty, 2005

BB091A	462963	5620167	679.67	Monodominant, *Centrosaurus apertus*		1988-05-02	Eberth & Getty, 2005
BB091B	463025	5619999	681.31	Monodominant, *Centrosaurus apertus*		1988-05-02	
BB091C	463279	5620143	681.03	Monodominant, *Centrosaurus apertus*		1988-05-02	
BB092	471061	5624020	676.98	Mixed faunal	P.J. Currie	1988-08-02	
BB093	470668	5623670	688.21	Mixed faunal	L.D. Watson	1983-05	
BB094	477111	5629460	674	Mixed faunal	P. May	1990-06-02	Brinkman, 1990; Eberth, 1990
BB095	477111	5629460	680	Mixed faunal	K. Aulenback	1990-06-16	
BB096	477182	5629682	689.59	Marine fauna	K. Aulenback	1990-06-16	Beavan & Russell, 1999; Brinkman et al., 2005
BB097	467705	5622390	676.09	Mixed faunal	J.C. Danis		Brinkman, 1990; Eberth, 1990
BB098	467377	5622510	663.49	Mixed faunal; eggshell locality	D. Brinkman		Brinkman, 1990; Eberth, 1990
BB099	467335	5622457	669.14	Mixed faunal	D. Brinkman	1990-06-02	
BB100	462563	5623135	654.11	Mixed faunal	J. Walper	long ago	Brinkman, 1990; Eberth, 1990
BB101	474782	5624890	725.48	Marine fauna	M. Klassen et al.	1990-07-23	
BB102	455537	5629186	678	Microsite (Class D BB)	L.J. Strong	1990-07-15	Brinkman, 1990; Eberth, 1990; includes Q061, Q130, Q144, Q152
BB103	477373	5631251	646.18	Microsite (Class D BB)	B. Nicholls	1990-07-02	Brinkman, 1990; Eberth, 1990
BB104	463724	5622515	678.96	Microsite (Class D BB)	P. Johnston		Brinkman, 1990; Eberth, 1990
BB105	463963	5622791	642.91	Microsite (Class D BB)	D. Brinkman	?	Brinkman, 1990; Eberth, 1990
BB106	471920	5623008	685.89	Microsite (Class D BB)	F. Cote		Brinkman, 1990; Eberth, 1990
BB107	463095	5624200	654.5	Microsite (Class D BB)	C. Page		Brinkman, 1990; Eberth, 1990
BB108	456043	5627192	671.25	Microsite (Class D BB)	W. Marshall		Brinkman, 1990; Eberth, 1990
BB109	459710	5622131	660	Microsite (Class D BB)	L.J. Strong	1991-06-05	
BB110	460264	5622340	687	Microsite (Class D BB)	L.J. Strong J. McCabe	1991-06-09	
BB111	460270	5622349	688	Microsite (Class D BB)	L.J. Strong	1991-06-10	
BB112	464698	5621254	676.74	Microsite (Class D BB)	D. Tanke		
BB113	474349	5624043	725.01	Microsite (Class D BB)	J. McCabe	1991-06-11	
BB114	473796	5623641	705.94	Mixed faunal	A. Mandryk	1991-08-02	
BB115	473630	5624062	713.17	Mixed faunal; estuarine channel	J. McCabe	1991-08-02	Brinkman, 1990; Eberth, 1990
BB116	463998	5624709	652.66	Microsite (Class D BB)	D. Heyd	1992-08-15	
BB117	463753	5622676	686.53	Microsite (Class D BB)	D. Eberth	Summer 1986	Brinkman, 1990; Eberth, 1990
BB118	463006	5622369	648.97	Microsite (Class D BB)	G. Dongl	Summer 1985	Brinkman, 1990; Eberth, 1990
BB119	466170	5621068	721.3	Microsite (Class D BB)	D. Brinkman	Summer 1985	Brinkman, 1990; Eberth, 1990
BB120	468465	5621694	697.61	Microsite (Class D BB)	D. Sabo	Shown in 1987	
BB121	464281	5622573	656.77	Microsite (Class D BB)	M. Cross	Summer 1987	Brinkman, 1990; Eberth, 1990
BB122	463809	5621504	665.01	Microsite (Class D BB)	H. Dompierre	1994-06-18	

BB123	463803	5621492	665.46	Mixed faunal	J. McCabe	1994-06-21	
BB124	462963	5622310	648.16	Mixed faunal	J. McCabe	1994-06-11	
BB125	463469	5624333	668.68	Mixed faunal	J. McCabe	?	
BB126	463980	5621500	681.32	Mixed faunal	?	?	
BB127	460626	5620366	703.15	Mixed faunal	P.J. Currie	1995-08-01	
BB128	465480	5622747	667.99	*Centrosaurus apertus* plus mixed faunal	M. Ryan	1993-07-02	Eberth & Getty, 2005
BB129	462670	5621129	668.92	Mixed faunal	P.J. Currie	1996-08-03	
BB130	461455	5620681	704.9	*Centrosaurus apertus* plus mixed faunal	P.J. Currie	1996-07-02	C. M. Brown et al., 2020
BB131	472002	5621988	715.21	Microsite (Class D BB)	P.J. Currie	1996-08-07	
BB132	469967	5623523	669.06	Mixed faunal	D. Tanke	1996-08-27	
BB133	466293	5622532	674.34	Mixed faunal	D. Tanke	1997-07-04	
BB134	464481	5621386	681.51	Mixed faunal	D. Tanke	1997-06-01	
BB135	463348	5620034	685.06	Mixed faunal	P.J. Currie	1998-07-19	Brinkman et al., 1998
BB136	462936	5620176	671.05	Mixed faunal	P.J. Currie	2009-06-15	
BB137	463345	5621230	667.04	Microsite (Class D BB)	P.J. Currie	1998-07-21	Brinkman et al., 1998
BB138	463030	5621887	648.73	Monodominant, *Coronosaurus brinkmani* (Oldman Formation)	P.J. Currie	1998-08-10	Ryan & Russell, 2005
BB139	462726	5621225	667.92	Microsite (Class D BB)	P.J. Currie	1998-08-23	
BB140	470861	5622443	663.45	Mixed faunal	P.J. Currie. S. Wright	1999-07-14	Above Q083
BB141	470850	5622378	672.29	Mixed faunal	S. Wright	1999-07-14	Just above BB140
BB142	460022	5629307	696.44	Microsite (Class D BB)	C. Coy	1999-08-23	
BB143	459934	5622212	682	Mixed faunal	P.J. Currie	2000-07-12	
BB144	462185	5621510	659.1	Mixed faunal	P.J. Currie	2000-07-12	
BB145	465674	5623129	666.3	Mixed faunal	P.J. Currie. K. Kucher	2000-07-13	
BB146	465560	5623015	676.63	Microsite (Class D BB)	P.J. Currie	2000-07-14	
BB146A	465644	5623040	676.76	Microsite (Class D BB)	P.J. Currie	2000-07-14	
BB146B	465485	5622985	677	Microsite (Class D BB)		2010-05-27	
BB147	473180	5623493	696.61	Mixed faunal	P.J. Currie	2000-07-25	
BB148	473300	5623480	714.54	Mixed faunal	G. Johnson	2000-07-24	
BB149	463838	5620565	693.75	Mixed faunal	D. Tanke	2001-03-14	
BB150	458037	5630722	660.76	Mixed faunal	P. Druckenmiller	2001-08-12	
BB151	458256	5630708	667.42	Mixed faunal	P. Druckenmiller	2001-08-12	
BB152	463401	5621378	675.05	Monodominant, Ceratopsidae	M. Getty		Eberth & Getty, 2005

BB153	461912	5624740	665.66	Mixed faunal	P.J. Currie	2002-07-09	
BB154	463889	5624794	660.05	Mixed faunal	P.J. Currie	2002-07-30	
BB155	463667	5624740	671.67	Mixed faunal	P.J. Currie	2002-07-30	
BB156	459453	5627146	669.76	Monodominant, *Styracosaurus*	D. Marsh; M. Ryan	2002-07-31	Eberth & Getty, 2005
BB157	459461	5627183	685.47	Mixed faunal	P.J. Currie	2002-07-31	
BB158	463013	5624673	676.05	Mixed faunal	E. Felber	2002-07-28	
BB159	468802	5622241	669.69	Mixed faunal	B. Coultes	2002-08-04	
BB160	468539	5622505	674.65	Microsite (Class D BB)	B. Coultes	2002-08-04	
BB161	462814	5624489	656.57	Microsite (Class D BB)	E. Felber	2002-07-28	
BB162	462777	5624622	654.24	Monodominant, *Centrosaurus apertus*	P.J. Currie	2002-07-11	Eberth & Getty, 2005
BB163	463059	5624648	669.81	Mixed faunal	P.J. Currie	2002-07-28	
BB164	472179	5622476	698.62	Mixed faunal	P.J. Currie	2002-08-15	
BB165	471487	5622282	679.07	Monodominant, Ceratopsidae	D. Tanke	2002-08-19	Eberth & Getty, 2005
BB166	458016	5630725	654.39	Monodominant, *Centrosaurus apertus*			Eberth & Getty, 2005
BB167	474698	5626642	707.58	Monodominant, Ceratopsidae cf, *Styracosaurus*	P.J. Currie	2002-08-26	
BB168	463553	5621225	668.63	Monodominant, *Centrosaurus apertus*	D. Tanke; M. Getty	2002-09-12	Eberth & Getty, 2005
BB169	464716	5625072	664.27	Mixed faunal	P.J. Currie	2004-08-01	
BB170	471132	5624097	679.12	Mixed faunal	P.J. Currie	Many years ago	
BB171	459618	5629718	664.44	Mixed faunal	E. Felber	2005-07-07	
BB172	466385	5624206	655.41	Mixed faunal	P.J. Currie	2005-07-27	
BB173	464377	5624895	654.94	Mixed faunal	T.E. Guldberg	2005-07-28	
BB173A	464413	5624935	651.84	Mixed faunal	T.E. Guldberg	2005-07-28	
BB174	464545	5624996	665.63	Mixed faunal	P.J. Currie	2005-07-28	
BB175	458293	5629222	674.05	Mixed faunal	P.J. Currie	2005-07-29	
BB176	458545	5630378	665.76	Mixed faunal	P.J. Currie	2005-07-31	
BB177	463006	5624843	696.78				
BB178	463353	5624294	658.18		R. Pryor	2005-10-18	Eberth & Getty, 2005
BB179	458691	5627859	670.7		D. Eberth	2005-10-18	
BB180	471134	5622271	669.88	Monodominant, *Centrosaurus apertus*	P.J. Currie	2005-10-20	C. M. Brown, Herridge-Berry, et al., 2020
BB181	471144	5622294	676.3			2015-06-15	
BB182	468535	5622444	667.2	Mixed faunal	D. Tanke	2005-10-22	
BB183	462936	5620176	671.01				
BB184	465845	5621722	707.4	Mixed faunal	P.J. Currie	2006-06-26	
BB185	473753	5624018	666.19	Hadrosauridae? Mixed faunal	J. Achenbach	2006-07-04	
BB186	475438	5625755	695.54	Hadrosauridae; Ankylosauridae;	P.J. Currie	2006-07-07	

				Tyrannosauridae			
BB187	462480	5622820	688.29	Mixed faunal	P.J. Currie	2006-07-08	
BB188	465415	5623387	668.12	Monodominant, *Centrosaurus apertus*	W. Sloboda	2006-07-19	Eberth & Getty, 2005
BB189	465138	5623247	664.29	Mixed faunal incl, *Corythosaurus* skull	W. Sloboda	2002-07-19	
BB190	472379	5623176	687.73	Mixed faunal	M. Archer; H. Godthelp	2006-07-20	A.D.-P. thesis
BB191	466087	5621517	694.08	Mixed faunal	P.J. Currie	2007-05-21	
BB192	463194	5620319	705.17			2007-05-24	
BB193	463408	5620479	700.08			2007-05-24	
BB194	472277	5621647	718.79	Mixed faunal	P.J. Currie	2007-05-25	
BB195	460321	5621273	682.73	Mixed faunal	P. Druckenmiller	2007-05-28	
BB196	474140	5624198	701.59	Mixed faunal	D. Brinkman	2007-05-15	
BB197	463358	5621094	672.82	Mixed faunal	P.J. Currie	2007-06-14	
BB198	477274	5630532	697.56	Microsite Class D	P. Makovicky	2007-06-15	
BB199	463797	5621103	678.29	Mixed faunal	E. Koppelhus	2007-06-25	
BB200	458564	5629325	682.15	Mixed faunal	D. Tanke	2007-06-26	
BB201	458593	5629541	677.07	Microsite Class D	E. Koppelhus	2007-06-26	
BB202	477184	5629682	689.28	Mixed faunal	E. Koppelhus	2002-05	
BB203	477406	5631065	679.5				
BB204	471347	5622443	674.19	Mixed faunal; Class C	P.J. Currie	2007-09-29	
BB205	460605	5619668	697	Mixed faunal; Class B	A.P. Carabajal	2008-06-18	
BB206	462434	5620174	685	Monodominant, *Centrosaurus apertus*	E. Felber	2008-06-24	Eberth & Getty, 2005
BB207	462437	5620106	674	?Ceratopsidae	E. Felber	2008-06-24	
BB208	463016	5619913	669	Mixed faunal Class B	E. Felber	2008-06-24	
BB209	460766	5619688	703	Mixed faunal Class B	P.J. Currie	2009-06-22	
BB210	463058	5621880	664.07	Mixed faunal Class D	R. Sissons	2009-06-27	
BB211	460629	5617379	710	Mixed faunal Class D	D. Cretin. C. Cretin		
BB212	463825	5621785	680				
BB213	474262	5624049	708	Mixed faunal Class D			
BB214	460736	5617610	715	Mixed faunal Class D	T. Miyashita		
BB216	469976	5623365	669	Mixed faunal		2010-05-27	
BB217	469476	5623844	678	Ceratopsidae; Centrosaurus monodominant		2010-05-27	Eberth & Getty, 2005
BB218	471389	5624871	692	Mixed faunal		2010-05-27	
BB219	471382	5624905	680	Mixed faunal		2010-05-27	
BB219A	471375	5624812	678.6			2008-06-14	

BB220	457878	5629170	670	Mixed faunal		2010-05-27	
BB221	473074	5624880	637			2010-05-27	
BB222	473339	5625419	685.1	Microsite		2010-05-27	
BB223	473470	5625447	660			2010-05-27	
BB224	473437	5625478	665			2010-05-27	
BB225	473606	5625495	667			2010-05-27	
BB226	474343	5626159	705			2010-05-27	
BB227	474292	5625998	690			2010-05-27	
BB228	474280	5626020	697			2010-05-27	
BB229	474158	5626209	710			2010-05-27	
BB230	458385	5629431	683.4	Mixed faunal		2010-05-27	
BB231	472821	5624888	681.3	Ceratopsidae		2010-05-27	
BB232	472825	5624835	668			2010-05-27	
BB233	470304	5623777	681.6	Microsite		2010-05-27	
BB234	470270	5623682	683			2010-05-27	
BB235	474575	5626337	687.9		J. Scott	2011-06-10	
BB236	471349	5624272	690.3	Turtle braincase		2011-06-07	
BB237	465101	5625329	679.1	Mixed faunal	E. Koppelhus	2012-07-04	
BB238	465713	5625486	647.3			2012-07-04	
BB239	472110	5622359	705.2			2012-07-08	
BB240	469356	5623211	652.9	Microsite		2013-05-29	
BB241	471793	5621113	710.4	Mixed faunal	E. Felber	2014-05-26	
BB242	471661	5621003	668.6			2014-05-26	
BB243	471304	5624751	681.7			2014-06-08	
BB244	469383	5623618	728.3	Mixed faunal	A. van der Reest	2014-06-09	6 m above BB041A
BB245	472681	5623791	685.3			2014-06-10	
BB246	473074	5623973	633.3		G. Funston	2015-05-25	
BB247	470230	5621894	693.2	Mixed faunal		2014-06-23	
BB248	475645	5627184	682.6			2014-06-25	
BB249	490576	5632801	697.9	Microsite		2014-06-27	
BB250	490543	5632897	671.6	Microsite		2014-06-27	
BB251	438709	5640189	656.4			2015-05-21	
BB252	438411	5630979	667.3			2015-05-22	
BB253	473120	5625083	673.4	Microsite		2015-05-31	
BB254	469576	5623744	673.9	Mixed faunal		2015-06-08	
BB255	473454	5624159	668.2			2017-05-26	
BB256	459274	5627409	607.1			2019-05-26	

BB257	459322	5627396	666.7			2019-05-26	
BB258	471548	5622202	692.2	Mixed faunal		2019-05-28	
BB259	458062	5630434	655.7			2019-06-22	
BB260	457899	5631165	650.1			2019-06-22	
BB261	469102	5624135	658.5	?Monodominant, Ceratopsidae		2019-06-23	
BB261A	469130	5624100	659.8			2019-06-23	
BB262	469045	5623842	649.9	Microsite		2019-06-23	
BB262B	468858	5623853	651.2			2019-06-23	
BB263	471212	5622573	664.1			2019-06-24	
BB264	465419	5621212	690				
BB265	466268	5622119	694.4	Mixed faunal Class C			
BB266	463533	5621437	662.4	Class C/D			
BB267	463337	5624558	656.8	Mixed faunal Class B			
BB268	465018	5622145	668.4	Mixed faunal			
BB269	466408	5623486	661.9	Mixed faunal			
BB270	464851	5621323	680.9	Microsite			
BB272	464013	5620374	704.4	Class C; phosphatized			
BB273	465197	5621201	696.6	Mixed faunal Class C			
BB274	464540	5622440	675				
BB275	458567	5629627	678	Mixed faunal			
BB276	464470	5621826	686.6	Mixed faunal Class C			
BB277	457917	5630412	665.5				
BB278	457902	5630166	663.3				
BB279	460084	5629352	688.7				
BB280	459620	5629073	696.7				
BB281	463823	5623633	638	Coronosaurus brinkmani plus mixed faunal	C.M. Brown		
BB282	463522	5621413	**667.4**	Class B/D	M. Rhodes		
BB300	467310	5621138	**710**	Hadrosaur dominated			Eberth et al., 2015
BB301	462695	5624747	**695.7**	Monodominant, *Styracosaurus albertensis*		2010-05-27	C. M. Brown et al., 2020
BB303	472236	5623173	688	Mixed faunal Class B/D	H. Larsson; A. Demers-Potvin	2022-08-11	A.D.-P. thesis
BB304	468200	5622419	669	Mixed faunal	A.Demers-Potvin et al.	2023-08-10	
BB305	467903	5622355	**667.1**	Mixed faunal	H. Larsson	2023-08-11	

BB306	472509	5622411	719	Mixed faunal with microsite	L.-P. Bateman ; A. Mueller	2023-08-13	
BB307	472248	5622842	659	Mixed faunal	H. Larsson; A. Howenstine	2023-08-13	
BB308	464160	5620315	**721.4**	Mixed faunal	D. Tanke	1998	
BB309	471444	5621748	691	Mixed faunal	UALVP crew	2019-07-01	
L1116	466950	5619330		Microsite in Lethbridge Coal Zone			Brinkman et al., 1998
L1117	465670	5619330		Microsite below LCZ			Brinkman et al., 1998
L1118	462990	5622810					Brinkman et al., 1998
L1120	478550	5632500		Microsite			Brinkman et al., 1998
L1122	473100	5622950		Microsite below LCZ			Brinkman et al., 1998

Elevation in bold indicates elevation estimated solely from TMP DEM.

Table 3. Uncollected specimen quarries marked in Dinosaur Provincial Park

Quarry Number	UTM East	UTM North	Elevation (MASL)	Identification	Elements / Remarks	Discovered/Collected by	Date discovered
U004	465639	5625563	654.1	Hadrosauridae	Abandoned skeleton		2010-05-27
U006	465935	5622241	667.79	Hadrosauridae	Partial appendicular skeleton	P. Dodson	1984-06-02
U008	465807	5622167	667.8	Hadrosauridae	Partial skeleton		1984-08-19
U011	458536	5627994	657.66	Hadrosauridae	Partial skeleton	P.J. Currie	1984-08-30
U012	465473	5621796	691.3	Hadrosauridae	Most of skeleton eroded	P.J. Currie	2010-05-27
U013	466639	5623530	664.79	Ornithischia	Pelvic region	P.J. Currie	1984-08-08
U015	459116	5629385	682	?Nodosauridae	Partial skeleton, osteoderms	D.A. Russell	1984-08-02
U020	464412	5621096	680.1	Hadrosauridae	Limb bones in BB046	L.J. Strong	1985-06-09
U022	459174	5627269	650.38	Hadrosauridae	Skeleton possibly in bonebed	L. Krause	1985-08-08
U023	459172	5627232	650.63	Ceratopsidae	Limb bones. possibly in bonebed	L. Krause	1985-08-08
U026	464022	5620564	692.29	Hadrosauridae	Partial appendicular skeleton	L. Krause	1985-06-13
U029	459194	5627519	665.6	Hadrosauridae	Partial skeleton	P.J. Currie	1985-08-25
U030	459192	5627503	667.6	Ornithomimidae	Phalanges, fibula	L.J. Strong	1985-08-25
U031	464029	5623223	655.8	Hadrosauridae	Small vertebra series	S. Clarke	1985-08-17
U032	463595	5622167	661.78	Ornithomimidae	Foot elements in BB066	L.J. Strong	1985-08-31
U034	456173	5627058	670.82	Hadrosauridae	Vertebra. limb bones	L.J. Strong	19785-08-29
U036	463928	5617423	707.93	Hadrosauridae	Limb bones	G. MacCrimmon	1986-06-11
U038	465194	5621097	708.59	Hadrosauridae	Limb bones	L.J. Strong	1986-06-27
U039	465109	5620865	696.38	Hadrosauridae	Partial postcranial skeleton	J. McCabe	1986-06-27
U044	467864	5624564	653.3	Hadrosauridae	Partial postcranial skeleton	J. Shultis	1986-07-18
U046	468063	5624479	652.89	Ceratopsidae	Jugal & partial skeleton	G.L.P. Danis. J. Shultis	1986-07-23
U048	460523	5620558	694.59	Tyrannosauridae	Phalanges, broken bones	P.J. Currie	1986-07-24
U049	460525	5620552	694.69	Hadrosauridae	Partial skull & jaws	P. Harrop	1986-08-03
U050	460151	5620376	685.27	Hadrosauridae	Partial postcranial skeleton	B. Buoy	1986-08-06
U053	466583	5622536	674	Ceratopsidae	Partial skull & skeleton in BB061	Many people	1981 & 1982
U054	466538	5622506	674	Ceratopsidae	Partial skull & skeleton in BB061	M. Klassen	1986-08-11
U055	465882	5620706	714.4	Hadrosauridae	Maxilla & partial skeleton	J. McCabe	1986-08-09
U059	468078	5624637	680.29	Hadrosauridae	Partial postcranial skeleton	J. McCabe. D. Tanke	1986-09-15
U063	464702	5621257	676.6	Hadrosauridae	Limb bones	D. Tanke	1991-06-02
U066	460053	5619762	702.96	Hadrosauridae	3 ribs	L.J. Strong	1991-06-15
U067	460011	5619740	702.7	unidentified	4 bones	L.J. Strong	1991-06-15
U068	460147	5619801	706.39	?probably Hadrosauridae	Many bone fragments	L.J. Strong	1991-06-24

U070	474215	5623969	708.2	Hadrosauridae	Ilium, femur	D. Tanke	1991-06-16
U071	473790	5623694	710.3	Hadrosauridae	Partial postcranial skeleton	C. Makinson	1991-07-08
U073	473489	5624180	677.04	Crocodile	Lower jaw, partial skeleton	J. McCabe	1991-07-02
U078	465336	5621154	691.8	Hadrosauridae	Partial postcranial skeleton	V. Marsovski	1994-06-16
U079	465294	5621121	694.6	Hadrosauridae	Partial postcranial skeleton	V. Marsovski	1994-06-15
U080	460653	5619810	687.43	Hadrosauridae	Partial postcranial skeleton	D. Demetrick	
U081	464009	5621506	685.86	Hadrosauridae	Ribs & vertebrae	J. McCabe	1994-06-26
U082	463932	5621433	672.96	Hadrosauridae	Tendons, skin impressions	J.R.M.	1994-07-17
U083	460628	5620159	683.23	Ornithomimidae	Metatarsals, phalanges	M. Dunsmore	1994-08-02
U084	465373	5621074	704.29	Hadrosauridae	Partial postcranial skeleton	P.J. Currie. G.L.P. Danis	1994-10-04
U087	463729	5621184	668.68	Tyrannosauridae	Partial postcranial skeleton	W. Sloboda	1996-07-02
U088	463949	5620648	693.23	Hadrosauridae	Partial postcranial skeleton		1996-07-22
U090	462837	5621193	671.83	Hadrosauridae	Articulated tail	D. Trexler	1996-07-25
U091	463110	5621491	670.1	Lambeosaurinae	Uncollected remains of Q107	W. Sloboda	1996-07-23
U094	471358	5622446	673.6	*Basilemys*	Partial carapace in BB204	P.J. Currie	1996-08-07
U097	465083	5621131	704.17	Hadrosauridae	Partial postcranial skeleton	D. Trexler	1996-08-29
U098	477244	5630454	678.47	Hadrosauridae	Partial postcranial skeleton	W. Sloboda	1997-07-04
U099	477282	5630550	692.86	Hadrosauridae	Sacral vertebrae, right ischium	W. Sloboda	1997-07-02
U102	463149	5620647	675.03	Tyrannosauridae	Skeleton eroding from hillside	P.J. Currie	1997-08-23
U108	460224	5622185		Ornithomimidae	Partial skeleton	J. Vipond	2000-07-02
U110	465016	5621135	697.86	*Euoplocephalus tutus*	Scutes & limb bones	D. Tanke	2000-09-04
U115	458801	5629836	663.55	Hadrosauridae	Articulated proximal caudals	G. Rigoza	1998-06
U117	458272	5630260	656.1	Hadrosauridae	Partial postcranial skeleton	A. Rasmussen	2002-07-02
U118	458733	5629703	672.68	Hadrosauridae	Paired dentaries	D. Brinkman	1998-06
U119	459125	5629972	664.82	Hadrosauridae	Associated skeleton in siltstone	D. Brinkman	2010-05-27
U121	459161	5630364	676.97	*Paratarpon apogerontus*	Vertebrae & fin	M. Mitchell	2002-07-05
U122	462142	5624581	658.88	Hadrosauridae	Partial postcranial skeleton	E. Koppelhus	2002-07-09
U123	461944	5624736	667.17	Hadrosauridae	Partial postcranial skeleton	P.J. Currie	2002-07-09
U125	457740	5630215	665.17	Nodosauridae	2 caudal vertebrae, osteoderms	D. Tanke	2002-07-15
U127	458374	5629323	669.89	Hadrosauridae	Associated hind leg	D. Tanke	2002-07-16
U128	463929	5620663	693.82	Ankylosauridae	Mostly osteoderms	D. Tanke	2002-07-20
U129	463825	5620695	686.77	Hadrosauridae	2 caudals	D. Tanke	Summer 1997
U130	464048	5620511	695.16		Back of skull	D. Tanke	2002-07-20
U131	464225	5620612	690.06	Hadrosauridae	Partial postcranial skeleton	D. Tanke	2002-07-22
U133	463628	5624477	683.02	Hadrosauridae	Partial postcranial skeleton	P.J. Currie	2002-07-30
U134	463500	5624379	668.24	Tyrannosauridae	Hind limb & foot bones	E. Felber	2002-07-28

U135	458558	5629813	667.33	*Leidyosuchus canadensis*	Skull	P. Druckenmiller	2001-08-12
U136	466836	5622420	664.04	Hadrosauridae	Articulated caudals	P.J. Currie	2002-08-02
U137	467020	5622104	691.37	Hadrosauridae	Partial postcranial skeleton	P.J. Currie. E. Koppelhus	2002-08-03
U138	467761	5622572	676.06	Ceratopsidae	Articulated caudals	B. Coultis	2002-08-04
U139	468548	5622456	672.49	Hadrosauridae	Partial postcranial skeleton	P.J. Currie	2002-08-04
U140	459799	5621769	674.98	Hadrosauridae	Partial postcranial skeleton	P.J. Currie	2002-08-12
U143	462895	5624723	683.26	Hadrosauridae	Partial postcranial skeleton	P.J. Currie	2002-07-28
U144	464650	5620865	699.67	Ankylosauridae	Scutes & limb bones	D. Tanke	2002-08-20
U145	464433	5620975	682.01	Hadrosauridae	Partial postcranial skeleton	B. Noble	2002-08-20
U146	466270	5622495	671.56	Hadrosauridae	Dentary, 2 dorsals & ribs	B. Cooley	2002-08-20
U147	456101	5628780	654.24	Hadrosauridae	Partial postcranial skeleton	B. Cooley	2002-08-21
U148	456094	5628783	654.21	Hadrosauridae	Arm bones, vertebrae, ribs	D. Tanke	2002-08-25
U149	474694	5626651	709.1	cf. *Styracosaurus*	Partial postcranial skeleton	E. Koppelhus	2002-08-26
U150	474525	5626445	705	Hadrosauridae	2 femora, tibia	E. Koppelhus	2002-08-26
U151	490374	5632638	674.86	cf. *Daspletosaurus*	Partial skull with teeth	D. Tanke	2002-08-27
U152	464392	5622705	672.31	Hadrosauridae	Partial postcranial skeleton	S. Hummel	2002-08-28
U154	465623	5621069	698.17	Hadrosauridae	Partial postcranial skeleton	W. Grady	2003-07-07
U155	473045	5623416	710.8	Tyrannosauridae	Partial postcranial skeleton	D. Brinkman	1998-06
U156	473453	5623936	707.86	*Corythosaurus casuarius*	Partial postcranial skeleton	Many people	Summer 1982
U157	465949	5621431	700.29	Ceratopsidae	Articulated postcranial skeleton	Unknown	2010-05-27
U158	463034	5621865	660.09	Hadrosauridae	Skull & postcranial skeleton	M. Getty	2003-07-02
U159	471079	5623992	672.46	Hadrosauridae	Partial postcranial skeleton	P.J. Currie	1988-08-02
U160	473280	5623501	709.79	Coelurosauria	Articulated foot	P.J. Currie	2004-07-25
U161	473513	5625381	667.6	Hadrosauridae	Limb bones in a bonebed	P.J. Currie	2004-08-07
U162	465273	5622341	662.77	Coelurosauria	Partial postcranial skeleton	D. Brinkman	2004-07-02
U163	457510	5629463	662.72	Hadrosauridae	Limb bones	P.J. Currie	2004-08-10
U164	474675	5626636	705.59	Hadrosauridae	Partial skeleton in BB167	D. Tanke	2004-10-17
U165	474533	5626454	708.26	Hadrosauridae	Limb bones, might be U150	P.J. Currie	2004-10-17
U166	472050	5624713	727.73	Fish?	7 vertebrae	E. Koppelhus. D. Tanke	2004-10-18
U169	466117	5623756	662.08	Hadrosauridae	Tibia	W. Sloboda	2005-07-27
U170	463808	5620717	687.95	Hadrosauridae	Lower leg bones	H. Larsson	2005-07-09
U171	464262	5624983	671.4	Hadrosauridae	Limb bones & vertebra	P.J. Currie	2005-07-28
U173	460604	5617765	715.79	Tyrannosauridae	Associated foot bones	C.Cretin	circa 1997
U174	460531	5617707	713.44	Hadrosauridae	Limb bones, vertebrae	D. Cretin	circa 1997
U175	466678	5623521	664.76		Vertebrae, ribs, pubis	B. Spencer	2010-05-27

U176	459415	5629262	682.81	Hadrosauridae	Badly eroded ribs & vertebrae	D. Tanke	2010-05-27
U177	459147	5629595	671.23	Ankylosauridae	Vertebrae, ribs, scute	D. Tanke	2010-05-27
U178	458531	5629804	666.79	Hadrosauridae	Limb bones	D. Tanke	2010-05-27
U179	459031	5629475	682.81	*Leidyosuchus canadensis*	Partial skull	D. Tanke	2010-05-27
U180	459912	5621635	674.24	Hadrosauridae	Rib & manual phalanx	D. Tanke	2010-05-27
U181	459998	5621341	703.7	Hadrosauridae	2 dentaries, 1 quadrate	D. Tanke	2010-05-27
U182	460545	5621574	697.61	Hadrosauridae	Pterygoid & quadrate	D. Tanke	2010-05-27
U183	465602	5622014	679.12	Hadrosauridae	Eroded articulated skeleton	?J. Walper	pre-1976
U184	460435	5619781	693.18	Hadrosauridae	Eroded limb elements	D. Badamgarav	2006-05-19
U185	465970	5622793	651.98	Hadrosauridae	Partial postcranial skeleton		2010-05-27
U186	463881	5620506	696.94	Ankylosauridae	Osteoderms & vertebrae	D. Tanke	2004-09-01
U187	458062	5629378	661.98	Hadrosauridae	Disarticulated skeleton	D. Tanke	1985-09-14
U188	458036	5629823	661.34	Hadrosauridae	2 arm bones	D. Tanke	2006-06-21
U189	458366	5629051	682.65	Champsosauridae	Partial postcranial skeleton	D. Tanke	circa 1999
U190	465760	5621899	688.61	Hadrosauridae	Partial skull & jaws	D. Tanke	1990s
U191	465504	5621984	673.71	Hadrosauridae	Eroded foot	D. Tanke	2010-05-27
U192	473941	5623931	703.1	Hadrosauridae	3 ribs, femur, other bones	C. Luckwell	2006-07-03
U193	473866	5623838	702.3	*Prosaurolophus maximus*	Jaws with teeth	D. Tanke	2006-07-03
U194	472727	5622207	744.63	Ornithomimidae	Phalanges & metatarsal ends	D. Brinkman	2006-07-03
U195	472077	5622705	692	Plesiosauria; Hadrosauridae	Partial postcranial skeleton with gastroliths; humerus, metatarsal	P. Voigt	summer 2001
U196	472030	5622659	692.95	Plesiosauria	Partial postcranial skeleton	N. Schroeder	mid June 2002
U197	472660	5623221	689.23	Hadrosauridae	Skull & partial skeleton	D. Brinkman	2010-05-27
U198	474077	5623896	696.23	Crocodilia	Skull	W. Sloboda	2006-07-18
U199	474083	5623893	697.79	Ankylosauridae	Eroded skull & neck plates	W. Sloboda	2006-07-18
U200	474192	5624034	701.49	Tyrannosauridae	3 articulated vertebrae, tooth	W. Sloboda	2006-07-18
U201	474170	5624010	702.11	Hadrosauridae	Skull bones	W. Sloboda	August 2001
U202	474243	5624040	704.13	Ceratopsidae	Partial postcranial skeleton; small individual	W. Sloboda	August 2001
U203	465321	5623354	668.6	Hadrosauridae	Partial postcranial skeleton	W. Sloboda	June 2002
U204	465193	5623314	681.2	Hadrosauridae	Badly shattered skeleton	W. Sloboda	2006-07-19
U205	465154	5623339	680.25	Hadrosauridae	Vertebrae & ribs	W. Sloboda	June 2002
U207	465111	5623334	679.2	Hadrosauridae	Partial postcranial skeleton	M. Archer	2006-07-19
U208	471309	5621986	679.46	Hadrosauridae	Partial postcranial skeleton	P.J. Currie	2006-07-20
U209	474185	5623892	704.33	Hadrosauridae	Partial postcranial skeleton	P.J. Currie	2007-05-17
U210	463534	5620549	695.46	Hadrosauridae	Weathered femur & sacrum	H. Godthelp	2007-05-16
U211	463542	5620576	691.71	Hadrosauridae	2 femora & tibia	H. Godthelp	2007-05-16

U212	463150	5620243	703.23	Hadrosauridae	Metatarsals & phalanges	C. Isaacs	2007-05-16
U213	475348	5625734	687.13	Hadrosauridae	Partial skeleton; juvenile	P.J. Currie	2007-05-19
U214	475367	5625610	695.31	*Centrosaurus apertus*	Partial skull	P. Druckenmiller	2007-05-20
U215	474114	5624198	701.21	Tyrannosauridae	Maxilla, premaxilla, other frags	D. Brinkman	2007-05-15
U216	477417	5631075	676.76	Hadrosauridae	Partial postcranial skeleton	D. Tanke	2007-06-15
U217	477372	5630534	666.82	Hadrosauridae	Partial postcranial skeleton	P. Gignac	2007-06-15
U218	458323	5631202	682.26	Plesiosauria	Vertebrae, rib fragments	D. Tanke	June 2003
U219	458561	5630934	686.73	Plesiosauria	Vertebrae, rib fragments	D. Tanke	June 2003
U220	457894	5629219	661.68	Hadrosauridae	Partial postcranial skeleton	P.J. Currie	2007-06-17
U221	463854	5621492	674.22	Ceratopsidae	Partial postcranial skeleton	D. Tanke	2003-08-29
U222	460498	5619558	698.47	Hadrosauridae	Partial postcranial skeleton	E. Koppelhus	2007-06-25
U223	458574	5629328	682.18	Ornithomimidae	Partial postcranial skeleton	D. Tanke	2006-06-22
U224	458330	5629481	674.87	Hadrosauridae	Articulated caudals	D. Tanke	2006-06-30
U225	473594	5624065	713.08	*Myledaphus bipartitus*	String of vertebrae	D. Tanke	June 2003
U226	463804	5622094	663.11	Hadrosauridae	6 or more anterior caudals	D. Tanke	2007-06-28
U227	464164	5621205	679.73	Ceratopsidae	Partial postcranial skeleton	D. Tanke	2001-08-25
U228	459114	5628366	690.91	Hadrosauridae	Dentary & partial skeleton	D. Tanke	2007-06-28
U229	460652	5617329	729.98	Small theropod	Bag collected by D, Tanke	M. Tounissoux	2004-06
U230	462350	5622945	672	Tyrannosauridae	Small scattered skull	H. Godthelp	2004-06
U232	460879	5620475	692	Hadrosauridae	North side of South Sandhill Pocket	E. Koppelhus	2008-06-23
U233	460778	5620312	690	Ornithomimidae		P.J. Currie	2008-06-23
U234	463445	5620676	684	?Hadrosauridae	Near Q214	P.J. Currie	2008-06-24
U236	464341	5621337	670.82	Hadrosauridae	Footprint	D. Zelenitsky	2009-05-10
U237	465251	5621124	703.17	Hadrosauridae	Footprint	P.J. Currie	2006-05-15
U238	458460	5629736	675	Hadrosauridae	Skull, jaws & partial skeleton	A. Barrera	2009-07-08
U239	463975	5620765	683	Hadrosauridae	Partial postcranial skeleton	D. Tanke	2009-07-08
U240	465064	5623068	667	Crocodilia	Partial scattered skeleton	D. Tanke	2009-06-25
U241	465282	5622514	675	Hadrosauridae	Partial scattered skeleton	P.J. Currie	2009-07-06
U242	466050	5621199	710	Hadrosauridae	Eroded skeleton incl, jaw	P.J. Currie	2009-07-06
U243	465473	5622951	672	Hadrosauridae	Partial postcranial skeleton	E. Koppelhus	2009-07-09
U244	474226	5626107	688	Hadrosauridae			2010-05-27
U245	471494	5624728		Hadrosauridae	Partial postcranial skeleton		2010-05-27
U246	472949	5624983	700.6	Hadrosauridae			2010-05-27
U248	473358	5625364	666.2	Hadrosauridae			2010-05-27
U249	473356	5625367	674.5	Hadrosauridae			2010-05-27
U249a	470021	5623346	674.5	Hadrosauridae			1989-12-30
U250	458472	5629566	678.9	Hadrosauridae			2010-05-27

U251	458464	5629242	683.2	Hadrosauridae			2010-05-27
U256	469171	5623419	663.1	Hadrosauridae	Ribs & limbs		2013-05-29
U257	459223	5629462	663.5	Hadrosauridae	Sacrum & limbs		2013-06-04
U259	459415	5629260	633.1			B. Maybury	2015-05-25
U260	459882	5629273	633.5			J. Scott	2015-05-25
U261	469084	5622006	674.5	Hadrosauridae	Partial postcranial skeleton		2014-06-23
U262	468920	5621988	692.8	Ceratopsidae	Skull, postcranial UALVP 56469		2014-06-23
U263	469737	5622148	669	Hadrosauridae	Hind leg		2014-06-24
U264	476911	5629045	701.5	Hadrosauridae			2014-06-26
U265	438895	5631073	665.5	Hadrosauridae		E. Koppelhus	2015-05-22
U266	441261	5630148	668	Centrosaurinae		S. Persons	2015-05-23
U267	465457	5621222	695.6	Tyrannosauridae	Ilia	Y.-N. Lee	2015-06-17
U268	473494	5623961	699.6				2017-05-26
U269	474261	5626091	701				1989-12-30
U270	440887	5630360	669.2				2017-05-28
U271	457915	5630427	631				2017-05-28
U273	469840	5623745	669.8	Hadrosauridae	Femur & tibia		2019-05-27
U274	468651	5623800	653.9	Hadrosauridae	Associated skeleton; adult		2019-06-23
U275	463264	5621159	665.5	Hadrosauridae			
U276	465827	5623736	662.9	Hadrosauridae			
U277	465326	5620940	694.4	Hadrosauridae			
U278	464751	5621230	675.2	Hadrosauridae			
U279	465336	5621338	689.7	Hadrosauridae			2021-07-14
U280	465213	5621158	701.5	Hadrosauridae			
U281	464527	5622550	675.7	Hadrosauridae	6 bones	J. Acorn	
U283	465960	5622289	668.5	Hadrosauridae	6+ bones; adult	R. Sissons	2023-06-16
U284	463390	5620796	681.6	Hadrosauridae	5 caudals	E. Koppelhus	2023-06-20
U285	457883	5630157	657.1	Hadrosauridae	11 caudals; adult	J. Vipond; S. Vipond	2023-06-24
U287	461554	5619637	**669**	Hadrosauridae	Articulated tail	L. Liboiron	2023
U288	464862	5620841	**690**	Hadrosauridae	Skeleton with skin	I. Walker	2022
U289	465415	5620826	**704.65**	Ankylosauria	Skull	L. Liboiron	2023
U290	460898	5618458	NA	Amiidae	Skeleton	L. Liboiron	2023
U291	467713	5624765	663	Hadrosauridae	Partial skeleton	L.-P. Bateman; A. Mueller	2022-08-15
U292	467690	5624775	665	Hadrosauridae	Disarticulated skeleton	H.C.E. Larsson	2022-08-15
U293	467764	5624695	655	Hadrosauridae	Associated skeleton	H.C.E. Larsson	2022-08-19

U294	465863	5621950	672	Ornithomimidae	Articulated tail	H.C.E. Larsson et al.	2023-08-21

Elevation in bold indicates elevation estimated solely from TMP DEM.

Table 4. Invertebrate localities marked in Dinosaur Provincial Park*

Quarry Number	UTM East	UTM North	Elevation (MASL)	Identification	Discovered (collected) by	Year collected	References
GSC Inv 4996	ND	ND	ND	Invertebrates	C.H. Sternberg	1915	
GSC Inv 16457	ND	ND	ND	Invertebrates	L.S. Russell	1931	
GSC Inv 16458	ND	ND	ND	Invertebrates	L.S. Russell	1931	
GSC Inv 41605	ND	ND	ND	Invertebrates	C.H. Sternberg		
L1203	464031	5622365	658.38	Clams (unionids)			Johnston & Hendy, 2005
L1209	465790	5621920	692	Unionids	B. McQuorcodale		Johnston & Hendy, 2005
Ammonites	473643	5625906	749.9	Ammonites			
Clam01	465590	5621684	692.8			2010	
Clam02	474421	5626041	666	Unionids		2010	
Clam03	466235	5622835	654.8			2010	
Clam04	473609	5625464	663			2010	
Clam05	470022	5623806	685.8			2010	
Clam06	471511	5624195	657.3	Unionids		2014. 2021	
Clam07				Unionids	H. Larsson et al.		This thesis
Oystr1	466062	5621662				2010	
Oystr2	466286	5621340				2010	
Picidiid clams 01	473117	5623765	658.6	Picidiids		2014	

*Includes quarries lacking locality data

Table 5. Major plant localities from Dinosaur Provincial Park

Quarry Number	UTM East	UTM North	Elevation (MASL)	Identification	Discovered (collected) by	Year collected
GSC Plant 1774/2159	457499	5631434	664.1	Plant site	C.H. Sternberg	1913
Bell Plants	457491	5631425	630.2	Plant site	C.H. Sternberg	1913
Cycad	462869	5620384	767	Plant site		2017
Q220*	462202	5621241	660.2	*Cercidiphyllum* (katsura leaves)	W. Sloboda	1994
Q221*	464070	5622334	663.7	Plant site	P.J. Currie; C. Coy	1995
HCEL Plants 2017	474004	5625763	673	Plant site	H.C.E. Larsson et al.	2017
HCEL Plants 2022	470290	5623635	688	Plant site	A.Mueller; L.-P. Bateman	2022

*Leaves found among skeleton quarries

Table 6. Oldman-Dinosaur Park formation contacts in and around Dinosaur Provincial Park

Contact Number	UTM East	UTM North	Elevation (MASL)
Contact 001	458870.22	5627339.85	640.33
Contact 002	458796.78	5627495.42	641.93
Contact 003	458102.1	5628366.38	642.42
Contact 004	458268.38	5628188.41	645.05
Contact 005	458304.92	5628177.27	645.53
Contact 006	459448.14	5626713.5	646.07
Contact 007	458493.72	5627978.6	646.24
Contact 008	459559.28	5626549.39	646.67
Contact 009	458373.77	5628081.06	646.75
Contact 010	458671.47	5627751.52	647.19
Contact 011	457798.76	5628869.1	647.26
Contact 012	458582.77	5627865.52	647.92
Contact 013	457678.28	5628971.54	648.31
Contact 014	459029.56	5627148.45	648.41
Contact 015	464928.36	5623825.71	648.49
Contact 016	459903.32	5626126.39	648.57
Contact 017	457732.45	5629094.11	648.67
Contact 018	459991.95	5625877.07	648.87
Contact 019	464895.25	5623795.5	649.03
Contact 020	464916.6	5623849.98	649.38
Contact 021	457622.84	5629078.58	649.55
Contact 022	464872.36	5623831.52	649.91
Contact 023	459316.81	5626859.45	650.42
Contact 024	459770.37	56262352.36	650.54
Contact 025	459190.8	5626972.44	650.85
Contact 026	464340.65	5623410.13	651.43
Contact 027	463829.4	5623478.15	651.66
Contact 028	464125.32	5623731.3	651.73
Contact 029	464068.39	5623415.3	651.91
Contact 030	464135.92	5623422.8	652.34
Contact 031	464103.66	5623418.44	652.39
Contact 032	464285.74	5623418.48	652.86
Contact 033	473130.08	5624026.29	653.13
Contact 034	464552.61	5623694.87	653.13
Contact 035	464521.1	5623696.26	653.28
Contact 036	463433.14	5622864.52	653.42
Contact 037	464197.88	5623424.93	653.46
Contact 038	464524.28	5623673.3	653.53
Contact 039	464481.43	5623600.58	653.87
Contact 040	464268.12	5623434.38	653.89
Contact 041	464445.53	5623553.26	653.95
Contact 042	464030.24	5623404.78	654
Contact 043	460505.01	5624957.89	654.12
Contact 044	461489.29	5621631.47	654.49
Contact 045	464281.02	5623423.67	654.6
Contact 046	463364.43	5624283	654.65
Contact 047	463459.34	5622983.51	654.68
Contact 048	462115.12	5624550.03	654.74
Contact 049	464139.82	5623558.92	654.8
Contact 050	464138.64	5623565.47	655
Contact 051	460473.36	5625503.91	655.08
Contact 052	461645.81	5621673.02	655.08
Contact 053	463896.99	5623243.86	655.12

Contact 054	464757.89	5623985.64	655.14
Contact 055	464146.65	5623698.1	655.21
Contact 056	464554.18	5623719.95	655.27
Contact 057	464226.17	5623704.44	655.28
Contact 058	463886.79	5623553.98	655.6
Contact 059	461956.01	5624553.67	655.69
Contact 060	465366.87	5623486.24	655.87
Contact 061	462307.09	5624411.87	655.94
Contact 062	463101.42	5624247.46	656.01
Contact 063	463884.38	5623584.2	656.05
Contact 064	463898.561	5623539.74	656.06
Contact 065	464363.14	5623770.64	656.08
Contact 066	463504.67	5623268.02	656.15
Contact 067	460637.41	5622069.89	656.16
Contact 068	463924.73	5623606.83	656.22
Contact 069	464479.43	5623402.82	656.25
Contact 070	464061.45	5623572.96	656.25
Contact 071	467685.12	5622773.79	656.34
Contact 072	464501.35	5623405.36	656.38
Contact 073	464164.9	5623613.1	656.47
Contact 074	471379.5	5622950.81	656.57
Contact 075	462847.92	5624258.37	656.6
Contact 076	475145.12	5625623.68	656.99
Contact 077	463914.26	5623532.54	657.08
Contact 078	462054.93	5621542.08	657.1
Contact 079	462103.64	5624685.94	657.15
Contact 080	463973.25	5623613.06	657.17
Contact 081	463564.21	5623189.31	657.19
Contact 082	464528.76	5623421.18	657.21
Contact 083	464491.35	5622220.08	657.23
Contact 084	462474.68	5624366.82	657.48
Contact 085	461237.68	5624758.06	657.59
Contact 086	463977.1	5623444.01	657.59
Contact 087	470869.43	5622482.8	657.9
Contact 088	462481.38	5621569.56	657.91
Contact 089	462700.4	5623228.93	657.92
Contact 090	462706.8	5623292.96	657.93
Contact 091	462352.27	5621524.36	657.95
Contact 092	467036.37	5623029.51	658.09
Contact 093	463254.67	5622957.44	658.12
Contact 094	463974.83	5623480.68	658.15
Contact 095	463969.69	5623492.8	658.31
Contact 096	463251.67	5622948.21	658.36
Contact 097	462202.26	5621235.87	658.38
Contact 098	462852.06	5622207.37	658.44
Contact 099	459872.36	5621943.18	658.52
Contact 100	474773.67	5625312.31	658.63
Contact 101	461417.37	5624613.41	658.67
Contact 102	464548.39	5623401.72	658.81
Contact 103	473634.02	5624328.68	658.96
Contact 104	464671.83	5623403.64	659.02
Contact 105	463934.04	5623528.9	659.07
Contact 106	473987.5	5624698.52	659.08
Contact 107	462744.75	5623181.64	659.2
Contact 108	467257.23	5623031.94	659.33
Contact 109	461277.73	5621727.28	659.33

Contact 110	464622.68	5623405.07	659.44
Contact 111	465514.96	5623341.56	659.49
Contact 112	460061.67	5621971.99	659.51
Contact 113	462190.92	5621335.57	659.52
Contact 114	463009.86	5622583.04	659.55
Contact 115	460450.51	5622000.8	659.55
Contact 116	465700.62	5623402.83	659.56
Contact 117	463055.95	5622443.24	659.59
Contact 118	460877.01	5622050.88	659.6
Contact 119	463087.45	5623183.03	659.61
Contact 120	465743.06	5623090.42	659.65
Contact 121	460301.8	5621862.45	659.79
Contact 122	462333.7	5621097.29	659.93
Contact 123	462781.01	5621976.5	659.96
Contact 124	461793.59	5621665.26	660.1
Contact 125	469616.96	5622181.76	660.11
Contact 126	460809.78	5621976.52	660.26
Contact 127	470369.47	5622365.75	660.29
Contact 128	465401.95	5622477.37	660.32
Contact 129	465978.81	5623135.08	660.4
Contact 130	465665.52	5622963.68	660.55
Contact 131	463150.58	5623060.7	660.56
Contact 132	468364.02	5622533.27	660.69
Contact 133	460517.13	5622118.32	660.77
Contact 134	463018.68	5623111.99	660.78
Contact 135	463749.03	5622099.78	660.8
Contact 136	463433.15	5623231.72	660.81
Contact 137	460346.12	5621962.52	660.94
Contact 138	463166.45	5622975.98	661.08
Contact 139	461048.49	5621576.83	661.1
Contact 140	463759.93	5622114.94	661.11
Contact 141	460852.2	5621803.33	661.23
Contact 142	474404.07	5624989.17	661.23
Contact 143	462597.98	5621697.07	661.28
Contact 144	463113.13	5622979.2	661.3
Contact 145	463829.91	5622404.97	661.43
Contact 146	464559.99	5622233.55	661.51
Contact 147	468800.79	5622492.28	661.62
Contact 148	463196.9	5623000.27	661.68
Contact 149	461073.13	5621708.37	661.7
Contact 150	464000.13	5622830.91	661.77
Contact 151	468035.1	5622654.22	662.09
Contact 152	460192.03	5622042.61	662.17
Contact 153	464628.61	5622007.05	662.17
Contact 154	465486.78	5622754.83	662.19
Contact 155	463917.24	5621179.41	662.35
Contact 156	462602.63	5621655.9	662.36
Contact 157	472620.75	5623866.48	662.54
Contact 158	469105.69	5622036.78	662.79
Contact 159	462851.27	5622086.94	662.91
Contact 160	472186.86	5623651.47	663.03
Contact 161	460363.61	5622167.82	663.17
Contact 162	471847.63	5623372.67	663.2
Contact 163	462385.74	5621119.13	663.24
Contact 164	461841.96	5620811.29	663.49
Contact 165	462124	5620953.21	663.56

Contact 166	461888.76	5620480.92	663.73
Contact 167	466475.2	5623067.19	663.94
Contact 168	462625.18	5621175.88	664.44
Contact 169	464628.01	5622011.98	664.68
Contact 170	461725.31	5620482.65	664.73
Contact 171	463664.49	5622285.58	664.75
Contact 172	462986.78	5620966.64	665.39
Contact 173	461895.34	5620875.46	665.55
Contact 174	462068.24	5621082.82	665.63
Contact 175	462988.1	5620881.98	665.74
Contact 176	464372.07	5621453.97	666.17
Contact 177	464372.37	5621454.75	666.19
Contact 178	471599.88	5620911.25	666.24
Contact 179	462486.07	5621249.08	666.24
Contact 180	461729.6	5619996.9	666.27
Contact 181	471599.88	5620911.29	666.31
Contact 182	463760.58	5621618.88	666.36
Contact 183	462450.36	5620238.2	666.83
Contact 184	471532.07	5621004.39	667.7
Contact 185	462699.47	5621125.47	668.26
Contact 186	471532.03	5621004.7	668.26
Contact 187	461683.06	5620555.58	668.42
Contact 188	462663.97	5619769.78	668.77
Contact 189	463268.03	5620136.31	668.9
Contact 190	461575.18	5620009.46	669.35
Contact 191	463060.04	5619185.25	669.35
Contact 192	463060.19	5619185.27	669.36
Contact 193	463355	5619848.72	669.53
Contact 194	463041.22	5620807.8	669.61
Contact 195	463283.9	5620639.61	669.76
Contact 196	462438.68	5619863.67	669.93
Contact 197	462724.05	5619517.42	670.06
Contact 198	462899.91	5619305.59	670.77
Contact 199	464746.52	5621382.6	670.84
Contact 200	463394.73	5619988.44	671.47
Contact 201	464756.97	5621390.83	671.5
Contact 202	463438.31	5620324.21	671.67
Contact 203	463371.79	5620247.4	672.26
Contact 204	471521.31	5620669.86	672.64
Contact 205	471521.3	5620669.88	672.65
Contact 206	463745.08	5619584.46	675.79
Contact 207	470377.16	5619170.4	677.12
Contact 208	469836.65	5620456.64	677.23
Contact 209	463971.57	5619523.29	678.13
Contact 210	470435.85	5619215.5	678.8
Contact 211	470387.78	5618975.64	679.93
Contact 212	470463.4	5618783.21	680.72
Contact 213	465573.01	5622536.26	661.35
Contact 214	465835.01	5622685.17	661.77
Contact 215	465958.28	5622784.17	661
Contact 216	466867.89	5622856.73	657.12
Contact 217	465477.94	5622358.22	663.25
Contact 218	466132.47	5622438.73	665.71
Contact 219	462568.1	5623139.94	654.11
Contact 220	466746.94	5622579.26	664.41
Contact 221	466846.48	5622412.37	662.64

Contact 222	466946.64	5622358.56	667.57
Contact 223	465784.59	5622333.21	663.97
Contact 224	463590.66	5622157.26	660.85
Contact 225	464346.28	5621337.96	672.28
Contact 226	463088.68	5622040.64	661.77
Contact 227	463055.36	5621886.75	664.07
Contact 228	462507	5621269.9	666.3
Contact 229	462542.84	5621186.94	663.15
Contact 230	462658.69	5621191.64	664.74
Contact 231	462721.14	5621121.41	666.2
Contact 232	463123.19	5621094.89	668.25
Contact 233	463399.76	5621298.73	665.81
Contact 234	463298.66	5621334.01	668
Contact 235	463049.91	5621452.06	664.39
Contact 236	462977.54	5621472.1	664.94
Contact 237	463131.18	5621670.91	665.33
Contact 238	463601.8	5621275.73	667.52
Contact 239	464041.09	5622349.17	661.99

Appendix III. Fossil occurrences reported from main quarry of Lake Diefenbaker Bonebed

Subclass/clade	**Superorder/order**	**Lower-level taxon**	**Element**	**Frequency**
Dinosauria	Ornithischia	*Centrosaurus apertus*	Parietal (lateral bar)	1
		Centrosaurinae cf. *Centrosaurus*	Parietal (median bar)	1
			Nasal	1
			Squamosal	2
			Syncervical	1
			Scapula	2
			Ischium	1
		Ceratopsidae Indet	Parietal	1
			Squamosal	1
			Epiparietal	1
			Other frill element	9
			Maxilla	1
			Quadrate	3
			Braincase	2
			Other skull element	4
			Dentary	4
			Angular	1
			Surangular-articular	1
			Tooth	1
			Cervical	1
			Dorsal	2
			Caudal	4
			Vertebra Indet	5
			Rib	1
			Scapula	2
			Ulna	1
			Radius	1
			Ischium	1
			Fibula	1
			Metatarsal	3
			Phalanx	1
			Ungual	1
			Other limb element	2
			Unidentified element	8
			Total	71
		Lambeosaurinae	Humerus	1
			Pubis	1
			Ischium	2
		Hadrosaurinae	Maxilla	1
		Hadrosauridae Indet	Maxilla	1
			Squamosal	1
			Dentary	2
			Cervical	1

			Caudal	2
Subclass/clade	**Superorder/order**	**Lower-level taxon**	**Element**	**Frequency**
			Vertebra Indet	5
			Scapula	1
			Humerus	2
			Ulna	1
			Metacarpal	1
			Femur	3
			Tibia	1
			Metatarsal	3
			Phalanx	3
			Ungual	2
			Other limb element	1
			Total	35
		Ornithischia Indet	Other skull element	1
			Tooth	1
			Caudal	1
			Chevron	1
			Vertebra Indet	8
			Rib	45
			Femur	1
			Tibia	1
			Phalanx	3
			Other limb element	9
			Unidentified element	15
			Total	86
	Theropoda	Tyrannosauridae	Caudal	1
			Phalanx	1
			Tooth	8
			Unidentified element	1
		Elmisaurinae cf. *Citipes elegans*	Metatarsal II	1
		Theropoda Indet	Metacarpal	1
			Phalanx	1
			Unidentified element	1
			Total	15
Dinosauria	Indet	Indet	Other skull element	2
			Vertebra Indet	3
			Chevron	2
			Rib	31
			Other limb element	6
			Unidentified element	28
			Total	72
Crocodylia	Indet	Indet	Braincase	1
			Radius	1
			Femur	1

Subclass/clade	Superorder/order	Lower-level taxon	Element	Frequency
			Rib	1
Choristodera	Neochoristodera	*Champsosaurus* sp.	Braincase	1
			Other skull element	1
			Dorsal	2
			Caudal	1
			Rib	4
			Coracoid	2
			Humerus	1
			Ilium	2
			Tibia	1
Testudines	Cryptodira	Trionychidae	Carapace fragment	4
	Indet	Indet	Carapace fragment	3
			Plastron	1
			Scapula	1
Reptilia Indet	Indet	Indet	Other skull element	1
			Caudal	1
			Rib	5
			Unidentified element	15
			Total	50
Osteichthyes Indet	Indet	Indet	Unidentified element	2
Miscellaneous	Miscellaneous	Miscellaneous	Unidentified element	5
			Grand Total	337

Only the collection assembled by the McGill University crew (2012-2018 macrofossils and microfossils found at the main bonebed layer) is included.

Appendix IV. Large-scale mapping of Dinosaur Provincial Park outcrops – preliminary dataset acquired in August 2021

Introduction

This appendix documents an initial attempt at mapping the geological record of Dinosaur Provincial Park over a large spatial scale. It was originally intended to be one of my thesis chapters, but the latter became focused on less extensive mapping projects (see Chapter 3). As a result, the present text mostly consists of the Material and methods section, which remains the only detailed record of an ambitious but ultimately inefficient uninhabited aerial vehicle (UAV) mapping workflow. Our original hypothesis was that we would be able to combine tens of thousands of images acquired from separate commercial-grade UAVs in the field into a single giant 3-D point cloud of the badlands of Dinosaur Provincial Park. However, despite the measurement of ground control points in the field (see below), the geolocation accuracy of the resulting models produced by structure-from-motion (SfM) photogrammetry proved insufficient. Furthermore, the fact that each of these UAVs had to remain stationary for each image capture eventually made me realize that they simply weren't designed to cover the amount of ground that we wanted. Drone mapping technology has advanced remarkably, even since 2021, and we are now experimenting mapping projects of a similar scale in the Park with bigger and more autonomous UAVs.

The mapped area of the present appendix extended over the entire eastern left bank of the Red Deer River located within the Park (Figure 1). This region of the Park is known as the Happy Jack's area since it is named after the ranch that existed by the river long before the Park was founded in 1955. Only a solitary cabin remains of that ranch, and it is located a few hundred metres away from the camp that served as our annual field headquarters. This made the Happy Jack's area the most easily accessible region of the Park for our crew and it was also convenient from a scientific point of view since it has very steep exposures of the Belly River Group compared with other areas such as the Core or the Steveville Badlands. As a result, the horizontal distances between exposures of the Oldman Formation at river level and exposures of the Lethbridge Coal Zone (and occasionally Bearpaw Formation) near prairie level are among the smallest in the entire Park, which facilitates the interpretation of potential 3-D digital outcrop models. Most of the images at the source of the Bonebed 190 digital reconstruction were also acquired during that same field season (see Chapter 3). The Happy Jack's area also encompasses the exposures that hosted the HCEL Plant 2022 site, as well as the Clam04 and Clam06 invertebrate localities, although all these were the focus of their own individual mapping projects in later field seasons.

Material and methods

Image acquisition in the field

Drone flights were conducted in Dinosaur Provincial Park during the 2021 field season in late August. Prior to fieldwork, all pilots conducted online training to obtain a Pilot certificate for basic operations with small remotely piloted aircraft systems (RPAS) from Transport Canada.

Mapping material. Two commercial-grade survey drone makes were used during fieldwork: one of them was a DJI Mavic 2 Pro equipped with a Hasselblad L1D-20c 16.8 megapixel (MP) digital camera with a 10.26 mm focal length and pixel size of 2.53 x 2.53 µm, the other five were smaller DJI Mavic Air2s equipped with a DJI FC3411 20 MP digital camera with a 8.38 mm focal length and pixel size of 2.51 x 2.51 μm. Both cameras had a 72 dpi vertical and horizontal resolution. Each drone had its associated remote controller and four batteries that each had a 30-minute life in the field, all fitting inside a satchel. The batteries were recharged at the end of each mission with a gasoline-powered generator at camp. In theory, this meant that up to 720 minutes of flying could be spent daily, whether for capturing images dedicated to mapping or recording videos dedicated to science outreach.

Even though each photograph captured by these cameras has geotags, the vertical and horizontal accuracies of their estimated geospatial position can fluctuate wildly at the 10^1 m scale, especially in DJI drones. For this reason, Ground Control Points (GCPs) were used to increase image geolocation accuracy. These must be sufficiently visible to be detected on images taken more than 50 m above ground during image processing. Therefore, crosses were formed out of pairs of Jacob's staffs, as well as their sheaths. Considering that the four sets of staffs could each be split in 4 ~1-m long stakes, and that each of these sets had 1 orange sheath, a maximum of 10 GCPs were available for each daily flying mission. The optimal number of GCPs to use for drone mapping projects has been shown to vary between 5 and 8, where a higher number did not significantly improve geolocation accuracy in a similar mathematical pattern to a collector curve or a species-area relationship. We ensured all GCPs on a given mission day were spread evenly across x, y and z axes: this means that they were often placed near the corners and the center of a given mapping area (along x and y axes), as well as near river level, near prairie level and at intermediate elevations along the z axis. The GCPs were usually laid on very flat and accessible ground from which they would be easily visible from the air. In some cases, they were laid directly against metal stakes that mark historical fossil quarries across Dinosaur Provincial Park. Most of those stakes (n=111) were planted by Levi, C. M. and Ray Sternberg in 1935 and

1936, in an effort to relocate quarries excavated during fossil collecting expeditions going as far back as 1912 (Currie 2005; Tanke 2005).

The geospatial positions of each GCP were measured with a SXBlue II + GNSS GPS receiver (Geneq. Inc., Montréal, Québec, Canada). This model contains a Space Based Augmentation System (SBAS) that improves positional accuracy by using real-time differential corrections. Geographical coordinates and elevation were recorded once the receiver achieved a differential position (which was known once the DGPS and DIFF lights were turned on), where it could reach a 2-DRMS accuracy of 60 cm. Since 2-DRMS stands for twice the distance root mean square error, it means that measurements with this GPS fall within 60 cm of their true position 95% of the time (within 2 standard deviations from the true position). Such estimates of position error (EPE) are usually a reliable indicator of horizontal accuracy, but *vertical* accuracy should conservatively be estimated to be at least twice as low, in this case 1.2 m. This resulted in an accuracy at least 6 times lower than that of the differential GPS receiver previously used to measure the position 650 of Dinosaur Provincial Park's quarries (MacDonald *et al*. 2005). Nonetheless, it remains far higher than that of recreational GPS receivers, which can often reach 10-20 m. As a result, the GPS receiver model used in this study is considered a compromise between the accuracy it can reach and the time constraints imposed by drone battery management. Furthermore, the relative geolocation accuracy is more crucial than the absolute geolocation accuracy to the palaeontological investigation at hand. Since the GPS receiver was constantly carried around the mapping area by one of the crew members, it is the kinematic positional errors that applied to this study, i.e. 10 mm vertically and 20 mm horizontally. Horizontal (Easting and Northing) coordinates were measured in the NAD83 coordinate system (UTM zone 12N). Vertical coordinates (absolute elevation) were measured along the EGM96 geoid. These vertical and horizontal coordinate systems are consistent with those used in recent surveys of the fossil quarries of Dinosaur Provincial Park (Currie & Koppelhus 2005: supp. CD-ROM), thus facilitating the comparison of our respective results. The GPS receiver was plugged to the cell phone of a crew member, on which measurements could be read via the MapIt app.

Flight protocol. For each daily mission, a crew of 10 set out with 6 drones, with Jacob's staffs serving as Ground Control Points, and a GPS receiver. Each morning, a topographic map was studied to design flight paths for each drone, accounting for vegetation cover, terrain obstacles and technical limitations. Additional information on local ground cover was obtained from a set of photomosaics created during an aerial survey conducted in the Park by TMP staff in 2015 (Caleb Brown, pers. comm.), which did not involve photogrammetry. During a flying training session undertaken without GCPs at the start of the field season in the Steveville badlands, it was estimated that covering a ~1 km^2 area daily was a realistic objective considering the complexity of the local topography and the technical limitations of the 6 drones at our disposal (Figures 1, 2).

Eight of the 10 crew members formed four pairs consisting in one drone pilot and one visual observer who together ensured they maintained constant line of sight of the aircraft. The larger drone (DJI Mavic 2 Pro, henceforth labeled Drone 1) was consistently flown 80 m above ground (relative to launching point) with the camera constantly oriented straight down at a 90° roll angle (along the Y axis), ensuring nadir shots. As such, its function was solely to create a base map along a path following a grid pattern. This model alone had the Pix4Dcapture app already installed, which enabled the pilot to trace flight paths on the associated remote controller's screen. This app also indicated the expected image resolution for any position the drone occupied above ground, which enabled the pilot to consistently aim for a Ground Sampling Distance (GSD) of 4-5 cm/pixel. Since the camera specifications remained constant throughout fieldwork, and since the camera's *absolute* height was kept constant, the only variable affecting GSD that fluctuated was the camera's distance from the terrain, or *relative* height. The drone's flight parameters (i.e. height, camera angle, etc.) were set on a cell phone plugged to the remote controller.

The other 5 drones (labeled Drones 2-6) were flown 40-50 m above ground in more irregular patterns, almost in free flight, with their cameras oriented at a ~45° roll angle, ensuring oblique shots. As such, they had the dual functions of capturing 'close-ups' and more detailed photographs of steeper slopes in the same mapping area as that covered by Drone 1. For each drone, regardless of its purpose, photographs were taken aiming for 60-80% minimal frontal and side overlap. This means that a given number of photographs taken by Drone 1 covered a far greater area than an equal number of photographs taken by Drones 2-6. As a result, the 'nadir' team was tasked with mapping the entire ~1 km^2 covered daily while the 4 'oblique' teams were tasked with mapping less extensive transects, usually including 2 to 3 of the GCPs. The irregular flight paths of the 'oblique' teams also meant that the extent of frontal overlap was not as consistent as that of the 'nadir' flight paths.

The remaining pair was tasked with the daily geolocation of all GCPs. Therefore, these workers often covered more ground than the rest of the crew since they had to tread across the entire mapping area daily. During the very first missions, the 'GPS' team had the additional task of placing all GCPs across the mapping area. However, this was found to impose great physical strain, so that task was assigned to the pilots for the remaining missions: following the flight paths established *a priori*, each pilot-observer pair placed GCPs for their assigned flying area, so they could be marked later by the GPS team. This process required intense coordination between all teams since each had to know when the GCPs were suitably placed to begin image capture, as well as the time when the GCPs could be removed (usually by the same team that placed them earlier). Fortunately, radio communication was maintained at all times between neighbouring teams when located within 1-2 km^2 despite the uneven terrain.

Drone camera parameters had to be adjusted due to sudden weather fluctuations throughout the survey period. The cameras were initially set on Program mode with ISO 100 (the basic ISO for landscape shots) for all drones, with F-stop and shutter speed fluctuating wildly. After the advent of smoke from wildfires in the Rockies that led to blurry photos, shutter speed was manually increased to 1/500 and ISO raised to 400 to maintain brightness levels. When battery levels dropped to 20%, pilot-observer pairs were advised to identify a sufficiently flat and open patch to ensure a safe landing and battery change.

Over 9 days of surveys with 6 drones spread among a field crew of 10, ~7 km^2 of badlands were mapped including a ~6.5 km^2 continuous area that followed the easternmost third of the left bank of the Red Deer River, and the remaining ~0.5 km^2 covering the vicinity of Bonebed 190 (Figures 1, 2). Photos were also taken during the training session in the Steveville badlands, but they did not lead to a sufficiently accurate map. A total of 38,109 photographs were taken, amounting to ~349 Gb. Such extensive data storage necessitated that each memory card be copied on field hard drives and then emptied on a daily basis. The metadata for each flight day is summarized in Table 1 and GCP measurements are provided in Table 2.

From photogrammetry to map generation

The raw image data acquired in the field was transformed in the GeoAnalytics lab at McGill University's Geographic Information Center using Pix4Dmapper (Lausanne, Switzerland), a photogrammetry software specialized for UAV-based mapping projects. Image selection and alignment led to the creation of a point cloud and, optionally a 3-D mesh, followed by the creation of a Digital Surface Model (DSM), an orthomosaic and, optionally, a Digital Elevation Model (DEM). In summary, it takes a collection of 2-D images to form a single 3-D model of the surveyed landscape, which in turn gets flattened into a single 2-D surface whose *x*, *y*, and *z* distances are corrected for perspective. The DSM includes vegetation in its computed surface, while the DEM does not, making the latter more accurate when measurements at ground level alone are required. The orthomosaic consists in a mosaic of the photographs of the landscape wrapped on the surface of the DSM. Together, the orthomosaic and the DEM provide similar image data to the TMP photomosaic, but with far greater absolute and relative geolocation accuracy.

For each major step in the mapping process, a quality report presents a statistical summary of camera matching and calibration and absolute geolocation accuracy. The parameters for each step in the mapping process were left at their default settings unless specified otherwise in the following paragraphs.

Step 1: image selection and alignment. For each project, a selection of photographs covering a given mapped area was made, often combined from separate drone flights. Considering that the workstation used for the start of image processing had 64 Gb of RAM and considering that Pix4Dmapper performs optimally for projects based on fewer than 2,000 images, the continuous transect of outcrops spanning the eastern left bank of the Red Deer River in Dinosaur Provincial Park had to be divided into 7 projects. This constraint eventually led to the creation of a project covering the entire study area on a workstation with 238.4 Gb of RAM and a GeForce RTX 3070 GPU. Considering that this particular project was composed of 15,339 images, it was run on Pix4Dmatic, a SfM photogrammetry software that is adapted for projects of >2,000 images (Figure 2B). The following steps in the digital reconstruction of the Park apply equally to Pix4Dmatic and Pix4Dmapper, albeit on a much larger scale for the former program.

Prior to creating separate projects on Pix4Dmapper, all ~38,000 images captured in the field were inspected individually. Images that were too blurry, or which contained a sizable portion of sky in the background, were deemed of insufficient quality. Crucially, inspection of the images ensured that the GCPs present on some of them were sufficiently visible to be marked later in the photogrammetric process. To compare the effects of different photo combinations on the model's relative accuracy, resolution and file size, many projects often covered the same region. As an example, five different projects were created to render the same region surrounding Bonebed 190: one was solely composed of images from drone 1; another included images from drones 1 and 4, the latter consisting in nadir shots taken ~40 m above ground and concentrated on a smaller area in the immediate vicinity of the fossil quarries. A third project only included images from drone 3, which were all taken at an oblique angle, while a fourth combined images from all 3 drones used to survey the region. Finally, a fifth project was a merging of 2 subprojects, one of which contained all nadir shots, the other containing all oblique shots.

Once all the images used to create a project were selected, they were imported into Pix4Dmapper to begin their alignment and matching. Vertical and horizontal coordinate systems were maintained constant for each project and were consistent with those selected for the geolocation of GCPs in the field (WGS84, zone 12N / EGM96 geoid). The *3D Maps* project type was also selected. Before beginning image alignment, a flight path composed of all selected images could be viewed at its exact geographical location. The software then matched each image by identifying the pixels they have in common, designated as Automatic tie points (ATPs). This is also the step where each photograph is calibrated to become an orthophoto. Image matching and camera calibration eventually led to a sparse 3-D point cloud composed of thousands of ATPs. Since all images were geolocated, the point cloud was already georeferenced, albeit with low vertical accuracy.

What follows is an overview of the parameters that were selected by trial and error to optimize this workflow. The *Aerial Grid or Corridor* image pair matching parameter was always selected as it was consistent with our flight paths. The *Geometrically Verified Matching* parameter was also checked since it is considered useful for discarding geometrically inconsistent matches when many similar features (such as brown to gray to ochre rocky outcrops in the present study) are a common occurrence in the project. The *Standard (default)* camera calibration method was retained since the *Alternative* method is optimized for relatively flat terrain (which does not apply to this study), and the *Accurate Geolocation and Orientation* method requires RTK/PPK geotags, which were not available for this project. Lastly, the internal camera parameters optimization option was switched from *All (default)* to *All Prior*, despite the former theoretically being best suited for cameras used with UAVs as was our case. This decision was made because GCP elevations on some initial point cloud results for Bonebed 190 displayed offsets in elevation ranging up to 25 m relative to measurements made on GCPs in the field, which resulted in a difference between initial and optimized camera parameters of almost 45% as seen in the quality report. If this difference ranges higher than 5%, the *All Prior* parameter, in which computed position values are kept close to the initial values, is advised.

Not all attempted projects were successful at this stage. The dataset assembled during the drone training session in the Steveville badlands resulted in two subregions of the same valley transect lying at highly divergent angles, as well as displaying massive holes in the point cloud.

Step 2: GCP marking and point cloud densification. The inclusion of the geotags of each photograph during image import facilitated their geospatial alignment along the *x* and *y* axes prior to their matching. However, the import of GCP measurements was crucial to aligning the sparse point cloud more accurately along the *z* axis. While individual camera geotags have accuracies ranging within tens of metres, especially in the *z* axis, our GCPs were marked with an accuracy of 0.6 m in the *x* and *y* axes and ~1.2 m in the *z* axis. The location of each GCP was found efficiently by searching the point cloud for the required Easting and Northing coordinates. For any ATP clicked in the model, an image panel appeared showing a sequence of all the photographs on which said point was identified during Step 1. In this way, each cross-shaped GCP was identified among the images. The GCP's coordinates and accuracy (both horizontal and vertical) were written in a Selection panel lying above the Image panel. The point associated with these coordinates was then marked at the center of each cross since all GPS measurements in the field were made with the receiver laid directly at that same location. Since the GCPs contributed supplemental georeferencing information to the model, the entire project had to be reoptimized, leading to slight changes in vertical and horizontal position. It must be mentioned that none of the GCPs in the model remained at the initial position recorded in the field: instead, their computed position always differed slightly from their initial position, especially along the *z* axis.

Once the model was georeferenced with sufficient accuracy, the second step of the photogrammetry process consisted of the formation of a densified point cloud, which forms the basis of the DSM (Figure 3). The one major parameter that was modified from its default settings was the selection of the Point Cloud Classification option. Classifying point clouds into different land use types is widely known to improve the generation of a DEM, which is one of the desired outputs from this project. As its surface was represented by a far higher point density, the densified point cloud could be edited to control the quality of its relative geolocation accuracy. This is where the model was inspected thoroughly for points that represent noise from the few images that displayed a little sky background. More importantly, the relative positions of the surfaces assembled from different drone models were also inspected. Densified point clouds formed from different drone datasets achieved maximum relative geolocation accuracy when a given surface captured by Drone 1 (such as a slope along a coulee) lay at the same approximate height as the same surface captured by one or more of drones 2-6. Any overlapping surface that had a vertical offset >1 m relative to the 'base map' surface created from Drone 1 had its points selected and disabled from the point cloud. In this way, they were no longer accounted for leading up to DSM generation. The point cloud could be exported as a .las file, with the option to merge all its tiles into a single file.

A 3-D textured mesh was created optionally from the densified point cloud since it could become a useful reference point for eventual geological exploration of the orthomosaic, especially for steep and near-vertical surfaces. It was possible to generate the mesh at a higher resolution than the default setting, although it significantly increased computing time and file size. The mesh could be exported as .ply, .fbx, .obj, .3Dpdf and .dxf files, the latter including an option with polylines for GIS analysis.

Step 3: DSM, orthomosaic and DEM generation. Once the densified point cloud was edited, it was ready to be transformed into a DSM, which would then form the foundation of the orthomosaic and (optionally) the DEM. For each of these 2-D imagery types, the mapping area was generated in separate square tiles of equal surface area exported as .GeoTIFF files, as well as a merger of all tiles. During initial experiments, the DSM and orthomosaic resolution was customized to 1 cm/pixel, which usually equalled 2-3 times the project's average measured GSD. However, inspection of the entire orthomosaic and of individual tiles showed that projects processed at the initial GSD provided sufficient information for a highly reduced computing time. Therefore, the initial GSD was maintained in later projects. The selection of the *Merge tiles* option was a prerequisite for generating the DEM, so it was maintained despite resulting in increased computing time. A transparent orthomosaic was expected from this project, since the empty areas occupying much of the tiles lying on the fringes of the mapping area would not appear in uniform white or black colour. As a result, the *GeoTIFF Without Transparency* option was unselected from its default setting, which approximately halved the size of the datasets generated during this step of the mapping process. Contour lines were optionally generated from the DEM, set at 5-m intervals and a 10-cm resolution and exported in .shp and .pdf file formats.

Each orthomosaic was inspected upon completion in the *Mosaic Editor* to verify the quality of its orthophotos. This is also where DSMs and DEMs could be inspected. The mosaic could be edited by drawing polygons around blurry areas. These delimited regions were then corrected in the *Mosaic Editor* using the Ortho projection, which greatly improved their sharpness, and thus our ability to identify lithological units among the outcrops for future research. The Ortho projection was always chosen over the Planar projection since the former relies on the same algorithm that was used for generating the entire unedited orthomosaic. In this way, it accounts for the spatial positions of all cameras whose photos covered the edited region (or of a customized selection), which improves its correction for perspective. In contrast, the Planar projection uses a single camera position for its correction which, while reducing computing time, could lead to distortions when all edited regions are viewed within the merged edited orthomosaic. The *Save* option in the Mosaic Editor only saves an internal copy of the edited orthomosaic within the Pix4D project. The *Export* option must be selected to save an updated copy on the designated directory. Both saving and exporting the orthomosaic require significantly more computing time with an increase in the abundance of edited regions.

Orthomosaics for each subproject were displayed in QGIS version Tisler (Figure 4). The orthomosaic created from the Pix4Dmatic project did not have a higher resolution than any of the less extensive orthomosaics created from Pix4Dmapper.

Figures

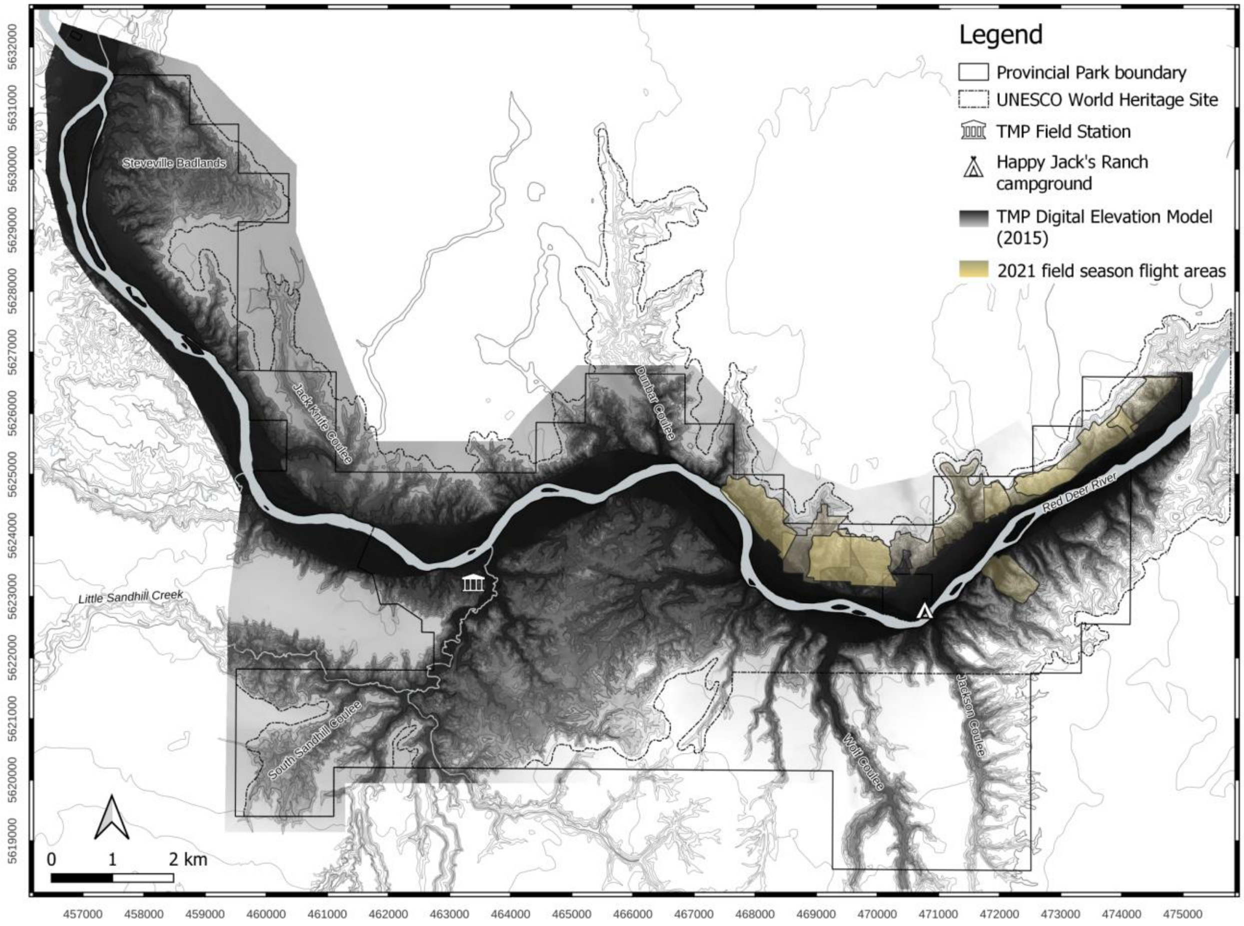

Figure 1. Dinosaur Provincial Park flight areas – August 2021 field season. Each polygon represents a different area covered on each flight day, presented in greater detail in Figure 2. DEM courtesy of Royal Tyrrell Museum of Palaeontology. Coordinates in NAD83 coordinate system, UTM zone 12N.

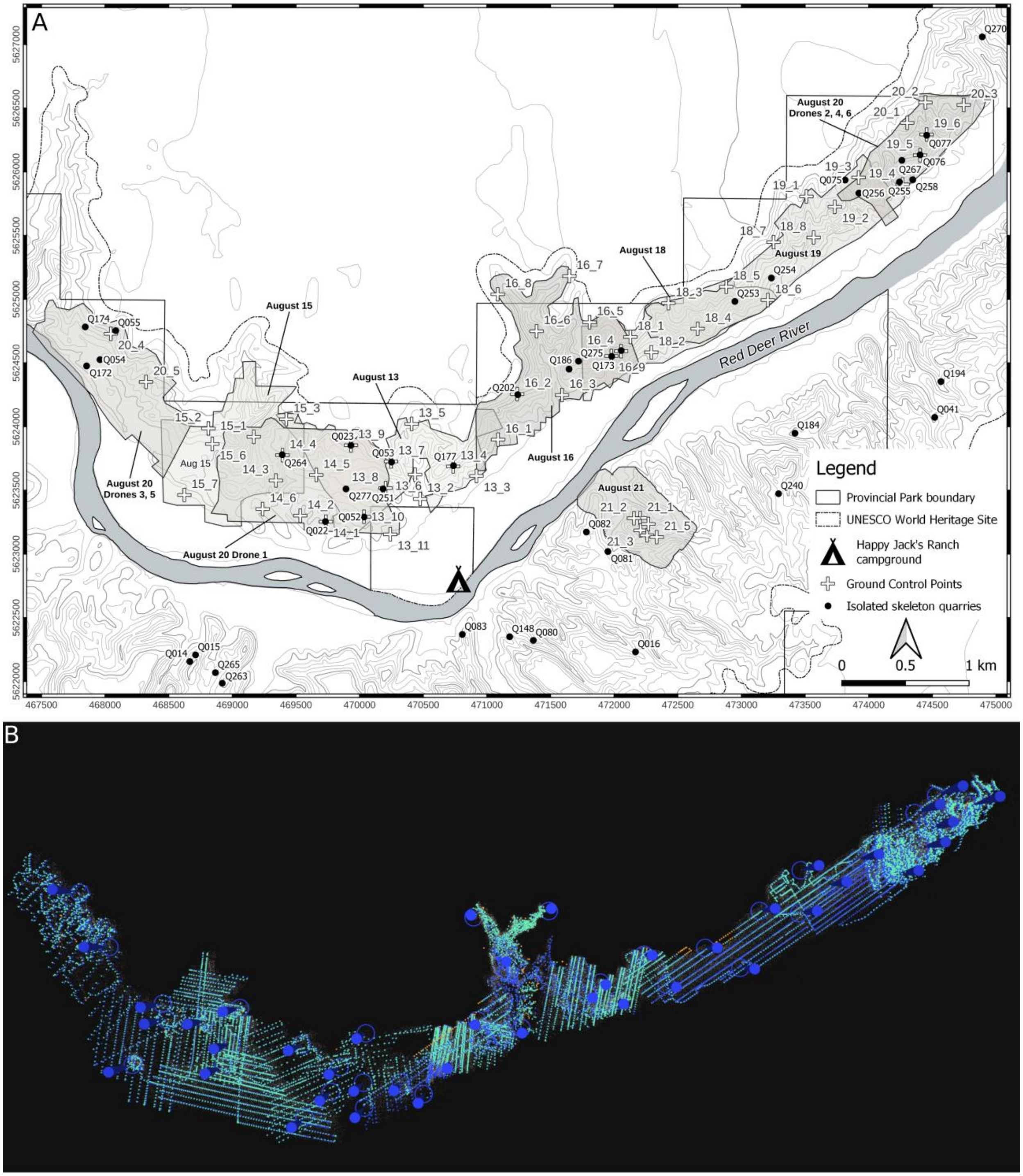
A
B
Legend
Provincial Park boundary
UNESCO World Heritage Site
Happy Jack's Ranch campground
Ground Control Points
Isolated skeleton quarries
0
0.5
1 km
Red Deer River
August 13
August 15
August 16
August 18
August 19
August 20 Drones 2, 4, 6
August 20 Drones 3, 5
August 20 Drone 1
August 21
Aug 15
13_2
13_3
13_4
13_5
13_6
13_7
13_8
13_9
13_10
13_11
14_1
14_2
14_3
14_4
14_5
14_6
15_1
15_2
15_3
15_6
15_7
16_1
16_2
16_3
16_4
16_5
16_6
16_7
16_8
16_9
18_1
18_2
18_3
18_4
18_5
18_6
18_7
18_8
19_1
19_2
19_3
19_4
19_5
19_6
20_1
20_2
20_3
20_4
20_5
21_1
21_2
21_3
21_5
Q014
Q015
Q016
Q022
Q023
Q041
Q052
Q053
Q054
Q055
Q075
Q076
Q077
Q080
Q081
Q082
Q083
Q148
Q172
Q173
Q174
Q177
Q184
Q186
Q194
Q202
Q240
Q251
Q253
Q254
Q255
Q256
Q258
Q263
Q264
Q265
Q267
Q270
Q275
Q277
5627000
5626500
5626000
5625500
5625000
5624500
5624000
5623500
5623000
5622500
5622000
467500
468000
468500
469000
469500
470000
470500
471000
471500
472000
472500
473000
473500
474000
474500
475000

Figure 2. Dinosaur Provincial Park eastern left bank flight plans. A, extents of surveyed areas and ground control point (GCP) locations for each flight day. Some GCPs were placed intentionally against stakes marking excavated skeleton quarries. B, GCP locations plotted along each selected camera location during image alignment on Pix4Dmatic. Coordinates in NAD83 coordinate system, UTM zone 12N.

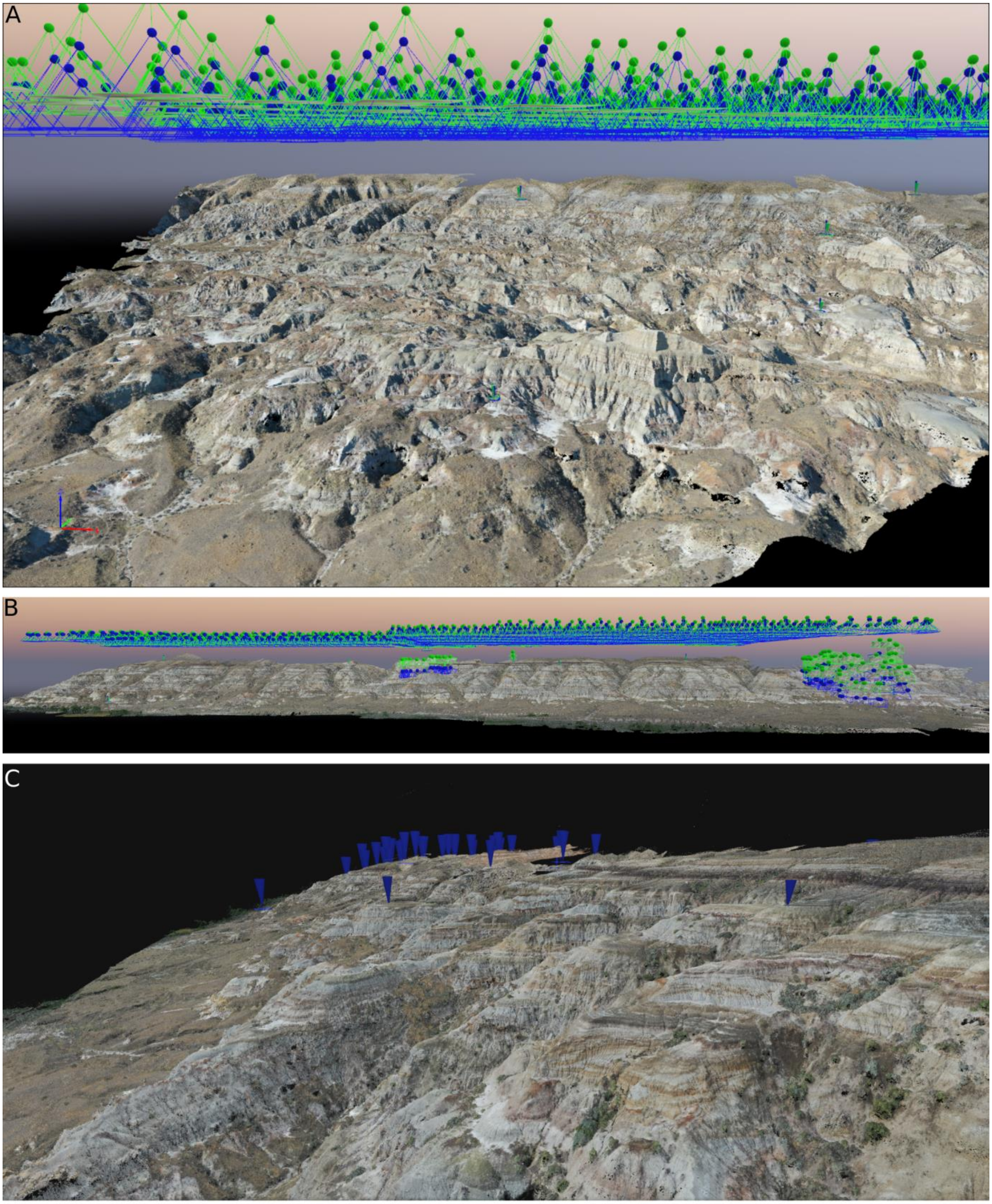
A
B
C

Figure 3. Examples of dense point clouds and camera alignments on Pix4Dmapper and Pix4Dmatic. A, Pix4Dmapper project created from Drone 1 photos taken on August 13 (outcrops located just West of Happy Jack's Ranch access road), viewed from Southeast. B, Pix4Dmapper project created from Drone 1 (August 19) and smaller drones (#x and x) covering outcrops located between Q253 and Q258 (see Figure 2), viewed from Southeast. C, Pix4Dmatic project covering entire study area, Q253-Q258 area viewed from Northeast at angle almost parallel to ground surface at river level. Note Lethbridge Coal Zone clearly visible as dark band just below prairie level. Pins on ground surface represent ground control points (GCPs). Blue represents initial camera/GCP locations, green represents calibrated locations after geolocation corrected by GCP inclusion.

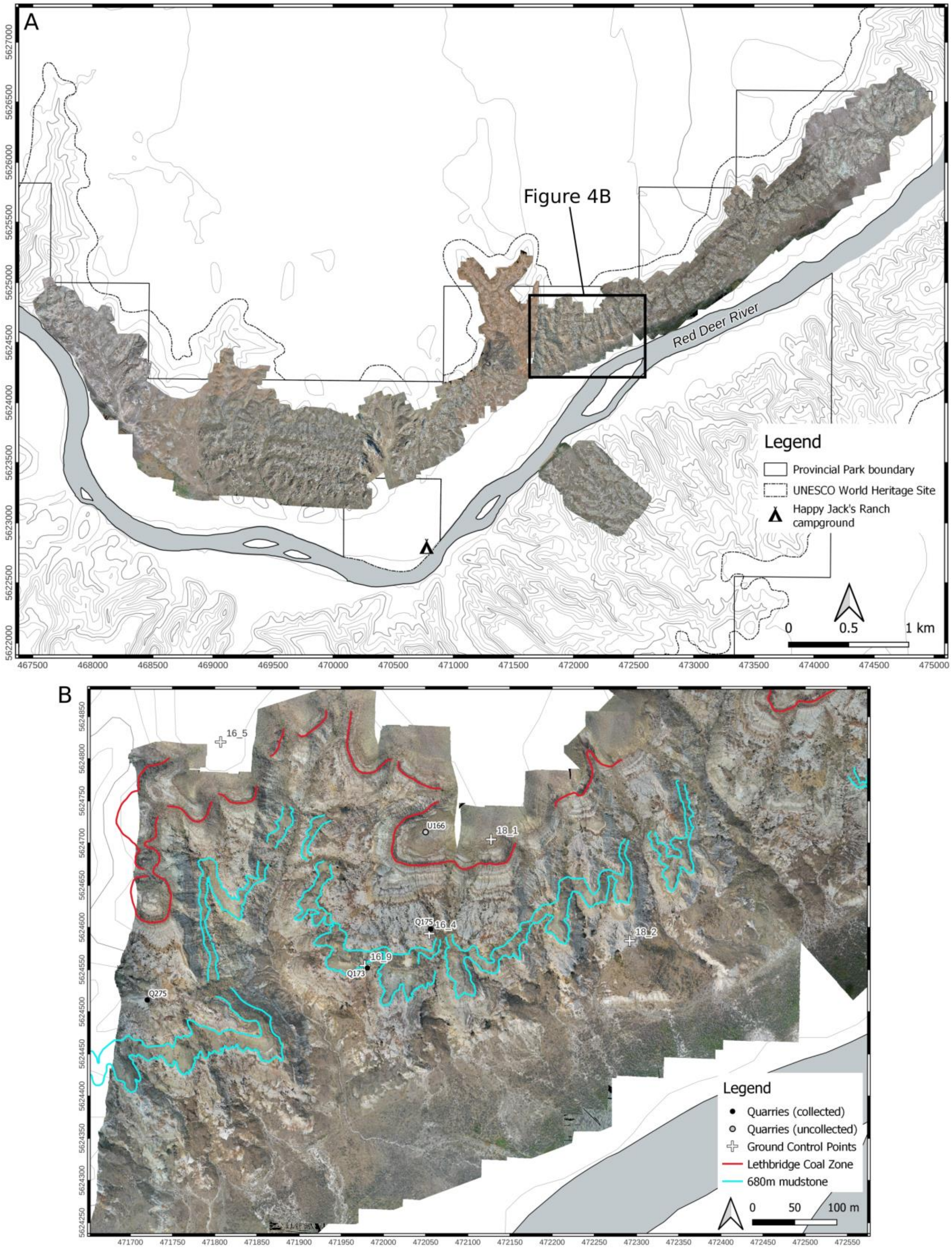
A
Figure 4B
Red Deer River
Legend
Provincial Park boundary
UNESCO World Heritage Site
Happy Jack's Ranch campground
0
0.5
1 km
5627000
5626500
5626000
5625500
5625000
5624500
5624000
5623500
5623000
5622500
5622000
467500
468000
468500
469000
469500
470000
470500
471000
471500
472000
472500
473000
473500
474000
474500
475000
B
16_5
U166
18_1
Q175
16_4
18_2
16_9
Q173
Q275
Legend
Quarries (collected)
Quarries (uncollected)
Ground Control Points
Lethbridge Coal Zone
680m mudstone
0
50
100 m
5624850
5624800
5624750
5624700
5624650
5624600
5624550
5624500
5624450
5624400
5624350
5624300
5624250
471700
471750
471800
471850
471900
471950
472000
472050
472100
472150
472200
472250
472300
472350
472400
472450
472500
472550

Figure 4. Preliminary orthomosaic of Dinosaur Provincial Park outcrops created from several Pix4Dmatic projects each covering a ~1 km^2 area, projected on QGIS. A, overview of area mapped during 2021 field season. B, inset of Figure 4A showing preliminary tracing of potential marker beds.

Tables

Table 1. Metadata for each mapped transect of Dinosaur Provincial Park outcrops in Happy Jack's area, eastern left bank, Dinosaur Provincial Park 2021 field season. This does not include the more large-scale project created on Pix4Dmatic.

Transect	Q174-Q264	Q264-Q052	Q052-Q177	Q052-Q177	Q202-Q175	Q175-BB253	BB231-Q258	Q255-BB167
Drones	1-6	1-5	1	1-6	1-6	1,2,5	1,2,6	1-6
Area (km^2)	2.138	1.285	1.133	1.384	1.499	0.845	0.993	1.027
Number of marked GCPs	9	7	9	9	7	7	8	7
Camera position(s)	Nadir, oblique	Nadir, oblique	Nadir	Nadir, oblique	Nadir, oblique	Nadir, oblique	Nadir, oblique	Nadir, oblique
Average GSD (cm)	2.39	2.16	3.06	2.98	1.39	2.13	2.21	2.14
No. images calibrated; %	2,515; 98	3,687; 95	888; 99	1,052; 97	4,591; 97	1,812; 99	1,805; 99	3,531; 98
Project size (Gb)	56.9	56.8	25.8	28.6	67.7	52.5	51.3	36.3

Table 2. Ground control point measurements for each flight day, Dinosaur Provincial Park 2021 field season. Each GCP numbered sequentially by date within August 2021. Horizontal coordinates in WGS84 / Universal Transverse Mercator zone 12 N, EGM96 geoid. Orthometric height is elevation above mean global sea level.

GCP	Easting (m)	Northing (m)	Orthometric height (m)	Horizontal accuracy (m)	Vertical accuracy (m)	Notes
13-2	470475.441	5623432.469	645.01	0.6	1.2	
13-3	470918.365	5623613.44	643.88	0.6	1.2	
13-4	470735.276	5623687.949	689.46	0.6	1.2	Q177 stake
13-5	470408.552	5624021.613	705.98	0.6	1.2	
13-6	470435.845	5623623.946	646.22	0.6	1.2	
13-7	470246.741	5623726.979	688.6	0.6	1.2	Q053 stake
13-8	470204.287	5623517.908	661.84	0.6	1.2	20 m E of Q251
13-9	469932.464	5623854.279	704.32	0.6	1.2	Q023 stake
13-10	470034.289	5623293.052	667.96	0.6	1.2	Q052 stake
13-11	470240.796	5623154.69	636.51	0.6	1.2	
14-1	469735.642	5623254.176	654.08	0.6	1.2	Q022 stake
14-2	469533.621	5623301.108	651.52	0.6	1.2	
14-3	469342.163	5623577.597	664.79	0.6	1.2	
14-4	469393.814	5623776.638	698.21	0.6	1.2	
14-5	469659.482	5623620.919	658.88	0.6	1.2	
14-6	469237.891	5623353.38	664.48	0.6	1.2	
15-1	469168.307	5623920.044	687.37	0.6	1.2	
15-2	468811.716	5623986.274	687.87	0.6	1.2	
15-3	469423.877	5624058.209	718.74	0.6	1.2	
15-6	468842.369	5623864.002	663.02	0.6	1.2	
15-7	468622.915	5623463.813	636.33	0.6	1.2	
16-1	471087.515	5623898.586	630.41	0.6	1.2	
16-2	471238.195	5624255.892	674.33	0.6	1.2	Q202 stake

16-3	471590.603	5624248.553	642	0.6	1.2	
16-4	472054.338	5624592.653	686.22	0.6	1.2	Q175 stake
16-5	471807.01	5624819.888	727.88	0.6	1.2	
16-6	471390.06	5624749.234	647.73	0.6	1.2	
16-7	471648.278	5625181.858	723.84	0.6	1.2	
16-8	471085.093	5625039.553	728.7	0.6	1.2	
16-9	471977.962	5624554.707	682.25	0.6	1.2	Q173 stake
18-1	472127.609	5624704.336	724.56	0.6	1.2	
18-2	472291.981	5624584.114	656.58	0.6	1.2	
18-3	472426.618	5624969.586	711.67	0.6	1.2	
18-4	472655.948	5624769.078	651.45	0.6	1.2	
18-5	472880.822	5625098.456	721.4	0.6	1.2	
18-6	473207.55	5624994.121	641.45	0.6	1.2	
18-7	473252.245	5625448.825	710.98	0.6	1.2	
18-8	473567.347	5625485.099	688.83	0.6	1.2	
19-1	473510.839	5625807.305	717.12	0.6	1.2	
19-2	473733.569	5625726.395	708.32	0.6	1.2	
19-3	473920.771	5625956.359	724.27	0.6	1.2	
19-4	474266.475	5625902.307	666.08	0.6	1.2	
19-5	474403.653	5626130.918	695.6	0.6	1.2	Q076 stake
19-6	474455.287	5626293.719	669.99	0.6	1.2	Q077 stake
20-1	474302.597	5626384.616	718.92	0.6	1.2	
20-2	474445.682	5626545.466	717.11	0.6	1.2	
20-3	474746.953	5626525.783	689.46	0.6	1.2	
20-4	468045.245	5624728.773	697.65	0.6	1.2	Q055 stake (not found)
20-5	468321.8	5624351.5	675.5	0.6	1.2	
21-1	472204.335	5623283.116	688.68	0.6	1.2	BB190 core
21-2	472155.629	5623281.098	688.38	0.6	1.2	BB190 core
21-3	472207.955	5623186.403	689.56	0.6	1.2	BB190 core
21-4	472259.432	5623146.742	686.38	0.6	1.2	BB190 core

21-5	472334.569	5623133.399	687.28	0.6	1.2	BB190 core
21-6	472268.563	5623236.068	688.35	0.6	1.2	BB190 core

Appendix V

Justification of trophic links in Dinosaur Provincial Park food webs

This appendix presents in greater detail the reasons for the trophic links between the nodes which compose the Dinosaur Provincial Park food webs. It lays the foundation for the food web presented in this thesis, but also for a second manuscript where food webs from a greater number of temporal intervals within the Belly River Group of Dinosaur Provincial Park (e.g. Oldman Formation, Lethbridge Coal Zone) will be compared.

DETRITUS & CARRION

Fossil record: clearly no direct fossil evidence of these nodes in DPP but they are retained from the Messel food web because they are important food sources for several taxa that are less (or not at all) reliant on predation

Trophic links

- Dung and leaf litter considered part of 'Detritus' node since it's decomposing
- Carrion retained because it could represent the carcass of an animal that is not usually by the consumer (e.g. ankylosaur carcass scavenged by pterosaurs)
- Decaying wood gets distinct node because it may have been distinct food source for megaherbivores, particularly hadrosaurs and ceratopsians, as shown from coprolite content from Two Medicine Formation (Chin 2007)

BACTERIA

Fossil record: nonexistent in DPP

Keep the bacteria from Messel food web that have links to DPP nodes, e.g. those that are eaten by bivalves, fungi (Labandeira & Dunne 2014)

PLANTS

The versions of the food web presented in this thesis have plant nodes selected at a low taxonomic resolution. This appendix presents an alternative selection of nodes resolved at a higher taxonomic resolution, usually at the family level. This more complete version of the Dinosaur Provincial Park food web is in preparation for a second manuscript.

- Several taxa (most notably Cycadaceae and angiosperm families) divided into 3 nodes: leaves, shoots and fruits/seeds to reflect modularity of their anatomy and the fact that different modules on the same plant can feed very different consumers
    - Shoots require their own node because they are more digestible than tree leaves for many animals so support different dietary niches
- Inconvenient: I will tend to make feasible links for DPP while Messel food web relies much more on realized links because of better soft-tissue fossil preservation, so it will lead to underestimation of omnivores' PATL

Would it be worth making a figure with photos of fossils from BB234 plant site showing new fossil records of certain nodes (isopods, dragonfly, pines)?

Algae

Possible fossilized algae now found at BB234 so it's reasonable to keep some algae nodes from Messel, especially Chlorophyta as a major staple resource

- Dinoflagellates not detected in pollen samples from Oldman Fm, so they may reflect increasingly saline water as Bearpaw transgression progresses throughout DPF (Braman 2005)

Bryophytes (Anthocerotaceae, Sphaerocarpaceae, Sphagnaceae)

Fossil record: palynoflora (Jarzen 1982; Braman 2005)

Trophic links : all hornwort, liverwort, moss families seem to have aquatic species, so it makes sense to maintain links with terrestrial and aquatic bivalves and snails as seen in Messel food web (Labandeira & Dunne 2014)

Lycopodiophytes

Fossil record: palynoflora (Jarzen 1982; Braman 2005)

Trophic links: *Selaginella* and relatives eaten by birds, insects (Labandeira & Dunne 2014); Lycopodiaceae also tentatively reported from pollen assemblages but appear to lack natural predators so not included in network

- Very little information on Isoetaceae (quillwort) predators but birds and muskrats are known to eat them at least (Environment and Climate Change Canada 2012)

Equisetum

Fossil record: fossil stems common across DPP, especially at Q213 (Braman *et al.* 1995)

Trophic links: see Mallon (2019) on horsetail digestibility, seems to suit hadrosaurs at least

- A few insect groups also known to feed on horsetails (Poinar, Jr. 2014)

Polypodiales – Ferns

Nodes: Osmundaceae, Schizaeaceae, Gleicheniaceae, Cyatheaceae (tree ferns), Dicksoniaceae, Polypodiaceae, Matoniaceae, Marsileaceae

Fossil record: palynoflora (Jarzen 1982; Braman 2005)

Trophic links: poor nutritional value, likely consumed in bulk by megaherbivores (Mallon 2019)

- Direct evidence of heavy fern consumption by nodosaur *Borealopelta* (Brown *et al.* 2020*c*)
- Insect feeding evidence (Fuentes-Jacques *et al.* 2022)

Cycadaceae

Fossil record: palynoflora (Jarzen 1982; Braman 2005)

Trophic links: few insects known to actually feed on cycad leaves, mostly beetles, butterflies and thrips (Schneider *et al.* 2002)

- Among megaherbivores, nodosaurids at least definitely fed on cycad leaves (Brown *et al.* 2020*c*); arguable that other megaherbivores also ate their leaves given that extant native herbivorous mammals still do so, e.g. kangaroos (Schneider *et al.* 2002)
- Extant birds and mammals (e.g. opossums, squirrels) eat cycad fruits and stems (Schneider *et al.* 2002), so it's reasonable to have links between DPP omnivorous/herbivorous theropods and mammals as well as thescelosaurs and pachycephalosaurs
- elephants even known to eat cones (Schneider *et al.* 2002), so add a node for that cycad part and connect to herbivores with relatively strong bites (ceratopsids incl juveniles, hadrosaurs)

Caytoniaceae

Fossil record: palynoflora (Jarzen 1982; Braman 2005)

Trophic links: appearance of large tree with leaf module named *Sagenopteris* (Retallack & Dilcher 1988); high diversity of insect damage types on well preserved leaves from Early Cretaceous Spain (Sender *et al.* 2022)

Coniferophyta
Fossil record: pollen and recently macroflora for Pinaceae, macroflora for *Sequoia*/*Metasequoia*; wood (Ramanujam 1972; Braman *et al.* 1995); exclusively pollen for Podocarpaceae, Cupressaceae and Cheirolepidiaceae (Jarzen 1982; Braman 2005)
Trophic links: stomach contents in hadrosaur (Currie *et al.* 1995)

Ginkgos (*Baiera digitata*, *Ginkgoites* sp., *Ginkgo* sp.)
Fossil record: macroflora (Koppelhus 2005)
Trophic links: few insect predators compared to other gymnosperms in the present (Honda 1997) but evidence of margin feeding in Jurassic suggests other herbivorous taxa besides homopterans (Na *et al.* 2018); hadrosaurs proposed to be frequent ginkgo consumers (Mallon 2019)

- very likely *Ginkgo* sp. representative found at new DPP plant site in 2017/18

Angiosperms
Fossil record: most species known from pollen (Jarzen 1982; Braman 2005), leaf macrofossils relatively rare (Koppelhus 2005) but at least new fossil leaf sites recently found; lack of petrified wood referred to angiosperms may indicate that woody dicots usually grew as shrubs and rarely reached size of large trees, so canopy seemed dominated by conifers

- Maybe more conservative not to include new leaf morphotypes from new plant sites yet in case those belong to families already included in food web

Trophic links

- The only angiosperm fruit/seed nodes connected to megaherbivores with wide snouts for bulk feeding should be families known to produce large fruits (e.g. *Artocarpus*) or at least grapes of small fruit (e.g. *Vitis*)
    - Fruit dispersal syndromes likely analogous to those observed in extant tropical forests (Gautier-Hion *et al.* 1985)
- Restrict families solely producing nuts/small seeds (e.g. Fagaceae) to birds, mammals, soft-shelled turtles and narrow-snouted herbivorous dinosaurs like thescelosaurs, pachycephalosaurs, ornithomimids
- Families that only produce very small seeds (e.g. *Acer*, Salicaceae) should be restricted to birds, small mammals and smallest herbivorous/omnivorous dinosaurs (when they fall on the ground in case of the latter)
- Taxa that lack sufficient info on fruit consumers should have their fruit/seed nodes deleted

- *Angiosperms known from leaf macroflora*
    - *Artocarpus* (Moraceae; breadfruit/jackfruit): leaves from Oldman Fm; fleshy zoochorous fruit
    - *Cercidiphyllum* (Cercidiphyllaceae; katsura tree): leaves found in DPF Q220, almost no information on fruit consumers, so fruit node discarded

  - *Dombeyopsis nebrascensis* (Sterculiaceae): fruit unknown, so discarded node
  - *Menispermites* (Menispermaceae; moonseeds): fruits produced in drupes, fleshy and zoochorous
  - *Platanus* (sycamores): fruits produced as spiky seed capsules, nonfleshy zoochory, likely only accessible to birds and mammals after dispersal
  - *Vitis* (Vitaceae; grapes): fleshy and zoochorous fruit
  - *Trapa* sp. (aquatic plant similar to water chestnut)
  - *Cobbania corrugata* (aquatic plant similar to water lettuce): most common monocot in DPP palaeobotanical record (Stockey *et al.* 2007)

- *Angiosperms known from palynoflora*
  - Buxaceae (boxwood): DPP pollen most similar to a herbaceous species *Pachysandra*
  - Gunneraceae (gunneras): small orange gooseberry-like fruit
  - Salicaceae (willows, poplar, aspen): poplar-like leaf possibly found at BB234 Plant; fruit is dehiscent capsule containing seeds, possibly only accessible to birds, mammals and small herbivorous/omnivorous dinosaurs like orodromines and caenagnathid *Citipes*
  - Droseraceae (Venus flytrap)
  - Olacaceae (tallowwood): can be trees, shrubs or vines; small to medium-sized fleshy fruit (Gautier-Hion *et al.* 1985)
  - Loranthaceae (showy mistletoes): climbing shrub so node for stems/shoots is irrelevant; fruits consist of berries, birds and monkeys seem to be only vertebrates to eat them in modern tropical forests (Gautier-Hion *et al.* 1985), perhaps small herbivorous/omnivorous dinosaurs such as orodromines, ornithomimids, caenagnathid *Citipes* and juvenile hadrosaurs also ate them
  - Sapindaceae (soapberries, maples): very variable fruit anatomy, either fleshy berries or nonfleshy samaras
  - Proteaceae (proteas); fruit can be either drupes, follicles or nuts similar to *Macadamia*
  - Compositae (sunflowers)
  - Fagaceae (beeches, oaks, chestnuts): possible microphyll oak leaf found at BB234 plant site; fruits usually as nuts, nonfleshy zoochory
  - Betulaceae (birches, alders): possible birch leaf found at BB234 plant site; fruits usually as catkins likely only accessible to DPP birds, nonfleshy zoochory
  - Ulmaceae (elms): fruits as samaras, possibly only accessible to birds, mammals and small herbivorous/omnivorous dinosaurs like orodromines and caenagnathid *Citipes*
  - Chenopodiaceae (goosefoots): usually herbs and shrubs, rarely trees; family includes sugar beets
  - Liliaceae (lilies): usually herbaceous plants
  - Cyperaceae (sedges and reeds)
  - Sparganiaceae (bur-reeds)

  - Families that don’t exist as trees (e.g. Compositae, Gunneraceae, Buxaceae) have shoots and tree leaves collapsed into one node

LICHEN & FUNGI

Fossil record: nonexistent
Trophic links largely based on Messel (Labandeira & Dunne 2014); links between fungi and certain plant species removed

DEMOSPONGIAE (SPONGES)

Nonexistent in DPP but freshwater sponges reported from Messel (Labandeira & Dunne 2014); links based on that same food web

MOLLUSCS

Bivalves

Fossil record: abundance of bivalves in DPP, especially freshwater assemblages dominated by Unionidae and Sphaeriidae (Johnston & Hendy 2005)

- Sharp turnover at LCZ contact where unionid- and sphaeriid-dominated assemblages are replaced by more diverse brackish assemblage, including the marine *Mactra*

Trophic links

- Freshwater bivalve links based on Messel (Labandeira & Dunne 2014)
- Brackish and marine bivalve links based on Paja biota food web (Cortés & Larsson 2023)

Gastropods

Fossil record: freshwater snails occasionally found in DPP (Johnston & Hendy 2005); terrestrial pulmonate snails not found in DPP yet but two species reported from Foremost and Oldman Fm along nearby Milk River (Russell 1941; Johnston & Hendy 2005)
Trophic links based on Messel food web and well-documented extant species like *Planogyra* (VanVleet 2014)

- Rare ichnofossil evidence of snail trophic interactions with discovery of snail shells in dinosaur coprolites from Two Medicine Formation, suggests the snails were key recycling agents in Mesozoic nonmarine communities (Chin *et al.* 2009)

Ammonites

Fossil record: ammonites rarely found in DPP, always at highest stratigraphic horizons; they are thus included in LCZ food web
Trophic links inferred from Paja biota network and other ecomorphological inferences (Kruta *et al.* 2011; Cortés & Larsson 2023)

ARTHROPODS

Crustaceans and millipedes

Fossil record:

- Most widespread fossils are actually ichnofossils as crayfish coprolites found in microfossil bulk samples (Brinkman data)
- very rare millipede fossil in nodule from DPP (Johnston & Hendy 2005)

Trophic links:

- branchiopods and ostracods included in food web because of their importance as zooplankton for aquatic community; aquatic crustacean links inferred from Messel
- Millipedes are among the earliest detritivores in history of complex terrestrial ecosystems (Hopkin & Read 1992)

Insects

Fossil record:

- new dragonfly and hymenopteran wings from BB234 plant site (this study), aphid in amber (McKellar *et al.* 2019)
- Most other insects, arachnids and chelicerates represent families reported from nearby Grassy Lake Amber in Foremost Fm (Pike 1994; McKellar *et al.* 2008)
- 'Isopods' reported from BB234 plant site might be maggots (fly larvae)

Trophic links:

- Diets largely based on extant relatives and Messel food web links, including literature and databases on plant-herbivore interactions (Labandeira & Dunne 2014; Fuentes-Jacques *et al.* 2022; Biological Records Centre 2024)
- ants also get distinct node from main Hymenoptera node because of their distinct ecological role; diet largely based on Messel food web while ignoring giant *Formicium* lineage (the only one that ate larger prey)
- Orthopterans get exceptional inclusion even if not found in Grassy Lake Amber due to their importance as food source for several tetrapods, especially mammals and lizards
- Ichnofossil evidence of dung beetle burrows near location of coprolites attributed to hadrosaurs in Two Medicine Formation (Chin & Gill 1996); this detritivorous interaction was almost certainly occurring in coeval DPF biota as well

CHONDRICHTHYANS

Fossil record: only 3 species known from paralic depositional environments of DPF (excluding LCZ): *Hybodus* and orectolobid sharks and ray *Myledaphus bipartitus*; the others are only known from brackish-to-marine-dominated facies of LCZ (Beavan & Russell 1999, Brinkman *et al.* 2005*b*). Nodes representing the latter are: Odontaspididae (including *Odontaspis aculeatus* and *Carcharias steineri*), Cretoxyrhinidae (*Archaeolamna japonensis judithensis* and *Cretolamna* sp.), *Archaeotriakis* sp., *Protoplatyrhina renae*, Sclerorhynchidae and *Elasmodus greenoughii*.

- *Myledaphus* is only DPP elasmobranch to be represented by fairly complete skeleton (Neuman & Brinkman 2005), the others are only known from isolated teeth

Sharks

Fossil record

- *Hybodus montanensis* only occurs from 20 m above OF-DPF contact upwards, may suggest affinity for brackish water but definitely part of more coastal assemblage (Brinkman 1990)
- Orectolobids (carpet sharks): *Squatirhina* is one of the few sharks found below LCZ, as low as Oldman Formation

Trophic links

- Hybodonts clearly very successful shark group due to their persistence for much of Jurassic and Cretaceous (e.g. Villalobos-Segura et al., 2023), likely active generalist pursuit predator due to fusiform body shape, direct evidence of hybodont preying on ammonite (Vullo 2011)
- Orectolobid diet based on extant carpet sharks such as the spotted wobbegong *Orectolobus maculatus* (Compagno 2002), so links distributed to nodes representing small benthic fish, crayfish and rays such as *Myledaphus*
- *Squatina* diet based on extant angelsharks, which mainly consists of benthic fish, crustaceans and molluscs (Froese & Pauly 2024*a*)
- Odontaspididae: diet based on extant sand tiger sharks, which mostly prey on teleosts but complement that diet with houndsharks (Triakidae), angelsharks (Squatinidae) and rays (Compagno 2002)
- Cretoxyrhinidae: the largest sharks found in DPP by far, apex predator of LCZ marine community since *Tylosaurus* skeleton collected just off DPP eastern border was in Bearpaw Formation (Caldwell 2005); diet based on extant great white shark, so generalist pursuit predator (Compagno 2002), likely the only natural enemy of marine turtle *Kimurachelys slobodae*, plesiosaur *Fluvionectes sloanae*, and medium-sized mosasaur *Plioplatecarpus* sp.; bite marks on elasmosaur paddle from Niobrara Chalk (from WIS just like Bearpaw Sea, slightly older) attributed to *Cretoxyrhina mantelli* (Everhart 2005)
- *Archaeotriakis* diet based on extant leopard sharks such as *Triakis semifasciata* (Compagno 1984): prey mainly consists of benthic invertebrates (crayfish, clams) and is complemented by small fish

Other chondrichthyans

Fossil record

- *Myledaphus* is by far the most abundant chondrichthyan in the DPP fossil record, but that may be wild overestimation because each individual has extensive tooth plates in jaws and each tooth is among the most resistant elements of any vertebrate microfossil assemblage

Trophic links

- *Myledaphus* diet modeled on extant guitarfish so links distributed to bottom-dwelling molluscs, crayfish and small fish (Schneider 1990)
- Sclerorhynchid diet based on extant sawfish: small fish and benthic invertebrates (Froese & Pauly 2024*b*)

- *Elasmodus* diet based on extant *Chimaera monstrosa*, which feeds mainly on benthic invertebrates (Froese & Pauly 2024*c*)

OSTEICHTHYANS

Fossil record: very few skeletons, mostly based on teeth, jaw elements and centra
Trophic links:
What is the rule I choose to determine trophic links in and out of those fish? Settle for the fish species or family's maximum body size, otherwise every prey will be connected to every predator

Chondrosteans

Fossil record: Acipenseridae (sturgeons) and Polyodontidae (paddlefish), mostly represented by denticles in vertebrate microfossil localities (Brinkman 1990), but also a few isolated macrofossil elements like skulls and cleithra; only two fairly complete sturgeon skeletons known from DPP, one of which is articulated and was described as holotype of *Anchiacipenser acanthaspis* (Sato *et al.* 2018)

Trophic links:

- *Anchiacipenser* diet based on extant lake sturgeon *Acipenser fulvescens* and Atlantic sturgeon *A. oxyrhynchus* (Scott & Crossman 1973): largely carnivorous, feed on crustaceans, molluscs, zooplankton, occasionally algae, rarely small bottom-dwelling fish; this means that *Notogoneus* sp. is considered too large to be viable prey based on sturgeon gape size, only fish nodes going into the sturgeon are therefore the 4 acanthomorphs, many or all of which could be bottom-dwellers
- Extant paddlefish diet (*Polyodon spathula*) inferred for the DPP polyodontid, so filter-feeding zooplanktivore (Hoxmeier & Devries 1997)

Holosteans

Fossil record: at least 3 holostean-grade fishes recognized in DPP: Lepisosteidae (gar), Amiidae (bowfin), *Belonostomus longirostris* (Aspidorhynchiformes, likely within Teleostomorpha), all known from isolated elements such as skull and jaw bones, scales and centra (Brinkman 1990; Neuman & Brinkman 2005); gar scales in particular are often overrepresented in vertebrate microfossil localities; distinctive isolated scales hint at presence of between one and two more holosteans, termed Holostean A and B (Brinkman 1990; Neuman & Brinkman 2005)

Trophic links:

- Extant gar are generalist carnivores, largely piscivorous in adult stages, large longnose gar *Lepisosteus osseus* individuals known to feed on pikes (Scott & Crossman 1973), so almost all DPP fishes with estimated body length <1 m are considered DPP gar prey; Amiidae constitute exception because those are never reported among extant gar prey
- DPP amiid considered part of Amiinae, same clade as extant bowfin *Amia calva* (Grande & Bemis 1998); opportunistic predator with wide gape, could catch prey as large as pickerel but also known to eat plant material (Scott & Crossman 1973); close extinct

relative *Cyclurus* connected to molluscs in Messel food web (Labandeira & Dunne 2014), but DPP amiid lacks crushing teeth on palatal bones (Neuman & Brinkman 2005), therefore molluscs not included in its diet; in a way, DPP amiid diet is more similar to extant bowfin's

- Nothing known about feeding anatomy of Holosteans A and B, so Holostei (other) node assigned similar links to Lepisosteidae and Amiidae combined
- *Belonostomus* seems to be rare freshwater species among a clade largely composed of marine species going back to Jurassic (Brito 1997); *B. longirostris* one of the most gracile species of its clade with very narrow snout, fish prey likely restricted to smallest species (Neuman & Brinkman 2005)

***Enchodus* sp.**
Fossil record: only known in DPP from teeth recovered in LCZ vertebrate microfossil localities (Brinkman *et al.* 2005*b*), so only present in LCZ version
Trophic links: large marine fish known throughout Cretaceous oceans, likely a key generalist predator, could eat most fishes and rays in LCZ assemblage, even some sharks (Everhart 2013)

Teleosts
Fossil record:

- Most of the Park's teleosts only known from isolated skull, mandible elements and centra from several DPP vertebrate microfossil localities (Brinkman 1990, 2019; Neuman & Brinkman 2005)
- prioritize nodes for taxa that actually have jaw or skull elements; only include taxa based solely on centra if they represent a truly unique group (e.g. Hiodontidae)
- This means that this network has 15 teleost nodes overall

Elopomorphs
Fossil record: Elopomorphs are rare teleost group from DPP to be represented by species whose closest extant relatives have marine rather than freshwater habitat, yet the present species are almost always found in non-marine beds: *Paratarpon apogerontus* and *Paralbula casei*

- *Paratarpon* is the only teleost from the Park to be represented by more than one near-complete skeleton; only described specimen is from Manyberries area (Bardack 1970), but others are known from DPP (Neuman & Brinkman 2005); originally thought to be characteristic of coastal community (Brinkman 1990) but now
- *Paralbula* known solely from tooth plates with flat, irregular teeth (Neuman & Brinkman 2005); considered same species as *Paralbula casei* placed within Albulidae (Estes 1969)

Trophic links

- *Paratarpon* similar to extant tarpon *Elops* and *Megalops* so diet likely restricted to small fish and crustaceans (Neuman & Brinkman 2005); maximum body length estimated at 1.5 m (Bardack 1970), so it was the largest teleost by far known from the Park
- *Paralbula*: tooth plates with irregularly stacked teeth imply crushing function (Estes 1969), as seen in diet of modern relative bonefish *Albula vulpes* based on mollusks and crustaceans (Crabtree *et al.* 1998)

Osteoglossomorphs

Fossil record: at least 3 species in DPP

  - *Coriops* known from tooth-bearing elements, *Cretophareodus* known from tooth-bearing elements and a rare articulated skeleton (Guo-Qing 1996), hiodontids only known from isolated centra (Brinkman 2019)
    - Frequent occurrence (but low abundance) in many microsites in Oldman and lower DPF but not a single hiodontid centrum found in any microsite more than 40 m above OF-DPF contact; suggests that absence of hiodontids in LCZ fossil record is genuine and does not reflect collecting bias

Trophic links

- *Coriops* dentition is particularly similar to that of extant bonytongues (arowanas) (Neuman & Brinkman 2005, Froese & Pauly 2024*d*); implies diet of microcrustaceans (juveniles), terrestrial and aquatic insects, small fishes, frogs, crustaceans and plant
  - Elect not to include ?*Wilsonichthys* (only centra indicative of its presence in DPP)
- *Cretophareodus* has smaller teeth, likely fed on softer prey, so no decapods among its links
- Hiodontidae: DPP hiodontids much smaller than extant *Hiodon* relatives based on study of fossil centrum growth patterns (Newbrey *et al.* 2007), so they are considered prey for almost every other (semi)aquatic vertebrate; Food restricted to microcrustaceans and insects (Scott & Crossman 1973); hiodontids known to be surface feeders, so likely out of reach of benthic predators like *Myledaphus* and *Squatirhina*

Clupeomorphs

Fossil record

- Clupeomorphs represented by centra assigned to medium-sized ellimmichthyiforms *Diplomystus* and *Horseshoeichthys* (Brinkman 2019); *Diplomystus* only reported from Onefour but it was almost certainly present in DPP as well

Trophic links

- Both are herring-like with more complete skeletons known from Green River Formation and Horseshoe Canyon Formation respectively (Grande 1984; Newbrey *et al.* 2010)
- Diet largely similar to modern herring (Scott & Crossman 1973); both species have large heads that could allowing for relatively wide gape, and one complete *Diplomystus* skeleton from Green River preserved while attempting to swallow fish more than half its own body length (Grande 1984)

Ostariophysans

Fossil record: at least two major ostariophysan clades represented in DPP

- Centra assigned to extinct gonorynchid genus *Notogoneus* (Brinkman 2019); most of them come from Onefour but a few sampled from L2371 (Wolf Coulee microsite), a locality very high in section in DPF
- Characiformes detected on basis of dentaries very similar to extant tetra *Charax* species found in Onefour area (Newbrey *et al.* 2009); only DPP occurrence consists of rare centra similar to extant minnow *Cyprinus cyprinus* found in L2371 (Brinkman 2019)

Trophic links

- Rare *Notogoneus* skeleton from Two Medicine Formation shows it reached standard length of 40 cm (Grande & Grande 1999)
- Only extant relative of *Notogoneus* is beaked salmon *Gonorynchus gonorynchus* which feeds on benthic and burrowing marine invertebrates (Froese & Pauly 2024*e*); *Notogoneus* looks more like pelagic predator but skull anatomy poorly preserved; stick to beaked salmon diet for now, which means it becomes prey to bottom-dwelling predators like *Myledaphus* and *Squatirhina*
- Characiformes considered the smallest fish on average in this food web, extant tetras largely feed on insect larvae, shrimps and odonate nymphs (Froese & Pauly 2024*f*)

Esocoids

Fossil record: 2 species (*Estesesox foxi* and *Oldmanesox canadensis*) based on isolated dentaries and vomers with C-shaped tooth bases that enable teeth to fold backwards, which is apomorphic for Esocoidea (Wilson *et al.* 1992; Neuman & Brinkman 2005)

- Esocoids originally classified as part of Esocidae (Wilson *et al.* 1992), but family now considered uncertain (Brinkman *et al.* 2014)

Trophic links

- taxonomic uncertainty combined with apparently small body size means diet likely more similar to extant pickerel than to large extant pikes so only smallest fish and frogs form vertebrate diet (Raney 1942; Scott & Crossman 1973)

Acanthomorphs

Fossil record

- Acanthomorphs represented by at least 4 distinct taxa distinguished by dentary tooth plate anatomy, similar to extant beryciforms (Neuman & Brinkman 2005); several more morphotaxa exist based on isolated centrum anatomy but are not retained here since several morphotypes might belong to the same taxon (Brinkman 2019)

Trophic links

- Plates formed of very small short teeth typical of extant perciforms, so generalist diet attributed to all 4 acanthomorphs including molluscs, insect nymphs and the network's smallest fishes (Scott & Crossman 1973)

AMPHIBIANS

Most fossils found in screen-washed samples from vertebrate microfossil localities; marked decrease in abundance up-section for Anura in particular coinciding with increasing shoreline proximity (and thus likely salinity) (Brinkman 1990; Cullen & Evans 2016)

Caudata - Salamanders

Fossil record: 5 nodes in DPP network distinguished by jaw and centrum anatomy: albanerpetontid *Albanerpeton* spp., scapherpetontids *Scapherpeton tectum* and *Lisserpeton bairdi*, batrachosauroidid *Opisthotriton kayi*, and sirenid *Habrosaurus prodilatus* (Gardner 2005)

- all nodes known from DPP except for sirenid *Habrosaurus* sp. and scapherpetontid *Lisserpeton bairdi*, which are only known from DPF of Irvine (Gardner 2005)

Trophic links

- o Sirenids, batrachosauroidids and scapherpetontids all considered fully aquatic based on elongated bodies and reduced limbs (Wilson *et al.* 2014*a*)
    - o *Opisthotriton* had pedicellate teeth as shown from more complete Paleocene relatives (Estes 1975), so probably consumed softer prey than other salamanders; therefore it differs from other aquatic salamanders in missing molluscs and crustaceans from its diet
    - o *Habrosaurus* had stout bulbous non-pedicellate teeth more suitable for eating hard-bodied arthropods and molluscs (Gardner 2003); diet can realistically be inferred from modern greater siren *Siren lacertina*, which includes more aquatic plants than other salamanders (Hanlin 1978)
    - o Scapherpetontids also had non-pedicellate teeth and could still reach relatively large body size (Estes 1976) so their diet is also inferred from greater siren, although less durophagous
- o Albanerpetontids considered the only terrestrial amphibian family from DPP based on robust skull, powerful limbs and girdles (Wilson *et al.* 2014*a*), the DPP taxon that likely had the most similar lifestyle to extant salamandrids; therefore they eat terrestrial as well as aquatic insects and their much smaller body size constrains them to *Tyrrellbatrachus brinkmani* among its frog prey

Anurans - Frogs

Fossil record: 3 nodes in DPP network distinguished by maxilla anatomy: *Hensonbatrachus kermiti*, *Tyrrellbatrachus brinkmani* and an unnamed species (Anura indet 1) (Gardner *et al.* 2016)

Trophic links

- currently include frog larvae, otherwise links connecting to aquatic predatory insect nymphs and larvae would be deleted and it would lack consistency with Messel food web
- DPP frog diet based on extant frogs (Stewart & Sandison 1972), mostly insectivorous but also includes aquatic plants and small fishes
- o Edentulisum in *Tyrrellbatrachus brinkmani* likely indicated it was a small invertebrate (insect) specialist compared with other DPP frogs (Gardner 2015; Paluh *et al.* 2021)
- o Currently impossible to tell whether smaller DPP frogs were fully terrestrial with a scansorial niche (like extant poison dart frogs for example), so they all get a semiaquatic habit for now

TESTUDINES

Adocus sp.

Fossil record: rare turtle in DPP (only represented by isolated shell fragments), but more skulls and skeletons found in time-equivalent Oldman Formation in Manyberries area and more recent Hell Creek Formation (Brinkman 2005)

Trophic links:

- Hydrodynamic shell indicates it was likely aquatic
- Skull with complex triturating surface similar to extant herbivorous turtles (Meylan & Gaffney 1989; Brinkman 2005), so diet composed of aquatic plants as well as terrestrial angiosperm shoots and fruits

Baenidae

Fossil record: 3 nodes in DPP network: *Plesiobaena antiqua*, *Boremys pulchra*, *Neurankylus eximius*

- *Plesiobaena* particularly abundant in skeleton assemblage, *Boremys* also fairly well represented, *Neurankylus* much rarer in DPP but more common elsewhere in Alberta (Brinkman 2005)

Trophic links:

- All have hydrodynamic shell indicative of aquatic lifestyle, *Neurankylus* shell and size particularly similar to extant river turtle *Dermatemys* (Brinkman 2005); *Boremys* shell less streamlined than *Plesiobaena* shell but still within range of extant freshwater turtles
- Both *Plesiobaena* and *Boremys* have robust lower jaws with broad and flat triturating surfaces, suggesting they were durophagous (Brinkman & Nicholls 1991; Brinkman 2003, 2005); therefore their main prey were likely crustaceans and molluscs but links are also connecting them to aquatic insects, carrion (dead fish) and some plant material as observed in possibly the closest extant analogue, the common map turtle *Graptemys geographica* (Donato 2000); therefore *Plesiobaena* and *Boremys* interpreted as durophagous omnivores
- *Neurankylus* skull noted to have deep lower jaw with narrow triturating surface with sharp ridges, likely indicating cutting rather than crushing function, though herbivory or omnivory could not be determined (Brinkman & Nicholls 1993; Brinkman 2005); therefore we elect to give it a generalist omnivorous diet without molluscs or crustaceans
    - Plant food perhaps comparable to extant *Dermatemys*, with significant component of terrestrial vegetation compared to other freshwater turtles (Bishop *et al.* 2022); *Artocarpus* proposed as one of the few woody dicots it fed on because it's part of Moraceae (same family as *Dermatemys* preferred leaves)

Trionychidae – soft-shelled turtles

Fossil record: 5 nodes in DPP network, though these species clearly were not equally abundant in community (Gardner *et al.* 1995; Brinkman 2005):

- *Axestemys foveatus* (by far the most common by numbers of shells and skeletons)
- *Axestemys splendida* (by far the largest, respectable number of skeletons, a few skulls)
- *Axestemys allani* (very rare skeletons)
- *"Apalone" latus* (very rare shells)

- Trionychidae gen. sp. indet (very rare large shells)

Trophic links

- Trionychids are among the more generalist and opportunistic DPP aquatic predators: studies of stomach contents reveal (possibly accidental) ingestion of plant material and seeds (Meylan 2006); maybe attribute links to all angiosperm fruits/seeds but restrict links to angiosperm leaves/shoots to aquatic plants
    - Trionychids usually hunt underwater but occasionally on land if concealed by vegetation
    - Large fish often seem to be eaten as carrion, at least for species of the size of *Apalone spinifera* and *A. mutica* (Williams & Christiansen 1981), which are of similar size to *Axestemys foveatus* and *A. allani*
- smaller species like *Apalone mutica* seem to consume more fruit and nuts in their diet than larger (more carnivorous) species like *Apalone ferox* (Williams & Christiansen 1981; Meylan 2006; Albers 2012) but that difference is not reflected in trophic link distribution; frogs and medium to large fish often reported in soft-shelled turtle stomach contents, but never salamanders
- *Axestemys splendida* specimens have similar size to *Palaeomyda messeliana* '*Trionyx messelianus'* from Messel so it seems reasonable to infer links to trophic analogues from Messel food web (Gardner *et al.* 1995; Labandeira & Dunne 2014; Cadena 2016); this means *A. splendida* exceptionally consumes larger fishes like gar, bowfin and *Coriops*, as well as the only possibly aquatic bird known from DPP (Ornithurine A); supported by broader, more robust skull at jaw joint than other trionychids (Gardner *et al.* 1995)
- Little evidence of niche partitioning between *Axestemys foveatus, A. allani* and *"Apalone" latus* based on total size, although rare skeletons of *A. allani* suggest it had narrower, more elongated head and longer neck; that said, its differences in prey preference may not be reflected in a trophic network that lacks quantification of link strength

Chelydridae – snapping turtles

Fossil record: limited to shell fragments (Brinkman 2005)

Trophic links: since all chelydrid shell remains from the Park are most similar to common snapping turtle *Chelydra serpentina* (Brinkman 2005), the diet of that ancient relative was likely more similar to that extant species than to the alligator snapping turtle *Macrochelys temminckii*

- *C. serpentina* stomach contents show that plant material seems limited to aquatic angiosperms (Punzo 1975) while alligator snapping turtles have fruits and nuts as well (DiLaura *et al.* 1999); retain links to mammals as in alligator turtle

Macrobaenidae – *Judithemys sukhanovi*

Fossil record: an articulated skeleton and five complete shells (Parham & Hutchison 2003)

Trophic links: another aquatic turtle due to shell similar to extant marine turtles and reduced plastron

- diet omnivorous to herbivorous due to upturned beak similar to snapping turtles (Parham & Hutchison 2003); similar links to DPP chelydrid but with more angiosperm resources

Basilemys variolosa
Fossil record: shells and limb elements known from DPP but best skull only known from Horseshoe Canyon Formation (Brinkman 1998, 2005)
Trophic links

- The only fully terrestrial turtle known from DPP: short digits on both hands and feet indicate terrestrial lifestyle (Holroyd & Hutchison 2002)
- Heavily roofed skull, jaws with triturating surface of ridges and pits (Brinkman 2005), so diet very likely analogous to large extant tortoises (e.g. Galapagos and Aldabra tortoises (Grubb 1971; Blake *et al.* 2021)): angiosperm-based diet largely consisted of, sedges, herbaceous dicots and fruits

Kimurachelys slobodae
Fossil record: all fossils collected in LCZ, only one maxilla found in DPP, more complete mandibles collected in Onefour and Manyberries (Brinkman *et al.* 2015); therefore restricted to LCZ network
Trophic links: mandible most similar to olive Ridley sea turtle *Lepidochelys olivacea* (Brinkman *et al.* 2015), so likely carnivorous species feeding on snails, crustaceans

SQUAMATA

Fossil record: mainly isolated dentaries and skull elements, no articulated specimens (Gao & Fox 1996); one of the major tetrapod clades for which it is necessary to include specimens found in Belly River Group outside DPP, e.g. Irvine locality (Caldwell 2005):

- Lizards found in Oldman (including Irvine) and DPF: teiids *Socognathus unicuspis* and *Glyptogenys ornata*, varanoids *Palaeosaniwa canadensis* and *Parasaniwa* n. sp.
- DPP Oldman Fm only: teiid *Sphenosiagon simplex*
- Irvine Oldman Fm only: anguid *Odaxosaurus priscus*, scincid *Orthrioscincus mixtus*, teiids *Leptochamops thrinax*, and *Gerontoseps irvinensis*
- DPF only: xenosaurid *?Exostinus sp.,* helodermatid *Labrodioctes* cf. *montanensis*

Elect to include all terrestrial squamates in each DPP time zone because of abundant lizard jaw fragments at vertebrate microfossil localities throughout Oldman and DPF, little solid evidence of faunal turnover

- Lizard body masses estimated from tooth midshaft diameter due to incomplete tooth rows in several dentaries (Longrich *et al.* 2012)

Anguidae and Scincidae
Fossil record: Anguidae represented by *Odaxosaurus priscus*; Scincidae represented by *Orthrioscincus mixtus* (Gao & Fox 1996)

- most complete jaw elements for both families come from Irvine; a few more anguid fragments reported from more recently screen washed DPP bulk samples

Trophic links: likely insectivorous like extant relatives such as anguid glass lizard *Ophisaurus* (Graham 2023) and skinks (Manicom & Schwarzkopf 2011)

Teiidae

Fossil record: most diverse and abundant lizard family in Belly River Group fossil assemblage (Gao & Fox 1996; Caldwell 2005)

- The most likely family to have some species turnover between Oldman and DPF due to its higher overall diversity but strong evidence still lacking due to lack of species-level identifications for most bulk-sampled vertebrate microfossil localities

Trophic links

- Teiids with generalist dentitions all seem closely related to extant species that include fruits in their diet, especially late in their ontogeny (Vitt & de Carvalho 1992; Silva *et al.* 2020)
- *Socognathus unicuspis* was probably ecological analog of extant large omnivorous teiid *Tupinambis* (Gao & Fox 1996; Silva *et al.* 2020); the largest of all DPP teiids, so could likely eat all other teiids, scincid, anguid and xenosaurid, as well as smallest birds and mammals
- *Glyptogenys ornata* noted to have deep robust jaw with thick blunt teeth indicative of durophagy (likely beetle specialization) (Gao & Fox 1996)
- *Gerontoseps irvinensis* much smaller than other teiids; teeth get thicker and blunter posteriorly but remain unicuspid, suggesting crushing function so maybe dietary preferences for hard-shelled insects (Gao & Fox 1996)
- *Leptochamops thrinax* has straighter, more cylindrical and tricuspid teeth, so very different dentition from other teiids; looks most similar to extant *Kentropyx* (Vitt & de Carvalho 1992; Gao & Fox 1996); the latter is known to eat smaller lizards, so *Leptochamops* gets links to scincid and smaller teiids
- No attempt to infer diet of *Sphenosiagon simplex* but it has very similar dentition to *Leptochamops* while apparently reaching smaller body size, so it has similar diet without larger vertebrate prey

Xenosauridae - ?*Exostinus* sp.

Fossil record: very rare fragments from DPP vertebrate microfossi localities

Trophic links: largely insectivorous like extant relative *Xenosaurus* (Ballinger *et al.* 1995), although small teiids also reported in the latter's diet; therefore ?*Exostinus* sp. likely consumed smallest DPP teiids on occasion based on estimated body masses between predator and prey

Varanoidea

Fossil record: 3 nodes in DPP network, all represented by skull and dentary elements

- Helodermatid *Labrodioctes* cf. *montanensis* (very rare identified elements)
- *Parasaniwa* n. sp. (rather small-bodied)
- *Palaeosaniwa canadensis* (also known from several vertebrae)

Trophic links:

- *Labrodioctes* was second largest terrestrial lizard in DPP, likely close relative (with similar estimated body size) to extant gila monster *Heloderma suspectum*, so likely similar generalist diet ranging from insects to lizards, salamanders, small birds and mammals (Beck 2005)

- *Parasaniwa* was still a small lizard according to body mass estimates, so diet likely similar to small-bodied extant varanids (or juveniles of larger species), so strong insect component as well as smaller lizards, mammals and birds (Cross *et al.* 2020; Mazzotti *et al.* 2020); decaying fruits also reported among mainly carnivorous *Varanus bengalensis* (Karunarathna *et al.* 2017), so detritus included
- *Palaeosaniwa* by far the largest terrestrial lizard in DPP, closest extinct analogue to medium-sized monitor lizards though nowhere near maximum size of Komodo dragon *Varanus komodoensis* (Longrich *et al.* 2012; Purwandana *et al.* 2016)
    - Essentially same diet as *Parasaniwa*, with addition of larger birds, mammals, reptiles, as well as small turtles and fishes <50 cm long based on stomach contents of *V. bengalensis* and *V. niloticus* (Karunarathna *et al.* 2017; Mazzotti *et al.* 2020); aquatic salamanders or tritons never reported in extant diets so not included among links

Mosasauria – *Plioplatecarpus* sp.
Fossil record: only a few teeth in LCZ vertebrate microfossil localities (Brinkman *et al.* 2005*b*; Caldwell 2005), so restricted to LCZ network; may indicate that plioplatecarpines tolerated brackish water, possibly freshwater
Trophic links: relatively small mosasaur species with more vermiform body plan, but still large enough to consume every LCZ fish, ammonite and aquatic tetrapod, except plesiosaurs, *Kimurachelys* and largest sharks (Schulp *et al.* 2013)

PLESIOSAURIA & CHORISTODERA

Elasmosauridae – *Fluvionectes sloanae*
Fossil record: occasional skeletons and isolated elements found throughout most of DPF but not Oldman Fm, may indicate tolerance to freshwater (Sato *et al.* 2005)

- Lowest definite occurrence is isolated vertebra 13.5 m above OF-DPF contact but possible plesiosaur vertebra also known from BB076 just above contact (Sato *et al.* 2005), so plesiosaurs excluded from Oldman network but included in lowermost DPF networks
- Average size of DPP individuals inferior to that observed in marine sediments of Bearpaw Sea, indicating either juveniles venturing into estuaries or distinct species (Sato *et al.* 2005); DPP may have been too far inland at time of Oldman Fm, so elasmosaurids excluded from Oldman Fm network
- more complete DPP specimens all referred to *Fluvionectes sloanae* holotype from Onefour described from associated postcranial skeleton (Campbell *et al.* 2021), estimated to reach almost 7m length, a more comparable size to fully marine elasmosaurid relatives

Trophic links: body plan likely similar to better-known elasmosaurids, therefore highly piscivorous diet but likely limited to small to medium-sized fishes due to relatively small skull size, as shown from stomach contents of a marine relative (Cicimurri & Everhart 2001); include larger molluscs following elasmosaurid diets proposed for Paja biota network (Cortés & Larsson 2023)

Polycotylidae – *Trinacromerum* sp.

Fossil record: much less abundant than elasmosaurs in DPP, only a few teeth tentatively assigned to Polycotylidae from LCZ microsites (Beavan & Russell 1999; Sato *et al.* 2005); eventually decide whether to include in LCZ network at all

***Cteniogenys* sp.**

Fossil record: fragmentary dentaries and maxillae from vertebrate microfossil localities in Oldman and DPF (Gao & Brinkman 2005)

Trophic links: most realistic anatomical reconstructions obtained from distant relatives from Mid-Jurassic *Cteniogenys antiquus* (Evans 1990) and complete skeletons of *Hyphalosaurus* from Yixian Fm (Early Cretaceous China) (Gao & Ksepka 2008); anatomy of the latter in particular suggests DPP *Cteniogenys* was semiaquatic carnivore, largely piscivorous diet complemented by insects

- *Hyphalosaurus* rarely exceeded 1 m total length with skull usually <10 cm; assuming DPP *Cteniogenys* had similar anatomy, it likely had a smaller fish prey size range than champsosaurs

Champsosauridae

Fossil record: a few skulls and skeletons reported from DPP (Gao & Fox 1998), tooth and centrum record from vertebrate microfossil localities better reflects broad stratigraphic distribution (Brinkman 1990)

- Two species now recognized in DPP: *Champsosaurus natator* and more gracile *C. lindoei* (Russell 1956; Gao & Fox 1998)

Trophic links: closest trophic analogue is probably gharial *Gavialis gangeticus*, champsosaurs may have hunted similarly by spending more time underwater than more generalist crocodilians (Matsumoto *et al.* 2022), so were likely piscivores

- reduced limbs and more hydrodynamic ribcage compared to crocodilians may suggest a more aquatic lifestyle than them, may explain coexistence through niche partitioning
- analysis of neural anatomy of *C. lindoei* confirms champsosaurs were well adapted for sensing movement underwater (Dudgeon *et al.* 2020)
- *C. natator* has larger and more robust skull than *C. lindoei*, so it could catch larger prey, e.g. gar, *Paralbula*, *Habrosaurus*
- insects and crustaceans cited among juvenile gharial diet (Bouchard 2009), so these are included among champsosaur prey; soft-shelled turtles and birds also cited among adult gharial diets (Whitaker & Basu 1982), so DPP species interpreted to dive or swim near river bottom are included among *C. natator* prey, but not *C. lindoei*

CROCODILIA & PTEROSAURIA

Crocodilians

Fossil record: 3 nodes in DPP network

- *Leidyosuchus canadensis*, by far the best skeletal record, known from several skulls and mandibles (Wu *et al.* 2001)

- At least two globidontan alligatoroids: *Albertochampsa langstoni*, known from single skull (Erickson 1972), and isolated dentaries assigned to cf. *Stangerochampsa* based on similarities to the latter better known from Horseshoe Canyon Formation (Wu *et al.* 1996; Wu 2005)

Trophic links

- All 3 DPP crocodilians have clear extant trophic analogues in alligators and caimans, so their trophic links are largely derived from these taxa (Magnusson *et al.* 1987; Saalfeld *et al.* 2011), with some variability
- Inferred Eocene croc diets based on trophic links for Messel food web and predictions from morphology (skull shape and body size) also accounted for (Labandeira & Dunne 2014; Hastings & Hellmund 2017)
- Links to insect prey retained because they are still found in adult stomach contents, albeit in much smaller proportions than in juveniles (Saalfeld *et al.* 2011)
- *Leidyosuchus* is by far the largest of the three, with the most generalist dentition, so most similar to *Alligator mississippiensis* and *Asiatosuchus* in ability to hunt medium-sized mammals (Shoop & Ruckdeschel 1990; Hastings & Hellmund 2017); therefore it gets links to smallest ornithischians and theropods as well as juvenile megaherbivores and tyrannosaurs (assuming hatchling size); at the same time it remains connected to bivalves, crustaceans
- Globidontans have rounder teeth (as their name suggests), which is indicative of durophagous diet, however, their general skull morphology is closer to that of generalist alligatoroids, therefore their trophic links are based on relatively long-snouted taxa such as *Diplocynodon*, and extant caimans (e.g. *Caiman crocodilus*, *Paleosuchus trigonatus*) than to more specialized taxa such as *Allognathosuchus* (Magnusson *et al.* 1987; Hastings & Hellmund 2017)
    - o If problematic globidontan dentaries belong to cf *Stangerochampsa*, that species has a slightly shorter and more robust skull than *Albertochampsa*, therefore its closest extant analogue may be Cuvier's dwarf caiman *Paleosuchus palpebrosus*, although differences in prey proportions cannot be reflected in current network
    - o *Albertochampsa* estimated to be twice weight of cf *Stangerochampsa*, therefore the former could realistically have preyed on the latter, as well as on smaller champsosaur (*C. lindoei*)

Cryodrakon boreas

Fossil record: one associated skeleton and a few isolated remains such as elongated cervicals, metacarpals, femur, humeri in DPP, all well preserved large pterosaur remains assigned to this new species distinct from *Quetzalcoatlus* (Currie & Godfrey 2005; Hone *et al.* 2019)

- Insufficient fossil evidence of another azhdarchid taxon in DPP for now (Hone *et al.* 2019), so no node for smaller pterosaur species

Trophic links: *Cryodrakon* was among the larger azhdarchids to exist, similar size to *Quetzalcoatlus* (Witton 2008; Hone *et al.* 2019); cranial material unknown from DPP but likely had a ~1 m long skull as seen in close relatives; decent locomotory ability on land compared with other pterosaurs due to wrist joints (Witton & Naish 2008)

- Probably terrestrial stalker, often compared to storks and ground hornbills foraging on small prey with long beaks as extant analogues (Witton & Naish 2008); large head means they likely did not feed on very small lizards or mammals
- Links distributed to lizards >0.3 kg (*Socognathus* teiid estimated body mass); non-bird dinosaurs up to 20 kg (*Stegoceras* estimated body mass) except for *Dromaeosaurus* and *Saurornitholestes* because of defensive abilities; juvenile megaherbivores and tyrannosaurs (assuming hatchling size); birds >1.5 kg (estimated *Palintropus* sp. B body mass) and mammals >0.4 kg (*Cimolomys* estimated body mass)
- Smaller semiaquatic reptiles lacking shells (*Champsosaurus lindoei*, *Cteniogenys*) also proposed as prey
- Large size and flying locomotion means that *Cryodrakon* probably lacked any natural enemies, therefore it could technically be considered an apex predator in DPP alongside tyrannosaurids; if there were smaller pterosaur species in DPP network, they could have been likely prey for dromaeosaurids and juvenile tyrannosaurids at least
- *Cryodrakon* likely an important scavenger in DPP ecosystem: long neck and beak made it ideally suited to pick at carcasses

ORNITHISCHIA

Rules on herbivorous dinosaur diets

Woody dicots should only be attributed to taxa that are known to have suitable masticatory anatomy to process tough angiosperm leaves (e.g. hadrosaurs, ceratopsids, nodosaurs), while those that don't should be restricted to shoots, herbaceous plants and fruits/seeds (e.g. ornithomimids, ankylosaurids, *Caenagnathus*, troodontids)

- Note: that distinction is lost in low-resolution version of food web where all angiosperm leaves are included in same node
- Angiosperm leaves should therefore be linked to low-browsing herbivores that can feasibly digest them especially when accounting for saplings, plus it seemed that most DPP angiosperms were shrubs at their tallest
- Distinction between leaves and shoots therefore concerns nutritional content more than feeding height
- DPP megaherbivore assemblage proposed to be a classic dinosaurian example of chronofauna, with distinct ecological niches for each family defined by interspecific competition (Ryan & Evans 2005; Mallon *et al.* 2012; Mallon 2019)

Ankylosauridae

Fossil record: rare skeleton occurrences compared to other large DPP dinosaurs (Béland & Russell 1978; Dodson 1983; Currie & Russell 2005)

- 4 nodes in DPP network based on 4 species according to latest taxonomic revisions based on scute arrangement and tail club shape (Arbour & Currie 2013; Penkalski & Blows 2013): *Euoplocephalus tutus*, *Dyoplosaurus acutosquameus*, *Scolosaurus cutleri*, *Anodontosaurus lambei*

- unclear whether ankylosaurids underwent faunal turnover through Belly River Group: *Euoplocephalus* found throughout DPF but other stratigraphic ranges likely underestimated due to lack of diagnostic material (Arbour & Currie 2013); *Scolosaurus* quarry location unclear between 2 candidate sites, could be from Oldman Formation (Arbour & Currie 2013)

Trophic links:

- Likely fern consumers due to feeding height <1 m, wide rostrum suggestive of high plant intake (Mallon *et al.* 2013; Mallon 2019), even direct evidence from Early Cretaceous Australian ankylosaurid relative with cololite containing angiosperm fruits and seeds (Molnar & Clifford 2001)
- Low coronoid process on ankylosaurid mandibles suggests their bite force was insufficient to process woody dicot browse (Mallon 2019)
- Ankylosaurid teeth more cusped than nodosaurid teeth, suggesting greater ability to pierce fruit tissue, although tooth microwear evidence does not support diet partitioning between these families (Mallon & Anderson 2014)
- These lines of evidence together suggest ankylosaurids have links distributed to ferns, cycad shoots and seeds, Caytoniaceae shoots and seeds, and angiosperm shoots and fruits/seeds, but not to woody leaves (including cycads and Caytoniaceae)

Nodosauridae

Fossil record: rare skulls and skeletons, similar situation to ankylosaurids (Currie & Russell 2005); some evidence of faunal turnover between 2 species that each get a node in DPP network (Mallon *et al.* 2012): *Edmontonia rugosidens* (MAZ1, more abundant skeletal remains) and *Panoplosaurus mirus* (MAZ-1b)

Trophic links

- Most detailed evidence of nodosaur diet comes from Early Cretaceous Alberta relative *Borealopelta markmitchelli* cololite, reveals diet dominated (at time of death) by ferns, with a few cycad leaf remains, lycopod possibly referred to *Selaginella* (Brown *et al.* 2020*c*)
- Low feeding height, narrower rostrum for nodosaurids than ankylosaurids suggests more selective browsing for the former (Mallon 2019)
- Higher coronoid process for nodosaurs than for ankylosaurs suggests the former could generate higher bite force necessary to break woody dicot matter therefore higher mechanical advantage (Mallon & Anderson 2013; Mallon 2019); teeth also more blade-shaped suggesting enhanced shearing ability for slicing leaves (Mallon & Anderson 2014)
- These lines of evidence together suggest nodosaurids have links distributed to ferns, all cycad and Caytoniaceae leaves, shoots and seeds, and angiosperm leaves, shoots and fruits/seeds

Thescelosauridae – Orodrominae

Fossil record: very rare dinosaurs in DPP, only represented by isolated dentary, centra, femur, definitely underrepresented due to taphonomic bias against small-bodied tetrapods (Brown *et al.*

2013*b*, *a*), posterior postcranial skeleton collected in Oldman Fm in nearby Pinhorn Reserve along Milk River (Brown *et al.* 2013*a*)

- Marked decrease in abundance noted from lower to upper DPF suggests preference for inland habitat (Brinkman 1990)

Trophic links: among the smallest DPP ornithischians, bipedal runners, likely prey for fast-running theropods especially dromaeosaurids

- Morphology: low skull and dentaries with narrow rostrum and beak indicative of selective forager targeting high-quality plant material, likely fruits and shoots (Wyenberg-Henzler *et al.* 2021; Hudgins *et al.* 2022), so angiosperm shoot and fruit/seed nodes assigned (except Fagaceae nuts which would have been too hard to crack)
- Tooth wear facets oblique, formed through orthal to orthopalinal chewing (Hudgins *et al.* 2022)
- Direct evidence from gut contents of neornithischian with similar skull morphology to *Thescelosaurus* shows it ate cycad seeds; DPP orodromine skull only known from anterior dentary fragment but still reasonable to propose it ate cycad and caytoniaceae seeds

Hadrosauridae

Fossil record: by far the clade with the highest skeleton abundance in DPP throughout Belly River Group sedimentary succession (Béland & Russell 1978; Dodson 1983; Currie & Russell 2005), though juveniles heavily underrepresented due to taphonomic size bias

- Strong evidence of faunal turnover among both lambeosaurines and saurolophines throughout Belly River Group (Ryan & Evans 2005; Mallon *et al.* 2012; Mallon 2019)
    - Oldman Formation: *Brachylophosaurus canadensis* (lambeosaurine), cf. *Hypacrosaurus stebingeri* (saurolophine)
    - DPF MAZ1: lambeosaurines *Corythosaurus casuarius*, *C. intermedius* (MAZ-1b), *Parasaurolophus walkeri, Lambeosaurus lambei*, *L. clavinitialis* (MAZ-1b); saurolophine *Gryposaurus notabilis*
    - DPF MAZ2: lambeosaurine *L. lambei*, saurolophine *Prosaurolophus maximus*
    - DPF LCZ : *L. lambei*, *L. magnicristatus*, *P. maximus*
    - Taxonomy note : *L. clavinitialis* considered junior synonym of *L. lambei* (Horner *et al.* 2004) so it does not get its own node in the network, however *Corythosaurus intermedius* is sufficiently different from *C. casuarius* in anatomy and stratigraphic distribution to warrant its own node (Mallon 2019)
- Juvenile hadrosaur abundance estimated with survivorship curve (Wyenberg-Henzler *et al.* 2021)

Trophic links

- Tooth battery made hadrosaurs the only DPP dinosaurs capable of mastication, therefore granting access to tougher foods than most other herbivores; that, along with highest feeding height by far, especially in bipedal posture, made them the dominant tree leaf browsers (including conifer leaves) (Mallon *et al.* 2013; Mallon & Anderson 2014; Mallon 2019)

- Direct evidence from rarely preserved stomach contents: conifer leaves, seeds, fruits, leaf fragments (Currie *et al.* 1995; Tweet *et al.* 2008)
- Crustacean cuticle found in coprolites attributed to hadrosaur *Maiasaura* from Two Medicine Formation, similar age to DPF (Chin *et al.* 2017), could have been accidentally ingested while foraging for aquatic plants
- Other coprolites from Two Medicine Formation attributed to hadrosaurs suggest intentional ingestion of wood decayed by fungi (Chin 2007); more evidence for intentional decaying wood ingestion than accidental ingestion of branches and twigs because of lack of leaf remains in coprolite
- Juveniles had much lower feeding height and less developed jaw muscles, so were likely restricted to softer plants, strong evidence for ontogenetic niche shifts (or at least expansion) in hadrosaurs (Wyenberg-Henzler *et al.* 2021, 2022)
    - Small herbivore niche occupancy by juvenile hadrosaurs may explain relatively low diversity of small-bodied ornithischians across dinosaur faunas, hypothesis competing with taphonomic size bias (Codron *et al.* 2012, Brown *et al.* 2013*b*; Schroeder *et al.* 2021)
- This evidence together suggests that hadrosaurs were probably the most generalist herbivores of DPP community, likely closest analogues to extant elephants, perhaps even filled similar role as ecosystem engineers, e.g. bipedal hadrosaur felling small tree to access leaves; juveniles for each species worthy of distinct node to track ontogenetic niche expansion with diet restricted to most nutritious plant matter (i.e. shoots and fruits of angiosperms, cycads and Caytoniaceae); adults also connected to crayfish (Decapoda), decaying wood and fungi nodes because of aforementioned coprolite evidence
- Mixed evidence for dietary niche partitioning between coeval lambeosaurine and saurolophine species (Mallon & Anderson 2013): mean skull length ratio respects Hutchinsonian ratio necessary for species in very close phylogenetic proximity to coexist and saurolophines have more steeply inclined tooth facets than lambeosaurines implying higher shearing capacity, however there's no significant difference in beak shape; therefore we decide there's not enough evidence to have different series of trophic links for species of those two subfamilies

Pachycephalosauridae

Fossil record: 3 species currently recognized in DPP following taxonomic revisions: *Stegoceras validum*, *Foraminacephale brevis* and (more recently) *Sphaerotholus lyonsi* (Schott & Evans 2017; Dyer *et al.* 2022; Woodruff *et al.* 2023)

- Most fossils consist of frontoparietal skull domes mostly ex situ (Evans *et al.* 2013), very rare skull and postcranial skeleton for *S. validum* holotype (Gilmore 1924*b*)
- No evidence of species turnover among pachycephalosaurids, so *S. lyonsi* is assumed to have existed throughout DPF despite currently being known from a single squamosal

Trophic links: both species small-bodied and bipedal, likely prey for several theropods especially dromaeosaurs and juvenile tyrannosaurs

- Morphology: wider rostrum than thescelosaurids indicative of more generalist feeding strategy targeting high- and low-quality foods (Hudgins *et al.* 2022); jaw better adapted to process tougher tissue, proposed to eat leaves, shoots, seeds, fruits, perhaps even insects (Maryańska *et al.* 2004; Wyenberg-Henzler *et al.* 2021)
- These characteristics mean that links are distributed to very diverse food assemblage including ferns and hard-shelled arthropods

Ceratopsia

Fossil record: abundant skeletons and ceratopsid-dominated bonebeds in DPP, catastrophic assemblages indicative of herding behaviour (Currie & Dodson 1984; Currie & Russell 2005; Eberth & Getty 2005)

- Strong evidence of faunal turnover for both centrosaurines and chasmosaurines throughout Belly River Group
    - Oldman Formation: centrosaurine *Coronosaurus brinkmani*, indeterminate chasmosaurine
    - DPF MAZ-1: centrosaurine *Centrosaurus apertus*, chasmosaurines *Chasmosaurus russelli* and *Mercuriceratops gemini* (MAZ-1a), and *C. belli* (MAZ-1b)
    - DPF MAZ-2 : centrosaurine *Styracosaurus albertensis*, chasmosaurines *C. belli* and possibly *C. irvinensis* basal lineage (Campbell *et al.* 2019)
    - DPF LCZ : centrosaurine cf. *Achelousaurus horneri*, *Chasmosaurus irvinensis*
    - Enigmatic centrosaurine *Spinops sternbergorum* either from OF or lowermost DPF, only known quarry lost
    - Some species far more elusive than others, e.g. *Mercuriceratops* and *Spinops*
- Lack of stratigraphic overlap between *Centrosaurus* and *Styracosaurus* means that anagenesis cannot be rejected as mode of speciation in Centrosaurinae, however cladogenesis seems more supported among Chasmosaurinae due to taxonomic referral of *Chasmosaurus* sp. skulls in mid-DPF to lineage leading to *Chasmosaurus irvinensis* (thus overlap with *C. russelli* - *C. belli* lineage in DPF MAZ-2) (Campbell *et al.* 2019)
- Only two leptoceratopsid jaw elements found in DPP, assigned to *Unescoceratops koppelhusae* (Ryan *et al.* 2012)
- Juvenile ceratopsid abundance estimated with survivorship curve (Wyenberg-Henzler *et al.* 2021)

Trophic links

- Morphology: massive skull could generate extremely high bite forces, beak and tooth rows perfect for slicing fibrous or woody vegetation (Mallon & Anderson 2013, 2014, 2015; Mallon 2019); therefore any woody angiosperm material clearly part of ceratopsid diet, though we add cycad leaves due to cycad presence confirmed in pollen record, as well as ferns, cycad cones; slightly greater feeding height than ankylosaurs has little ecological significance, they probably had access to same vegetation strata (Mallon *et al.* 2013)
    - It could be argued that cycads should not be included in ceratopsian diet since this herbivorous dinosaur clade (particularly Ceratopsidae) seems to radiate

        coincidently with angiosperms, therefore probably the most specialized one on angiosperms, at expense of other woody plant foods
    - Decaying wood could easily have been additional plant source for ceratopsids due to their high bite force, and the fact that Two Medicine Formation coprolites could be attributed to ceratopsids despite higher likelihood they belonged to hadrosaurs (Chin 2007)
    - Only taxa bearing largest fruits (*Artocarpus* and Sapindaceae) added to ceratopsid links (adult and juvenile) among angiosperm seed and fruit nodes
    - Differences in cranial depth between coeval centrosaurines and chasmosaurines constitute limited evidence for dietary niche partitioning (Mallon & Anderson 2013); centrosaurines appear to have taller skulls than chasmosaurines (indicative of higher stress resistance) but this morphological disparity is likely insufficient to attribute different combination of trophic links (similar situation to hadrosaurs)
    - Only one juvenile ceratopsid skeleton from DPP is well preserved, a specimen of *Chasmosaurus* (Currie *et al.* 2016); skull already well developed to shear resistant plant material, although narrower beak indicative of selective feeding combined with very low feeding height suggests more exclusive ontogenetic niche from adults (Wyenberg-Henzler *et al.* 2021)
        - Therefore, juvenile ceratopsids get distinct nodes in DPP network to reflect ontogenetic niche expansion; they ate angiosperm shoots but not leaves, as well as decaying wood with fungi, essentially high-energy plant tissues following similar logic to hadrosaurs
        - Leptoceratopsids had similar size and skull morphology to juvenile ceratopsids (Wyenberg-Henzler *et al.* 2021), therefore interpreted to have same trophic links

THEROPODA

Tyrannosauridae

Fossil record: best-documented theropods in DPP by far in terms of skulls and skeletons (Russell 1970, Currie 2003*a*; Currie & Russell 2005)

- Relatively complete ontogenetic series for the most common species *Gorgosaurus libratus* (Therrien *et al.* 2021; Voris *et al.* 2022) means we have strong evidence of ontogenetic niche shifts in tyrannosaurids
    - Juvenile body mass and density estimated from survivorship curves for each species (Erickson *et al.* 2004; Schroeder *et al.* 2021); confirms that juveniles are still vastly underrepresented in tyrannosaur fossil record (similar pattern to other dinosaur megafauna)
- Therefore 9 nodes in DPP network: albertosaurine *Gorgosaurus libratus*, and tyrannosaurines *Daspletosaurus torosus* and *Daspletosaurus* sp., each of which gets 3 nodes for each ontogenetic dietary category: subadult/adult, juvenile, young juvenile
- Stratigraphic distribution: *Gorgosaurus* found throughout Belly River Group but apparent faunal turnover between *Daspletosaurus torosus* (Oldman Fm only) and *Daspletosaurus* sp. (DPF only) (Currie & Russell 2005), therefore usually 2 species coexisting

    - *D. torosus* only known from holotype in DPP, but other fairly complete skeleton collected in Manyberries (Currie 2003*a*)

Trophic links: undoubtedly the main apex predators of the DPP community, the only predators capable of taking on full-size megaherbivores

- Fused nasals unique among theropods, suggests enhanced resistance to stress from struggling prey; rounder teeth in cross-section than other apex predator theropods suggests enhanced crushing and piercing ability rather than slicing (Holtz 2004)
- Bite marks on DPP hadrosaur and ceratopsian bones attributed to tyrannosaurs (Jacobsen 1998)
- Allometric growth hints at ontogenetic dietary shifts:
    - Skull gets progressively wider to accommodate enlarged adductor musculature and mandibles get progressively deeper to resist greater stress (Therrien *et al.* 2021; Voris *et al.* 2022); adults and subadults could likely crush bone but juveniles skulls still too gracile for that
    - Postcrania: legs become relatively shorter as animal grows, suggests enhanced cursorial ability as a pursuit predator in juvenile stage compared with adult, supported by occurrence of *Citipes* skeletons (apparently fast-running animal) in juvenile *Gorgosaurus* stomach contents (Therrien *et al.* 2023)
- Evidence of ontogenetic niche shifts combined with lack of medium-sized adult theropods strongly suggests that juvenile tyrannosaurids owned an entire predatory ecospace in DPP and other Late Cretaceous ecosystems (Holtz 2021; Schroeder *et al.* 2021)
- Enigma around *Gorgosaurus* and *Daspletosaurus* coexistence: only major anatomical difference between the two is that the latter appeared stockier, a bit heavier at adult size, but otherwise very little evidence of dietary niche partitioning; at a stretch one could argue that adult *Daspletosaurus* should only get links to adult megaherbivores and should be the only nodes connected to ankylosaurs…
    - Alternatively, it can be argued that absence of niche partitioning may have been irrelevant due to lack of competition for food resources given how rare *Daspletosaurus* seemed to be relative to *Gorgosaurus* (in DPF at least); this hypothesis is supported by the fact that *Daspletosaurus* does seem to be at the northern edge of its range (the most northerly tyrannosaurine of its time) while albertosaurines appeared close to the southern edge of their own range (Farlow & Pianka 2002), therefore DPP a region of range overlap?
- Could adults run as fast as juveniles? This could determine whether fast-running prey such as ornithomimids and smaller caenagnathids should be included in adult tyrannosaur links
    - Full-size adult *Gorgosaurus* (e.g. CMN 2120, AMNH 5458) has body mass ~2,500 kg and estimated top speed (accounting for mass) ~38 km/h (Dececchi *et al.* 2020)
    - Subadult *Gorgosaurus* (e.g. AMNH 5664) has body mass ~678 kg and est top speed almost 50 km/h, closer to *Struthiomimus* and *Ornithomimus* top speeds

    - estimated ~62 km/h (Dececchi *et al.* 2020); if subadults hunted by ambush, they could realistically have caught ornithomimids
    - What is more established is that longer hindlimbs of tyrannosaurs relative to other large theropods optimized their energy expenditure for locomotion while searching for prey, a key advantage given their megaherbivore prey certainly reached higher top speeds than sauropods in other ecosystems (Dececchi *et al.* 2020)
- How does this evidence translate into DPP network links?
    - Adult and subadult node has a high range of body mass (and therefore top speed): all ceratopsids and hadrosaurs (adult and juvenile), possibly all ankylosaurs (at least for *Daspletosaurus*), juveniles of other tyrannosaur species; *Unescoceratops*; all small theropods and ornithischians included when accounting for subadult tyrannosaurs in this node; otherwise include medium to large turtles, crocodilians and choristoderes as occasional prey
    - Juvenile stage: max body mass estimated between 335-460 kg, so include all small theropods (including young juvenile tyrannosaurs of other species), juvenile megaherbivores, all small ornithischians, birds >1 kg (ornithurine A and above), mammals >1 kg (*Meniscoessus* and *Didelphodon* sp.), lizards >1 kg (*Labrodioctes* and *Palaeosaniwa*), all crocs and turtles except *Basilemys*
    - Young juvenile (hatchling) stage: max body mass estimated around 32 kg (after a few years), so likely preyed on all mammals, birds >1 kg (ornithurine A and above), smallest theropods (i.e. *Citipes*, *Richardoestesia* and *Hesperonychus*), smallest ornithischians (orodromines and *Foraminacephale*), all lizards, *Cteniogenys*, frogs and *Albanerpeton*

Ornithomimidae

Fossil record: a few spectacular articulated skeletons, but mostly isolated limb and vertebra elements (Russell 1972*a*)

- 5 nodes in DPP network: *Ornithomimus edmontonicus*, *Struthiomimus altus* (the most common ornithomimids)
    - Much rarer species: *Rativates evadens* known from associated skull and skeleton (McFeeters *et al.* 2016), cf *Qiupalong* known from 2 isolated elements (North American occurrence of Chinese taxon)(McFeeters *et al.* 2017), and enigmatic large unnamed ornithomimid known from a few fragments (Longrich 2008)
    - No discernible faunal turnover among ornithomimids, all species poorly sampled (Cullen *et al.* 2021)

Trophic links: angiosperm shoots, fruits/seeds and aquatic leaves are unquestionably part of their diet; likely herbivorous, insufficient evidence for plant-dominated omnivory (Barrett 2005)

- Lack of teeth in mandible combined with likely weak adductor musculature makes consumption of woody angiosperms (and large nuts like Fagaceae) unlikely; still include herbaceous angiosperms and shoots in their diet
- Low-energy plants such as ferns excluded from links, in any case ornithomimid rostra are very narrow suggesting selective feeding habit more suited to browsing leaves and fruits

- Direct evidence: stomach contents of an Asian ornithomimid reveal omnipresence of plant material and gastroliths similar to extant herbivorous birds (Kobayashi *et al.* 1999)
- Interestingly no evidence of dietary niche partitioning among ornithomimids, certainly not among the most common species; more diverse faunas from Asia with better preserved skeletons show very little ecomorphological variation in ornithomimosaurs, except for deinocheirids

Caenagnathidae

Fossil record: caenagnathids likely less abundant than theropods of similar body size since their isolated remains are much more rarely recovered in vertebrate microsites (Funston 2020)

- 3 nodes in DPP network: *Caenagnathus collinsi* (large), *Chirostenotes pergracilis* (medium), *Citipes elegans* (small) (Funston 2020)
- All species seemed to coexist due to vastly overlapping stratigraphic distributions (Cullen *et al.* 2021)

Trophic links: perhaps the single most enigmatic group in the network for dietary inferences due to lack of teeth, variability in beak function (as seen in birds) and lack of direct evidence such as fossil stomach contents

- Caenagnathid skull anatomy highly convergent with that of extant frugivores, new study suggests craniomandibular morphology primarily adapted for processing plant rather than animal food (Funston, pers. comm.); therefore, caenagnathids might be considered plant-dominated omnivores rather than meat-dominated omnivores, a slight shift in paradigm from past research; however, diet fractions not accounted for in this network, so animal prey is likely overrepresented in caenagnathid trophic levels
- Very low bite forces for caenagnathids suggest that they did not eat any woody angiosperm material (e.g. tree leaves), so likely no links to angiosperm leaf nodes
- Among oviraptorosaurs, caenagnathids had generally shallower dentaries than oviraptorids, better suited to slicing food than to crushing (Ma *et al.* 2017)
- Gastroliths in Early Cretaceous relative *Caudipteryx zoui* strongly indicative of herbivory (Ji *et al.* 1998)
- Sharp pointed beak for *Chirostenotes* and *Citipes* indicative of more predatory lifestyle? *Chirostenotes* mandible in particular very similar to that of extant predatory turtles such as *Chelydra serpentina*, overall interpreted as omnivorous (Funston & Currie 2014; Funston 2020)
- Longer, shallower mandible in *Caenagnathus* (Sternberg 1940*b*; Funston 2020) suggests it would have been less resistant to stress than those of smaller DPP caenagnathids
- Lack of mandibular kinesis in caenagnathids means restrictions to potential prey size (Funston & Currie 2014)
- Fusion of tarsometatarsus in *Citipes* implies more cursorial behaviour than other caenagnathids (Funston 2020), could be interpreted as better pursuit predators and/or faster at fleeing from their own predators, which would make sense given how small they were
    - Additional direct evidence that *Citipes* was prey for juvenile *Gorgosaurus* (Therrien *et al.* 2023)

Overall differences in body size, skull morphology and cursorial ability strongly suggests dietary niche partitioning among caenagnathids, following similar pattern to megaherbivores (Funston 2020)

- How is that reflected in their trophic links? Omnivory is a reasonable interpretation, to varying degrees between species
    - Maybe make *Chirostenotes* and *Citipes* eat solely angiosperm shoots, fruits/seeds and root nodes, then add aquatic plants for *Caenagnathus* given that the latter is understood to be more herbivorous?
    - Relatively shallow dentary makes it unlikely that caenagnathids could crush molluscs (Funston & Currie 2014), and probably not medium to large angiosperm nuts like Fagaceae either; probably robust enough to slice rhizomes at least
    - *Citipes* is only caenagnathid proposed to eat smallest seeds (including those of angiosperms, cycads and Caytoniaceae) like extant Galliformes
    - For predation: lack of mandibular kinesis implies very limited prey size compared to more carnivorous theropods so exclude any dinosaur, any lizard >20 cm (*Socognathus* and larger), every mammal >0.2 kg (anything heavier than *Turgidodon*) for *Caenagnathus* and *Chirostenotes*, every mammal >0.1 kg for *Citipes* due to smaller size; only include birds <0.48 kg (Ornithurine D est. mass) for *Chirostenotes*; also exclude *Hensonbatrachus* from *Citipes* diet due to the latter's smaller size

    Caenagnathids are a great example of the effect of node selection on trophic levels in a network: collapsing plants into fewer nodes results in very high TL increase for them in particular

Troodontidae and problematic paravians

- *Fossil record*: 5 nodes in DPP network: 3 troodontids *Stenonychosaurus inequalis* (by far the best documented), cf *Paronychodon*, cf *Pectinodon*, and cf *Richardoestesia gilmorei* and cf *R. isosceles* (Sankey *et al.* 2002)
- *Stenonychosaurus inequalis* the only species with confirmed cranial remains (Russell 1969; Currie & Zhao 1993); cf. *R. gilmorei* known mostly from teeth and partial dentary (Currie *et al.* 1990); others known only from rare teeth (Sankey *et al.* 2002; Larson & Currie 2013)
- No evidence of faunal turnover in Belly River Group either due to persistence of *Stenonychosaurus* remains (Cullen *et al.* 2021); other taxa occasionally recovered throughout DPP in vertebrate microsites (Brinkman 1990)

Trophic links

- *Stenonychosaurus* braincases suggest particularly high brain-body mass ratio relative to other dinosaurs, as well as excellent eyesight due to large orbits, potentially nocturnal (Russell 1969)
    - Stable isotope ratio evidence: Troodontidae Ba/Ca and Sr/Ca ratios plot closer to megaherbivores than to other theropods, suggesting at least plant-dominated omnivory (Cullen & Cousens 2023)
    - Possible direct evidence of carnivory: fossil gastric pellets from Egg Mountain containing metatherian and multituberculate remains are attributed to *Troodon*

    formosus due to presence of shed teeth and nesting evidence at same locality (Freimuth *et al.* 2021)
  - Troodontid teeth appeared poorly adapted to resist stress from struggling prey, therefore limited to softer/smaller prey than dromaeosaurids (Torices *et al.* 2018); those teeth fit in long slender jaws (Currie 1987), which is consistent with low stress resistance
    - Fruits and seeds likely part of diet but do not include angiosperm fruit nodes from families that only produce nuts (e.g. Fagaceae)
  - Also restrict them from angiosperm fruit nodes for families that only produce small seeds (e.g. Salicaceae, Compositae)
  - Trophic links: all mammals, all birds and lizards <2 kg, frogs, *Albanerpeton*, angiosperm shoots and some fruits/seeds
- *Pectinodon* has most similar teeth to *Stenonychosaurus* and similar estimated body size (Brown *et al.* 2013*b*), therefore it gets same trophic links
- *Paronychodon* has more conical teeth lacking serrations, most similar to those of Asian non-denticulate troodontid *Byronosaurus jaffei* (Norell *et al.* 2000; Larson 2008), possibly means enhanced piercing ability, therefore similar diet to *Stenonychosaurus* and *Pectinodon* but with only a few fruits/seeds, as well as fish, crayfish and insects
- cf. *Richardoestesia gilmorei* has teeth most similar to dromaeosaurs out of all DPP theropods known largely from tooth morphs (Sankey *et al.* 2002; Larson 2008), so likely carnivorous, probably preyed on all mammals and birds, *Hesperonychus*, lizards <1 kg, land amphibians
- *R. isosceles* has straighter teeth than cf. *R. gilmorei*, adapted for piercing, indicative of piscivory, supported by stable isotopes (Frederickson *et al.* 2018); therefore same diet as *R. gilmorei* but with fish as well

Dromaeosauridae

Fossil record: extremely rare skeletons, known mostly from teeth and postcranial fragments such as iconic pedal claw II (Colbert & Russell 1969; Brinkman 1990; Currie 1995; Currie & Evans 2020)

- 3 nodes in DPP network: velociraptorine *Saurornitholestes langstoni* (by far the most abundant from teeth), dromaeosaurine *Dromaeosaurus albertensis*, and microraptorine *Hesperonychus elizabethae* (Longrich & Currie 2009)

Trophic links

- *Dromaeosaurus* and *Saurornitholestes* teeth had fewer and larger serrations indicates that these theropods preyed on larger animals compared with other theropods of similar body size
- *Dromaeosaurus* and *Saurornitholestes* likely hypercarnivores feeding not just on mammals, birds and lizards but also small ornithischians and all small to medium-sized theropods (including all ornithomimids and young juvenile tyrannosaurs); as for megaherbivores, they certainly hunted juveniles, but could only realistically tackle adults if hunting in packs (still unlikely due to huge size)

- Sickle-claw combined with evidence of primary feathers in all paravians together support ‘raptor prey restraint’ hunting tactic, ideal for jumping onto and grasping small to medium-sized prey, maybe not as ideal for large prey (Fowler *et al.* 2011)
- Tooth marks on pterosaur bone attributed to dromaeosaur may hint at predation on pterosaurs, but more likely scavenging because the bone is attributed to large azhdarchid *Cryodrakon* (Currie & Jacobsen 1995)
- *Hesperonychus* had very different diet due to much 10x smaller body size
  - Dentition not preserved (or at least isolated ‘bird’ teeth of problematic affinity or teeth attributed to juvenile *Saurornitholestes*); gasping claws meant it could likely catch prey of almost equal size such as largest birds and mammals, and probably lizards < 2 kg
  - Exceptional stomach content record of close relative *Microraptor* species from Early Cretaceous China show that microraptorines had wide prey range, from small mammals to lizards, even small teleosts and birds (Hone et al., 2022 and references therein); therefore all these prey are also attributed to *Hesperonychus* (including all birds, all land amphibians, all acanthomorphs, Characiformes and Hiodontidae)

Ornithurae – Birds

Fossil record

- Overall 9 nodes in DPP network: *Palintropus* sp. A,B and ornithurines A-G, most known from fragmentary coracoids, rare cases of femur (*Palintropus* sp. A,B), sternum (ornithurine B), dorsal and sacrum (*Palintropus* sp. A,B) (Longrich 2009; Mohr *et al.* 2020)
  - Add ornithurines B and C from Irvine (Longrich 2009) since I added other vertebrates unique to that locality (e.g. *Habrosaurus*, Cimolestidae, teiids)
  - add birds unique to more distant localities like Onefour and Devil’s Coulee (ornithurines D and F) (Longrich 2009) Bird diversity may still be underrepresented
  - ‘bird’ teeth often reported from vertebrate microfossil localities (Brinkman *et al.* 2005*b*), some could tentatively be assigned to Hesperornithiformes, however they could also belong to one of the non-avian theropods so we decide not to add a tenth bird node to network

Trophic links

  - *Palintropus* species A seems more closely related to *Apsaravis* than to Galliformes, proposed to be the size of a peacock (Longrich 2009), likely spent more time on the ground than other birds?
  - Ornithurine A can reasonably be interpreted as a diving bird due to its coracoid being very similar to *Pasquiaornis* from Sask as well as having pachyostosis (Longrich 2009), so very different niche from other DPP birds; it’s really the only one whose diet can reasonably be deemed more specialized than omnivore, restrict it to same fish prey as *Hesperonychus*
  - Ornithurine B is very small around size of house sparrow (*Passer domesticus*); sternum most similar to that of Charadriiformes (Longrich 2009)

- Ornithurine C coracoid has similar anatomy to *Palintropus* and *Apsaravis* but is much smaller (size of solitary sandpiper *Tringa solitaria*) (Longrich 2009)
- Ornithurine E coracoid has scapular cotyle similar to *Lithornis* or heron *Ardea* (Longrich 2009)
- Ornithurine G assigned to cf. *Cimolopteryx* but the similarities of that family to Neornithes clade Charadriiformes may simply reflect convergence or retention of plesiomorphic traits, thus we refrain from attributing a gull-like life history to that group

With current knowledge, it's impossible to infer much about the ecology of most DPP birds; Ornithurine A is the only one that can be inferred to have distinct lifestyle; therefore it seems parsimonious to interpret all DPP birds as omnivorous with shoots, fruits, seeds and insects forming bulk of diet; Ornithurine A is the only one interpreted as more piscivorous because of evidence for diving behaviour

MAMMALS

For all taxa, fossil record dominated by isolated teeth (Fox 2005), few dentaries reveal invaluable information about diet although lack of postcranial remains means inferences of locomotion and niche occupancy (either scansorial or burrowing or even swimming) remain highly uncertain

Multituberculates

Fossil record: a few jaw elements, mostly teeth found across Belly River Group (Fox 2005; Sankey *et al.* 2005)

- 5 nodes in DPP network: *Meniscoessus major*, *Cimolomys clarki* (both in family Cimolomyidae), *Mesodma primaeva* (fam. Neoplagiaulacidae), *Cimolodon* spp. (fam. Cimolodontidae), *Cimexomys* spp. (some species problematic due to relative lack of material so collapsed into same node; same issue with *Pediomys* in metatherians)

Trophic links: feeding ecology still debated but likely varying between insectivory, frugivory and folivory (Wilson *et al.* 2012; Robson 2018); dentition still suggests consumption of relatively large insects, so no ants or flies for any multituberculate trophic links

- *Cimolodon* and *Mesodma* lean towards animal-dominated omnivory, with *Mesodma* leaning most towards insect-based carnivory: they have mesiodistally shorter and apicobasally taller premolars indicating they retained a slicing function and thus took part in grinding cycle alongside molars (Wilson 2013); later study confirms that Neoplagiaulacidae (of which *Mesodma* is the only DPP member) were the multituberculate family that relied most on animal food (Weaver & Wilson 2021)
  - Stable isotope ratio evidence: neoplagiaulacid Ba/Ca and Sr/Ca ratios plot closer to tyrannosaurs and dromaeosaurs than to megaherbivores, independent evidence for animal-dominated omnivory or even insectivory (Cullen & Cousens 2023)
  - Perhaps restrict shoots from *Mesodma* links, only include fruits/seeds among plant food
- *Cimolomys* and *Meniscoessus* lean towards plant-dominated omnivory because of more distally elongate molars and higher surface complexity (Wilson 2013)

- No sufficient reason to attribute different trophic links to multituberculate nodes (except for *Mesodma*), possibly another example of trophic link attribution that would benefit from index of link strength to discern any dietary differences

Metatherians

Fossil record: some well-preserved jaws, mostly teeth (Fox 1979*a*, *b*; Sankey *et al.* 2005; Scott & Fox 2015); metatherian abundance increases relative to eutherians at higher stratigraphic intervals in greater proximity to Bearpaw Sea (Sankey *et al.* 2005)

- 6 nodes in DPP network: *Alphadon halleyi*, *Turgidodon praesagus* (*T. russelli* too fragmentary), *Pediomys* spp., *Eodelphis browni*, *E. cutleri*, *Didelphodon* sp. (the latter known from single dentary fragment in DPP, oldest occurrence of the genus)

Trophic links:

- Make *Didelphodon* sp. more carnivorous than other stagodontids (no fruits, just seeds and shoots); relatively large body mass (1.7 kg) means it likely ate small vertebrates as part of its diet (Wilson 2013; Wilson *et al.* 2016)
- *Eodelphis cutleri* has more robust jaw than *E. browni* (Fox 1981), the former could likely crush snail and crustacean shells, *Eodelphis* diet in general likely analogous to extant American opossum *Didelphis virginiana* (Hopkins & Forbes 1980) so one of the most generalist mammals: links to every bird smaller than Ornithurine D, every mammal smaller than *Cimolomys*, every lizard smaller than *Socognathus*, but plant material another important component
- *Alphadon* and *Turgidodon* seem to plot towards animal-dominated omnivory more than plant-dominated omnivory in lower molar morphospace (Wilson 2013) but smaller body sizes than stagodontids (*Eodelphis* and *Didelphodon*) means they are restricted to smaller prey, e.g. *Alphadon* limited to insects; omnivorous extant marsupial with 50-50 plant/insect diet like *Philander opossum* may be accurate trophic analogue (Martina & Waters 2014)
- *Pediomys*: increased shearing and crushing capacity for molars, therefore more omnivorous than other metatherians such as alphadontids or stagodontids although omnivory still animal-dominated (Wilson 2013)

Eutherians

Fossil record: Very rare remains in DPP (a few jaws, mostly teeth), clearly less common than metatherians or multituberculates (Fox 1979*c*; Sankey *et al.* 2005); eutherian abundance decreases relative to metatherians at higher stratigraphic intervals in greater proximity to Bearpaw Sea (Sankey *et al.* 2005)

- 3 nodes recognized in DPP: *Gypsonictops lewisi*, *Paranyctoides sternbergi* and Cimolestidae (the latter only known from tooth from Irvine microsite, formerly classified among Peradectidae)

Trophic links

- *Gypsonictops lewisi* close relatives of Leptictidae, so likely insectivorous, trophic links reasonably inferred largely from more recent relative *Leptictidium* from Messel (Labandeira & Dunne 2014; Eberle *et al.* 2023); flatter molars less adapted for shearing than in other mammals so diet more specialized towards softer insects and only plant families that have pulpy fruits (Fox 2005)

- *Paranyctoides sternbergi*: dentary most similar to fam. Nyctitheriidae (part of Eulipotyphla or Euarchonta) (Fox 2005; Manz & Bloch 2015; Manz *et al.* 2015), interpreted as scansorial and insectivorous, still eating fruits occasionally; DPP animal with dentition most similar to extant shrew such as *Sorex cinereus* (McCay & Storm 1997) and to Messel eulipotyphlans (Labandeira & Dunne 2014)
- Cimolestids likely more carnivorous than other eutherians with little plant matter in diet (Wilson 2013), although DPF cimolestid probably didn't eat any vertebrates due to its likely small body size; this means that cimolestid trophic links to plants only include smaller fruits and nuts (no small seeds) while *Paranyctoides* gets almost all fruits, nuts and seeds

Silhouette image acknowledgements

Species silhouettes used in the figures were provided by the following: A. Bell and L. Chiappe 2015, dx.doi.org/10.1371/journal.pone.0141690, I. Contreras, A. Farke, N. Tamura (vectorized by M. Keesey), L. Weaver and S. Werning (all CC-BY 3.0: https://creativecommons.org/licenses/by/3.0/), E. Schumacher (CC-BY-NC 3.0: https://creativecommons.org/licenses/by-nc/3.0/), E. Willoughby, G.E. Robertson and S. Sampson et al. (CC-BY-SA 3.0: https://creativecommons.org/licenses/by-sa/3.0/), Namu Wiki (CC-BY-NC-SA 2.0: https://creativecommons.org/licenses/by-nc-sa/2.0/kr/), S. Hartman (CC-BY-NC-SA 3.0: https://creativecommons.org/licenses/by-nc-sa/3.0/), M. Cavalcanti, P. Pilatti and D. Astúa, M. Dempsey, G. Paola-Munoz, E. Pinheiro-Giareta, E. Price, Sheatherius and Tree of Life App (CC-BY 4.0: https://creativecommons.org/licenses/by/4.0/), and M. Hodiono (image modified from Unsplash).

Appendix VI

Reference tables for nodes and links in Dinosaur Provincial Park, Serengeti, and Komodo food webs

Due to a different citation style, this appendix has a distinct reference list from the previous appendices. Some plant nodes are only represented in the most high-resolution version of the food webs (see Appendix V).

Dinosaur Provincial Park ecological network

Nodes in **bold** excluded from food webs with node selection restricted to fully terrestrial organisms.
*Plant nodes collapsed into nodes at lower taxonomic resolution in the food web version presented in this study.

Taxon	Occurrence references	Body size			Trophic link references
		Mass (kg)	Length (m)	References	
Detritus	NA	NA	NA	NA	(1)
Decayed wood	NA	NA	NA	NA	(2)
Carrion	NA	NA	NA	NA	This study
Sulphate-reducing bacteria	(1)	NA	NA	NA	(1)
Enterobacteriaceae	(1)	NA	NA	NA	(1)
Iron-oxidizing bacteria	(1)	NA	NA	NA	(1)
Iron-reducing bacteria	(1)	NA	NA	NA	(1)
Vibroid bacteria	(1)	NA	NA	NA	(1)
Manganese-reducing bacteria	(1)	NA	NA	NA	(1)
Rods	(1)	NA	NA	NA	(1)
Coccibacilli	(1)	NA	NA	NA	(1)
Coccoid bacteria	(1)	NA	NA	NA	(1)
Curved rod bacteria	(1)	NA	NA	NA	(1)
Hydrogen bacteria	(1)	NA	NA	NA	(1)
Ammonia-oxidizing bacteria	(1)	NA	NA	NA	(1)
Phosphate-reducing bacteria	(1)	NA	NA	NA	(1)
Methanogens	(1)	NA	NA	NA	(1)
Sulfur-oxidizing bacteria	(1)	NA	NA	NA	(1)
Gram-positive anaerobes	(1)	NA	NA	NA	(1)
Bacillariophyta	(1)	NA	NA	NA	(1)
Dinoflagellata	(3)	NA	NA	NA	(1)
Chlorophyta	(3)	NA	NA	NA	(1)
Anthocerotaceae*	(3,4)	NA	NA	NA	Same as Sphaerocarpaceae
Sphaerocarpaceae*	(3,4)	NA	NA	NA	(1)
Sphagnaceae*	(3,4)	NA	NA	NA	(1,5)
Lycopodiaceae*	(3,4)	NA	NA	NA	(6)
Selaginellaceae*	(3,4)	NA	NA	NA	(1,6,7)
Isoetaceae*	(3)	NA	NA	NA	(6,8)
Equisetum sp.	(9)	NA	NA	NA	(10)
Osmundaceae*	(3,4)	NA	NA	NA	(1,6,7)
Schizaeaceae*	(3,4)	NA	NA	NA	(1,6,7)

Gleicheniaceae*	(3,4)	NA	NA	NA	(1,6,7)
Cyatheaceae*	(3,4)	NA	NA	NA	(6,7)
Dicksoniaceae*	(3,4)	NA	NA	NA	(6,7)
Polypodiaceae*	(3,4)	NA	NA	NA	(1,6,7)
Matoniaceae*	(3)	NA	NA	NA	(7)
Marsileaceae*	(3)	NA	NA	NA	(6,7)
Cycadaceae	(3,4)	NA	NA	NA	(7,11)
Caytoniaceae*	(3,4)	NA	NA	NA	(12,13)
Pinaceae*	(3); this study	NA	NA	NA	(14)
Podocarpaceae*	(3,15)	NA	NA	NA	(14,16)
Cupressaceae*	(3,15)	NA	NA	NA	(14,16)
Sequoia sp.*	(9,17)	NA	NA	NA	(14,16)
Metasequoia sp.*	(18)	NA	NA	NA	(14,16)
*Elatocladus albertaensis**	(17,18)	NA	NA	NA	Same as other conifers
Cheirolepidiaceae*	(3)	NA	NA	NA	(19)
*Baiera digitata**	(18)	NA	NA	NA	(20,21)
Ginkgoites sp.*	(9,18)	NA	NA	NA	(20,21)
Ginkgo sp.*	This study	NA	NA	NA	(20,22,23)
Ephedraceae*	(3,4)	NA	NA	NA	(1,24,25)
Artocarpus sp.*	(17,18)	NA	NA	NA	(26)
Cercidiphyllum sp.*	(4,14,18)	NA	NA	NA	(1)
*Dombeyopsis nebrascensis**	(17,18)	NA	NA	NA	(1,14)
Menispermites sp.*	(17,18)	NA	NA	NA	(1)
Platanus sp.*	(9,17)	NA	NA	NA	(1,14,27)
*Vitis stantoni**	(9,17)	NA	NA	NA	(1,14)
Buxaceae*	(3)	NA	NA	NA	(1,14)
Gunneraceae*	(3,4)	NA	NA	NA	Same as herbaceous plants
Salicaceae*	(3)	NA	NA	NA	(1,14,27)
Droseraceae*	(3)	NA	NA	NA	(14,28)
Olacaceae*	(3)	NA	NA	NA	(1)
Loranthaceae*	(3,4)	NA	NA	NA	(1,14)
Sapindaceae*	(3)	NA	NA	NA	(1,14)
Proteaceae*	(3,4)	NA	NA	NA	(14)
Compositae*	(3)	NA	NA	NA	(14)
Fagaceae*	(3)	NA	NA	NA	(1,14,27)
Betulaceae*	(3)	NA	NA	NA	(1,14,27)
Ulmaceae*	(3)	NA	NA	NA	(1,14,27)
Chenopodiaceae*	(3)	NA	NA	NA	(14)

Liliaceae*	(3,4)	NA	NA	NA	(14)
Zingiberaceae	(18)	NA	NA	NA	(14)
Cyperaceae*	(3)	NA	NA	NA	(1)
Sparganiaceae*	(3)	NA	NA	NA	(1)
Trapa sp.*	(18)	NA	NA	NA	(1,29)
*Cobbania corrugata**	(9,30)	NA	NA	NA	(1,30)
Lichen	(1)	NA	NA	NA	(1)
Fungi	(3)	NA	NA	NA	(1)
Demospongiae	(1)	NA	NA	NA	(1)
Unionidae	(31)	NA	0.12	This study	(1)
Sphaeriidae	(31)	NA	0.015	(31)	(1)
Anomia micronema	(31)	NA	0.075	(32)	(33,34)
***Brachidontes* sp.**	(31)	NA	0.04	(35)	(34)
Crassostrea subtrigonalis	(31)	NA	0.1	(33)(Ostreidae)	(33)(Ostreidae)
Mactra alta	(31)	NA	0.1	(36)	(33,34)
Corbula subtrigonalis	(31)	NA	0.02	(37)	(33,34)
Hydrobiidae	(31)	NA	NA	NA	(1)
Pleuroceridae	(31)	NA	NA	NA	(1)
Viviparidae	(31)	NA	NA	NA	(1)
Pulmonate snails	(31,38)	NA	NA	NA	(1,39,40)
Ammonoidea	This study	NA	NA	NA	(33,41,42)
Branchiopoda	(1)	NA	NA	NA	(1)
Ostracoda	(1)	NA	NA	NA	(1)
Decapoda	This study	NA	NA	NA	(1)
Acari	(43)	NA	NA	NA	(14)
Araneidae	(43)	0.0051086	NA	(44)	(1)
Pseudoscorpionida	(43)	0.00000212	NA	(44)	(45)
Diplopoda	(31)	0.00075	NA	(46)	(47)
Collembola	(43)	NA	NA	NA	(48)
Anisoptera	This study	0.0003673	NA	(44)	(1,49)
Blattodea	(43)	0.005	NA	(50)	(1)
Isoptera	(43)	0.0000075	NA	(46)	(1,51,52)
Phasmatodea	(43)	0.001061	NA	(44)	(1)
Orthoptera	NA	0.0038951	NA	(44)	(1,6,51,53)
Psocodea	(43)	NA	NA	(44)	(54)
Thysanoptera	(43)	NA	NA	NA	(6,14)
Aphidoidea	(55)	NA	NA	NA	(1,6,55)
Hemiptera (other)	(43)	0.00094	NA	(50)	(1,6)

Coleoptera	(43)	0.0019	NA	(50)	(1,6,56,57)
Neuroptera	(43)	0.00014405	NA	(44)	(48)
Diptera	(43)	0.00016517	NA	(44)	(1,6)
Formicidae	(43)	0.0007	NA	(50)	(1)
Hymenoptera (other)	(43)	0.001665	NA	(44)	(1,6)
Lepidoptera	(43)	0.00091	NA	(44)	(1,6,11)
Trichoptera	(43)	0.0006	NA	(50)	(1,58)
Hybodus montanensis	(59–61)	NA	2	(62)	(41,63)
***Squatina* sp.**	(59,60)	NA	1.75	(64)(angelshark)	(64)(angelshark)
Orectolobidae	(59,60); this study	NA	1.475	(65) (spotted wobbegong)	(65)(spotted wobbegong)
Odontaspididae	(59,60)	NA	3.6	(65)(sand tiger sharks)	(65)(sand tiger sharks)
Cretoxyrhinidae	(59,60)	NA	6	(65)(great white shark)	(65,66)
***Archaeotriakis* sp.**	(59,60)	NA	1.6	(67) (leopard shark)	(67) (leopard shark)
Myledaphus bipartitus	(59–61)	NA	1.5	(68)	(69,70)
Protoplatyrhina renae	(59,60)	NA	NA	NA	(70)
Sclerorhynchidae	(59,60)	NA	2.5	(71)(common sawfish)	(71)(common sawfish)
Elasmodus greenoughii	(59,60)	2.5	0.5	(72)(*Chimaera*)	(72)(*Chimaera*)
Anchiacipenser acanthaspis	(61)	110.174	1.2	(73,74)	(75)
Polyodontidae	(61)	70	2.5	(76,77)	(78)
Lepisosteidae	(61)	18	1.8	(79)(Gar)	(1,75,79,80)(Gar)
Amiidae	(61)	6.6	0.61	(75)(Bowfin)	(1,75)(Bowfin)
Holostei (other)	(61)	NA	NA	NA	*Lepisosteus* and Amiidae
Belonostomus longirostris	(61)	NA	0.75	(81)	(68,82)
***Enchodus* sp.**	(59,60)	NA	1	(83)	(84)
Paratarpon apogerontus	(68,85,86)	NA	1.5	(68,86)	(68,87)(*Megalops*)
Paralbula casei	(68,85)	7	0.75	(88)(bonefish)	(89,90)(bonefish)
Coriops amnicolus	(68,85)	NA	0.6	(91)(bonytongue)	(68,91)(bonytongue)
Cretophareodus alberticus	(68)	NA	0.3	(68)	(92,93)
Hiodontidae	(85)	NA	0.2	(94)	(75)(mooneyes)
***Diplomystus* sp.**	(85)	NA	0.4	(93)	(75,93)(herrings)
***Horseshoeichthys* sp.**	(85)	NA	0.27	(95)	(75)(herrings)
***Notogoneus* sp.**	(85)	NA	0.5	(96)	(96,97)(*Gonorynchus*)
Characiformes	(85,98)	0.03	0.1	(99)(tetra)	(99)(tetra)
Estesesox foxi	(85,100)	NA	0.3	(75)(chain pickerel)	(68,75,101) (chain pickerel)
Oldmanesox canadensis	(85,100)	NA	0.3	(75)(chain pickerel)	(68,75,101)(chain pickerel)
Acanthomorpha #1-4	(68)	NA	NA	NA	(75)(perches)
***Albanerpeton* spp.**	(102); This study	NA	0.2	(103)	(103–106)
Scapherpeton tectum	(61)	NA	0.7	(103)	(103)

Lisserpeton bairdi	(102)	NA	0.7	(103)	(103,107,108)
Opisthotriton kayi	(61)	NA	0.35	(103)	(103,109)
Habrosaurus prodilatus	(102)	NA	1.6	(103)	(103,110,111)
Hensonbatrachus kermiti	(112)	NA	0.1	(113)	(1,114,115)
Tyrrellbatrachus brinkmani	(112)	NA	0.035	(113)	(1,114–116)
Anura indet 1	(112)	NA	0.07	(112)	(1,114,115)
Adocus sp.	This study	7.6	0.39	(117,118)	(117,119,120)
Axestemys foveatus	(121); this study	3.7	0.3	(117,118)	(122–124)
Axestemys allani	(121); this study	3.38	0.291	(117,118)	(122–124)
Axestemys splendida	(121); this study	13.7	0.49	(117,118)	(1,125–127)
“Apalone” latus	(121)	3.3	0.2875	(118)	(122–124)
Trionychidae gen. sp. indet	(117)	13.7	0.49	(117,118)	(1,125–127)
Chelydridae	(61,117)	11.46	0.439	(128)	(117,129–131)
Plesiobaena antiqua	(132); this study	3.7	0.3	(118,132)	(117,132,133)
Boremys pulchra	(134); this study	3.7	0.3	(118,134)	(117,133,134)
Neurankylus eximius	This study	18	0.54	(118)	(117,120,135)
Judithemys sukhanovi	(136)	10	0.435	(118,136)	(117,136)
Kimurachelys slobodae	(137)	NA	NA	NA	(137,138)
cf _Cteniogenys_ sp.	(139)	NA	NA	NA	(139–141)
Champsosaurus natator	(142)	NA	2	(143)	(144–148)
Champsosaurus lindoei	(142)	NA	1.3	This study	(144–148)
Fluvionectes sloanae	(59,149,150)	NA	6.9	(150)	(33,151)
Plioplatecarpus sp.	(59,152)	NA	5.5	(153)	(153)
Leidyosuchus canadensis	(61,154)	97	2.69	(154,155)	(154,156–159)
Albertochampsa langstoni	(160)	39.14	2.1	(155)	(156,159,161)
cf. _Stangerochampsa_	(161)	16.27	1.65	(155)	(156,159,161)
Basilemys variolosa	(117); this study	190	1.3	(117,118)	(117,162–164)
Odaxosaurus priscus	(165)	0.05	0.14	(165,166)	(1,167)
Orthrioscincus mixtus	(165)	0.03	0.113	(165,166)	(168)
Leptochamops thrinax	(152,165)	0.06	0.15	(165,166)	(165,169)
Socognathus unicuspis	(152,165)	0.3	0.27	(165,166)	(165,170)
Sphenosiagon simplex	(152,165)	0.03	0.114	(165,166)	(165,169)
Glyptogenys ornata	(152,165)	0.0815	0.17	(165,166)	(165)
Gerontoseps irvinensis	(152,165)	0.044	0.133	(165,166)	(165)
?*Exostinus* sp.	(165)	0.075	0.16	(165,166)	(171)
Labrodioctes cf. *montanensis*	(165)	3.4	0.67	(165,166)	(172)
Parasaniwa sp.	(165)	0.5	0.33	(165,166)	(1,173–176)
Palaeosaniwa canadensis	(165)	6	0.82	(166)	(51,173–176)

Cryodrakon boreas	(177); this study	250	NA	(177,178)	(179)
Orodrominae	(61,180); this study	13	NA	(181)	(182,183)
Stegoceras validum	(184,185)	25.135	NA	(181,186,187)	(182,183,188,189)
Foraminacephale brevis	(184,185)	13	NA	(181,190)	Same as *S. validum*
Sphaerotholus lyonsi	(191)	13	NA	Same as *F. brevis*	Same as *S. validum*
Unescoceratops koppelhusae	(192)	130	NA	(181,190)	(183,193)
Ornithomimus edmontonicus	(194); this study	178.508	NA	(195)	(196–198)
Struthiomimus altus	(194); this study	178.508	NA	(195)	(196–198)
Rativates evadens	(194,199)	120.26	NA	(199,200); this study	(196–198)
cf. *Qiupalong*	(194,201)	131	NA	(202)	Same as *Ornithomimus*
Large unnamed ornithomimid	(203)	370	NA	(181)	Same as *Ornithomimus*
Caenagnathus collinsi	(194); this study	96	NA	(204)	(205–209)
Chirostenotes pergracilis	(194); this study	63.872	NA	(181,186,195,204)	(205–209)
Citipes elegans	(194)	19.8	NA	(210)	(205–209)
Richardoestesia cf. *R. gilmorei*	(211,212); this study	10.3284	NA	(186)	(212–214)
Richardoestesia isosceles	(211); this study	10.1954	NA	(186)	(213–215)
cf. *Paronychodon*	(213); this study	45	NA	(186)	(213,214)
cf. *Pectinodon*	(211); this study	47.3759	NA	(186)	(211,216)
Stenonychosaurus inequalis	(61,194); this study	57.447	NA	(195)	(216–220)
Dromaeosaurus albertensis	(61); this study	15.06	NA	(181,186)	(219,221–223)
Saurornitholestes langstoni	(61,194); this study	21.789	NA	(181,186,224)	(219,222,223,225)
Hesperonychus elizabethae	(194,226)	2.33	NA	(181,186)	(227)
Palintropus sp. A	(228)	2.54	NA	(181)	(1,229,230)
Palintropus sp. B	(228)	1.48	NA	(181)	(1,229)
Ornithurine A	(228)	1.64	NA	(181)	(228)
Ornithurine B	(228)	0.1	NA	(181)	(1,229)
Ornithurine C	(228)	0.12	NA	(181)	(1,229)
Ornithurine D	(228)	0.48	NA	(181)	(1,229)
Ornithurine E	(228)	0.18	NA	(181)	(1,229)
Ornithurine F	(228)	0.11	NA	(181)	(1,229)
Ornithurine G	(231)	2.5	NA	(181,231)	(1,229)
Meniscoessus major	(232,233)	1.42	NA	(234)	(235–238)
Mesodma primaeva	(232,233)	0.0535	NA	(239)	(216,235–238)
Cimolomys clarki	(232,233)	0.472	NA	(234)	(235–238)
Cimolodon spp.	(232,233)	0.179	NA	(239)	(235–238)
Cimexomys spp.	(232,233)	0.051	NA	(239)	(235–238,240)
Alphadon halleyi	(232,233,241)	0.0665	NA	(242)	(237,243)
Turgidodon praesagus	(232,233,241)	0.1984	NA	(242)	(237,243)

Pediomys spp.	(232,233)	0.0588	NA	(242)	(237)
Eodelphis browni	(232,233,244)	0.4432	NA	(242)	(243,245,246)
Eodelphis cutleri	(232,233,244)	0.5316	NA	(242)	(243,245,246)
Didelphodon sp.	(244)	1.636	NA	(242)	(237,245,247)
Gypsonictops lewisi	(232,233,248)	0.0961	NA	(234)	(1,233,249)
Paranyctoides sternbergi	(232,233,248)	0.0262	NA	(234)	(1,250–252)
Cimolestidae	(248)	0.04	NA	(239)	(237)
Euoplocephalus tutus	(253,254)	1617.9	NA	(186)	(255–259)
Scolosaurus cutleri	(253)	2374.58	NA	(181,187,260,261)	(255–259)
Dyoplosaurus acutosquameus	(253)	2194.89	NA	(195)	(255–259)
Anodontosaurus lambei	(253)	2164.816	NA	(186)	(255–259)
Edmontonia rugosidens	(254,262); this study	3180.67	NA	(190,263,264)	(7,255,256,258,259)
Panoplosaurus mirus	(254,262); this study	1486.424	NA	(181,195)	(7,255,256,258,259)
Corythosaurus casuarius	(254,262); this study	3515.045	NA	(187,195,261,264)	(2,16,255,256,258,259,265,266)
Corythosaurus intermedius	(262,267)	2928.647	NA	(181,186,255,263)	(2,16,255,256,258,259,265,266)
Parasaurolophus walkeri	(254,262); this study	3785.365	NA	(181,186,187,255,261)	(2,16,255,256,258,259,265,266)
Lambeosaurus clavinitialis	(254,262); this study	4442.3925	NA	(190,195)	(2,16,255,256,258,259,265,266)
Lambeosaurus lambei	(254,262); this study	3299.6792	NA	(181,186,195,255)	(2,16,255,256,258,259,265,266)
Lambeosaurus magnicristatus	(254,262)	3092.027	NA	(195,255,263)	(2,16,255,256,258,259,265,266)
Brachylophosaurus canadensis	(254,262)	4458.36	NA	(195)	(2,16,255,256,258,259,265,266)
Gryposaurus notabilis	(254,262)	4717.051	NA	(255)	(2,16,255,256,258,259,265,266)
Prosaurolophus maximus	(254,262); this study	4181.47	NA	(255)	(2,16,255,256,258,259,265,266)
cf. *Hypacrosaurus*	(255)	3586.5	NA	(74)	(2,16,255,256,258,259,265,266)
Juvenile hadrosaurs	Same as adults	120	NA	(183,268); this study	(183,269)
Coronosaurus brinkmani	(270); this study	2000	NA	(190)	(255,256,258,259)
Centrosaurus apertus	(254,262); this study	2125.548	NA	(181,186,187,255,261)	(255,256,258,259)
Styracosaurus albertensis	(254,262,271)	4160.968	NA	(195,255)	(255,256,258,259)
cf. *Achelousaurus*	(272)	3187.77	NA	(255)	(255,256,258,259)
Spinops sternbergorum	(273)	1896.318	NA	(186)	(255,256,258,259)
Mercuriceratops gemini	(274)	1500	NA	(190); this study	(255,256,258,259)
Chasmosaurus belli	(262,275); this study	2863.418	NA	(181,255,260,263)	(255,256,258,259)
Chasmosaurus russelli	(262,275); this study	2213.03	NA	(181,186,187,261)	(255,256,258,259)
Chasmosaurus irvinensis	(262,275); this study	2704.38	NA	(255)	(255,256,258,259)
Juvenile ceratopsids	(276); Same as adults	160	NA	(183)	(183)
Gorgosaurus libratus	(254,277,278)	2513.39	NA	(195,210,279)	(210,277,280–283)
G. libratus (juvenile)	(284); same as adults	335	NA	(210)	(210,280,283,284)
G. libratus (young juvenile)	Same as adults	34.79	NA	(186,285)	(277,280,283)
Daspletosaurus torosus	(254,277,278)	2744.971	NA	(268,277,285); this study	(210,277,280–283)

D. torosus (juvenile)	Same as adults	423.33	NA	(186,285); this study	Same as *Gorgosaurus*
D. torosus (young juvenile)	Same as adults	30.13	NA	(186,285)	Same as *Gorgosaurus*
Daspletosaurus sp.	(254,277,278)	2989.271	NA	(268,285); this study	(210,277,280–283)
Daspletosaurus sp. (juvenile)	Same as adults	461	NA	(186,285); this study	Same as *Gorgosaurus*
Daspletosaurus sp. (young juvenile)	Same as adults	32.81	NA	(186,285)	Same as *Gorgosaurus*

Serengeti ecological network

*Species/life stages included in cenogram and histogram but not in food web

Scientific name	Common name	Body mass (kg)	Body mass reference	Trophic interaction references
Thripidae	Thrips	NA	NA	(51)
Coleoptera	Rove- and ground beetles	0.0019	(50)	(51)
Araneidae	Orb-weaver spiders	NA	(44)	(51)
Formicidae	Ants	0.0007	(50)	(51)
Hodotermes sp.	Harvester termites	0.0000075	(46)	(51)
Diptera	Flies	0.00016517	(44)	(51)
Orthoptera	Crickets	0.0038951	(44)	(51)
Heteroptera	Herbivorous true bugs	0.00094	(50)	(51)
Tettigoniidae	Katydids	NA	(44)	(51)
Mantidae	Praying mantids	NA	(44)	(51)
Chilopoda	Centipedes	NA	(44)	(51)
Blattodea	Cockroaches	0.005	(50)	(51)
Phrynobatrachus mababiensis	Dwarf puddle frog	0.11	(74)	(51)
Diplopoda	Millipedes	0.00075	(46)	(51)
Crocidura sp.	Shrew	0.01	(286)	(51)
Pipistrellus nanus	Banana pipistrelle	0.01	(287)	(51)
Scorpiones	Scorpions	NA	NA	(51)
Empidonax wrightii	Gray flycatcher	0.01	(286)	(51)
Apalis flavida	Yellow-breasted apalis	0.01	(74)	(51)
Eremomela icteropygialis	Yellow-bellied eremomela	0.01	(74)	(51)
Sylvietta whytii	Red-faced crombec	0.01	(74)	(51)
Charadrius tricollaris	Three-banded plover	0.04	(74)	(51)
Micropteropus pusillus	Dwarf epauletted fruit bat	0.04	(287)	(51)
Rhabdomys pumilio	Four-striped grass mouse	0.04	(288)	(289)
Steatomys pratensis	Fat mouse	0.03	(287)	(51)
Xenopus muelleri	Mueller’s clawed frog	0.08	(74)	(51)

Anas capensis	Cape teal	0.59	(290)	(51)
Lydodactylus capensis	Cape dwarf gecko	0.18	(74)	(51)
Decapoda	Crabs	NA	NA	(51)
Pelomys fallax	Creek rat	0.15	(287)	(51)
Perciformes	Fish e.g. catfish	NA	NA	(51)
Psammophis angolensis	Dwarf sand snake	0.512	(286)	(51)
Glaucidium perlatum	Pearl-spotted owlet	0.09	(74)	(51)
Pterocles gutturalis	Yellow-throated sandgrouse	0.4	(74)	(51)
Poecilogale albinucha	Striped weasel	0.31	(288)	(51)
Pedetes capensis	East African spring hare	4	(287)	(289)
Tockus nasutus epirhinus	African grey hornbill	NA	NA	(51)
Francolinus coqui	Coqui francolin	NA	NA	(51)
*Mungos mungo**	Banded mongoose	1.26	(288)	(287)
Rhamphiophis oxyrhynchus	Rufous beaked snake	1.528	(286)	(51)
Atelerix albiventris	Four-toed African hedgehog	1.6	(287)	(51)
*Genetta genetta**	Common genet	1.756	(288)	(287)
*Lepus saxatilis victoriae**	Savanna hare	1.764	(288)	(287)
*Genetta maculate**	Blotched genet	1.95	(288)	(287)
Tachybaptus ruficollis	Little grebe	0.15	(290)	(51)
Eupodottis senegalensis	White-bellied bustard	1	(74)	(51)
*Nandinia binotata**	Tree civet	2.167	(288)	(287)
Heterohyrax brucei	Bush hyrax	2.45	(288)	(51)
Procavia johnstoni	Rock hyrax	2.95	(288)	(289)
Asio capensis	African marsh owl	0.39	(74)	(51)
Helogale parvula	Dwarf mongoose	0.3	(74)	(51)
Necrosyrtes monachus	Hooded vulture	2.25	(290)	(51)
Pronolagus rupestris	Smith's red rock hare	2.25	(74)	(51)
*Herpestes ichneumon**	Ichneumon mongoose	2.98	(288)	(287)
*Atilax paludinosus**	Marsh mongoose	3.6	(288)	(287)
*Ichneumia albicauda**	White-tailed mongoose	3.628	(288)	(287)
Haliaeetus vocifer	African fish eagle	3.63	(290)	(51)
Otolemur crassicaudatus	Greater bush baby	1.1	(287)	(51)
Leptoptilos crumeniferus	Marabou stork	8.9	(290)	(51)
Bucorvus leadbeateri	Southern ground hornbill	6.18	(74)	(51)
Otocyon megalotis	Bat-eared fox	4.098	(288)	(51)
*Felis silvestris lybica**	East African wild cat	4.573	(288)	(287)
*Cercopithecus mitis albogularis**	Sykes' monkey	5.041	(288)	(287)
*Chlorocebus pygerythrus**	Vervet monkey	5.3	(288)	(287)

Lutra maculicollis	Spot-necked otter	6.5	(287)	(51)
*Proteles cristatus**	Aardwolf	8.139	(288)	(287)
Psammobates pardalis	Leopard tortoise	18	(291)	(51)
Gyps africanus	White-backed vulture	7.2	(290)	(51)
Gyps rueppellii	Lappet-faced vulture	8.5	(290)	(51)
*Mellivora capensis**	Honey badger	9	(288)	(287)
Varanus niloticus	Nile monitor lizard	22.4	(74)	(51)
Ardeotis kori	Kori bustard	15.2	(74)	(51)
Colobus guereza	Black-and-white colobus monkey	9.93	(288)	(51)
Canis mesomelas	Black-backed jackal	8.43	(288)	(51,289)
Canis aureus	Common jackal	9.66	(288)	(289)
*Canis adustus**	Side-striped jackal	10.392	(288)	(287)
Smutsia temminckii	Ground pangolin	11.9	(288)	(51)
Leptailurus serval	Serval cat	12	(288)	(51,289)
Aonyx capensis	African clawless otter	19.32	(288)	(51)
Caracal caracal	Caracal	13.75	(74)	(289)
Papio anubis	Olive baboon	17.73	(288)	(289)
Madoqua kirkii	Kirk’s dikdik	5.3	(74)	(51)
*Raphicerus campestris**	Steenbok	11.662	(288)	(287)
*Civettictis civetta**	African civet	12.076	(288)	(287)
*Oreotragus oreotragus**	Klipspringer	13.487	(288)	(287)
Hystrix cristata	Crested porcupine	14.9	(288)	(51)
*Sylvicapra grimmia**	Gray duiker	15.639	(288)	(287)
Ourebia ourebi	Oribi	17.19	(288)	(51)
Gazella thomsoni	Thomson’s gazelle	20.5	(74)	(289)
Lycaon pictus	African wild dog	22	(288)	(51,289)
Dendroaspis polylepis	Black mamba	30.76	(74)	(51)
Hyaena hyaena	Striped hyena	35.07	(288)	(51,287)
Crocuta crocuta	Spotted hyena	63.37	(288)	(289)
Orycteropus afer	Aardvark	56.18	(288)	(51)
Acinonyx jubatus	Cheetah	50.58	(288)	(289)
Panthera pardus	Leopard	55	(74)	(51,289)
Tragelaphus scriptus	Bushbuck	43.25	(74)	(289)
Redunca redunca	Bohor reedbuck	58.06	(288)	(51)
Gazella granti	Grant’s gazelle	55	(74)	(289)
Aepyceros melampus	Impala	52.59	(288)	(289)
Phacochoerus africanus	Common warthog	82.5	(74)	(289)
Potamochoerus larvatus	Bushpig	97.5	(74)	(51,289)

*Tragelaphus imberbis**	Lesser kudu	94.32	(288)	(287)
Struthio camelus	Ostrich	145	(290)	(51)
Panthera leo	Adult lion	161.5	(74)	(51,289,292,293)
P. leo (juvenile)	Juvenile lion	66 (18 months)	(287,294)	(51,289,292,293)
P. leo (young juvenile)	Young juvenile lion	33 (8 months)	(287,294)	(51,289,292,293)
Damaliscus lunatus	Topi	127.19	(288)	(51)
Alcelaphus buselaphus	Kongoni	160.94	(288)	(289)
Connochaetes taurinus	Brindled gnu (common wildebeest)	180	(74)	(289)
Kobus ellipsiprymnus	Waterbuck	210	(74)	(289)
*Hippotragus equinus**	Roan antelope	264.174	(288)	(287)
Equus burchelli	Plains zebra	400	(74)	(289)
Syncerus caffer	Buffalo	592.67	(288)	(51)
Taurotragus oryx	Common eland	570	(74)	(51)
Crocodilus niloticus	Nile crocodile	889.32	(74)	(51)
Giraffa camelopardalis	Maasai giraffe	964.65	(288)	(51)
Diceros bicornis	Black rhinoceros	1180.51	(74)	(51)
Hippopotamus amphibius	Hippopotamus	1536.31	(288)	(51)
Loxodonta africana	African elephant	3940	(74)	(51)

Komodo ecological network

Scientific name	Common name	Body mass	Body mass reference	Trophic interaction references
Fungi	Fungi	NA	NA	(1)
Demospongiae	Sponges	NA	NA	(1)
Medusozoa	Jellyfish	NA	NA	(295)
Asperitas trochus	Land snails	NA	NA	(39)
Bivalvia	Marine clam	NA	NA	(33)
Branchiopoda	Zooplankton	NA	NA	(1)
Diplopoda	Millipedes	0.00075	(46)	(47)
Odonata	Dragonflies	0.0003673	(44)	(1,49)
Gastrimargus lumbokensis	Crickets	0.0038951	(44)	(51)
Stenocatanops exinsula	Crickets	0.0038951	(44)	(51)
Valanga nigricornis	Crickets	0.0038951	(44)	(51)
Austracris guttulosa	Crickets	0.0038951	(44)	(51)
Blattodea	Cockroaches	0.005	(50)	(1)
Heteroptera	True bugs	0.00094	(50)	(1)
Trox sp.	Carrion beetle	NA	NA	(296)
Scarabidae indet	Carrion beetle	NA	NA	(296)
Coleoptera (other)	Beetles	0.0019	(50)	(1)
Diptera	Flies	0.00016517	(44)	(1)
Araneidae	Spiders	NA	NA	(1)
Brachyura	Crabs	NA	NA	(51)
Teleostei	Fishes	NA	NA	(1,51)
Anura	Frogs	0.1	(74)	(1)
Gekko gecko	Tokay gecko	0.054	(286)	(297)
Hemidactylus frenatus	Common house gecko	0.0033	(286)	(298)
Hemidactylus platyurus	Flat-tailed house gecko	0.0038	(286)	(298)
Lepidodactylus intermedius	Scaly-toed gecko	NA	NA	(297)
Sphenomorphus melanopogon	Lesser Sunda dark-throated skink	NA	NA	(168)
Trimeresurus insularis	White-lipped pit viper	0.4145	(286)	(296,299)
Coelognathus subradiatus	Indonesian ratsnake	0.015	(286)	Same as other snakes
Dendrelaphis pictus	Common bronzeback	1.13	(286)	(300)
Naja sputatrix	Indonesian cobra	NA	NA	(296,301)
Daboia siamensis	Siamese Russell's viper	1.306	(286)	(296)
Eretmochelys imbricata	Hawksbill sea turtle	67	(286)	(302)
Megapodius reinwardt	Orange-footed scrubfowl	0.6964	(296)	(303)
Gallus varius	Green junglefowl	0.683	(296)	(296)

Geopelia maugeus	Barred dove	NA	NA	(304)
Ducula aenea	Green imperial pigeon	NA	NA	(304)
Corvus macrorhynchos	Large-billed crow	0.545	(286)	(296,305)
Haliastur indus	Brahminy kite	NA	NA	(296,306)
Icthyophaga leucogaster	White-bellied sea eagle	2.7515	(286)	(296,307)
Crocidura sp.	Shrew	0.01	(286)	(51)
Hipposideros diadema	Diadem roundleaf bat	0.05	(308)	(308)
Pteropus vampyrus	Large flying-fox	1.027	(288)	(296,309)
Mus musculus	House mouse	0.0215	(74)	(51)
Rattus sp.	Rats	0.28	(286)	(51)
Komodomys rintjanus	Komodo rat	0.2	(310)	(51)
Macaca fascicularis	Crab-eating macaque	4.569	(288)	(296,311)
Paradoxurus musangus	Southeast Asian palm civet	3.1	(296)	(296,312)
?*Arctogalidia* sp.	Small-toothed palm civet	2.5	(313)	(296,313)
Sus scrofa	Wild boar	50	(296)	(296)
Cervus timorensis	Rusa sambar deer	70	(296)	(296)
Bubalis bubalis	Water buffalo	400	(296)	(296)
Varanus komodoensis	Adult Komodo dragon	80	(175)	(175,296)
V. komodoensis (subadult)	Subadult Komodo dragon	25	(175)	(175,296)
V. komodoensis (juvenile)	Juvenile Komodo dragon	10	(175)	(175,296)
V. komodoensis (young juvenile)	Young juvenile Komodo dragon	1	(175)	(175,296)

Appendix VI references

1. Labandeira CC, Dunne JA. Data from: Highly resolved middle Eocene food webs show early development of modern trophic structure after the end-Cretaceous extinction [Internet]. Dryad Digital Repository; 2014. Available from: https://datadryad.org/stash/dataset/doi:10.5061/dryad.ps0f0
2. Chin K. The paleobiological implications of herbivorous dinosaur coprolites from the Upper Cretaceous Two Medicine Formation of Montana: why eat wood? PALAIOS. 2007;22(5):554–66.
3. Braman DR. Campanian Palynomorphs. In: Currie PJ, Koppelhus EB, editors. Dinosaur Provincial Park: A Spectacular Ancient Ecosystem Revealed. Bloomington: Indiana University Press; 2005. p. 101–30.
4. Jarzen DM. Palynology of Dinosaur Provincial Park (Campanian) Alberta. Syllogeus. 1982;38:1–69.
5. Raman A. Insect-bryophyte interactions: a little explored territory in the domain of insect-plant interactions: Current Science (00113891). Curr Sci 00113891. 2018 Aug 25;115(4):614–6.
6. Fuentes-Jacques LJ, Hanson-Snortum P, Hernández-Ortiz V, Díaz-Castelazo C, Mehltreter K. A global review and network analysis of phytophagous insect interactions with ferns and lycophytes. Plant Ecol. 2022 Jan 1;223(1):27–40.
7. Brown CM, Greenwood DR, Kalyniuk JE, Braman DR, Henderson DM, Greenwood CL, et al. Dietary palaeoecology of an Early Cretaceous armoured dinosaur (Ornithischia; Nodosauridae) based on floral analysis of stomach contents. R Soc Open Sci. 2020;7(6):200305.
8. Environment and Climate Change Canada. Engelmann's quillwort (*Isoetes engelmannii*): recovery strategy [Internet]. 2012 [cited 2024 Mar 22]. Available from: https://www.canada.ca/en/environment-climate-change/services/species-risk-public-registry/recovery-strategies/engelmanns-quillwort.html
9. Braman DR, Johnston PA, Haglund WM. Upper Cretaceous Paleontology, Stratigraphy and Depositional Environments at Dinosaur Provincial Park and Drumheller, Alberta. Drumheller, Alberta: Royal Tyrrell Museum of Palaeontology; 1995. 119 p. (Canadian Paleontology Conference Field Trip Guidebook 4, Canadian Paleontology Conference V).
10. Poinar, Jr. G. Insect Herbivores of Horsetails: Bionomics, Dispersal, and Co-Evolution. Am Entomol. 2014 Dec 1;60(4):235–40.
11. Schneider D, Wink M, Sporer F, Lounibos P. Cycads: their evolution, toxins, herbivores and insect pollinators. Naturwissenschaften. 2002 Jul 1;89(7):281–94.
12. Retallack GJ, Dilcher DL. Reconstructions of Selected Seed Ferns. Ann Mo Bot Gard. 1988;75(3):1010–57.
13. Sender LM, Wappler T, García-Ávila M, Santos AA, Diez JB. First plant-insect interactions on Cretaceous Caytoniales (genus *Sagenopteris*) from the Lower Cretaceous (Albian) of Spain. Cretac Res. 2022 Oct;138:105295.
14. Biological Records Centre. Biological Records Centre. 2024 [cited 2024 Mar 23]. BRC - Database of Insects and their Food Plants. Available from: https://dbif.brc.ac.uk/hosts.aspx

15. Ramanujam CGK. Fossil coniferous woods from the Oldman Formation (Upper Cretaceous) of Alberta. Can J Bot. 1972;50(3):595–602.
16. Currie PJ, Koppelhus EB, Muhammad AF. “Stomach” contents of a hadrosaur from the Dinosaur Park Formation (Campanian, Upper Cretaceous) of Alberta, Canada. In: Sun AL, Wang YQ, editors. Sixth Symposium on Mesozoic Terrestrial Ecosystems and Biota: Short Papers. Beijing: China Ocean Press; 1995. p. 111–4.
17. Bell WA. Uppermost Cretaceous and Paleocene Plants of Western Canada. Ottawa: Geological Survey of Canada, Paper 65-35; 1965. 46 p.
18. Koppelhus EB. Paleobotany. In: Currie PJ, Koppelhus EB, editors. Dinosaur Provincial Park: A Spectacular Ancient Ecosystem Revealed. Bloomington: Indiana University Press; 2005. p. 131–8.
19. Escapa I, Leslie A. A new Cheirolepidiaceae (Coniferales) from the Early Jurassic of Patagonia (Argentina): Reconciling the records of impression and permineralized fossils. Am J Bot. 2017;104(2):322–34.
20. Na YL, Sun CL, Wang H, Dilcher DL, Yang ZY, Li T, et al. Insect herbivory and plant defense on ginkgoalean and bennettitalean leaves of the Middle Jurassic Daohugou Flora from Northeast China and their paleoclimatic implications. Palaeoworld. 2018 Jun 1;27(2):202–10.
21. Wachtler M. Ginkgo from the Lower Jurassic of Middle Europe. In: Wachtler M, Wachtler N, editors. The Fossil Flora of Early Jurassic. Innichen, Italy: Dolomythos-Museum; 2024. p. 55–66.
22. Honda H. Ginkgo and Insects. In: Hori T, Ridge RW, Tulecke W, Del Tredici P, Trémouillaux-Guiller J, Tobe H, editors. *Ginkgo biloba*, A Global Treasure: From Biology to Medicine [Internet]. Tokyo: Springer Japan; 1997 [cited 2024 Mar 22]. p. 243–50. Available from: https://doi.org/10.1007/978-4-431-68416-9_19
23. Royer DL, Hickey LJ, Wing SL. Ecological conservatism in the “living fossil” *Ginkgo*. Paleobiology. 2003;29(1):84–104.
24. Wooten RC, Crawford CS. Food, ingestion rates, and assimilation in the desert millipede *Orthoporus ornatus* (Girard) (Diplopoda). Oecologia. 1975 Sep 1;20(3):231–6.
25. Xu W, He Z, Wei C. A new cicada species of *Psalmocharias* Kirkaldy feeding on an *Ephedra* plant from China (Hemiptera: Cicadidae). Zootaxa. 2017 Jul 7;4290:367–72.
26. Gautier-Hion A, Duplantier JM, Quris R, Feer F, Sourd C, Decoux JP, et al. Fruit characters as a basis of fruit choice and seed dispersal in a tropical forest vertebrate community. Oecologia. 1985 Feb 1;65(3):324–37.
27. Woodland Trust. A-Z Guide - British Trees - Woodland Trust [Internet]. 2024 [cited 2024 Mar 25]. Available from: https://www.woodlandtrust.org.uk/trees-woods-and-wildlife/british-trees/a-z-of-british-trees/
28. Crowder AA, Pearson MC, Grubb PJ, Langlois PH. *Drosera* L. J Ecol. 1990;78(1):233–67.
29. Dray FA, Thompson CR, Habeck DH, Balciunas JK, Center TD. A survey of the fauna associated with *Pistia Stratiotes* L. (Waterlettuce) in Florida [Internet]. U.S. Army Engineer Waterways Experiment Station; 1988 Apr [cited 2024 Mar 25]. Available from: https://erdc-library.erdc.dren.mil/jspui/handle/11681/6310
30. Stockey RA, Rothwell GW, Johnson KR. *Cobbania corrugata* gen. et comb. nov. (Araceae): a floating aquatic monocot from the Upper Cretaceous of western North America. Am J Bot. 2007;94(4):609–24.

31. Johnston PA, Hendy AJW. Paleoecology of Mollusks from the Upper Cretaceous Belly River Group. In: Dinosaur Provincial Park: A Spectacular Ancient Ecosystem Revealed. Bloomington: Indiana University Press; 2005. p. 139–66.
32. Smithsonian Environmental Research Center. Nemesis. 2024 [cited 2024 Apr 6]. *Anomia simplex*. Available from: https://invasions.si.edu/nemesis/species_summary/79798
33. Cortés D, Larsson HCE. Top of the food chains: an ecological network of the marine Paja Formation biota from the Early Cretaceous of Colombia reveals the highest trophic levels ever estimated. Zool J Linn Soc. 2023 Sep 16;zlad092.
34. Zagata C, Young C, Sountis J, Kuehl M. Animal Diversity Web. 2008 [cited 2024 Mar 19]. *Mytilus edulis*. Available from: https://animaldiversity.org/accounts/Mytilus_edulis/
35. da Costa Fernandes F. *Brachidontes pharaonis*. CABI Compend. 2010 Jun 14;CABI Compendium:109127.
36. Tyler L. Marine Life Information Network. 2024 [cited 2024 Apr 6]. BIOTIC Species Information for *Mactra stultorum*. Available from: https://www.marlin.ac.uk/biotic/browse.php?sp=6364
37. Tyler L. Marine Life Information Network. 2024 [cited 2024 Apr 6]. BIOTIC Species Information for *Corbula gibba*. Available from: https://www.marlin.ac.uk/biotic/browse.php?sp=4397
38. Russell LS. *Prograngerella*, a New Ancestral Land Snail from the Upper Cretaceous of Alberta. J Paleontol. 1941;15(3):309–11.
39. VanVleet K. Animal Diversity Web. 2014 [cited 2024 Mar 19]. *Planogyra asteriscus*. Available from: https://animaldiversity.org/accounts/Planogyra_asteriscus/
40. Chin K, Hartman JH, Roth B. Opportunistic exploitation of dinosaur dung: fossil snails in coprolites from the Upper Cretaceous Two Medicine Formation of Montana. Lethaia. 2009 Jun;42(2):185–98.
41. Vullo R. Direct evidence of hybodont shark predation on Late Jurassic ammonites. Naturwissenschaften. 2011;98(6):545–9.
42. Kruta I, Landman N, Rouget I, Cecca F, Tafforeau P. The Role of Ammonites in the Mesozoic Marine Food Web Revealed by Jaw Preservation. Science. 2011;331(6013):70–2.
43. McKellar RC, Wolfe AP, Tappert R, Muehlenbachs K. Correlation of Grassy Lake and Cedar Lake ambers using infrared spectroscopy, stable isotopes, and palaeoentomology. Can J Earth Sci. 2008;45(9):1061–82.
44. Sohlström EH, Marian L, Barnes AD, Haneda NF, Scheu S, Rall BC, et al. Applying generalized allometric regressions to predict live body mass of tropical and temperate arthropods. Ecol Evol. 2018;8(24):12737–49.
45. Del-Claro K, Tizo-Pedroso E. Natural history and social behavior in neotropical pseudoscorpions. In: Oliveira PS, Rico-Gray V, editors. Tropical Biology and Conservation Management - Volume XI: Case Studies. Oxford: EOLSS Publications; 2009. p. 177–93.
46. Carbone C, Mace GM, Roberts SC, Macdonald DW. Energetic constraints on the diet of terrestrial carnivores. Nature. 1999 Nov;402(6759):286–8.
47. Hopkin SP, Read HJ. The Biology of Millipedes. Oxford University Press; 1992. 248 p.
48. Grimaldi DA, Engel MS. Evolution of the insects. Cambridge [U.K.] ; New York: Cambridge University Press; 2005. 755 p.

49. Kondratieff BC. Dragonflies and Damselflies (Odonata). In: Capinera JL, editor. Encyclopedia of Entomology [Internet]. Dordrecht: Springer Netherlands; 2008 [cited 2024 Mar 25]. p. 1242–6. Available from: https://doi.org/10.1007/978-1-4020-6359-6_986
50. Shine R. Food Habits, Habitats and Reproductive Biology of Four Sympatric Species of Varanid Lizards in Tropical Australia. Herpetologica. 1986;42(3):346–60.
51. de Visser SN, Freymann BP, Olff H. The Serengeti food web: empirical quantification and analysis of topological changes under increasing human impact. J Anim Ecol. 2011;80(2):484–94.
52. Scheffrahn RH. Termites (Isoptera). In: Capinera JL, editor. Encyclopedia of Entomology [Internet]. Dordrecht: Springer Netherlands; 2008 [cited 2024 Mar 25]. p. 3737–47. Available from: https://doi.org/10.1007/978-1-4020-6359-6_2400
53. Capinera JL. Grasshoppers, Katydids and Crickets (Orthoptera). In: Capinera JL, editor. Encyclopedia of Entomology [Internet]. Dordrecht: Springer Netherlands; 2008 [cited 2024 Mar 25]. p. 1694–712. Available from: https://doi.org/10.1007/978-1-4020-6359-6_1168
54. Baz A. Bark-Lice, Book-Lice or Psocids (Psocoptera). In: Capinera JL, editor. Encyclopedia of Entomology [Internet]. Dordrecht: Springer Netherlands; 2008 [cited 2024 Feb 19]. p. 381–99. Available from: https://doi.org/10.1007/978-1-4020-6359-6_236
55. McKellar RC, Jones E, Engel MS, Tappert R, Wolfe AP, Muehlenbachs K, et al. A direct association between amber and dinosaur remains provides paleoecological insights. Sci Rep. 2019;9(1):17916.
56. Riddick EW. Ground Beetle (Coleoptera: Carabidae) Feeding Ecology. In: Capinera JL, editor. Encyclopedia of Entomology [Internet]. Dordrecht: Springer Netherlands; 2008 [cited 2024 Mar 25]. p. 1742–7. Available from: https://doi.org/10.1007/978-1-4020-6359-6_1201
57. Chin K, Gill BD. Dinosaurs, Dung Beetles, and Conifers: Participants in a Cretaceous Food Web. PALAIOS. 1996;11(3):280–5.
58. Slack HD. The Food of Caddis Fly (Trichoptera) Larvae. J Anim Ecol. 1936;5(1):105–15.
59. Brinkman DB, Braman DR, Neuman AG, Ralrick PE, Sato T. A Vertebrate Assemblage from the Marine Shales of the Lethbridge Coal Zone. In: Currie PJ, Koppelhus EB, editors. Dinosaur Provincial Park: A Spectacular Ancient Ecosystem Revealed. Bloomington: Indiana University Press; 2005. p. 486–500.
60. Beavan NR, Russell AP. An elasmobranch assemblage from the terrestrial-marine transitional Lethbridge Coal Zone (Dinosaur Park Formation: Upper Campanian), Alberta, Canada. J Paleontol. 1999;73(3):494–503.
61. Brinkman DB. Paleoecology of the Judith River Formation (Campanian) of Dinosaur Provincial Park, Alberta, Canada: Evidence from vertebrate microfossil localities. Palaeogeogr Palaeoclimatol Palaeoecol. 1990;78(1):37–54.
62. Villalobos-Segura E, Stumpf S, Türtscher J, Jambura PL, Begat A, López-Romero FA, et al. A Synoptic Review of the Cartilaginous Fishes (Chondrichthyes: Holocephali, Elasmobranchii) from the Upper Jurassic Konservat-Lagerstätten of Southern Germany: Taxonomy, Diversity, and Faunal Relationships. Diversity. 2023 Mar;15(3):386.
63. Maisey JG. What is an 'elasmobranch'? The impact of palaeontology in understanding elasmobranch phylogeny and evolution. J Fish Biol. 2012;80(5):918–51.

64. Froese R, Pauly D. Fishbase. 2024 [cited 2023 Apr 5]. Species Summary: *Squatina squatina*. Available from: https://fishbase.se/summary/Squatina-squatina.html
65. Compagno LJV. FAO Species Catalogue. Sharks of the World. An Annotated and Illustrated Catalogue of Shark Species Known to Date. Volume 2. Bullhead, mackerel and carpet sharks (Heterodontiformes, Lamniformes and Orectolobiformes). Rome: Food & Agriculture Org.; 2002. 288 p.
66. Everhart MJ. Bite marks on an elasmosaur (Sauropterygia; Plesiosauria) paddle from the Niobrara Chalk (Upper Cretaceous) as probable evidence of feeding by the lamniform shark, *Cretoxyrhina mantelli*. PalArch Found. 2005;2(2):14–24.
67. Compagno LJV. FAO Species Catalogue. Vol. 4. Sharks of the World. An Annotated and Illustrated Catalogue of Shark Species Known to Date. Part 2 - Carcharhiniformes [Internet]. Rome: Food & Agriculture Org.; 1984. 655 p. Available from: http://ibimm.org.br/wp-content/uploads/2017/05/Sharks-of-The-World-VOL.4-PARTE-II.pdf
68. Neuman AG, Brinkman DB. Fishes of the Fluvial Beds. In: Currie PJ, Koppelhus EB, editors. Dinosaur Provincial Park: A Spectacular Ancient Ecosystem Revealed. Bloomington: Indiana University Press; 2005. p. 167–85.
69. Sullivan T. Florida Museum - Discover Fishes. 2023 [cited 2023 Jun 8]. *Rhinobatos lentiginosus*. Available from: https://www.floridamuseum.ufl.edu/discover-fish/species-profiles/rhinobatos-lentiginosus/
70. Froese R, Pauly D. Fishbase. 2024 [cited 2023 Apr 5]. Species Summary: *Rhinobatos rhinobatos*. Available from: https://fishbase.se/summary/Rhinobatos-rhinobatos.html
71. Froese R, Pauly D. Fishbase. 2024 [cited 2023 May 14]. Species Summary: *Pristis pristis*. Available from: https://www.fishbase.se/summary/8940
72. Froese R, Pauly D. Fishbase. 2024 [cited 2023 May 14]. Species Summary: *Chimaera monstrosa*. Available from: https://fishbase.se/summary/Chimaera-monstrosa.html
73. Sato H, Murray AM, Vernygora O, Currie PJ. A rare, articulated sturgeon (Chondrostei: Acipenseriformes) from the Upper Cretaceous of Dinosaur Provincial Park, Alberta, Canada. J Vertebr Paleontol. 2018;38(4):(1)-(15).
74. Hone DWE, O'Gorman EJ. Data from: Body Size Distribution of the Dinosaurs [Internet]. figshare; 2013 [cited 2023 Apr 4]. Available from: http://dx.doi.org/10.6084/m9.figshare.627530
75. Scott WB, Crossman EJ. Freshwater fishes of Canada [Internet]. Bulletin, Fisheries Board of Canada; 1973. 966 p. Available from: https://publications.gc.ca/site/eng/9.870340/publication.html
76. Jerome J. Animal Diversity Web. 2004 [cited 2024 Feb 19]. *Polyodon spathula* (American paddlefish). Available from: https://animaldiversity.org/accounts/Polyodon_spathula/
77. Froese R, Pauly D. Fishbase. 2024 [cited 2024 Apr 5]. Species Summary: *Polyodon spathula*. Available from: https://fishbase.mnhn.fr/summary/174
78. Hoxmeier RHJ, Devries DR. Habitat Use, Diet, and Population Structure of Adult and Juvenile Paddlefish in the Lower Alabama River. Trans Am Fish Soc. 1997;126(2):288–301.
79. Rudy B. Animal Diversity Web. 2003 [cited 2024 Feb 19]. *Lepisosteus osseus* (Gar). Available from: https://animaldiversity.org/accounts/Lepisosteus_osseus/

80. Echelle AA. Food Habits of Young-of-Year Longnose Gar in Lake Texoma, Oklahoma. Southwest Nat. 1968;13(1):45–50.
81. Brito PM. Révision des Aspidorhynchidae (Pisees, Actinopterygii) du Mésozoïque: ostéologie, relations phylogénétiques, données environnementales et biogéographiques. Geodiversitas. 1997;19(4):681–772.
82. Kogan I, Licht M. A *Belonostomus tenuirostris* (Actinopterygii: Aspidorhynchidae) from the Late Jurassic of Kelheim (southern Germany) preserved with its last meal. Paläontol Z. 2013;87(4):543–8.
83. Chida M, Brinkman DB, Murray AM. A large, new dercetid fish (Teleostei: Aulopiformes) from the Campanian Bearpaw Formation of Alberta, Canada. Cretac Res. 2023 Oct 1;150:105579.
84. Everhart MJ. *Enchodus* sp. The sabre-toothed fish of the Cretaceous [Internet]. 2013 [cited 2023 May 15]. Available from: http://oceansofkansas.com/Enchodus.html
85. Brinkman DB. Teleost abdominal centra from the Belly River Group of Alberta, Canada. Paludicola. 2019;12(3):109–52.
86. Bardack D. A New Teleost from the Oldman Formation (Cretaceous) of Alberta [Internet]. Vol. Publications in Palaeontology 3. National Museums of Canada; 1970. 8 pp. Available from: https://www.biodiversitylibrary.org/item/111125
87. Luna S, Reyes R, Froese R. Species Summary: *Megalops atlanticus* [Internet]. 2005 [cited 2024 Apr 2]. Available from: https://fishbase.mnhn.fr/summary/Megalops-atlanticus.html
88. Reeves S. Animal Diversity Web. 2011 [cited 2024 Apr 3]. *Albula vulpes* (Macabi). Available from: https://animaldiversity.org/accounts/Albula_vulpes/
89. Estes R. Studies on Fossil Phyllodont Fishes: Interrelationships and Evolution in the Phyllodontidae (Albuloidei). Copeia. 1969;1969(2):317–31.
90. Crabtree R, Stevens C, Snodgrass D, Stengard F. Feeding habits of bonefish, *Albula vulpes* from waters of the Florida Keys. Fish Bull. 1998;96(4):754–66.
91. Froese R, Pauly D. Fishbase. 2024 [cited 2024 Apr 2]. Species Summary: *Scleropages jardinii*. Available from: https://fishbase.mnhn.fr/summary/Scleropages-jardinii.html
92. Guo-Qing L. A new species of Late Cretaceous osteoglossid (Teleostei) from the Oldman Formation of Alberta, Canada, and its phylogenetic relationships. In: Arratia G, Viohl G, editors. Mesozoic Fishes: Systematics and Paleoecology. Munich: Verlag Dr. Friedrich Pfeil; 1996. p. 285–98.
93. Grande L. Paleontology of the Green River Formation, with a review of the fish fauna. Second edition. Laramie, Wyoming: The Geological Survey of Wyoming; 1984. 333 p.
94. Newbrey MG, Wilson MVH, Ashworth AC. Centrum growth patterns provide evidence for two small taxa of Hiodontidae in the Cretaceous Dinosaur Park Formation. Can J Earth Sci. 2007 Jun 29;44(6):721–32.
95. Newbrey MG, Murray AM, Brinkman DB, Wilson MVH, Neuman AG. A new articulated freshwater fish (Clupeomorpha, Ellimmichthyiformes) from the Horseshoe Canyon Formation, Maastrichtian, of Alberta, Canada. Can J Earth Sci. 2010 Sep 21;47(9):1183–96.
96. Grande L, Grande T. A new species of †*Notogoneus* (Teleostei: Gonorynchidae) from the Upper Cretaceous Two Medicine Formation of Montana, and the poor Cretaceous record of freshwater fishes from North America. J Vertebr Paleontol. 1999 Dec 13;19(4):612–22.

97. Froese R, Pauly D. Species Summary: *Gonorynchus gonorynchus* [Internet]. 2024 [cited 2024 Apr 2]. Available from: https://fishbase.mnhn.fr/summary/Gonorynchus-gonorynchus.html
98. Newbrey MG, Murray AM, Wilson MVH, Brinkman DB, Neuman AG. Seventy-five-million-year-old tropical tetra-like fish from Canada tracks Cretaceous global warming. Proc R Soc B Biol Sci. 2009 Nov 7;276(1674):3829–33.
99. Froese R, Pauly D. Fishbase. 2024 [cited 2024 Apr 3]. Species Summary: *Charax pauciradiatus*. Available from: https://fishbase.mnhn.fr/summary/27858
100. Wilson MVH, Brinkman DB, Neuman AG. Cretaceous Esocoidei (Teleostei): early radiation of the pikes in North American fresh waters. J Paleontol. 1992;66(5):839–46.
101. Raney EC. The Summer Food and Habits of the Chain Pickerel (*Esox niger*) of a Small New York Pond. J Wildl Manag. 1942;6(1):58–66.
102. Gardner JD. Lissamphibians. In: Currie PJ, Koppelhus EB, editors. Dinosaur Provincial Park: A Spectacular Ancient Ecosystem Revealed. Bloomington: Indiana University Press; 2005. p. 186–201.
103. Wilson GP, DeMar DG Jr, Carter G. Extinction and survival of salamander and salamander-like amphibians across the Cretaceous-Paleogene boundary in northeastern Montana, USA. In: Wilson GP, Clemens WA, Horner JR, Hartman JH, editors. Through the End of the Cretaceous in the Type Locality of the Hell Creek Formation in Montana and Adjacent Areas [Internet]. Geological Society of America; 2014 [cited 2024 Mar 24]. p. 271–97. Available from: https://doi.org/10.1130/2014.2503(10)
104. Gardner JD. Albanerpetontid Amphibians from the Upper Cretaceous (Campanian and Maastrichtian) of North America. 2000;349–88.
105. McGowan G, Evans SE. Albanerpetontid amphibians from the Cretaceous of Spain. Nature. 1995;373(6510):143–5.
106. Wentz A. Animal Diversity Web. 2001 [cited 2024 Mar 12]. *Ambystoma tigrinum* (Eastern Tiger Salamander). Available from: https://animaldiversity.org/accounts/Ambystoma_tigrinum/
107. Estes R. A New Fossil Salamander from Montana and Wyoming. Copeia. 1965;1965(1):90–5.
108. Estes R. Middle Paleocene Lower Vertebrates from the Tongue River Formation, Southeastern Montana. J Paleontol. 1976;50(3):500–20.
109. Estes R. Lower Vertebrates from the Fort Union Formation, Late Paleocene, Big Horn Basin, Wyoming. Herpetologica. 1975;31(4):365–85.
110. Gardner JD. Revision of *Habrosaurus* Gilmore (Caudata; Sirenidae) and relationships among sirenid salamanders. Palaeontology. 2003;46(6):1089–122.
111. Hanlin HG. Food Habits of the Greater Siren, *Siren lacertina*, in an Alabama Coastal Plain Pond. Copeia. 1978;1978(2):358–60.
112. Gardner JD, Redman CM, Cifelli RL. The hopping dead: Late Cretaceous frogs from the middle – late Campanian (Judithian) of western North America. Foss Impr. 2016;72(1–2):78–107.
113. Gardner JD. An edentulous frog (Lissamphibia; Anura) from the Upper Cretaceous (Campanian) Dinosaur Park Formation of southeastern Alberta, Canada. Can J Earth Sci. 2015;52(8):569–80.
114. Stewart MM, Sandison P. Comparative Food Habits of Sympatric Mink Frogs, Bullfrogs, and Green Frogs. J Herpetol. 1972;6(3/4):241–4.

115. Porter G. Animal Diversity Web. 2023 [cited 2024 Mar 12]. *Lithobates clamitans* (Green Frog). Available from: https://animaldiversity.org/accounts/Lithobates_clamitans/
116. Paluh DJ, Riddell K, Early CM, Hantak MM, Jongsma GF, Keeffe RM, et al. Rampant tooth loss across 200 million years of frog evolution. Wittkopp PJ, editor. eLife. 2021 Jun 1;10:e66926.
117. Brinkman DB. Turtles: Diversity, Paleoecology, and Distribution. In: Currie PJ, Koppelhus EB, editors. Dinosaur Provincial Park: A Spectacular Ancient Ecosystem Revealed. Bloomington: Indiana University Press; 2005. p. 202–20.
118. Pough FH. The Advantages of Ectothermy for Tetrapods. Am Nat. 1980;115(1):92–112.
119. Meylan PA, Gaffney ES. The Skeletal Morphology of the Cretaceous Cryptodiran Turtle, *Adocus*, and the Relationships of the Trionychoidea. Am Mus Novit. 1989;2941:1–60.
120. Bishop ND, Polisar J, Eliazar PJ, Carthy RR, Bjorndal KA. Diet of *Dermatemys mawii*, an Aquatic Turtle That Relies Heavily on Terrestrial Vegetation. Chelonian Conserv Biol. 2022 Jun;21(1):37–45.
121. Gardner JD, Russell AP, Brinkman DB. Systematics and taxonomy of soft-shelled turtles (Family Trionychidae) from the Judith River Group (mid-Campanian) of North America. Can J Earth Sci. 1995;32(5):631–43.
122. Albers J. Animal Diversity Web. 2012 [cited 2024 Feb 14]. *Apalone mutica* (Smooth Softshelled Turtle). Available from: https://animaldiversity.org/accounts/Apalone_mutica/
123. Cochran PA, McConville DR. Feeding by *Trionyx spiniferus* in Backwaters of the Upper Mississippi River. J Herpetol. 1983;17(1):82–6.
124. Williams TA, Christiansen JL. The Niches of Two Sympatric Softshell Turtles, *Trionyx muticus* and *Trionyx spiniferus*, in Iowa. J Herpetol. 1981;15(3):303–8.
125. Meylan PA. Biology and Conservation of Florida Turtles. St. Petersburg, Florida: Ch-e-lon-ian Re-search Foun-da-tion; 2006.
126. Cadena E. *Palaeoamyda messeliana* nov. comb. (Testudines, Pan-Trionychidae) from the Eocene Messel Pit and Geiseltal localities, Germany, taxonomic and phylogenetic insights. PeerJ. 2016 Oct 27;4:e2647.
127. Stewart H. Animal Diversity Web. 2009 [cited 2024 Feb 14]. *Apalone ferox* (Florida Softshell Turtle). Available from: https://animaldiversity.org/accounts/Apalone_ferox/
128. Regis KW, Meik JM. Allometry of sexual size dimorphism in turtles: a comparison of mass and length data. PeerJ. 2017;5:e2914.
129. Aresco MJ, Gunzburger MS. Ecology and Morphology of *Chelydra serpentina* in Northwestern Florida. Southeast Nat. 2007 Sep;6(3):435–48.
130. Punzo F. Studies on the Feeding Behavior, Diet, Nesting Habits and Temperature Relationships of *Chelydra serpentina osceola* (Chelonia: Chelydridae). J Herpetol. 1975;9(2):207–10.
131. DiLaura P, Pruitt J, Munsey D, Good G, Meyer B, Urban K. Animal Diversity Web. 1999 [cited 2024 Feb 14]. *Macrochelys temminckii* (Alligator Snapping Turtle). Available from: https://animaldiversity.org/accounts/Macrochelys_temminckii/
132. Brinkman DB. Anatomy and systematics of *Plesiobaena antiqua* (Testudines; Baenidae) from the mid-Campanian Judith River Group of Alberta, Canada. J Vertebr Paleontol. 2003 Apr 11;23(1):146–55.
133. Donato M. Animal Diversity Web. 2000 [cited 2024 Apr 5]. *Graptemys geographica* (Common Map Turtle, Northern Map Turtle). Available from: https://animaldiversity.org/accounts/Graptemys_geographica/

134. Brinkman DB, Nicholls EL. Anatomy and relationships of the turtle *Boremys pulchra* (Testudines: Baenidae). J Vertebr Paleontol. 1991;11(3):302–15.
135. Brinkman DB, Nicholls EL. The skull of *Neurankylus eximius* (Testudines: Baenidae) and a reinterpretation of the relationships of this taxon. J Vertebr Paleontol. 1993;13(3):273–81.
136. Parham JF, Hutchison JH. A new eucryptodiran turtle from the Late Cretaceous of North America (Dinosaur Provincial Park, Alberta, Canada). J Vertebr Paleontol. 2003;23(4):783–98.
137. Brinkman DB, Densmore M, Rabi M, Ryan MJ, Evans DC. Marine turtles from the Late Cretaceous of Alberta, Canada. Can J Earth Sci. 2015 Aug 1;52(8):581–9.
138. Herbst P. Animal Diversity Web. 1999 [cited 2024 Mar 15]. *Lepidochelys olivacea* (Pacific Ridley; Olive Ridley Sea Turtle). Available from: https://animaldiversity.org/accounts/Lepidochelys_olivacea/
139. Gao KQ, Brinkman DB. Choristoderes from the Park and Its Vicinity. In: Currie PJ, Koppelhus EB, editors. Dinosaur Provincial Park: A Spectacular Ancient Ecosystem Revealed. Bloomington: Indiana University Press; 2005. p. 221–34.
140. Evans SE. The skull of *Cteniogenys*, a choristodere (Reptilia: Archosauromorpha) from the Middle Jurassic of Oxfordshire. Zool J Linn Soc. 1990 Jul;99(3):205–37.
141. Gao KQ, Ksepka DT. Osteology and taxonomic revision of *Hyphalosaurus* (Diapsida: Choristodera) from the Lower Cretaceous of Liaoning, China. J Anat. 2008 Jun;212(6):747–68.
142. Gao KQ, Fox RC. New choristoderes (Reptilia: Diapsida) from the Upper Cretaceous and Palaeocene, Alberta and Saskatchewan, Canada, and phylogenetic relationships of Choristodera. Zool J Linn Soc. 1998;124(4):303–53.
143. Russell LS. The Cretaceous reptile *Champsosaurus natator* Parks. Bull Natl Mus Can. 1956;145:1–51.
144. Matsumoto R, Fujiwara S ichi, Evans SE. Feeding behaviour and functional morphology of the neck in the long-snouted aquatic fossil reptile *Champsosaurus* (Reptilia: Diapsida) in comparison with the modern crocodilian *Gavialis gangeticus*. J Anat. 2022;240(5):893–913.
145. Dudgeon TW, Maddin HC, Evans DC, Mallon JC. The internal cranial anatomy of *Champsosaurus* (Choristodera: Champsosauridae): Implications for neurosensory function. Sci Rep. 2020 Apr 28;10(1):7122.
146. Erickson BR. Aspects of some anatomical structures of Champsosaurus (Reptilia: Eosuchia). J Vertebr Paleontol. 1985 Jun 1;5(2):111–27.
147. Whitaker R, Basu D. The Gharial *Gavialis gangeticus* - A Review. Bombay Nat Hist Soc J. 1982;79:531–48.
148. Bouchard K. Animal Diversity Web. 2009 [cited 2024 Apr 6]. *Gavialis gangeticus* (Gharial). Available from: https://animaldiversity.org/accounts/Gavialis_gangeticus/
149. Sato T, Eberth DA, Nicholls EL, Manabe M. Plesiosaurian Remains from Non-marine to Paralic Sediments. In: Currie PJ, Koppelhus EB, editors. Dinosaur Provincial Park: A Spectacular Ancient Ecosystem Revealed. Bloomington: Indiana University Press; 2005. p. 249–76.
150. Campbell JA, Mitchell MT, Ryan MJ, Anderson JS. A new elasmosaurid (Sauropterygia: Plesiosauria) from the non-marine to paralic Dinosaur Park Formation of southern Alberta, Canada. PeerJ. 2021;9:e10720.

151. Cicimurri DJ, Everhart MJ. An Elasmosaur with Stomach Contents and Gastroliths from the Pierre Shale (Late Cretaceous) of Kansas. Trans Kans Acad Sci. 2001;104(3):129–43.
152. Caldwell MW. The Squamates: Origins, Phylogeny, and Paleoecology. In: Currie PJ, Koppelhus EB, editors. Dinosaur Provincial Park: A Spectacular Ancient Ecosystem Revealed. Bloomington: Indiana University Press; 2005. p. 235–48.
153. Schulp AS, Vonhof HB, Lubbe JHJL van der, Janssen R, Baal RR van. On diving and diet: resource partitioning in type-Maastrichtian mosasaurs. Neth J Geosci. 2013 Sep;92(2–3):165–70.
154. Wu XC, Russell AP, Brinkman DB. A review of *Leidyosuchus canadensis* Lambe, 1907 (Archosauria: Crocodylia) and an assessment of cranial variation based upon new material. Can J Earth Sci. 2001;38(12):1665–87.
155. O'Brien HD, Lynch LM, Vliet KA, Brueggen J, Erickson GM, Gignac PM. Crocodylian Head Width Allometry and Phylogenetic Prediction of Body Size in Extinct Crocodyliforms. Integr Org Biol. 2019;1(1):1–15.
156. Saalfeld DT, Conway WC, Calkins GE. Food Habits of American Alligators (*Alligator mississippiensis*) in East Texas. Southeast Nat. 2011 Dec;10(4):659–72.
157. Shoop CR, Ruckdeschel CA. Alligators as Predators on Terrestrial Mammals. Am Midl Nat. 1990;124(2):407–12.
158. Hastings AK, Hellmund M. Evidence for prey preference partitioning in the middle Eocene high-diversity crocodylian assemblage of the Geiseltal-Fossillagerstätte, Germany utilizing skull shape analysis. Geol Mag. 2017 Jan;154(1):119–46.
159. Magnusson WE, da Silva EV, Lima AP. Diets of Amazonian Crocodilians. J Herpetol. 1987;21(2):85–95.
160. Erickson BR. *Albertochampsa langstoni*, gen. et. sp. nov., a new alligator from the Cretaceous of Alberta. Vol. 2. Saint Paul, Minnesota: The Science Museum of Minnesota; 1972. 13 p.
161. Wu XC. Crocodylians. In: Currie PJ, Koppelhus EB, editors. Dinosaur Provincial Park: A Spectacular Ancient Ecosystem Revealed. Bloomington: Indiana University Press; 2005. p. 277–91.
162. Brinkman DB. The skull and neck of the Cretaceous turtle *Basilemys* (Trionychoidea, Nanhsiungchelyidae), and the interrelationships of the genus. Paludicola. 1998;1(4):150–7.
163. Blake S, Tapia PI, Safi K, Ellis-Soto D. Chapter 11 - Diet, behavior, and activity patterns. In: Gibbs JP, Cayot LJ, Aguilera WT, editors. Galapagos Giant Tortoises [Internet]. Academic Press; 2021 [cited 2024 Mar 15]. p. 207–39. (Biodiversity of World: Conservation from Genes to Landscapes). Available from: https://www.sciencedirect.com/science/article/pii/B9780128175545000253
164. Grubb P. The growth, ecology and population structure of giant tortoises on Aldabra. Philos Trans R Soc Lond B Biol Sci. 1971 Mar 4;260(836):327–72.
165. Gao KQ, Fox RC. Taxonomy and evolution of Late Cretaceous lizards (Reptilia: Squamata) from Western Canada. Bull Carnegie Mus Nat Hist. 1996;33:1–107.
166. Longrich NR, Bhullar BAS, Gauthier JA. Mass extinction of lizards and snakes at the Cretaceous–Paleogene boundary. Proc Natl Acad Sci. 2012;109(52):21396–401.
167. Graham A. Animal Diversity Web. 2023 [cited 2024 Mar 18]. *Ophisaurus ventralis* (Eastern Glass Lizard). Available from: https://animaldiversity.org/accounts/Ophisaurus_ventralis/

168. Manicom C, Schwarzkopf L. Diet and prey selection of sympatric tropical skinks. Austral Ecol. 2011;36(5):485–96.
169. Vitt LJ, de Carvalho CM. Life in the trees: the ecology and life history of *Kentropyx striatus* (Teiidae) in the lavrado area of Roraima, Brazil, with comments on the life histories of tropical teiid lizards. Can J Zool. 1992;70(10):1995–2006.
170. Silva OD da, Costa TM da, Silva-Alves VD, Fermiano EC, Seba M de FR, Nogueira OM, et al. Diet and food ontogeny of the lizard *Tupinambis matipu* Silva et al. 2018 (Squamata: Teiidae) in Central Brazil. Res Soc Dev. 2020 Nov 25;9(11):e52391110073–e52391110073.
171. Ballinger RE, Lemos-Espinal J, Sanoja-Sarabia S, Coady NR. Ecological Observations of the Lizard, *Xenosaurus grandis* in Cuautlapan, Veracruz, Mexico. Biotropica. 1995;27(1):128–32.
172. Beck DD. Biology of Gila Monsters and Beaded Lizards. Berkeley & Los Angeles: University of California Press; 2005. 260 p.
173. Mazzotti FJ, Nestler JH, Cole JM, Closius C, Kern WH, Rochford MR, et al. Diet of Nile Monitors (*Varanus niloticus*) Removed from Palm Beach and Broward Counties, Florida, USA. J Herpetol. 2020 May;54(2):189–95.
174. Cross SL, Craig MD, Tomlinson S, Bateman PW. I don't like crickets, I love them: invertebrates are an important prey source for varanid lizards. J Zool. 2020;310(4):323–33.
175. Purwandana D, Ariefiandy A, Imansyah MJ, Seno A, Ciofi C, Letnic M, et al. Ecological allometries and niche use dynamics across Komodo dragon ontogeny. Sci Nat. 2016 Mar 2;103(3):27.
176. Karunarathna DMSS, Surasinghe T, Botejue M, Gabadage D, Dissanayake D. Dietary habits and the predators of the Bengal Monitor *Varanus bengalensis* in Sri Lanka. Biawak. 2017 Jun 30;11:28–39.
177. Hone DWE, Habib MB, Therrien F. *Cryodrakon boreas*, gen. et sp. nov., a Late Cretaceous Canadian azhdarchid pterosaur. J Vertebr Paleontol. 2019;39(3):e1649681.
178. Witton MP. A new approach to determining pterosaur body mass and its implications for pterosaur flight. Zitteliana. 2008;B28:143–58.
179. Witton MP, Naish D. A Reappraisal of Azhdarchid Pterosaur Functional Morphology and Paleoecology. PLOS ONE. 2008;3(5):e2271.
180. Brown CM, Evans DC, Ryan MJ, Russell AP. New data on the diversity and abundance of small-bodied ornithopods (Dinosauria, Ornithischia) from the Belly River Group (Campanian) of Alberta. J Vertebr Paleontol. 2013;33(3):495–520.
181. Brown CM, Evans DC, Campione NE, O'Brien LJ, Eberth DA. Evidence for taphonomic size bias in the Dinosaur Park Formation (Campanian, Alberta), a model Mesozoic terrestrial alluvial-paralic system. Palaeogeogr Palaeoclimatol Palaeoecol. 2013;372:108–22.
182. Hudgins MN, Currie PJ, Sullivan C. Dental assessment of *Stegoceras validum* (Ornithischia: Pachycephalosauridae) and *Thescelosaurus neglectus* (Ornithischia: Thescelosauridae): paleoecological inferences. Cretac Res. 2022;130:105058.
183. Wyenberg-Henzler T, Patterson RT, Mallon JC. Size-mediated competition and community structure in a Late Cretaceous herbivorous dinosaur assemblage. Hist Biol. 2021;34(11):2230–40.

184. Schott RK, Evans DC. Cranial variation and systematics of *Foraminacephale brevis* gen. nov. and the diversity of pachycephalosaurid dinosaurs (Ornithischia: Cerapoda) in the Belly River Group of Alberta, Canada. Zool J Linn Soc. 2017;179:865–906.

185. Dyer A, Powers M, Currie P. Problematic putative pachycephalosaurids: Synchrotron µCT imaging shines new light on the anatomy and taxonomic validity of *Gravitholus albertae* from the Belly River Group (Campanian) of Alberta, Canada. Vertebr Anat Morphol Palaeontol. 2022;10(1):65–110.

186. Schroeder K, Lyons SK, Smith FA. The influence of juvenile dinosaurs on community structure and diversity. Science. 2021;371(6532):941–4.

187. Seebacher F. A new method to calculate allometric length-mass relationships of dinosaurs. J Vertebr Paleontol. 2001;21:51–60.

188. Maryańska T, Chapman RE, Weishampel DB. Pachycephalosauria. In: Dodson P, Weishampel DB, Osmólska H, editors. The Dinosauria. Second Edition. Berkeley & Los Angeles: University of California Press; 2004. p. 464–77.

189. Gilmore CW. On *Troodon validus*, an ornithopodous dinosaur from the Belly River Cretaceous of Alberta, Canada. Bull Univ Alta Dep Geol. 1924;1:1–43.

190. Paul GS. The Princeton Field Guide to Dinosaurs: 2nd Edition [Internet]. 2nd Edition. Princeton: Princeton University Press; 2016 [cited 2023 May 5]. 360 p. (Princeton field guides). Available from: https://www.degruyter.com/document/doi/10.1515/9781400883141/html

191. Woodruff DC, Schott RK, Evans DC. Two new species of small-bodied pachycephalosaurine (Dinosauria, Marginocephalia) from the uppermost Cretaceous of North America suggest hidden diversity in well-sampled formations. Pap Palaeontol. 2023;9(6):e1535.

192. Ryan MJ, Evans DC, Currie PJ, Brown CM, Brinkman D. New leptoceratopsids from the Upper Cretaceous of Alberta, Canada. Cretac Res. 2012;35:69–80.

193. Varriale FJ. Dental microwear reveals mammal-like chewing in the neoceratopsian dinosaur *Leptoceratops gracilis*. PeerJ. 2016;4:e2132.

194. Cullen TM, Zanno L, Larson DW, Todd E, Currie PJ, Evans DC. Anatomical, morphometric, and stratigraphic analyses of theropod biodiversity in the Upper Cretaceous (Campanian) Dinosaur Park Formation. Can J Earth Sci. 2021;58(9):870–84.

195. Benson RBJ, Hunt G, Carrano MT, Campione N. Data from: Cope's rule and the adaptive landscape of dinosaur body size evolution [Internet]. Dryad; 2018 [cited 2023 Jun 13]. p. 10396132 bytes. Available from: https://datadryad.org/stash/dataset/doi:10.5061/dryad.1t3r4

196. Kobayashi Y, Lu JC, Dong ZM, Barsbold R, Azuma Y, Tomida Y. Herbivorous diet in an ornithomimid dinosaur. Nature. 1999 Dec;402(6761):480–1.

197. Barrett PM. The Diet of Ostrich Dinosaurs (theropoda: Ornithomimosauria). Palaeontology. 2005;48(2):347–58.

198. Russell DA. Ostrich Dinosaurs from the Late Cretaceous of Western Canada. Can J Earth Sci. 1972 Apr 1;9(4):375–402.

199. McFeeters B, Ryan MJ, Schröder-Adams C, Cullen TM. A new ornithomimid theropod from the Dinosaur Park Formation of Alberta, Canada. J Vertebr Paleontol. 2016 Nov 1;36(6):e1221415.

200. Christiansen P, Fariña † RA. Mass Prediction in Theropod Dinosaurs. Hist Biol. 2004 Jun 1;16(2–4):85–92.

201. McFeeters B, Ryan MJ, Schröder-Adams C, Currie PJ. First North American occurrences of *Qiupalong* (Theropoda: Ornithomimidae) and the palaeobiogeography of derived ornithomimids. FACETS. 2017 Jan 1;2:355–73.
202. Farlow JO, Coroian D, Currie PJ, Foster JR, Mallon JC, Therrien F. "Dragons" on the landscape: Modeling the abundance of large carnivorous dinosaurs of the Upper Jurassic Morrison Formation (USA) and the Upper Cretaceous Dinosaur Park Formation (Canada). Anat Rec. 2022;306(7):1669–96.
203. Longrich NR. A New, Large Ornithomimid from the Cretaceous Dinosaur Park Formation of Alberta, Canada: Implications for the Study of Dissociated Dinosaur Remains. Palaeontology. 2008;51(4):983–97.
204. Funston GF, Persons WS, Bradley GJ, Currie PJ. New material of the large-bodied caenagnathid *Caenagnathus collinsi* from the Dinosaur Park Formation of Alberta, Canada. Cretac Res. 2015;54:179–87.
205. Lamanna MC, Sues HD, Schachner ER, Lyson TR. A new large-bodied oviraptorosaurian theropod dinosaur from the latest Cretaceous of western North America. Plos One. 2014;9.
206. Funston GF. Caenagnathids of the Dinosaur Park Formation (Campanian) of Alberta, Canada: anatomy, osteohistology, taxonomy, and evolution. Vertebr Anat Morphol Palaeontol. 2020;8:105–53.
207. Funston GF, Currie PJ. A previously undescribed caenagnathid mandible from the late Campanian of Alberta, and insights into the diet of *Chirostenotes pergracilis* (Dinosauria: Oviraptorosauria). Can J Earth Sci. 2014 Feb 1;51(2):156–65.
208. Ji Q, Currie PJ, Norell MA, Ji SA. Two feathered dinosaurs from northeastern China. Nature. 1998 Jun;393(6687):753–61.
209. Ma W, Wang J, Pittman M, Tan Q, Tan L, Guo B, et al. Functional anatomy of a giant toothless mandible from a bird-like dinosaur: *Gigantoraptor* and the evolution of the oviraptorosaurian jaw. Sci Rep. 2017 Nov 24;7(1):16247.
210. Therrien F, Zelenitsky DK, Tanaka K, Voris JT, Erickson GM, Currie PJ, et al. Exceptionally preserved stomach contents of a young tyrannosaurid reveal an ontogenetic dietary shift in an iconic extinct predator. Sci Adv. 2023 Dec 8;9(49):eadi0505.
211. Larson DW, Currie PJ. Multivariate Analyses of Small Theropod Dinosaur Teeth and Implications for Paleoecological Turnover through Time. PLOS ONE. 2013;8(1):e54329.
212. Currie PJ, Rigby, Jr. JK, Sloan RE. Theropod teeth from the Judith River Formation of southern Alberta, Canada. In: Carpenter K, Currie PJ, editors. Dinosaur Systematics: Perspectives and Approaches [Internet]. Cambridge: Cambridge University Press; 1990. p. 107–25. Available from: https://books.google.ca/books?hl=en&lr=&id=6ZV1KcVNM18C&oi=fnd&pg=PA5&dq=Dinosaur+Systematics:+Perspectives+and+Approaches&ots=q3zk9WOdzd&sig=2f_JiPYBqqCG8FzBA3CeTgWvNIM&redir_esc=y#v=onepage&q=Dinosaur%20Systematics%3A%20Perspectives%20and%20Approaches&f=false
213. Sankey JT, Brinkman DB, Guenther M, Currie PJ. Small theropod and bird teeth from the late Cretaceous (late Campanian) Judith River Group, Alberta. J Paleontol. 2002;76(4):751–63.
214. Larson DW. Diversity and variation of theropod dinosaur teeth from the uppermost Santonian Milk River Formation (Upper Cretaceous), Alberta: a quantitative method

supporting identification of the oldest dinosaur tooth assemblage in Canada. Can J Earth Sci. 2008 Dec 1;45(12):1455–68.

215. Frederickson JA, Engel MH, Cifelli RL. Niche Partitioning in Theropod Dinosaurs: Diet and Habitat Preference in Predators from the Uppermost Cedar Mountain Formation (Utah, U.S.A.). Sci Rep. 2018 Dec 14;8(1):17872.

216. Cullen TM, Cousens BL. New biogeochemical insights into Mesozoic terrestrial paleoecology and evidence for omnivory in troodontid dinosaurs. GSA Bull [Internet]. 2023 Nov 15 [cited 2024 Feb 14]; Available from: https://doi.org/10.1130/B37077.1

217. Currie PJ. Bird-like characteristics of the jaws and teeth of troodontid theropods (Dinosauria, Saurischia). J Vertebr Paleontol. 1987;7(1):72–81.

218. Russell DA. A new specimen of *Stenonychosaurus* from the Oldman Formation (Cretaceous) of Alberta. Can J Earth Sci. 1969 Aug 1;6(4):595–612.

219. Torices A, Wilkinson R, Arbour VM, Ruiz-Omeñaca JI, Currie PJ. Puncture-and-Pull Biomechanics in the Teeth of Predatory Coelurosaurian Dinosaurs. Curr Biol. 2018 May 7;28(9):1467-1474.e2.

220. Freimuth WJ, Varricchio DJ, Brannick AL, Weaver LN, Wilson Mantilla GP. Mammal-bearing gastric pellets potentially attributable to *Troodon formosus* at the Cretaceous Egg Mountain locality, Two Medicine Formation, Montana, USA. Palaeontology. 2021;64(5):699–725.

221. Currie PJ. New information on the anatomy and relationships of *Dromaeosaurus albertensis* (Dinosauria: Theropoda). J Vertebr Paleontol. 1995;15(3):576–91.

222. Currie PJ, Jacobsen AR. An azhdarchid pterosaur eaten by a velociraptorine theropod. Can J Earth Sci. 1995 Jul 1;32(7):922–5.

223. Fowler DW, Freedman EA, Scannella JB, Kambic RE. The predatory ecology of *Deinonychus* and the origin of flapping in birds. Plos One. 2011;6.

224. Christiansen P. Strength indicator values of theropod long bones, with comments on limb proportions and cursorial potential. Gaia. 1998;15:241–55.

225. Currie PJ, Evans DC. Cranial Anatomy of New Specimens of *Saurornitholestes langstoni* (Dinosauria, Theropoda, Dromaeosauridae) from the Dinosaur Park Formation (Campanian) of Alberta. Anat Rec. 2020;303(4):691–715.

226. Longrich NR, Currie PJ. A microraptorine (Dinosauria–Dromaeosauridae) from the Late Cretaceous of North America. Proc Natl Acad Sci. 2009;106(13):5002–7.

227. Hone DWE, Alexander Dececchi T, Sullivan C, Xing X, Larsson HCE. Generalist diet of *Microraptor zhaoianus* included mammals. J Vertebr Paleontol. 2022 Aug 31;42(2):e2144337.

228. Longrich NR. An ornithurine-dominated avifauna from the Belly River Group (Campanian, Upper Cretaceous) of Alberta, Canada. Cretac Res. 2009;30(1):161–77.

229. Coleman TS, Boag DA. Canada goose foods: their significance to weight gain. Wildfowl. 1987;38:82–8.

230. Norell MA, Clarke JA. Fossil that fills a critical gap in avian evolution. Nature. 2001 Jan;409(6817):181–4.

231. Mohr SR, Acorn JH, Funston GF, Currie PJ. An ornithurine bird coracoid from the Late Cretaceous of Alberta, Canada. Can J Earth Sci. 2020;58(2):134–40.

232. Sankey JT, Brinkman DB, Fox RC, Eberth DA. Patterns of Distribution of Mammals in the Dinosaur Park Formation and Their Paleobiological Significance. In: Currie PJ,

Koppelhus EB, editors. Dinosaur Provincial Park: A Spectacular Ancient Ecosystem Revealed. Bloomington: Indiana University Press; 2005. p. 436–49.
233. Fox RC. Late Cretaceous Mammals. In: Currie PJ, Koppelhus EB, editors. Dinosaur Provincial Park: A Spectacular Ancient Ecosystem Revealed. Bloomington: Indiana University Press; 2005. p. 417–49.
234. Codron D, Carbone C, Müller DWH, Clauss M. Ontogenetic niche shifts in dinosaurs influenced size, diversity and extinction in terrestrial vertebrates. Biol Lett. 2012 Apr 18;8(4):620–3.
235. Robson SV. An Analysis of North American Taeniolabidoid Multituberculate (Mammalia, Allotheria) Dentitions Using Mammalian Dietary Proxies [Master's Thesis]. [Calgary]: University of Calgary; 2018.
236. Wilson GP, Evans AR, Corfe IJ, Smits PD, Fortelius M, Jernvall J. Adaptive radiation of multituberculate mammals before the extinction of dinosaurs. Nature. 2012 Mar;483(7390):457–60.
237. Wilson GP. Mammals across the K/Pg boundary in northeastern Montana, U.S.A.: dental morphology and body-size patterns reveal extinction selectivity and immigrant-fueled ecospace filling. Paleobiology. 2013;39(3):429–69.
238. Weaver LN, Wilson GP. Shape disparity in the blade-like premolars of multituberculate mammals: functional constraints and the evolution of herbivory. J Mammal. 2021 Aug 1;102(4):967–85.
239. Wilson GP. Data from: Mammals across the K/Pg boundary in northeastern Montana, U.S.A.: dental morphology and body-size patterns reveal extinction selectivity and immigrant-fueled ecospace filling [Internet]. Dryad; 2013 [cited 2023 Apr 4]. p. 15529899 bytes. Available from: http://datadryad.org/stash/dataset/doi:10.5061/dryad.gv06d
240. Montellano M, Weil A, Clemens WA. An exceptional specimen of *Cimexomys judithae* (Mammalia: Multituberculata) from the Campanian Two Medicine Formation of Montana, and the phylogenetic status of *Cimexomys*. J Vertebr Paleontol. 2000;20(2):333–40.
241. Fox RC. Mammals from the Upper Cretaceous Oldman Formation, Alberta. I. *Alphadon* Simpson (Marsupialia). Can J Earth Sci. 1979;16:91–102.
242. Gordon CL. A First Look at Estimating Body Size in Dentally Conservative Marsupials. J Mamm Evol. 2003 Jun 1;10(1):1–21.
243. Martina LS, Waters M. Animal Diversity Web. 2014 [cited 2024 Mar 7]. *Philander opossum* (gray four-eyed opossum). Available from: https://animaldiversity.org/accounts/Philander_opossum/
244. Scott CS, Fox RC. Review of Stagodontidae (Mammalia, Marsupialia) from the Judithian (Late Cretaceous) Belly River Group of southeastern Alberta, Canada. Can J Earth Sci. 2015;52(8):682–95.
245. Hopkins DD, Forbes RB. Dietary Patterns of the Virginia Opossum in an Urban Environment. The Murrelet. 1980;61(1):20–30.
246. Fox RC. Mammals from the Upper Cretaceous Oldman Formation, Alberta. V. *Eodelphis* Matthew, and the evolution of the Stagodontidae (Marsupialia). Can J Earth Sci. 1981;18(2):350–65.

247. Wilson GP, Ekdale EG, Hoganson JW, Calede JJ, Vander Linden A. A large carnivorous mammal from the Late Cretaceous and the North American origin of marsupials. Nat Commun. 2016 Dec 8;7:13734.
248. Fox RC. Mammals from the Upper Cretaceous Oldman Formation, Alberta. III. Eutheria. Can J Earth Sci. 1979;16:114–25.
249. Eberle JJ, Clemens WA, Erickson GM, Druckenmiller PS. A new tiny eutherian from the Late Cretaceous of Alaska. J Syst Palaeontol. 2023 Jan;21(1):2232359.
250. Manz CL, Bloch JI. Systematics and Phylogeny of Paleocene-Eocene Nyctitheriidae (Mammalia, Eulipotyphla?) with Description of a new Species from the Late Paleocene of the Clarks Fork Basin, Wyoming, USA. J Mamm Evol. 2015 Sep 1;22(3):307–42.
251. Manz CL, Chester SGB, Bloch JI, Silcox MT, Sargis EJ. New partial skeletons of Palaeocene Nyctitheriidae and evaluation of proposed euarchontan affinities. Biol Lett. 2015 Jan;11(1):20140911.
252. McCay TS, Storm GL. Masked Shrew (*Sorex cinereus*) Abundance, Diet and Prey Selection in an Irrigated Forest. Am Midl Nat. 1997;138(2):268–75.
253. Arbour VM, Currie PJ. *Euoplocephalus tutus* and the Diversity of Ankylosaurid Dinosaurs in the Late Cretaceous of Alberta, Canada, and Montana, USA. PLOS ONE. 2013;8(5):e62421.
254. Currie PJ, Russell DA. The Geographic and Stratigraphic Distribution of Articulated and Associated Dinosaur Remains. In: Currie PJ, Koppelhus EB, editors. Dinosaur Provincial Park: A Spectacular Ancient Ecosystem Revealed. Bloomington: Indiana University Press; 2005. p. 537–69.
255. Mallon JC. Competition structured a Late Cretaceous megaherbivorous dinosaur assemblage. Sci Rep. 2019;9(1):15447.
256. Mallon JC, Anderson JS. The Functional and Palaeoecological Implications of Tooth Morphology and Wear for the Megaherbivorous Dinosaurs from the Dinosaur Park Formation (Upper Campanian) of Alberta, Canada. PLOS ONE. 2014;9(6):e98605.
257. Molnar RE, Clifford HT. An ankylosaurian cololite from the Lower Cretaceous of Queensland, Australia. In: Carpenter K, editor. The Armored Dinosaurs. Indiana University Press; 2001. p. 399–412.
258. Mallon JC, Evans DC, Ryan MJ, Anderson JS. Feeding height stratification among the herbivorous dinosaurs from the Dinosaur Park Formation (upper Campanian) of Alberta, Canada. BMC Ecol. 2013 Apr 4;13(1):14.
259. Mallon JC, Anderson JS. Skull Ecomorphology of Megaherbivorous Dinosaurs from the Dinosaur Park Formation (Upper Campanian) of Alberta, Canada. PLoS ONE. 2013 Jul 10;8(7):e67182.
260. Maidment S, Henderson DM, Barrett PM. What drove reversions to quadrupedality in ornithischian dinosaurs? Testing hypotheses using centre of mass modelling. Naturwissenschaften. 101:989–1001.
261. Paul GS. Dinosaur models: the good, the bad, and using them to estimate the mass of dinosaurs. In: Wolberg DL, Stump E, Rosenberg GD, editors. Dinofest International. Phoenix: The Academy of Natural Sciences, Arizona State University; 1997. p. 129–42.
262. Mallon JC, Evans DC, Ryan MJ, Anderson JS. Megaherbivorous dinosaur turnover in the Dinosaur Park Formation (upper Campanian) of Alberta, Canada. Palaeogeogr Palaeoclimatol Palaeoecol. 2012 Sep 15;350–352:124–38.

263. Paul GS. The Princeton Field Guide to Dinosaurs: 1st Edition. 1st edition. Princeton: Princeton University Press; 2010.
264. Colbert EH. The weights of dinosaurs. Am Mus Novit. 1962;2076:1–16.
265. Tweet JS, Chin K, Braman DR, Murphy NL. Probable gut contents within a specimen of *Brachylophosaurus canadensis* (Dinosauria: Hadrosauridae) from the Upper Cretaceous Judith River Formation of Montana. PALAIOS. 2008;23(9):624–35.
266. Chin K, Feldmann RM, Tashman JN. Consumption of crustaceans by megaherbivorous dinosaurs: dietary flexibility and dinosaur life history strategies. Sci Rep. 2017;7(1):11163.
267. Eberth DA, Evans DC, Ramezani J, Kamo SL, Brown CM, Currie PJ, et al. Calibrating geologic strata, dinosaurs, and other fossils at Dinosaur Provincial Park (Alberta, Canada) using a new CA-ID-TIMS U–Pb geochronology. Can J Earth Sci. 2023 Dec 1;60(12):1627–46.
268. Campione NE. Package "MASSTIMATE." CRAN; 2020.
269. Wyenberg-Henzler T, Patterson RT, Mallon JC. Ontogenetic dietary shifts in North American hadrosaurids (Dinosauria: Ornithischia). Cretac Res. 2022;135:105177.
270. Ryan MJ, Russell AP. A new centrosaurine ceratopsid from the Oldman Formation of Alberta and its implications for centrosaurine taxonomy and systematics. Can J Earth Sci. 2005;42(7):1369–87.
271. Brown CM, Holmes R, Currie P. A subadult individual of *Styracosaurus albertensis* (Ornithischia: Ceratopsidae) with comments on ontogeny and intraspecific variation in Styracosaurus and Centrosaurus. Vertebr Anat Morphol Palaeontol. 2020;8:67–95.
272. Ryan MJ, Eberth DA, Brinkman DB, Currie PJ, Tanke DH. A New *Pachyrhinosaurus*-Like Ceratopsid from the Upper Dinosaur Park Formation (Late Campanian) of Southern Alberta, Canada. In: Ryan MJ, Eberth DA, Chinnery-Allgeier BJ, Ralrick PE, editors. New Perspectives on Horned Dinosaurs: The Royal Tyrrell Museum Ceratopsian Symposium. Bloomington: Indiana University Press; 2010. p. 141–55.
273. Farke AA, Ryan MJ, Barrett PM, Tanke DH, Braman DR, Loewen MA, et al. A New Centrosaurine from the Late Cretaceous of Alberta, Canada, and the Evolution of Parietal Ornamentation in Horned Dinosaurs. Acta Palaeontol Pol. 2011;56(4):691–702.
274. Ryan MJ, Evans DC, Currie PJ, Loewen MA. A new chasmosaurine from northern Laramidia expands frill disparity in ceratopsid dinosaurs. Naturwissenschaften. 2014;101(6):505–12.
275. Campbell JA, Ryan MJ, Schröder-Adams CJ, Holmes RB, Evans DC. Temporal range extension and evolution of the chasmosaurine ceratopsid *'Vagaceratops' irvinensis* (Dinosauria: Ornithischia) in the Upper Cretaceous (Campanian) Dinosaur Park Formation of Alberta. Vertebr Anat Morphol Palaeontol. 2019;7:83–100.
276. Currie PJ, Holmes RB, Ryan MJ, Coy C. A juvenile chasmosaurine ceratopsid (Dinosauria, Ornithischia) from the Dinosaur Park Formation, Alberta, Canada. J Vertebr Paleontol. 2016 Mar 3;36(2):e1048348.
277. Russell DA. Tyrannosaurs From the Late Cretaceous of Western Canada. National Museums of Canada, Publications in Palaeontology 1. Ottawa: National Museums of Canada; 1970. 34 p.
278. Currie PJ. Cranial anatomy of tyrannosaurid dinosaurs from the Late Cretaceous of Alberta,Canada. Acta Palaeontol Pol. 2003;48(2):191–226.

279. Snively E, O'Brien H, Henderson DM, Mallison H, Surring LA, Burns ME, et al. Lower rotational inertia and larger leg muscles indicate more rapid turns in tyrannosaurids than in other large theropods. PeerJ. 2019 Feb 21;7:e6432.
280. Therrien F, Zelenitsky DK, Voris JT, Tanaka K. Mandibular force profiles and tooth morphology in growth series of *Albertosaurus sarcophagus* and *Gorgosaurus libratus* (Tyrannosauridae: Albertosaurinae) provide evidence for an ontogenetic dietary shift in tyrannosaurids. Can J Earth Sci. 2021;58(9):812–28.
281. Jacobsen AR. Feeding behaviour of carnivorous dinosaurs as determined by tooth marks on dinosaur bones. Hist Biol. 1998 Jan;13(1):17–26.
282. Farlow JO, Pianka ER. Body Size Overlap, Habitat Partitioning and Living Space Requirements of Terrestrial Vertebrate Predators: Implications for the Paleoecology of Large Theropod Dinosaurs. Hist Biol. 2002 Mar 1;16(1):21–40.
283. Dececchi TA, Mloszewska AM, Jr TRH, Habib MB, Larsson HCE. The fast and the frugal: Divergent locomotory strategies drive limb lengthening in theropod dinosaurs. PLoS ONE. 2020 May 13;15(5):e0223698.
284. Voris JT, Zelenitsky DK, Therrien F, Ridgely RC, Currie PJ, Witmer LM. Two exceptionally preserved juvenile specimens of *Gorgosaurus libratus* (Tyrannosauridae, Albertosaurinae) provide new insight into the timing of ontogenetic changes in tyrannosaurids. J Vertebr Paleontol. 2022;41(6):e2041651.
285. Erickson GM, Makovicky PJ, Currie PJ, Norell MA, Yerby SA, Brochu CA. Gigantism and comparative life-history parameters of tyrannosaurid dinosaurs. Nature. 2004 Aug;430(7001):772.
286. Myhrvold N, Baldridge E, Chan B, Sivam D, Freeman DL, Ernest SKM. Data from: An amniote life-history database to perform comparative analyses with birds, mammals, and reptiles [Internet]. Figshare; 2016 [cited 2024 Mar 21]. Available from: https://figshare.com/collections/An_amniote_life-history_database_to_perform_comparative_analyses_with_birds_mammals_and_reptiles/3308127
287. Kingdon J. The Kingdon field guide to African mammals. Second edition. Princeton, NJ: Princeton University Press; 2015. 640 p.
288. Jones KE, Bielby J, Cardillo M, Fritz SA, O'Dell J, Orme DL. PanTHERIA: a species-level database of life history, ecology, and geography of extant and recently extinct mammals [Internet]. Wiley; 2016 [cited 2024 Jan 29]. Available from: https://figshare.com/collections/PanTHERIA_a_species-level_database_of_life_history_ecology_and_geography_of_extant_and_recently_extinct_mammals/3301274
289. Baskerville EB, Dobson AP, Bedford T, Allesina S, Anderson TM, Pascual M. Spatial Guilds in the Serengeti Food Web Revealed by a Bayesian Group Model. PLOS Comput Biol. 2011 Dec 29;7(12):e1002321.
290. Dunning Jr JB. CRC Handbook of Avian Body Masses. CRC Press; 2008. 668 p.
291. Baker HH, Grubb JN. Animal Diversity Web. 2011 [cited 2024 Jul 21]. *Psammobates pardalis* (Leopard Tortoise). Available from: https://animaldiversity.org/accounts/Psammobates_pardalis/
292. Harrington E. Animal Diversity Web. 2004 [cited 2024 Aug 1]. *Panthera leo* (lion). Available from: https://animaldiversity.org/accounts/Panthera_leo/

293. Bothma J d. P, Walker C. The African lion. In: Larger Carnivores of the African Savannas. Berlin, Heidelberg: Springer; 1999. p. 23–59.
294. Smuts GL, Robinson GA, Whyte IJ. Comparative growth of wild male and female lions (*Panthera leo*). J Zool. 1980;190(3):365–73.
295. Graham WM, Kroutil RM. Size-based Prey Selectivity and Dietary Shifts in the Jellyfish, *Aurelia aurita*. J Plankton Res. 2001 Jan 1;23(1):67–74.
296. Auffenberg W. The Behavioral Ecology of the Komodo Monitor. Gainesville: University Presses of Florida; 1981. 406 p.
297. Aowphol A, Thirakhupt K, Nabhitabhata J, Voris HK. Foraging ecology of the Tokay gecko, *Gekko gecko* in a residential area in Thailand. Amphib-Reptil. 2006;27(4):491–503.
298. Wu K. Animal Diversity Web. 2017 [cited 2024 Mar 19]. *Hemidactylus frenatus* (Chichak, Common House Gecko). Available from: https://animaldiversity.org/accounts/Hemidactylus_frenatus/
299. Orlov N, Ananjeva N, Barabanov A, RYABOV S, KHALIKOV R. Diversity of vipers (Azemiopinae, Crotalinae) in East, Southeast, and South Asia: annotated checklist and natural history data (Reptilia: Squamata: Serpentes: Viperidae). Faun Abh Staatl Mus Für Tierkd Dresd. 2002 Nov 15;23:177–218.
300. Vogel G, van Rooijen J. Contributions to a review of the *Dendrelaphis pictus* (Gmelin, 1789) complex - 2. the eastern forms (Serpentes: Colubridae). Herpetozoa. 2008;21(1/2):3–29.
301. Ramirez J. Animal Diversity Web. 2001 [cited 2024 Mar 19]. *Naja naja* (Indian Cobra). Available from: https://animaldiversity.org/accounts/Naja_naja/
302. Edelman M. Animal Diversity Web. 2004 [cited 2024 Mar 19]. *Eretmochelys imbricata* (Hawksbill). Available from: https://animaldiversity.org/accounts/Eretmochelys_imbricata/
303. Howard L. Animal Diversity Web. 2004 [cited 2024 Mar 19]. Megapodiidae (megapodes). Available from: https://animaldiversity.org/accounts/Megapodiidae/
304. Smith B. Animal Diversity Web. 2022 [cited 2024 Mar 19]. *Streptopelia turtur* (European turtle dove). Available from: https://animaldiversity.org/accounts/Streptopelia_turtur/
305. Kurosawa R, Kono R, Kondo T, Kanai Y. Diet of Jungle Crows in an Urban Landscape. Glob Environ Res. 2003;7:193–8.
306. Manakadan R, Natarajan V. Brahminy Kite *Haliastur indus* (Boddaert) preying on bats. J Bombay Nat Hist Soc. 1949;89(3):367.
307. Corbett L, Hertog T. Diet and breeding of White-bellied Sea-Eagles *Haliaeetus leucogaster* in subtropical river habitats in the Northern Territory, Australia. Corella. 2011;37(2):41–8.
308. Pavey CR, Burwell CJ. The diet of the diadem leaf-nosed bat, *Hipposideros diadema*: confirmation of a morphologically-based prediction of carnivory. J Zool. 1997;243(2):295–303.
309. Kunz TH, Jones DP. *Pteropus vampyrus*. Mamm Species. 2000;642:1–6.
310. Veatch EG, Tocheri MW, Sutikna T, McGrath K, Wahyu Saptomo E, Jatmiko, et al. Temporal shifts in the distribution of murine rodent body size classes at Liang Bua (Flores, Indonesia) reveal new insights into the paleoecology of *Homo floresiensis* and associated fauna. J Hum Evol. 2019 May 1;130:45–60.

311. Bonadio C. Animal Diversity Web. 2000 [cited 2024 Jul 21]. *Macaca fascicularis* (long-tailed macaque). Available from: https://animaldiversity.org/accounts/Macaca_fascicularis/
312. Nelson J. Animal Diversity Web. 2013 [cited 2024 Mar 19]. *Paradoxurus hermaphroditus* (Asian palm civet). Available from: https://animaldiversity.org/accounts/Paradoxurus_hermaphroditus/
313. Bauer C. Animal Diversity Web. 2013 [cited 2024 Mar 19]. *Arctogalidia trivirgata* (small-toothed palm civet). Available from: https://animaldiversity.org/accounts/Arctogalidia_trivirgata/

BIBLIOGRAPHY

AGRAWAL, A. A. and ZHANG, X. 2021. The evolution of coevolution in the study of species interactions. *Evolution*, **75**, 1594–1606.

ALBERS, J. 2012. Apalone mutica *(Smooth Softshelled Turtle)*. Animal Diversity Web. Downloaded from https://animaldiversity.org/accounts/Apalone_mutica/ on 14 February 2024.

ALLAIN, R., VULLO, R., ROZADA, L., ANQUETIN, J., BOURGEAIS, R., GOEDERT, J., LASSERON, M., MARTIN, J. E., PÉREZ-GARCÍA, A., FABRÈGUES, C. P. D., ROYO-TORRES, R., AUGIER, D., BAILLY, G., CAZES, L., DESPRES, Y., GAILLIÈGUE, A., GOMEZ, B., GOUSSARD, F., LENGLET, T., VACANT, R., MAZAN and TOURNEPICHE, J.-F. 2022. Vertebrate paleobiodiversity of the Early Cretaceous (Berriasian) Angeac-Charente Lagerstätte (southwestern France): implications for continental faunal turnover at the J/K boundary. *Geodiversitas*, **44**, 683–752.

ALROY, J., ABERHAN, M., BOTTJER, D. J., FOOTE, M., FÜRSICH, F. T., HARRIES, P. J., HENDY, A. J. W., HOLLAND, S. M., IVANY, L. C., KIESSLING, W., KOSNIK, M. A., MARSHALL, C. R., MCGOWAN, A. J., MILLER, A. I., OLSZEWSKI, T. D., PATZKOWSKY, M. E., PETERS, S. E., VILLIER, L., WAGNER, P. J., BONUSO, N., BORKOW, P. S., BRENNEIS, B., CLAPHAM, M. E., FALL, L. M., FERGUSON, C. A., HANSON, V. L., KRUG, A. Z., LAYOU, K. M., LECKEY, E. H., NÜRNBERG, S., POWERS, C. M., SESSA, J. A., SIMPSON, C., TOMAŠOVÝCH, A. and VISAGGI, C. C. 2008. Phanerozoic Trends in the Global Diversity of Marine Invertebrates. *Science*, **321**, 97–100.

ARBOUR, V. M. and CURRIE, P. J. 2013. *Euoplocephalus tutus* and the Diversity of Ankylosaurid Dinosaurs in the Late Cretaceous of Alberta, Canada, and Montana, USA. *PLOS ONE*, **8**, e62421.

——— and EVANS, D. C. 2017. A new ankylosaurine dinosaur from the Judith River Formation of Montana, USA, based on an exceptional skeleton with soft tissue preservation. *Royal Society Open Science*, **4**, 161086.

———, BURNS, M. E. and SISSONS, R. L. 2009. A redescription of the ankylosaurid dinosaur *Dyoplosaurus acutosquameus* Parks, 1924 (Ornithischia: Ankylosauria) and a revision of the genus. *Journal of Vertebrate Paleontology*, **29**, 1117–1135.

ARCHIBALD, J. D., CLEMENS, W. A., PADIAN, K., ROWE, T., MACLEOD, N., BARRETT, P. M., GALE, A., HOLROYD, P., SUES, H.-D., ARENS, N. C., HORNER, J. R., WILSON, G. P., GOODWIN, M. B., BROCHU, C. A., LOFGREN, D. L., HURLBERT, S. H., HARTMAN, J. H., EBERTH, D. A., WIGNALL, P. B., CURRIE, P. J., WEIL, A., PRASAD, G. V. R., DINGUS, L., COURTILLOT, V., MILNER, A., MILNER, A., BAJPAI, S., WARD, D. J. and SAHNI, A. 2010. Cretaceous Extinctions: Multiple Causes. *Science*, **328**, 973–973.

BAKKER, R. T. 1978. Dinosaur feeding behaviour and the origin of flowering plants. *Nature*, **274**, 661–663.

BALLINGER, R. E., LEMOS-ESPINAL, J., SANOJA-SARABIA, S. and COADY, N. R. 1995. Ecological Observations of the Lizard, *Xenosaurus grandis* in Cuautlapan, Veracruz, Mexico. *Biotropica*, **27**, 128–132.

BAMFORTH, E. L. 2013. Paleoecology and paleoenvironmental trends immediately prior to the end-Cretaceous extinction in the latest Maastrichtian (66Ma) Frenchman Formation, Saskatchewan, Canada.Unpublished Ph.D. Thesis, McGill University, Montreal, 405pp.

——— and KOPPELHUS, E. B. 2018. New absolute paleoclimate estimates from Dinosaur Provincial Park, Alberta (Campanian, Late Cretaceous): Preliminary results based on a new fossil leaf assemblage. *6th Annual Meeting Canadian Society of Vertebrate Paleontology Abstracts*, **6**, 10–11.

BAMFORTH, E. L., BUTTON, C. L. and LARSSON, H. C. E. 2014. Paleoclimate estimates and fire ecology immediately prior to the end-Cretaceous mass extinction in the Frenchman Formation (66Ma), Saskatchewan, Canada. *Palaeogeography, Palaeoclimatology, Palaeoecology*, **401**, 96–110.

BANKER, R. M. W., DINEEN, A. A., SORMAN, M. G., TYLER, C. L. and ROOPNARINE, P. D. 2022. Beyond functional diversity: The importance of trophic position to understanding functional processes in community evolution. *Frontiers in Ecology and Evolution*, **10**, 983374.

BARBA-MONTOYA, J., REIS, M. dos, SCHNEIDER, H., DONOGHUE, P. C. J. and YANG, Z. 2018. Constraining uncertainty in the timescale of angiosperm evolution and the veracity of a Cretaceous Terrestrial Revolution. *New Phytologist*, **218**, 819–834.

BARDACK, D. 1970. *A New Teleost from the Oldman Formation (Cretaceous) of Alberta*. Publications in Palaeontology 3. National Museums of Canada, 1–20 pp.

BARDET, N., FALCONNET, J., FISCHER, V., HOUSSAYE, A., JOUVE, S., PEREDA SUBERBIOLA, X., PÉREZ-GARCÍA, A., RAGE, J.-C. and VINCENT, P. 2014. Mesozoic marine reptile palaeobiogeography in response to drifting plates. *Gondwana Research*, **26**, 869–887.

BARNARD, P. L., DUGAN, J. E., PAGE, H. M., WOOD, N. J., HART, J. A. F., CAYAN, D. R., ERIKSON, L. H., HUBBARD, D. M., MYERS, M. R., MELACK, J. M. and IACOBELLIS, S. F. 2021. Multiple climate change-driven tipping points for coastal systems. *Scientific Reports*, **11**, 15560.

BARNES, C. R. 1988. Stratigraphy and Palaeontology of the Ordovician-Silurian boundary interval, Anticosti. *Bulletin of the British Museum, Natural History, Geology Series*, **43**, 195–219.

BARNETT, R., WESTBURY, M. V., SANDOVAL-VELASCO, M., VIEIRA, F. G., JEON, S., ZAZULA, G., MARTIN, M. D., HO, S. Y. W., MATHER, N., GOPALAKRISHNAN, S.,

RAMOS-MADRIGAL, J., DE MANUEL, M., ZEPEDA-MENDOZA, M. L., ANTUNES, A., BAEZ, A. C., DE CAHSAN, B., LARSON, G., O'BRIEN, S. J., EIZIRIK, E., JOHNSON, W. E., KOEPFLI, K.-P., WILTING, A., FICKEL, J., DALÉN, L., LORENZEN, E. D., MARQUES-BONET, T., HANSEN, A. J., ZHANG, G., BHAK, J., YAMAGUCHI, N. and GILBERT, M. T. P. 2020. Genomic Adaptations and Evolutionary History of the Extinct Scimitar-Toothed Cat, *Homotherium latidens*. *Current Biology*, **30**, 5018-5025.e5.

BARNOSKY, A. D., HADLY, E. A. and BELL, C. J. 2003. Mammalian Response to Global Warming on Varied Temporal Scales. *Journal of Mammalogy*, **84**, 354–368.

———, MATZKE, N., TOMIYA, S., WOGAN, G. O. U., SWARTZ, B., QUENTAL, T. B., MARSHALL, C., MCGUIRE, J. L., LINDSEY, E. L., MAGUIRE, K. C., MERSEY, B. and FERRER, E. A. 2011. Has the Earth's sixth mass extinction already arrived? *Nature*, **471**, 51–57.

———, HADLY, E. A., GONZALEZ, P., HEAD, J., POLLY, P. D., LAWING, A. M., ERONEN, J. T., ACKERLY, D. D., ALEX, K., BIBER, E., BLOIS, J., BRASHARES, J., CEBALLOS, G., DAVIS, E., DIETL, G. P., DIRZO, R., DOREMUS, H., FORTELIUS, M., GREENE, H. W., HELLMANN, J., HICKLER, T., JACKSON, S. T., KEMP, M., KOCH, P. L., KREMEN, C., LINDSEY, E. L., LOOY, C., MARSHALL, C. R., MENDENHALL, C., MULCH, A., MYCHAJLIW, A. M., NOWAK, C., RAMAKRISHNAN, U., SCHNITZLER, J., SHRESTHA, K. D., SOLARI, K., STEGNER, L., STEGNER, M. A., STENSETH, N. C., WAKE, M. H. and ZHANG, Z. 2017. Merging paleobiology with conservation biology to guide the future of terrestrial ecosystems. *Science*, **355**, eaah4787.

BARRETT, P. M. 2005. The Diet of Ostrich Dinosaurs (theropoda: Ornithomimosauria). *Palaeontology*, **48**, 347–358.

———. 2014. Paleobiology of Herbivorous Dinosaurs. *Annual Review of Earth and Planetary Sciences*, **42**, 207–230.

———, MCGOWAN, A. J. and PAGE, V. 2009. Dinosaur diversity and the rock record. *Proceedings of the Royal Society B: Biological Sciences*, **276**, 2667–2674.

BARRICK, R. E., FISCHER, A. G. and SHOWERS, W. J. 1999. Oxygen Isotopes from Turtle Bone: Applications for Terrestrial Paleoclimates? *PALAIOS*, **14**, 186–191.

BARRY, J. C., JOHNSON, N. M., RAZA, S. M. and JACOBS, L. L. 1985. Neogene mammalian faunal change in southern Asia: Correlations with climatic, tectonic, and eustatic events. *Geology*, **13**, 637–640.

BASCOMPTE, J., JORDANO, P. and OLESEN, J. M. 2006. Asymmetric Coevolutionary Networks Facilitate Biodiversity Maintenance. *Science*, **312**, 431–433.

BEAVAN, N. R. and RUSSELL, A. P. 1999. An elasmobranch assemblage from the terrestrial-marine transitional Lethbridge Coal Zone (Dinosaur Park Formation: Upper Campanian), Alberta, Canada. *Journal of Paleontology*, **73**, 494–503.

BECK, D. D. 2005. *Biology of Gila Monsters and Beaded Lizards*. University of California Press, Berkeley & Los Angeles.

BEHRENSMEYER, A. K. 1982. Time Resolution in Fluvial Vertebrate Assemblages. *Paleobiology*, **8**, 211–227.

BEHRENSMEYER, A. K. and HOOK, R. W. 1992. Paleoenvironmental Contexts and Taphonomic Modes. *In* BEHRENSMEYER, A. K., DAMUTH, J. D., DIMICHELE, W. A., POTTS, R., SUES, H.-D. and WING, S. L. (eds.) *Terrestrial Ecosystems through Time*, The University of Chicago Press, Chicago, 15–136 pp.

BEHRENSMEYER, A. K., WESTERN, D. and BOAZ, D. E. D. 1979. New perspectives in vertebrate paleoecology from a recent bone assemblage. *Paleobiology*, **5**, 12–21.

———, KIDWELL, S. M. and GASTALDO, R. A. 2000. Taphonomy and paleobiology. *Paleobiology*, **26**, 103–147.

———, TODD, N. E., POTTS, R. and MCBRINN, G. E. 1997. Late Pliocene Faunal Turnover in the Turkana Basin, Kenya and Ethiopia. *Science*, **278**, 1589–1594.

———, DAMUTH, J. D., DIMICHELE, W. A., POTTS, R., SUES, H.-D. and WING, S. L. 1992. *Terrestrial Ecosystems through Time*. The University of Chicago Press, Chicago and London.

BÉLAND, P. and RUSSELL, D. A. 1978. Paleoecology of Dinosaur Provincial Park (Cretaceous), Alberta, interpreted from the distribution of articulated vertebrate remains. *Canadian Journal of Earth Sciences*, **15**, 1012–1024.

BENSON, R. B. J. 2018. Dinosaur Macroevolution and Macroecology. *Annual Review of Ecology, Evolution, and Systematics*, **49**, 379–408.

BENSON, R. B. J., BUTLER, R., CLOSE, R. A., SAUPE, E. and RABOSKY, D. L. 2021. Biodiversity across space and time in the fossil record. *Current Biology*, **31**, R1225–R1236.

———, MANNION, P. D., BUTLER, R. J., UPCHURCH, P., GOSWAMI, A. and EVANS, S. E. 2013. Cretaceous tetrapod fossil record sampling and faunal turnover: Implications for biogeography and the rise of modern clades. *Palaeogeography, Palaeoclimatology, Palaeoecology*, **372**, 88–107.

BENTON, M. J. 1979. Ecological succession among late Palaeozoic and mesozoic tetrapods. *Palaeogeography, Palaeoclimatology, Palaeoecology*, **26**, 127–150.

———. 2008. How to find a dinosaur, and the role of synonymy in biodiversity studies. *Paleobiology*, **34**, 516–533.

———. 2010. The origins of modern biodiversity on land. *Philosophical Transactions: Biological Sciences*, **365**, 3667–3679.

BENTON, M. J., WILLS, M. A. and HITCHIN, R. 2000. Quality of the fossil record through time. *Nature*, **403**, 534–537.

———, TVERDOKHLEBOV, V. P. and SURKOV, M. V. 2004. Ecosystem remodelling among vertebrates at the Permian–Triassic boundary in Russia. *Nature*, **432**, 97–100.

BENTON, M. J., WILF, P. and SAUQUET, H. 2022. The Angiosperm Terrestrial Revolution and the origins of modern biodiversity. *New Phytologist*, **233**, 2017–2035.

———, ZHANG, Q., HU, S., CHEN, Z.-Q., WEN, W., LIU, J., HUANG, J., ZHOU, C., XIE, T., TONG, J. and CHOO, B. 2013. Exceptional vertebrate biotas from the Triassic of China, and the expansion of marine ecosystems after the Permo-Triassic mass extinction. *Earth-Science Reviews*, **125**, 199–243.

BIANUCCI, G., LAMBERT, O., URBINA, M., MERELLA, M., COLLARETA, A., BENNION, R., SALAS-GISMONDI, R., BENITES-PALOMINO, A., POST, K., DE MUIZON, C., BOSIO, G., DI CELMA, C., MALINVERNO, E., PIERANTONI, P. P., VILLA, I. M. and AMSON, E. 2023. A heavyweight early whale pushes the boundaries of vertebrate morphology. *Nature*, **620**, 824–829.

BIBI, F. and CANTALAPIEDRA, J. L. 2023. Plio-Pleistocene African megaherbivore losses associated with community biomass restructuring. *Science*, **380**, 1076–1080.

BIOLOGICAL RECORDS CENTRE. 2024. *BRC - Database of Insects and their Food Plants*. Biological Records Centre. Downloaded from https://dbif.brc.ac.uk/hosts.aspx on 23 March 2024.

BISHOP, N. D., POLISAR, J., ELIAZAR, P. J., CARTHY, R. R. and BJORNDAL, K. A. 2022. Diet of *Dermatemys mawii*, an Aquatic Turtle That Relies Heavily on Terrestrial Vegetation. *Chelonian Conservation and Biology*, **21**, 37–45.

BLACKBURN, T. M. and GASTON, K. J. 2002. Scale in macroecology. *Global Ecology and Biogeography*, **11**, 185–189.

BLAKE, S., TAPIA, P. I., SAFI, K. and ELLIS-SOTO, D. 2021. Chapter 11 - Diet, behavior, and activity patterns. *In* GIBBS, J. P., CAYOT, L. J. and AGUILERA, W. T. (eds.) *Galapagos Giant Tortoises*, Academic Press, 207–239 pp.

BLANCO, F., CALATAYUD, J., MARTÍN-PEREA, D. M., DOMINGO, M. S., MENÉNDEZ, I., MÜLLER, J., FERNÁNDEZ, M. H. and CANTALAPIEDRA, J. L. 2021. Punctuated ecological equilibrium in mammal communities over evolutionary time scales. *Science*, **372**, 300–303.

BOND, W. J. and SCOTT, A. C. 2010. Fire and the spread of flowering plants in the Cretaceous. *The New Phytologist*, **188**, 1137–1150.

BOUCHARD, K. 2009. Gavialis gangeticus *(Gharial)*. Animal Diversity Web. Downloaded from https://animaldiversity.org/accounts/Gavialis_gangeticus/ on 6 April 2024.

BOUCOT, A. J. 1990. Community evolution: its evolutionary and biostratigraphic significance. *In* MILLER III, W. (ed.) *Paleocommunity Temporal Dynamics: The Long-Term Development of Multispecies Assemblages*, Vol. 5. 48–70 pp.

———, XU, C., SCOTESE, C. R. and MORLEY, R. J. 2013. *Phanerozoic Paleoclimate: An Atlas of Lithologic Indicators of Climate*. SEPM (Society for Sedimentary Geology), Tulsa, Oklahoma, U.S.A.

BOWEN, G. J., MAIBAUER, B. J., KRAUS, M. J., RÖHL, U., WESTERHOLD, T., STEIMKE, A., GINGERICH, P. D., WING, S. L. and CLYDE, W. C. 2015. Two massive, rapid releases of carbon during the onset of the Palaeocene–Eocene thermal maximum. *Nature Geoscience*, **8**, 44–47.

BRAMAN, D. R. 2005. Campanian Palynomorphs. *In* CURRIE, P. J. and KOPPELHUS, E. B. (eds.) *Dinosaur Provincial Park: A Spectacular Ancient Ecosystem Revealed*, Indiana University Press, Bloomington, 101–130 pp.

———, JOHNSTON, P. A. and HAGLUND, W. M. 1995. *Upper Cretaceous Paleontology, Stratigraphy and Depositional Environments at Dinosaur Provincial Park and Drumheller, Alberta*. *Canadian Paleontology Conference Field Trip Guidebook 4, Canadian Paleontology Conference V*. Royal Tyrrell Museum of Palaeontology, Drumheller, Alberta.

BRETT-SURMAN, M. K. 1997. Ornithopods. *In* FARLOW, J. O. and BRETT-SURMAN, M. K. (eds.) *The Complete Dinosaur*, Indiana University Press, Bloomington, 330–346 pp.

BRINKMAN, D. B. 1990. Paleoecology of the Judith River Formation (Campanian) of Dinosaur Provincial Park, Alberta, Canada: Evidence from vertebrate microfossil localities. *Palaeogeography, Palaeoclimatology, Palaeoecology*, **78**, 37–54.

BRINKMAN, D. B. 1998. The skull and neck of the Cretaceous turtle *Basilemys* (Trionychoidea, Nanhsiungchelyidae), and the interrelationships of the genus. *Paludicola*, **1**, 150–157.

———. 2003. Anatomy and systematics of *Plesiobaena antiqua* (Testudines; Baenidae) from the mid-Campanian Judith River Group of Alberta, Canada. *Journal of Vertebrate Paleontology*, **23**, 146–155.

BRINKMAN, D. B. 2005. Turtles: Diversity, Paleoecology, and Distribution. *In* CURRIE, P. J. and KOPPELHUS, E. B. (eds.) *Dinosaur Provincial Park: A Spectacular Ancient Ecosystem Revealed*, Indiana University Press, Bloomington, 202–220 pp.

———. 2019. Teleost abdominal centra from the Belly River Group of Alberta, Canada. *Paludicola*, **12**, 109–152.

BRINKMAN, D. B. and NICHOLLS, E. L. 1991. Anatomy and relationships of the turtle *Boremys pulchra* (Testudines: Baenidae). *Journal of Vertebrate Paleontology*, **11**, 302–315.

——— and ———. 1993. The skull of *Neurankylus eximius* (Testudines: Baenidae) and a reinterpretation of the relationships of this taxon. *Journal of Vertebrate Paleontology*, **13**, 273–281.

BRINKMAN, D. B., RYAN, M. J. and EBERTH, D. A. 1998. The paleogeographic and stratigraphic distribution of ceratopsids (Ornithischia) in the upper Judith River Group of Western Canada. *PALAIOS*, **13**, 160–169.

———, RUSSELL, A. P. and PENG, J.-H. 2005*a*. Vertebrate Microfossil Sites and Their Contribution to Studies of Paleoecology. *In* CURRIE, P. J. and KOPPELHUS, E. B. (eds.) *Dinosaur Provincial Park: A Spectacular Ancient Ecosystem Revealed*, Indiana University Press, Bloomington, 88–98 pp.

———, NEWBREY, M. G. and NEUMAN, A. G. 2014. Diversity and paleoecology of actinopterygian fish from vertebrate microfossil localities of the Maastrichtian Hell Creek Formation of Montana. *In* WILSON, G. P., CLEMENS, W. A., HORNER, J. R. and HARTMAN, J. H. (eds.) *Through the End of the Cretaceous in the Type Locality of the Hell Creek Formation in Montana and Adjacent Areas*, Special Paper 503. Geological Society of America, 247–270 pp.

———, RUSSELL, A. P., EBERTH, D. A. and PENG, J. 2004. Vertebrate palaeocommunities of the lower Judith River Group (Campanian) of southeastern Alberta, Canada, as interpreted from vertebrate microfossil assemblages. *Palaeogeography, Palaeoclimatology, Palaeoecology*, **213**, 295–313.

———, BRAMAN, D. R., NEUMAN, A. G., RALRICK, P. E. and SATO, T. 2005*b*. A Vertebrate Assemblage from the Marine Shales of the Lethbridge Coal Zone. *In* CURRIE, P. J. and KOPPELHUS, E. B. (eds.) *Dinosaur Provincial Park: A Spectacular Ancient Ecosystem Revealed*, Indiana University Press, Bloomington, 486–500 pp.

BRINKMAN, D. B., DENSMORE, M., RABI, M., RYAN, M. J. and EVANS, D. C. 2015. Marine turtles from the Late Cretaceous of Alberta, Canada. *Canadian Journal of Earth Sciences*, **52**, 581–589.

BRITO, P. M. 1997. Révision des Aspidorhynchidae (Pisees, Actinopterygii) du Mésozoïque: ostéologie, relations phylogénétiques, données environnementales et biogéographiques. *Geodiversitas*, **19**, 681–772.

BROWN, B. 1914*a*. Article XXXV. - *Corythosaurus casuarius*, a new crested dinosaur from the Belly River Cretaceous, with provisional classification of the family Trachodontidae. *Bulletin of the American Museum of Natural History*, **33**, 559–565.

———. 1914*b*. Article XXXIV. A complete skull of *Monoclonius* from the Belly River Cretaceous of Alberta. *Bulletin of the American Museum of Natural History*, **33**, 549–558, pl. XXXVIII–XL.

———. 1916*a*. Article XXXVIII. - *Corythosaurus casuarius*: skeleton, musculature and epidermis; second paper. *Bulletin of the American Museum of Natural History*, **35**, 709–726, pl. XIII–XXII.

———. 1916*b*. Article XXX VII.- A new crested trachodont dinosaur *Prosaurolophus maximus*. *Bulletin of the American Museum of Natural History*, **35**, 701–708.

———. 1917. Article X. A complete skeleton of the horned dinosaur *Monoclonius*, and description of a second skeleton showing skin impressions. *Bulletin of the American Museum of Natural History*, **37**, 281–306, pl. XI–XIX.

——— and SCHLAIKJER, E. M. 1937. The skeleton of *Styracosaurus* with the description of a new species. *American Museum Novitates*, **955**, 1–12.

BROWN, C. M. 2013. Advances in Quantitative Methods in Dinosaur Palaeobiology: A Case Study in Horned Dinosaur Evolution.Unpublished Ph.D. Thesis, University of Toronto, Toronto, 443pp.

———, HOLMES, R. and CURRIE, P. 2020*a*. A subadult individual of *Styracosaurus albertensis* (Ornithischia: Ceratopsidae) with comments on ontogeny and intraspecific variation in Styracosaurus and Centrosaurus. *Vertebrate Anatomy Morphology Palaeontology*, **8**, 67–95.

———, CURRIE, P. J. and THERRIEN, F. 2022*a*. Intraspecific facial bite marks in tyrannosaurids provide insight into sexual maturity and evolution of bird-like intersexual display. *Paleobiology*, **48**, 12–43.

———, EVANS, D. C., RYAN, M. J. and RUSSELL, A. P. 2013*a*. New data on the diversity and abundance of small-bodied ornithopods (Dinosauria, Ornithischia) from the Belly River Group (Campanian) of Alberta. *Journal of Vertebrate Paleontology*, **33**, 495–520.

BROWN, C. M., CAMPIONE, N. E., MANTILLA, G. P. W. and EVANS, D. C. 2022*b*. Size-driven preservational and macroecological biases in the latest Maastrichtian terrestrial vertebrate assemblages of North America. *Paleobiology*, **48**, 210–238.

BROWN, C. M., EVANS, D. C., CAMPIONE, N. E., O'BRIEN, L. J. and EBERTH, D. A. 2013*b*. Evidence for taphonomic size bias in the Dinosaur Park Formation (Campanian, Alberta), a model Mesozoic terrestrial alluvial-paralic system. *Palaeogeography, Palaeoclimatology, Palaeoecology*, **372**, 108–122.

———, HERRIDGE-BERRY, S., CHIBA, K., VITKUS, A. and EBERTH, D. A. 2020*b*. High-resolution (centimetre-scale) GPS/GIS-based 3D mapping and spatial analysis of in situ fossils in two horned-dinosaur bonebeds in the Dinosaur Park Formation (Upper Cretaceous) at Dinosaur Provincial Park, Alberta, Canada. *Canadian Journal of Earth Sciences*, **58**, 225–246.

———, CAMPIONE, N. E., GIACOMINI, H. C., O'BRIEN, L. J., VAVREK, M. J. and EVANS, D. C. 2013*c*. Ecological modelling, size distributions and taphonomic size bias in dinosaur faunas: a comment on Codron et al. (2012). *Biology Letters*, **9**, 20120582.

BROWN, C. M., HENDERSON, D. M., VINTHER, J., FLETCHER, I., SISTIAGA, A., HERRERA, J. and SUMMONS, R. E. 2017. An Exceptionally Preserved Three-Dimensional Armored Dinosaur Reveals Insights into Coloration and Cretaceous Predator-Prey Dynamics. *Current Biology*, **27**, 2514–2521.

———, GREENWOOD, D. R., KALYNIUK, J. E., BRAMAN, D. R., HENDERSON, D. M., GREENWOOD, C. L. and BASINGER, J. F. 2020*c*. Dietary palaeoecology of an Early Cretaceous armoured dinosaur (Ornithischia; Nodosauridae) based on floral analysis of stomach contents. *Royal Society Open Science*, **7**, 200305.

BROWN, J. H. and MAURER, B. A. 1989. Macroecology: The Division of Food and Space Among Species on Continents. *Science*, **243**, 1145–1150.

BROWN, S. A. E., SCOTT, A. C., GLASSPOOL, I. J. and COLLINSON, M. E. 2012. Cretaceous wildfires and their impact on the Earth system. *Cretaceous Research*, **36**, 162–190.

BRUSATTE, S. L., BUTLER, R. J., PRIETO-MARQUEZ, A. and NORELL, M. A. 2012. Dinosaur morphological diversity and the end-Cretaceous extinction. *Nature Communications*, **3**, 8.

BRUSATTE, S. L., BUTLER, R. J., BARRETT, P. M., CARRANO, M. T., EVANS, D. C., LLOYD, G. T., MANNION, P. D., NORELL, M. A., PEPPE, D. J., UPCHURCH, P. and WILLIAMSON, T. E. 2015. The extinction of the dinosaurs. *Biological Reviews*, **90**, 628–642.

BURGESS, S. D. and BOWRING, S. A. 2015. High-precision geochronology confirms voluminous magmatism before, during, and after Earth's most severe extinction. *Science Advances*, **1**, e1500470.

BUTLER, R. J., BARRETT, P. M., KENRICK, P. and PENN, M. G. 2009. Diversity patterns amongst herbivorous dinosaurs and plants during the Cretaceous: implications for hypotheses of dinosaur/angiosperm co-evolution. *Journal of Evolutionary Biology*, **22**, 446–459.

CADENA, E. 2016. *Palaeoamyda messeliana* nov. comb. (Testudines, Pan-Trionychidae) from the Eocene Messel Pit and Geiseltal localities, Germany, taxonomic and phylogenetic insights. *PeerJ*, **4**, e2647.

CALDWELL, M. W. 2005. The Squamates: Origins, Phylogeny, and Paleoecology. *In* CURRIE, P. J. and KOPPELHUS, E. B. (eds.) *Dinosaur Provincial Park: A Spectacular Ancient Ecosystem Revealed*, Indiana University Press, Bloomington, 235–248 pp.

CAMPBELL, J. A., MITCHELL, M. T., RYAN, M. J. and ANDERSON, J. S. 2021. A new elasmosaurid (Sauropterygia: Plesiosauria) from the non-marine to paralic Dinosaur Park Formation of southern Alberta, Canada. *PeerJ*, **9**, e10720.

———, RYAN, M. J., SCHRÖDER-ADAMS, C. J., HOLMES, R. B. and EVANS, D. C. 2019. Temporal range extension and evolution of the chasmosaurine ceratopsid *'Vagaceratops' irvinensis* (Dinosauria: Ornithischia) in the Upper Cretaceous (Campanian) Dinosaur Park Formation of Alberta. *Vertebrate Anatomy Morphology Palaeontology*, **7**, 83–100.

CAPLAN, M. L. and BUSTIN, R. M. 1999. Devonian–Carboniferous Hangenberg mass extinction event, widespread organic-rich mudrock and anoxia: causes and consequences. *Palaeogeography, Palaeoclimatology, Palaeoecology*, **148**, 187–207.

CARON, D., MAIORANO, L., THUILLER, W. and POLLOCK, L. J. 2022. Addressing the Eltonian shortfall with trait-based interaction models. *Ecology Letters*, **25**, 889–899.

———, BROSE, U., LURGI, M., BLANCHET, F. G., GRAVEL, D. and POLLOCK, L. J. 2024. Trait-matching models predict pairwise interactions across regions, not food web properties. *Global Ecology and Biogeography*, **33**, e13807.

CARON, J.-B. and JACKSON, D. A. 2008. Paleoecology of the Greater Phyllopod Bed community, Burgess Shale. *Palaeogeography, Palaeoclimatology, Palaeoecology*, **258**, 222–256.

CARR, T. D., VARRICCHIO, D. J., SEDLMAYR, J. C., ROBERTS, E. M. and MOORE, J. R. 2017. A new tyrannosaur with evidence for anagenesis and crocodile-like facial sensory system. *Scientific reports*, **7**.

CARVALHO, M. R., JARAMILLO, C., PARRA, F. de la, CABALLERO-RODRÍGUEZ, D., HERRERA, F., WING, S., TURNER, B. L., D'APOLITO, C., ROMERO-BÁEZ, M., NARVÁEZ, P., MARTÍNEZ, C., GUTIERREZ, M., LABANDEIRA, C., BAYONA, G., RUEDA, M., PAEZ-REYES, M., CÁRDENAS, D., DUQUE, Á., CROWLEY, J. L., SANTOS, C. and SILVESTRO, D. 2021. Extinction at the end-Cretaceous and the origin of modern Neotropical rainforests. *Science*, **372**, 63–68.

CEBALLOS, G., EHRLICH, P. R., BARNOSKY, A. D., GARCÍA, A., PRINGLE, R. M. and PALMER, T. M. 2015. Accelerated modern human–induced species losses: Entering the sixth mass extinction. *Science Advances*, **1**, e1400253.

CHEN, M., STRÖMBERG, C. A. E. and WILSON, G. P. 2019. Assembly of modern mammal community structure driven by Late Cretaceous dental evolution, rise of flowering plants, and dinosaur demise. *Proceedings of the National Academy of Sciences*, **116**, 9931–9940.

CHEN, Z.-Q. and BENTON, M. J. 2012. The timing and pattern of biotic recovery following the end-Permian mass extinction. *Nature Geoscience*, **5**, 375–383.

CHIARENZA, A. A., FIORILLO, A. R., TYKOSKI, R. S., MCCARTHY, P. J., FLAIG, P. P. and CONTRERAS, D. L. 2020. The first juvenile dromaeosaurid (Dinosauria: Theropoda) from Arctic Alaska. *PLOS ONE*, **15**, e0235078.

———, MANNION, P. D., LUNT, D. J., FARNSWORTH, A., JONES, L. A., KELLAND, S.-J. and ALLISON, P. A. 2019. Ecological niche modelling does not support climatically-driven dinosaur diversity decline before the Cretaceous/Paleogene mass extinction. *Nature Communications*, **10**, 1091.

CHIN, K. 2007. The paleobiological implications of herbivorous dinosaur coprolites from the Upper Cretaceous Two Medicine Formation of Montana: why eat wood? *PALAIOS*, **22**, 554–566.

——— and GILL, B. D. 1996. Dinosaurs, Dung Beetles, and Conifers: Participants in a Cretaceous Food Web. *PALAIOS*, **11**, 280–285.

———, HARTMAN, J. H. and ROTH, B. 2009. Opportunistic exploitation of dinosaur dung: fossil snails in coprolites from the Upper Cretaceous Two Medicine Formation of Montana. *Lethaia*, **42**, 185–198.

———, FELDMANN, R. M. and TASHMAN, J. N. 2017. Consumption of crustaceans by megaherbivorous dinosaurs: dietary flexibility and dinosaur life history strategies. *Scientific Reports*, **7**, 11163.

CICIMURRI, D. J. and EVERHART, M. J. 2001. An Elasmosaur with Stomach Contents and Gastroliths from the Pierre Shale (Late Cretaceous) of Kansas. *Transactions of the Kansas Academy of Science*, **104**, 129–143.

CLACK, J. A., BENNETT, C. E., CARPENTER, D. K., DAVIES, S. J., FRASER, N. C., KEARSEY, T. I., MARSHALL, J. E., MILLWARD, D., OTOO, B. K. A., REEVES, E. J., ROSS, A. J., MARCELLO, R., SMITHSON, K. Z., SMITHSON, T. R. and WALSH, S. A. 2017. Phylogenetic and environmental context of a Tournaisian tetrapod fauna. *Nature Ecology & Evolution*, **1**.

CLOSE, R. A., BENSON, R. B., ALROY, J., BEHRENSMEYER, A. K., BENITO, J., CARRANO, M. T., CLEARY, T. J., DUNNE, E. M., MANNION, P. D., UHEN, M. D. and BUTLER, R. J. 2019. Diversity dynamics of Phanerozoic terrestrial tetrapods at the local-community scale. *Nature Ecology & Evolution*, **3**, 590–597.

CODRON, D., CARBONE, C. and CLAUSS, M. 2013. Ecological Interactions in Dinosaur Communities: Influences of Small Offspring and Complex Ontogenetic Life Histories. *PLOS ONE*, **8**, e77110.

———, ———, MÜLLER, D. W. H. and CLAUSS, M. 2012. Ontogenetic niche shifts in dinosaurs influenced size, diversity and extinction in terrestrial vertebrates. *Biology Letters*, **8**, 620–623.

CODRON, J., BOTHA-BRINK, J., CODRON, D., HUTTENLOCKER, A. K. and ANGIELCZYK, K. D. 2017. Predator–prey interactions amongst Permo-Triassic terrestrial vertebrates as a deterministic factor influencing faunal collapse and turnover. *Journal of Evolutionary Biology*, **30**, 40–54.

COHEN, J. E. and ŁUCZAK, T. 1992. Trophic levels in community food webs. *Evolutionary Ecology*, **6**, 73–89.

———, JONSSON, T. and CARPENTER, S. R. 2003. Ecological community description using the food web, species abundance, and body size. *Proceedings of the National Academy of Sciences*, **100**, 1781–1786.

COLBERT, E. H. and RUSSELL, D. A. 1969. The small Cretaceous dinosaur *Dromaeosaurus*. *American Museum Novitates*, 1–49.

COMPAGNO, L. J. V. 1984. *FAO Species Catalogue. Vol. 4. Sharks of the World. An Annotated and Illustrated Catalogue of Shark Species Known to Date. Part 2 - Carcharhiniformes*. Food & Agriculture Org., Rome.

———. 2002. *FAO Species Catalogue. Sharks of the World. An Annotated and Illustrated Catalogue of Shark Species Known to Date. Volume 2. Bullhead, mackerel and carpet sharks (Heterodontiformes, Lamniformes and Orectolobiformes)*. Food & Agriculture Org., Rome.

CONDAMINE, F. L., GUINOT, G., BENTON, M. J. and CURRIE, P. J. 2021. Dinosaur biodiversity declined well before the asteroid impact, influenced by ecological and environmental pressures. *Nature Communications*, **12**, 3833.

CONGREVE, C. R. 2013. Cladal Turnover: the end-Ordovician as a large-scale analogue of species turnover. *Palaeontology*, **56**, 1285–1296.

———, FALK, A. R. and LAMSDELL, J. C. 2018. Biological hierarchies and the nature of extinction. *Biological Reviews*, **93**, 811–826.

———, PATZKOWSKY, M. E. and WAGNER, P. J. 2021. An early burst in brachiopod evolution corresponding with significant climatic shifts during the Great Ordovician Biodiversification Event. *Proceedings of the Royal Society B: Biological Sciences*, **288**, 20211450.

CONWAY MORRIS, S. 1995. Ecology in deep time. *Trends in Ecology & Evolution*, **10**, 290–294.

COOMBS, W. P. 1978. The families of the ornithischian dinosaur order Ankylosauria. *Palaeontology*, **21**, 143–170.

CORTÉS, D. and LARSSON, H. C. E. 2023. Top of the food chains: an ecological network of the marine Paja Formation biota from the Early Cretaceous of Colombia reveals the highest trophic levels ever estimated. *Zoological Journal of the Linnean Society*, zlad092.

CRABTREE, R., STEVENS, C., SNODGRASS, D. and STENGARD, F. 1998. Feeding habits of bonefish, *Albula vulpes* from waters of the Florida Keys. *Fishery Bulletin*, **96**, 754–766.

CROSS, S. L., CRAIG, M. D., TOMLINSON, S. and BATEMAN, P. W. 2020. I don’t like crickets, I love them: invertebrates are an important prey source for varanid lizards. *Journal of Zoology*, **310**, 323–333.

CRUTZEN, P. J. 2006. The “Anthropocene”. *In* EHLERS, E. and KRAFFT, T. (eds.) *Earth System Science in the Anthropocene*, Springer, Berlin, Heidelberg, 13–18 pp.

CULLEN, T. M. and EVANS, D. C. 2016. Palaeoenvironmental drivers of vertebrate community composition in the Belly River Group (Campanian) of Alberta, Canada, with implications for dinosaur biogeography. *BMC Ecology*, **16**, 52.

——— and COUSENS, B. L. 2023. New biogeochemical insights into Mesozoic terrestrial paleoecology and evidence for omnivory in troodontid dinosaurs. *GSA Bulletin*.

———, ZANNO, L., LARSON, D. W., TODD, E., CURRIE, P. J. and EVANS, D. C. 2021. Anatomical, morphometric, and stratigraphic analyses of theropod biodiversity in the Upper Cretaceous (Campanian) Dinosaur Park Formation. *Canadian Journal of Earth Sciences*, **58**, 870–884.

CURRANO, E. D., WILF, P., WING, S. L., LABANDEIRA, C. C., LOVELOCK, E. C. and ROYER, D. L. 2008. Sharply increased insect herbivory during the Paleocene-Eocene Thermal Maximum. *Proceedings of the National Academy of Sciences*, **105**, 1960–1964.

CURRIE, P. J. 1981. Hunting dinosaurs in Alberta's great bonebed. *Canadian Geographic*, **101**, 34–39.

———. 1985. Cranial anatomy of *Stenonychosaurus inequalis* (Saurischia, Theropoda) and its bearing on the origin of birds. *Canadian Journal of Earth Sciences*, **22**, 1643–1658.

———. 1987. Bird-like characteristics of the jaws and teeth of troodontid theropods (Dinosauria, Saurischia). *Journal of Vertebrate Paleontology*, **7**, 72–81.

———. 1991. The Sino-Canadian Dinosaur Expeditions. *Geotimes*, **36**, 18–21.

———. 1995. New information on the anatomy and relationships of *Dromaeosaurus albertensis* (Dinosauria: Theropoda). *Journal of Vertebrate Paleontology*, **15**, 576–591.

———. 2003*a*. Cranial anatomy of tyrannosaurid dinosaurs from the Late Cretaceous of Alberta,Canada. *Acta Palaeontologica Polonica*, **48**, 191–226.

———. 2003*b*. Allometric growth in tyrannosaurids (Dinosauria: Theropoda) from the Upper Cretaceous of North America and Asia. *Canadian Journal of Earth Sciences*, **40**, 651–665.

———. 2005. History of Research. *In* CURRIE, P. J. and KOPPELHUS, E. B. (eds.) *Dinosaur Provincial Park: A Spectacular Ancient Ecosystem Revealed*, Indiana University Press, Bloomington, 3–33 pp.

——— and RUSSELL, D. A. 1982. A giant pterosaur (Reptilia: Archosauria) from the Judith River (Oldman) Formation of Alberta. *Canadian Journal of Earth Sciences*, **19**, 894–897.

——— and PADIAN, K. 1983. A new pterosaur record from the Judith River (Oldman) Formation of Alberta. *Journal of Paleontology*, **57**, 599–600.

——— and DODSON, P. 1984. Mass death of a herd of ceratopsian dinosaurs. *Third Symposium on Mesozoic Terrestrial Ecosystems*, 61–66.

——— and RUSSELL, D. A. 1988. Osteology and relationships of *Chirostenotes pergracilis* (Saurischia, Theropoda) from the Judith River (Oldman) Formation of Alberta, Canada. *Canadian Journal of Earth Sciences*, **25**, 972–986.

——— and ZHAO, X.-J. 1993. A new troodontid (Dinosauria, Theropoda) braincase from the Dinosaur Park Formation (Campanian) of Alberta. *Canadian Journal of Earth Sciences*, **30**, 2231–2247.

——— and JACOBSEN, A. R. 1995. An azhdarchid pterosaur eaten by a velociraptorine theropod. *Canadian Journal of Earth Sciences*, **32**, 922–925.

——— and KOPPELHUS, E. B. 2005. *Dinosaur Provincial Park: A Spectacular Ancient Ecosystem Revealed*. Bloomington & Indianapolis.

——— and RUSSELL, D. A. 2005. The Geographic and Stratigraphic Distribution of Articulated and Associated Dinosaur Remains. *In* CURRIE, P. J. and KOPPELHUS, E. B. (eds.) *Dinosaur Provincial Park: A Spectacular Ancient Ecosystem Revealed*, Indiana University Press, Bloomington, 537–569 pp.

——— and GODFREY, S. J. 2005. Pterosaurs. *In* CURRIE, P. J. and KOPPELHUS, E. B. (eds.) *Dinosaur Provincial Park: A Spectacular Ancient Ecosystem Revealed*, Indiana University Press, Bloomington, 292–311 pp.

——— and EVANS, D. C. 2020. Cranial Anatomy of New Specimens of *Saurornitholestes langstoni* (Dinosauria, Theropoda, Dromaeosauridae) from the Dinosaur Park Formation (Campanian) of Alberta. *The Anatomical Record*, **303**, 691–715.

———, RIGBY, JR., J. K. and SLOAN, R. E. 1990. Theropod teeth from the Judith River Formation of southern Alberta, Canada. *In* CARPENTER, K. and CURRIE, P. J. (eds.) *Dinosaur Systematics: Perspectives and Approaches*, Cambridge University Press, Cambridge, 107–125 pp.

———, KOPPELHUS, E. B. and MUHAMMAD, A. F. 1995. ‘Stomach’ contents of a hadrosaur from the Dinosaur Park Formation (Campanian, Upper Cretaceous) of Alberta, Canada. *Sixth Symposium on Mesozoic Terrestrial Ecosystems and Biota: Short Papers*, **6**, 111–114.

———, HOLMES, R. B., RYAN, M. J. and COY, C. 2016. A juvenile chasmosaurine ceratopsid (Dinosauria, Ornithischia) from the Dinosaur Park Formation, Alberta, Canada. *Journal of Vertebrate Paleontology*, **36**, e1048348.

DAI, X., DAVIES, J. H. F. L., YUAN, Z., BRAYARD, A., OVTCHAROVA, M., XU, G., LIU, X., SMITH, C. P. A., SCHWEITZER, C. E., LI, M., PERROT, M. G., JIANG, S., MIAO, L., CAO, Y., YAN, J., BAI, R., WANG, F., GUO, W., SONG, H., TIAN, L., DAL CORSO, J., LIU, Y., CHU, D. and SONG, H. 2023. A Mesozoic fossil lagerstätte from 250.8 million years ago shows a modern-type marine ecosystem. *Science*, **379**, 567–572.

DAL CORSO, J., BERNARDI, M., SUN, Y., SONG, H., SEYFULLAH, L. J., PRETO, N., GIANOLLA, P., RUFFELL, A., KUSTATSCHER, E., ROGHI, G., MERICO, A., HOHN, S., SCHMIDT, A. R., MARZOLI, A., NEWTON, R. J., WIGNALL, P. B. and BENTON, M. J.

2020. Extinction and dawn of the modern world in the Carnian (Late Triassic). *Science Advances*, **6**, eaba0099.

DAMUTH, J. D. 1982. Analysis of the preservation of community structure in assemblages of fossil mammals. *Paleobiology*, **8**, 434–446.

DARWIN, C. 1859. *On the Origin of Species*. John Murray, London.

DASHZEVEG, D., NOVACEK, M. J., NORELL, M. A., CLARK, J. M., CHIAPPE, L. M., DAVIDSON, A., MCKENNA, M. C., DINGUS, L., SWISHER, C. and ALTANGEREL, P. 1995. Extraordinary preservation in a new vertebrate assemblage from the Late Cretaceous of Mongolia. *Nature*, **374**, 446–449.

DAVIS, C. C., WEBB, C. O., WURDACK, K. J., JARAMILLO, C. A. and DONOGHUE, M. J. 2005. Explosive Radiation of Malpighiales Supports a Mid-Cretaceous Origin of Modern Tropical Rain Forests. *The American Naturalist*, **165**, E36–E65.

DECECCHI, T. A., MLOSZEWSKA, A. M., JR, T. R. H., HABIB, M. B. and LARSSON, H. C. E. 2020. The fast and the frugal: Divergent locomotory strategies drive limb lengthening in theropod dinosaurs. *PLOS ONE*, **15**, e0223698.

DEGRANGE, F. J. 2020. A revision of skull morphology in Phorusrhacidae (Aves, Cariamiformes). *Journal of Vertebrate Paleontology*, **40**, e1848855.

DELMAS, E., BESSON, M., BRICE, M.-H., BURKLE, L. A., DALLA RIVA, G. V., FORTIN, M.-J., GRAVEL, D., GUIMARÃES JR., P. R., HEMBRY, D. H., NEWMAN, E. A., OLESEN, J. M., PIRES, M. M., YEAKEL, J. D. and POISOT, T. 2019. Analysing ecological networks of species interactions. *Biological Reviews*, **94**, 16–36.

DIETL, G. P. and FLESSA, K. W. 2011. Conservation paleobiology: putting the dead to work. *Trends in Ecology & Evolution*, **26**, 30–37.

DIETL, G. P., KIDWELL, S. M., BRENNER, M., BURNEY, D. A., FLESSA, K. W., JACKSON, S. T. and KOCH, P. L. 2015. Conservation Paleobiology: Leveraging Knowledge of the Past to Inform Conservation and Restoration. *Annual Review of Earth and Planetary Sciences*, **43**, 79–103.

DILAURA, P., PRUITT, J., MUNSEY, D., GOOD, G., MEYER, B. and URBAN, K. 1999. Macrochelys temminckii *(Alligator Snapping Turtle)*. Animal Diversity Web. Downloaded from https://animaldiversity.org/accounts/Macrochelys_temminckii/ on 14 February 2024.

DIMICHELE, W. A., HOTTON, C. L., LABANDEIRA, C. C. and SUES, H.-D. 2023. A paleontological perspective on ecosystem assembly rules in the Paleozoic terrestrial realm. *Evolving Earth*, **1**, 100020.

———, BEHRENSMEYER, A. k., OLSZEWSKI, T. d., LABANDEIRA, C. c., PANDOLFI, J. m., WING, S. l. and BOBE, R. 2004. Long-Term Stasis in Ecological Assemblages: Evidence from the Fossil Record. *Annual Review of Ecology, Evolution, and Systematics*, **35**, 285–322.

DOBZHANSKY, T. 1937. *Genetics and the origin of species*. Columbia University Press, New York.

DODSON, P. 1971. Sedimentology and taphonomy of the Oldman Formation (Campanian), Dinosaur Provincial Park, Alberta (Canada). *Palaeogeography, Palaeoclimatology, Palaeoecology*, **10**, 21–74.

———. 1975. Taxonomic Implications of Relative growth in Lambeosaurine Hadrosaurs. *Systematic Biology*, **24**, 37–54.

———. 1983. A Faunal Review of the Judith River (Oldman) Formation, Dinosaur Provincial Park, Alberta, Canada. *The Mosasaur*, **1**, 89–118.

DODSON, P. and CURRIE, P. J. 1988. The smallest ceratopsid skull–Judith River Formation of Alberta. *Canadian Journal of Earth Sciences*, **25**, 926–930.

———, BEHRENSMEYER, A. K., BAKKER, R. T. and MCINTOSH, J. S. 1980. Taphonomy and Paleoecology of the Dinosaur Beds of the Jurassic Morrison Formation. *Paleobiology*, **6**, 208–232.

DONATO, M. 2000. Graptemys geographica *(Common Map Turtle, Northern Map Turtle)*. Animal Diversity Web. Downloaded from https://animaldiversity.org/accounts/Graptemys_geographica/ on 5 April 2024.

DUDGEON, T. W., MADDIN, H. C., EVANS, D. C. and MALLON, J. C. 2020. The internal cranial anatomy of *Champsosaurus* (Choristodera: Champsosauridae): Implications for neurosensory function. *Scientific Reports*, **10**, 7122.

DUNNE, J. A. and YEAKEL, J. 2015. Modern Lessons from Ancient Food Webs. *American Scientist*, **103**, 188.

———, LABANDEIRA, C. C. and WILLIAMS, R. J. 2014. Highly resolved early Eocene food webs show development of modern trophic structure after the end-Cretaceous extinction. *Proceedings of the Royal Society B: Biological Sciences*, **281**, 20133280.

———, WILLIAMS, R. J., MARTINEZ, N. D., WOOD, R. A. and ERWIN, D. H. 2008. Compilation and Network Analyses of Cambrian Food Webs. *PLOS Biology*, **6**, e102.

DURING, M. A. D., SMIT, J., VOETEN, D. F. A. E., BERRUYER, C., TAFFOREAU, P., SANCHEZ, S., STEIN, K. H. W., VERDEGAAL-WARMERDAM, S. J. A. and VAN DER LUBBE, J. H. J. L. 2022. The Mesozoic terminated in boreal spring. *Nature*, **603**, 91–94.

DYER, A., POWERS, M. and CURRIE, P. 2022. Problematic putative pachycephalosaurids: Synchrotron µCT imaging shines new light on the anatomy and taxonomic validity of *Gravitholus albertae* from the Belly River Group (Campanian) of Alberta, Canada. *Vertebrate Anatomy Morphology Palaeontology*, **10**, 65–110.

EBERLE, J. J., CLEMENS, W. A., ERICKSON, G. M. and DRUCKENMILLER, P. S. 2023. A new tiny eutherian from the Late Cretaceous of Alaska. *Journal of Systematic Palaeontology*, **21**, 2232359.

EBERTH, D. A. 1990. Stratigraphy and sedimentology of vertebrate microfossil sites in the uppermost Judith River Formation (Campanian), Dinosaur Provincial Park, Alberta, Canada. *Palaeogeography, Palaeoclimatology, Palaeoecology*, **78**, 1–36.

———. 2005. The Geology. *In* CURRIE, P. J. and KOPPELHUS, E. B. (eds.) *Dinosaur Provincial Park: A Spectacular Ancient Ecosystem Revealed*, Indiana University Press, Bloomington, 54–82 pp.

———. 2015. Origins of dinosaur bonebeds in the Cretaceous of Alberta, Canada. *Canadian Journal of Earth Sciences*, **52**, 655–681.

EBERTH, D. A. 2018. Stratigraphy and paleoenvironmental evolution of the dinosaur-rich Baruungoyot-Nemegt succession (Upper Cretaceous), Nemegt Basin, southern Mongolia. *Palaeogeography, Palaeoclimatology, Palaeoecology*, **494**, 29–50.

EBERTH, D. A. and HAMBLIN, A. P. 1993. Tectonic, stratigraphic, and sedimentologic significance of a regional discontinuity in the upper Judith River Group (Belly River wedge) of southern Alberta, Saskatchewan, and northern Montana. *Canadian Journal of Earth Sciences*, **30**, 174–200.

——— and CURRIE, P. J. 2005. Vertebrate Taphonomy and Taphonomic Modes. *In* CURRIE, P. J. and KOPPELHUS, E. B. (eds.) *Dinosaur Provincial Park: A Spectacular Ancient Ecosystem Revealed*, Indiana University Press, Bloomington, 453–477 pp.

EBERTH, D. A. and GETTY, M. A. 2005. Ceratopsian Bonebeds: Occurrence, Origins, and Significance. *In* CURRIE, P. J. and KOPPELHUS, E. B. (eds.) *Dinosaur Provincial Park: A Spectacular Ancient Ecosystem Revealed*, Indiana University Press, Bloomington, 501–536 pp.

EBERTH, D. A., SHANNON, M. and NOLAN, B. G. 2007. A bonebeds database: classification, biases, and patterns of occurrence. *In* ROGERS, R. R., EBERTH, D. A. and FIORILLO, A. R. (eds.) *Bonebeds: Genesis, Analysis, and Paleobiological Significance*, University of Chicago Press, Chicago, IL, 103–219 pp.

———, BRINKMAN, D. B. and BARKAS, V. 2010. A Centrosaurine Mega-Bonebed from the Upper Cretaceous of Southern Alberta: Implications for Behavior and Death Events. *In* RYAN, M. J., CHINNERY-ALLGEIER, B. J. and EBERTH, D. A. (eds.) *New Perspectives on Horned Dinosaurs*, Indiana University Press, Bloomington & Indianapolis, 495–508 pp.

———, EVANS, D. C. and LLOYD, D. W. H. 2015. Occurrence and Taphonomy of the First Documented Hadrosaurid Bonebed from the Dinosaur Park Formation (Belly River Group, Campanian) at Dinosaur Provincial Park, Alberta, Canada. *In* EBERTH, D. A. and EVANS, D. C. (eds.) *Hadrosaurs*, Indiana University Press, Bloomington, 502–523 pp.

———, ———, BRINKMAN, D. B., THERRIEN, F., TANKE, D. H. and RUSSELL, L. S. 2013. Dinosaur biostratigraphy of the Edmonton Group (Upper Cretaceous), Alberta, Canada: evidence for climate influence. *Canadian Journal of Earth Sciences*, **50**, 701–726.

EBERTH, D. A., EVANS, D. C., RAMEZANI, J., KAMO, S. L., BROWN, C. M., CURRIE, P. J. and BRAMAN, D. R. 2023. Calibrating geologic strata, dinosaurs, and other fossils at Dinosaur Provincial Park (Alberta, Canada) using a new CA-ID-TIMS U–Pb geochronology. *Canadian Journal of Earth Sciences*, **60**, 1627–1646.

EHRLICH, P. R. and RAVEN, P. H. 1964. Butterflies and plants: a study in coevolution. *Evolution*, **18**, 586–608.

EKLÖF, A., JACOB, U., KOPP, J., BOSCH, J., CASTRO-URGAL, R., CHACOFF, N. P., DALSGAARD, B., DE SASSI, C., GALETTI, M., GUMARÃES, P. R., LOMÁSCOLO, S. B., MARTÍN GONZÁLEZ, A. M., PIZO, M. A., RADER, R., RODRIGO, A., TYLIANAKIS, J.

M., VÁZQUEZ, D. P. and ALLESINA, S. 2013. The dimensionality of ecological networks. *Ecology Letters*, **16**, 577-583.

ELDREDGE, N. and GOULD, S. J. 1972. Punctuated equilibria: an alternative to phyletic gradualism. *In* SCHOPF, T. J. M. (ed.) *Models in Paleobiology*, Freeman, Cooper & Co., 82–115 pp.

ENVIRONMENT AND CLIMATE CHANGE CANADA. 2012. *Engelmann's quillwort (*Isoetes engelmannii*): recovery strategy*. Downloaded from https://www.canada.ca/en/environment-climate-change/services/species-risk-public-registry/recovery-strategies/engelmanns-quillwort.html on 22 March 2024.

ERICKSON, B. R. 1972. Albertochampsa langstoni*, gen. et. sp. nov., a new alligator from the Cretaceous of Alberta*. Vol. 2. The Science Museum of Minnesota, Saint Paul, Minnesota.

ERICKSON, G. M., MAKOVICKY, P. J., CURRIE, P. J., NORELL, M. A., YERBY, S. A. and BROCHU, C. A. 2004. Gigantism and comparative life-history parameters of tyrannosaurid dinosaurs. *Nature*, **430**, 772.

ERWIN, D. H. 2007. Disparity: Morphological Pattern and Developmental Context. *Palaeontology*, **50**, 57–73.

ERWIN, D. H. 2015. Novelty and Innovation in the History of Life. *Current Biology*, **25**, R930–R940.

ESTES, R. 1969. Studies on Fossil Phyllodont Fishes: Interrelationships and Evolution in the Phyllodontidae (Albuloidei). *Copeia*, **1969**, 317–331.

———. 1975. Lower Vertebrates from the Fort Union Formation, Late Paleocene, Big Horn Basin, Wyoming. *Herpetologica*, **31**, 365–385.

———. 1976. Middle Paleocene Lower Vertebrates from the Tongue River Formation, Southeastern Montana. *Journal of Paleontology*, **50**, 500–520.

EVANS, D. C. and REISZ, R. R. 2007. Anatomy and Relationships of *Lambeosaurus magnicristatus*, a crested hadrosaurid dinosaur (Ornithischia) from the Dinosaur Park Formation, Alberta. *Journal of Vertebrate Paleontology*, **27**, 373–393.

———, BAVINGTON, R. and CAMPIONE, N. E. 2009. An unusual hadrosaurid braincase from the Dinosaur Park Formation and the biostratigraphy of *Parasaurolophus* (Ornithischia: Lambeosaurinae) from southern Alberta. *Canadian Journal of Earth Sciences*, **46**, 791–800.

———, MCGARRITY, C. T. and RYAN, M. J. 2015. A Skull of *Prosaurolophus maximus* from Southeastern Alberta and the Spatiotemporal Distribution of Faunal Zones in the Dinosaur Park Formation. *In* EBERTH, D. A. and EVANS, D. C. (eds.) *Hadrosaurs*, Indiana University Press, Bloomington, 200–207 pp.

———, SCHOTT, R. K., LARSON, D. W., BROWN, C. M. and RYAN, M. J. 2013. The oldest North American pachycephalosaurid and the hidden diversity of small-bodied ornithischian dinosaurs. *Nature Communications*, **4**, 1828.

EVANS, S. E. 1990. The skull of *Cteniogenys*, a choristodere (Reptilia: Archosauromorpha) from the Middle Jurassic of Oxfordshire. *Zoological Journal of the Linnean Society*, **99**, 205–237.

EVERHART, M. J. 2005. Bite marks on an elasmosaur (Sauropterygia; Plesiosauria) paddle from the Niobrara Chalk (Upper Cretaceous) as probable evidence of feeding by the lamniform shark, *Cretoxyrhina mantelli*. *PalArch Foundation*, **2**, 14–24.

———. 2013. Enchodus *sp. The sabre-toothed fish of the Cretaceous*. Downloaded from http://oceansofkansas.com/Enchodus.html on 15 May 2023.

FAGERSTROM, J. A. 1987. *The Evolution of Reef Communities*. Wiley-Interscience, New York.

FANTI, F., CURRIE, P. J. and BURNS, M. E. 2015. Taphonomy, age, and paleoecological implication of a new *Pachyrhinosaurus* (Dinosauria: Ceratopsidae) bonebed from the Upper Cretaceous

(Campanian) Wapiti Formation of Alberta, Canada. *Canadian Journal of Earth Sciences*, **52**, 250–260.

FANTI, F., BELL, P. R., CURRIE, P. J. and TSOGTBAATAR, K. 2018. The Nemegt Basin — One of the best field laboratories for interpreting Late Cretaceous terrestrial ecosystems. *Palaeogeography, Palaeoclimatology, Palaeoecology*, **494**, 1–4.

FARLOW, J. O. 1976. A Consideration of the Trophic Dynamics of a Late Cretaceous Large-Dinosaur Community (Oldman Formation). *Ecology*, **57**, 841–857.

———. 1993. On the rareness of big, fierce animals: speculations about the body sizes, population densities, and geographic ranges of predatory mammals and large carnivorous dinosaurs. *American Journal of Science*, **293-A**, 167–199.

——— and PIANKA, E. R. 2002. Body Size Overlap, Habitat Partitioning and Living Space Requirements of Terrestrial Vertebrate Predators: Implications for the Paleoecology of Large Theropod Dinosaurs. *Historical Biology*, **16**, 21–40.

———, COROIAN, I. D. and FOSTER, J. R. 2010. Giants on the landscape: modelling the abundance of megaherbivorous dinosaurs of the Morrison Formation (Late Jurassic, western USA). *Historical Biology*, **22**, 403–429.

———, COROIAN, D., CURRIE, P. J., FOSTER, J. R., MALLON, J. C. and THERRIEN, F. 2022. “Dragons” on the landscape: Modeling the abundance of large carnivorous dinosaurs of the Upper Jurassic Morrison Formation (USA) and the Upper Cretaceous Dinosaur Park Formation (Canada). *The Anatomical Record*, **306**, 1669–1696.

FIELD, D. J., BERCOVICI, A., BERV, J. S., DUNN, R., FASTOVSKY, D. E., LYSON, T. R., VAJDA, V. and GAUTHIER, J. A. 2018. Early Evolution of Modern Birds Structured by Global Forest Collapse at the End-Cretaceous Mass Extinction. *Current Biology*, **28**, 1825–1831.

FIORILLO, A. R., MCCARTHY, P. J. and FLAIG, P. P. 2016. A multi-disciplinary perspective on habitat preferences among dinosaurs in a Cretaceous Arctic greenhouse world, North Slope, Alaska (Prince Creek Formation: lower Maastrichtian). *Palaeogeography, Palaeoclimatology, Palaeoecology*, **441**, 377–389.

FOSTER, G. L. and ROHLING, E. J. 2013. Relationship between sea level and climate forcing by CO_2 on geological timescales. *Proceedings of the National Academy of Sciences*, **110**, 1209–1214.

FOSTER, J. R. 2003. *Paleoecological Analysis of the Vertebrate Fauna of the Morrison Formation (Upper Jurassic), Rocky Mountain Region, U.S.A.: Bulletin 23*. New Mexico Museum of Natural History and Science.

FOWLER, D. W. 2017. Revised geochronology, correlation, and dinosaur stratigraphic ranges of the Santonian-Maastrichtian (Late Cretaceous) formations of the Western Interior of North America. *PLOS ONE*, **12**, e0188426.

FOWLER, D. W. and FOWLER, E. A. F. 2020. Transitional evolutionary forms in chasmosaurine ceratopsid dinosaurs: evidence from the Campanian of New Mexico. *PeerJ*, **8**, e9251.

———, FREEDMAN, E. A., SCANNELLA, J. B. and KAMBIC, R. E. 2011. The predatory ecology of *Deinonychus* and the origin of flapping in birds. *Plos One*, **6**.

FOX, R. C. 1979*a*. Mammals from the Upper Cretaceous Oldman Formation, Alberta. I. *Alphadon* Simpson (Marsupialia). *Canadian Journal of Earth Sciences*, **16**, 91–102.

———. 1979*b*. Mammals from the Upper Cretaceous Oldman Formation, Alberta. II. *Pediomys* Marsh (Marsupialia). *Canadian Journal of Earth Sciences*, **16**, 103–113.

———. 1979*c*. Mammals from the Upper Cretaceous Oldman Formation, Alberta. III. Eutheria. *Canadian Journal of Earth Sciences*, **16**, 114–125.

———. 1981. Mammals from the Upper Cretaceous Oldman Formation, Alberta. V. *Eodelphis* Matthew, and the evolution of the Stagodontidae (Marsupialia). *Canadian Journal of Earth Sciences*, **18**, 350–365.

———. 2005. Late Cretaceous Mammals. *In* CURRIE, P. J. and KOPPELHUS, E. B. (eds.) *Dinosaur Provincial Park: A Spectacular Ancient Ecosystem Revealed*, Indiana University Press, Bloomington, 417–449 pp.

FRASER, D., SOUL, L. C., TÓTH, A. B., BALK, M. A., ERONEN, J. T., PINEDA-MUNOZ, S., SHUPINSKI, A. B., VILLASEÑOR, A., BARR, W. A., BEHRENSMEYER, A. K., DU, A., FAITH, J. T., GOTELLI, N. J., GRAVES, G. R., JUKAR, A. M., LOOY, C. V., MILLER, J. H., POTTS, R. and LYONS, S. K. 2021. Investigating Biotic Interactions in Deep Time. *Trends in Ecology & Evolution*, **36**, 61–75.

FREDERICKSON, J. A. and TUMARKIN-DERATZIAN, A. R. 2014. Craniofacial ontogeny in *Centrosaurus apertus*. *PeerJ*, **2**, e252.

FREDERICKSON, J. A., ENGEL, M. H. and CIFELLI, R. L. 2018. Niche Partitioning in Theropod Dinosaurs: Diet and Habitat Preference in Predators from the Uppermost Cedar Mountain Formation (Utah, U.S.A.). *Scientific Reports*, **8**, 17872.

FREIMUTH, W. J., VARRICCHIO, D. J., BRANNICK, A. L., WEAVER, L. N. and WILSON MANTILLA, G. P. 2021. Mammal-bearing gastric pellets potentially attributable to *Troodon formosus* at the Cretaceous Egg Mountain locality, Two Medicine Formation, Montana, USA. *Palaeontology*, **64**, 699–725.

FRICKE, E. C., HSIEH, C., MIDDLETON, O., GORCZYNSKI, D., CAPPELLO, C. D., SANISIDRO, O., ROWAN, J., SVENNING, J.-C. and BEAUDROT, L. 2022. Collapse of terrestrial mammal food webs since the Late Pleistocene. *Science*, **377**, 1008–1011.

FROESE, R. and PAULY, D. 2024*a*. *Species Summary:* Squatina squatina. Fishbase. Downloaded from https://fishbase.se/summary/Squatina-squatina.html on 5 April 2023.

——— and ———. 2024*b*. *Species Summary:* Pristis pristis. Fishbase. Downloaded from https://www.fishbase.se/summary/8940 on 14 May 2023.

——— and ———. 2024*c*. *Species Summary:* Chimaera monstrosa. Fishbase. Downloaded from https://fishbase.se/summary/Chimaera-monstrosa.html on 14 May 2023.

——— and ———. 2024*d*. *Species Summary:* Scleropages jardinii. Fishbase. Downloaded from https://fishbase.mnhn.fr/summary/Scleropages-jardinii.html on 2 April 2024.

——— and ———. 2024*e*. *Species Summary:* Gonorynchus gonorynchus. Downloaded from https://fishbase.mnhn.fr/summary/Gonorynchus-gonorynchus.html on 2 April 2024.

——— and ———. 2024*f*. *Species Summary:* Charax pauciradiatus. Fishbase. Downloaded from https://fishbase.mnhn.fr/summary/27858 on 3 April 2024.

FU, D., TONG, G., DAI, T., LIU, W., YANG, Y., ZHANG, Y., CUI, L., LI, L., YUN, H., WU, Y., SUN, A., LIU, C., PEI, W., GAINES, R. R. and ZHANG, X. 2019. The Qingjiang biota—A Burgess Shale–type fossil Lagerstätte from the early Cambrian of South China. *Science*, **363**, 1338–1342.

FUENTES, A. J., CLYDE, W. C., WEISSENBURGER, K., BERCOVICI, A., LYSON, T. R., MILLER, I. M., RAMEZANI, J., ISAKSON, V., SCHMITZ, M. D. and JOHNSON, K. R. 2019. Constructing a time scale of biotic recovery across the Cretaceous–Paleogene boundary, Corral Bluffs, Denver Basin, Colorado, U.S.A. *Rocky Mountain Geology*, **54**, 133–153.

FUENTES-JACQUES, L. J., HANSON-SNORTUM, P., HERNÁNDEZ-ORTIZ, V., DÍAZ-CASTELAZO, C. and MEHLTRETER, K. 2022. A global review and network analysis of phytophagous insect interactions with ferns and lycophytes. *Plant Ecology*, **223**, 27–40.

FUNSTON, G. F. 2020. Caenagnathids of the Dinosaur Park Formation (Campanian) of Alberta, Canada: anatomy, osteohistology, taxonomy, and evolution. *Vertebrate Anatomy Morphology Palaeontology*, **8**, 105–153.

FUNSTON, G. F. and CURRIE, P. J. 2014. A previously undescribed caenagnathid mandible from the late Campanian of Alberta, and insights into the diet of *Chirostenotes pergracilis* (Dinosauria: Oviraptorosauria). *Canadian Journal of Earth Sciences*, **51**, 156–165.

FUNSTON, G. F. and CURRIE, P. J. 2020. New material of *Chirostenotes pergracilis* (Theropoda, Oviraptorosauria) from the Campanian Dinosaur Park Formation of Alberta, Canada. *Historical Biology*, **0**, 1–15.

FÜRSICH, F. T. and ABERHAN, M. 1990. Significance of time-averaging for palaeocommunity analysis. *Lethaia*, **23**, 143–152.

———, SHA, J., JIANG, B. and PAN, Y. 2007. High resolution palaeoecological and taphonomic analysis of Early Cretaceous lake biota, western Liaoning (NE-China). *Palaeogeography, Palaeoclimatology, Palaeoecology*, **253**, 434–457.

GAO, K.-Q. and FOX, R. C. 1996. Taxonomy and evolution of Late Cretaceous lizards (Reptilia: Squamata) from Western Canada. *Bulletin of Carnegie Museum of Natural History*, **33**, 1–107.

——— and ———. 1998. New choristoderes (Reptilia: Diapsida) from the Upper Cretaceous and Palaeocene, Alberta and Saskatchewan, Canada, and phylogenetic relationships of Choristodera. *Zoological Journal of the Linnean Society*, **124**, 303–353.

——— and BRINKMAN, D. B. 2005. Choristoderes from the Park and Its Vicinity. *In* CURRIE, P. J. and KOPPELHUS, E. B. (eds.) *Dinosaur Provincial Park: A Spectacular Ancient Ecosystem Revealed*, Indiana University Press, Bloomington, 221–234 pp.

——— and KSEPKA, D. T. 2008. Osteology and taxonomic revision of *Hyphalosaurus* (Diapsida: Choristodera) from the Lower Cretaceous of Liaoning, China. *Journal of Anatomy*, **212**, 747–768.

GARCÍA-GIRÓN, J., CHIARENZA, A. A., ALAHUHTA, J., DEMAR, D. G., HEINO, J., MANNION, P. D., WILLIAMSON, T. E., WILSON MANTILLA, G. P. and BRUSATTE, S. L. 2022. Shifts in food webs and niche stability shaped survivorship and extinction at the end-Cretaceous. *Science Advances*, **8**, eadd5040.

GARDNER, J. D. 2003. Revision of *Habrosaurus* Gilmore (Caudata; Sirenidae) and relationships among sirenid salamanders. *Palaeontology*, **46**, 1089–1122.

———. 2005. Lissamphibians. *In* CURRIE, P. J. and KOPPELHUS, E. B. (eds.) *Dinosaur Provincial Park: A Spectacular Ancient Ecosystem Revealed*, Indiana University Press, Bloomington, 186–201 pp.

GARDNER, J. D. 2015. An edentulous frog (Lissamphibia; Anura) from the Upper Cretaceous (Campanian) Dinosaur Park Formation of southeastern Alberta, Canada. *Canadian Journal of Earth Sciences*, **52**, 569–580.

GARDNER, J. D., RUSSELL, A. P. and BRINKMAN, D. B. 1995. Systematics and taxonomy of soft-shelled turtles (Family Trionychidae) from the Judith River Group (mid-Campanian) of North America. *Canadian Journal of Earth Sciences*, **32**, 631–643.

———, REDMAN, C. M. and CIFELLI, R. L. 2016. The hopping dead: Late Cretaceous frogs from the middle – late Campanian (Judithian) of western North America. *Fossil Imprint*, **72**, 78–107.

GATES, T. A. and SAMPSON, S. D. 2007. A new species of *Gryposaurus* (Dinosauria: Hadrosauridae) from the late Campanian Kaiparowits Formation, southern Utah, USA. *Zoological Journal of the Linnean Society*, **151**, 351–376.

GATES, T. A., SAMPSON, S. D., ZANNO, L. E., ROBERTS, E. M., EATON, J. G., NYDAM, R. L., HUTCHISON, J. H., SMITH, J. A., LOEWEN, M. A. and GETTY, M. A. 2010. Biogeography of terrestrial and freshwater vertebrates from the late Cretaceous (Campanian) Western Interior of North America. *Palaeogeography, Palaeoclimatology, Palaeoecology*, **291**, 371–387.

GAUTIER-HION, A., DUPLANTIER, J.-M., QURIS, R., FEER, F., SOURD, C., DECOUX, J.-P., DUBOST, G., EMMONS, L., ERARD, C., HECKETSWEILER, P., MOUNGAZI, A., ROUSSILHON, C. and THIOLLAY, J.-M. 1985. Fruit characters as a basis of fruit choice and seed dispersal in a tropical forest vertebrate community. *Oecologia*, **65**, 324–337.

GHIENNE, J.-F., DESROCHERS, A., VANDENBROUCKE, T. R. A., ACHAB, A., ASSELIN, E., DABARD, M.-P., FARLEY, C., LOI, A., PARIS, F., WICKSON, S. and VEIZER, J. 2014. A Cenozoic-style scenario for the end-Ordovician glaciation. *Nature Communications*, **5**, 4485.

GILMORE, C. W. 1923. A new species of *Aspideretes* from the Belly River Cretaceous of Alberta, Canada. *Transactions of the Royal Society of Canada, Section 4, Series 3*, **17**, 1–10.

———. 1924*a*. A new coelurid dinosaur from the Belly River Cretaceous of Alberta. *Canada Department of Mines Geological Survey Bulletin (Geological Series)*, **38**, 1–12.

———. 1924*b*. On *Troodon validus*, an ornithopodous dinosaur from the Belly River Cretaceous of Alberta, Canada. *Bulletin of the University of Alberta Department of Geology*, **1**, 1–43.

———. 1946. Notes on recently mounted reptile fossil skeletons in the United States National Museum. *Proceedings of the United States National Museum*, **96**, 195–203, pl. 12–19.

GINGERICH, P. D. and GUNNELL, G. F. 1995. Rates of evolution in Paleocene-Eocene mammals of the Clarks Fork Basin, Wyoming, and a comparison with Neogene Siwalik lineages of Pakistan. *Palaeogeography, Palaeoclimatology, Palaeoecology*, **115**, 227–247.

GODFREY, S. J. and HOLMES, R. 1995. Cranial morphology and systematics of *Chasmosaurus* (Dinosauria: Ceratopsidae) from the Upper Cretaceous of western Canada. *Journal of Vertebrate Paleontology*, **15**, 726–742.

GOTELLI, N. J., GRAVES, G. R. and RAHBEK, C. 2010. Macroecological signals of species interactions in the Danish avifauna. *Proceedings of the National Academy of Sciences*, **107**, 5030–5035.

GOULD, S. J. 1985. The Paradox of the First Tier: An Agenda for Paleobiology. *Paleobiology*, **11**, 2–12.

——— and ELDREDGE, N. 1977. Punctuated Equilibria: The Tempo and Mode of Evolution Reconsidered. *Paleobiology*, **3**, 115–151.

GRAHAM, A. 2023. Ophisaurus ventralis *(Eastern Glass Lizard)*. Animal Diversity Web. Downloaded from https://animaldiversity.org/accounts/Ophisaurus_ventralis/ on 18 March 2024.

GRANDE, L. 1984. *Paleontology of the Green River Formation, with a review of the fish fauna*. The Geological Survey of Wyoming, Laramie, Wyoming.

——— and BEMIS, W. E. 1998. A Comprehensive Phylogenetic Study of Amiid Fishes (Amiidae) Based on Comparative Skeletal Anatomy. An Empirical Search for Interconnected Patterns of Natural History. *Journal of Vertebrate Paleontology*, **18**, 1–696.

——— and GRANDE, T. 1999. A new species of †*Notogoneus* (Teleostei: Gonorynchidae) from the Upper Cretaceous Two Medicine Formation of Montana, and the poor Cretaceous record of freshwater fishes from North America. *Journal of Vertebrate Paleontology*, **19**, 612–622.

GRANGE, S. and DUNCAN, P. 2006. Bottom-up and top-down processes in African ungulate communities: resources and predation acting on the relative abundance of zebra and grazing bovids. *Ecography*, **29**, 899–907.

GRAVEL, D., POISOT, T., ALBOUY, C., VELEZ, L. and MOUILLOT, D. 2013. Inferring food web structure from predator–prey body size relationships. *Methods in Ecology and Evolution*, **4**, 1083–1090.

———, BAISER, B., DUNNE, J. A., KOPELKE, J.-P., MARTINEZ, N. D., NYMAN, T., POISOT, T., STOUFFER, D. B., TYLIANAKIS, J. M., WOOD, S. A. and ROSLIN, T. 2019. Bringing Elton and Grinnell together: a quantitative framework to represent the biogeography of ecological interaction networks. *Ecography*, **42**, 401–415.

GRIMALDI, D. 1999. The Co-Radiations of Pollinating Insects and Angiosperms in the Cretaceous. *Annals of the Missouri Botanical Garden*, **86**, 373–406.

GROFF, D. V., HAMLEY, K. M., LESSARD, T. J. R., GREENAWALT, K. E., YASUHARA, M., BRICKLE, P. and GILL, J. L. 2020. Seabird establishment during regional cooling drove a terrestrial ecosystem shift 5000 years ago. *Science Advances*, **6**, eabb2788.

GRUBB, P. 1971. The growth, ecology and population structure of giant tortoises on Aldabra. *Philosophical Transactions of the Royal Society of London. B, Biological Sciences*, **260**, 327–372.

GUO-QING, L. 1996. A new species of Late Cretaceous osteoglossid (Teleostei) from the Oldman Formation of Alberta, Canada, and its phylogenetic relationships. *In* ARRATIA, G. and VIOHL, G. (eds.) *Mesozoic Fishes: Systematics and Paleoecology*, Verlag Dr. Friedrich Pfeil, Munich, 285–298 pp.

GUTHRIE, R. D. 2006. New carbon dates link climatic change with human colonization and Pleistocene extinctions. *Nature*, **441**, 207–209.

HALL, S. J. and RAFFAELLI, D. 1991. Food-Web Patterns: Lessons from a Species-Rich Web. *Journal of Animal Ecology*, **60**, 823–841.

HANLIN, H. G. 1978. Food Habits of the Greater Siren, *Siren lacertina*, in an Alabama Coastal Plain Pond. *Copeia*, **1978**, 358–360.

HAQ, B. U. 2014. Cretaceous eustasy revisited. *Global and Planetary Change*, **113**, 44–58.

HARMON, L. J., ANDREAZZI, C. S., DÉBARRE, F., DRURY, J., GOLDBERG, E. E., MARTINS, A. B., MELIÁN, C. J., NARWANI, A., NUISMER, S. L., PENNELL, M. W., RUDMAN, S. M., SEEHAUSEN, O., SILVESTRO, D., WEBER, M. and MATTHEWS, B. 2019. Detecting the macroevolutionary signal of species interactions. *Journal of Evolutionary Biology*, **32**, 769–782.

HARTMAN, J. H., JOHNSON, K. R. and NICHOLS, D. J. 2002. *The Hell Creek Formation and the Cretaceous-Tertiary Boundary in the Northern Great Plains: An Integrated Continental Record of the End of the Cretaceous*. Geological Society of America.

HASSLER, A., MARTIN, J. E., AMIOT, R., TACAIL, T., GODET, F. A., ALLAIN, R. and BALTER, V. 2018. Calcium isotopes offer clues on resource partitioning among Cretaceous predatory dinosaurs. *Proceedings of the Royal Society B: Biological Sciences*, **285**, 20180197.

HASTINGS, A. K. and HELLMUND, M. 2017. Evidence for prey preference partitioning in the middle Eocene high-diversity crocodylian assemblage of the Geiseltal-Fossillagerstätte, Germany utilizing skull shape analysis. *Geological Magazine*, **154**, 119–146.

HAUTMANN, M. 2020. What is macroevolution? *Palaeontology*, **63**, 1–11.

HAY, W. W. 2017. Toward understanding Cretaceous climate—An updated review. *Science China Earth Sciences*, **60**, 15.

——— and FLOEGEL, S. 2012. New thoughts about the Cretaceous climate and oceans. *Earth-Science Reviews*, **115**, 262–272.

HEAD, J. J., BLOCH, J. I., HASTINGS, A. K., BOURQUE, J. R., CADENA, E. A., HERRERA, F. A., POLLY, P. D. and JARAMILLO, C. A. 2009. Giant boid snake from the Palaeocene neotropics reveals hotter past equatorial temperatures. *Nature*, **457**, 715–717.

HENDERSON, D. M. and TANKE, D. H. 2010. Estimating past and future dinosaur skeletal abundances in Dinosaur Provincial Park, Alberta, Canada. *Canadian Journal of Earth Sciences*, **47**, 1291–1304.

HENDRY, A. P. 2016. *Eco-evolutionary Dynamics*. Princeton University Press.

HERMAN, A. B. and SPICER, R. A. 1997. New quantitative palaeoclimate data for the Late Cretaceous Arctic: evidence for a warm polar ocean. *Palaeogeography, Palaeoclimatology, Palaeoecology*, **128**, 227–251.

HERMAN, A. B., SPICER, R. A. and SPICER, T. E. V. 2016. Environmental constraints on terrestrial vertebrate behaviour and reproduction in the high Arctic of the Late Cretaceous. *Palaeogeography, Palaeoclimatology, Palaeoecology*, **441**, 317–338.

HOLMES, R. B. and RYAN, M. J. 2013. The postcranial skeleton of *Styracosaurus albertensis*. *Kirtlandia*, **58**, 5–37.

HOLMES, R. B., FORSTER, C., RYAN, M. and SHEPHERD, K. M. 2001. A new species of *Chasmosaurus* (Dinosauria: Ceratopsia) from the Dinosaur Park Formation of southern Alberta. *Canadian Journal of Earth Sciences*, **38**, 1423–1438.

HOLMES, R. B., PERSONS, W. S., RUPAL, B. S., QURESHI, A. J. and CURRIE, P. J. 2020. Morphological variation and asymmetrical development in the skull of *Styracosaurus albertensis*. *Cretaceous Research*, **107**, 104308.

HOLROYD, P. A. and HUTCHISON, J. H. 2002. Patterns of geographic variation in latest Cretaceous vertebrates: Evidence from the turtle component. *In The Hell Creek Formation and the Cretaceous-Tertiary Boundary in the Northern Great Plains: An Integrated Continental Record of the End of the Cretaceous*, Geological Society of America.

HOLTZ, T. R. 2004. Tyrannosauroidea. *In The Dinosauria*, University of California Press, Berkeley & Los Angeles, 111–136 pp.

HOLTZ, T. R. 2021. Theropod guild structure and the tyrannosaurid niche assimilation hypothesis: implications for predatory dinosaur macroecology and ontogeny in later Late Cretaceous Asiamerica. *Canadian Journal of Earth Sciences*, **58**, 778–795.

HONDA, H. 1997. Ginkgo and Insects. *In* HORI, T., RIDGE, R. W., TULECKE, W., DEL TREDICI, P., TRÉMOUILLAUX-GUILLER, J. and TOBE, H. (eds.) Ginkgo Biloba*, A Global Treasure: From Biology to Medicine*, Springer Japan, Tokyo, 243–250 pp.

HONE, D. W. E. and RAUHUT, O. W. M. 2010. Feeding behaviour and bone utilization by theropod dinosaurs. *Lethaia*, **43**, 232–244.

HONE, D. W. E., HABIB, M. B. and THERRIEN, F. 2019. *Cryodrakon boreas*, gen. et sp. nov., a Late Cretaceous Canadian azhdarchid pterosaur. *Journal of Vertebrate Paleontology*, **39**, e1649681.

HONE, D. W. E., ALEXANDER DECECCHI, T., SULLIVAN, C., XING, X. and LARSSON, H. C. E. 2022. Generalist diet of *Microraptor zhaoianus* included mammals. *Journal of Vertebrate Paleontology*, **42**, e2144337.

HONG, S. K. and LEE, Y. I. 2012. Evaluation of atmospheric carbon dioxide concentrations during the Cretaceous. *Earth and Planetary Science Letters*, **327–328**, 23–28.

HOORN, C., WESSELINGH, F. P., STEEGE, H. ter, BERMUDEZ, M. A., MORA, A., SEVINK, J., SANMARTÍN, I., SANCHEZ-MESEGUER, A., ANDERSON, C. L., FIGUEIREDO, J. P., JARAMILLO, C., RIFF, D., NEGRI, F. R., HOOGHIEMSTRA, H., LUNDBERG, J., STADLER, T., SÄRKINEN, T. and ANTONELLI, A. 2010. Amazonia Through Time: Andean Uplift, Climate Change, Landscape Evolution, and Biodiversity. *Science*, **330**, 927–931.

HOPKIN, S. P. and READ, H. J. 1992. *The Biology of Millipedes*. Oxford University Press.

HOPKINS, D. D. and FORBES, R. B. 1980. Dietary Patterns of the Virginia Opossum in an Urban Environment. *The Murrelet*, **61**, 20–30.

HORNER, J. R. 1992. *Cranial Morphology of* Prosaurolophus *(Ornithischia: Hadrosauridae) with Description of two New Hadrosaurid Species and an Evaluation of Hadrosaurid Phylogenetic Relationships*. Museum of the Rockies, Bozeman, Montana.

HORNER, J. R., VARRICCHIO, D. J. and GOODWIN, M. B. 1992. Marine transgressions and the evolution of Cretaceous dinosaurs. *Nature*, **358**, 59–61.

———, WEISHAMPEL, D. B. and FORSTER, C. A. 2004. Hadrosauridae. *In* DODSON, P., WEISHAMPEL, D. B. and OSMÓLSKA, H. (eds.) *The Dinosauria*, University of California Press, Berkeley & Los Angeles, 438–463 pp.

HORTAL, J., DE BELLO, F., DINIZ-FILHO, J. A. F., LEWINSOHN, T. M., LOBO, J. M. and LADLE, R. J. 2015. Seven Shortfalls that Beset Large-Scale Knowledge of Biodiversity. *Annual Review of Ecology, Evolution, and Systematics*, **46**, 523–549.

HOXMEIER, R. H. J. and DEVRIES, D. R. 1997. Habitat Use, Diet, and Population Structure of Adult and Juvenile Paddlefish in the Lower Alabama River. *Transactions of the American Fisheries Society*, **126**, 288–301.

HU, S., ZHANG, Q., CHEN, Z.-Q., ZHOU, C., LÜ, T., XIE, T., WEN, W., HUANG, J. and BENTON, M. J. 2011. The Luoping biota: exceptional preservation, and new evidence on the Triassic recovery from end-Permian mass extinction. *Proceedings of the Royal Society B: Biological Sciences*, **278**, 2274–2282.

HUANG, Y., CHEN, Z.-Q., ROOPNARINE, P. D., BENTON, M. J., ZHAO, L., FENG, X. and LI, Z. 2023. The stability and collapse of marine ecosystems during the Permian-Triassic mass extinction. *Current Biology*, **33**, 1059-1070.e4.

———, ———, ———, ———, YANG, W., LIU, J., ZHAO, L., LI, Z. and GUO, Z. 2021. Ecological dynamics of terrestrial and freshwater ecosystems across three mid-Phanerozoic mass extinctions from northwest China. *Proceedings of the Royal Society B: Biological Sciences*, **288**, 20210148.

HUDGINS, M. N., CURRIE, P. J. and SULLIVAN, C. 2022. Dental assessment of *Stegoceras validum* (Ornithischia: Pachycephalosauridae) and *Thescelosaurus neglectus* (Ornithischia: Thescelosauridae): paleoecological inferences. *Cretaceous Research*, **130**, 105058.

IBRAHIM, N., SERENO, P. C., VARRICCHIO, D. J., MARTILL, D. M., DUTHEIL, D. B., UNWIN, D. M., BAIDDER, L., LARSSON, H. C. E., ZOUHRI, S. and KAOUKAYA, A. 2020. Geology and paleontology of the Upper Cretaceous Kem Kem Group of eastern Morocco. *ZooKeys*, **928**, 1–216.

JABLONSKI, D. 1986. Background and Mass Extinctions: The Alternation of Macroevolutionary Regimes. *Science*, **231**, 129–133.

———. 2005. Mass Extinctions and Macroevolution. *Paleobiology*, **31**, 192–210.

——— and SEPKOSKI, J. J. 1996. Paleobiology, Community Ecology, and Scales of Ecological Pattern. *Ecology*, **77**, 1367–1378.

——— and EDIE, S. M. 2023. Perfect storms shape biodiversity in time and space. *Evolutionary Journal of the Linnean Society*, **2**, kzad003.

———, ROY, K. and VALENTINE, J. W. 2006. Out of the Tropics: Evolutionary Dynamics of the Latitudinal Diversity Gradient. *Science*, **314**, 102–106.

JACOBSEN, A. R. 1998. Feeding behaviour of carnivorous dinosaurs as determined by tooth marks on dinosaur bones. *Historical Biology*, **13**, 17–26.

JARAMILLO, C. and CÁRDENAS, A. 2013. Global Warming and Neotropical Rainforests: A Historical Perspective. *Annual Review of Earth and Planetary Sciences*, **41**, 741–766.

JARAULA, C. M. B., GRICE, K., TWITCHETT, R. J., BÖTTCHER, M. E., LEMETAYER, P., DASTIDAR, A. G. and OPAZO, L. F. 2013. Elevated $p\mathrm{CO}_2$ leading to Late Triassic extinction, persistent photic zone euxinia, and rising sea levels. *Geology*, **41**, 955–958.

JARZEN, D. M. 1982. Palynology of Dinosaur Provincial Park (Campanian) Alberta. *Syllogeus*, **38**, 1–69.

JERZYKIEWICZ, T., CURRIE, P. J., EBERTH, D. A., JOHNSTON, P. A., KOSTER, E. H. and ZHENG, J.-J. 1993. Djadokhta Formation correlative strata in Chinese Inner Mongolia: an overview of the stratigraphy, sedimentary geology, and paleontology and comparisons with the type locality in the pre-Altai Gobi. *Canadian Journal of Earth Sciences*, **30**, 2180–2195.

JESSOP, T. S., ARIEFIANDY, A., FORSYTH, D. M., PURWANDANA, D., WHITE, C. R., BENU, Y. J., MADSEN, T., HARLOW, H. J. and LETNIC, M. 2020. Komodo dragons are not ecological analogs of apex mammalian predators. *Ecology*, **101**, e02970.

JI, Q., CURRIE, P. J., NORELL, M. A. and JI, S.-A. 1998. Two feathered dinosaurs from northeastern China. *Nature*, **393**, 753–761.

JOHNSON, K. R. and HICKEY, L. J. 1990. Megafloral change across the Cretaceous/Tertiary boundary in the northern Great Plains and Rocky Mountains, U.S.A. *In Geological Society of America Special Papers*, Vol. 247. Geological Society of America, 433–444 pp.

———, NICHOLS, D. J., ATTREP, M. and ORTH, C. J. 1989. High-resolution leaf-fossil record spanning the Cretaceous/Tertiary boundary. *Nature*, **340**, 708.

JOHNSTON, P. A. and HENDY, A. J. W. 2005. Paleoecology of Mollusks from the Upper Cretaceous Belly River Group. *In Dinosaur Provincial Park: A Spectacular Ancient Ecosystem Revealed*, Indiana University Press, Bloomington, 139–166 pp.

JUDSON, O. P. 2017. The energy expansions of evolution. *Nature Ecology & Evolution*, **1**, 0138.

KAMMERER, C. F., VIGLIETTI, P. A., BUTLER, E. and BOTHA, J. 2023. Rapid turnover of top predators in African terrestrial faunas around the Permian-Triassic mass extinction. *Current Biology*, **33**, 2283-2290.e3.

KARUNARATHNA, D. M. S. S., SURASINGHE, T., BOTEJUE, M., GABADAGE, D. and DISSANAYAKE, D. 2017. Dietary habits and the predators of the Bengal Monitor *Varanus bengalensis* in Sri Lanka. *Biawak*, **11**, 28–39.

KAUFFMAN, E. G. and CALDWELL, W. G. E. 1993. The Western Interior Basin in space and time. *In* CALDWELL, W. G. E. and KAUFFMAN, E. G. (eds.) *Evolution of the Western Interior Basin*, Geological Association of Canada, St. John’s, Newfoundland, 1–30 pp.

KÉFI, S., BERLOW, E. L., WIETERS, E. A., JOPPA, L. N., WOOD, S. A., BROSE, U. and NAVARRETE, S. A. 2015. Network structure beyond food webs: mapping non-trophic and trophic interactions on Chilean rocky shores. *Ecology*, **96**, 291–303.

KELLER, G., MATEO, P., PUNEKAR, J., KHOZYEM, H., GERTSCH, B., SPANGENBERG, J., BITCHONG, A. M. and ADATTE, T. 2018. Environmental changes during the Cretaceous-Paleogene mass extinction and Paleocene-Eocene Thermal Maximum: Implications for the Anthropocene. *Gondwana Research*, **56**, 69–89.

KEMPF, H. L., CASTRO, I. O., DINEEN, A. A., TYLER, C. L. and ROOPNARINE, P. D. 2020. Comparisons of Late Ordovician ecosystem dynamics before and after the Richmondian invasion reveal consequences of invasive species in benthic marine paleocommunities. *Paleobiology*, **46**, 320–336.

KIDWELL, S. M. and FLESSA, K. W. 1995. The quality of the fossil record: Populations, Species, and Communities. *Annual Review of Ecology and Systematics*, **26**, 269–299.

——— and HOLLAND, S. M. 2002. The Quality of the Fossil Record: Implications for Evolutionary Analyses. *Annual Review of Ecology and Systematics*, **33**, 561–588.

KIESSLING, W., RAJA, N. B., RODEN, V. J., TURVEY, S. T. and SAUPE, E. E. 2019. Addressing priority questions of conservation science with palaeontological data. *Philosophical Transactions of the Royal Society B: Biological Sciences*, **374**, 20190222.

KIRWAN, M. L. and MEGONIGAL, J. P. 2013. Tidal wetland stability in the face of human impacts and sea-level rise. *Nature*, **504**, 53–60.

KNAPP, A., KNELL, R. J., FARKE, A. A., LOEWEN, M. A. and HONE, D. W. E. 2018. Patterns of divergence in the morphology of ceratopsian dinosaurs: sympatry is not a driver of ornament evolution. *Proceedings of the Royal Society B: Biological Sciences*, **285**, 20180312.

KNAUST, D. and DESROCHERS, A. 2019. Exceptionally preserved soft-bodied assemblage in Ordovician carbonates of Anticosti Island, eastern Canada. *Gondwana Research*, **71**, 117–128.

KNOLL, A. H. and NOWAK, M. A. 2017. The timetable of evolution. *Science Advances*, **3**, e1603076.

KOBAYASHI, Y., LU, J.-C., DONG, Z.-M., BARSBOLD, R., AZUMA, Y. and TOMIDA, Y. 1999. Herbivorous diet in an ornithomimid dinosaur. *Nature*, **402**, 480–481.

KOPPELHUS, E. 2005. Paleobotany. *In* CURRIE, P. J. and KOPPELHUS, E. B. (eds.) *Dinosaur Provincial Park: A Spectacular Ancient Ecosystem Revealed*, Indiana University Press, Bloomington, 131–138 pp.

KRAUSE, D. W., HOFFMANN, S., HU, Y., WIBLE, J. R., ROUGIER, G. W., KIRK, E. C., GROENKE, J. R., ROGERS, R. R., ROSSIE, J. B., SCHULTZ, J. A., EVANS, A. R., KOENIGSWALD, W. von and RAHANTARISOA, L. J. 2020. Skeleton of a Cretaceous mammal from Madagascar reflects long-term insularity. *Nature*, 1–7.

KRUTA, I., LANDMAN, N., ROUGET, I., CECCA, F. and TAFFOREAU, P. 2011. The Role of Ammonites in the Mesozoic Marine Food Web Revealed by Jaw Preservation. *Science*, **331**, 70–72.

LABANDEIRA, C. C. and CURRANO, E. D. 2013. The Fossil Record of Plant-Insect Dynamics. *Annual Review of Earth and Planetary Sciences*, **41**, 287–311.

LABANDEIRA, C. C. and DUNNE, J. A. 2014. Data from: Highly resolved middle Eocene food webs show early development of modern trophic structure after the end-Cretaceous extinction.

LALAND, K. N., ULLER, T., FELDMAN, M. W., STERELNY, K., MÜLLER, G. B., MOCZEK, A., JABLONKA, E. and ODLING-SMEE, J. 2015. The extended evolutionary synthesis: its structure, assumptions and predictions. *Proceedings of the Royal Society B: Biological Sciences*, **282**, 20151019.

LAMBE, L. M. 1902. New genera and species from the Belly River series (Mid-Cretaceous). *Geological Survey of Canada, Contributions to Canadian Palaeontology*, **3**, 25–81.

———. 1904. On the squamoso-parietal crest of the horned dinosaurs *Centrosaurus apertus* and *Monoclonius canadensis* from the Cretaceous of Alberta. *Transactions of the Royal Society of Canada*, **2 (Sec. 4)**, 3–12.

———. 1913. A new genus and species of Ceratopsia from the Belly River Formation of Alberta. *The Ottawa Naturalist*, **27**, 109–116.

———. 1914*a*. On the fore-limb of a carnivorous dinosaur from the Belly River Formation of Alberta, and a new genus of Ceratopsia from the same horizon, with remarks on the integument of some Cretaceous herbivorous dinosaurs. *The Ottawa Naturalist*, **27**, 129–135.

———. 1914*b*. On *Gryposaurus notabilis*, a new genus and species of trachodont dinosaur from the Belly River Formation of Alberta, with a description of the skull of *Chasmosaurus belli*. *The Ottawa Naturalist*, **27**, 147–155.

———. 1914*c*. On a new genus and species of carnivorous dinosaur from the Belly River Formation of Alberta, with a description of the skull of *Stephanosaurus marginatus* from the same horizon. *Ottawa Naturalist*, **28**, 13–20.

———. 1915. On *Eoceratops canadensis*, gen. nov., with remarks on other genera of Cretaceous horned dinosaurs. *Canadian Geological Survey Museum Bulletin*, **12**, 1–49.

———. 1917. *The Cretaceous Theropodous Dinosaur* Gorgosaurus. Geological Survey of Canada, Ottawa.

———. 1918. The Cretaceous genus *Stegoceras*, typifying a new family referred provisionally to the Stegosauria. *Transactions of the Royal Society of Canada*, **12**, 23–36.

———. 1919. Description of a new genus and species (*Panoplosaurus mirus*) of an armoured dinosaur from the Belly River beds of Alberta. *Transactions of the Royal Society of Canada*, **3 (Sec. 4)**, 39–50.

LAMSDELL, J. C., MCCOY, V. E., PERRON-FELLER, O. A. and HOPKINS, M. J. 2020. Air Breathing in an Exceptionally Preserved 340-Million-Year-Old Sea Scorpion. *Current Biology*, **30**, 4316-4321.e2.

———, CONGREVE, C. R., HOPKINS, M. J., KRUG, A. Z. and PATZKOWSKY, M. E. 2017. Phylogenetic Paleoecology: Tree-Thinking and Ecology in Deep Time. *Trends in Ecology & Evolution*, **32**, 452–463.

LANGSTON JR., W. 1965. Pre-Cenozoic vertebrate paleontology in Alberta: Its past and future. *In* FOLINSBEE, R. E. and ROSS, D. M. (eds.) *Vertebrate Paleontology in Alberta*, University of Alberta, Edmonton, 9–31 pp.

LARSON, D. W. 2008. Diversity and variation of theropod dinosaur teeth from the uppermost Santonian Milk River Formation (Upper Cretaceous), Alberta: a quantitative method supporting identification of the oldest dinosaur tooth assemblage in Canada. *Canadian Journal of Earth Sciences*, **45**, 1455–1468.

——— and CURRIE, P. J. 2013. Multivariate Analyses of Small Theropod Dinosaur Teeth and Implications for Paleoecological Turnover through Time. *PLOS ONE*, **8**, e54329.

LARSSON, H. C. E. and DEMERS-POTVIN, A. V. 2024. The first highly resolved ecological network for successive palaeocommunities of the Late Cretaceous (Campanian) Belly River Group of Dinosaur Provincial Park, Alberta. *Canadian Society of Vertebrate Palaeontology Annual Meeting Abstracts 2024*, **12**, 23.

LEACH, C. T., HOFFMAN, E. and DODSON, P. 2021. The promise of taphonomy as a nomothetic discipline: taphonomic bias in two dinosaur-bearing faunas in North America1. *Canadian Journal of Earth Sciences*, **58**, 852–869.

LEBLANC, A. R. H., REISZ, R. R., EVANS, D. C. and BAILLEUL, A. M. 2016. Ontogeny reveals function and evolution of the hadrosaurid dinosaur dental battery. *BMC Evolutionary Biology*, **16**, 152.

LEE, M. S. Y. and YATES, A. M. 2018. Tip-dating and homoplasy: reconciling the shallow molecular divergences of modern gharials with their long fossil record. *Proceedings of the Royal Society B: Biological Sciences*, **285**, 20181071.

LEE, S., LEE, Y.-N., CURRIE, P. J., SISSONS, R., PARK, J.-Y., KIM, S.-H., BARSBOLD, R. and TSOGTBAATAR, K. 2022. A non-avian dinosaur with a streamlined body exhibits potential adaptations for swimming. *Communications Biology*, **5**, 1–9.

LEGENDRE, S. and HARTENBERGER, J.-L. 1992. The Evolution of Mammalian Faunas in Europe during the Eocene and Oligocene. *In Eocene-Oligocene Climatic and Biotic Evolution*, 516–528 pp.

LEHMAN, T. M. 1987. Late Maastrichtian paleoenvironments and dinosaur biogeography in the western interior of North America. *Palaeogeography, Palaeoclimatology, Palaeoecology*, **60**, 189–217.

———. 2001. Late Cretaceous Dinosaur Provinciality. *In* TANKE, D. H. and CARPENTER, K. (eds.) *Mesozoic Vertebrate Life*, Indiana University Press, Bloomington, 310–328 pp.

LENZ, O. K. and WILDE, V. 2018. Changes in Eocene plant diversity and composition of vegetation: the lacustrine archive of Messel (Germany). *Paleobiology*, **44**, 709–735.

LOEWEN, M. A., IRMIS, R. B., SERTICH, J. J. W., CURRIE, P. J. and SAMPSON, S. D. 2013. Tyrant Dinosaur Evolution Tracks the Rise and Fall of Late Cretaceous Oceans. *PLOS ONE*, **8**, e79420.

LONGRICH, N. R. 2008. A New, Large Ornithomimid from the Cretaceous Dinosaur Park Formation of Alberta, Canada: Implications for the Study of Dissociated Dinosaur Remains. *Palaeontology*, **51**, 983–997.

———. 2009. An ornithurine-dominated avifauna from the Belly River Group (Campanian, Upper Cretaceous) of Alberta, Canada. *Cretaceous Research*, **30**, 161–177.

——— and CURRIE, P. J. 2009. A microraptorine (Dinosauria–Dromaeosauridae) from the Late Cretaceous of North America. *Proceedings of the National Academy of Sciences*, **106**, 5002–5007.

———, BHULLAR, B.-A. S. and GAUTHIER, J. A. 2012. Mass extinction of lizards and snakes at the Cretaceous–Paleogene boundary. *Proceedings of the National Academy of Sciences*, **109**, 21396–21401.

LOWI-MERRI, T. M. and EVANS, D. C. 2020. Cranial variation in *Gryposaurus* and biostratigraphy of hadrosaurines (Ornithischia: Hadrosauridae) from the Dinosaur Park Formation of Alberta, Canada. *Canadian Journal of Earth Sciences*, **57**, 765–779.

LULL, R. S. 1933. A revision of the Ceratopsia or horned dinosaurs. *Memoirs of the Peabody Museum of Natural History*, **3**, 1–175.

——— and WRIGHT, N. E. 1942. *Hadrosaurian dinosaurs of North America*. Geological Society of America, Boulder, Colorado.

LUQUE, J., FELDMANN, R. M., VERNYGORA, O., SCHWEITZER, C. E., CAMERON, C. B., KERR, K. A., VEGA, F. J., DUQUE, A., STRANGE, M., PALMER, A. R. and JARAMILLO, C. 2019. Exceptional preservation of mid-Cretaceous marine arthropods and the evolution of novel forms via heterochrony. *Science Advances*, **5**, eaav3875.

LYELL, C. 1830. *Principles of geology*. Vol. 1. John Murray, London.

———. 1832. *Principles of geology*. Vol. 2. John Murray, London.

LYONS, S. K., AMATANGELO, K. L., BEHRENSMEYER, A. K., BERCOVICI, A., BLOIS, J. L., DAVIS, M., DIMICHELE, W. A., DU, A., ERONEN, J. T., TYLER FAITH, J., GRAVES, G. R., JUD, N., LABANDEIRA, C., LOOY, C. V., MCGILL, B., MILLER, J. H., PATTERSON, D., PINEDA-MUNOZ, S., POTTS, R., RIDDLE, B., TERRY, R., TÓTH, A., ULRICH, W., VILLASEÑOR, A., WING, S., ANDERSON, H., ANDERSON, J., WALLER, D. and GOTELLI, N. J. 2016. Holocene shifts in the assembly of plant and animal communities implicate human impacts. *Nature*, **529**, 80–83.

LYSON, T. R., MILLER, I. M., BERCOVICI, A. D., WEISSENBURGER, K., FUENTES, A. J., CLYDE, W. C., HAGADORN, J. W., BUTRIM, M. J., JOHNSON, K. R., FLEMING, R. F., BARCLAY, R. S., MACCRACKEN, S. A., LLOYD, B., WILSON, G. P., KRAUSE, D. W. and CHESTER, S. G. B. 2019. Exceptional continental record of biotic recovery after the Cretaceous–Paleogene mass extinction. *Science*, **366**, 977–983.

MA, W., WANG, J., PITTMAN, M., TAN, Q., TAN, L., GUO, B. and XU, X. 2017. Functional anatomy of a giant toothless mandible from a bird-like dinosaur: *Gigantoraptor* and the evolution of the oviraptorosaurian jaw. *Scientific Reports*, **7**, 16247.

MACDONALD, M., CURRIE, P. J. and SPENCER, W. A. 2005. Precise Mapping of Fossil Sites in the Park Using Survey Grade GPS Technology. *In* CURRIE, P. J. and KOPPELHUS, E. B. (eds.)

Dinosaur Provincial Park: A Spectacular Ancient Ecosystem Revealed, Indiana University Press, Bloomington, 478–485 pp.

MAGNUSSON, W. E., DA SILVA, E. V. and LIMA, A. P. 1987. Diets of Amazonian Crocodilians. *Journal of Herpetology*, **21**, 85–95.

MAIDMENT, S. C. R. and MUXWORTHY, A. 2019. A chronostratigraphic framework for the Upper Jurassic Morrison Formation, western U.S.A. *Journal of Sedimentary Research*, **89**, 1017–1038.

———, DEAN, C. D., MANSERGH, R. I. and BUTLER, R. J. 2021. Deep-time biodiversity patterns and the dinosaurian fossil record of the Late Cretaceous Western Interior, North America. *Proceedings of the Royal Society B: Biological Sciences*, **288**, 20210692.

MALLON, J. C. 2019. Competition structured a Late Cretaceous megaherbivorous dinosaur assemblage. *Scientific Reports*, **9**, 15447.

——— and ANDERSON, J. S. 2013. Skull Ecomorphology of Megaherbivorous Dinosaurs from the Dinosaur Park Formation (Upper Campanian) of Alberta, Canada. *PLoS ONE*, **8**, e67182.

——— and ———. 2014. The Functional and Palaeoecological Implications of Tooth Morphology and Wear for the Megaherbivorous Dinosaurs from the Dinosaur Park Formation (Upper Campanian) of Alberta, Canada. *PLOS ONE*, **9**, e98605.

——— and ———. 2015. Jaw mechanics and evolutionary paleoecology of the megaherbivorous dinosaurs from the Dinosaur Park Formation (upper Campanian) of Alberta, Canada. *Journal of Vertebrate Paleontology*, **35**, e904323.

———, EVANS, D. C., RYAN, M. J. and ANDERSON, J. S. 2012. Megaherbivorous dinosaur turnover in the Dinosaur Park Formation (upper Campanian) of Alberta, Canada. *Palaeogeography, Palaeoclimatology, Palaeoecology*, **350–352**, 124–138.

———, ———, ——— and ———. 2013. Feeding height stratification among the herbivorous dinosaurs from the Dinosaur Park Formation (upper Campanian) of Alberta, Canada. *BMC Ecology*, **13**, 14.

———, OTT, C. J., LARSON, P. L., IULIANO, E. M. and EVANS, D. C. 2016. *Spiclypeus shipporum* gen. et sp. nov., a Boldly Audacious New Chasmosaurine Ceratopsid (Dinosauria: Ornithischia) from the Judith River Formation (Upper Cretaceous: Campanian) of Montana, USA. *PLOS ONE*, **11**, e0154218.

MANICOM, C. and SCHWARZKOPF, L. 2011. Diet and prey selection of sympatric tropical skinks. *Austral Ecology*, **36**, 485–496.

MANN, D. H., GROVES, P., REANIER, R. E., GAGLIOTI, B. V., KUNZ, M. L. and SHAPIRO, B. 2015. Life and extinction of megafauna in the ice-age Arctic. *Proceedings of the National Academy of Sciences*, **112**, 14301–14306.

MANNION, P. D., UPCHURCH, P., BENSON, R. B. J. and GOSWAMI, A. 2014. The latitudinal biodiversity gradient through deep time. *Trends in Ecology & Evolution*, **29**, 42–50.

MANZ, C. L. and BLOCH, J. I. 2015. Systematics and Phylogeny of Paleocene-Eocene Nyctitheriidae (Mammalia, Eulipotyphla?) with Description of a new Species from the Late Paleocene of the Clarks Fork Basin, Wyoming, USA. *Journal of Mammalian Evolution*, **22**, 307–342.

———, CHESTER, S. G. B., BLOCH, J. I., SILCOX, M. T. and SARGIS, E. J. 2015. New partial skeletons of Palaeocene Nyctitheriidae and evaluation of proposed euarchontan affinities. *Biology Letters*, **11**, 20140911.

MARSHALL, C. R. 1990. Confidence Intervals on Stratigraphic Ranges. *Paleobiology*, **16**, 1–10.

———. 1994. Confidence Intervals on Stratigraphic Ranges: Partial Relaxation of the Assumption of Randomly Distributed Fossil Horizons. *Paleobiology*, **20**, 459–469.

———. 1997. Confidence Intervals on Stratigraphic Ranges with Nonrandom Distributions of Fossil Horizons. *Paleobiology*, **23**, 165–173.

———. 2023. Forty years later: The status of the “Big Five” mass extinctions. *Cambridge Prisms: Extinction*, **1**, e5.

MARTIN, D., MCKENNA, H. and LIVINA, V. 2017. The human physiological impact of global deoxygenation. *The Journal of Physiological Sciences*, **67**, 97–106.

MARTINA, L. S. and WATERS, M. 2014. Philander opossum *(gray four-eyed opossum)*. Animal Diversity Web. Downloaded from https://animaldiversity.org/accounts/Philander_opossum/ on 7 March 2024.

MARTÍNEZ-BOTÍ, M. A., FOSTER, G. L., CHALK, T. B., ROHLING, E. J., SEXTON, P. F., LUNT, D. J., PANCOST, R. D., BADGER, M. P. S. and SCHMIDT, D. N. 2015. Plio-Pleistocene climate sensitivity evaluated using high-resolution CO_2 records. *Nature*, **518**, 49-54.

MARYAŃSKA, T., CHAPMAN, R. E. and WEISHAMPEL, D. B. 2004. Pachycephalosauria. *In* DODSON, P., WEISHAMPEL, D. B. and OSMÓLSKA, H. (eds.) *The Dinosauria*, University of California Press, Berkeley & Los Angeles, 464–477 pp.

MATSUMOTO, R., FUJIWARA, S. and EVANS, S. E. 2022. Feeding behaviour and functional morphology of the neck in the long-snouted aquatic fossil reptile *Champsosaurus* (Reptilia: Diapsida) in comparison with the modern crocodilian *Gavialis gangeticus*. *Journal of Anatomy*, **240**, 893–913.

MATTHEW, W. D. and BROWN, B. 1923. Preliminary notices of skeletons and skulls of Deinodontidae from the Cretaceous of Alberta. *American Museum Novitates*, **89**, 1–10.

MAYHEW, P. J., BELL, M. A., BENTON, T. G. and MCGOWAN, A. J. 2012. Biodiversity tracks temperature over time. *Proceedings of the National Academy of Sciences*, **109**, 15141–15145.

MAZZOTTI, F. J., NESTLER, J. H., COLE, J. M., CLOSIUS, C., KERN, W. H., ROCHFORD, M. R., SUAREZ, E., BRUBAKER, R., PLATT, S. G., RAINWATER, T. and KETTERLIN, J. K. 2020. Diet of Nile Monitors (*Varanus niloticus*) Removed from Palm Beach and Broward Counties, Florida, USA. *Journal of Herpetology*, **54**, 189–195.

MCCAY, T. S. and STORM, G. L. 1997. Masked Shrew (*Sorex cinereus*) Abundance, Diet and Prey Selection in an Irrigated Forest. *The American Midland Naturalist*, **138**, 268–275.

MCFEETERS, B., RYAN, M. J., SCHRÖDER-ADAMS, C. and CULLEN, T. M. 2016. A new ornithomimid theropod from the Dinosaur Park Formation of Alberta, Canada. *Journal of Vertebrate Paleontology*, **36**, e1221415.

———, ———, ——— and CURRIE, P. J. 2017. First North American occurrences of *Qiupalong* (Theropoda: Ornithomimidae) and the palaeobiogeography of derived ornithomimids. *FACETS*, **2**, 355–373.

MCGILL, B. J. 2010. Matters of Scale. *Science*, **328**, 575–576.

MCKELLAR, R. C., WOLFE, A. P., TAPPERT, R. and MUEHLENBACHS, K. 2008. Correlation of Grassy Lake and Cedar Lake ambers using infrared spectroscopy, stable isotopes, and palaeoentomology. *Canadian Journal of Earth Sciences*, **45**, 1061–1082.

———, JONES, E., ENGEL, M. S., TAPPERT, R., WOLFE, A. P., MUEHLENBACHS, K., COCKX, P., KOPPELHUS, E. B. and CURRIE, P. J. 2019. A direct association between amber and dinosaur remains provides paleoecological insights. *Scientific Reports*, **9**, 17916.

MEYLAN, P. A. 2006. *Biology and Conservation of Florida Turtles*. Ch-e-lon-ian Re-search Foun-da-tion, St. Petersburg, Florida.

MEYLAN, P. A. and GAFFNEY, E. S. 1989. The Skeletal Morphology of the Cretaceous Cryptodiran Turtle, *Adocus*, and the Relationships of the Trionychoidea. *American Museum Novitates*, **2941**, 1–60.

MITCHELL, J. S., ROOPNARINE, P. D. and ANGIELCZYK, K. D. 2012. Late Cretaceous restructuring of terrestrial communities facilitated the end-Cretaceous mass extinction in North America. *Proceedings of the National Academy of Sciences*, **109**, 18857–18861.

MOHR, S. R., ACORN, J. H., FUNSTON, G. F. and CURRIE, P. J. 2020. An ornithurine bird coracoid from the Late Cretaceous of Alberta, Canada. *Canadian Journal of Earth Sciences*, **58**, 134–140.

MOLNAR, R. E. and CLIFFORD, H. T. 2001. An ankylosaurian cololite from the Lower Cretaceous of Queensland, Australia. *In* CARPENTER, K. (ed.) *The Armored Dinosaurs*, Indiana University Press, 399–412 pp.

MONTEFELTRO, F. C., LAUTENSCHLAGER, S., GODOY, P. L., FERREIRA, G. S. and BUTLER, R. J. 2020. A unique predator in a unique ecosystem: modelling the apex predator within a Late Cretaceous crocodyliform-dominated fauna from Brazil. *Journal of Anatomy*, **237**, 323–333.

MORRIS, J. L., LEAKE, J. R., STEIN, W. E., BERRY, C. M., MARSHALL, J. E. A., WELLMAN, C. H., MILTON, J. A., HILLIER, S., MANNOLINI, F., QUIRK, J. and BEERLING, D. J. 2015. Investigating Devonian trees as geo-engineers of past climates: linking palaeosols to palaeobotany and experimental geobiology. *Palaeontology*, **58**, 787–801.

MOYSIUK, J. and CARON, J.-B. 2019. A new hurdiid radiodont from the Burgess Shale evinces the exploitation of Cambrian infaunal food sources. *Proceedings of the Royal Society B: Biological Sciences*, **286**, 20191079.

NA, Y.-L., SUN, C.-L., WANG, H., DILCHER, D. L., YANG, Z.-Y., LI, T. and LI, Y.-F. 2018. Insect herbivory and plant defense on ginkgoalean and bennettitalean leaves of the Middle Jurassic Daohugou Flora from Northeast China and their paleoclimatic implications. *Palaeoworld*, **27**, 202–210.

NEUMAN, A. G. and BRINKMAN, D. B. 2005. Fishes of the Fluvial Beds. *In* CURRIE, P. J. and KOPPELHUS, E. B. (eds.) *Dinosaur Provincial Park: A Spectacular Ancient Ecosystem Revealed*, Indiana University Press, Bloomington, 167–185 pp.

NEWBREY, M. G., WILSON, M. V. H. and ASHWORTH, A. C. 2007. Centrum growth patterns provide evidence for two small taxa of Hiodontidae in the Cretaceous Dinosaur Park Formation. *Canadian Journal of Earth Sciences*, **44**, 721–732.

NEWBREY, M. G., MURRAY, A. M., WILSON, M. V. H., BRINKMAN, D. B. and NEUMAN, A. G. 2009. Seventy-five-million-year-old tropical tetra-like fish from Canada tracks Cretaceous global warming. *Proceedings of the Royal Society B: Biological Sciences*, **276**, 3829–3833.

NEWBREY, M. G., MURRAY, A. M., BRINKMAN, D. B., WILSON, M. V. H. and NEUMAN, A. G. 2010. A new articulated freshwater fish (Clupeomorpha, Ellimmichthyiformes) from the Horseshoe Canyon Formation, Maastrichtian, of Alberta, Canada. *Canadian Journal of Earth Sciences*, **47**, 1183–1196.

NICHOLLS, E. L. and RUSSELL, A. P. 1981. A new specimen of *Struthiomimus altus* from Alberta, with comments on the classificatory characters of Upper Cretaceous ornithomimids. *Canadian Journal of Earth Sciences*, **18**, 518–526.

——— and ———. 1990. Paleobiogeography of the Cretaceous Western Interior Seaway of North America: the vertebrate evidence. *Palaeogeography, Palaeoclimatology, Palaeoecology*, **79**, 149–169.

NOPCSA, F. 1928. Palaeontological notes on reptiles. *Geologica Hungarica, Seria Palaeontologica*, **1**, 1–84.

NORELL, M. A., MAKOVICKY, P. J. and CLARK, J. M. 2000. A New Troodontid Theropod from Ukhaa Tolgod, Mongolia. *Journal of Vertebrate Paleontology*, **20**, 7–11.

———, ——— and CURRIE, P. J. 2001. The beaks of ostrich dinosaurs. *Nature*, **412**, 873–874.

O'CONNOR, J. K. 2019. The trophic habits of early birds. *Palaeogeography, Palaeoclimatology, Palaeoecology*, **513**, 178–195.

———, ZHOU, Z. and XU, X. 2011. Additional specimen of *Microraptor* provides unique evidence of dinosaurs preying on birds. *Proceedings of the National Academy of Sciences of the United States of America*, **108**, 19662–19665.

O'CONNOR, J. K., ZHENG, X., DONG, L., WANG, X., WANG, Y., ZHANG, X. and ZHOU, Z. 2019. *Microraptor* with Ingested Lizard Suggests Non-specialized Digestive Function. *Current Biology*, **29**, 2423-2429.e2.

O'CONNOR, L. M. J., POLLOCK, L. J., BRAGA, J., FICETOLA, G. F., MAIORANO, L., MARTINEZ-ALMOYNA, C., MONTEMAGGIORI, A., OHLMANN, M. and THUILLER, W. 2020. Unveiling the food webs of tetrapods across Europe through the prism of the Eltonian niche. *Journal of Biogeography*, **47**, 181–192.

O'KEEFE, F. R., DUNN, R. E., WEITZEL, E. M., WATERS, M. R., MARTINEZ, L. N., BINDER, W. J., SOUTHON, J. R., COHEN, J. E., MEACHEN, J. A., DESANTIS, L. R. G., KIRBY, M. E., GHEZZO, E., COLTRAIN, J. B., FULLER, B. T., FARRELL, A. B., TAKEUCHI, G. T., MACDONALD, G., DAVIS, E. B. and LINDSEY, E. L. 2023. Pre–Younger Dryas megafaunal extirpation at Rancho La Brea linked to fire-driven state shift. *Science*, **381**, eabo3594.

OLSEN, P. E., REMINGTON, C. L., CORNET, B. and THOMSON, K. S. 1978. Cyclic Change in Late Triassic Lacustrine Communities. *Science*, **201**, 729–733.

OLSON, E. C. 1952. The Evolution of a Permian Vertebrate Chronofauna. *Evolution*, **6**, 181–196.

ORESKA, M. P. J. and CARRANO, M. T. 2019. Paleocommunity mixing increases with marine transgression in Dinosaur Park Formation (Upper Cretaceous) vertebrate microfossil assemblages. *Paleobiology*, **45**, 136–153.

OSBORN, H. F. 1905. *Tyrannosaurus* and other Cretaceous carnivorous dinosaurs. *Bulletin American Museum of Natural History*, **Vol. XXI**, 259–265.

——— and LAMBE, L. M. 1902. On Vertebrates of the Mid-Cretaceous of the North-West Territory. *Geological Survey of Canada, Contributions to Canadian Palaeontology*, **3**, 7–21.

OSTROM, J. H. 1961. Cranial morphology of the hadrosaurian dinosaurs of North America. *Bulletin of the American Museum of Natural History*, **122**, 33–186.

———. 1963. *Parasaurolophus cyrtocristatus*, a Crested Hadrosaurian from New Mexico. *Fieldiana: Geology*, **14**, 143–168.

PALUH, D. J., RIDDELL, K., EARLY, C. M., HANTAK, M. M., JONGSMA, G. F., KEEFFE, R. M., MAGALHÃES SILVA, F., NIELSEN, S. V., VALLEJO-PAREJA, M. C., STANLEY, E. L. and BLACKBURN, D. C. 2021. Rampant tooth loss across 200 million years of frog evolution. *eLife*, **10**, e66926.

PARDO, J. D., SMALL, B. J., MILNER, A. R. and HUTTENLOCKER, A. K. 2019. Carboniferous–Permian climate change constrained early land vertebrate radiations. *Nature Ecology & Evolution*, **3**, 200–206.

PARHAM, J. F. and HUTCHISON, J. H. 2003. A new eucryptodiran turtle from the Late Cretaceous of North America (Dinosaur Provincial Park, Alberta, Canada). *Journal of Vertebrate Paleontology*, **23**, 783–798.

PARKS, W. A. 1919. Preliminary Description of a New Species of Trachodont Dinosaur of the Genus *Kritosaurus*. *Kritosaurus incurvimanus*. *Transactions of the Royal Society of Canada*, **3**, 51–63.

———. 1920. *The Osteology of the Trachodont Dinosaur* Kritosaurus incurvimanus. University Library, Toronto.

———. 1921. The head and forelimb of a specimen of *Centrosaurus apertus*. *Transactions of the Royal Society of Canada*, **series 4**.

———. 1922. Parasaurolophus walkeri*, a New Genus and Species of Crested Trachodont Dinosaur*. University Library, Toronto.

———. 1923. Corythosaurus intermedius*, a New Species of Trachodont Dinosaur*. University Library, Toronto.

———. 1924. Dyoplosaurus acutosquameus*, a New Genus and Species of Armoured Dinosaur, with Notes on a Skeleton of* Prosaurolophus maximus. University Library, Toronto.

———. 1928. Struthiomimus samueli*, a New Species of Ornithomimidae from the Belly River formation of Alberta*. University Library, Toronto.

———. 1931. *A Genus and Two New Species of Trachodont Dinosaurs from the Belly River Formation of Alberta*. University Library, Toronto.

———. 1933. New species of *Champsosaurus* from the Belly River Formation of Alberta, Canada. *Transactions of the Royal Society of Canada, sect. 4, ser. 3*, **27**, 121–137.

———. 1935. *New Species of Trachodont Dinosaurs from the Cretaceous Formations of Alberta, with Notes on Other Species*. University Library, Toronto.

PAULINA CARABAJAL, A., CURRIE, P. J., DUDGEON, T. W., LARSSON, H. C. E. and MIYASHITA, T. 2021. Two braincases of *Daspletosaurus* (Theropoda: Tyrannosauridae): anatomy and comparison1. *Canadian Journal of Earth Sciences*, **58**, 885–910.

PENG, J., BRINKMAN, Donald., RUSSELL, A. P., ALBERTA., and PROVINCIAL MUSEUM OF ALBERTA. 2001. *Vertebrate microsite assemblages (exclusive of mammals) from the Foremost and Oldman formations of the Judith River group (Campanian) of Southeastern Alberta: an illustrated guide*. Curatorial Section, Provincial Museum of Alberta, Edmonton: 54 pp.

PENKALSKI, P. 2018. Revised systematics of the armoured dinosaur *Euoplocephalus* and its allies. *Neues Jahrbuch für Geologie und Paläontologie - Abhandlungen*, 261–306.

——— and BLOWS, W. T. 2013. *Scolosaurus cutleri* (Ornithischia: Ankylosauria) from the Upper Cretaceous Dinosaur Park Formation of Alberta, Canada. *Canadian Journal of Earth Sciences*, **50**, 171–182.

PIKE, E. M. 1994. Historical changes in insect community structure as indicated by hexapods of Upper Cretaceous Alberta (Grassy Lake) amber. *The Canadian Entomologist*, **126**, 695–702.

PIMIENTO, C., GRIFFIN, J. N., CLEMENTS, C. F., DANIELE, S., VARELA, S., UHEN, M. D. and JARAMILLO, C. 2017. The Pliocene marine megafauna extinction and its impact on functional diversity. *Nature Ecology & Evolution*, **1**, 1100–1106.

PIRES, M. M., RINDEL, D., MOSCARDI, B., CRUZ, L. R., GUIMARÃES, P. R., DOS REIS, S. F. and PEREZ, S. I. 2020. Before, during and after megafaunal extinctions: Human impact on Pleistocene-Holocene trophic networks in South Patagonia. *Quaternary Science Reviews*, **250**, 106696.

POINAR, JR., G. 2014. Insect Herbivores of Horsetails: Bionomics, Dispersal, and Co-Evolution. *American Entomologist*, **60**, 235–240.

POISOT, T., STOUFFER, D. B. and KÉFI, S. 2016. Describe, understand and predict: why do we need networks in ecology? *Functional Ecology*, **30**, 1878–1882.

———, CANARD, E., MOUILLOT, D., MOUQUET, N. and GRAVEL, D. 2012. The dissimilarity of species interaction networks. *Ecology Letters*, **15**, 1353–1361.

POLLY, P. D., ERONEN, J. T., FRED, M., DIETL, G. P., MOSBRUGGER, V., SCHEIDEGGER, C., FRANK, D. C., DAMUTH, J., STENSETH, N. C. and FORTELIUS, M. 2011. History matters: ecometrics and integrative climate change biology. *Proceedings of the Royal Society B: Biological Sciences*, **278**, 1131–1140.

PUNZO, F. 1975. Studies on the Feeding Behavior, Diet, Nesting Habits and Temperature Relationships of *Chelydra serpentina osceola* (Chelonia: Chelydridae). *Journal of Herpetology*, **9**, 207–210.

PURWANDANA, D., ARIEFIANDY, A., IMANSYAH, M. J., SENO, A., CIOFI, C., LETNIC, M. and JESSOP, T. S. 2016. Ecological allometries and niche use dynamics across Komodo dragon ontogeny. *The Science of Nature*, **103**, 27.

QVARNSTRÖM, M., FIKÁČEK, M., WERNSTRÖM, J. V., HULD, S., BEUTEL, R. G., ARRIAGA-VARELA, E., AHLBERG, P. E. and NIEDŹWIEDZKI, G. 2021. Exceptionally preserved beetles in a Triassic coprolite of putative dinosauriform origin. *Current Biology*, **31**, P3374-3381.E5.

RAHBEK, C., BORREGAARD, M. K., ANTONELLI, A., COLWELL, R. K., HOLT, B. G., NOGUES-BRAVO, D., RASMUSSEN, C. M. Ø., RICHARDSON, K., ROSING, M. T., WHITTAKER, R. J. and FJELDSÅ, J. 2019. Building mountain biodiversity: Geological and evolutionary processes. *Science*, **365**, 1114–1119.

RAJA, N. B., DUNNE, E. M., MATIWANE, A., KHAN, T. M., NÄTSCHER, P. S., GHILARDI, A. M. and CHATTOPADHYAY, D. 2022. Colonial history and global economics distort our understanding of deep-time biodiversity. *Nature Ecology & Evolution*, **6**, 145–154.

RAMANUJAM, C. G. K. 1972. Fossil coniferous woods from the Oldman Formation (Upper Cretaceous) of Alberta. *Canadian Journal of Botany*, **50**, 595–602.

RAMEZANI, J., BEVERIDGE, T. L., ROGERS, R. R., EBERTH, D. A. and ROBERTS, E. M. 2022. Calibrating the zenith of dinosaur diversity in the Campanian of the Western Interior Basin by CA-ID-TIMS U–Pb geochronology. *Scientific Reports*, **12**, 16026.

RANEY, E. C. 1942. The Summer Food and Habits of the Chain Pickerel (*Esox niger*) of a Small New York Pond. *The Journal of Wildlife Management*, **6**, 58–66.

RAUP, D. M. and SEPKOSKI, J. J. 1984. Periodicity of extinctions in the geologic past. *Proceedings of the National Academy of Sciences*, **81**, 801–805.

RAY, D. C., VAN BUCHEM, F. S. P., BAINES, G., DAVIES, A., GRÉSELLE, B., SIMMONS, M. D. and ROBSON, C. 2019. The magnitude and cause of short-term eustatic Cretaceous sea-level change: A synthesis. *Earth-Science Reviews*, **197**, 102901.

VAN DER REEST, A. J. and CURRIE, P. J. 2017. Troodontids (Theropoda) from the Dinosaur Park Formation, Alberta, with a description of a unique new taxon: implications for deinonychosaur diversity in North America. *Canadian Journal of Earth Sciences*, **54**, 919–935.

———, WOLFE, A. P. and CURRIE, P. J. 2016. A densely feathered ornithomimid (Dinosauria: Theropoda) from the Upper Cretaceous Dinosaur Park Formation, Alberta, Canada. *Cretaceous Research*, **58**, 108–117.

RETALLACK, G. J. and DILCHER, D. L. 1988. Reconstructions of Selected Seed Ferns. *Annals of the Missouri Botanical Garden*, **75**, 1010–1057.

RIPPLE, W. J., ESTES, J. A., BESCHTA, R. L., WILMERS, C. C., RITCHIE, E. G., HEBBLEWHITE, M., BERGER, J., ELMHAGEN, B., LETNIC, M., NELSON, M. P., SCHMITZ, O. J., SMITH, D. W., WALLACH, A. D. and WIRSING, A. J. 2014. Status and Ecological Effects of the World's Largest Carnivores. *Science*, **343**, 1241484.

ROBSON, S. V. 2018. An Analysis of North American Taeniolabidoid Multituberculate (Mammalia, Allotheria) Dentitions Using Mammalian Dietary Proxies.Master's Thesis, University of Calgary, Calgary, 251pp.

ROLLAND, J. and CONDAMINE, F. L. 2019. The contribution of temperature and continental fragmentation to amphibian diversification. *Journal of Biogeography*, **46**, 1857–1873.

———, DANIELE, S., DOLPH, S., ANTOINE, G., OLIVIER, B. and NICOLAS, S. 2018. The impact of endothermy on the climatic niche evolution and the distribution of vertebrate diversity. *Nature Ecology & Evolution*, **2**, 459–464.

———, HENAO-DIAZ, L. F., DOEBELI, M., GERMAIN, R., HARMON, L. J., KNOWLES, L. L., LIOW, L. H., MANK, J. E., MACHAC, A., OTTO, S. P., PENNELL, M., SALAMIN, N., SILVESTRO, D., SUGAWARA, M., UYEDA, J., WAGNER, C. E. and SCHLUTER, D. 2023. Conceptual and empirical bridges between micro- and macroevolution. *Nature Ecology & Evolution*, **7**, 1181–1193.

ROOPNARINE, P. D. 2006. Extinction cascades and catastrophe in ancient food webs. *Paleobiology*, **32**, 1–19.

———. 2010. Networks, Extinction and Paleocommunity Food Webs. *The Paleontological Society Papers*, **16**, 143–161.

——— and ANGIELCZYK, K. D. 2015. Community stability and selective extinction during the Permian-Triassic mass extinction. *Science*, **350**, 90–93.

——— and DINEEN, A. A. 2018. Coral Reefs in Crisis: The Reliability of Deep-Time Food Web Reconstructions as Analogs for the Present. *In* TYLER, C. L. and SCHNEIDER, C. L. (eds.) *Marine Conservation Paleobiology*, Springer International Publishing, Cham, 105–141 pp.

——— and BANKER, R. M. W. 2021. Ecological stasis on geological time scales. *Science*, **372**, 237–238.

———, ANGIELCZYK, K. D., WEIK, A. and DINEEN, A. 2019. Ecological persistence, incumbency and reorganization in the Karoo Basin during the Permian-Triassic transition. *Earth-Science Reviews*, **189**, 244–263.

———, ANGIELCZYK, K. D., OLROYD, S. L., NESBITT, S. J., BOTHA-BRINK, J., PEECOOK, B. R., DAY, M. O. and SMITH, R. M. H. 2017. Comparative ecological dynamics of Permian-

Triassic communities from the Karoo, Luangwa, and Ruhuhu Basins of southern Africa. *Journal of Vertebrate Paleontology*, **37**, 254–272.

ROSE, K. D. 2012. The importance of Messel for interpreting Eocene Holarctic mammalian faunas. *Palaeobiodiversity and Palaeoenvironments*, **92**, 631–647.

ROSSI, L., SPORTA CAPUTI, S., CALIZZA, E., CAREDDU, G., OLIVERIO, M., SCHIAPARELLI, S. and COSTANTINI, M. L. 2019. Antarctic food web architecture under varying dynamics of sea ice cover. *Scientific Reports*, **9**, 12454.

ROYER, D. L., BERNER, R. A., MONTAÑEZ, I. P., TABOR, N. J. and BEERLING, D. J. 2004. CO_2 as a primary driver of Phanerozoic climate. *GSA Today*, **14**, 4.

RUDWICK, M. J. S. 1997. *Georges Cuvier, Fossil Bones, and Geological Catastrophes: New Translations & Interpretations of the Primary Texts*. The University of Chicago Press.

RUSSELL, D. A. 1969. A new specimen of *Stenonychosaurus* from the Oldman Formation (Cretaceous) of Alberta. *Canadian Journal of Earth Sciences*, **6**, 595–612.

———. 1970. *Tyrannosaurs From the Late Cretaceous of Western Canada*. National Museums of Canada, Ottawa.

———. 1972*a*. Ostrich Dinosaurs from the Late Cretaceous of Western Canada. *Canadian Journal of Earth Sciences*, **9**, 375–402.

———. 1972*b*. A Pterosaur from the Oldman Formation (Cretaceous) of Alberta. *Canadian Journal of Earth Sciences*, **9**, 1338–1340.

RUSSELL, L. S. 1940. Edmontonia rugosidens *(Gilmore), an Armoured Dinosaur from the Belly River Series of Alberta*. University Library, Toronto.

———. 1941. *Prograngerella*, a New Ancestral Land Snail from the Upper Cretaceous of Alberta. *Journal of Paleontology*, **15**, 309–311.

———. 1956. The Cretaceous reptile *Champsosaurus natator* Parks. *Bulletin of the National Museum of Canada*, **145**, 1–51.

———. 1966. Dinosaur hunting in Western Canada. *Royal Ontario Museum Life Sciences Contributions*, **70**, 1–37.

RYAN, M. J. and RUSSELL, A. P. 2001. Dinosaurs of Alberta (exclusive of Aves). *In* TANKE, D. H. and CARPENTER, K. (eds.) *Mesozoic Vertebrate Life*, Indiana University Press, Bloomington, 279–297 pp.

RYAN, M. J. and RUSSELL, A. P. 2005. A new centrosaurine ceratopsid from the Oldman Formation of Alberta and its implications for centrosaurine taxonomy and systematics. *Canadian Journal of Earth Sciences*, **42**, 1369–1387.

RYAN, M. J. and EVANS, D. C. 2005. Ornithischian Dinosaurs. *In Dinosaur Provincial Park: A Spectacular Ancient Ecosystem Revealed*, Indiana University Press, Bloomington, 312–348 pp.

RYAN, M. J., HOLMES, R. and RUSSELL, A. P. 2007. A revision of the late campanian centrosaurine ceratopsid genus *Styracosaurus* from the Western Interior of North America. *Journal of Vertebrate Paleontology*, **27**, 944–962.

RYAN, M. J., RUSSELL, A. P., EBERTH, D. A. and CURRIE, P. J. 2001. The Taphonomy of a *Centrosaurus* (Ornithischia: Ceratopsidae) Bone Bed from the Dinosaur Park Formation (Upper Campanian), Alberta, Canada, with Comments on Cranial Ontogeny. *Palaios*, **16**, 482–506.

———, EBERTH, D. A., BRINKMAN, D. B., CURRIE, P. J. and TANKE, D. H. 2010. A New *Pachyrhinosaurus*-Like Ceratopsid from the Upper Dinosaur Park Formation (Late Campanian) of Southern Alberta, Canada. *In* RYAN, M. J., EBERTH, D. A., CHINNERY-ALLGEIER, B. J. and RALRICK, P. E. (eds.) *New Perspectives on Horned Dinosaurs: The Royal Tyrrell Museum Ceratopsian Symposium*, Indiana University Press, Bloomington, 141–155 pp.

RYAN, M. J., EVANS, D. C., CURRIE, P. J., BROWN, C. M. and BRINKMAN, D. 2012. New leptoceratopsids from the Upper Cretaceous of Alberta, Canada. *Cretaceous Research*, **35**, 69–80.

SAALFELD, D. T., CONWAY, W. C. and CALKINS, G. E. 2011. Food Habits of American Alligators (*Alligator mississippiensis*) in East Texas. *Southeastern Naturalist*, **10**, 659–672.

SAIGO, M., ZILLI, F. L., MARCHESE, M. R. and DEMONTE, D. 2015. Trophic level, food chain length and omnivory in the Paraná River: a food web model approach in a floodplain river system. *Ecological Research*, **30**, 843–852.

SALLAN, L., FRIEDMAN, M., SANSOM, R. S., BIRD, C. M. and SANSOM, I. J. 2018. The nearshore cradle of early vertebrate diversification. *Science*, **362**, 460–464.

SAMPSON, S. D., RYAN, M. J. and TANKE, D. H. 1997. Craniofacial ontogeny in centrosaurine dinosaurs (Ornithischia: Ceratopsidae): taxonomic and behavioral implications. *Zoological Journal of the Linnean Society*, **121**, 293–337.

———, LOEWEN, M. A., FARKE, A. A., ROBERTS, E. M., FORSTER, C. A., SMITH, J. A. and TITUS, A. L. 2010. New Horned Dinosaurs from Utah Provide Evidence for Intracontinental Dinosaur Endemism. *PLOS ONE*, **5**, e12292.

SANDOM, C. J., EJRNÆS, R., HANSEN, M. D. D. and SVENNING, J.-C. 2014. High herbivore density associated with vegetation diversity in interglacial ecosystems. *Proceedings of the National Academy of Sciences*, **111**, 4162–4167.

SANKEY, J. T., BRINKMAN, D. B., GUENTHER, M. and CURRIE, P. J. 2002. Small theropod and bird teeth from the late Cretaceous (late Campanian) Judith River Group, Alberta. *Journal of Paleontology*, **76**, 751–763.

———, BRINKMAN, D. B., FOX, R. C. and EBERTH, D. A. 2005. Patterns of Distribution of Mammals in the Dinosaur Park Formation and Their Paleobiological Significance. *In* CURRIE,

P. J. and KOPPELHUS, E. B. (eds.) *Dinosaur Provincial Park: A Spectacular Ancient Ecosystem Revealed*, Indiana University Press, Bloomington, 436–449 pp.

SATO, H., MURRAY, A. M., VERNYGORA, O. and CURRIE, P. J. 2018. A rare, articulated sturgeon (Chondrostei: Acipenseriformes) from the Upper Cretaceous of Dinosaur Provincial Park, Alberta, Canada. *Journal of Vertebrate Paleontology*, **38**, (1)-(15).

SATO, T., EBERTH, D. A., NICHOLLS, E. L. and MANABE, M. 2005. Plesiosaurian Remains from Non-marine to Paralic Sediments. *In* CURRIE, P. J. and KOPPELHUS, E. B. (eds.) *Dinosaur Provincial Park: A Spectacular Ancient Ecosystem Revealed*, Indiana University Press, Bloomington, 249–276 pp.

SCHERER, C. R. and VOICULESCU-HOLVAD, C. 2024. Reanalysis of a dataset refutes claims of anagenesis within *Tyrannosaurus*-line tyrannosaurines (Theropoda, Tyrannosauridae). *Cretaceous Research*, **155**, 105780.

SCHEYER, T. M., ROMANO, C., JENKS, J. and BUCHER, H. 2014. Early Triassic Marine Biotic Recovery: The Predators' Perspective. *PLOS ONE*, **9**, e88987.

SCHNEIDER, D., WINK, M., SPORER, F. and LOUNIBOS, P. 2002. Cycads: their evolution, toxins, herbivores and insect pollinators. *Naturwissenschaften*, **89**, 281–294.

SCHNEIDER, W. 1990. *FAO species identification sheets for fishery purposes. Field guide to the commercial marine resources of the Gulf of Guinea.* FAO, Rome.

SCHOENE, B., EDDY, M. P., SAMPERTON, K. M., KELLER, C. B., KELLER, G., ADATTE, T. and KHADRI, S. F. R. 2019. U-Pb constraints on pulsed eruption of the Deccan Traps across the end-Cretaceous mass extinction. *Science*, **363**, 862–866.

SCHOTT, R. K. and EVANS, D. C. 2017. Cranial variation and systematics of *Foraminacephale brevis* gen. nov. and the diversity of pachycephalosaurid dinosaurs (Ornithischia: Cerapoda) in the

Belly River Group of Alberta, Canada. *Zoological Journal of the Linnean Society*, **179**, 865–906.

SCHROEDER, K., LYONS, S. K. and SMITH, F. A. 2021. The influence of juvenile dinosaurs on community structure and diversity. *Science*, **371**, 941–944.

SCHULP, A. S., VONHOF, H. B., LUBBE, J. H. J. L. van der, JANSSEN, R. and BAAL, R. R. van. 2013. On diving and diet: resource partitioning in type-Maastrichtian mosasaurs. *Netherlands Journal of Geosciences*, **92**, 165–170.

SCOTESE, C. R., SONG, H., MILLS, B. J. W. and VAN DER MEER, D. G. 2021. Phanerozoic paleotemperatures: The earth's changing climate during the last 540 million years. *Earth-Science Reviews*, **215**, 103503.

SCOTT, C. S. and FOX, R. C. 2015. Review of Stagodontidae (Mammalia, Marsupialia) from the Judithian (Late Cretaceous) Belly River Group of southeastern Alberta, Canada. *Canadian Journal of Earth Sciences*, **52**, 682–695.

SCOTT, W. B. and CROSSMAN, E. J. 1973. *Freshwater fishes of Canada*. Bulletin, Fisheries Board of Canada.

SECORD, R., BLOCH, J. I., CHESTER, S. G. B., BOYER, D. M., WOOD, A. R., WING, S. L., KRAUS, M. J., MCINERNEY, F. A. and KRIGBAUM, J. 2012. Evolution of the Earliest Horses Driven by Climate Change in the Paleocene-Eocene Thermal Maximum. *Science*, **335**, 959–962.

SEILACHER, A., REIF, W.-E., WESTPHAL, F., RIDING, R., CLARKSON, E. N. K., WHITTINGTON, H. B. and MORRIS, S. C. 1985. Sedimentological, ecological and temporal patterns of fossil Lagerstätten. *Philosophical Transactions of the Royal Society of London. B, Biological Sciences*, **311**, 5–24.

SELDEN, P. A. and NUDDS, J. R. 2012. *Evolution of Fossil Ecosystems*. Manson, London, UK.

SENDER, L. M., WAPPLER, T., GARCÍA-ÁVILA, M., SANTOS, A. A. and DIEZ, J. B. 2022. First plant-insect interactions on Cretaceous Caytoniales (genus *Sagenopteris*) from the Lower Cretaceous (Albian) of Spain. *Cretaceous Research*, **138**, 105295.

SEPKOSKI, J. J., BAMBACH, R. K., RAUP, D. M. and VALENTINE, J. W. 1981. Phanerozoic marine diversity and the fossil record. *Nature*, **293**, 435–437.

SERENO, P. C. 1999. The evolution of dinosaurs. *Science*, **284**, 2137–47.

SERENO, P. C., WILSON, J. A. and CONRAD, J. L. 2004. New dinosaurs link southern landmasses in the Mid–Cretaceous. *Proceedings of the Royal Society of London. Series B: Biological Sciences*, **271**, 1325–1330.

SHAW, J. O., COCO, E., WOOTTON, K., DAEMS, D., GILLREATH-BROWN, A., SWAIN, A. and DUNNE, J. A. 2021. Disentangling ecological and taphonomic signals in ancient food webs. *Paleobiology*, **47**, 385–401.

SHEEHAN, P. M. 1996. A new look at Ecologic Evolutionary Units (EEUs). *Palaeogeography, Palaeoclimatology, Palaeoecology*, **127**, 21–32.

———, FASTOVSKY, D. E., HOFFMANN, R. G., BERGHAUS, C. B. and GABRIEL, D. L. 1991. Sudden Extinction of the Dinosaurs: Latest Cretaceous, Upper Great Plains, U.S.A. *Science*, **254**, 835–839.

SHOOP, C. R. and RUCKDESCHEL, C. A. 1990. Alligators as Predators on Terrestrial Mammals. *The American Midland Naturalist*, **124**, 407–412.

SILVA, O. D. da, COSTA, T. M. da, SILVA-ALVES, V. D., FERMIANO, E. C., SEBA, M. de F. R., NOGUEIRA, O. M., MUDREK, J. R., BARBOSA, A. P. D., GUSMÃO, A. C., MUNIZ, C. C., CARNIELLO, M. A., SANTOS-FILHO, M. dos and SILVA, D. J. da. 2020. Diet and food ontogeny of the lizard *Tupinambis matipu* Silva et al. 2018 (Squamata: Teiidae) in Central Brazil. *Research, Society and Development*, **9**, e52391110073–e52391110073.

SIMPSON, G. G. 1944. *Tempo and Mode in Evolution*. Columbia University Press.

SINCLAIR, A. R. E., MDUMA, S. and BRASHARES, J. S. 2003. Patterns of predation in a diverse predator–prey system. *Nature*, **425**, 288–290.

SINGH, S. A., ELSLER, A., STUBBS, T. L., RAYFIELD, E. J. and BENTON, M. J. 2024. Predatory synapsid ecomorphology signals growing dynamism of late Palaeozoic terrestrial ecosystems. *Communications Biology*, **7**, 1–19.

SMITH, F. A., TOMÉ, C. P., ELLIOTT SMITH, E. A., LYONS, S. K., NEWSOME, S. D. and STAFFORD, T. W. 2016. Unraveling the consequences of the terminal Pleistocene megafauna extinction on mammal community assembly. *Ecography*, **39**, 223–239.

SMITH, J. J., HASIOTIS, S. T., KRAUS, M. J. and WOODY, D. T. 2009. Transient dwarfism of soil fauna during the Paleocene–Eocene Thermal Maximum. *Proceedings of the National Academy of Sciences*, **106**, 17655–17660.

SONG, H., KEMP, D. B., TIAN, L., CHU, D., SONG, H. and DAI, X. 2021. Thresholds of temperature change for mass extinctions. *Nature Communications*, **12**, 4694.

SPIEKMAN, S. N. F., NEENAN, J. M., FRASER, N. C., FERNANDEZ, V., RIEPPEL, O., NOSOTTI, S. and SCHEYER, T. M. 2020. Aquatic Habits and Niche Partitioning in the Extraordinarily Long-Necked Triassic Reptile *Tanystropheus*. *Current Biology*, S0960982220310174.

SREEKAR, R., KATABUCHI, M., NAKAMURA, A., CORLETT, R. T., SLIK, J. W. F., FLETCHER, C., HE, F., WEIBLEN, G. D., SHEN, G., XU, H., SUN, I.-F., CAO, K., MA, K., CHANG, L.-W., CAO, M., JIANG, M., GUNATILLEKE, I. A. U. N., ONG, P., YAP, S., GUNATILLEKE, C. V. S., NOVOTNY, V., BROCKELMAN, W. Y., XIANG, W., MI, X., LI, X., WANG, X., QIAO, X., LI, Y., TAN, S., CONDIT, R., HARRISON, R. D. and KOH, L. P. 2018. Spatial scale changes the relationship between beta diversity, species richness and latitude. *Royal Society Open Science*, **5**, 181168.

STANLEY, S. M. 1975. A theory of evolution above the species level. *Proceedings of the National Academy of Sciences*, **72**, 646–650.

STEENWEG, R., HEBBLEWHITE, M., BURTON, C., WHITTINGTON, J., HEIM, N., FISHER, J. T., LADLE, A., LOWE, W., MUHLY, T., PACZKOWSKI, J. and MUSIANI, M. 2023. Testing umbrella species and food-web properties of large carnivores in the Rocky Mountains. *Biological Conservation*, **278**, 109888.

STEIN, W. E., BERRY, C. M., HERNICK, L. V. and MANNOLINI, F. 2012. Surprisingly complex community discovered in the mid-Devonian fossil forest at Gilboa. *Nature*, **483**, 78–81.

———, ———, MORRIS, J. L., HERNICK, L. V., MANNOLINI, F., STRAETEN, C. V., LANDING, E., MARSHALL, J. E. A., WELLMAN, C. H., BEERLING, D. J. and LEAKE, J. R. 2019. Mid-Devonian *Archaeopteris* Roots Signal Revolutionary Change in Earliest Fossil Forests. *Current Biology*, **30**, 421-431.E2.

STERNBERG, C. H. 1917. *Hunting Dinosaurs in the Bad Lands of the Red Deer River, Alberta, Canada*. World Company Press, Lawrence, Kansas.

STERNBERG, C. M. 1932. Two new theropod dinosaurs from the Belly River formation of Alberta. *Canadian Field Naturalist*, **46**, 99–105.

———. 1935. *Hooded Hadrosaurs of the Belly River Series of the Upper Cretaceous: A Comparison, with Descriptions of New Species*. National Museums of Canada, Ottawa.

———. 1936. Preliminary map 969A, Steveville sheet, Alberta.

———. 1940*a*. Ceratopsidae from Alberta. *Journal of Paleontology*, **14**, 468–480.

———. 1950. Steveville west of the 4th meridian, with notes on fossil localities.

———. 1953. A new hadrosaur from the Oldman Formation of Alberta: Discussion of nomenclature. *Bulletin of the National Museum of Canada*, **128**, 275–286.

STERNBERG, R. M. 1940*b*. A toothless bird from the Cretaceous of Alberta. *Journal of Paleontology*, **14**, 81–85.

STEWART, M. M. and SANDISON, P. 1972. Comparative Food Habits of Sympatric Mink Frogs, Bullfrogs, and Green Frogs. *Journal of Herpetology*, **6**, 241–244.

STIGALL, A. L., EDWARDS, C. T., FREEMAN, R. L. and RASMUSSEN, C. M. Ø. 2019. Coordinated biotic and abiotic change during the Great Ordovician Biodiversification Event: Darriwilian assembly of early Paleozoic building blocks. *Palaeogeography, Palaeoclimatology, Palaeoecology*, **530**, 249–270.

STOCKEY, R. A., ROTHWELL, G. W. and JOHNSON, K. R. 2007. *Cobbania corrugata* gen. et comb. nov. (Araceae): a floating aquatic monocot from the Upper Cretaceous of western North America. *American Journal of Botany*, **94**, 609–624.

STRAUSS, D. and SADLER, P. M. 1989. Classical confidence intervals and Bayesian probability estimates for ends of local taxon ranges. *Mathematical Geology*, **21**, 411–427.

SUES, H. D. 1978. A new small theropod dinosaur from the Judith River Formation (Campanian) of Alberta Canada. *Zoological Journal of the Linnean Society*, **62**, 381–400.

SWAIN, A., DEVEREUX, M. and FAGAN, W. F. 2021. Deciphering trophic interactions in a mid-Cambrian assemblage. *iScience*, **24**, 102271.

TANKE, D. H. 2005. Identifying Lost Quarries. *In* CURRIE, P. J. and KOPPELHUS, E. B. (eds.) *Dinosaur Provincial Park: A Spectacular Ancient Ecosystem Revealed*, Indiana University Press, Bloomington, 34–53 pp.

TENNANT, J. P., MANNION, P. D., UPCHURCH, P., SUTTON, M. D. and PRICE, G. D. 2017. Biotic and environmental dynamics through the Late Jurassic–Early Cretaceous transition: evidence for protracted faunal and ecological turnover. *Biological Reviews*, **92**, 776–814.

THERRIEN, F., ZELENITSKY, D. K., VORIS, J. T. and TANAKA, K. 2021. Mandibular force profiles and tooth morphology in growth series of *Albertosaurus sarcophagus* and *Gorgosaurus libratus* (Tyrannosauridae: Albertosaurinae) provide evidence for an ontogenetic dietary shift in tyrannosaurids. *Canadian Journal of Earth Sciences*, **58**, 812–828.

———, ———, TANAKA, K., VORIS, J. T., ERICKSON, G. M., CURRIE, P. J., DEBUHR, C. L. and KOBAYASHI, Y. 2023. Exceptionally preserved stomach contents of a young tyrannosaurid reveal an ontogenetic dietary shift in an iconic extinct predator. *Science Advances*, **9**, eadi0505.

THOMAS, R. G., EBERTH, D. A., DEINO, A. L. and ROBINSON, D. 1990. Composition, radioisotopic ages, and potential significance of an altered volcanic ash (bentonite) from the Upper Cretaceous Judith River Formation, Dinosaur Provincial Park, southern Alberta, Canada. *Cretaceous Research*, **11**, 125–162.

THOMPSON, R. M., HEMBERG, M., STARZOMSKI, B. M. and SHURIN, J. B. 2007. Trophic Levels and Trophic Tangles: The Prevalence of Omnivory in Real Food Webs. *Ecology*, **88**, 612–617.

TORICES, A., WILKINSON, R., ARBOUR, V. M., RUIZ-OMEÑACA, J. I. and CURRIE, P. J. 2018. Puncture-and-Pull Biomechanics in the Teeth of Predatory Coelurosaurian Dinosaurs. *Current Biology*, **28**, 1467-1474.e2.

TÓTH, A. B., LYONS, S. K., BARR, W. A., BEHRENSMEYER, A. K., BLOIS, J. L., BOBE, R., DAVIS, M., DU, A., ERONEN, J. T., FAITH, J. T., FRASER, D., GOTELLI, N. J., GRAVES, G. R., JUKAR, A. M., MILLER, J. H., PINEDA-MUNOZ, S., SOUL, L. C., VILLASEÑOR, A. and ALROY, J. 2019. Reorganization of surviving mammal communities after the end-Pleistocene megafaunal extinction. *Science*, **365**, 1305–1308.

TRUJILLO, K. and KOWALLIS, B. 2015. Recalibrated legacy 40Ar/39Ar ages for the Upper Jurassic Morrison Formation, Western Interior, U.S.A. *Geology of the Intermountain West*, **2**, 1–8.

TUMARKIN-DERATZIAN, A. R. 1997. Sedimentology, Taphonomy, and Faunal Review of a Multigeneric Bonebed (Bonebed 47) in the Dinosaur Park Formation (Campanian) of Southern Alberta, Canada.Unpublished B.Sc. Thesis, Lafayette College, Easton, PA, 107pp.

TWEET, J. S., CHIN, K., BRAMAN, D. R. and MURPHY, N. L. 2008. Probable gut contents within a specimen of *Brachylophosaurus canadensis* (Dinosauria: Hadrosauridae) from the Upper Cretaceous Judith River Formation of Montana. *PALAIOS*, **23**, 624–635.

TYSON, H. L. 1977. Functional craniology of the Ceratopsia (Reptilia: Ornithischia) with special reference to *Eoceratops*.M.Sc. thesis, University of Alberta, Edmonton, 339pp.

UPCHURCH, P., HUNN, C. A. and NORMAN, D. B. 2002. An analysis of dinosaurian biogeography: evidence for the existence of vicariance and dispersal patterns caused by geological events. *Proceedings of the Royal Society of London. Series B: Biological Sciences*, **269**, 613–621.

VAN ROY, P., DALEY, A. C. and BRIGGS, D. E. G. 2015. Anomalocaridid trunk limb homology revealed by a giant filter-feeder with paired flaps. *Nature*, **522**, 77–80.

VAN VALEN, L. M. 1973. A new evolutionary law. *Evolutionary Theory*, **1**, 1–30.

VAN VALKENBURGH, B. and MOLNAR, R. E. 2002. Dinosaurian and Mammalian Predators Compared. *Paleobiology*, **28**, 527–543.

———, HAYWARD, M. W., RIPPLE, W. J., MELORO, C. and ROTH, V. L. 2016. The impact of large terrestrial carnivores on Pleistocene ecosystems. *Proceedings of the National Academy of Sciences of the United States of America*, **113**, 862–867.

VANVLEET, K. 2014. Planogyra asteriscus. Animal Diversity Web. Downloaded from https://animaldiversity.org/accounts/Planogyra_asteriscus/ on 19 March 2024.

VAVREK, M. J. 2010. Palaeomacroecology: Large Scale Patterns in Species Diversity Through the Fossil Record.Unpublished Ph.D. Thesis, McGill University, Montreal, 222pp.

——— and LARSSON, H. C. E. 2010. Low beta diversity of Maastrichtian dinosaurs of North America. *Proceedings of the National Academy of Sciences of the United States of America*, **107**, 8265–8268.

VERMEIJ, G. J. and LEIGHTON, L. R. 2003. Does global diversity mean anything? *Paleobiology*, **29**, 3–7.

VIGLIETTI, P. A., BENSON, R. B. J., SMITH, R. M. H., BOTHA, J., KAMMERER, C. F., SKOSAN, Z., BUTLER, E., CREAN, A., ELOFF, B., KAAL, S., MOHOI, J., MOLEHE, W., MTALANA, N., MTUNGATA, S., NTHERI, N., NTSALA, T., NYAPHULI, J., OCTOBER, P., SKINNER, G., STRONG, M., STUMMER, H., WOLVAARDT, F. P. and ANGIELCZYK, K. D. 2021. Evidence from South Africa for a protracted end-Permian extinction on land. *Proceedings of the National Academy of Sciences*, **118**, e2017045118.

VILLALOBOS-SEGURA, E., STUMPF, S., TÜRTSCHER, J., JAMBURA, P. L., BEGAT, A., LÓPEZ-ROMERO, F. A., FISCHER, J. and KRIWET, J. 2023. A Synoptic Review of the Cartilaginous Fishes (Chondrichthyes: Holocephali, Elasmobranchii) from the Upper Jurassic Konservat-Lagerstätten of Southern Germany: Taxonomy, Diversity, and Faunal Relationships. *Diversity*, **15**, 386.

VISSER, J. 1986. Sedimentology and taphonomy of a *Styracosaurus* bonebed in the Late Cretaceous Judith River Formation, Dinosaur Provincial Park, Alberta.Unpublished M.Sc. Thesis, University of Calgary, Calgary, 150pp.

VITT, L. J. and DE CARVALHO, C. M. 1992. Life in the trees: the ecology and life history of *Kentropyx striatus* (Teiidae) in the lavrado area of Roraima, Brazil, with comments on the life histories of tropical teiid lizards. *Canadian Journal of Zoology*, **70**, 1995–2006.

VORIS, J. T., ZELENITSKY, D. K., THERRIEN, F., RIDGELY, R. C., CURRIE, P. J. and WITMER, L. M. 2022. Two exceptionally preserved juvenile specimens of *Gorgosaurus libratus* (Tyrannosauridae, Albertosaurinae) provide new insight into the timing of ontogenetic changes in tyrannosaurids. *Journal of Vertebrate Paleontology*, **41**, e2041651.

VRBA, E. S. 1993. Turnover pulses, the Red Queen, and related topics. *American Journal of Science*, **293-A**, 418–452.

VULLO, R. 2011. Direct evidence of hybodont shark predation on Late Jurassic ammonites. *Naturwissenschaften*, **98**, 545–549.

WALL, W. P. and GALTON, P. M. 1979. Notes on pachycephalosaurid dinosaurs (Reptilia: Ornithischia) from North America, with comments on their status as ornithopods. *Canadian Journal of Earth Sciences*, **16**, 1176–1186.

WANG, D., QIN, M., LIU, L., LIU, L., ZHOU, Y., ZHANG, Y., HUANG, P., XUE, J., ZHANG, S. and MENG, M. 2019. The Most Extensive Devonian Fossil Forest with Small Lycopsid Trees Bearing the Earliest Stigmarian Roots. *Current Biology*, **29**, 2604-2615.e2.

WANG, S. C. and DODSON, P. 2006. Estimating the diversity of dinosaurs. *Proceedings of the National Academy of Sciences*, **103**, 13601–13605.

WEAVER, L. N. and WILSON, G. P. 2021. Shape disparity in the blade-like premolars of multituberculate mammals: functional constraints and the evolution of herbivory. *Journal of Mammalogy*, **102**, 967–985.

WEAVER, L. N., KELSON, J. R., HOLDER, R. M., NIEMI, N. A. and BADGLEY, C. 2024. On the role of tectonics in stimulating the Cretaceous diversification of mammals. *Earth-Science Reviews*, **248**, 104630.

WESTON, T. C. 1899. *Reminiscences among the rocks in connection with the Geological Survey of Canada*. Warwick Bro’s & Rutter, Toronto.

WHITAKER, R. and BASU, D. 1982. The Gharial *Gavialis gangeticus* - A Review. *Bombay Natural History Society Journal*, **79**, 531–548.

WHITE, M. A., BELL, P. R., CAMPIONE, N. E., SANSALONE, G., BROUGHAM, T., BEVITT, J. J., MOLNAR, R. E., COOK, A. G., WROE, S. and ELLIOTT, D. A. 2022. Abdominal contents reveal Cretaceous crocodyliforms ate dinosaurs. *Gondwana Research*, **106**, 281–302.

WHITE, P. D., FASTOVSKY, D. E. and SHEEHAN, P. M. 1998. Taphonomy and suggested structure of the dinosaurian assemblage of the Hell Creek Formation (Maastrichtian), eastern Montana and western North Dakota. *PALAIOS*, **13**, 41–51.

WHITLOCK, J., TRUJILLO, K. and HANIK, G. 2018. Assemblage-level structure in Morrison Formation dinosaurs, Western Interior, USA. *Geology of the Intermountain West*, **5**, 9–22.

WIENS, D. and WORSLEY, T. 2016. Reproductive failure: a new paradigm for extinction. *Biological Journal of the Linnean Society*, **119**, 1096–1102.

WIGNALL, P. B. 2001. Large igneous provinces and mass extinctions. *Earth-Science Reviews*, **53**, 1–33.

——— and HALLAM, A. 1993. Griesbachian (Earliest Triassic) palaeoenvironmental changes in the Salt Range, Pakistan and southeast China and their bearing on the Permo-Triassic mass extinction. *Palaeogeography, Palaeoclimatology, Palaeoecology*, **102**, 215–237.

WILCOX, T. M., SCHWARTZ, M. K. and LOWE, W. H. 2018. Evolutionary Community Ecology: Time to Think Outside the (Taxonomic) Box. *Trends in Ecology & Evolution*, **33**, 240–250.

WILF, P. 2000. Late Paleocene–early Eocene climate changes in southwestern Wyoming: Paleobotanical analysis. *GSA Bulletin*, **112**, 292–307.

WILLIAMS, R. J. and MARTINEZ, N. D. 2000. Simple rules yield complex food webs. *Nature*, **404**, 180–183.

WILLIAMS, R. J. and MARTINEZ, N. D. 2004. Limits to Trophic Levels and Omnivory in Complex Food Webs: Theory and Data. *The American Naturalist*, **163**, 458–468.

WILLIAMS, T. A. and CHRISTIANSEN, J. L. 1981. The Niches of Two Sympatric Softshell Turtles, *Trionyx muticus* and *Trionyx spiniferus*, in Iowa. *Journal of Herpetology*, **15**, 303–308.

WILLIS, K. J. and BIRKS, H. J. B. 2006. What Is Natural? The Need for a Long-Term Perspective in Biodiversity Conservation. *Science*, **314**, 1261–1265.

WILSON, G. P. 2013. Mammals across the K/Pg boundary in northeastern Montana, U.S.A.: dental morphology and body-size patterns reveal extinction selectivity and immigrant-fueled ecospace filling. *Paleobiology*, **39**, 429–469.

———, DEMAR, D. G., Jr. and CARTER, G. 2014*a*. Extinction and survival of salamander and salamander-like amphibians across the Cretaceous-Paleogene boundary in northeastern Montana, USA. *In* WILSON, G. P., CLEMENS, W. A., HORNER, J. R. and HARTMAN, J. H. (eds.) *Through the End of the Cretaceous in the Type Locality of the Hell Creek Formation in Montana and Adjacent Areas*, Special Paper 503. Geological Society of America, 271–297 pp.

———, CLEMENS, W. A., HORNER, J. R. and HARTMAN, J. H. 2014*b*. *Through the End of the Cretaceous in the Type Locality of the Hell Creek Formation in Montana and Adjacent Areas*. Geological Society of America.

———, EKDALE, E. G., HOGANSON, J. W., CALEDE, J. J. and VANDER LINDEN, A. 2016. A large carnivorous mammal from the Late Cretaceous and the North American origin of marsupials. *Nature Communications*, **7**, 13734.

———, EVANS, A. R., CORFE, I. J., SMITS, P. D., FORTELIUS, M. and JERNVALL, J. 2012. Adaptive radiation of multituberculate mammals before the extinction of dinosaurs. *Nature*, **483**, 457–460.

WILSON, J. P., RYAN, M. J. and EVANS, D. C. 2020. A new, transitional centrosaurine ceratopsid from the Upper Cretaceous Two Medicine Formation of Montana and the evolution of the '*Styracosaurus*-line' dinosaurs. *Royal Society Open Science*, **7**, 200284.

WILSON, M. V. H., BRINKMAN, D. B. and NEUMAN, A. G. 1992. Cretaceous Esocoidei (Teleostei): early radiation of the pikes in North American fresh waters. *Journal of Paleontology*, **66**, 839–846.

WILSON, P. K. and MOORE, J. R. 2016. Assessing the Control of Preservational Environment on Taphonomic and Ecological Patterns in an Oligocene Mammal Fauna from Badlands National Park, South Dakota. *PLOS ONE*, **11**, e0157585.

WING, S. L., SUES, H.-D., POTTS, R., DIMICHELE, W. A. and BEHRENSMEYER, A. K. 1992. Evolutionary Palaeoecology. *In* BEHRENSMEYER, A. K., DAMUTH, J. D., DIMICHELE, W. A., POTTS, R., SUES, H.-D. and WING, S. L. (eds.) *Terrestrial Ecosystems through Time*, The University of Chicago Press, Chicago and London, 1–13 pp.

WING, S. L., HARRINGTON, G. J., SMITH, F. A., BLOCH, J. I., BOYER, D. M. and FREEMAN, K. H. 2005. Transient Floral Change and Rapid Global Warming at the Paleocene-Eocene Boundary. *Science*, **310**, 993–996.

WITTON, M. P. 2008. A new approach to determining pterosaur body mass and its implications for pterosaur flight. *Zitteliana*, **B28**, 143–158.

——— and NAISH, D. 2008. A Reappraisal of Azhdarchid Pterosaur Functional Morphology and Paleoecology. *PLOS ONE*, **3**, e2271.

WOOD, J. M., THOMAS, R. G. and VISSER, J. 1988. Fluvial processes and vertebrate taphonomy: the Upper Cretaceous Judith River formation, South-Central dinosaur Provincial Park, Alberta, Canada. *Palaeogeography, Palaeoclimatology, Palaeoecology*, **66**, 127–143.

WOODRUFF, D. C. 2019. What factors influence our reconstructions of Morrison Formation sauropod diversity? *Geology of the Intermountain West*, **6**, 93–112.

———, SCHOTT, R. K. and EVANS, D. C. 2023. Two new species of small-bodied pachycephalosaurine (Dinosauria, Marginocephalia) from the uppermost Cretaceous of North America suggest hidden diversity in well-sampled formations. *Papers in Palaeontology*, **9**, e1535.

———, CARR, T. D., STORRS, G. W., WASKOW, K., SCANNELLA, J. B., NORDÉN, K. K. and WILSON, J. P. 2018. The Smallest Diplodocid Skull Reveals Cranial Ontogeny and Growth-Related Dietary Changes in the Largest Dinosaurs. *Scientific Reports*, **8**, 14341.

WOODWARD, H. N., FOWLER, E. A. F., FARLOW, J. O. and HORNER, J. R. 2015. *Maiasaura*, a model organism for extinct vertebrate population biology: a large sample statistical assessment of growth dynamics and survivorship. *Paleobiology*, **41**, 503–527.

WOOLLER, M. J., BATAILLE, C., DRUCKENMILLER, P., ERICKSON, G. M., GROVES, P., HAUBENSTOCK, N., HOWE, T., IRRGEHER, J., MANN, D., MOON, K., POTTER, B. A., PROHASKA, T., RASIC, J., REUTHER, J., SHAPIRO, B., SPALETA, K. J. and WILLIS, A. D. 2021. Lifetime mobility of an Arctic woolly mammoth. *Science*, **373**, 806–808.

WOOLLEY, C. H., BOTTJER, D. J., CORSETTI, F. A. and SMITH, N. D. 2024. Quantifying the effects of exceptional fossil preservation on the global availability of phylogenetic data in deep time. *PLOS ONE*, **19**, e0297637.

WU, X.-C. 2005. Crocodylians. *In* CURRIE, P. J. and KOPPELHUS, E. B. (eds.) *Dinosaur Provincial Park: A Spectacular Ancient Ecosystem Revealed*, Indiana University Press, Bloomington, 277–291 pp.

———, BRINKMAN, D. B. and RUSSELL, A. P. 1996. A new alligator from the Upper Cretaceous of Canada and the relationship of early eusuchians. *Palaeontology*, **39**, 351–375.

———, RUSSELL, A. P. and BRINKMAN, D. B. 2001. A review of *Leidyosuchus canadensis* Lambe, 1907 (Archosauria: Crocodylia) and an assessment of cranial variation based upon new material. *Canadian Journal of Earth Sciences*, **38**, 1665–1687.

WU, Y., GE, Y., HU, H., STIDHAM, T. A., LI, Z., BAILLEUL, A. M. and ZHOU, Z. 2023. Intra-gastric phytoliths provide evidence for folivory in basal avialans of the Early Cretaceous Jehol Biota. *Nature Communications*, **14**, 4558.

WYENBERG-HENZLER, T., PATTERSON, R. T. and MALLON, J. C. 2021. Size-mediated competition and community structure in a Late Cretaceous herbivorous dinosaur assemblage. *Historical Biology*, **34**, 2230–2240.

———, ——— and ———. 2022. Ontogenetic dietary shifts in North American hadrosaurids (Dinosauria: Ornithischia). *Cretaceous Research*, **135**, 105177.

XING, L., BELL, P. R., IV, W. S. P., JI, S., MIYASHITA, T., BURNS, M. E., JI, Q. and CURRIE, P. J. 2012. Abdominal Contents from Two Large Early Cretaceous Compsognathids (Dinosauria: Theropoda) Demonstrate Feeding on Confuciusornithids and Dromaeosaurids. *PLOS ONE*, **7**, e44012.

———, PERSONS, W. S., BELL, P. R., XU, X., ZHANG, J., MIYASHITA, T., WANG, F. and CURRIE, P. J. 2013. Piscivory in the Feathered Dinosaur *Microraptor*. *Evolution*, **67**, 2441–2445.

YANG, S., HE, H., JIN, F., ZHANG, F., WU, Y., YU, Z., LI, Q., WANG, M., O'CONNOR, J. K., DENG, C., ZHU, R. and ZHOU, Z. 2020. The appearance and duration of the Jehol Biota: Constraint from SIMS U-Pb zircon dating for the Huajiying Formation in northern China. *Proceedings of the National Academy of Sciences*, **117**, 14299–14305.

YODZIS, P. 1998. Local trophodynamics and the interaction of marine mammals and fisheries in the Benguela ecosystem. *Journal of Animal Ecology*, **67**, 635–658.

ZACHOS, J., PAGANI, M., SLOAN, L., THOMAS, E. and BILLUPS, K. 2001. Trends, Rhythms, and Aberrations in Global Climate 65 Ma to Present. *Science*, **292**, 686–693.

ZANNO, L. E., DRYMALA, S., NESBITT, S. J. and SCHNEIDER, V. P. 2015. Early crocodylomorph increases top tier predator diversity during rise of dinosaurs. *Scientific Reports*, **5**, 9276.

ZAZULA, G. D., MACPHEE, R. D. E., METCALFE, J. Z., REYES, A. V., BROCK, F., DRUCKENMILLER, P. S., GROVES, P., HARINGTON, C. R., HODGINS, G. W. L., KUNZ, M. L., LONGSTAFFE, F. J., MANN, D. H., MCDONALD, H. G., NALAWADE-CHAVAN, S. and SOUTHON, J. R. 2014. American mastodon extirpation in the Arctic and Subarctic predates human colonization and terminal Pleistocene climate change. *Proceedings of the National Academy of Sciences*, **111**, 18460–18465.

ZELENITSKY, D. K., THERRIEN, F., ERICKSON, G. M., DEBUHR, C. L., KOBAYASHI, Y., EBERTH, D. A. and HADFIELD, F. 2012. Feathered Non-Avian Dinosaurs from North America Provide Insight into Wing Origins. *Science*, **338**, 510–514.

ZHANG, M., DAI, S., DU, B., JI, L. and HU, S. 2018. Mid-Cretaceous Hothouse Climate and the Expansion of Early Angiosperms. *Acta Geologica Sinica - English Edition*, **92**, 2004–2025.

ZHENG, X., WANG, X., SULLIVAN, C., ZHANG, X., ZHANG, F., WANG, Y., LI, F. and XU, X. 2018. Exceptional dinosaur fossils reveal early origin of avian-style digestion. *Scientific Reports*, **8**, 14217.

ZHOU, Z. 2014. The Jehol Biota, an Early Cretaceous terrestrial Lagerstätte: new discoveries and implications. *National Science Review*, **1**, 543–559.

———, BARRETT, P. M. and HILTON, J. 2003. An exceptionally preserved Lower Cretaceous ecosystem. *Nature*, **421**, 807–814.

2008. *The Jehol Fossils: The Emergence of Feathered Dinosaurs, Beaked Birds and Flowering Plants*. *In* CHANG, M., CHEN, P., WANG, Y., WANG, Y. and MIAO, D. (eds.) Elsevier: Academic Press, London.

2021. *IPCC, 2021: Climate Change 2021: The Physical Science Basis. Contribution of Working Group I to the Sixth Assessment Report of the Intergovernmental Panel on Climate Change*. *In* MASSON-DELMOTTE, V., ZHAI, P., PIRANI, A., CONNORS, S. L., PÉAN, C., BERGER, S., CAUD, N., CHEN, Y., GOLDFARB, L., GOMIS, M. I., HUANG, M., LEITZELL, K., LONNOY, E., MATTHEWS, J. B. R., MAYCOCK, T. K., WATERFIELD, T., YELEKÇI, O., YU, R. and ZHOU, B. (eds.) Cambridge University Press, Cambridge, United Kingdom and New York, NY, USA.